

IRON AND STEEL DIVISION

1948

A. I. M. E.

BENDIX LIBRARY

TN
1
A5
Vol. 176
N/C

TRANSACTIONS

OF THE

AMERICAN INSTITUTE OF MINING AND METALLURGICAL ENGINEERS

(INCORPORATED)

Volume 176

*American Institute of Mining, Metallurgical
and Petroleum Engineers*

IRON AND STEEL DIVISION

1948

TECHNICAL PAPERS, DISCUSSIONS AND SYMPOSIA PRESENTED BEFORE THE DIVISION
AT MEETINGS HELD AT CHICAGO, OCTOBER 20-22, 1947, NEW YORK, FEBRUARY
15-19, 1948, AND SAN FRANCISCO, FEBRUARY 13-17, 1949, ALSO THE
HOWE LECTURE.

PUBLISHED BY THE INSTITUTE
AT THE OFFICE OF THE SECRETARY
29 WEST 39TH STREET
NEW YORK 18, N.Y.

Notice

This volume is the twenty-first of a series containing papers and discussions presented before the Iron and Steel Division of the American Institute of Mining and Metallurgical Engineers since its organization in 1928; one volume each year, as follows:

1928, Iron and Steel Technology in 1928 (later listed as Volume 80 of the TRANSACTIONS); 1929 (vol. 84), 1930 (vol. 90), 1931 (vol. 95), 1932 (vol. 100), 1933, 1934, 1935, 1936, 1937, 1938, 1939, 1940, 1941, 1942, 1943, 1944, 1945, 1946, and 1947, TRANSACTIONS of the American Institute of Mining and Metallurgical Engineers, Iron and Steel Division.

This volume contains papers and discussions presented at the meetings at Chicago, Oct. 20-22, 1947; New York, Feb. 15-19, 1948 and San Francisco, Feb. 13-17, 1949; also the Howe Lecture for the New York Meeting, February 15-19, 1948.

Papers on iron and steel subjects published by the Institute prior to 1928 are to be found in many volumes of the TRANSACTIONS of the Institute; in Vols. 37 to 45, inclusive; 47, 50 and 51, 53, 56, 58, 62, 67 to 71, inclusive; 73 and 75. Vol. 67 was devoted exclusively to iron and steel.

Iron and steel papers published in the TRANSACTIONS before the year 1936 may be found by consulting the general indexes to Vols. 1 to 35 (1871-1904), Vols. 36 to 55 (1905-1916), Vols. 56 to 72 (1917-1935), and Vols. 73 to 117 (1926-1935).

COPYRIGHT, 1949, BY THE
AMERICAN INSTITUTE OF MINING AND METALLURGICAL ENGINEERS
(INCORPORATED)

PRINTED IN THE UNITED STATES OF AMERICA

THE MAPLE PRESS COMPANY, YORK, PA.

FOREWORD

THE 1948 Transactions of the Iron and Steel Division is the twenty-first consecutive annual volume published for this group since its organization as a division of the AIME. The twenty-four papers of this volume comprise six papers on steelmaking problems, four papers on the subject of gases in steel, three papers on sulphur in ironmaking and ten papers on physical metallurgy.

Of especial interest to all members is the excellent Howe Memorial Lecture delivered by Robert B. Sosman at the annual 1948 meeting. The lecture is entitled, "Temperatures in the Open-hearth Furnace." It is a subject which was a major interest to Dr. Sosman for many years.

These papers were published during the period from September, 1947 to December, 1948 in Metals Technology, and include all iron and steel papers for the year, and all physical metallurgy papers except those published after June, 1948. A few of the papers published in this 1948 volume will be presented at the 1949 Annual Meeting of the AIME and the discussion of these papers will by necessity be published in the next volume of Transactions.

This is the last volume of Iron and Steel Division Transactions in which papers embracing the production and metallurgy of iron and steel will be separated from papers covering the nonferrous metals. The 1950 volume will be of new format and larger size than the present and the past series of Transactions, and in addition, its contents will be broadened to include papers covering all metals, both in the ferrous and in the non-ferrous fields.

This volume of Transactions represents only the formal technical papers presented at the regular meetings of the Iron and Steel Division and does not include the proceedings of the three important conferences—Open Hearth Steel, Blast Furnace, Coke Oven and Raw Materials, and Electric Furnace Steel—sponsored by standing committees of the Iron and Steel Division. I wish to compliment the chairmen and executive committees of these three important groups for successful and outstanding work in their respective operating fields.

It is also a pleasure for me to compliment the chairman of the Publications Committee, Mr. H. W. Johnson, and his committee, for the high quality of papers published in this issue of Transactions.

Gilbert Solèr, *Chairman,*
Iron and Steel Division

Welland, Ontario,
November 1, 1948.

AIME OFFICERS AND DIRECTORS

For the year ending February 1949

PRESIDENT

W. E. WRATHER, Washington, D. C.

PAST PRESIDENTS AND DIRECTORS

LOUIS S. CATES, New York, N. Y.

CLYDE WILLIAMS, Columbus, Ohio

VICE-PRESIDENT AND TREASURER

ANDREW FLETCHER, New York, N. Y.

VICE-PRESIDENTS AND DIRECTORS

H. J. BROWN, Boston, Mass.

ERLE V. DAVELER, New York, N. Y.

C. HARRY BENEDICT, Lake Linden, Mich.

D. H. McLAUGHLIN, New York, N. Y.

ROBERT W. THOMAS, Ray, Ariz.

DIRECTORS

N. G. ALFORD, Pittsburgh, Pa.

ARTHUR JOHN BLAIR, Birmingham, Ala.

OLIVER BOWLES, Washington, D. C.

W. E. BREWSTER, Chicago, Ill.

R. J. ENNIS, Schumacher, Ont., Canada

J. B. HAFFNER, Kellogg, Idaho

A. B. KINZEL, New York, N. Y.

PHILIP KRAFT, New York, N. Y.

WILLIAM W. MEIN, Sr., San Francisco, Calif.

C. V. MILLIKAN, Tulsa, Okla.

D. D. MOFFAT, Salt Lake City, Utah

A. J. PHILLIPS, Barber, N. J.

RUSSELL B. PAUL, New York, N. Y.

W. B. PLANK, Easton, Pa.

EARLE E. SCHUMACHER, Murray Hill, N. J.

JOHN R. SUMAN, Houston, Texas

C. P. WATSON, Los Angeles, Calif.

CLYDE E. WEED, New York, N. Y.

DIVISION CHAIRMEN—Directors Ex-officiis

A. A. SMITH, JR. (Institute of Metals), Barber, N. J.

IRWIN W. ALCORN (Petroleum), Houston, Texas

GILBERT SOLER (Iron and Steel), Welland, Ont., Canada

CLAYTON G. BALL (Coal), Chicago, Ill.

CURTIS L. WILSON (Mineral Industry Education), Rolla, Mo.

RICHARD W. SMITH (Industrial Minerals), Washington, D. C.

JOHN F. MYERS (Minerals Beneficiation), Copperhill, Tenn.

SECRETARY

A. B. PARSONS, New York, N. Y.

STAFF IN NEW YORK

Assistant Secretaries

EDWARD H. ROBBE

E. J. KENNEDY, JR.

ERNEST KIRKENDALL

WILLIAM H. STRANG

Assistant to the Secretary

H. NEWELL APPLETON

Advertising Manager

"Mining and Metallurgy"

WHEELER SPACKMAN

Assistant Treasurer

H. A. MALONEY

CONTENTS

	PAGE
Foreword, by Gilbert Soler.	3
AIME Officers and Directors.	4
Iron and Steel Division Officers and Committees	7
R. W. Hunt Award	11
Howe Lectures and Lecturers.	10
Photograph of Robert B. Sosman, Howe Lecturer 1948.	14

TECHNICAL PAPERS AND DISCUSSIONS

Howe Lecture

Temperatures in the Open-hearth Furnace. By ROBERT B. SOSMAN. (<i>Metals Tech.</i> , Aug. 1948, T.P. 2435)	15
---	----

Steelmaking

Direct Oxidation in the Basic Open Hearth Process. By E. B. HUGHES and F. G. NORRIS. (<i>Metals Tech.</i> , June 1948, T.P. 2380). With discussion	52
Operation of Oxygen-enriched Open-hearth Furnaces. By J. S. MARSH. (<i>Metals Tech.</i> , Aug. 1948, T.P. 2416). With discussion.	78
Role of Thermochemical Factors in Basic Open Hearth Production Rate. By T. E. BROWER and B. M. LARSEN. (<i>Metals Tech.</i> , Oct. 1948, T.P. 2451)	92
Structure, Segregation and Solidification of Semikilled Steel Ingots. By MICHAEL TENENBAUM. (<i>Metals Tech.</i> , Sept. 1947, T.P. 2273). With discussion.	108
Origin of Silicate Inclusions in Basic Electric-arc-furnace Steel of Higher Carbon Contents. By AXEL HULTGREN. (<i>Metals Tech.</i> , Aug. 1948, T.P. 2418)	173
A Method for Determining the Origin of Surface Defects in Rolled Steel Products. By C. L. MEYETTE and V. L. ELLIOTT. (<i>Metals Tech.</i> , June 1948, T.P. 2368). With discussion	201

Gases in Steel

Sampling and Analysis of Steel for Hydrogen. By G. DERGE, W. PEIFER and J. H. RICHARDS. (<i>Metals Tech.</i> , June 1948, T.P. 2362). With discussion	219
Apparatus for the Hot-extraction Analysis for Hydrogen in Steel. By C. E. SIMS and G. A. MOORE. (<i>Metals Tech.</i> , June 1948, T.P. 2369). With discussion.	248
A Quantitative Experimental Investigation of the Hydrogen and Nitrogen Contents of Steel during Commercial Melting. By C. E. SIMS, G. A. MOORE and D. W. WILLIAMS. (<i>Metals Tech.</i> , Feb. 1948, T.P. 2347). With discussion	260
Effect of Hydrogen on the Ductility of Cast Steels. By C. E. SIMS, G. A. MOORE and D. W. WILLIAMS. (<i>Metals Tech.</i> , Oct. 1948, T.P. 2454)	283

Sulphur in Ironmaking

Kinetics of the Transfer of Sulphur across a Slag-metal Interface. By LO-CHING CHANG and K. M. GOLDMAN. (<i>Metals Tech.</i> , June 1948, T.P. 2367). With discussion	309
Some Correlations between Variables Affecting Sulphur in Blast Furnace Iron. By T. E. BROWER and B. M. LARSEN. (<i>Metals Tech.</i> , Sept. 1948, T.P. 2465).	330
Tracer Study of Sulphur in the Coke Oven. By S. E. EATON, R. W. HYDE and B. S. OLD. (<i>Metals Tech.</i> , Oct. 1948, T.P. 2453).	343

Transformation of Austenite		PAGE
Anisothermal Formation of Bainite and Proeutectoid Constituents in Steels. By LEONARD D. JAFFE. (<i>Metals Tech.</i> , Dec. 1947, T.P. 2290). With discussion.		363
Austenite Transformation Above and Within the Martensite Range. By R. T. HOWARD, JR. and M. COHEN. (<i>Metals Tech.</i> , Sept. 1947, T.P. 2283). With discussion.		384
X ray Determination of Retained Austenite by Integrated Intensities. By B. L. AVERBACH and M. COHEN. (<i>Metals Tech.</i> , Feb. 1948, T.P. 2342). With discussion.		401
An Evaluation of Quenching Oils by Means of the End Quench Test. By C. A. SIEBERT and G. SANDOZ. (<i>Metals Tech.</i> , April 1948, T.P. 2353). With discussion.		416

Properties of Steel

Notch-tensile Characteristics of a Partially Austempered, Low Alloy Steel. By G. SACHS, L. J. EBERT and W. F. BROWN, JR. (<i>Metals Tech.</i> , Feb. 1948, T.P. 2321).	424
Influence of Strain Aging on the Fracture Stress of Low-carbon Steel. By D. J. MCADAM, JR., G. W. GEIL, D. H. WOODARD and W. D. JENKINS. (<i>Metals Tech.</i> , Jan. 1948, T.P. 2318). With discussion.	436
Anelastic Properties of Iron. By T'ING-SUI KE. (<i>Metals Tech.</i> , June 1948, T.P. 2370). With discussion.	448
Testing Gun Steel and Other Alloys and Metals for Resistance to Surface Cracking. By E. INGERSON. (<i>Metals Tech.</i> , Aug. 1947, T.P. 2223). With discussion.	477
Wear Tests on Grinding Balls. By T. E. NORMAN and C. M. LOEB, JR. (<i>Metals Tech.</i> , April 1948, and <i>Mining Tech.</i> , May 1948, T.P. 2319). With discussion.	490
Behavior of Metal Cavity Liners in Shaped Explosive Charges. By G. B. CLARK and W. H. BRUCKNER. (<i>Mining Tech.</i> , May 1947, and <i>Metals Tech.</i> , Aug. 1947, T.P. 2158). With discussion.	527

TECHNICAL NOTES

Note on the Distribution of Sulphur between Molten Iron and Slag. By TERKEL ROSENQVIST. (<i>Metals Tech.</i> , Oct. 1948, T.N. 7)	541
Contents of Vol. 175, Institute of Metals Division, 1948	543
Index	547

IRON AND STEEL DIVISION

Established as a Division February 22, 1928

(By-laws printed in the 1939 TRANSACTIONS Volume of the Division)

Officers and Committees for Year ending February 1949

GILBERT SOLER, *Chairman*, Welland, Ontario
T. S. WASHBURN, *Past Chairman*, Chicago, Ill.
T. B. COUNSELMAN, *Vice Chairman*, New York, N. Y.
T. L. JOSEPH, *Vice Chairman*, Minneapolis, Minn.
ERNEST KIRKENDALL, *Secretary*, 29 West 39th Street, New York 18, N. Y.

Past Chairmen

RALPH H. SWEETSER, 1928
G. B. WATERHOUSE, 1929
W. J. MACKENZIE, 1930
F. M. BECKET, 1931
F. N. SPELLER, 1932
JOHN JOHNSTON, 1933
L. F. REINARTZ, 1934

A. B. KINZEL, 1935
C. E. WILLIAMS, 1936
FRANCIS B. FOLEY, 1937
J. T. MACKENZIE, 1938
J. HUNTER NEAD, 1939
FRANK T. SISCO, 1940

C. H. HERTY, Jr., 1941
E. C. SMITH, 1942
H. W. GRAHAM, 1943
W. A. HAVEN, 1944
ERLE G. HILL, 1945
W. E. BREWSTER, 1946
T. S. WASHBURN, 1947

Executive Committee

Until 1949

M. GENSAMER
H. E. PHELPS
H. K. WORK

Until 1950

W. A. STEELE
F. M. WASHBURN
E. C. WRIGHT

Until 1951

C. G. HOGBERG
E. D. MARTIN
C. S. SMITH

Blast Furnace, Coke Oven and Raw Materials

T. L. JOSEPH, *Chairman*
T. F. PLIMPTON, *Vice Chairman*
C. L. WYMAN, *Vice Chairman*
W. S. UNGER, *Secretary*

Program

Subcommittee

E. J. GARDNER, *Chairman*
F. D. DEVANEY
K. C. MCCUTCHEON
J. M. STAPLETON

Finance

Subcommittee

E. F. MITCHELL, *Chairman*
T. B. COUNSELMAN
J. W. FERREE
M. F. MORGAN
A. S. NICHOLS
R. H. SWEETSER
C. L. WYMAN

Papers

Subcommittee

R. W. CAMPBELL, *Chairman*
G. W. HEWITT
C. F. HOFFMAN
R. A. LINDGREN

Open Hearth Steel

C. R. FONDERSMITH, *Chairman*
W. C. KITTO, *Past-Chairman*
E. G. HILL, *Vice Chairman*
ERNEST KIRKENDALL, *Secretary-Treasurer*

T. A. CLEARY
CLYDE DENLINGER
J. J. GOLDEN
H. M. GRIFFITH
H. G. GRIM

L. A. LAMBING
B. D. MCCARTHY
A. P. MILLER
E. L. RAMSEY
L. F. REINARTZ
A. E. REINHARD

A. H. SOMMER
A. W. THORNTON
F. L. TOY
D. N. WATKINS
T. T. WATSON

IRON AND STEEL DIVISION

Bessemer Steel

G. M. YOCOM, *Chairman*
H. C. DUNKLE, *Vice-Chairman*

S. J. DOUGHERTY
K. L. FETTERS

H. W. GRAHAM
E. C. PENROD
E. B. STORY

A. W. THORNTON
F. L. TOY

Electric Furnace Steel*Executive Committee*

J. B. CAINE, *Chairman*
W. J. REAGAN, *Past-Chairman*
ERNEST KIRKENDALL, *Secretary*

C. W. BRIGGS
FRANK GARRATT
M. E. GOETZ

G. A. LILLIEQVIST
J. S. MARSH
T. J. McLOUGHLIN

W. M. PATTERSON
H. E. PHELPS
H. A. SCHWARTZ

Conference Committee

NORMAN I. STOTZ, *Chairman*
J. A. BOWERS, *Vice-Chairman*

F. W. BROOKE
E. J. CHELIUS
S. W. EWING
W. M. FARNSWORTH
J. W. HARVEY

R. J. KNERR
CHARLES LOCKE
M. J. MEINEN
ALDEN SAFFORD

C. E. SIMS
C. C. SPENCER
E. C. TROY
H. F. WALTHER
R. J. WILCOX

Physical Chemistry of Steelmaking

B. M. LARSEN, *Chairman*
W. O. PHILBROOK, *Secretary*

F. H. ALLISON, JR.
H. R. BELDING
M. B. BEVER
C. W. BRIGGS
W. S. DEBENHAM
GERHARD DERGE

L. G. EKHOLM
H. B. EMERICK
A. G. FORREST
H. J. FORSYTH
J. J. GOLDEN
T. L. JOSEPH
L. A. LAMBING

J. S. MARSH
SHADBURN MARSHALL
D. L. MCBRIDE
C. E. SIMS
C. R. TAYLOR
M. TENENBAUM

Membership

N. F. TISDALE, *Chairman*
VERNON JONES
C. L. LABEKA
J. C. MURRAY
R. E. PENROD

H. J. CUTLER
SAMUEL EPSTEIN
J. W. HALLEY
H. E. JOHNSON

C. E. SIMS
J. M. STAPLETON
S. P. WATKINS
T. T. WATSON

Mining and Metallurgy

C. G. HOGBERG, *Chairman*

W. E. MAHIN

A. C. RICHARDSON

Howe Memorial Lecture

GILBERT SOLER, *Chairman*
C. H. HERTY, JR.
J. T. MACKENZIE

M. A. GROSSMANN

L. F. REINARTZ

Robert W. Hunt Medal and Prize

GILBERT SOLER, *Chairman*
C. D. KING
K. C. McCUTCHEON

JOHN CHIPMAN

H. K. WORK

J. E. Johnson, Jr. Award

FORDYCE COBURN, *Chairman*
C. G. HOGBERG
P. R. NICHOLS

C. F. HOFFMAN

L. F. SATTELE

Programs

J. B. AUSTIN
WALTER CRAFTS
M. W. LIGHTNER

H. B. EMERICK, *Chairman*
G. B. McMEANS
W. O. PHILBROOK
O. R. RICE

M. TENENBAUM
G. L. VON PLANCK
T. B. WINKLER

Publications

A. G. FORREST
W. E. MAHIN

H. W. JOHNSON, *Chairman*
B. R. QUENEAU
C. S. SMITH

M. TENENBAUM
F. M. WASHBURN

Nominating

F. B. FOLEY

T. S. WASHBURN, *Chairman*
H. W. GRAHAM
E. G. HILL

L. F. REINARTZ

Division Organization

C. S. SMITH

H. K. WORK, *Chairman*
T. S. WASHBURN

GILBERT SOLER, *ex-officio*

The Howe Memorial Lecture

THE Howe Memorial Lecture was authorized in April 1923, in memory of Henry Marion Howe, as an annual address to be delivered by invitation under the auspices of the Institute by an individual of recognized and outstanding attainment in the science and practice of iron and steel metallurgy or metallography, chosen by the Board of Directors upon recommendation of the Iron and Steel Division.

So far, only American metallurgists have been invited to deliver the Howe lecture. It is believed that this lecture would gain in importance and significance were it possible to include metallurgists from other countries, but the Institute has not yet been able to do this on account of lack of special funds to support this lectureship.

The titles of the lectures and the lecturers are as follows:

- 1924 What's Steel? By Albert Sauveur.
- 1925 Austenite and Austenitic Steels. By John A. Mathews.
- 1926 Twenty-five Years of Metallography. By William Campbell.
- 1927 Alloy Steels. By Bradley Stoughton.
- 1928 Significance of the Simple Steel Analysis. By Henry D. Hibbard.
- 1929 Studies of Hadfield's Manganese Steel with the High-power Microscope. By John Howe Hall.
- 1930 The Future of the American Iron and Steel Industry. By Zay Jeffries.
- 1931 On the Art of Metallography. By Francis F. Lucas.
- 1932 On the Rates of Reactions in Solid Steel. By Edgar C. Bain.
- 1933 Steelmaking Processes. By George B. Waterhouse.
- 1934 The Corrosion Problem with Respect to Iron and Steel. By Frank N. Speller.
- 1935 Problems of Steel Melting. By E. C. Smith.
- 1936 Correlation between Metallography and Mechanical Testing. By H. F. Moore.
- 1937 Progress in Improvement of Cast Iron and Use of Alloys in Iron. By Paul D. Merica.
- 1938 On the Allotropy of Stainless Steels. By Frederick Mark Becket.
- 1939 Some Things We Don't Know about the Creep of Metals. By H. W. Gillett.
- 1940 Slag Control. By C. H. Herty, Jr.
- 1941 Some Complexities of Impact Strength. By Alfred V. de Forest.
- 1942 Time as a Factor in the Making and Treating of Steel. By John Johnston.
- 1943 The Development of Research and Quality Control in the Modern Steel Plant. By Leo F. Reinartz.
- 1944 Gray Iron—Steel Plus Graphite. By J. T. MacKenzie.
- 1945 Toughness and Fracture of Hardened Steels. By Marcus A. Grossmann.
- 1946 The Blast-furnace Process and Means of Control. By T. L. Joseph.
- 1947 Factors Which Determine Iron and Steel Making Processes. By H. W. Graham.
- 1948 Temperatures in the Open-hearth Furnace. By Robert B. Sosman.

Robert W. Hunt Award

THE Robert W. Hunt award was established in 1920 by the partners and employees of the distinguished metallurgist and testing engineer for whom it was named. Recipients are nominated by a continuing committee of four members of the Iron and Steel Division, together with the Chairman of the Division as member ex-officio.

The award is made for the best original paper or papers on iron and steel contributed to the Institute during the year under review and consists of a gold medal, a silver medal, or a money prize, together with a certificate. The only condition attached to the award is that the money prize shall not be given to anyone who was more than 40 years of age when the paper that merited the award was presented.

Awards have been made as follows:

- 1920 Robert Woolston Hunt: Manufacture of Steel Rails. TRANSACTIONS (1920) **62**, 174.
- 1926 Charles Lewis Kinney, Jr.: Economic Significance of Metalloids in Basic Pig Iron in Basic Open-hearth Practice. TRANSACTIONS (1924) **70**, 136.
- 1928 Charles H. Herty, Jr.: Some Factors Affecting the Elimination of Sulphur in the Basic Open-hearth Process. (Co-authors: A. R. Belyea, E. H. Burkart and C. C. Miller.) TRANSACTIONS (1925) **71**, 512. Chemical Equilibrium of Manganese, Carbon and Phosphorus in the Basic Open-hearth Process. TRANSACTIONS (1926) **73**, 1107. Desulphurizing Action of Manganese in Iron. (Co-author: J. M. Gaines, Jr.) TRANSACTIONS (1927) **75**, 434.
- 1928 John A. Mathews: Austenite and Austenitic Steels. TRANSACTIONS (1925) **71**, 568.
- 1929 Edgar Collins Bain and William E. Griffiths: An Introduction to the Iron-chromium-nickel Alloys. TRANSACTIONS (1927) **75**, 166.
- 1930 James Aston: A New Development in Wrought Iron Manufacture. TRANSACTIONS (1929) **84**, 166.
- 1931 Edmund S. Davenport: Transformation of Austenite at Constant Subcritical Temperatures. (Co-author: E. C. Bain.) TRANSACTIONS (1930) **90**, 117.
- 1932 Howard Scott: Transformational Characteristics of Iron-manganese Alloys. TRANSACTIONS (1931) **95**, 284.
- 1933 Clarence E. Sims and Gustaf A. Lillieqvist: Inclusions—Their Effect, Solubility and Control in Cast Steel. TRANSACTIONS (1932) **100**, 154.
- 1934 Cyril Stanley Smith and Earl W. Palmer: The Precipitation-hardening of Copper Steels. TRANSACTIONS (1933) **105**, 133.
- 1936 Carl C. Henning: Manufacture and Properties of Bessemer Steel. TRANSACTIONS (1935) **116**, 137.
- 1937 William F. Holbrook and Thomas L. Joseph: Relative Desulphurizing Powers of Blast-furnace Slags. TRANSACTIONS (1936) **120**, 99.
- 1938 Thomas S. Washburn and John H. Nead: Structure of Rimmed-steel Ingots. TRANSACTIONS (1937) **125**, 378.
- 1939 Kenneth Charles McCutcheon and John Chipman: Evolution of Gases from Rimming-steel Ingots. TRANSACTIONS (1938) **131**, 206.
- 1940 Axel Hultgren and Gösta Phragmén: Solidification of Rimming-steel Ingots. TRANSACTIONS (1939) **135**, 133.

- 1941 Alden B. Greninger and Alexander R. Troiano: Crystallography of Austenite Decomposition, *TRANSACTIONS* (1940) **140**, 307.
- 1941 George E. Steudel: Effect of the Volume and Properties of Bosh and Hearth Slag on Quality of Iron. *TRANSACTIONS* (1940) **140**, 65.
- 1942 Harold K. Work: Photocell Control for Bessemer Steelmaking. *TRANSACTIONS* (1941) **145**, 132.
- 1943 Marcus A. Grossmann: Hardenability Calculated from Chemical Composition. *TRANSACTIONS* (1942) **150**, 227.
- 1944 Clarence David King: The Washing of Pittsburgh Coking Coals and Results Obtained on Blast Furnaces. *TRANSACTIONS* (1944) **158**, 67.
- 1945 Edwin Chester Wright: Manufacture and Properties of Killed Bessemer Steel. *TRANSACTIONS* (1944) **158**, 107.
- 1947 Harry K. Ihrig: The Effect of Various Elements on the Hot-workability of Steel. *TRANSACTIONS* (1946) **167**, 749.
- 1948 B. M. Larsen and T. E. Brower: Oxygen in Liquid Open-hearth Steel—Oxygen Content During the Refining Period. *TRANSACTIONS* (1947) **172**, 137. Oxygen in Liquid Open-hearth Steel—Effect of Special Additions, Stirring Methods and Tapping. *TRANSACTIONS* (1947) **172**, 164.

TECHNICAL PAPERS,
DISCUSSIONS
AND
TECHNICAL NOTES



R. B. SOSMAN

Henry Marion Howe Memorial Lecturer, 1948

Temperatures in the Open-hearth Furnace

BY ROBERT B. SOSMAN,* MEMBER AIME

(New York Meeting, February 1948)

HOWE MEMORIAL LECTURE

THE chance that a Howe Memorial Lecturer will be able to refer back to a personal contact with the distinguished metallurgist for whom this lectureship is named grows steadily smaller. I did not have the pleasure of his personal acquaintance, but I did receive from him in 1916, quite unexpectedly, a letter commenting on a paper that I had recently published²⁷ on "Types of Prismatic Structure in Igneous Rocks." The paper was written for geologists and petrologists, but it had an application, naturally, to the crystallization of iron and steel in a mold. The letter impressed me at the time, and still does, with the breadth of Professor Howe's interests and his perseverance in keeping up with the progress of any branch of knowledge that had metallurgical connotations.

SCOPE OF THE LECTURE

During several years preceding the date mentioned I had worked in collaboration with Arthur L. Day and E. T. Allen⁸ at the Geophysical Laboratory, Carnegie Institution of Washington, on the temperature scale as defined by the nitrogen thermometer at high temperatures. Later (1928-1947) I had the opportunity of helping to apply this experience to the pyrometric problems of the steel industry. Because of the range of its temperatures, the multiplicity of the methods used, and

the variety of its purposes, pyrometry in the open-hearth process has always offered a fertile field for both research and development. I am therefore devoting an hour to the subject of temperatures in the basic open-hearth furnace, the furnace that makes most of our steel in the United States.

I would direct your attention particularly to the choice of the first two words in the title of the Lecture.

One sometimes hears or reads of the "temperature of such-and-such a furnace," as if it were a single, measurable, characteristic quantity. I need hardly emphasize to any one who has ever operated a furnace or a kiln that "temperature of the furnace" is a meaningless phrase. Even if we confine our attention to the space enclosed by the roof, walls, and hearth of an open-hearth furnace, it is doubtful whether any such space has ever been so uniform in temperature that the phrase would have a meaning. In any furnace, there are many different temperatures, capable of being measured at many different places, and actually being measured for several different purposes.

These pyrometric purposes, methods, and results, if given in detail, would expand this lecture into a book on the basic open-hearth process. I must therefore confine myself to a statement of the range of temperatures as they have been observed in various parts of the furnace, indicating in a general way why they are measured, and mentioning the methods that are available without attempting to describe these

Manuscript received at the office of the Institute June 8, 1948. Issued as TP 2435 in METALS TECHNOLOGY, August 1948.

* Professor of Ceramics, School of Ceramics, Rutgers University, New Brunswick, New Jersey. Formerly Assistant Director, Research Laboratory, United States Steel Corporation.

²⁷ References are at the end of the paper.

methods fully. The viewpoint will be that of the physicist rather than that of the engineer.

In most of the work that I shall mention from first-hand knowledge, I have had only the role of advisor, coordinator, diplomatic expediter, or contact man between plant and laboratory—necessary but not primary functions. The real work has been done by my colleagues in the Research Laboratory of the United States Steel Corporation; those most directly concerned with open-hearth pyrometry have been J. W. Bain, B. M. Larsen, L. Rumford II, W. E. Shenk, and L. O. Sordahl, while valuable work on various aspects of pyrometry applicable in the open-hearth has also been done by K. Heindlhofer, J. Mrvosh, J. W. Percy, R. H. H. Pierce, Jr., C. Siddall, and R. B. Snow. We are indebted also to the many plant men and instrument company men who cooperated so cordially with us.

PYROMETRIC METHODS

A very brief listing of the methods of temperature measurement available for practical open-hearth pyrometry must suffice here. For ease of remembrance it is convenient to classify them as (1) "look," (2) "approach," and (3) "touch" methods. The first includes the two optical methods of brightness and color, which are usable as far away as the object can be seen. On nearer approach we can feel the radiant heat from the object and can use either the total radiation pyrometer, or partial radiation instruments such as the photo-electric pyrometer. Finally, for actual contact of thermometer with object, we depend mainly upon the thermo-electric pyrometer, with either the platinum-rhodium-platinum couple above 1250°C ,* or the base-metal couples (Chromel-Alumel, iron-constantan) below 1250°C .¹

* The Fahrenheit equivalent of every Centigrade temperature mentioned in the Lecture will be found in Table 2, page 50.

PYROMETRIC PURPOSES

Industrial pyrometry has five general purposes: (1) maintenance of the quality of the product; (2) protection of equipment against damage by excessive temperature; (3) control of efficiency in operations; (4) acquisition of new information about the process, that is, research; (5) guidance in improving the process, that is, development.

THE BASIC OPEN-HEARTH FURNACE

Fig 1 is a diagrammatic plan to illustrate the mode of operation of a basic open-hearth furnace fired with atomized liquid fuel (oil or tar) and forced air. Fig 2 and 3 contain generalized horizontal and vertical sections, omitting many details of the supporting steel framework, to show the construction of such a furnace. Its usual capacity is between 75 and 250 tons of steel, and its raw materials are cold steel scrap plus either cold pig iron or liquid crude iron from the blast furnace.

The principal variations from the design shown in Fig 2 and 3 are due to (1) use of gaseous fuel (natural gas, by-product coke-oven gas, producer gas) in place of liquid fuel, requiring that the ports be of different shape, and (in particular, for producer gas) that a double regenerator be used so that the gas can be preheated as well as the air; (2) use of a central furnace structure which can be tilted forward or back around a longitudinal axis, so that both slag and steel can be independently poured out of the furnace without the opening of sealed tap holes.²

THE BATH

The body of liquid metal on the hearth is often referred to as the "open-hearth bath." When completely liquefied soon after the beginning of a heat it is an alloy of iron, carbon, and manganese, with minor amounts of various other impurities. Its minimum temperature is therefore a few degrees lower than the austenite-cementite

eutectic in the iron-carbon system (Fig 4), at 1130°C . The actual temperature of the liquid metal early in the heat must occasionally be close to this figure, especially if

occasionally does, change over from a liquid with a few austenite crystals in suspension (just under the curve BC), to a paste of crystals wet with liquid metal (just above

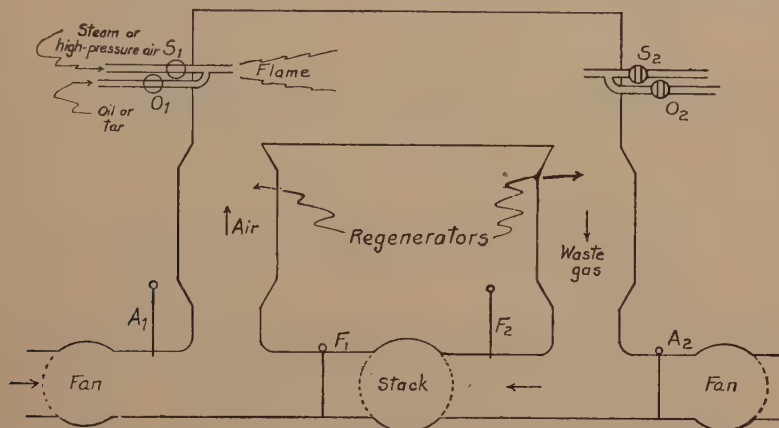


FIG 1—DIAGRAMMATIC PLAN TO ILLUSTRATE THE OPERATION OF AN OPEN-HEARTH FURNACE BURNING LIQUID FUEL.

A_1 and A_2 : Valves for air

F_1 and F_2 : Valves for waste gas

O_1 and O_2 : Valves for oil or tar

S_1 and S_2 : Valves for steam or high-pressure air for atomizing the fuel.

As shown in the drawing, when A_1 , F_2 , O_1 , and S_1 are open, A_2 , O_2 , F_1 , and S_2 are closed. On reversal of the furnace, A_2 , O_2 , F_1 , and S_2 are opened, and A_1 , F_2 , O_1 , and S_1 are closed.

cold pig iron or charcoal is included in the charge, by virtue of the principle that a liquid in contact with the crystalline phases of a eutectic mixture can not long be kept hotter than the melting temperature of the eutectic.

At the end of a heat in which a pure ingot-iron or low-metalloid steel is being produced, the minimum temperature is the melting point of pure iron, for which the best present value is 1535°C . If the metal is saturated with oxygen this is lowered to 1524°C .

A bath of composition intermediate between zero carbon and 4.3 pct carbon has a minimum temperature that can be below the temperature of the liquidus curves AB and BC in Fig 4, but must be above that of the solidus curves AH and JE . If the temperature of the metal in the furnace does not rise fast enough to keep up with its changing composition, the bath can, and

curve JE). These facts are all simple deductions from the phase equilibrium diagram.

The minimum liquid metal temperature that we have actually observed in a furnace is about 1200°C .

These minimum working temperatures are not the minimum finishing temperatures for the steel in the furnace. The steelmaker has to provide enough extra temperature above the liquidus to take care of the heat losses during tapping and pouring. The principal loss is the heat stored in the refractory lining of the ladle. Next in magnitude is the loss by radiation from the unprotected surface of the liquid metal during tapping. When tapping is complete and the surface is covered with a few inches of slag, the loss by radiation and air convection is relatively small.

Fig 5 and 6 represent the results of some unpublished calculations made in 1931 to show the relative importance of the several

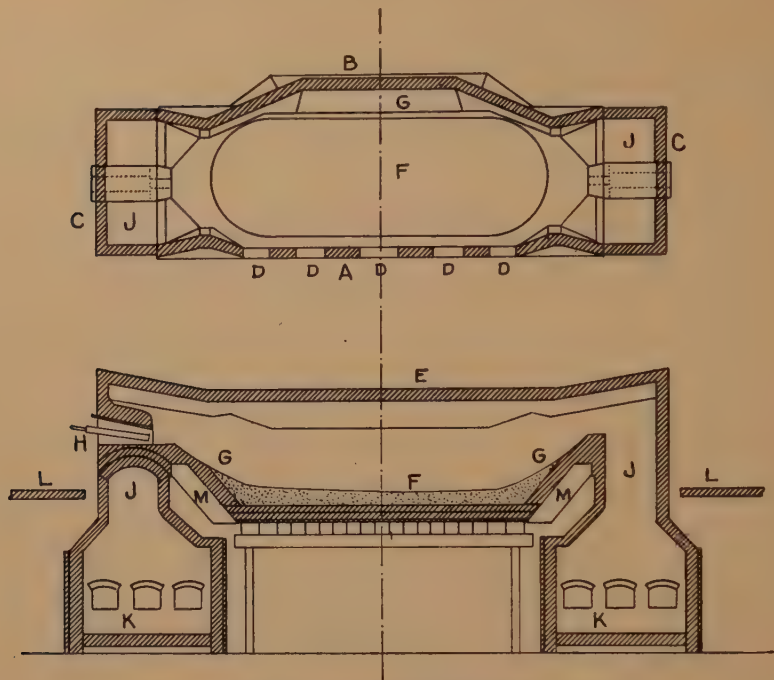


FIG 2—OPEN-HEARTH FURNACE, BURNING LIQUID FUEL.

Upper part: horizontal section through furnace and ports.

Lower part: vertical section through furnace; left half of section is through burner housing right half of section is at rear of burner housing.

- A. Front wall
- B. Back wall
- C. End walls
- D. Doors
- E. Arched roof
- F. Hearth
- G. Banks
- H. Burner
- J. Down-takes for waste gas
- K. Slag pockets, opening into regenerator chambers
- L. Charging floor
- M. Cooling boxes

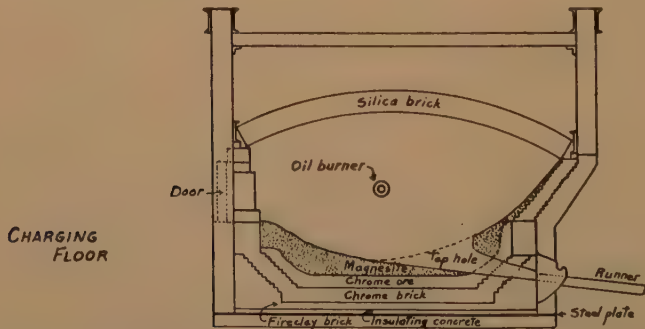


FIG 3—OPEN-HEARTH FURNACE, BURNING LIQUID FUEL. VERTICAL TRANSVERSE SECTION ON CENTER LINE OF FURNACE, SHOWING CONSTRUCTION OF BOTTOM.

PIT

causes of loss of heat. The data on which the calculations are based are: liquid steel density 7.0, heat capacity 0.19, total emissivity 0.20; brick density 2.0, heat

steel that has been much overheated in the furnace, and has then been allowed to cool in the ladle until it reached a prescribed pouring temperature, is not the same steel

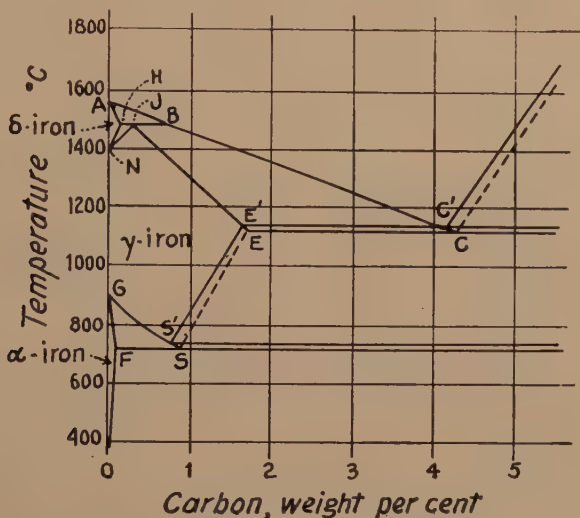


FIG 4—COMPOSITION-TEMPERATURE PHASE EQUILIBRIUM DIAGRAM FOR THE SYSTEM CARBON-IRON.

capacity 0.225, conductivity 3.75×10^{-3} ; all in cgs units.

Being roughly proportional to the area of external surface of the cylinder of liquid metal, the drop in temperature during tapping and pouring is relatively large for steel coming from a small furnace, and small for steel from a large furnace. Though naturally influenced by many minor variables, the calculated order of magnitude, on the assumption that it is inversely proportional to the two-thirds power of the tonnage, is as shown in Table 1.

Pyrometry of the steel bath has for its primary purpose the control of quality. (See p. 16.) The importance of correct finishing temperatures for liquid steel has long been recognized. Upon the temperature of the metal as it runs into the ingot mold depends the manner in which it will crystallize, with all the structure-sensitive properties that are linked with that crystallization. And pouring temperature is not the only controlling temperature. A

as the one that has been tapped at just the right temperature to attain the prescribed figure for pouring without any imposed delay. The hotter steel has had opportunity in the furnace to approach a different chemical equilibrium from the colder one.

TABLE 1—*Calculated Effect of Furnace Tonnage (Ladle Capacity) on Loss of Temperature in Steel between Tapping and Pouring*

Capacity Tons	Loss °C	Loss °F
50	86	154
60	76	137
75	66	118
100	54	97
110	51	91
150	41	74

Each open-hearth shop learns by experience the best initial pouring temperature for each grade of steel that it makes. Addition of the appropriate figure for lost temperature, taken from data such as those in Table 1, will then give the minimum

finishing temperature to be attained in the furnace. The maximum permissible under good practice is not much higher than this.

The maximum attainable temperature of the open-hearth bath beneath a silica roof does not depend upon the properties of the

bath and slag, but upon the properties of the roof, as we shall see later. The highest such temperature that has been reliably recorded by Mr. Sordahl is 1657°C (3014°F).

This may seem a relatively low maximum

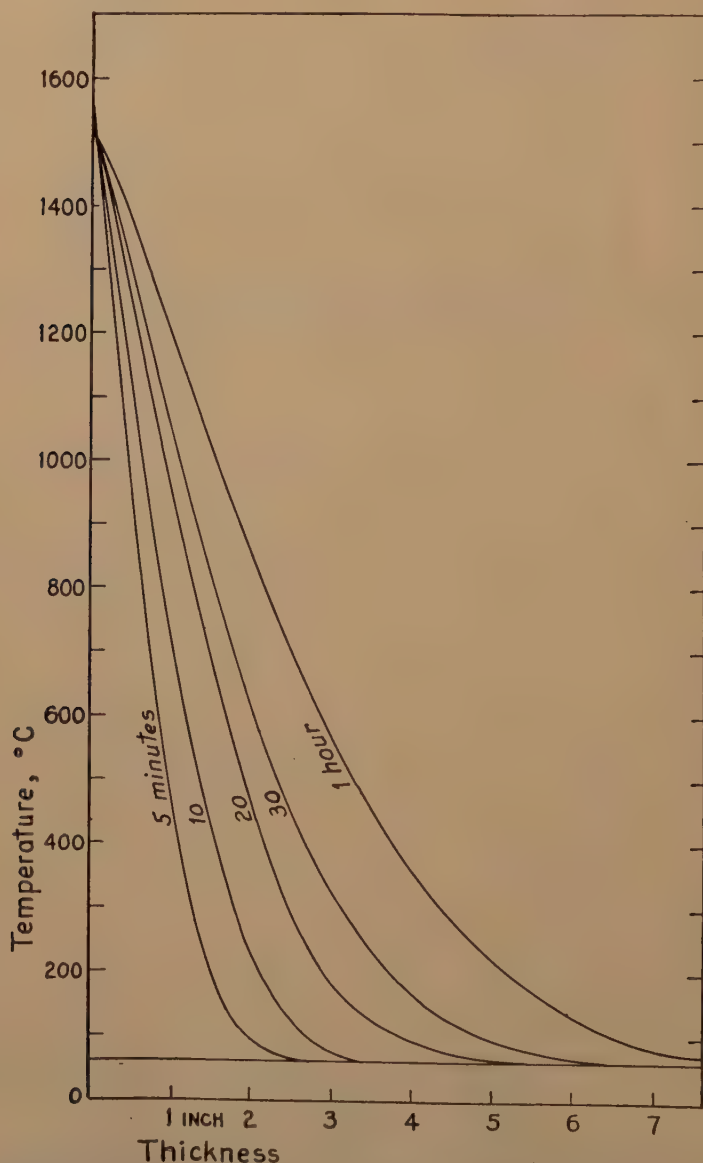


FIG 5—DISTRIBUTION OF TEMPERATURE IN THE $7\frac{1}{2}$ IN. FIRECLAY BRICK LINING OF A LADLE CONTAINING STEEL AT AN INITIAL TEMPERATURE OF 1585°C .

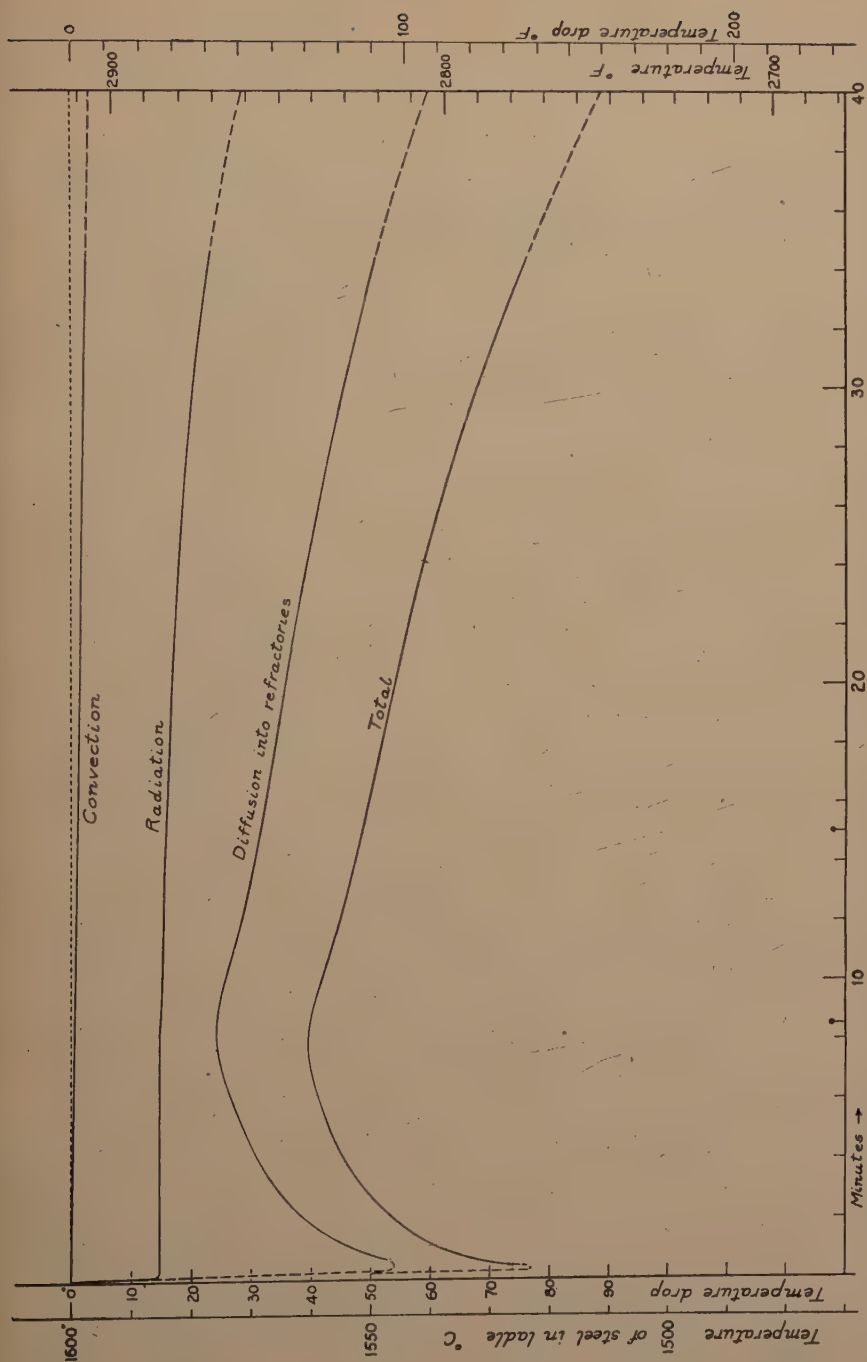


FIG 6—CALCULATED MAXIMUM DROP IN TEMPERATURE OF 100 TONS OF STEEL TAPPED AT 1600°C AT $11\frac{3}{4}$ TONS PER MIN. INTO LADLE WITH $7\frac{1}{2}$ IN. FIRECLAY BRICK LINING; POURED DURING PERIOD BEGINNING 15 MIN. AND ENDING 40 MIN. AFTER BEGINNING OF TAP.

to some of you who are accustomed to tapping-temperatures read with the optical pyrometer, but we believe that the present scale is in error on the high side; I shall have more to say about this in the discussion of bath pyrometry.

BATH PYROMETRY

The human eye, aided by the old-fashioned copper-cobalt blue glass, is such a sensitive pyrometer, thanks to its sensitivity both to brightness and to color, that steel has been made for generations without the aid of a bath pyrometer. Changing conditions in the industrial world, bearing particularly on employees' reliability, made it inevitable that an objective quantitative measurement would sooner or later have to be substituted for the subjective estimate of temperature made by the eye and brain of the experienced steelmelter.

The old-timer's estimate of temperature was seldom expressed in figures. It was expressed rather in the technical terms: "cold," "shady," "O.K.," "hot," "stinking hot." Very roughly, we find that these terms can be interpreted as a series of temperatures separated by about 15°C or 25°F . A heat that should have been tapped from a certain furnace at 1635°C (2975°F), let us say, would be recognized as "shady" by the pouring crew if it was only 1620°C (2950°F), and as distinctly "cold" if at 1605°C (2925°F), in which case it would leave a larger skull in the ladle than normal. It would be recognized as "hot" if at 1650°C (3000°F), and might then make some unsatisfactory ingots, while if tapped at 1665°C (3025°F) it would leave a very clean ladle and would cause some stickers in the ingot molds. (The terms are not absolute temperature terms; for a larger furnace, with less heat loss in the ladle, this whole series would be shifted downward.)

The pyrometer must therefore do better than $\pm 15^{\circ}\text{C}$, and $\pm 5^{\circ}\text{C}$ seems a not impossible goal both for precision and accuracy. It is worth noting that 3°C at

1650°C , the accuracy ultimately hoped for, is only 0.16 pct, considered as a percentage of the absolute temperature, which would be distinctly better than most measurements in applied physics.

The task of finding a satisfactory working method and equipment for open-hearth bath pyrometry falls naturally into three parts: (1) accurate measurement of the true temperature of the liquid metal, without regard to cost or convenience; (2) development of a device which will give reproducible and precise readings of some kind that can be correlated with temperature, but which at the same time is a device satisfactorily convenient and inexpensive to use; (3) calibration of (2) in terms of (1).

A systematic study of the subject was begun in the research laboratory of the United States Steel Corporation in 1934, when Mr. Lewis Rumford II reviewed the available methods in a memorandum and did some experimenting in the plants. In 1936 we organized a series of comparisons in open-hearth furnaces in the old Pencoyd Works near Philadelphia.²⁶ Preliminary tests showed that the accurate readings with which everything else should be compared could best be made with the platinum-rhodium-platinum thermocouple, capable of a precision of 1°C and an accuracy which we hoped could be held within the desired $\pm 3^{\circ}\text{C}$.

Step (1): For the comparisons at Pencoyd the basic readings were made by means of a so-called "dissolving-tube method." A platinum-rhodium-platinum thermocouple is enclosed in a small refractory porcelain tube of $\frac{3}{16}$ -in. (5 mm) bore and $\frac{1}{16}$ -in. (1.5 mm) wall. This is about as small and thin a tube as can be handled, and its use in the steel bath is only rendered possible by encasing it (loosely) in a tube made of Acheson artificial electrode graphite, $1\frac{3}{4}$ -in. od and 14 in. long, tapered for 4 in. at the closed end down to $\frac{1}{2}$ -in. diam. The graphite tube with its enclosed porcelain tube and thermocouple is set in a water-

cooled head, and the thermocouple wires are led out through a pipe inside one of the two water pipes. A packing of asbestos cord around the porcelain in the opening

mersed in the steel bath, the graphite quickly dissolves away below the slag level, leaving the porcelain in direct contact with the liquid metal and immersed therein to a

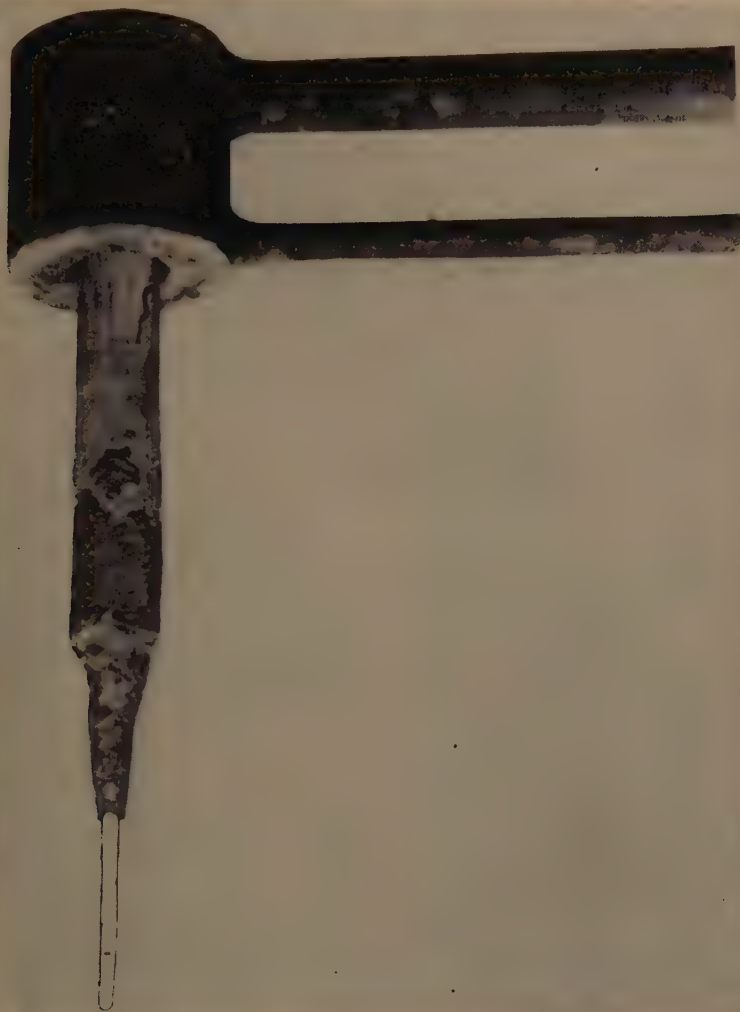


FIG 7—PHOTOGRAPH OF DISSOLVING-TUBE PYROMETER AFTER REMOVAL FROM LIQUID STEEL.

of the graphite sheath prevents the rise of gases which would carry spurts of steel up into the water-cooled head after the graphite has begun to dissolve away.

The combination is inserted through a door of the furnace, with a sheet-metal shield protecting the operators. When im-

depth of 6 to 8 in. (See Fig 7.) Within the slag layer the graphite remains to protect the porcelain. To secure an accuracy of 3°C in measuring the metal bath temperature at the point of immersion, the couple should be used only once or twice.

We found that inequalities in the metal

bath itself exceeded the range of accuracy of the thermocouple reading, but it was still possible to make a satisfactory comparison of methods. The platinum couple, used as described above, gives the most precise and most accurate readings obtainable, but the method could not be recommended for routine control of the furnace, for two reasons: (1) the couples are too easily contaminated and hence too expensive, and (2) the water-cooled head, introduced into the furnace near the bath, is an accident hazard.

The British metallurgists have subsequently made improvements in the thermocouple method and have sought to make it a workable shop method. In place of our temporarily graphite-protected porcelain tube for the thermocouple, Schofield and Grace²⁹ introduced a vitreous silica (fused quartz) tube with no protection. On account of the very low expansion coefficient and high strength of the material, such a tube can be introduced into liquid steel without cracking. The British also discarded water-cooling in favor of refractory insulation for the pipes carrying the extension-wires of the couple; though awkward looking and bulky, it is probably no heavier than the water-cooled system and is much less hazardous. A similar pyrometer, with vitreous silica and platinum couple, was subsequently developed in this country,³⁰ primarily for use in electric furnace baths, which are more accessible than the open-hearth bath, and the Brown Instrument Co. now has such a pyrometer in commercial form. For our measurements subsequent to the Pencoyd tests, we adopted the silica tube in place of porcelain, and likewise discarded the water-cooled support. Using much longer silica tubes than in the British and electric furnace types, Mr. Sordahl has made numerous measurements of open-hearth bath temperature at various depths down to the hearth surface itself.

Practical Plant Methods

Because of the inconvenience of having to open the furnace door and use a protecting shield, and also because of the considerable expense of using a new silica tube and of discarding a part or all of a platinum couple for every reading, we have not considered the method described above to be a practical plant method. There is no question, however, as to its accuracy and reliability.

Step (2), therefore, must next be taken: the selection of a convenient and precise plant method, inexpensive enough not to discourage frequent readings. In the comparisons at Pencoyd Works, and in other subsequent tests, we tried the following methods, with results briefly indicated below.²⁵

Test-spoon Method

Metal is held in or poured from a slag-coated test spoon, and the temperature of the clean dark liquid is read with an optical pyrometer. A correction for emissivity must be added to obtain true temperature.

Not all test-spoon readings are satisfactory. Only when the slag is thin enough to permit the dipping of a clean sample in a properly slagged spoon can the readings be taken. To obtain satisfactory readings, a routine of slagging, dipping, removing from furnace, and reading, must be adhered to with rhythmic precision, for the metal cools so rapidly that even half a second's departure is significant. With an experienced reader, however, surprisingly precise readings can be obtained. The fatal defect of the method is its subjectivity, with its dependence upon personal skill and attentiveness.

Our readings at Pencoyd by this method, though self-consistent, proved, when corrected for an emissivity of 0.40, to be 10 to 15°C higher than the probable true temperature deduced from thermocouple readings.

Bath-equalization Method of Larsen and Shenk

A photoelectric roof pyrometer is sighted on the inner surface of the roof through an opening in the back wall. Another pyrometer of the same type is sighted downward through a water-cooled opening in the roof upon the slag surface. The two pyrometer circuits are connected in opposition, with a relay also in circuit which will turn on the fuel as soon as the difference between the two pyrometers falls below a certain set minimum of 5 or 10°C.

The procedure in taking a bath temperature is to shut off the fuel and air supply, throw in the relay circuit, and wait. Within a period of 15 to 50 sec the slag, if not too viscous, will presumably have attained the temperature of the large mass of metal beneath it, in which most of the heat in the furnace is stored; at the same time the roof and slag will be rapidly equalizing in temperature by radiation. When metal, slag, and roof become equal in temperature within the prescribed tolerance, the fuel and air are automatically turned on. Meanwhile, the recorder of the roof pyrometer has been recording the roof temperature, and its minimum, shown on the chart when the returning flame causes a sudden rise, is the equalized bath temperature.

The bath temperature obtained in this way is in the nature of an average surface temperature of the metal and, if the bath is not homogeneous, readings at individual points, such as are obtained with thermocouple or spoon, will differ from it. This is probably the reason why we found that the equalization method gave a terminal temperature (just before tapping) that appeared more nearly correct than any other method, yet was more erratic than the results by the blowing-tube method (see below), which has the effect of stirring the bath vertically within a restricted area.

During the heats, the equalization temperature was 10 to 15°C above the probable true temperature. Its precision is high;

under favorable conditions, near tapping time, about $\pm 3^\circ\text{C}$. When more than one equalization temperature was taken during the tapping period, the reading was found to be diminishing at a rate equivalent to a loss of 3 to 5°C in the bath during the 4- to 6-min. tapping period.

Rod-boil Method

A cold steel rod is inserted through the wicket into the bath while it is still active, and an optical pyrometer is sighted on the surface of the metal as it boils up through the slag. (The boiling is caused by the escape of carbon monoxide from solution as a result of the local chilling.) Readings are made during reversal of the furnace, when the flame is off. There is no correction for emissivity.

The few readings which it was possible to secure at Pencoyd by this method were consistent with the equalization and the test-spoon methods, but it would be impracticable to depend upon it for control, as the conditions are so frequently unfavorable to production of a boil.

Slag Bubble Method

An optical pyrometer reading is made, during reversal, on the interior of a gas bubble just as it bursts. The slag surrounding the bubble has just risen from the surface of the metal, presumably carrying the metal temperature with it, and in fact the bubbles can often be observed to be appreciably darker than the main body of slag. This indicator of metal temperature was suggested by Mr. Larsen.

The relatively small number of readings that we made by this method were, like the rod-boil temperature, consistent with the equalization and the spoon methods. When the bath is quiet, no readings are obtainable.

Slag Surface Method

The temperature of the bath is inferred from a series of optical pyrometer readings made during reversal, taken on the brighter

areas of the slag as the bath is heated up towards the end of a heat. The results by this method, as might be expected, could not be used as a basis for estimating the

a tube made of vitreous silica (fused quartz), 2 in. or more in diam, and carrying the radiation receiver of a total radiation pyrometer in its open end, is inserted to

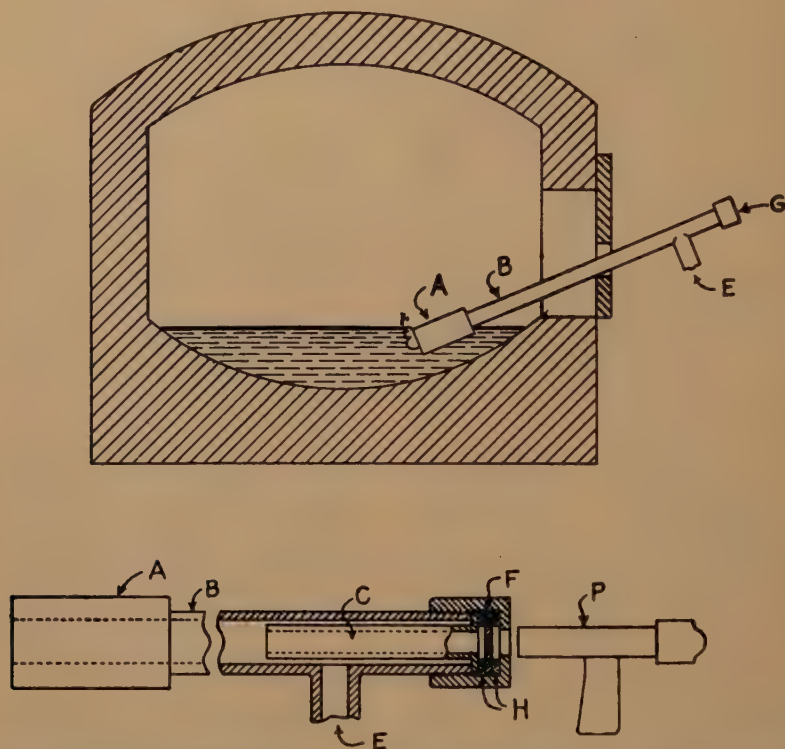


FIG 8—PRINCIPLE OF OPERATION OF BLOWING-TUBE PYROMETER. COLLINS AND OSELAND'S FORM AS USED IN EXPERIMENTS AT PENCYD.

- A. Welded steel tip
- B. Pipe
- C. Inner pipe to protect window against moisture and dirt
- E. Connection for introducing air
- F. Glass window
- G. Air-tight cap, carrying window
- H. Asbestos gaskets
- P. Optical pyrometer

true temperature of the bath, even though they were useful in showing the general course of temperature increase as influenced by fuel input and other factors.

Closed-tube Radiation Method

This method, while not adaptable to a large open-hearth furnace, has been used to some extent in small electric furnaces and should be included here. The closed end of

the depth of about 6 in. into the liquid steel. The silica tube is so transparent, especially to the infra-red wave-lengths that make up most of the energy at steel-making temperatures, that its inner surface quickly attains the radiating intensity of a blackbody or full radiator at the temperature of the liquid, and this temperature is then recorded by an automatic potentiometer.

Blowing-tube Pyrometer

The simple device of a viewing-tube with open end inserted beneath the surface of the liquid metal was first put into workable form and patented by Collins and Oseland⁶ at the Gary Works of the Carnegie-Illinois Steel Corporation. The pyrometer tube consisted of a 6-ft length of 2-in. steel pipe carrying a current of air under sufficient pressure to blow back the liquid steel from an orifice at the end of the pipe. Through a window at the other (outer) end the temperature of the steel was read with an optical pyrometer. (Fig 8.)

This type of pyrometer I have called a "blowing-tube pyrometer," after the special patentable feature of its operation.

In the form invented by Collins and Oseland the pyrometer, as tested at Pen-coyd, did not prove wholly practical under steel-plant conditions, because (1) it required two men for its operation, one to hold the tube in place while the other made the reading; (2) it depended upon the optical pyrometer, whose readings are subjective in that they involve judgment by an individual eye and brain without possibility of independent checking; (3) readings had to be made in haste under conditions of psychological stress which were bad for precision.

L. O. Sordahl²⁴ of our research laboratory put the blowing-tube pyrometer into more practical form by two changes: (1) the optical pyrometer was replaced with a Photronic cell, a photoelectric cell of the self-generative barrier-layer type, together with the necessary amplifier and current recorder; (2) an inner tube carrying a series of diaphragms was added, which together with the orifice define the beam of light to the Photronic cell. (See Fig 9.) In the earlier comparisons, a Weston Electrical Instrument Corporation Model 721 amplifier, raising the micro-amperes of the cell to milliamperes, was combined with an Esterline-Angus current recorder to make the

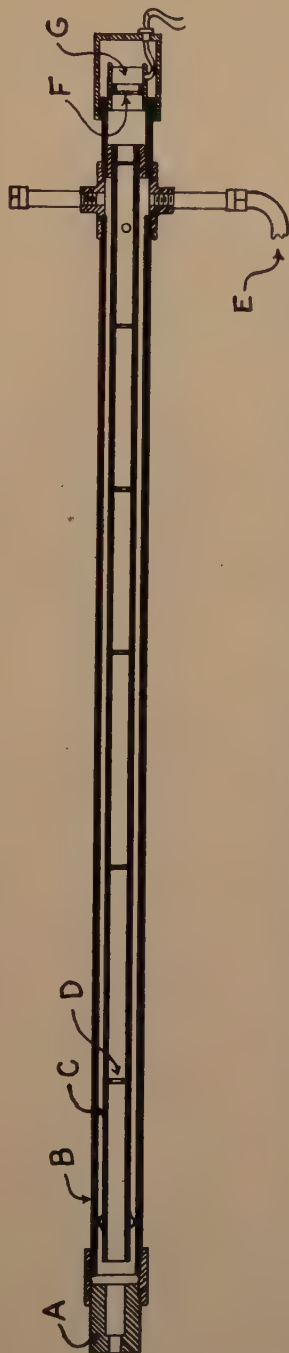


FIG 9—LONGITUDINAL SECTION OF SORDAHL PHOTOELECTRIC BLOWING-TUBE PYROMETER.

- A. Replaceable steel tip
- B. Outer pipe
- C. Inner pipe, carrying diaphragms D
- E. Hose connection for air supply
- F. Protective glass window
- G. Photronic cell

record. While this combination is entirely satisfactory to the physicist, it is not as well adapted to conditions of maintenance in the open-hearth shop as the Brown In-

Another form of the blowing-tube pyrometer is that invented and developed by the research group of the Leeds and Northrup Co.⁵ (Fig 10.) In this form the

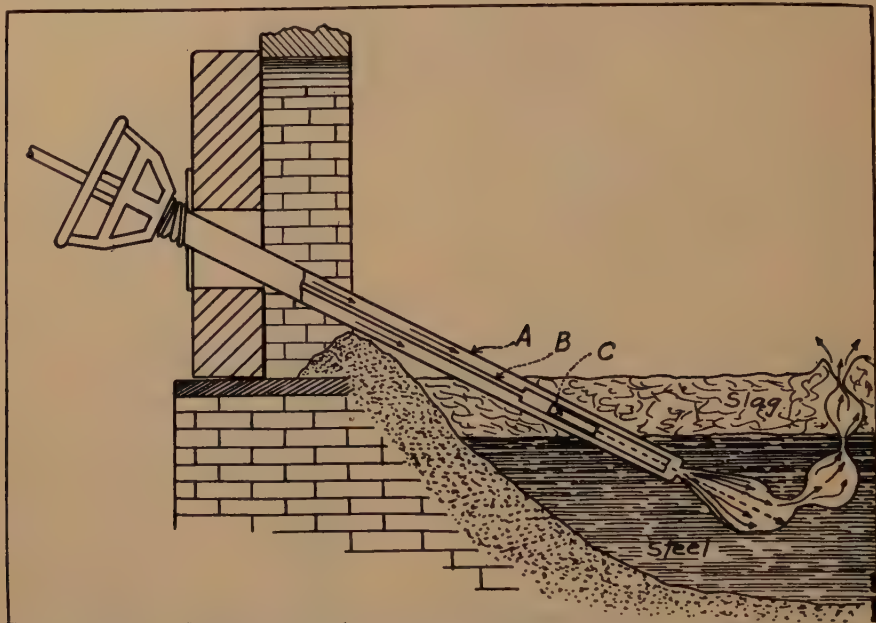


FIG 10—LEEDS AND NORTHROP'S FORM OF BLOWING-TUBE PYROMETER.

- A. Pyrometer tube
- B. Inner tube
- C. Radiation receiver (Rayotube)

strument Company's "Electronik" automatic potentiometer, which has been used as the recorder in our more recent work.

I shall not attempt to describe in detail the various difficulties met with in the development of the present form of the pyrometer. Nowhere more than in research work is it true that "Hindsight is better than foresight." Looking back, we can see that some of the difficulties were very real and are still with us though overcome sufficiently for present purposes. Others appear in retrospect to have been quite unnecessary. They all blend into the experience of any research man who, like Mr. Sordahl and the others who have been associated with him, have successfully evolved a working instrument or method out of sometimes unpromising material.

original optical pyrometer is replaced with a total radiation pyrometer having a very small and compact radiation receiver. In their first tentative form, the radiation receiver was mounted in the same position as the optical pyrometer window and the Photronic cell used in the two earlier forms. This combination was a failure for a reason difficult to foresee, namely, that the steel tube is likely to bend a little on account of unequal heating around its circumference at the point where it is in contact with the banks or with the door. This bending is of slight consequence to the earlier methods; the optical pyrometer requires only that the target be visible, while the Photronic cell receives the light over not quite the whole surface of a disk about 1.4 in. in diam, and a slight shifting produces no

error. The radiation receiver, on the other hand, concentrates the light and heat by means of a lens upon a small target consisting of a group of thermocouple junctions, and it cannot take care of a shifting target. Radiant heat from the inner wall of the pipe was another source of error for the radiation receiver, though of no consequence to the photo-electric cell.

The designers therefore seized the bull by the horns, so to speak, and thrust the radiation receiver right down the tube into the furnace, so near to the orifice of the blowing-tube that not only is there no error due to bending, but also the receiver needs to utilize only the middle part of the target area. It thus becomes independent of the diameter of the orifice. This is an advantage, because the orifice will occasionally be slightly reduced in diameter by picking up a thin "skull" of frozen liquid steel. This will constitute a direct error in the reading of the Photronic pyrometer, but will be without effect upon the accuracy of the radiation pyrometer.

The receiver can be successfully placed thus near the orifice by virtue of these facts: (1) it can be insulated with thin metal sheet insulation; (2) the reading can be taken within 10 sec; and (3) the receiver will endure a temperature of 150°C without harm while the Photronic cell must not be heated above 50°C.

CALIBRATION

Experience with these blowing-tube pyrometers has shown that it is possible to obtain a precise and reproducible reading, in either micro-amperes or microvolts, representing the intensity either of the visible light (Photronic instrument) or of the total radiation (radiation instrument) coming from the inside of a bubble in the liquid steel. This completes *Step* (2). We learned how to obtain an accurate measurement of the true temperature of the metal in *Step* (1). *Step* (3) can now be taken, by bringing the two sets of readings together

in order to find whether they can be consistently correlated with respect to the principal variables, namely, composition and temperature. This we have done only with our Photronic blowing-tube pyrometer.

The calibration of the blowing-tube pyrometer has not only involved the rather simple physical problem of calibrating an instrument, but has resulted in an unexpected coincidence that can easily lead to confusion of ideas, and has also brought up a problem in psychology and manufacturing control. The conclusions next to be presented are based upon many measurements by Mr. Sordahl during the past several years, made with the Photronic instrument in three plants, on plain and alloy steels with a wide range of carbon content (0.06 to 2.30 pct), in basic open-hearth, acid open-hearth, blown-metal, and electric furnaces, as well as in foundry ladles. This range of compositions and of conditions of manufacture has made it possible to cover a temperature range of about 250°C, from 1430 to 1680°C (2600–3050°F), thus giving considerable validity to the conclusions for all customary steel-making conditions.

EFFECT OF COMPOSITION

It was found early in the comparisons that the blowing-tube pyrometer readings maintained a constant relation to true temperature for all commonly made varieties of carbon steel and low-alloy steel. This result was very convenient, but in one respect unexpected. We had reason to expect that the percentage of carbon would have little if any influence, because published results by various earlier observers¹⁶ had shown that the emissivity of the liquid metal for wave-length 0.65μ as used for optical pyrometry, is the same for pure iron and for cast iron containing about 4 pct carbon. Steels with several per cent of certain oxidizable alloy metals such as manganese and chromium, on the other

hand, were known to be distinctly brighter to the optical pyrometer than pure iron and cast iron.¹¹ To the blowing-tube pyrometer, however, they proved identical with pure iron and with high-carbon iron.

in which i is photo-cell current, T is absolute temperature, and k and d are constants.

In presenting the data in this form, I am following a different succession in logic from that used by Mr. Sordahl in making

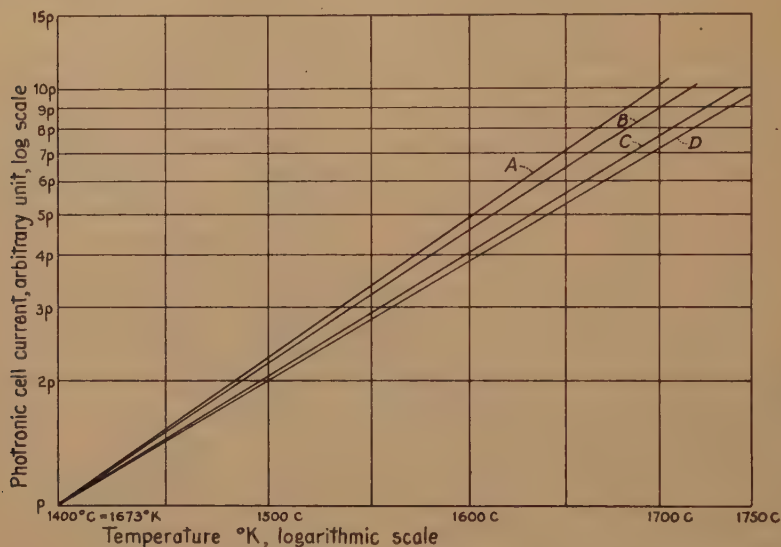


FIG 11—CALIBRATION CURVES OF PHOTRONIC PYROMETER.

- A. Graph of equation: $i = k_1 T^{14}$
 B. Graph of Fogle's photometric data for Type 3 Photronic cell.
 C. Graph of Larsen and Shenk's equation for Type 1 Photronic cell: $i = k_2 T^{12.34}$
 D. Graph of equation $i = k_3 T^{12}$
 (p has a different value for each curve and each cell.)

THE ABSOLUTE CALIBRATION

With composition thus satisfactorily disposed of as a variable, the entire body of comparisons, covering 250°C, can be combined in one calibration curve of the blowing-tube pyrometer as used in the bath. Photo-electric current is plotted against thermocouple temperature, using logarithmic scales because of the rapid increase of current with temperature. The curve proves to be very nearly a straight line, with a precision of 3°C. Our data fit curve B, in Fig 11. The current may be measured in any arbitrary unit, and is so represented in the Figure. The relationship is therefore of the form:

$$i = kT^d$$

the original measurements and in presenting them before the Open Hearth Conference.²⁶ I do this because the ideas now to be presented are less familiar to a general audience than they are to the steelmakers. The actual data consist, first, of blowing-tube current readings made just before tapping, combined with optical pyrometer readings on the same metal as it runs out of the furnace into the ladle; second, of blowing-tube current readings with the same Photronic cell, made alternately with platinum thermocouple readings in a steel bath, but in most cases not in the same furnace and bath as the first set. The first set served to establish a calibration curve of current against brightness temperature; the second set compared this brightness

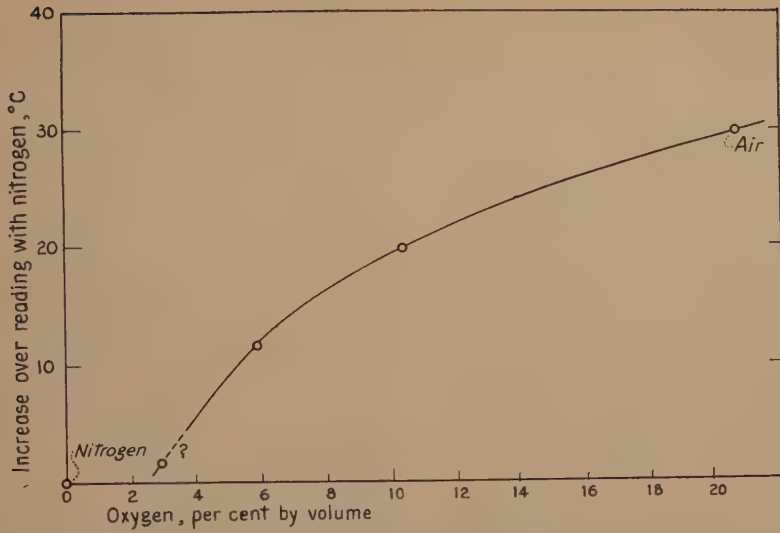


FIG 12—RELATION OF PERCENTAGE OF OXYGEN IN NITROGEN, TO APPARENT TEMPERATURE OF LIQUID STEEL, AS MEASURED BY BLOWING-TUBE PYROMETER.

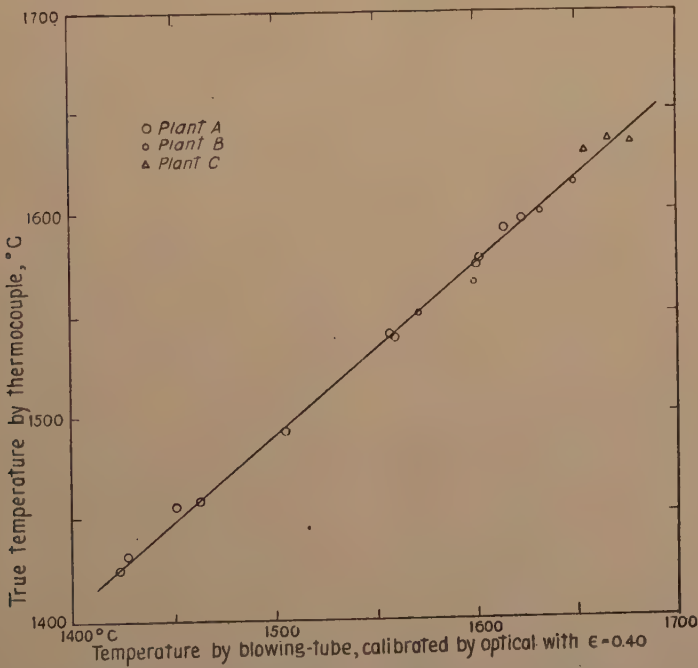


FIG 13—LINEAR RELATION BETWEEN TRUE TEMPERATURE, AS MEASURED BY THERMOCOUPLE, AND TEMPERATURE READ WITH BLOWING-TUBE PYROMETER CALIBRATED BY MEANS OF OPTICAL PYROMETER SIGHTED ON THE TAPPING STREAM AND CORRECTED FOR ASSUMED CONSTANT EMISSIVITY OF 0.40.

temperature scale against true (thermocouple) temperature.

Readings of both types were made over the entire range of temperature concerned, the actual points of the second set being shown in Fig 13. Care was taken to have the bath satisfactorily uniform in temperature and the readings were not used if a steep gradient was found in the liquid. These precautions seem to eliminate the possibility of any systematic error in the comparisons.

As far as the measurement of bath temperature is concerned, then, the job is finished, for we have calibrated the shop's blowing-tube and Photronic cell combination in terms of true temperature of the bath as measured by the platinum thermocouple.

It happens, however, as I have already indicated, that three collateral comparisons are also possible with the assembled data, and no conscientious physicist can ignore them; he must see whether they are mutually consistent, and if they are not consistent, he must find out why. The first of these comparisons involves brightness; the second, photometry; the third, emissivity.

To consider the first of these, we need to return for a moment to some practical operating details.

CHECKING SYSTEMS

To insure precision, any industrial pyrometer needs to be provided with some convenient means for checking from day to day, independent of its original and sometimes difficult absolute calibration. For a time, we depended upon a simple check of the Photronic cell alone, made by exposing it, alternately with a standard Photronic cell, to a constant illumination in a testing box containing a flashlight lamp, ammeter, and ground-glass screen. This is not completely satisfactory, however, for something might go wrong with the orifice, the protecting window, or the current recorder,

and still remain unnoticed even though the cell was correct. The designers of the Leeds and Northrup instrument⁵ took special pains to provide for an over-all check of their entire pyrometer, by balancing the working tube, through a galvanometer, against a standard tube of identical construction, both being sighted toward some steady high-temperature source such as the inside surface of the roof or walls of a furnace, whose true temperature does not need to be known.

We have found it convenient to supplement the Photronic cell check with an over-all check of the blowing-tube pyrometer as a whole, by sighting the tube on a spot on the inside of the furnace roof (with fuel turned off, to avoid variable flame reflection), and making a simultaneous reading either with an optical pyrometer on the same target, or with a radiation roof pyrometer which in turn has been set by calibration with an optical. This reading, it must be emphasized, need not be treated as an independent calibration of the blowing-tube pyrometer but only as a day-to-day check to assure consistency and precision.

BRIGHTNESS TEMPERATURE

Let us now see what additional information is obtainable from the method of routine checking just mentioned. The roof is very nearly a blackbody radiator, but whether it is exactly that or not, the red light of 0.65μ in the optical pyrometer and the predominantly red light that affects the Photronic cell represent so nearly the same emissivity in the roof that we are justified in trying out this check reading as an independent calibration of the blowing-tube pyrometer against true temperature.

There is no guarantee in principle that when sighted into a bubble in liquid metal the cell will experience the same illumination as when sighted on a blackbody. One logical expectation is that the cavity in the

liquid, being bounded in part by the relatively colder surface of the end of the steel tube, will show an average emissivity less than that of a perfect radiator. Accordingly, if a blowing-tube pyrometer has delivered a photo-current c in a bath of temperature T , and is then sighted upon a roof brick held at such a temperature that it again delivers current c , we might reasonably expect that an optical pyrometer sighted on the same brick should read a lower temperature, $T - a$.

The opposite possibility is that the inner surface of the bubble, exposed as it is to oxygen of the air at a rapidly rising temperature, will not behave exactly like steel exposed in the open to a cold surrounding atmosphere, but will react and undergo some increase of brightness. In that case, if the cell that delivers current c in the steel bath at T is sighted on a roof brick that likewise produces current c , an optical pyrometer sighted on the same brick will read a higher temperature, $T + b$.

Rather to our surprise, the optical read $T + b$ instead of $T - a$, and has done so consistently in all cases, thereby furnishing an interesting by-product of fact. There is no avoiding the conclusion that the bubble is brighter than a perfect radiator at the same temperature. The most reasonable explanation is reaction with oxygen of the air, as was quickly proved by a test using nitrogen from a cylinder in place of air. The brightness was found lower than that with air at the same steel temperature, by just the amount corresponding to the correction b , indicating that the bubble filled with nitrogen is close to being a perfect radiator, at least for the temperature of this test.

The explanation has been further confirmed by tests with mixtures of air and nitrogen. The results are shown in Fig 12. The difference is not proportional to the percentage of oxygen but rises less rapidly with a low percentage of oxygen, and the curve may conceivably be discontinuous, if a surface film is involved. It will be

interesting to learn, from further experiments, why the brightening effect is independent of alloy composition in a bubble, but is intensified by manganese and chromium on a smooth surface of flowing metal exposed in the open air.

PHOTOMETRIC CHECK

In the preceding paragraphs, I have been treating the Photronic pyrometer in our blowing-tube as a purely empirical device, to be calibrated by comparison. Let us now recall that the Photronic cell has an independent standing of its own in the instrument world, namely, as a photometer. Its spectral response curve is well known, and is not very different from the visual response curve of the human eye.³⁴ The distribution of energy in the spectrum of a blackbody or perfect radiator at a given temperature is also accurately known by the Wien-Planck formula.¹⁰ The photometric data are therefore at hand to convert the Photronic cell current reading directly into blackbody or brightness temperature.

Through the cooperation of Mr. M. E. Fogle and other technical men of the Weston Electrical Instrument Corporation, which makes the Photronic cell, we were able to secure cells especially selected for pyrometric use. The virtue of a special selection will be evident from the fact that the everyday Photronic cell is made and tested for use as a photographic exposure meter in daylight. At the end of our 80-in. pyrometric blowing-tube the light intensity is only a minute fraction of daylight. By testing at very low illumination, cells can be selected for equivalence of response in the steel bath, as they cannot be by the ordinary daylight test. The cells so selected are known as Type 3, Weston specification 668-12.

Fogle⁹ has made a photometric-pyrometric study of the Type 3 cell. Calculation from his data (represented by curve *B* in Fig 11) shows that the current follows fairly closely the formula on page 30

with d for the range 1400–1700°C decreasing from 13.5 to 12.3. Larsen and Shenk,¹⁸ with the aid of direct calibration in furnaces, found for the older cells of Type 1 a constant value for d of 12.34 for the range 1200–1750°C (curve C in Fig 11). Our data are consistent with either of these curves, for a change of 0.5 in d has hardly any appreciable effect on a temperature interpolated within 100°C. Only if temperatures near 1700° were extrapolated from some much lower calibration point, say 1400°, would the value of d come into question, as will be clear from Fig 11.

Since we are using Type 3 cells in the pyrometer, we have adopted the slope of Fogle's curve as a basis for interpolation and plotting of data. Each cell, however, has its own value of sensitivity to a standard illumination, hence there is no absolute correspondence of current and temperature.

EMISSIVITY

Another and more disturbing result of these comparisons is the new information obtained on the emissivity of liquid iron and steel.

An optical pyrometer sighted upon a smooth surface of liquid steel (which must be clean and should appear slightly gray in contrast with neighboring brighter portions of the surface that are rough or contaminated with slag or oxide) reads only a "brightness temperature" which is considerably lower than the true temperature. The early measurements indicated that both pure iron and iron with 4 pct carbon have an emissivity of 0.40 for wave-length 0.65μ .¹⁶ This means that a clean surface of the liquid near its melting point radiates only 40 pct as much red light as a black-body (a perfect absorber or perfect radiator) at the same temperature. In the absence of exact measurements at higher temperatures, it has been assumed during the past two decades that this emissivity is constant, and the pyrometer manufacturers have accordingly built instruments with a

special scale for use with cast iron and plain carbon steel, based upon the assumed constant emissivity of 0.40.

Optical pyrometer readings are customarily taken on the flowing stream during tapping of steel from the furnace, and again during the pouring process. We have supplemented these routine plant readings with optical pyrometer readings of our own. There is consequently a large body of data on the optical brightness of steels for which we have at the same time true thermocouple temperature and the blowing-tube readings. These data now show, as has been suspected for a number of years, that the emissivity ϵ is not constant at 0.40, but rises with temperature. The present data fit a curve that goes from 0.39 at 1425°C to 0.50 at about 1650°C. Of its course at still higher temperatures nothing is known. There is some indication in the data that the controlling variables in the variation of ϵ include not only the actual temperature, but the degree of superheat of the metal above the liquidus (see page 3 and Fig 4); additional very precise measurements will be necessary before this matter can be clarified completely. The meaning of these differences, in their effect on the temperature scale, can be shown thus: $+0.01$ in ϵ means -1°C at 1200° and -4°C at 1650°.

Increasing emissivity means increasing brightness relative to the perfect radiator, hence diminished correction for emissivity. The temperatures as now read optically in the steel plants are a little high near the melting point of iron, and become increasingly too high with rising temperature. What we now call 1650°C or 3002°F, after reading it with the optical pyrometer and using the conventional scale for steel, is actually only 1613°C (2935°F).

I referred above (page 29) to an unexpected coincidence that turned up in these comparisons. It is this: the extra brightness developed in the bubble of the blowing-tube pyrometer is exactly the same, within the limits of error of this comparison

(which is within $\pm 5^\circ\text{C}$), as the error due to the assumption of a constant emissivity of 0.40 for iron. In other words, a blowing-tube pyrometer calibrated in a steel bath with the aid only of an optical pyrometer and the present (supposedly erroneous) correction table for iron, will read correctly the true temperature of the open-hearth roof or of a blackbody.

While the data that I have cited and the conclusions therefrom are consistent throughout, it is fair to ask why the various laboratory determinations of the emissivity of liquid iron have indicated only a slight tendency to increase with temperature, less than the rather considerable change brought out by Sordahl's observations. An explanation may possibly be found in the very different conditions of observation at the furnace and in the laboratory. The brightness temperature of steel to which our observations apply is read on a rapidly flowing stream carrying as much as half a ton per second past the point observed. The laboratory measurement has usually been made on a few pounds, at most, of metal in not very vigorous motion. Some cinematography by British investigators¹³ has revealed rapid fluctuations in the furnace stream, too rapid to be observed visually, leading, perhaps, to an average brightness and emissivity that is different from the values for a quiet surface.

THE STEELMAKER'S TEMPERATURE SCALE

If further work confirms the values that we have found for emissivity of steel in a tapping stream, the temperature scale in the open-hearth shop needs correcting. This presents us with a minor problem in the fields of plant management and of commerce, as differentiated from those of physics and metallurgy. Should a plant that is thoroughly accustomed to the old scale change suddenly to the new? The difference is large enough to affect plant specifications on tapping and pouring

practice. All the instruments with scales based on emissivity 0.40 would have to be discarded or rebuilt. The plant men will be confused as to the source of the sudden change in temperature. If one plant changes and another does not, there will be endless confusion over comparative temperatures. All these are reasons for "leaving well enough alone."

On the other hand, I believe there is no permanent gain in adhering to incorrect data merely for the sake of convenience. An agreement among the technical men of the steel industry to change to a more correct scale on a predetermined date would probably take care of the matter satisfactorily, but the change should only be made after everyone is convinced, by as much independent confirmation as practicable, that the new data are the best obtainable.

Meanwhile, when a temperature is given for liquid steel in the open-hearth range, it should always be explicitly stated whether it is true temperature, or is a temperature on what we may call the "0.4 brightness scale."

I have devoted the larger part of this Lecture to bath pyrometry because the problems are new, interesting, and difficult. There are seven other regions of pyrometric interest in the furnace,—the slag, the roof, the walls, the bottom, the regenerators, the gases, and the flame,—but they must be treated much more briefly.

THE SLAG

Only by a passing chance is the slag ever at the same temperature as the steel bath beneath it. This will be obvious when we remember that all the thermal energy received by the bath, after it has been completely melted and has become covered with a layer of slag from one to ten inches deep, must be transmitted through this slag. The transmission is probably accomplished mainly by absorption of energy at the top surface of the slag and its transfer to the metal by convection. This process implies

not only a gradient of temperature in both slag and metal, but also a permanent difference of temperature at the boundary, well known to chemical engineers in their studies of the flow of heat across boundaries at much lower temperatures than ours.

The slag may normally be expected, therefore, to be hotter than the steel. Thermocouple measurements have shown it as high as 1760°C . Such a temperature can be attained only directly under an oil or tar flame, but I suspect that even in other areas of the bath the slag is as much as 50°C hotter than the metal. In the discussion of bath pyrometry I have mentioned the dark bubbles rising through the slag from the steel; a contrast of 10°C would be observable, and 50°C should be conspicuous.

The possible upper limit of slag temperature would be either the blackbody equivalent of the radiating flame, or the actual temperature of the flame gases in contact with the slag surface when the flame is directed downward sufficiently to touch the surface. In the latter case, the slag might locally reach a temperature as high as 1900°C . It sometimes happens that the flame of driven fuel (oil, tar) does touch the slag, and this may be one of the reasons why furnaces burning liquid fuels have heavier deposits of iron oxide in the regenerators than gas-fired furnaces, for the vapor pressure of iron and iron oxide from the slag may be expected to rise rapidly with temperature. Particularly if there is a little free carbon or carbon monoxide in the flame will there be volatilization, because of local reduction to iron on the slag surface.

The minimum temperature of the slag during normal operation should be attained at reversal of the furnace during the early part of a heat making a high-carbon steel. It is perhaps 10°C less than the minimum of the slag-covered bath, and may be estimated at 1110°C . Considerable inequalities may exist in the furnace, however, before the period when the ore boil and lime

boil begin to stir the bath and to equalize slag and metal.

In physico-chemical discussion of slag reactions we commonly assume that the slag is a homogeneous liquid solution of silica, iron oxides, lime, and magnesia, with minor amounts—occasionally increasing to major magnitude—of manganese oxides, alumina, alkalies, phosphorus pentoxide, chromium oxide, and other metal oxides. A silicate liquid, as can easily be observed by chilling it to a glass, can be quite transparent and colorless, which means that its absorbing power for that part of the energy spectrum that is visible to the eye is very low. What is its absorbing power for longer wave-lengths? It is conceivable that a furnace containing a quiet bath of steel covered with slag might be not unlike a basin containing mercury covered with water, difficult to heat by radiation because the liquid is transparent and the metal is reflecting. At the other extreme, the slag might be pictured as a liquid so opaque that it would itself reflect like a metal, and again be a poor heat absorber when its surface was smooth.

It is well known to the furnace men that when the steel bath becomes very quiet or "flat," and the slag takes on a mirror-like surface, the absorption of energy drops sharply and the fuel must be cut back to avoid damaging the walls and roof. The image of flame and roof can be seen reflected from the slag surface, but this would be true whether the slag were perfectly transparent or perfectly opaque, because even a transparent liquid reflects some of the incident light.

The ideal slag, from the standpoint of heat transfer into the bath, would seem to be somewhere between the two extremes of perfect transparency and complete opacity. Actually, many slags have somewhat the qualities of a mud, since they carry finely divided suspended crystals of calcium orthosilicate ($2\text{CaO}\cdot\text{SiO}_2$), periclase (MgO containing FeO and Fe_2O_3 in crystalline so-

lution), and magnesioferrite ($\text{MgO} \cdot \text{Fe}_2\text{O}_3$). The slag may even grade over into a wet sand or gravel, when it carries larger fragments of undissolved lime (CaO), as well as magnesia from the furnace banks.

In any event, its wide range of possible temperatures (1110–1900°C) and our present ignorance of its optical (to say nothing of its chemical) properties, mark the slag in the open-hearth furnace as a promising subject for research of value to the steelmaker.

THE ROOF

The principal purposes of open-hearth roof pyrometry are protection and operating efficiency. (See page 16.)

The temperature of the inner surface of the roof can fall very low during the charging period because of the large heat capacity and low temperature of the cold scrap. The roof often looks black during the early part of the charging period, but the impression is probably falsified by the contrast with the flame and with hotter parts of the furnace. A black object begins to be visible as a deep red in the dark at about 480 to 510°C. I doubt whether in continuous operation the roof ever cools to this temperature, but the minimum may reach 700 or even 600°C.

The maximum temperature of the silica roof is set by chemical, rather than physical, considerations.^{50,51} Liquid metallic iron has a measurable vapor pressure (0.1 mm or 0.13×10^{-3} atmosphere at 1650°C). The lower oxides are also volatile, though less so than the metal. Darken and Gurry⁷ find that the vapor in equilibrium with an oxide liquid having a composition near FeO (see Fig 14) contains the same proportion of iron and oxygen as the liquid itself; it is what the physical chemist calls a "constant-boiling mixture." Excess oxygen in the gas mixture in the furnace, accordingly, converts some of the volatile metal into solid or liquid oxide, in the form of impalpable dust or fog, some of which is so

fine that it travels all the way through the regenerators and comes out of the stack as brown smoke. The silica brick surface absorbs these vaporized or dusty oxides to form a liquid (L_b and B in Fig 15 and 16) whose fusion temperature is relatively low but which does not carry a high percentage of silica.¹² But just as soon as the temperature rises above the critical point where the two siliceous liquid phases A and B are in equilibrium, silica is dissolved to form the silica-rich liquid A , which is nearly pure silica.³ This occurs at a temperature not less than 1660°C nor above 1688°C (3020–3070°F). Both liquids flow along the surface of the roof, and if they are being produced rapidly enough, they will form stalactites or roof drips. At a slightly higher temperature, namely 1728°C, the pure silica (cristobalite) crystals themselves melt and join the other liquids. Rapid destruction of the roof follows if such a temperature is maintained.

Under normal working conditions, with a roof life of 150 to 300 heats for a stationary furnace melting scrap and blast furnace iron, only a few hundredths of an inch of thickness of silica is dissolved away at each heat. Many times this amount can be liquefied in a few minutes if the temperature exceeds the critical limit. On the other hand, rapid melting and working of the heat require that the temperature be maintained as high as possible to assure the transfer of heat from the flame or the roof surface to the bath. It has, therefore, been found well worth while in economically operated furnaces to maintain an automatic roof temperature control, or at least an automatic roof temperature indicator and recorder. This has usually taken the form of a radiation pyrometer sighted through an opening in the back wall and directed toward a point about midway of the inner surface of the roof. The middle point is chosen because it is least subject to unsymmetrical change with reversal of the furnace.

Photoelectric pyrometers (Photronic type as developed by Larsen and Shenk)¹⁷ have also been used for roof temperature indication, record, and control. The photo-

cell is more easily damaged by overheating and therefore has to be more carefully protected by water-cooling and by heat-absorbing glass. It also requires a longer

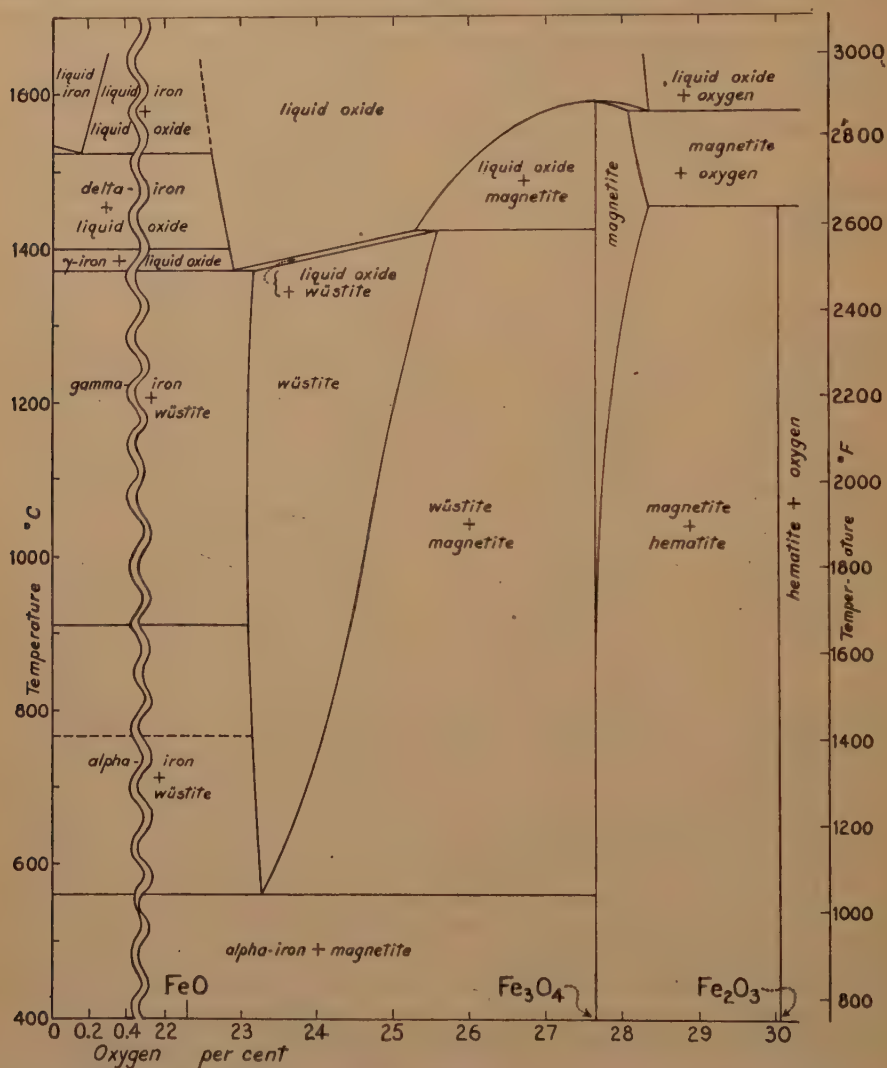


FIG 14—COMPOSITION-TEMPERATURE PHASE EQUILIBRIUM DIAGRAM FOR THE SYSTEM IRON-OXYGEN. (DARKEN AND GURRY (1946))

electric pyrometer has the advantages of greater sensitivity, less interference by carbon dioxide and water vapor, and speedier response to changing temperature. It has the disadvantage that the Photronic

tube, which makes it awkward on some furnaces because of interference with various operations along the pit side of the furnace.

Front wall pyrometers of the radiation

type have also been tried. The front wall is a more difficult place for working and servicing a pyrometer because of interference from doors and water pipes. It must be

necessary. The same is true of the so-called "H block" roof pyrometer, which consists of an inserted refractory block with a vertical cross-section like a capital letter H, and

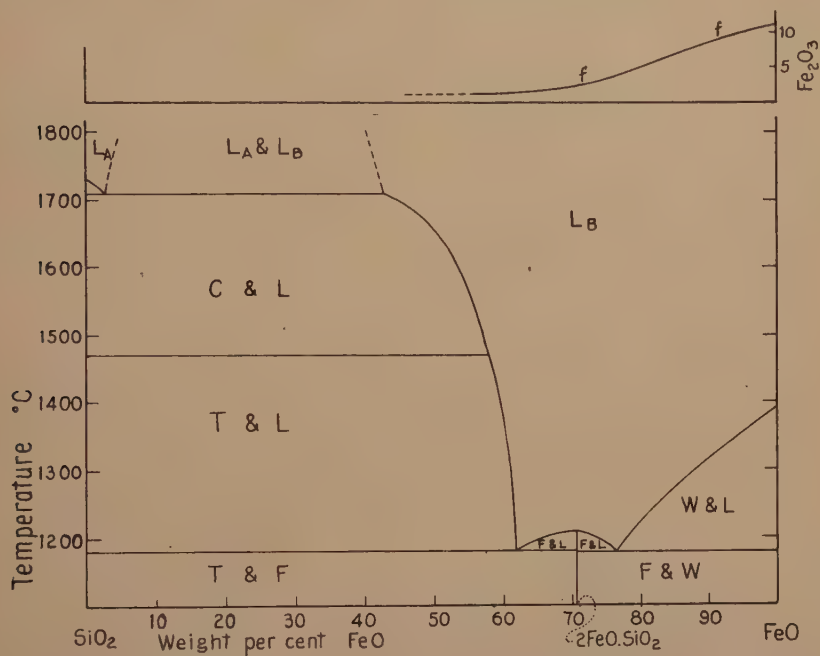


FIG 15—COMPOSITION-TEMPERATURE PHASE EQUILIBRIUM DIAGRAM FOR THE SYSTEM $\text{SiO}_2\text{-FeO}$. (BOWEN AND SCHAIRER (1932))

Phases: C: Cristobalite, SiO_2 .

F: fayalite, $2\text{FeO} \cdot \text{SiO}_2$.

L and L_B : iron-rich liquid B.

L_A : siliceous liquid A.

T: tridymite, SiO_2 .

W: wüstite, FeO crystalline solution

Curve *f* represents weight per cent Fe_2O_3 in liquid B in equilibrium at liquidus temperature.

mounted in such a way as to be completely protected by the buckstays of the furnace, else it will be damaged by the charging machine and the boxes of scrap, and the like, traveling across the front of the furnace.

Thermocouple pyrometers have also been tried in the open hearth roof, but have never been entirely satisfactory because the reading obtained is not the temperature of the inner face of the brick but a temperature somewhere along the gradient between the inner face and the outer surface. An empirical correction is therefore always

a radiation pyrometer sighted down into the upper chamber of the block. This temperature, like the thermocouple, requires a constantly changing empirical correction.

It must not be assumed that the temperature of the inner surface of the roof is always equal to the temperature of the slag, the gas, or anything else in the furnace space. The flame is certainly hotter than the roof surface at all times. It is also possible to heat the slag and steel to a temperature higher than the roof surface, because the transfer of heat is largely by radiation and if the roof surface is a good reflector, it can be cooler than

anything else in the vicinity. It probably would be entirely feasible, though perhaps not economically practicable, to use for the open-hearth roof a water-cooled sheet of

own temperature, its temperature when the flame is absent will still approach a value lower than that of the slag and bath. This is because there is a steady flow of heat by

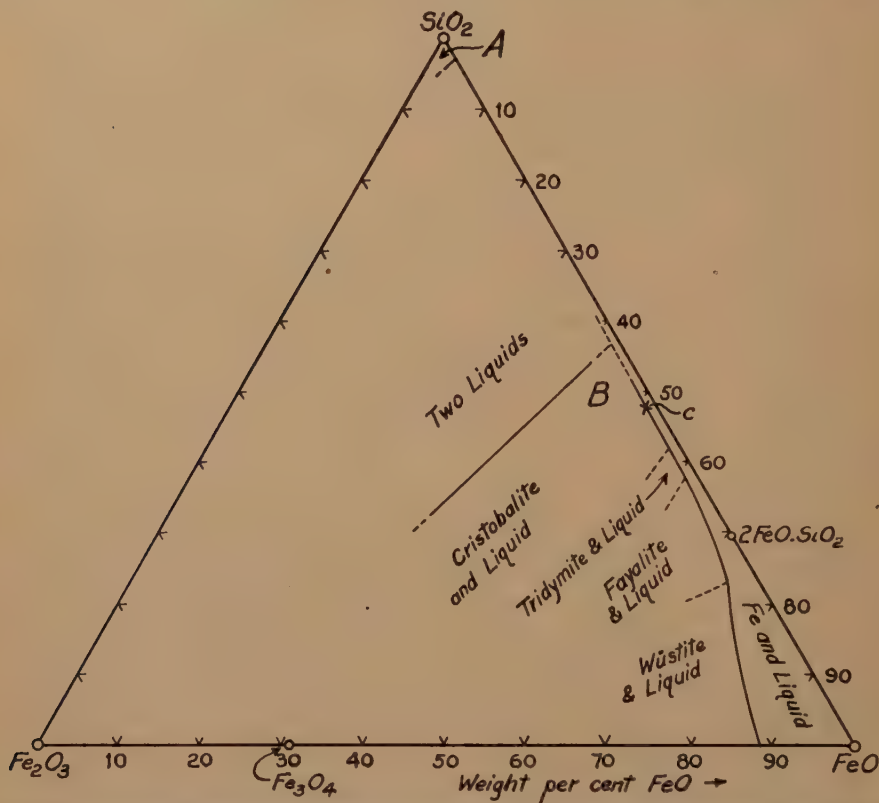


FIG 16—PROJECTION OF PARTIAL COMPOSITION-TEMPERATURE PHASE EQUILIBRIUM DIAGRAM FOR THE SYSTEM $\text{SiO}_2\text{-FeO-Fe}_2\text{O}_3$. (BOWEN AND SCHAIER (1932))

polished silver. If the proportions of the furnace were such that a relatively cool layer of gas could be made to travel slowly along the roof surface, the silver roof would gain heat only by contact with this gas layer, and the main body of the radiant heat of the flame would be almost completely reflected down to the slag to be absorbed there. Such a roof could even be designed to focus the radiant energy at any desired point or line.

If the roof surface of refractory brick is a perfect absorber, reflecting no heat whatever but radiating in accordance with its

conduction from the inner to the outer surface of the roof. The thermal equilibrium, therefore, with blackbody conditions existing inside the furnace, requires that the temperature of any area of the inner surface will depend upon the rate at which heat is being conducted away from that area.

The silica roof has a critical minimum as well as a critical maximum temperature. The minimum is set by the inversion temperature of cristobalite, at $200\text{--}275^\circ\text{C}$, a change in crystalline structure that is accompanied by a large and sudden volume change capable of shattering the brick.²⁸

This temperature is seldom if ever attained by cooling during normal continuous operation, but it must be passed through cautiously when the furnace is first heated up from the cold state.

With a basic roof (magnesia, chrome, or chrome-magnesia brick) the relatively low upper limit set by the chemistry of silica and the oxides of iron is raised, probably by at least 200°C .³² (A temperature of over 1750°C has been observed on an operating basic roof.) The melting temperature of the constituents of the brick is now so high (2800°C for magnesia, 2135°C for spinel, 2180°C for chromite) that even the eutectics are not easily attainable and the melting temperature of the brick no longer needs to be considered. Iron oxide is still the destructive agent, but whether there is a limiting liquidus temperature, as with silica, remains to be found by phase equilibrium studies of the system $\text{MgO-Al}_2\text{O}_3\text{-Cr}_2\text{O}_3\text{-Fe-O}$.

THE FURNACE WALLS

Logically, the four walls of a rectangular furnace inclosing a pool of steel and a flame might seem to be operating under nearly identical conditions. Actually, the four walls receive very different treatment and each has its own cycle of temperature.

The Backwall

The backwall is easiest to handle. In most plants it is entitled to the same consideration as the chapter on snakes in the book on Ireland: there is no backwall. Looking back over its history, it seems no more than a natural development from current practice that the rear bank, as a portion of the basic bottom, should grow upward, while the base of the arched roof was lowered to meet it. The result is the "sloping backwall," adopted in the design of nearly every modern open-hearth furnace. (See Fig 3.) In the tilting furnace, however, with its exceptionally high roof,

there is still a vertical section of brick-laid backwall.

The temperature in the re-entrant angle (roughly $80\text{--}90^{\circ}$ of arc) between the roof and the sloping bank might be expected to be higher than anywhere else in the furnace excepting the inside of the flame. The reason takes us back to the fundamental principles of radiant energy. A basic concept of the theory is the "blackbody" or holoradiator, an object or surface which absorbs all the radiant energy that strikes it, and re-radiates the energy according to the Wien-Planck Law.^{10,29} The wedge of space between two plane surfaces meeting at an acute angle is a fairly good blackbody; it approaches perfection as the angle becomes smaller, if the reflecting power is of the right magnitude. (See Fig 17.) For example, Mendenhall²⁰ shows that the emissivity or the absorptivity of a wedge with a 10° opening, in a material of reflectivity 0.7, is 0.998.

The geometrical explanation is simple: nearly every beam of radiant energy that enters the wedge and strikes one of the two surfaces is reflected, if reflected at all, across to the opposite surface, and then has to undergo several more cross reflections before it can escape from the entrance. There will be some absorption at every reflection, consequently the walls build up in temperature until the wedge is emitting nearly the blackbody radiation which is characteristic of the temperature of the two surfaces, regardless of the character of the original radiation or the true emissivity of the material. An everyday example is the extra brightness of a scratch or a crack in the polished surface of a hot piece of metal.

Since the wedge between the sloping backwall and the roof is a better absorber than the flatter and more exposed portions of walls and roof, its temperature should be a little higher. This is consistent with the fact that the silica roof always wears away most rapidly near the rear skew-back. It is

true that another plausible explanation can be offered for this type of roof wear, namely, that the flame and combustion gases may strike, superheat, and erode this

Front Wall and Doors

The front wall, together with the doors, which are usually five in number, constitute the barrier that incloses the furnace

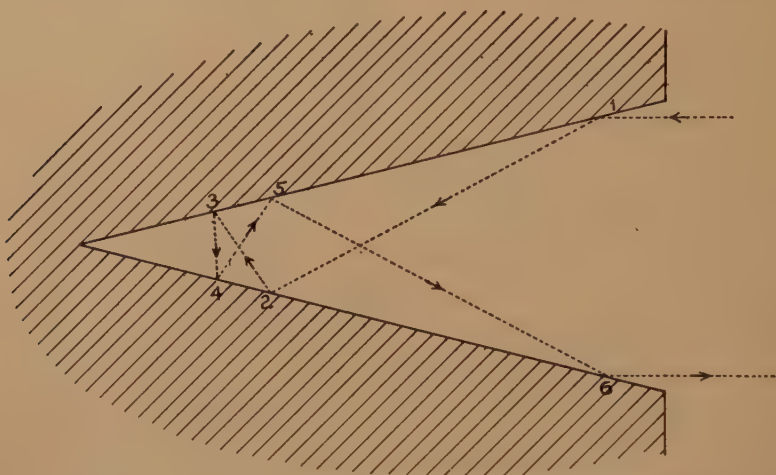


FIG 17—ABSORPTION OF RADIANT ENERGY BY A WEDGE-SHAPED OPENING WITH REFLECTING WALLS.

part of the roof, but the observation as to extra wear in this region is so general that it seems that some better explanation should be found for it than the rather accidental and variable one of flame erosion.

Endwalls

At the two ends of the furnace, the sometimes complicated construction that provides for the entrance of fuels and preheated air, and for the removal of waste gas, exposes the refractories not only to the sharp change in temperature that accompanies reversal of the furnace, but also to the direct impingement of the waste gas carrying its reactive load of iron oxides. These parts of the furnace, consequently, were the first to see the introduction, about 1914, of magnesia rammed into steel tubes as a replacement for silica brick, to be replaced a few years later by the more resistant types of chrome brick and chrome-magnesia brick that had been developed in the meantime.

heat at the side toward the charging floor. The banks of the furnace rise to or above the level of the sill plate of the doors, and the doors may occupy more than half the total front wall area. The fixed wall, therefore, is little more than a series of panels joined together near the roof by a series of arches.

In the modern furnace each door is independently water-cooled, partly for the comfort of the workmen, partly for the preservation of the door. Water-cooling of a lintel that supports the portion of wall above the door opening, which would otherwise be supported by an arch, is also frequent. Finally, the skewback steel member supporting the roof is sometimes protected by a water cooler. Through the front of the furnace as a whole, then, there is poured a large amount of heat that accomplishes nothing within the furnace but is thrown away with the warm water.

The flame is usually directed at a small angle toward the front from the center line of the furnace, but not enough to reach the

front wall. The front barrier hence receives much of its heat by radiation from flame, roof, banks, endwalls, and slag. Consequently, with a constant relatively large through-put of heat due to water-cooling, the front barrier as a whole should be a little cooler than the roof and banks. At the same time, there must be a differential within the barrier itself, the panels between the doors being the hottest parts. The differences are not conspicuous, amounting perhaps to 20°C at the most.

Another factor in furnace operation frequently works in a diametrically opposite direction as to the temperature of the front barrier. An excess of pressure within the furnace, especially during a period of active reaction in the bath, causing the furnace to "blow," drives the hot gases to the nearest available exits, namely, the wicket hole and the cracks around the doors. The inner face of the door may be thus bathed in flame, and consequently heated, by direct transfer, to a temperature temporarily higher than slag or roof.

The Bottom

The thermal history of the bottom differs radically, according to the process by which it is constructed. First of all, the furnace may have a "solid bottom," built on a heavy concrete foundation; or (more commonly) it may have a "pan bottom," built upon a platform of steel plates resting on I-beams, girders and columns. A structure of refractory brick is built up on the solid foundation, while in the case of the pan bottom, the brickwork is separated from the steel pan by a layer of refractory insulation. In either type of construction, the principal differences are in the granular refractory materials that are put on top of the brickwork. The bottom may be: (1) burned in; (2) partly rammed and partly burned; (3) fully rammed.

The hottest part of the career of a burned-in bottom (type 1) is at the very beginning of its life. It is built up by feeding

into the furnace thin layers of granular dead-burned magnesite mixed with slag, and firing each layer to the maximum temperature that the roof and walls of the furnace will stand. Any portion of it above the brickwork may therefore reach 1675 or even 1700°C while being built up, but will never again reach that temperature while in use.

In type (2) a layer of a wet plastic chrome ore mixture, or of a specially prepared magnesite, is rammed on top of the brickwork. Firing and building up of the upper layers of the magnesite bottom is then conducted as in type (1). The top surface of the rammed layer may reach 1675–1700°C, likewise the burned-in magnesite above it.

In type (3) the entire thickness of bottom above the brickwork is rammed with a dampened (not plastic) prepared magnesite, which is subsequently heated to the interior furnace temperature only at its top surface, the "hearth" of the furnace.

Pyrometry of the bottom has usually been for purposes of research and development, rather than control of quality or efficiency. Bottom pyrometry has been proposed as a means of insurance against break-outs, particularly in electric furnaces, but the installation is too difficult and the maintenance too troublesome to justify it.

In our experiments platinum-rhodium-platinum couples have been used for temperatures in or just below the magnesite section. They are protected with refractory porcelain tubes which must further be given a temporary protection with brick or pipe while rammed proprietary materials such as Plastic KN, Ramix, or Magnamix are being installed. Deeper in the brickwork Chromel-Alumel couples can be used, without protection except for insulators covering the two wires. Where possible, the couples are bent at right angles in order to run for a few inches parallel to an isothermal surface, in order to eliminate the error due to thermal conduction by the

wire, an error which may be considerable where the temperature gradient is steep. (Fig 18.) The couples are connected to multiple-point recorders, and an inde-

time of the heats, although corresponding fluctuations do not appear at higher levels, nearer the hot surface (Fig 19). The most likely explanation is that these fluctuations

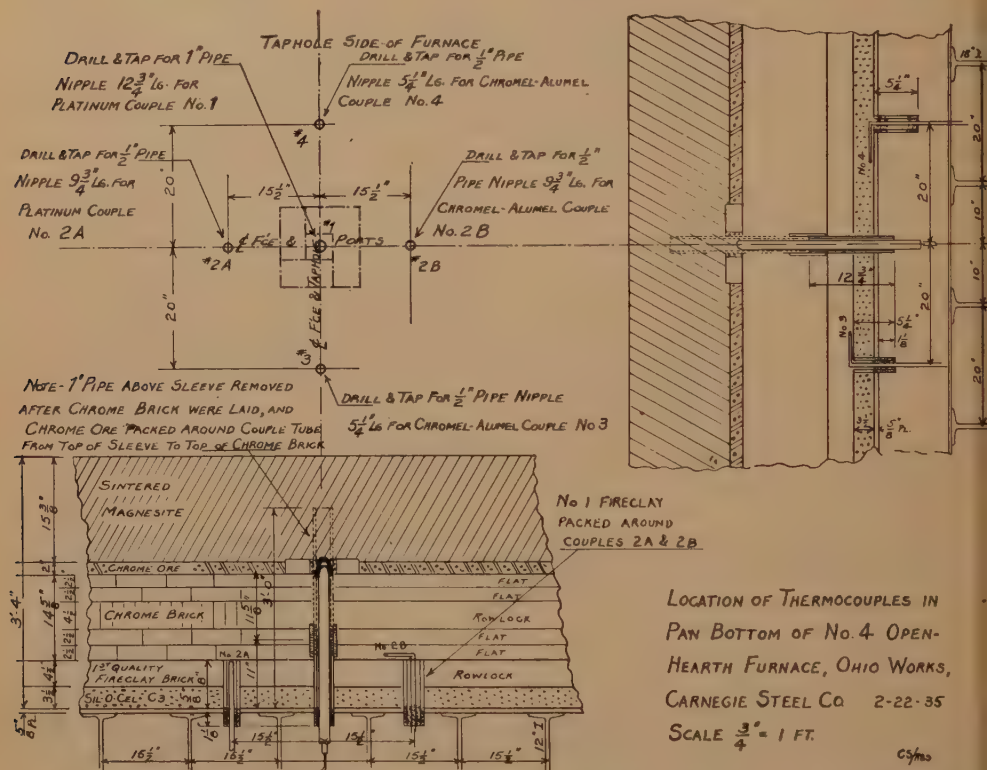


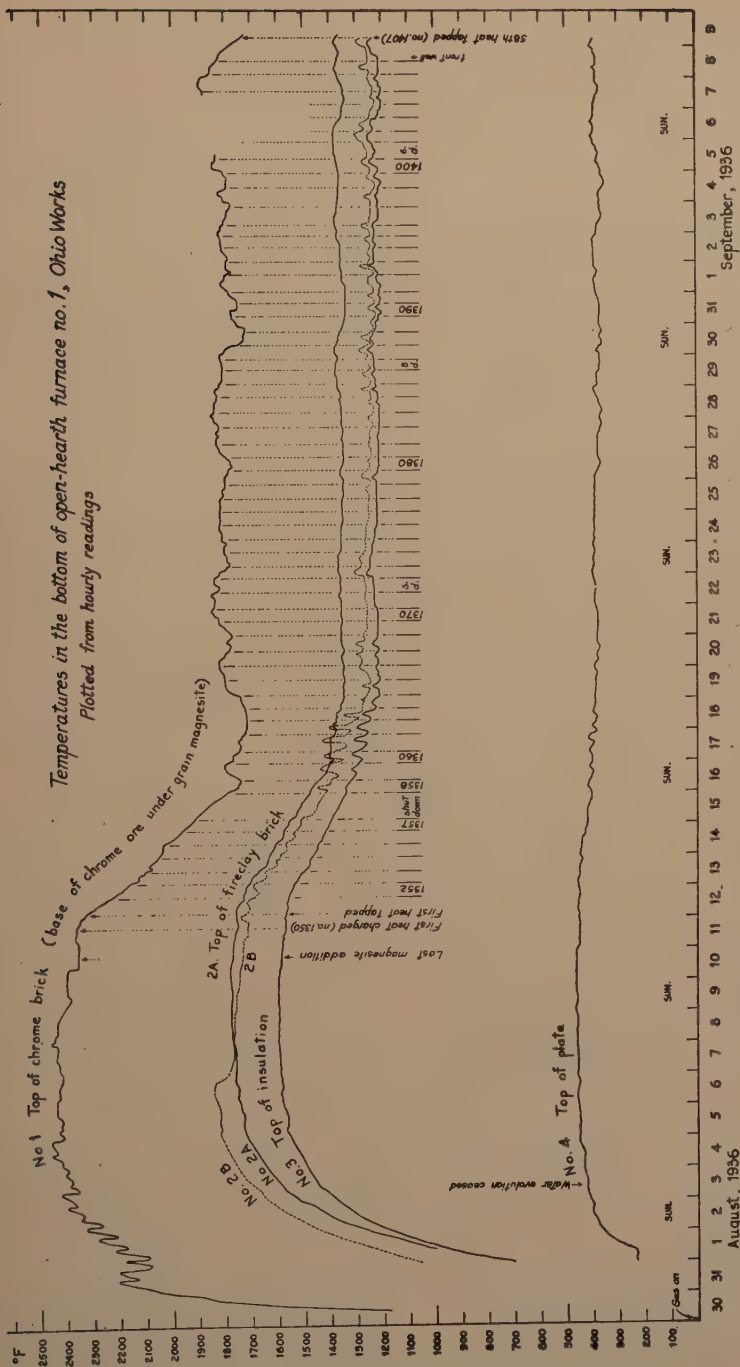
FIG 18—VERTICAL SECTION SHOWING ARRANGEMENT OF THERMOCOUPLES FOR MEASURING THE TEMPERATURE IN AN OPEN-HEARTH FURNACE BOTTOM.

pendent record is kept of the time of events in the operation of the furnace.

Fig 19, showing the temperatures during and after the burning-in of a new bottom, will serve to illustrate some of the results of a study of this kind. Note the abrupt permanent fall in temperature at the beginning of regular operations of charging and steelmaking, due probably to absorption of heat by the cold materials, whose effect is never subsequently overcome because of the continuing downward flow of heat. An unexpected result was the appearance, deep in the brickwork, of periodic fluctuations of temperature that match the

are connected with the rise and fall of the boundary of a mass of gas, perhaps carbon monoxide, evolved by the steel and slowly burning as air diffuses upward and carbon dioxide downward.

A few observations of the hearth surface temperature during operation have been obtained incidentally to the study of bath temperature, by taking readings with the protecting tube of the platinum thermocouple resting on the hearth. The maximum under these circumstances has been 1605°C. After tapping and before recharging the furnace the surface may reach 1650°C. Its minimum during operation must frequently



be below 900°C , because undissociated limestone (CaCO_3), whose dissociation pressure reaches one atmosphere at 897°C , lies in contact with the hearth for some time after the bath appears completely molten and covered with slag.

The Regenerators

Producer gas has so nearly disappeared from today's steelmaking plant that the two separate regenerator chambers, one for preheating the producer gas and one for preheating air, are now either replaced by a single chamber with a single arched roof, or they are used in parallel, both accessible to the same waste gas or air flow. This feature of the design does not, however, assure that the temperature will be distributed in accordance with the symmetry of the chambers.

Each regenerator chamber, for constructional reasons, is rectangular. The heat-absorbing checkerwork is built up of brick in a variety of designs, the entire mass resting upon a series of rider walls that form a set of flues beneath the checkerwork, while a clear head-room is left above it. At an infinitesimally slow rate of flow, either gas or air should distribute itself uniformly through all the vertical passages of the checkerwork; and the temperature over any horizontal plane should be uniform, though changing continuously with time. Actual conditions of flow lead to unsymmetrical distribution of gas or air and consequent unsymmetrical isothermal surfaces. The dissymmetry changes gradually as dust collects and clogs the passages that have been carrying the largest volume. Temperature distribution in the checkerwork is therefore extremely complex, undergoing cycles as follows: (1) the gas and air cycle, 10 to 20 min long; (2) the furnace cycle, 4 to 12 hr long; (3) the cleaning or dust-blowing cycle, 1 to 30 days long.

Pyrometry of the checkerwork is primarily for protection, secondarily as a control for efficient reversal of the furnace.

Reversal may be either by automatic control, or manually on a signal given by the pyrometers.

Protection is necessary because fireclay brick is almost universally used for the checkerwork, and such brick begins to soften and deform at a temperature which may be as low as 1175°C or as high as 1480°C depending upon the quality of the brick, but is in all cases lower than the temperature of about 1550°C which is easily attained if the furnace gases are allowed to flow uninterruptedly through one regenerator chamber. The iron oxide dust, furthermore, reacts with fireclay to form a liquid at a temperature as low as 1075°C . There must be some assurance, therefore, that the furnace is reversed before the hottest part of the checkerwork becomes overheated and damaged.

Obviously, the right temperature to measure for the sake of protecting the checkers is the temperature of this hottest spot. This is also the temperature best suited to control reversals, because of its sensitive response to changing conditions in the furnace. As a rule, the highest temperature is attained by the top course of bricks on that part of the checkerwork that is nearest the furnace. Larsen and Shenk¹⁹ found that this temperature can be satisfactorily measured by either a photoelectric (Photronic) pyrometer or a total radiation pyrometer, sighted across the top of the checkers from the bulkhead of the regenerator chamber. The pyrometer can also be sighted through a side wall of the chamber.

The maximum at the hottest point in the checkerwork is usually about 1000°C (1800°F). 1300°C (2400°F) is occasionally found and can perhaps be endured for a campaign, particularly if the upper courses are of high-heat-duty or super-duty fireclay brick. The hottest that we have observed in a furnace with silica roof is about 1375°C . In an all-basic furnace, burning more fuel and delivering gases for at least a part of

the time at a higher temperature than the silica furnace, the top checker brick have reached 1450°C . Such a temperature calls for either silica or basic brick for the top courses.

The minimum top temperature with efficient operation may be as low as 800°C . A minimum of 750°C has been observed.

The usual range of the instrumental temperature scale for the hottest part of the checkerwork, as set up in an automatic reversal mechanism of Larsen and Shenk's design,¹⁹ is $650\text{--}1400^{\circ}\text{C}$ or $1200\text{--}2600^{\circ}\text{F}$.

It is worth noting that a high temperature in the regenerators is not synonymous with efficient operation of the furnace; the optimum for a given furnace, so far as utilization of the heat is concerned, may be an intermediate, rather than a high, maximum.

Automatic reversal of the furnace can be based on various functions of temperature, time, and temperature difference. This is a large subject in itself, which I can only mention in passing, with the further remark that the temperature on which it is based can also be, and frequently is, measured by means of base-metal thermocouples in various places in the chamber. The disadvantages of the thermocouple in this service are (1) that it cannot be used economically at the hottest part of the checkerwork, and (2) that it reads a compromise temperature which is influenced partly by the passing gas or air and partly by the nearest bricks.

THE GASES

Accurate pyrometry of air and furnace gases is one of the most difficult of thermometric measurements.⁴ The gas is usually transparent, hence emits no visible light by which to judge its temperature. Its heat radiation is highly selective, dependent upon the percentage of carbon dioxide and water as well as upon the depth of the radiating mass, hence the radiation

pyrometer is useless. The contact (thermo-electric) method gives incorrect results because the thermometer may be as much influenced by radiation to and from its surroundings as it is by the temperature of the enveloping gas. Some form of suction pyrometer must therefore be used, the thermocouple being protected against radiation by a relatively nonconducting envelope, while a sample of the gas is drawn continuously past it to bring it up to the gas temperature. The whole apparatus should be of low heat capacity to favor accuracy when the gas temperature is changing rapidly.²²

Pyrometry of the furnace gases is consequently a research job, intended primarily to secure new information. I know of no furnace where it has been attempted for protection or control.

The effects of furnace leakage on temperature deserve a passing mention. Infiltration of cold air, through doors and through leaky regenerators and flues, might logically be expected to lead to cooler exit gases and cooler regenerators. Precisely the opposite is the usual effect. It must be remembered that we are not operating the furnace just to burn up oil or gas; we are trying to melt scrap and make steel, and the furnace has a job to do. If a leaky furnace leads to inefficient operation and greater waste of heat units, more fuel has to be burned and everything tends to run hotter. Sweeping statements like this must be made with caution, however; I know of several cases where stopping the air leakage slowed down the furnace instead of improving it. The answer, obviously, is to look more carefully into the conditions of combustion in such furnaces.

Fig 20 shows typical temperatures of gases in the downtakes and regenerators of an open-hearth furnace preheating both air and producer gas.²¹ The figure was selected to illustrate the large difference that can exist between the simple thermocouple reading and the true temperature.

THE FLAME

The complex of temperatures that characterizes the flame is the complex most difficult to analyze in the entire furnace.

radiation from flames is rendered probable by such facts as the "flame luminescence" of vitreous silica when hydrogen and oxygen are combining on its surface.²⁸ Such

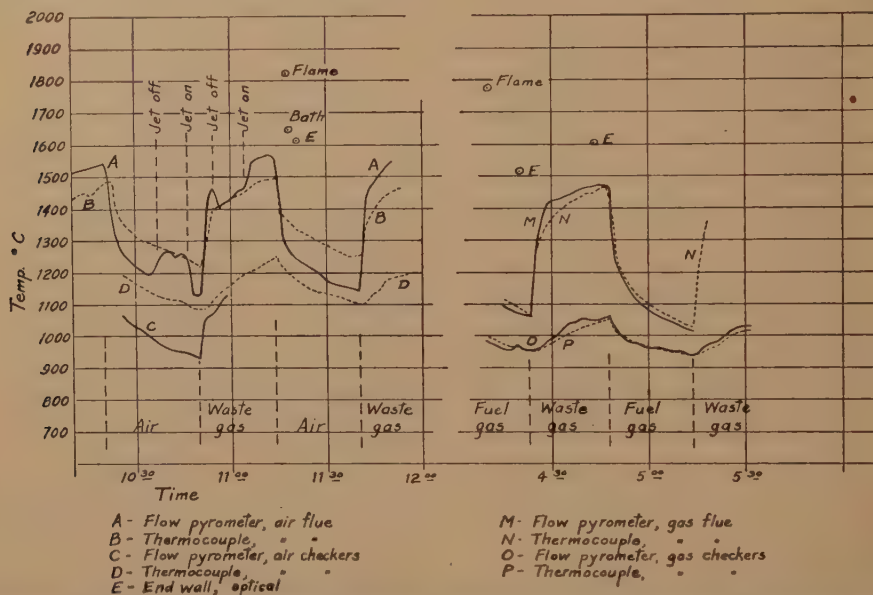


FIG 20—TEMPERATURE OF GASES AS READ BY A SUCTION PYROMETER IN THE DOWN-TAKES AND REGENERATORS OF AN OPEN-HEARTH FURNACE. (A. SCHACK (1929))

The problem is an inextricable mixture of the physics of radiation and the chemistry of combustion. As a field for research I believe it holds the best promise for returns in the improvement of the open-hearth process.

The temperature of an object in a steady thermal state, whether of heat storage or heat flow, is a relatively simple concept. The temperature is a measure of the mean energy of unsystematic molecular and atomic motion. The temperature of a flame cannot be so easily defined because the molecules in the flame are in process of reacting to form new molecules, with release of chemical energy. While most of this energy quickly becomes thermal energy, some of it can be converted directly into radiant energy without passing through the thermal stage characterized by irregular vibration. The general occurrence of such

radiation has a color and spectral distribution quite unrelated to the temperature of the water vapor produced or to the temperature of the surface.

Professor Hottel, however, who knows much more about the subject than I, considers that the non-thermal radiation from a hydrocarbon flame, if it can be detected at all, is a minor factor in the energy transfer. In his view, the subject can be handled satisfactorily on the basis of the principles of emission and absorption by gases and suspended solids, provided we can measure the temperature of the carbon particles in the flame and the temperature of the carbon dioxide and water vapor produced by combustion.

A simple calculation from the heat of combustion of the fuel and the heat capacity of the gases concerned will give the maximum average flame temperature.

Many such calculated temperatures can be found in the textbooks and in papers on combustion. Step reactions, however, as well as local concentrations of reacting constituents, are quite capable of yielding temperatures that are momentarily higher.

The temperature of the flame and the gases is so closely bound up with the problem of heat transfer from the source to the work that I wish to comment on one important aspect of the problem, concerned with surface temperatures, namely: the geometry of the furnace. To simplify the statement, let us picture a perfectly insulated operating open-hearth furnace, including regenerators, flues and stack. Let us suddenly close the valves on the incoming fuel and air, and plunge the whole thing, stack and all, into a perfect vacuum. The furnace will still continue to lose heat out the top of the stack, *by radiation*. The bath will radiate to the port roof, the port roof to the endwall, the endwall into the checkerwork, the checker brick surfaces into the flue, the flue to the inside of the stack, the inner surface of the stack, finally, to the universe. Each of these absorbing and emitting surfaces has behind it a material with a finite heat capacity, so it will take a little time to set up anything approaching a steady state of radiant flow, but radiation will inevitably drain the heat out of this perfectly insulated furnace through the only remaining opening. It is true that radiant heat energy is transferred with the speed of light, 186,000 miles per sec, but only in *straight lines*. What counts, then, is how many uninterrupted straight lines can you draw inside your furnace, and what points do they connect? While drawing these straight lines, remember also that specular reflection constitutes a straight path, as far as radiant energy is concerned.

In the actual, poorly insulated, furnace, the succession of absorbing and emitting walls has not only a heat capacity, but also a conductivity whereby some of the ab-

sorbed radiant energy reaches the outside world without being re-emitted. Furthermore, the masses of gas in the furnace are rather opaque to certain wave-lengths

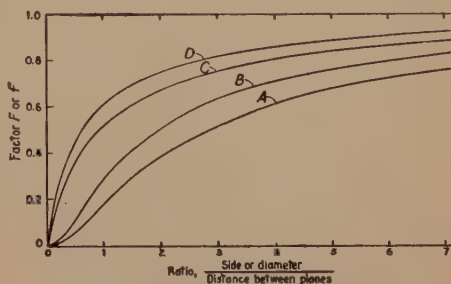


FIG 21—EFFECT OF ABSORBING AND RADIATING WALLS ON THE RADIANT HEAT TRANSFER BETWEEN PARALLEL PLANE SURFACES OF EQUAL AREA, DIRECTLY OPPOSED. (H. C. HOTTEL, (1930).) CURVES C AND D ARE MORE EXACT REPRESENTATIONS OF THE RADIATION FACTOR THAN THE CURVES ORIGINALLY PUBLISHED IN 1930. (PERSONAL COMMUNICATION FROM PROFESSOR HOTTEL.)

- A: direct radiation between disks
- B: direct radiation between rectangles, with ratio of sides 2:1
- C: total radiation between discs connected by non-conducting but reradiating walls
- D: total radiation between 2:1 rectangles connected by non-conducting but reradiating walls

characteristic of CO_2 and H_2O ; and the flame itself, if luminous with carbon particles, stops a considerable fraction of the spectrum though not all. The importance of straight-line radiation as a factor in temperature distribution, nevertheless, remains. Basically, it is a problem in geometry and topology, not physics.

The chemical engineers and the power engineers have gone deeper into this problem than the builders and users of metallurgical furnaces. Professor H. C. Hottel and collaborators at the Massachusetts Institute of Technology have published a series of papers on the subject, from which I take Fig 21 and 22 as easily understood examples.

Fig 21 illustrates how radically the conditions of heat transfer can be altered by absorption and reradiation. The ordinate

for curves *C* and *D* is the calculated value of the geometrical factor \bar{F} in the formula:

$$q = A\bar{F}\sigma(T_1^4 - T_2^4)$$

in which *q* is the rate of heat transfer in a system of black surfaces, *A* is the area of

that can be used for their measurement, will have given you a picture that can be useful to you in developing more efficient control of the process, a goal toward which all of us, as technical men, must direct our best effort.

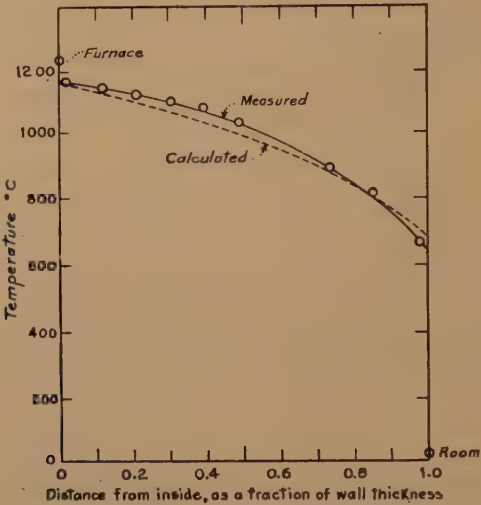


FIG 22—CALCULATED AND MEASURED DISTRIBUTION OF TEMPERATURE OVER THE SURFACE OF A CYLINDRICAL OPENING IN A FURNACE WALL. (HOTTEL AND KELLER(1932))
Temperature of inner surface of furnace wall, 1238°C.
Diameter of opening, 50.2 pct of wall thickness.

one of the two surfaces, \bar{F} is a factor allowing for the geometry of the system, σ is the Stefan-Boltzmann constant of radiation, and T_1 and T_2 are the absolute temperatures of the surfaces. When the system is not black and the heat source and heat sink have emissivities less than unity, the formulas become more complex.

Fig 22 shows that the geometrical deductions represent real facts as to temperature distribution.¹⁸ The curve of superficial temperature inside a round hole in a furnace wall, as measured with thermocouples, agrees closely, both in position and form, with the curve derived from considerations similar to those represented in Fig 21.

I trust that this hasty review of the temperatures found in the open-hearth furnace, together with the reasons why they are measured and some of the methods

TABLE 2—*Fahrenheit Equivalent of Every Centigrade Temperature Named in the Lecture*

Degrees		Degrees		Degrees	
C	F	C	F	C	F
200	392	1238	2260	1635	2977
275	527	1250	2282	1650	3002
480	896	1300	2372	1657	3015
510	950	1375	2507	1660	3020
600	1112	1400	2552	1665	3029
650	1202	1425	2597	1675	3047
700	1292	1430	2606	1680	3056
750	1382	1450	2642	1688	3070
800	1472	1480	2666	1700	3092
897	1647	1500	2732	1728	3142
900	1652	1524	2775	1750	3182
1000	1832	1535	2795	1760	3200
1075	1967	1550	2822	1800	3272
1110	2030	1585	2885	1900	3452
1130	2066	1600	2912	2135	3877
1175	2147	1605	2921	2180	3956
1200	2192	1613	2935	2800	5072
		1620	2948		

REFERENCES

1. The most recent detailed brief review of pyrometric methods in metallurgy will

- be found in the report of the Subcommittee on Pyrometry (Evans, Fairchild, Forsythe, Harrison, Peters, Roeser, Wensel, and Sosman) in *Metals Handbook*, Amer. Soc. for Met. (1948) 174-187.
2. For more complete descriptions of types of open-hearth furnace see "Basic Open-hearth Steelmaking," AIME (1944) 632 pp. A new edition of this book is planned for 1948.
 3. N. L. Bowen and J. F. Schairer: The System FeO-SiO_2 , *Amer. Jnl. Science* (1932) **24**, 177-213.
 4. (British) Inst. of Fuel, Symposium on Gas Temperature Measurement, *Jnl. Inst. Fuel* (1939) **12**, No. 64, pp. S1-S107.
 5. H. T. Clark: Methods of Temperature Measurement of Liquid Iron and Steel. AIME, *Proc. Elec. Furn. Steel Conf.* (1945) **3**, 81-88.
 6. F. L. Collins and C. Oseland: U. S. Pat. 2,020,019, Nov. 5, 1935.
 7. L. S. Darken and R. W. Gurry: The System Iron-oxygen. *Jnl. Amer. Chem. Soc.* (1945) **67**, 1398-1412. (1946) **68**, 798-816.
 8. A. L. Day, R. B. Sosman, and E. T. Allen: High Temperature Gas Thermometry. Carnegie Inst. Washington, Publ. 157. (1911).
 9. M. E. Fogle: Temperature Measurement and Control with Solid Photoelectric Cells. *Trans. Electrochem. Soc.* (1943) **83**, 77-86.
 10. W. E. Forsythe, et al.: Measurement of Radiant Energy. New York (1937).
 11. G. N. Goller: The Emissivity of Molten Stainless Steels. *Trans. Amer. Soc. Metals* (1944) **32**, 239-254.
 12. J. W. Greig: On Liquid Immiscibility in the System $\text{FeO-Fe}_2\text{O}_3\text{-Al}_2\text{O}_3\text{-SiO}_2$. *Amer. Jnl. Science* (1927) **14**, 473-484.
 13. J. A. Hall: A Photographic Investigation of the Brightness Temperatures of Liquid Steel Streams. *Jnl. Iron and Steel Inst.* (1947) **155**, 55-85.
 14. H. C. Hottel: Radiant Heat Transmission. *Mech. Eng.* (1930) **52**, 699-704.
 15. H. C. Hottel and J. D. Keller: Effect of Reradiation on Heat Transmission in Furnaces and through Openings. *Trans. Amer. Soc. Mech. Eng. (Iron and Steel Div.)* (1933) **55**, 39-49.
 16. D. Knowles and R. S. Sarjant: Emissivity of Molten Iron and Steel. *Jnl. Iron & Steel Inst.* (1947) **155**, 577-592.
 17. B. M. Larsen and W. E. Shenk: U. S. Pat. 2,054,382, Sep. 15, 1936.
 18. B. M. Larsen and W. E. Shenk: Temperature Measurement with Blocking-layer Photo-cells. *Jnl. Appl. Phys.* (1940) **11**, 555-560. *Amer. Inst. Phys.*, "Temperature, its Measurement and Control," etc., New York, 1941, p. 1150-1158.
 19. B. M. Larsen and W. E. Shenk: A Completely Automatic Control of Open-hearth Reversal. AIME, *Proc. Open Hearth Conf.* **28**, 228-239. TP 1830 (1945).
 20. C. E. Mendenhall: On the Emissive Power of Wedge-shaped Cavities and their Use in Temperature Measurements. *Astrophysical Jnl.* (1911) **33**, 91-97.
 21. A. Schack: Temperaturmessungen an Siemens-Martin-Oefen. *Archiv Eisen-huettenwesen* (1929) **3**, 7-12.
 22. Hermann Schmidt: Die Messung von Gastemperaturen. Mitt. Kaiser-Wilhelm Inst. Eisenforschung (1927) **9**, 227-238.
 23. F. H. Schofield and A. Grace: A "Quick-immersion" Thermocouple for Measuring the Temperature of Liquid Steel both before and after being Tapped from the Furnace. Iron and Steel Inst., Spec. Rep. (1939) **25**, 239-264.
 - Temperature, its Measurement and Control in Science and Industry, Amer. Inst. Phys. (1941) pp. 937-945.
 24. L. O. Sordahl: U. S. Pat. 2,184,169. Dec. 19, 1939.
 25. L. O. Sordahl and R. B. Sosman: Measuring Open-hearth Bath Temperatures. Instruments, **13**, 127-130, (1940); *Steel*, **106**, No. 21, pp. 44-47. 20 May 1940. Temperature, Its Measurement and Control in Science and Industry, Amer. Inst. Phys. N. Y. (1941) 927-936.
 26. L. O. Sordahl and J. W. Bain: AIME, *Proc. Open Hearth Conf.* (1947) **30**, 255-260.
 27. R. B. Sosman: Types of Prismatic Structure in Igneous Rocks. *Jnl. Geol.* (1916) **24**, 215-234.
 28. R. B. Sosman: The Properties of Silica. N. Y., 1927. (Amer. Chem. Soc. Monograph 37)
 29. R. B. Sosman: The Pyrometry of Solids and Surfaces. Cleveland, 1940. (Amer. Soc. Metals)
 30. R. B. Sosman: Silica as a Refractory in the Steel Industry. Year Book Amer. Iron and Steel Inst. (1929) **19**, 74-104.
 31. R. B. Sosman: Pyrometry and the Steel-maker's Refractories. *Jnl. Amer. Ceramic Soc.* (1938) **21**, 37-49.
 32. R. B. Sosman: The Outlook for an All-basic Open-hearth Furnace. AIME, *Proc. Open Hearth Conf.* (1945) **28**, 54-68.
 33. L. F. Weitzenkorn: A Method for the Determination of Bath Temperatures. AIME, *Proc. Elec. Furn. Steel* (1944) **2**, 143-151. *Proc. Open Hearth Conf.* (1945) **28**, 327-336.
 34. Weston Elec. Instr. Corp. Technical data on Weston Photronic cells, Newark, N. J. (1942).

Direct Oxidation in the Basic Open Hearth Process

BY EDWARD B. HUGHES* AND FRANK G. NORRIS* MEMBER AIME

(New York Meeting, February, 1948)

OXIDATION is characteristic of all processes for making steel from pig iron. This thought has been aptly expressed by H. W. Graham¹³ in the recent Howe Memorial Lecture, "The process of steel-making consists of using iron oxide to reduce the carbon content of the pig iron to the desired level."

Direct oxidation refers to the reaction that results from introducing oxygen either alone or mixed with other gases directly into the steel bath.

In working a heat, oxygen in some form is added to the steel to remove the undesirable constituents as oxides. There are two general methods of supplying this oxygen to the open hearth bath. The method in which the oxygen is added as a compound such as CO_2 or iron ore is designated an indirect method because the steel bath must first decompose the compound to attain oxygen in a usable form. The other method in which oxygen is added to the bath in the elemental or gaseous form, more or less diluted by other gases such as nitrogen, is a direct method because no decomposition is necessary before the oxygen reacts with iron to form FeO which is dissolved in the bath in a usable form. Bubble formation (at least of a macroscopic size) presents no problem in case of direct oxidation because the reacting agent (oxygen) is in the form of bubbles when entering the metal.

Regardless of whether oxygen is intro-

duced into the bath directly or indirectly, several reactions proceed concurrently. In the presence of the bath of molten iron, FeO is formed either by oxidation of iron by oxygen or reduction of oxides by iron. This FeO dissolved in the molten iron is the source of oxygen for the oxidation of manganese, carbon, silicon, and phosphorus if these are present. The oxidation of carbon from steel is the controlling steelmaking reaction.

The introduction of oxygen into the bath, its reaction in the elimination of impurities, and its control by the use of de-oxidizing additions have been subjects of importance since steel was first made by the bessemer process. Direct oxidation is, in a sense, an application of the bessemer principle to the open hearth process.

Graham¹³ states: "The use of oxygen or air jets introduced into the metal bath is essentially an effort to approach in the open hearth the turbulence, rapid interface reaction, and high production rate per hour that exists in the bessemer process."

The general subject, "Oxygen in Steel-making," was given new life by the studies of Herty and associates starting about 1925. The current interest in elemental oxygen is intimately related to the large scale production of oxygen developed during the war period. Some of the first applications were made during the early summer of 1946 at the Steel Co. of Canada using oxygen with the fuel. Such a use is of considerable interest and importance in contributing to faster heats but is not the subject of the present discussion which deals entirely with the introduction of elemental oxygen directly into the open hearth bath.

Manuscript received at the office of the Institute December 15, 1947. Issued as TP 2380 in METALS TECHNOLOGY, June 1948.

* Wheeling Steel Corporation, Steubenville, Ohio.

¹³ References are at the end of the paper.

A recent article¹² reviewing the current status of experiments with direct oxidation cites the following conclusions: 1. *Higher grade refractories are needed.* 2. *Oxygen must be cheaper in price.* 3. *Fumes and dust must be overcome.* There are certain operating conditions which support each of these three conclusions either separately or as a group. In substance, these conclusions infer that direct oxidation is interesting experimentally and may prove practical in the future but not now. One of the purposes of this report is to show what can be done with furnaces built of the usual brick and with oxygen at a cost of \$3.35 per 1000 cu ft. By selection of the proper stage of the heat for the direct oxidation and amount of oxygen used, the process is economical from the standpoint of oxygen and refractories and without the production of undue fumes. In many heats the fumes are no greater than those which accompany the melting of the usual scrap charge.

DESCRIPTION OF PRACTICE

The shop in which all of the present work was done has 11 open hearth furnaces 39.5 × 16.5 and 38 in. deep, tapping 160 tons, and fired with fuel oil.

The usual charge is 44 pct hot metal, 54 pct scrap, and 2 pct cold iron comprised mainly of ladle skulls. Sintered ore is charged with the heat. The flux charge is 135 lb of limestone per ton of ingots.

The commonest method of introduction of oxygen is with a $\frac{3}{4}$ in. standard pipe with a line pressure of 100 lb and about 75 lb at the discharge, resulting in a rate of flow of 500 cfm. The oxygen is 99.5 pct O.

No protection is used on the pipe.

The preferred depth of immersion is 6–10 in. From one to fourteen 20-ft lengths of pipe are used per heat.

The usual set-up using a special buggy to support and feed the pipe is one man at the furnace and one man at the line valve. When the buggy was not used, two to three men were needed to hold the hose and pipe.

The safety precaution is to clean the oil from the pipes before use and to avoid greasy gloves in handling the pipe before or during blowing.

The total time of oxygen flow for a heat is from 5 to 6 min. for one pipe up to 50 min. for several pipes. The overall elapsed time from start to finish of direct oxidation is from 5 min. to 3½ hr. In the latter case direct oxidation is supplemented by additions of ore.

The average carbon at melt is 0.30 pct and the average carbon at tap is 0.078 pct. Direct oxidation is used on all grades of 0.08 pct C and below. From Sept. 1, 1946 to Oct. 31, 1947, oxygen was introduced directly into the bath in 3899 heats. The recent monthly consumption of the shop is from 2,800,000 to 3,100,000 cu ft which is an average of 5000 cu ft per heat or 37 to 42 cu ft per ton. If more than this amount is used on some heats, other heats must be made with none. In fact, this distribution has been the immediate solution to the problem.

OBJECTIVES OF DIRECT OXIDATION

There are five general objectives that can be made the basis of allotting a limited supply of oxygen among heats.

1. To eliminate as much carbon as possible.
2. To replace as much ore as possible.
3. To replace as much cold iron as possible.
4. To make as fast heats as possible.
5. To make heats as economically as possible.

1. The effectiveness of direct oxidation in eliminating carbon is sometimes evaluated in terms of cubic feet of oxygen per point of carbon drop per ton. The way to make this figure as low as possible is to use no oxygen. There is some elimination of carbon, and because no oxygen is used the figure is zero. This same type of error is involved if a low rate of oxygen supply is compared with a faster rate. Direct oxidation at a low rate has a tendency to give less consumption per point of carbon.

2. If the objective is to replace as much

ore as possible, direct oxidation will be started early in the heat.

3. If the objective is to replace cold pig iron, the limited supply of oxygen available for direct oxidation will be used to raise the temperature of the bath and the carbon eliminated will be incidental. Such a program may be an alternative to heavy skull losses if cold iron is unavailable.

4. If the objective is to make as fast heats or the greatest production in a given period, the effect of carbon content on the rate of elimination under conditions of direct and indirect oxidation must be considered. The time saved by direct oxidation below 0.06 pct C is very great as shown by comparing the rate of carbon drop with direct and indirect oxidation. A comparison considering only oxygen consumption is unfavorable if the heat is blown to a low carbon content. The saving is in heat time because 0.03 to 0.04 pct C can be made by direct oxidation in about the same time as 0.08 or 0.10 pct C could be made by indirect sources of oxygen.

The saving of time is based on a comparison of the time of heat using direct oxidation with the time expected if that particular heat had been worked by conventional (indirect) methods. On a fast furnace it is more difficult to improve the heat time than on a slow furnace.

5. From an economical standpoint, the cost of all materials, the saving of fuel resulting from faster heats, from reduced fuel made possible by higher temperature, the differences in yield, and the value of increased production must all be considered. The proper balance will change as costs change from month to month. If separate costs were kept on individual furnaces or by grades, the difference in operating cost per furnace hour would be a basis for dispatching the oxygen supply among the different furnaces of the shop. If an unlimited supply of feed ore, cold iron, and oxygen were available for use in working heats, allocation by grades and furnaces

and stage of the heat could be based entirely on the economic factors.

DETERMINATION OF RATE OF CARBON ELIMINATION

Two series of heats were studied with special attention given to the practice used during refining. The heats were grouped according to whether oxygen was used at least partly for direct oxidation or ore for indirect oxidation. The change in carbon content with time for each method of oxidation is shown in Fig 1 entitled Carbon Elimination.

An accurate time of sample and carbon content was taken on each heat followed and a plot made of the data from each heat. The first sample was not at exactly the same carbon content on each heat. The curves were superimposed with reference to a common base point. The average is shown by the solid line and the spread of the observations by the shaded area.

The shaded areas about each curve show a tendency to diverge from the line and then converge so the end carbon is reached in about the same time for each heat. If the curve for a particular heat flattens out or the carbon hangs at some particular point, eventually the drop is faster than usual so that the given end point is reached in about the expected time. Conversely if there is rapid drop at the higher carbon contents, there is a tendency for a retarded drop later so that over a sufficiently extended range of carbon there is only a small difference in the time required for carbon elimination between two given values.

The rate for carbon elimination is defined as dc/dt or the slope of the carbon elimination curve. This value is not the same as that obtained by taking the carbon difference between two samples divided by the time interval between them.

Fig 2 shows the rate of carbon elimination plotted against carbon content for conditions of direct and indirect oxidation. Both scales are logarithmic. For direct

oxidation, the logarithm of the carbon drop is proportional to the logarithm of the carbon content from 0.20 to 0.03 pct carbon with the equation: $\text{Log } dc/dt = 1.727 \log C$

carbon for heats that are worked to lower values so that the true rate at 0.09 to 0.05 pct C can be determined from the carbon drop curve.

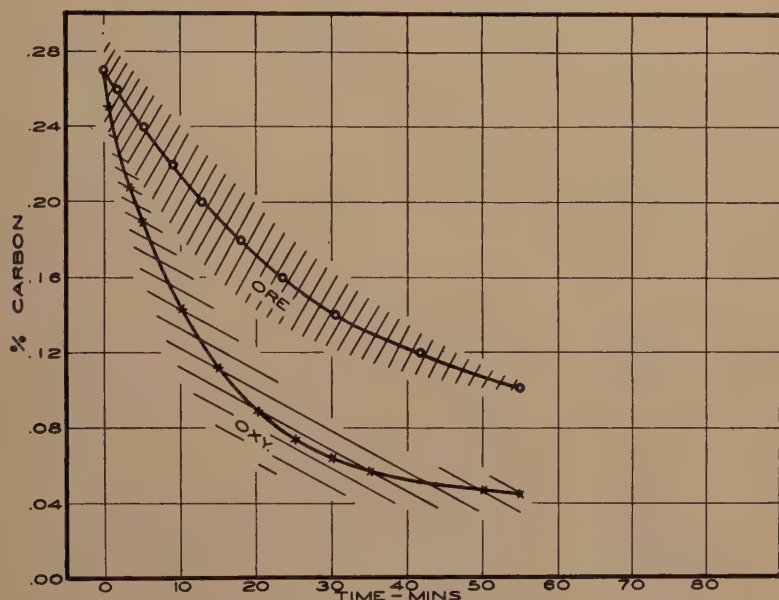


FIG 1—CARBON ELIMINATION.

-2.137 — where dc/dt is carbon drop measured in points of carbon per min. and C is points of carbon, in other words 0.25 pct carbon is 25 points.

The points that are obviously not on this line can be explained by operating conditions. The line represents normal carbon drop during the period of direct oxidation. The point 0.25 pct C and two points at 0.05 and 0.06 pct C were taken at the beginning of the blow and are not expected to represent conditions prevailing during the blowing period.

The lower rate at 0.15 pct C is believed to be caused by a general tendency to reduce the driving of the furnace for heats that will finish about 0.10 pct carbon rather than indicating that the true relation is semi-logarithmic. This view is supported (though of course not proved) by the log log relation existing below 0.09 pct

On this same chart are plotted the points for conditions of indirect oxidation. There is a linear relation between the two logarithms from 0.45 to 0.20 pct carbon and from 0.08 to 0.03 pct carbon. The relation for the line from 0.45 to 0.20 pct carbon is expressed by the formula $-\text{Log } dc/dt = 0.7884 \log C - 1.3665$; and that from 0.08 to 0.03 pct carbon by the formula $-\text{Log } dc/dt = 3.904 \log C - 4.327$.

These equations in integrated form show carbon as a function of time — $C =$

$[e^{a(1-b)t}]^{\frac{1}{1-b}}$ which is a mathematical expression of the relation shown in Fig 1.

The relation between carbon content and rate of elimination (Fig 2) is simple and straightforward and is based on carbon analysis only. It does not involve determination of other elements in the bath such as manganese or oxygen. The general

tendency for both carbon and manganese to be high early in the heat and to be eliminated more or less together leads to attempts to correlate the two. For uniform conditions this relation may be more or less satisfactory. Residual manganese can be

given conditions and is not of general application.

CONTROL OF CARBON ELIMINATION

There are several well recognized sources of oxygen in the open hearth process, such

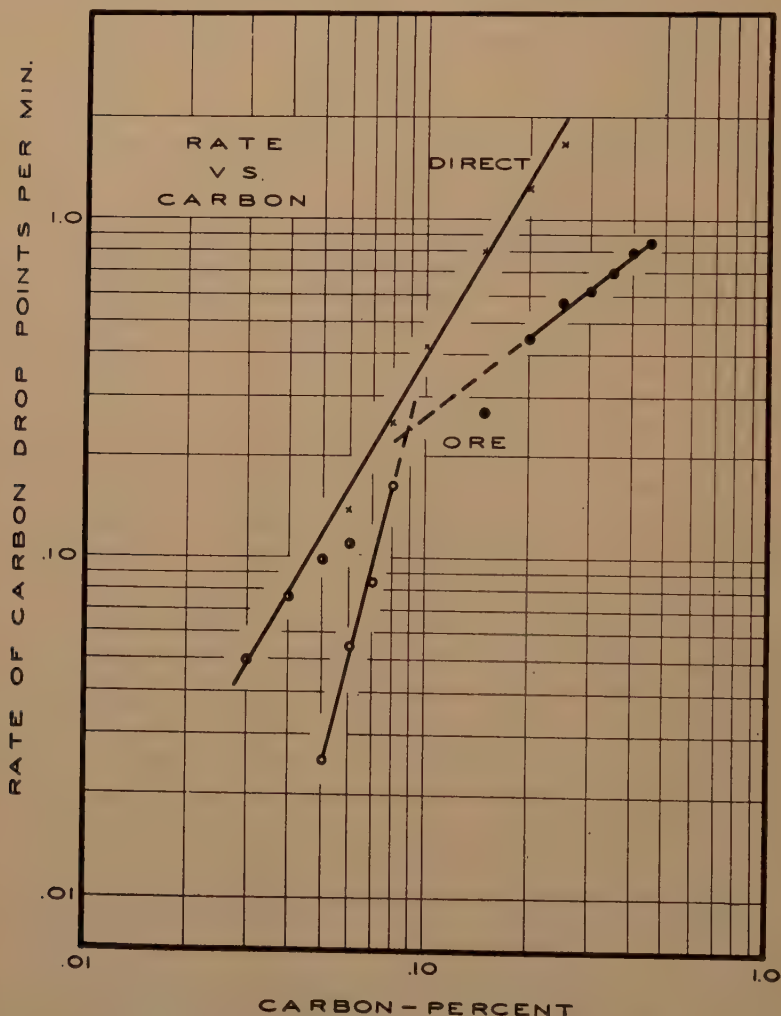


FIG 2—RELATION BETWEEN CARBON DROP AND CARBON CONTENT.

varied by changes in basicity, total manganese in the charge, and other factors which have no direct effect on the carbon content; therefore the relation between carbon and manganese is a special one for

as the CO_2 formed by the calcination of limestone, the oxidizing atmosphere acting directly on the unmelted scrap and on the slag at later stages of the heat. For a given practice (including lime charge, proportion

of hot metal, type of fuel) these sources of oxygen are considered approximately constant from heat to heat and the chief control of carbon elimination at the disposal of the operator is the amount of feed ore. Thus in the ordinary working of a heat by indirect oxidation, the rate of carbon drop is controlled by the first helper who is guided and limited by the desired carbon at the finish of the heat and by the temperature requirements or heat input of his particular furnace. The rate of carbon elimination usually proceeds as a series of steps or peaks, being very high immediately after an ore addition. These peaks, of course, are not disclosed by the usual study of a heat because samples are never taken immediately after an ore addition. In these conditions the carbon drop is primarily a function of the time since the last ore addition. Arbitrary limitations such as the lapse of a given period of time or the judgment of the samples as to when ore has worked through or when a steady state has been reached would tend to give samples showing a more nearly constant rate of carbon drop than actually prevails. All of these conditions are present and must be considered in estimating the effect of the oxygen introduced into the bath during periods of direct oxidation.

Several characteristic differences also become apparent. Oxygen is available in a continuous supply. The bath can be sampled at any time desired. The rate of carbon drop is an index of the rate at which the steel bath will accept oxygen.

CHEMICAL RELATION BETWEEN CARBON AND OXYGEN

After the reaction has occurred, the amount of oxygen that has reacted is readily computed. The answer is not the same as the oxygen required to cause the reaction to proceed, and failure to distinguish between the two leads to confusion.

If all of the carbon is oxidized to CO,

3.2 cu ft of gaseous oxygen is sufficient to react with 0.2 lb of carbon.

$$(0.2 \times \frac{16}{12} = 0.267 \text{ lb oxygen})$$

$$\frac{0.267}{0.083} = 3.2 \text{ cu ft})$$

Two tenths of a pound is selected because this amount is one point of carbon per ton.

Any CO₂ formed will increase the amount of oxygen required. If 10 pct of the carbon is oxidized to CO₂, the value 3.2 cu ft is increased to 3.25 cu ft.

To eliminate 0.01 pct carbon requires 3.25 cu ft of oxygen per ton of steel. For a 160 ton bath, 520 cu ft are required per point of carbon. 500 cfm is sufficient oxygen to eliminate carbon from a 160 ton bath at the rate of 0.0096 pct per min. Fig 2 shows that at 0.17 pct carbon the rate of elimination by direct oxidation is 0.96 points per minute. Above this carbon content, carbon is being eliminated faster than oxygen is being supplied by the lance. The physical effects of direct oxidation such as agitation are clearly in evidence at this range of carbon and contribute to the faster carbon drop. The oxidizing slag is needed chemically to supply the oxygen. Dumping ore or other indirect sources are not in themselves enough. The fast rates above 0.17 pct carbon (and probably to a lesser extent at lower carbon content) result from the combined chemical and physical effects of direct oxidation and the chemical effect of indirect oxidation.

A similar calculation shows that the elimination of one point of carbon per ton consumes the oxygen contained in 1.035 or 1.135 lb of ore, the exact amount depending on the amount of CO₂ formed.

Translated into terms of shop practice for 160 ton heats and boxes containing 4400 lb of ore, one box of ore contains sufficient oxygen to eliminate 1.27 or 2.4 points of carbon. Early in the heat this is about the carbon drop that results from a box of ore. At low carbon content the drop

is much less. This same decrease of carbon drop at low carbon content is found in heats made by direct oxidation.

EFFICIENCY OF DIRECT OXIDATION

The chemical relationship between amount of oxygen and points of carbon removed immediately invites a computation of efficiency based on the cubic feet of oxygen per point of carbon removed from the bath. Such computation is unsatisfactory because it leads to a variation of efficiency which is roughly proportional to the carbon content of the bath at the start of oxidation. In oxidizing the carbon from 1.00 to 0.90 pct, the oxygen consumption per point of carbon per ton of bath is 1 to 2 cu ft; from 0.25 to 0.10 pct C the consumption is 3 to 3.5 cu ft; from 0.10 to 0.05 pct it is about 15 cu ft; and below 0.05 pct it is 40 to 60 cu ft, the variation depending on the condition of the slag at start of oxidation.

These data are in general agreement with the findings of Slottman and Lounsberry⁶ who, in discussion of direct oxidation, state: "In carbon ranges above 0.40 pct, oxygen added directly to the bath reacts almost quantitatively with carbon and other alloying elements. With carbon contents below 0.25 the decarburizing efficiency of oxygen diminishes rapidly."

Because of the importance of carbon content as a guide to the progress of the refining process, it is sometimes used as a measure of the efficiency of the oxidation. This comparison is a convenient short-cut that gives reliable results if the conditions are approximately equal in the two processes or heats that are being compared. When conditions are widely different, such as direct or indirect oxidation methods, or different initial carbon content, or different amounts of other elements in the bath, carbon drop (that is, points per minute) can be used as a comparison only when certain innate characteristics of the refining procedure are known and accounted for.

If the differences between the shapes of the carbon drop curves of direct and indirect oxidation methods are known, the rating method based on the total carbon drop expressed in points of carbon eliminated per minute of oxidation appears less inviting. A cursory investigation of a carbon drop curve reveals that the speed of carbon removal, either by the direct or indirect method, depends on the carbon content of the bath. When traveling from one point to another, by automobile for example, the time necessary for the total trip is governed by the top speed of the car and the speed limits of the sections through which the traveling is done. The speed of the automobile at any one point may differ greatly from the average or computed speed between the two points. This fact must be recognized for proper interpretation of the point per minute method of rating carbon elimination.

Both of these methods for obtaining a rating of speed or efficiency take no account of the basic principle that a new process (direct oxidation) is being investigated to determine its potential value as a production tool and that it may partially replace a process (indirect oxidation) which has been in common use for many years. A method for comparing the efficiency of the new practice in terms of the old practice is proposed.

With the relation established in Fig 2, an expression can be derived for the efficiency of carbon elimination based on the speed of elimination by indirect oxidation. This relation is expressed by the formula—

$$\frac{R_d - R_i}{R_i}$$

in which R_d is the rate in points per minute of direct oxidation and R_i is the rate in points per minute of indirect oxidation.

Practical experience has influenced furnace operators to show a preference for starting direct oxidation at 0.15 to 0.10 pct carbon. This is in a shop with a definite

shortage of hot metal where it is not possible to charge heats to melt excessively high. With high melts there is an advantage to blow the bath at higher carbon contents.

ored heats, the benefits of direct oxidation are most pronounced below 0.08 pct carbon.

The shop in which the experiments were conducted shows a consumption of 150 cu

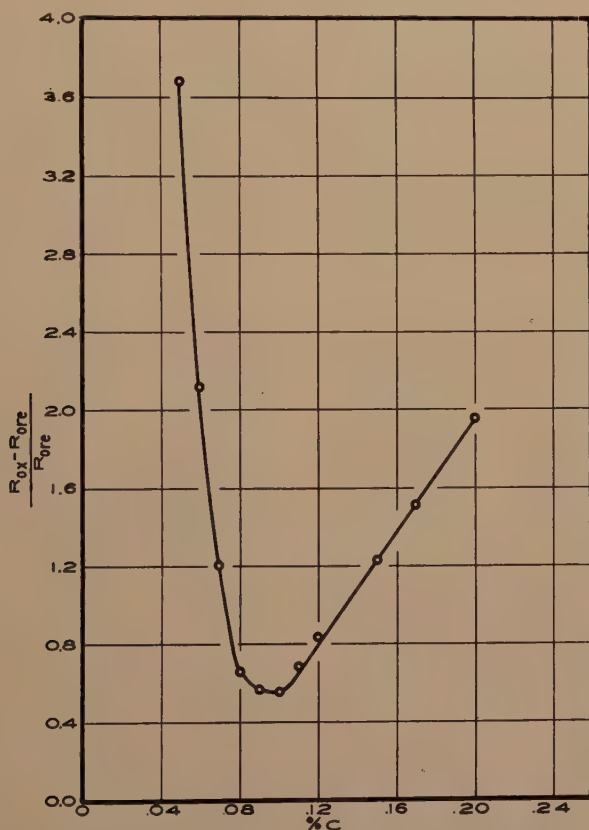


FIG 3—RELATION BETWEEN CARBON CONTENT AND THE COMPARATIVE RATE OF DIRECT OXIDATION.

Fig 3 affords a theoretical explanation of this practical observation. This figure shows the comparative rate of direct oxidation as a function of the carbon content. Starting at 0.20 pct carbon there is a linear decrease in the comparative rate of direct oxidation. The relation passes through a minimum at 0.10 pct carbon, has little change between 0.10 and 0.08 pct carbon, and increases very rapidly below 0.08 pct carbon. The actual rate of carbon elimination of course decreases markedly at the lower carbon contents, but compared with

ft of oxygen per ton of ingots produced with a saving of 3 to 5 gal of fuel per ton. The limiting factor in the direct oxidation practice is the supply of oxygen. As shown in Fig 3, the preferred practice with the available oxygen is to use ore for carbon elimination to near the tapping carbon with final elimination of carbon by direct oxidation, to use direct oxidation to eliminate carbon below 0.08 pct carbon, and to use oxygen to replace pig iron or other additions in getting heats to proper tapping temperature.

The measure of oxygen efficiency with

direct oxidation is the ratio of the carbon eliminated to the amount that would be eliminated by the same amount of oxygen added in the form of ore.

Efficiency, however, is not the only way of expressing the benefits of direct oxidation. If a box of ore is put into a heat, a certain time must elapse before further ore can be added effectively, this length of time depending on the individual furnace. No method is readily available to speed the reaction. This same furnace, however, will react favorably to direct oxidation shortly after an ore addition. Direct oxidation can be used to replace ore, and it also can be used at times when more ore could not be added. This is caused partly by increase in temperature and partly by agitation.

The shortening of furnace time is shown not by efficiency, but by comparison of carbon drop. The benefits of increased efficiency can be estimated in terms of the cost of oxygen. The benefits of faster carbon drop can be expressed in terms of the cost of furnace operation and refractory life. A representative figure used several years ago is \$60. per hr of furnace time. Using this estimate and recent increased costs gives a value not far from \$75. per hr, or \$1.25 per min. The difference in minutes for a given carbon elimination multiplied by \$1.25 gives the savings earned by faster work and can be expressed in terms of cost of oxygen. This comparison, of course, makes no assumption as to the method by which oxygen is used to save time and applies equally to use in direct oxidation or in burners to permit more fuel to be burned, or in jets to help to melt the scrap. The following table shows the furnace time equivalent

in value to 1000 cu ft of oxygen. This much saving in furnace time will just pay for the oxygen used.

THEORY OF CARBON ELIMINATION

The fundamental process of carbon elimination has received much study with still no general agreement concerning the detailed mechanism of this reaction. Comparison of the results of direct and indirect oxidation may lead to a better understanding of carbon elimination under both conditions.

In a recent paper, Kerlie¹⁴ shows an approximately linear relation between the rate of carbon removal (in the range from zero to 0.8 points per min.) and the free energy which is stated in terms of the carbon oxygen product.

Jay¹⁵ considers that the reactions take place within a gas phase in the molten steel bath and suggests a mechanism based on a chain reaction which involves the oxidation of all of the CO to CO₂. This formation of CO₂ (which later is reduced to CO) is stated to be the governing factor that determines the ultimate speed of carbon removal.

In view of Marsh's results, a plot of the rate against the logarithm of the carbon should be mentioned. For both direct and indirect oxidation a linear relation between rate and the logarithm of the carbon fits the data reasonably well down to about 0.12 pct C. Below this carbon content there is a distinct curvature in the direction to give actual rates of elimination higher than those that would fit the curve. This departure from the semilogarithmic relation simply means that the rate of elimination is never zero even down to 0.03 or 0.04 pct C, and that the actual rate approaches zero more slowly than required by the curve.

If both scales are logarithmic (Fig 2), this difficulty is avoided but there seems to be a departure from linearity if the reaction is not proceeding as fast as possible. The rate should, therefore, be considered as the

Cost Comparison.

Price of Oxygen		Time Saving Necessary to Justify Use of 1000 C.F. Oxygen (Minutes)
\$ per 1000 cu ft	\$ per ton	
3.35	80.40	2.68
0.63	15.	0.50
0.41	10.	0.333
0.21	5.	0.166

highest generally prevailing rate, rather than the rate which automatically and invariably accompanies a given carbon content. All of the large departures from

interface, in the other instance it diffuses from the gas metal interface which is beneath the slag surface. The oxygen content of the bath is controlled largely by the

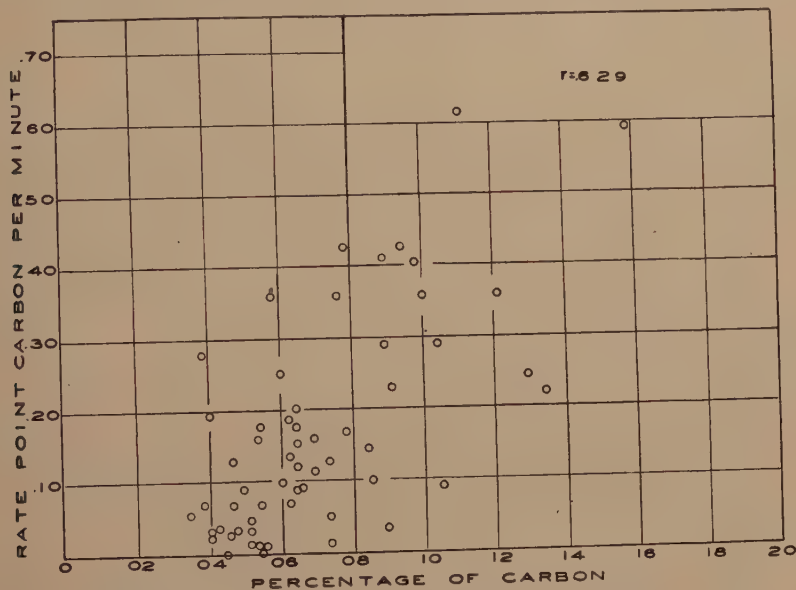


FIG 4—RELATION BETWEEN RATE AND CARBON CONTENT.

linearity are below the line, that is, in the direction of too low a rate for a given carbon content.

The fact that conditions of indirect oxidation require two lines is not entirely satisfying from the standpoint of simplicity. Three lines all on a log-log network would seem to be more satisfactory than use of a log-log relation for direct oxidation and a curvilinear relation on a semilog scale for indirect oxidation.

The log-log form of this equation is similar to that obtained by Nernst and many later workers on solution rates. It is the type expected if the thickness of the diffusion layer is decreased by increased carbon content. The general similarity of the relation for both direct and indirect oxidation suggests that the fundamental reaction mechanism is the same for the two cases. In the one instance, the oxygen diffuses into the bath from the slag metal

carbon content. If the oxygen supply were the controlling factor, the oxygen content of the metal would be high and nearly uniform during the period of direct oxidation.

MacKenzie³ has summarized previously published work (with indirect oxidation) and presents the generally accepted values for carbon drop as a function of the oxygen and the carbon content. In Fig 7 the observed rate (dc/dt) for a series of samples from direct oxidation heats is plotted against the rate computed from the carbon and oxygen content by MacKenzie's equation: $\text{rate} = 1.9 \text{ C} \cdot \text{O} - 0.005$. This computed value is the rate that the observed carbon and oxygen content would be expected to give with conditions of indirect oxidation. The grouping represented by lines 1-12 of Fig 7 is selected by the values of carbon-oxygen product actually prevailing rather than by equal intervals. This

grouping of points indicates that the relation between the rates with direct and indirect oxidation depends upon the car-

at various stages of the bath under conditions of indirect oxidation. These relations are summarized in Table I. The present

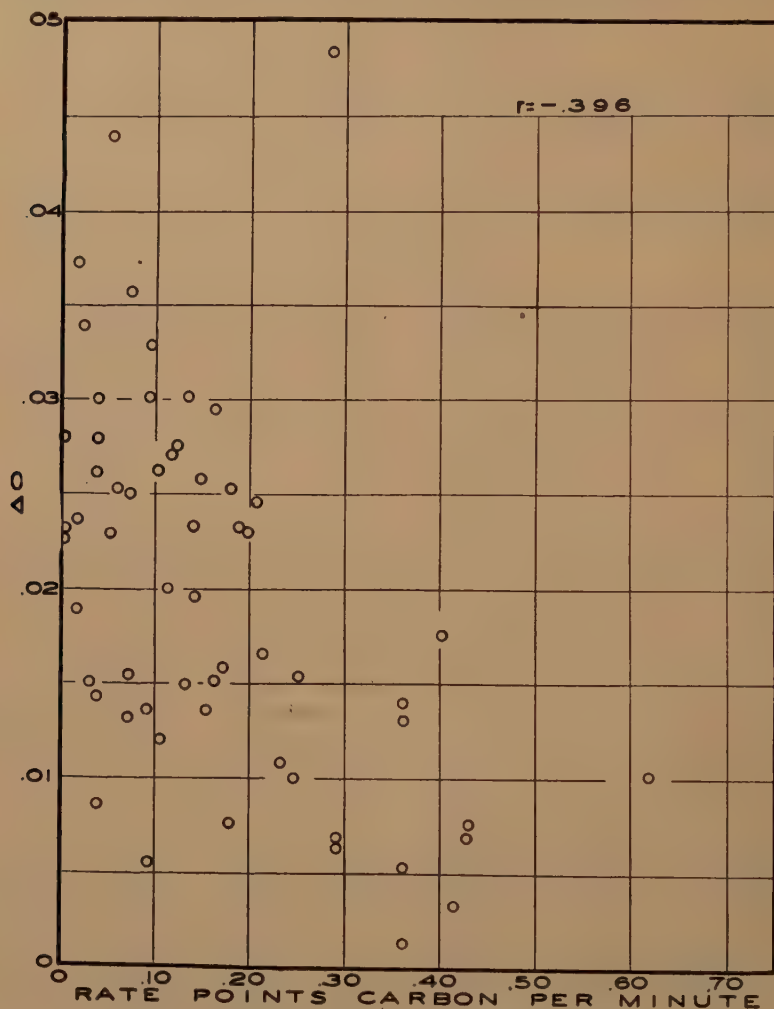


FIG 5—RELATION BETWEEN RATE AND DELTA OXYGEN.

bon-oxygen product. At low values of carbon-oxygen product, direct oxidation gives a faster carbon drop, while at high values elimination with ore is faster. Carbon elimination by direct oxidation is evidently quite different from indirect oxidation as summarized by MacKenzie's equation.

Brower and Larsen² have made a thorough study of carbon and oxygen relations

TABLE I—Relations among Carbon, Oxygen and Carbon Drop

Factors		Indirect Oxidation Brower and Larsen	Direct Oxidation Correlation Coeff.
C × O	$\frac{dc}{dt}$	No correl.	0.067
C	$\frac{dc}{dt}$	No correl.	0.629
C	C × O	Some correl.	0.152
ΔO	$\frac{dc}{dt}$		-0.396

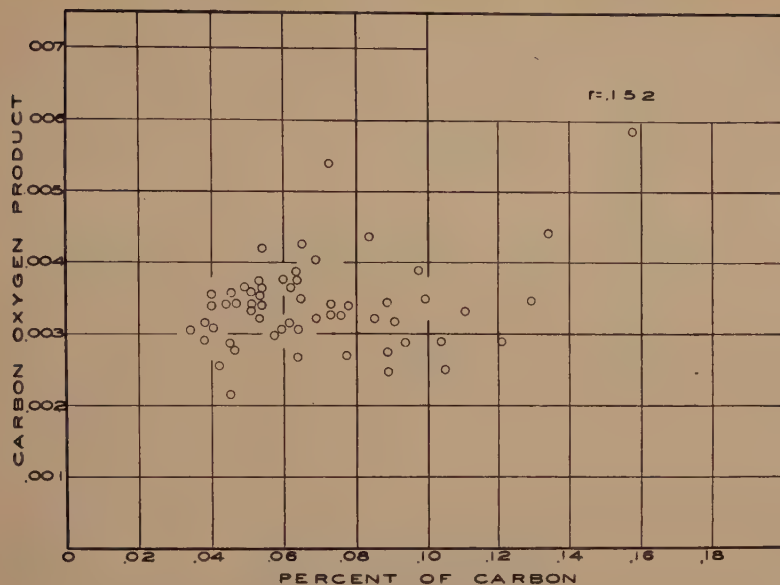


FIG 6—RELATION BETWEEN CARBON AND CARBON-OXYGEN PRODUCT.

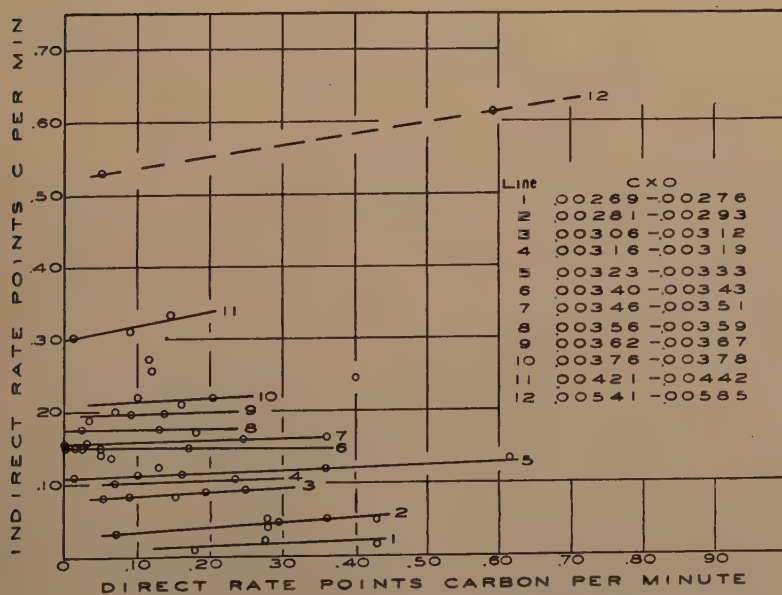


FIG 7—COMPARATIVE RATES AS AFFECTED BY CARBON-OXYGEN PRODUCT.

study of direct oxidation is in substantial agreement with most of the relations observed during the refining period with indirect oxidation. Even neglecting the

suggests that there is some other controlling factor.

The scatter diagram is shown in Fig 4. This figure represents instantaneous rates

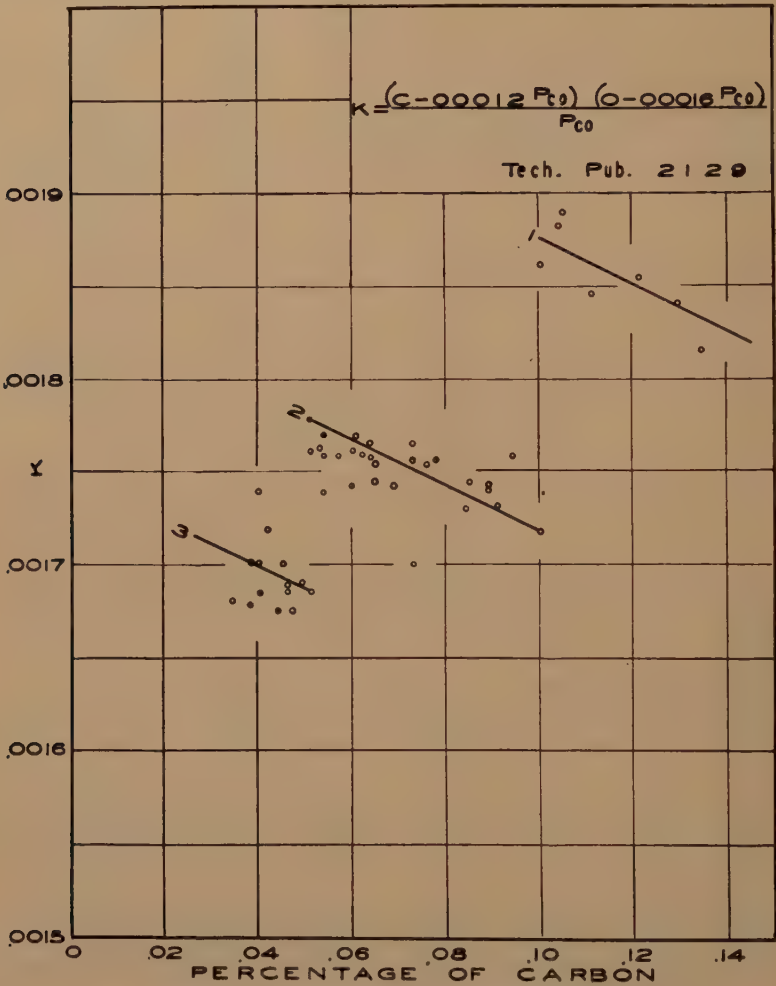


FIG 8—EFFECT OF CARBON ON K COMPUTED BY SIMS EQUATION.

departure from linearity the correlation between C and rate is 0.629 for direct oxidation.

A tendency for direct and indirect oxidation to give equal rates of carbon drop would appear as a pattern around the 45° line from the origin to the upper right corner of Fig 7. Absence of such a pattern

of individual points and includes the periods of lag sometimes observed. Fig 5 and 6 are the scatter diagrams for the other relations summarized in Table 1. The points on Fig 4, 5, and 6 represent conditions of direct oxidation.

Another discussion of indirect oxidation is that of Sims⁴ who has proposed an equa-

tion in the form of a carbon-oxygen product in which allowance is made for the carbon monoxide pressure. When applied to samples taken under conditions of direct

tion — $C \times O = 0.0193(\sqrt{C} - 0.09)$ and plotted in Fig 9 against the carbon-oxygen product observed in conditions of direct oxidation. The correlation between the two

$$\%C \times \%O = 0.0193(\sqrt{\%C} - 0.09)$$

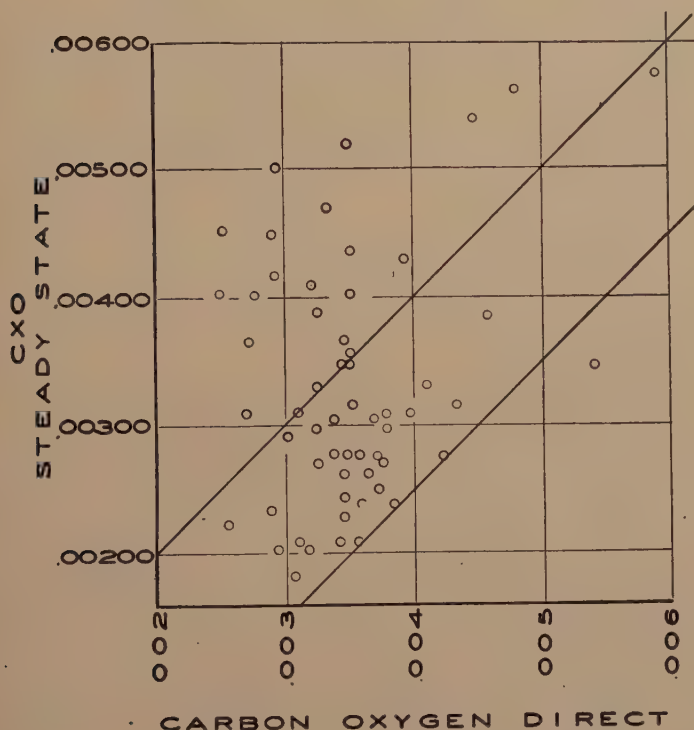


FIG 9—COMPARISON OF CARBON-OXYGEN PRODUCT.

oxidation,

$$K = \frac{(C - 0.0012P_{CO})(O - 0.0016P_{CO})}{P_{CO}}$$

appears as a discontinuous function of the carbon content. The cause of the discontinuity is apparently related to the grouping of the data in computation of the CO pressure. Fig 8 shows a general tendency for K (computed from Sims equation) to increase with a large increase in carbon content with possibly a decrease with smaller changes in carbon.

The carbon-oxygen product for the steady state is computed by Sims equa-

conditions (steady state and direct oxidation) is 0.265. The carbon-oxygen product is more nearly constant for direct oxidation than for the steady state as computed by the above relation.

With the exception of 3 points the value of carbon oxygen product is from 0.0022 to 0.0046 or a range of 0.0024. The computed values have a range from 0.0018 to 0.0050 or 0.0032 and show more scatter within this range.

More than half of the computed steady state values are lower, but not more than 0.0015 lower, than the values observed with direct oxidation, that is the points lie

within the band between the two lines on Fig 9.

With indirect oxidation the carbon elimination is the chief source of agitation

from the heats of reaction if simplifying assumptions are made concerning radiation and other heat losses and the rate of fuel supply. If the computed effect does not

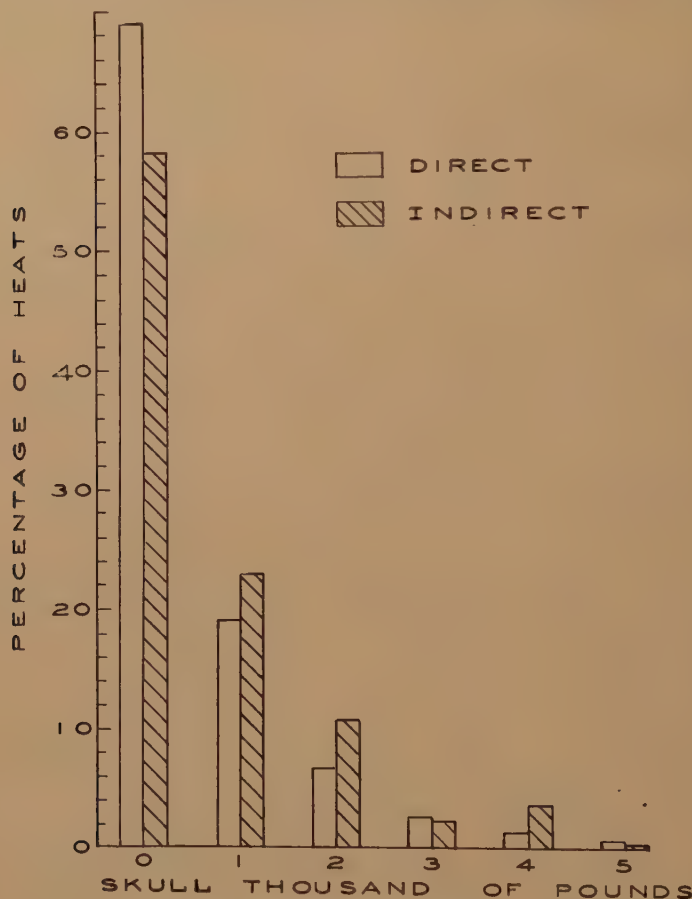


FIG 10—COMPARISON OF SKULL.

which, therefore, changes with changing rates. The CO pressure would thus be expected to be more closely related to the carbon content than under conditions of direct oxidation in which the agitation is more nearly independent of the evolution of CO from the elimination of carbon.

RELATION OF METHOD OF OXIDATION TO LADLE SKULL

The effect of direct oxidation on bath temperature can be computed directly

agree with observed temperatures, the discrepancy is not because of errors in the method of computation of the temperature effect, but is more likely because the assumed conditions have not prevailed in practice.

One practical result of the increased temperature accompanying direct oxidation is decreased ladle skull.

In Fig 10 a group of 411 heats made by indirect oxidation is compared with a group of 2154 heats made by direct oxidation.

Skulls on heats blown specifically for temperature and those blown for carbon reduction show no appreciable difference and therefore these two groups are both included in the 2154 direct oxidation heats. In other words, the important effect on skull is the use of direct oxidation rather than the reason for using it.

During the period that oxygen has been available, there has been a general improvement in skulls not shown by this comparison. The coldest heats are all in the group using direct oxidation which places this group at an initial disadvantage. A favorable effect would be shown if the two groups finished with an equal distribution of skulls. The actual improvement is even greater because the blown heats, though starting at a disadvantage, have turned out more favorably.

PROCESS APPLICATION

Theoretically and actually it is possible to replace all feed ore with oxygen fed directly into the bath; in other words, to conduct a bessemer or pneumatic process in an open hearth furnace. To the extent that pig iron or ferro silicon is used to increase the temperature near the end of

there is some evidence of a beneficial effect of direct oxidation on sulphur. Comparison of a large number of heats made by each practice shows no difference in sulphur related to method of oxidation.

Following is a comparison of groups selected because of similar specifications and time period. These differences are not significant.

Type of Oxidation			
Direct		Indirect	
No. Heats	Ave. S.	No. Heats	Ave. S.
216	0.0291	33	0.0298
186	0.0310	69	0.0309
209	0.0323	38	0.0324
207	0.0359	85	0.037

CONCLUSIONS

Direct oxidation is accompanied by an increase in temperature and rate of carbon elimination. Both of these effects may be managed so as to give faster and more effective steel production.

For given conditions of oxygen supply the carbon content governs the possible rate of carbon elimination as tabulated below:

Direct oxidation.....	0.25-0.03 pct C	log rate = 1.727 log C-2.1369
Indirect oxidation.....	0.45-0.20 pct C	log rate = 0.7884 log C-1.3665
Indirect oxidation.....	0.68-0.05 pct C	log rate = 3.904 log C-4.327

the heat, it is possible to replace these materials with oxygen. With these possibilities in mind it then becomes necessary to select the desired or ideal practice. Is it economically or otherwise desirable to use as much oxygen as possible? In view of the limited supply of open hearth feed ore and the unlimited ultimate availability of the element oxygen, a policy of conservation suggests an extended use of direct oxidation.

SULPHUR

On individual heats, or on heats using more than the average amount of oxygen,

Whether or not these rates are attained depends on conditions of furnace operation. In case of direct oxidation the rate of carbon elimination is considered independent of related factors such as carbon-oxygen product.

The decrease in ladle skull accompanying direct oxidation is shown by comparison of two groups of heats.

The effect of direct oxidation on sulphur elimination is not disclosed by comparison of similar groups of heats. In individual heats there may be an indirect effect related to agitation and faster solution of lime.

ACKNOWLEDGMENTS

The authors thank the Wheeling Steel Corp. for the facilities and equipment that made possible the present study and for permission to publish the results, and David Fleming who gave helpful suggestions for the preparation of the manuscript.

REFERENCES

1. F. Korber, W. Olsen, G. Thanheiser, and P. Bardenheuer: Influence of Carbon on Steelmaking Reactions, *Stahl und Eisen*—**56**, 181-208 (Feb. 13, 1936).
2. T. E. Brower and B. M. Larsen: Oxygen in Liquid Open Hearth Steel, Oxygen Content during the Refining Period, *Trans. AIME* (1947) **172**, 137; *Met. Tech.* Sept. 1946.
3. I. M. MacKenzie: The Rapid Determination of Reactive Oxygen in Open Hearth Steel. *Jnl. Iron and Steel Inst.* Advance copy, 5 pp. (Dec. 1946).
4. C. E. Sims: The Mechanism of the Carbon-Oxygen Reaction in Steelmaking, *Trans. AIME* (1947) **172**, 176; *Met. Tech.*, Jan. 1947, TP 2129.
5. M. W. Thring: Possibilities for the Extended Use of Oxygen in the British Iron and Steel Industry. *Jnl. Iron and Steel Institute* **156**, June 1947, 285-91.
6. George V. Slottman and F. B. Lounsbury: The Use of Oxygen in Open Hearth Practice for Carbon Reduction, Amer. Iron and Steel Inst. Preprint (May 1947). *Iron and Steel Engineer*—**24**, 85-8 (Aug. 1947).
7. Anon.: Oxygen and the Open Hearth Furnace, Canadian Met. and Metallurg. Ind. **10**, 16-22 (July 1947).
8. Anon.: Critical Points Mainly about Metallurgical Oxygen, *Metal Progress* **52**, 67-70, July 1947.
9. Walter E. Lobo: Low Cost Oxygen for Metallurgical Uses, *Iron Age* **160**, July 17, 1947, 49-55.
10. Anon.: Steelmaking Oxygen Presenting Problems to Delay Applications, *Iron Age* **160**, 113-115 (Aug. 7, 1947).
11. D. I. Brown: Electric Furnace Rimmed Steel, *Iron Age* **160**, 67-69, 149 (Aug. 7, 1947).
12. Anon.: Oxygen for Decarburization, *Steel* **121**, 126 (1947).
13. H. W. Graham: Factors Which Determine the Iron and Steel-making Processes, *Trans. AIME* (1947) **172**, 15; *T.P.* 2217, *Met. Tech.* Aug. 1947.
14. W. L. Kerlie: Some Aspects of the Refining of High Phosphorus Iron, *Jnl. Iron and Steel Inst.* **157**, 173-182 (1947).
15. A. H. Jay: The Mechanism of Carbon Removal in the Open Hearth Furnace, *Jnl. Iron and Steel Inst.* **157**, 167-172 (1947).
16. J. S. Marsh: Slag, Metal, Oxygen Relationships in the Basic Open Hearth and Electric Processes, *Proc. Elec. Furn. Steel Conf.* (1944) **2**, 126-136. *AIME* (1945).

DISCUSSION

(J. Chipman and C. Taylor presiding)

J. CHIPMAN—I shall open this paper for discussion. I might remark, before so doing, that another paper will deal with oxygen, but with oxygen-enriched blasts. Let us then try to divide the discussion of this general subject of the use of oxygen along the same lines as the paper, namely, the use of oxygen in the bath to be discussed now—and reserve the discussion of the use of oxygen in flame until after the next paper is presented.

T. S. WASHBURN*—The rate of carbon drop when oxygen is injected as shown in the first or second curve, seems to level off at 0.04 pct carbon. Did you find that to be the case, or did you find that by continuing to inject oxygen you could reduce the carbon down to 0.02 or even 0.01 pct?

C. R. TAYLOR—We have some evidence at our plant to indicate that the rate of carbon drop on production heats was in direct proportion to carbon content rather than being a logarithmic relationship, and I was wondering whether anyone else has made a similar finding.

B. M. LARSEN†—I wonder whether the authors considered the possibility that an increasing difference between direct and indirect oxidation is probably caused by the increasing need for storing up oxygen in the slag as the carbon becomes lower in the metal. Do the slags with direct oxidation go as high in iron oxide for a given carbon content?

H. W. JOHNSON‡—You mentioned there was variation in the rate at which the pipe was consumed. I wonder whether from your experience you could tell what are the factors that make for the longer life of pipes, such as pressure of oxygen and so forth.

M. TENENBAUM—I might make some comment with regard to Dr. Taylor's remark. We find that our rate of carbon drop is fairly constant over about 40 pct carbon. Below that we develop a relationship with the carbon content that is roughly linear down to 0.08 pct carbon.

* Inland Steel Company.

† U. S. Steel Corporation.

‡ Inland Steel Company.

C. E. SIMS*—Despite the excellent data in this paper, it does not appear logical to make a comparison of the rates of oxidation, by the two methods, as the authors have done. The so-called direct method, which is scarcely more direct than by oring, is, of course, much faster but it is merely a qualitative relationship. In the oring reaction there is a number of factors that control the rate of carbon oxidation such as, the concentration and availability of iron oxide in the slag, the temperature of the bath, the condition of the hearth, and the carbon content of the bath. The agitation produced by the boil is very important in facilitating the influx of iron oxide necessary to the maintenance of the boil.

With the direct method, there seems to be considerable evidence to indicate that the rate of carbon drop is merely a function of the rate at which oxygen can be introduced. The fact that oxygen is introduced as a gas facilitates CO evaluation and eliminates this bottleneck. One factor which makes the relationship imperfect, is that the oxygen is all put in at one place. It cannot diffuse fast enough to prevent some of it burning and vaporizing iron. If the rate of oxygen input were to be doubled, for example if another lance delivering the same amount of oxygen were to be introduced at the other end of the bath, it could confidently be expected that the rate of carbon drop would be approximately doubled. The relationship reported applies only to the particular conditions studied and cannot be generalized.

R. A. FLYNN†—Is there any difference in the relative rate of removal of elements, other than carbon, comparing the indirect oxidation and the direct oxidation processes? For example, does the rate of removal of phosphorus differ in the processes?

F. G. NORRIS (authors' reply)—These remarks will not be in the nature of a closure; I hope the discussion will be such that we will have to reserve that for the time when the paper is published and we get some written discussions. In other words, the subject is still wide open (even after the meeting is over).

First let me mention a little bit about what

we had in mind in making some of these comparisons. I certainly appreciated the remarks Dr. Sims made, because he has done a wonderful job in summarizing the relations under conditions of indirect oxidation. In making that comparison with his results as a reference point, we did not mean that there was any contradiction, necessarily. We just did that for purpose of information—to bring out the different conditions that exist in the bath and their effect on C elimination. It looks as if maybe with direct oxidation the bath is a little bit ahead of what it would be using indirect oxidation.

We know that in general the FeO in the slag will be lower when the heat is blown for a given rate or for a given point in the bath than it would be if that heat were worked with ore.

Sometimes the statement is made that the practical man would have a better understanding of the technical aspects of his job if he had more theory. Usually we have found that the man who is thinking about his job has a pretty fair understanding of the process and whatever else he may lack it is not theory. He has plenty of theories to explain whatever happens. They are not always couched in scientific terms and they do not start from the solution of a differential equation, but these theories have the merit of being based on observations of the process. I could cite instances, familiar to most of you, of learned dissertations which their authors consider logical and theoretically sound written by men who have never seen the process they are describing and have never been closer to operations than the front manager's office. The writer enjoys the distinction of having worked under the supervision of both Dr. Herty and Dr. Chipman, the two men who have done more than any others of our generation to bring science to the open hearth floor. I have also sat at the feet of the man who tapped the first ingot iron heat and of the man who first had the courage to risk a heat of good steel by adding ferrophosphorus when everyone knew that the only way to rephosphorize steel was by the addition of beef bones to the ladle. Having thus attempted to qualify myself as a witness, I would like to say that I know of no permanent contradiction between theory and practice. Apparent contradictions are due to: (1) faulty statement of

* Battelle Memorial Institute.

† American Brake Shoe Company.

the theory, (2) inadequate understanding of a good theory, or (3) inadequate information of the practice such as poor data or possibly misinterpretation of good data.

In the final discussion I shall try to polish up the language, but now I want to present the furnace man's theory of diffusion across the slag metal interface. In working a heat with ore the slag is ahead of the bath. First the slag is made, then it makes the boil. The bath is also last to get to temperature. When blowing a heat the bath gets ahead of the slag. Instead of getting the carbon down and then having to get hot, the bath is at proper temperature by the time the carbon is down.

At an A. S. M. meeting in Pittsburgh, Dr. Karl Fetters remarked that anyone who had trouble these days with phosphorus ought to be ashamed to admit it. He meant that present theory is adequate regarding the phosphorus reaction and the point is well taken. We are in more fortunate situation with respect to phosphorus than to any of the other elements, and our combination of raw materials and product is more favorable than many other shops. We do still miss heats (both rephosphorized and those with a maximum specification) and we are willing to admit it for the record.

Since adopting direct oxidation our iron is considerably lower in phosphorus. We have no information on the rate of phosphorus elimination because our first test is usually low enough. Based on this imperfect evidence, we can foresee no difficulty with phosphorus associated with direct oxidation. In fact, there may be less difficulty because heat and agitation combine to make faster solution of lime.

Of course, all elements are oxidized concurrently. You cannot work a heat and say, "We will blow this one for carbon, and this heat for temperature, and so forth." We prefer the term "direct oxidation" instead of specifying the type of gas, saying, "We are using air; nitrogen; artificial air; 95 pct oxygen; or 90 pct oxygen." Except for pure nitrogen, it is all direct oxidation. We also found that as long as oxygen is in, the bath does not care very much how it is done. Either a lance or a jet can be used for scrap melting. All kinds of combinations are possible.

Will you repeat your question, Mr. Washburn, on low carbon?

T. S. WASHBURN—That curve to which I referred was asymptotic at about 0.04 pct carbon. This would indicate you did not get below 0.04 pct carbon by introducing oxygen.

F. G. NORRIS—The curve quit at 0.04 pct carbon because we do not go lower than that on this specification.

T. S. WASHBURN—I got the impression it was practically flat at 0.04 pct carbon. I am talking about the first curve.

F. G. NORRIS—That is right. That first curve was flattening off at about 0.04 pct carbon. It does for both direct and indirect oxidation. Of course it flattens out when one gets down on the low carbon heats.

All the way through we have tried to answer the question, "What would have happened to that bath if you had not blown it?" You cannot give all the credit to direct oxidation simply because you are blowing the bath, because there would have been some drop without the direct oxidation. We tried to erase that as best we could by getting information on the two conditions. Below 3 pct carbon, I rather suspect one is going to slow down no matter what one does, and time will be gained by using direct oxidation compared to what it would be if that same thing were done with ore.

Dr. Taylor says he finds that the rate is proportional to carbon content instead of to the logarithm of the carbon. If that relation would fit our data we certainly would not have gone to the trouble of using a logarithmic scale. The curve represents full speed operation. This is the possibility of the process. If you do not operate full speed, the points are below the curve.

We did not get a very good fit at about 0.25 pct carbon, because we were just getting started. On the heats that are made to about an 0.08 to 0.10 specification, either consciously or unconsciously (and I suppose our fellows feel it is good practice) we start slowing up, just like a freight train before it comes to a station or like a man working to the end of the day. He cannot work up to quitting time and quit—he has to slow down a little bit.

So that is the way on these heats. If we are shooting for 0.08 pct carbon, we are going to slow down at about 0.10 pct carbon. But if the heat is scheduled to go down to 0.04 pct car-

bon, we pass right through 0.08 pct carbon and never know it—just like the Sunshine Special passes through Steubenville.

At some levels of carbon content, it does look as if a semilogarithmic relation might hold true. I imagine we could find portions there where the spread of the points would be such you could not decide whether it was linear or logarithmic. The main reason we have chosen a logarithmic ruling on both scales is that it seems to fit the entire range from 0.04–0.20 pct carbon reasonably well. It does not require any funny assumptions at lower carbon contents.

You may be interested in our first attempts to improve pipe life. The first heat we made we spent about two weeks hunting up sillimanite and coating the pipe with it. We wanted to dry it nicely and not too fast, so we put it on the roof of the furnace. I guess it cost us \$30. for that one pipe by the time we figured out the labor cost and all material, but we did this so as to have a real job of pipe protection. When we used the pipe the coating chipped off almost immediately. We found out later we did not have the right kind of sillimanite anyhow. We still had a heat we wanted to blow and we ran out of coated pipe—all we had was bare pipe. So we finished the first heat with bare pipe and have never tried anything else.

Of course, we have a pipe mill, you understand. Some of you who have to buy the pipe on the open market really have to put stopper rod sleeve brick around it to protect it. We just went ahead and blew the heat. It does not seem to make much difference whether we protect the pipe or not.

Later, we made the device you saw illustrated that fits into the furnace. This method did make a lot of difference in pipe life. If a man stands up there, the longer he stands the more tired he becomes, and he is going to ram that pipe in pretty fast. Those are the pipes that do not last very long. If you put them in too quickly and there is too great a depth of immersion, the pipe bends up on the end and slag starts squirting on the roof. That is not good. Oxygen does not get to the bath and the roof resents this treatment.

But with this control we have a little crank to feed the pipe. We try to keep the depth maybe about 6 in.—open hearth inches, of course. The pressure or the rate of blowing does

make some difference due to the cooling effect. If the flow can be kept fairly fast, one gets a little better pipe life.

With regard to this matter of multiple injection, the suggestion was made that if we use two pipes we would go twice as fast. If you use three, you do not go three times as fast; we have only five wicket holes, but we never used that many pipes. We also tried smaller pipes. Instead of putting in one $\frac{3}{4}$ -in pipe, we put in three $\frac{1}{4}$ -in. pipes, but that is not so good either because they bend—they are not stiff enough to penetrate through the slag.

I know that it ought to be that if you give that gas a chance to bubble around in more places, it ought to be better; but somehow it just does not work out that way. We have put the pipes in different doors. We tried two-door and four-door, but that does not make too much difference either.

We want to thank Mr. Tenenbaum for the information that the rate over 0.40 pct carbon is fairly constant and below 0.40 pct it varies directly with carbon content. We do not know too much about what happens over 0.40 pct carbon—we do not aim to melt our heats much higher than that. I do not say we do not start blowing any higher than that—sometimes we do—but the bath is pretty cold and there is usually a lot of lime down at 0.40 pct carbon.

Once in a while we will put in a pipe just to warm things up as much as anything. Of course, the oxygen does not know that is what we are doing—it thinks we are trying to eliminate carbon, too—so it goes ahead and eliminates carbon and warms up the bath all at once. But when you say a “constant rate,” I do not quite understand what you mean because that rate is going to be faster at 0.40 pct carbon. I suppose you mean it is just the same at 0.40 pct as it is at 0.60 pct.

M. TENENBAUM—It is just the same at 50 as it is at 150 pct.

F. G. NORRIS—You are out of my territory on the 150 pct carbon. I do not know about that. Is it pretty fast?

M. TENENBAUM—It is fast.

F. G. NORRIS—How many points per hour or points per minute?

M. TENENBAUM—It is of the order of two points per minute on a 150 ton heat.

F. G. NORRIS—I do not know how this would compare with the lower rates we have found at lower carbon.

J. CHIPMAN—This may not be quite the closure, but I hope it will appear in *Transactions* as a part of the closure, and I am sure it will be a classic. Speaking of classics, the author of the classic AIME paper on the rate of carbon removal is in the audience, and I wonder if Alex Feild would say a word on the subject.

A. L. FEILD*—I have been listening with much enjoyment to Frank Norris' presentation which, as our Chairman says, certainly bears the earmarks of a real classic. I have nothing to offer myself because I have not worked on gaseous oxygen in the open hearth, but I am an attentive listener.

G. V. SLOTTMAN†—I think I can contribute a bit about what happens in the very low carbon range—below the 0.4, 0.3 pct Mr. Hughes was talking about. We did some work in 1946 in making 0.2 pct carbon steels. In fact, we got down as low as 0.19 pct.

What we found when you plot the rate of carbon drop against the carbon content—and these were for heats with no ore in them; where the oxygen injected into the bath was the only oxidizing effect other than that which was coming from the furnace atmosphere—was a curve that had an S-shape. The rate of carbon drop remained fairly constant over 0.35 pct carbon and then it dropped almost in direct relationship to the carbon content. And when it got into the 0.05 pct range the rate of carbon drop began to slow up very appreciably so that from 0.05 pct on down it became increasingly difficult to remove the carbon.

Investigating that effect to see what was causing it, we plotted manganese against carbon content. This plot gives a curve which is roughly a parabola, and in the region from about 0.15 pct carbon on down, the manganese drops very rapidly with carbon. And in the region of about 0.03 pct carbon, manganese is being eliminated much faster than carbon. The amount of oxygen required to take out a

point of carbon is roughly four or five times the amount needed to take out a point of manganese.

In the higher carbon ranges the effect of manganese is therefore not very important. But when the rate of manganese elimination is in the order of five to six times the rate of carbon elimination, the effect of manganese elimination on the rate of carbon drop becomes very appreciable.

We found that if we took tangents to the carbon manganese curve and got the differential manganese drop with respect to carbon and corrected our carbon drop curves, we could then obtain a linear relationship between the rate of carbon drop and the carbon content. The relationship is further complicated because of the probability that there is a minimum carbon content which one can reach in practice by direct oxidation. By making a correction factor for this effect one obtains a straight line curve of the rate of carbon drop against carbon content.

W. J. REAGAN*—I was very much interested in some of the comments about the indirect results obtained by the use of oxygen, such as heating up the bath, eliminating skulls, and so on. I recall that at the electric furnace meeting one operator stated that they had been able to produce clean steels as they had a positive means of heating up the bath and producing a boil in the bath.

I would like to ask the authors whether or not they have found any similar results which they could attribute to the use of oxygen such as better rimming action, elimination of skulls, better ingot characteristics, and the like.

J. B. WAGSTAFF†—I would like to make an observation which might help us a step further on the carbon removal. I think if you will calculate the oxygen per unit drop of carbon as a function of the carbon content of the bath, you will not get a straight line in the low carbon range because a considerable amount of oxide is necessary to form iron oxide required for equilibrium in the slag. In fact, the oxygen per unit drop of carbon increases rapidly at low carbon concentration. Now, if you are putting the oxygen in at a constant rate, quite obvi-

* Rustless Iron and Steel Corporation.

† Air Reduction Company.

* Pennsylvania State College.

† Hydrocarbon Research, Inc.

ously the rate of carbon elimination in the bath drops off very rapidly in the low carbon range.

Another thing that may be of interest is when you plot the oxygen per unit drop of carbon against the inverse of the carbon content, I think you get something very close to a straight line. Just exactly why that is so I am not sure; perhaps somebody could tell me.

J. W. GAINES*—The question came up in earlier discussion this afternoon as to the effect of increasing the rate at which oxygen is added to the bath and its relation to the rate of carbon elimination. I think it is fair to say there is a connection there because if you compare heats made in furnaces of wide range of size—say from 50 tons to 250—and with oxygen injection rates running from, say, 15,000 cfhr up to as high as 75,000, you find that the ratio of carbon removed to oxygen input is substantially constant—that is within limits of open hearth accuracy. Now, that means that the more gas that is put in by and large, the more carbon there is eliminated.

One other point which bears on that same subject is a consideration of the effect of the purity of the decarburizing gas. Many of you know that a number of tests have been made where air has been used instead of oxygen, and where, also, intermediate purities have been employed, including 70 and 45 pct oxygen mixture.

If all of that information is surveyed, one finds that the trend with purity is very, very slight. The high purity oxygen will do a little bit faster job for the same volume per minute, but as compared with air it is a difference of 10 pct instead of a difference of five-fold. In other words, it seems to be primarily a matter of: (1) introducing gaseous material into the bath which will permit the normal bath reactions to proceed; and (2) supplying heat to the bath to make up for the heat demand of the endothermic reaction of carbon elimination.

I think it is also true that the sharper working furnace will show less difference between air and oxygen, than one which is more dependent on the heat producing action of the oxygen.

S. MARSHALL†—Most of our work with oxy-

gen has been reported in recent meetings, and there is not a great deal that I can add at this time. However, I should like to add something to Mr. Gaines' statements with regard to the required purity of the gas.

In some of our experiments, about 150 cf of oxygen introduced as air produced essentially the same carbon reduction rate as about 700 cf of oxygen supplied as the pure gas. And in heats where nitrogen was used to agitate the bath, the rate of carbon removal was intermediate to the rates resulting from standard ore practice and the use of pure oxygen. It appears that agitation alone is a big factor in the carbon reduction rate.

F. G. NORRIS—In the first place, I certainly want to thank all of the discussers of this paper and also the discussers of the discussion of the paper. Some of these last remarks scarcely require any answer at this time as they were in the nature of contributions of information.

We know that agitation is an important part of the reaction in the open hearth process. We know that there are some things that we like about agitation from the standpoint of the speed of reaction. There are other things we do not like about it. It splatters slag on the roof, and the roof does not like it, and just falls down and quits if it is continued.

One can see the difference between the effect of oxygen and air. One knows immediately when air is being blown and when it is not by merely looking at it—at least we can. By saying that, I do not mean we can see something nobody else can see. I mean, according to our practice—which is to start blowing at low carbon—we can tell the difference. If one starts blowing at high carbon not much difference can be seen because one splatters pretty badly anyhow.

If one is blowing relatively pure oxygen, there is some boil right at the end of the pipe, but it is not as pronounced as with air. We have tried a few heats with air, but we have gone back to pure oxygen—and it is not entirely on account of the failure of our air compressors.

We would like to comment on this matter of manganese, and the elimination of manganese late in the heat, and adjusting the carbon curve to take that into account. I do not exactly like the implication that is made when you apply a correction to the carbon curve, because we have

* Linde Air Products.

† Carnegie-Illinois Steel Corporation.

determined those carbon contents and I think they are correct within the limitations of our sampling method and our chemical analysis. I will stand on what those carbon values are uncorrected. If you want to have a manganese drop curve, that is quite another matter. I do not believe they are interchangeable; they may be concurrent.

This seems to me to be an effort to apportion the oxygen that is introduced and say part of it reacts with carbon and part with manganese and the rest to building up the slag. Let me point out some of the dangers or pitfalls into which one might fall in trying to estimate the carbon that would have been eliminated if the oxygen had not been used by the manganese.

Start by working with one practice—doing it in one shop—with a given source of hot or cold metal. That means there is a standardized charge, with a given manganese content, and all those factors affect residual manganese. With this standard practice concurrent reactions duplicated from heat to heat will be found which will give the illusion of constant cause and effect. But change any one of those things—change the basicity of the slag, change the proportion of pig iron in the charge, or change the amount of manganese in the pig iron—and the standardized behavior of carbon and manganese will be upset. I think they are independent of each other. They are dependent on a common cause, and that is the oxidizing influence. I can almost guarantee to finish up fairly low carbon at a pretty high manganese if starting with a charge selected for this purpose.

If one sets out to make a pure iron heat, one certainly does not use 2 pct manganese iron; it will be closer to about 0.80 or 0.90. Then there is an entirely different relation in the later stages of the heat between the final elimination of the carbon and manganese. There comes a time when the heat is worked on manganese instead of on carbon. You will get down to where you tap out because the carbon has gone down about as low as it is going to go.

In respect to the slag metal relations, in the case of ore compared to the case of direct oxidation; I do not think that the slag is in equilibrium with the bath in the case of direct oxidation. With direct oxidation heats I believe the predominate diffusion is from metal to slag. The oxygen first reacts with the oxidizable

elements, which means iron, carbon and manganese. There is a certain excess of it that will also cause agitation. But I do not think the point that is reached would be termed an equilibrium value in the distribution of iron oxide between slag and metal.

I certainly want to express our appreciation again for the interest that has been shown in this paper, and we hope that if we have failed to answer the discussion orally you will send in written discussion on this. If any of you who has not had the opportunity to read this paper—we sent it in too late to have it preprinted—will send us written discussion, we will undertake to give a more considered answer.

E. B. HUGHES and F. G. NORRIS (authors' closure)—It is, of course, the privilege of each author to select the method of presentation and interpretation of results that seem to him to be the most logical and effective.

To us it seems logical to use a normal heat made by established practice as a basis of comparison for a new practice. We realize that such a comparison is impossible because of the practical difficulty of determining what is normal practice or of locating such a heat. It is also impossible to carry the oxidation reaction to completion in any steelmaking process. The introduction of a given amount of reagent, in this case oxygen, does not insure that it will react with a stoichiometric equivalent weight of carbon. There is not any reason to expect that it will. Even if the reaction took place in a closed system, equilibrium would be established among all of the elements present which as a minimum would include Fe, C, Mn, P, and O.

Faced with the necessity of having to make a choice between two impossible ideals, we have preferred to attempt to establish normal practice for both conditions and make the comparison on this basis.

Computations of efficiency based on stoichiometric relations do not appeal to us because this method seems to imply that the ideal or 100 pct efficiency is the reaction of all of the oxygen with carbon and carbon alone.

If we understand Dr. Slottman's method, he recognizes the possibility of the reaction of oxygen with one element other than carbon, that is, manganese, and attempts to use carbon as the unit to express the combined results. It seems unfortunate that the combination is referred to as a correction. This nomenclature

carries an implication of error in the original data which is probably not intended.

It is true that the data are limited to specific conditions. These conditions are stated in the subject of the paper, "The Elimination of Carbon in the Basic Open Hearth Process." Some of those who have attempted to violate the relations summarized by this curve have been less successful in the application of direct oxidation.

Simply sticking a pipe in the furnace does not automatically insure that the rate of carbon elimination will be either that in Fig 10 or indeed any other value. The rate may not be that high if there is no effort to drive the furnace. If the operation proceeds without regard to furnace structure, a higher rate may be possible temporarily. The same remarks apply to the curves based on heats worked with ore.

Ordinarily we aim to make the specified carbon. Many of the heats are specified 0.04 max. carbon. Carbon elimination on these heats has a tendency to flatten off at about this value. The same tendency at higher levels is shown by heats specified 0.08 max. or 0.10 max. This tendency is incidental to operations and is not an inherent characteristic of direct oxidation. The lowest carbon heat we have made by direct oxidation finished 0.018 pct C. One box of ore was dumped at 0.75 C which was before the heat was melted. It melted 1 hr and 20 min. later at 0.25 C. Direct oxidation was started 1 hr and 50 min. later at 0.10 C. During the next 50 min. six pipes were used at 125-lb line pressure. Carbon down to 0.010 on a killed test is pretty hard to make in an open hearth furnace. If we had the job of making this order, we would prefer direct oxidation and have every reason to believe we would do a better job faster than by the use of feed ore.

In partial answer to Mr. Larsen's question about slag oxidation, the FeO on this heat was 37.6 pct. Such a heat worked entirely by indirect oxidation would probably carry a slag of 48 to 54 pct FeO.

In looking over our records in answer to this point, we notice that a week later we made a 0.03 C heat that had 26.5 pct FeO. This may not be the lowest FeO we have made at this carbon content, but it is lower than usual. This particular heat was charged with 31,400 lb of sintered Hanna ore. It melted soft, requiring a total of 45,000 extra metal. Direct oxidation

was started at 0.08 C at which time the slag pancake showed 2.4 CaO/SiO₂ ratio. No feed ore was used in making this heat. These are specific answers. The general answer is shown by the ratio of FeO in the slag to oxygen in the bath. For a given carbon content this ratio is lower for direct oxidation. On any one heat at the beginning of direct oxidation, the slag metal ratio is higher than at the end. This means that the oxygen increases in the metal as carbon is eliminated, but that it does not increase proportionately in the slag.

Ore dumped into a high carbon bath has a chilling effect. As the chilling proceeds there is a tendency to retard the reaction rate. The initially high carbon content tends to favor a fast rate of reaction. The net effect of these two compensating influences may lead to the conclusion of a constant rate above 0.40 C.

Extrapolation of our curve for indirect oxidation is not justified on the basis of our own data. With the supporting evidence given by Mr. Tenenbaum, extrapolation is no longer into a totally unknown region. The instantaneous value of 2 points per min. at 1.30 pct carbon is in substantial agreement with his value of 2 points per min. starting from 1.50 C. A constant rate of drop means that the carbon content is a linear function of the time. We have not observed this to be the case. In our experience more carbon is eliminated in a given time at high carbon than at low carbon.

It is true that when using one or two pipes in the open hearth bath diffusion is not fast enough to prevent the oxidation of iron. Neither is it in the Bessemer process. Preferential oxidation of carbon instead of iron seems to require more than multiple points of entry for the gas stream.

In reply to Professor Reagan's question, we have not found any difference in rimming action or ingot characteristics. We believe rimming action depends upon the composition and temperature of the steel in the ladle as modified by pouring rate and mold additions. The manner of arriving at this composition and temperature in the ladle is of secondary importance. There may be an indirect influence due to better pouring temperature and fewer skulls.

We thank Mr. Wagstaff for his remarks and also Dr. Gaines for his contribution to several of the questions which have been raised. We

certainly agree that the more oxygen that can be introduced effectively into the bath, the more carbon will be eliminated. There is no practical difference that we can observe between use of one and three pipes. The initial

faster to shape the slag when using direct oxidation.

Knowledge of the oxidation of carbon can be summarized somewhat as follows:

1. The equilibrium constant has been de-

TABLE 2—Comparison of Refining Processes

Conditions	Pre-dominate Source of Oxygen	Points of Entrance to Metal	Agitation	Source of Temp.	Rate of C Drop	Splash
Bessemer enriched blast.	Blast	Multiple	Indep. of reaction	Exothermic reactions. Includes Fe	Fastest refining known*	No effect because of design of equipment
Air.....	Blast	Multiple	Indep. of reaction	Exothermic reaction—chiefly Si content of Fe	Faster than O.H.	
Open hearth oxygen.	Blast	Few	Indep. of reaction	C reaction is exothermic	Fast	Limits speed of process
Air.....	Blast	Few	Indep. of reaction	Less temp. from reaction	Sl. slower than O	More than pure O
Nitrogen.....	Slag	More	Indep. of reaction	Chills bath	Faster than slag	
Box of lump ore...	Ore	Many localized	High—depends on reaction	Endothermic. Chills bath	Approaching Bessemer in speed	Of short duration
Oxidizing slag....	Ore and Fnc. Atm.	Entire bath area	Entirely limited by reaction	Fuel required to maintain reaction	Slow	Practically none

* This estimate is based on evidence given by Julius Strassberger, American Iron and Steel Institute, May 1948.

benefit of multiple points of injection is located between the number we have used and the number used in the Bessemer process.

We acknowledge our indebtedness to Dr. Marshall for his contribution concerning the effects of agitation that accompanies blowing with nitrogen which we have included in the tabular summary of various processes. We surmise that continued blowing with nitrogen would have a chilling effect and that its effectiveness would ultimately become less pronounced.

In answer to Mr. Flynn's question, it appears that oxidation in general is speeded up and that the effect of direct oxidation is not exclusively effective for carbon elimination. Manganese follows the carbon right down just as it would for heats worked by indirect methods. We have much less information on the rate of phosphorus elimination. As explained in the details of the oral discussion, our phosphorus level is pretty low. The question is probably directed to the possibility of working carbon so fast that the other elements are still high when the carbon is down. Naturally the slag has to be shaped up when the heat is tapped. This is not necessarily automatic, but in general it is easier and

terminated. This is independent of mechanism of the reaction or size or shape of the container.

2. The approach to equilibrium changes with various circumstances. In the open hearth it is approached more closely in case of direct oxidation possibly because of agitation.

3. The speed or rate of the reaction is influenced by both fundamental and practical considerations.

4. For a given carbon content temperature has the predominate effect. For relatively constant conditions of temperature and agitation, increased carbon content increases the speed. It is practically impossible to separate cause and effect relations among the three factors: carbon, temperature, agitation.

5. The practical factor that limits the speed of the reaction is the design of the process with respect to maintenance of temperature, effect of splash, and introduction of gas.

6. The fastest rate of carbon drop in the open hearth process is immediately after dumping ore into a hot bath of high carbon content. The initial speed is not maintained, chiefly because of the heat requirement.

R. J. RAUDEBAUGH*—Having carefully read

* Georgia Institute of Technology.

this paper I am left with the impression that it should be of definite interest and considerable value to the practical steelmaker. The conclusions are concisely stated and apparently well substantiated.

One question on which I would like further enlightenment pertains to Fig 1 in which the authors plot carbon elimination as a function of carbon content of the melt for both direct and indirect oxidation procedures. Assuming 0.10 pct carbon to be the desired end point, the spread in time to arrive at that condition appears to be considerable (between 10 and 25 min.) in the case of direct oxidation practice, whereas by indirect practice a time of about 55 min. seems to be consistently implied. Would this result in greater variation in FeO content of the bath at the time of tapping and hence possibly modified deoxidation practice? Would the variation in temperature of the melt vary to a greater extent than in the case of indirect practice?

I find it confusing to follow the discussion in the left-hand column of p. 55. The last paragraph apparently refers to points on Fig 2 associated with indirect practice, although such is not clearly stated to be the case.

Likewise on p. 55, the first paragraph in the right-hand column beneath the figure may be misleading. The dash preceding the word *Log* in the two equations cited is not to be taken as a negative sign. The equations are correctly expressed in the conclusions (p. 67).

Referring to the discussion concerned with the chemical relation between carbon and oxygen (right-hand column at the top of p. 57) I believe there is an error in the figure of 3.25 cf of oxygen cited for the amounts of that gas required to oxidize 0.2 pct of carbon to a 90 pct CO, 10 pct CO₂ condition. I believe 3.5 cf is more nearly correct.

Having voiced an opinion in my opening statement as to how I thought the practical steelmaker would probably react to this paper, I feel that I should close by speaking for myself and others here who might be in the academic field. The authors' description of direct oxidation as a workable modification of basic open hearth practice and the conditions under which it can be used most effectively brings the individual like myself to a better appreciation of current developments along this line.

F. G. NORRIS (authors' reply)—The authors appreciate Professor Raudebaugh's clarification of the several points that he mentions specifically. It is of course gratifying to have this assurance that the paper is of interest to readers from many fields.

With reference to the second paragraph, the oxygen content of the bath depends primarily on the carbon content. The relation is such that the carbon-oxygen product tends to be a constant. Because of these relations there is less variation in the oxygen content of the bath in case of direct oxidation. The increased rate, and therefore shorter time to reach a given carbon, is only incidental in affecting the oxygen content or the deoxidation practice.

With our practice, the temperature is under closer control with direct oxidation because of the ease with which the low carbon bath can be brought to proper tapping temperature.

S. FEIGENBAUM*—The authors present an interesting comparison of the effects produced by direct and indirect oxidation of the open hearth bath. The effectiveness of direct oxidation at carbon levels below 0.10 pct has become well recognized and seems at present to be the best justified metallurgical application for oxygen in open hearth practice.

The addition of ore for carbon reduction is attended initially by the absorption of heat from the bath while direct oxidation has an exothermic effect, so that oxygen may be used very late in the refining period when ore would prove troublesome. Metallurgically, the use of ore is advantageous because of direct conversion of the ferric content; and for some plants there may be merit in concurrent application of direct and indirect oxidation particularly at higher carbon contents. Furthermore the use of compressed air rather than oxygen for this purpose appears to warrant further consideration since agitation of the bath has been demonstrated to be a major factor in rate of carbon drop.

There is probably little reason to expect that sulphur elimination would be benefited by direct oxidation. Although the temperature effect is favorable oxidizing conditions toward the end of the refining period are unfavorable toward sulphur reduction and the net effect would be slight.

* Jones and Laughlin Steel Corporation.

Operation of Oxygen-enriched Open-hearth Furnaces*

By J. S. MARSH,† MEMBER AIME

(New York Meeting, February 1948)

JOSEPH PRIESTLEY prepared oxygen on Aug. 1, 1774, and noted with great surprise "that a candle burned in this air with a remarkable brilliant flame." On Aug. 2, 1774, some ironmaker possibly began to wonder if this substance could be used to increase his rate of production; at any rate, there is no disputing the fact that the notion of using oxygen for steelmaking in concentrations greater than that available in great abundance—as air—has been in existence for years. Action was delayed by the lack of enough oxygen at a cost within reach of the steelmaker. Within the last several years enough has been available to permit large-scale tests of its use for both combustion, with which this paper is concerned, and for decarburization. The literature is now enormous and easily available; it is sufficient here to cite three items of historic importance in that all are about 25 years old and in that all are remarkably consistent as far as they go, with what is known today.^{1,2,3}

SIGNIFICANCE OF HIGH-TEMPERATURE HEAT

The principal function of the open-hearth furnace is to supply sufficient high-temperature heat to melt the charge and then to increase its temperature to a range suitable for tapping, ordinarily in the neighborhood of 2900°F. That heat is required to make steel is understood by

Manuscript received at the office of the Institute Feb. 18, 1948. Issued as TP 2416, METALS TECHNOLOGY, Aug. 1948.

* The experimental oxygen heats herein reported were made under the joint sponsorship of the Bethlehem Steel Co., the Air Reduction Co., and the Koppers Co.

† Engineer, Bethlehem Steel Company.

^{1,2,3} References are at the end of the paper.

everybody; however, there seems to be some confusion now and then about the significance of high-temperature heat.

Transfer of energy—and heat is energy—is always from a point of higher potential to a point of lower potential and, other things being equal, the greater the potential difference, the greater is the rate of transfer of energy. In the open hearth the flame, of course, is the high-potential source. Perhaps the most satisfactory approach is through the notion of theoretical flame temperature, which is the ratio of heat input to the heat content of the combustion products,* the former is composed mainly of heat of combustion of the fuel plus sensible heat of the fuel plus sensible heat of the combustion air. Thus, flame temperature can be increased by increasing the value of the numerator, by decreasing the value of the denominator, or both. The first method is as old as the open-hearth process and, of course, makes use of preheated air; its possibilities have been by no means exhausted.

The second method can be put into effect only by changing the composition of the combustion air, since the combustion of a given quantity of fuel produces a definite quantity of product, and since the denominator includes the non-reactive fraction of the air, principally nitrogen. In other words, the denominator consists of the volume of exit gas multiplied by its heat capacity and that volume consists of carbon dioxide and water vapor as reaction

$$\begin{aligned} & \text{* Theoretical flame temperature} \\ & = \frac{\text{heat of combustion} + \text{sensible heat in fuel} + \text{sensible heat in air}}{\text{total quantity of combustion products} \times \text{their mean heat capacity}} \end{aligned}$$

products, possibly unconsumed oxygen, and nitrogen.

Unconsumed oxygen may be ignored here. It is clear that nitrogen gets a "free ride"; it dilutes the combustion products, increases the value of the denominator, and decreases the maximum possible flame temperature. *Oxygen, it must be emphasized, is not a fuel and it adds no heat*; increased flame temperature through the use of oxygen enrichment results from reduction of the quantity of heat carried away from the melting zone by nitrogen by reducing the fraction of nitrogen present.

INCREASING FLAME TEMPERATURE

These matters are elementary in the extreme; it is, therefore, very easy to overlook some of their implications. For example, 1000 Btu per cu ft gas may appear attractive to the operator of a gas furnace. Yet—and this is likely to be true—if the volume of combustion products is high, flame temperature may be lower than that of the 500 Btu gas he had been using. At all events, it appears that there are two ways, simple in principle, to increase flame temperature, therefore rate of melting: 1. Increase the heat content of the combustion air. 2. Decrease the fraction of inert matter. It is with the second of these that results reported here are concerned. Before proceeding, however, it will be useful to review briefly another aspect of heat transfer.

HEAT TRANSFER BY RADIATION

Transfer of heat from flame to charge is principally by radiation; energy passes through the furnace atmosphere from the luminous carbon particles and from the combustion gases such as carbon dioxide and water vapor. As is usual with radiation, upon striking the charge—or the furnace walls or roof—it may be absorbed or reflected. This fact is recognized by the existence of the terms *emissivity* and *absorptivity*, which are merely fractions in

terms of actual behavior and that of a theoretically perfect emitter and absorber (that is, a black body). In principle, these matters are related by:

$$\frac{q_{\text{net}}}{A} = \sigma \epsilon (T_1^4 - T_2^4)$$

where q_{net} = heat flow from flame to charge

A = area

σ = radiation constant

ϵ = emission-absorption factor

T_1 = absolute flame temperature

T_2 = absolute charge temperature

Actually, this equation is too simple to account quantitatively for heat flow in the open hearth. For one thing, flame temperature varies considerably over the volume that the flame occupies; for another, as written, the equation applies only to surfaces that "see" only each other and thus exchange energy only between each other. However, there is no need to introduce a complicating factor to account for shape and distribution in space of the radiating surfaces. Useful qualitative deductions are obtainable, nevertheless. First, since rate of heat transfer depends upon difference of fourth-power temperatures, the greatest benefit from oxygen enrichment must derive from its use when the charge is coldest, which is to say when there is the greatest temperature difference. Second, the charge cannot distinguish between changed emissivity and changed flame temperature; increase of either will increase rate of heat transfer. Both are effective in determining the heat flow pattern and changed furnace design may be necessary to produce the pattern yielding the highest overall melting rate. Third, oxygen enrichment does not necessarily endanger refractories such as the roof, because—and this is fortunate—the emission-absorption factor is not the same for all substances. Steel scrap is a far better absorber of radiation than is silica brick; therefore, even though both are exposed to the same

quantity of radiation, the charge is heated at the higher rate; in fact, much of the radiation received by the roof is returned to the charge by reflection. Fourth, because of the foregoing item, the relative placement of oxygen and fuel streams is not critical, in general. Fifth, more benefit should derive from introduction of oxygen by a stream contiguous to the fuel stream (that is, through the burner) than from the same quantity premixed with the air (that is, introduced at the air intake or in the checker zone). This is because the former is equivalent to a substantially greater enrichment (greater nitrogen impoverishment) in the flame zone.

In passing, another implication of the radiation equation favoring increased flame temperature in the first stages of the heat may be cited. Rate of heat absorption is a function of area of surface exposed. For example, assuming only downward radiation, on a 1-ton sphere of steel, an area of about 6 sq ft of surface would be exposed. As a cube, the area would be from 2.5 to 7.5 sq ft, depending upon its orientation. As 0.5-in. plate, the area would be about 100 sq ft. Thus, lighter scrap, which has higher surface-volume ratio, really is faster melting. In addition, the interior of the piece can be heated only by conduction and nothing can be done about thermal conductivity; consequently, the thinner the piece the less the effect of this limitation. Since maximum surface is exposed to the flame before melting has begun, the aforementioned reason for early enrichment follows. As melting progresses, the exposed surface becomes less and approaches a plane as a limit. In addition to the contraction of area, the exposed surface becomes slag and—unfortunately, this time—the absorptivity of slag is less than that of steel; it would appear then, that the advantage of enrichment is minimum once the heat is under cover. Analysis of the problem cannot stop at this point, however; the faster-melting light scrap is likely

to be so voluminous that a point is reached at which rate of charging cannot keep up with rate of melting. In this case, enrichment is of lessened, or even no, advantage. These things must be kept in mind.

By way of prefacing the following discussion, it must be stated that more space will be given to summarized findings and to conclusions than to detailed data, for it was felt that this system would be on the whole more useful.

INITIAL TESTS

The furnace chosen for the first tests is of modern construction 82 ft 7 in. long and 23 ft 6 in. wide having a hearth area of 880 sq ft. Checkers are two-pass, the chamber volume being about 8200 cu ft and containing about 3900 cu ft of checker brick. Heats average about 200 net tons. Oil is the only fuel and the grade of steel made is ordinarily common structural containing about 0.20 pct carbon. High-purity oxygen was piped to the shop in a 3-in. line from an adjacent plant at an average pressure of 170 psi. A special panel was installed for measurement and control of flow to the furnace; measurement was by orifice meter and control was by air-operated globe valves so arranged that reversal was automatic.

To evaluate the effect of oxygen enrichment, the furnace was made to compete with itself; that is, oxygen and non-oxygen heats were alternated. Data were recorded by special observers on the form shown in Fig 1. (As a matter of record, the first heat was made on Aug. 19, 1946.) The data shown are for a heat that was typical rather than outstanding in any way. Zero time was the end of tap of the preceding heat. Although mostly self-explanatory, some additional description may be useful. Proceeding from top to bottom, first seen is the record of oil flow, which was in the neighborhood of 500 gphr after charging was begun. The flow was decreased some-

usual. Had they been, such would have been noted. Similarly, the hot metal was charged in two ladles. The total charge time—start of scrap to finish hot metal—

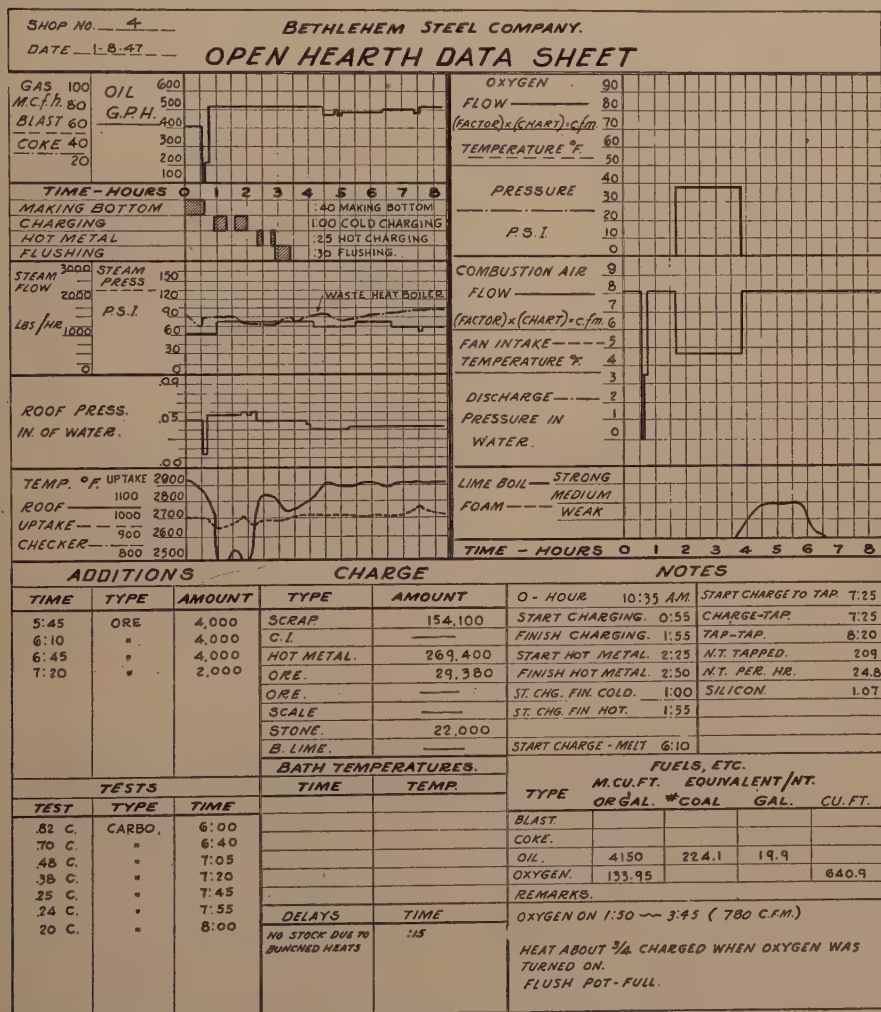


FIG 1—OPEN HEARTH DATA SHEET.

of 1 hr 55 min. was not unusual for oxygen heats.

The next three sections are concerned with items such as atomizing steam pressure, roof pressure, and roof temperature as measured by a radiation pyrometer sighted upon a block in the center of the main roof.

The sixth and seventh sections are of more interest; the former shows oxygen flow and the latter air flow. To be noted is the fact that when oxygen was used, the air flow was reduced to the extent required to yield

help in arriving at an understanding of the behavior of oxygen-enriched furnaces.

Burners

The first burner tested was of the type ordinarily used for the combined burning

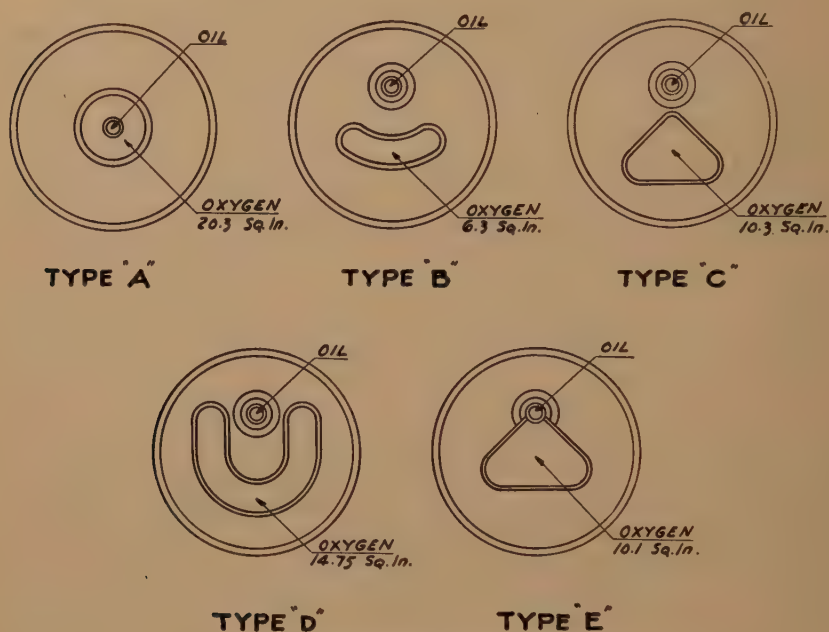


FIG 2—EXPERIMENTAL BURNER PROFILES.

a predetermined enrichment, which in this case was to 27 pct oxygen. Other details are shown at the bottom of the form; for example, the heat melted high and required $3\frac{1}{2}$ boxes of feed ore.

Data were collected on 241 heats from this furnace; of these, oxygen was used on 94; it may be added that all tons-per-hr figures are on a standardized tap-to-tap basis. Much of the work was exploratory in nature and involved experiment with burners of various design, variable enrichment, determination of the most satisfactory time for use of oxygen, and mode of its introduction. Since conclusions drawn from such experiments were upheld by subsequent work, it will be useful to state some of them at this point because they

of liquid fuel and coke-oven gas, which is to say it consisted of two concentric pipes within a water jacket; the inner carries the liquid fuel and the outer the gas, which, in this instance, was oxygen. It was stated in the introductory remarks that consideration of heating by radiation leads to the conclusion that the relative positions of fuel and oxygen streams are not critical and it subsequently developed that this burner performed as well as any other. However, various nozzle forms were tried; profiles are shown in Fig 2. The object, of course, was to increase the quantity of heat flowing downward as compared with that radiated upward toward the roof. As far as heat time was concerned, there was little to choose among these burners; conse-

quently, when the operators showed an inclination to favor Type C, this was adopted for nearly all subsequent work with full awareness that the matter of burner design had not been exhausted, but with the conviction that potential returns from possible improvements were small. In passing, some unplanned evidence for the correctness of the initial conclusion may be cited: on another test furnace, the fuel and oxygen orifices were recessed a few inches from the end of the water jacket; by some quirk of stream flow, the oxygen stream was inverted, for the hottest part of the flame was on top. Yet the roof was not burned and heat time usual with enrichment resulted.

Degree of Enrichment

The degree of enrichment first tested was arbitrarily established at 27 pct. Increase to 33 pct resulted in no gain. Enrichment to 25 pct was tried, with results nearly the same as for 27 pct. This suggests that the first increments of oxygen added produce the greatest effect. Quantitative information is given later.

Mode of Introduction of Oxygen

A few heats were made by introducing the oxygen at the air intake; results confirmed the preliminary analysis in that, as compared with burner injection, gain was small, more oxygen was consumed, and no fuel was saved. The remainder of the tests were therefore with burner injection.

Duration of Enrichment

For the initial heats, oxygen was turned on at the start of charge. However, owing to mechanical limitations, rate of heating exceeded rate of charging. The over-all effect of this was merely to waste oxygen; consequently, for subsequent heats, enrichment was delayed. By trial and error it was found that waiting until the scrap was about one-half charged resulted in no loss of heat time and substantial saving of oxy-

gen. Similarly, it was found that the most satisfactory time for stopping enrichment was about that of start of hot metal charging. This meant a total flow of oxygen for about 2 hr for all furnaces on hot metal charges. It will be noted that the end point found by experience is consistent with the conclusion from consideration of heat transfer.

The Personnel Factor

It is very well known that the productivity of an open-hearth furnace is highly dependent upon the skill and judgment of its operators. Ordinarily the pace is set by a number of factors, including the durability of refractories. Under special circumstances, however, furnace productivity can exceed by substantial amount that which can be maintained. This fact must be taken into account, especially if the number of tests is relatively small. For example, during the first tests, it quickly appeared that the alternate non-oxygen heats were being made in shorter time than usual; this suggested that the furnace "remembered"—that is that heat was stored and carried over. However, the immediately adjacent furnaces also began to produce heats in shorter time than usual; the inescapable conclusion, then, was that novelty and competition were responsible, rather than carry-over of heat. To repeat, such a pace cannot be maintained indefinitely. At all events, behavior was therefore judged by comparison of oxygen and non-oxygen heats on the same furnace rather than by comparison with previous behavior of that furnace. This practice was followed also with tests on other furnaces; otherwise, gains from enrichment would have been fictitiously high.

Other Details of the First Tests

Attempt was made to maintain a constant charge, which consisted of approximately 60 pct hot metal, 33 pct scrap and

7 pct (metallic) ore. Five different burners were used and enrichment ranged up to 33 pct oxygen. The highest enrichment permitted increased fuel flow (up to 650 gphr) but no production gain over that from 27 pct resulted, and refractories were endangered. On the average, the oxygen heats were 20 pct faster with a fuel saving of 10 pct, as compared with the alternated non-oxygen heats. The fuel saving is ascribable only to faster melting, because refining time was normal. Nothing unusual was noticed about refractory wear; to be sure, the furnace operators had to be more alert because of increased tempo, but that was all.

EFFECT OF FRACTION OF SCRAP CHARGED

Since the gain from oxygen enrichment results from faster melting, high-scrap charges should show most effect. The effect of variation of the fraction of scrap in the charge was investigated in a congested shop containing 21 furnaces. The test furnace is of about 725 sq ft hearth area and taps heats in the neighborhood of 135 tons; its fuel is oil. Oxygen was supplied to a special station by trailer truck. Of a total metallic charge of about 300,000 lb, aim scrap charges were 85,000, 100,000, and 125,000 lb, respectively. Results for the 100,000-lb scrap charge and an oxygen enrichment of 27 pct are given in Table 1. These data on individual heats are given as typical examples of those collected; space does not permit reproduction of them all and it is doubtful if such would be useful. There is another reason for reproducing Table 1; that is, that it contains several items of the sort that must be considered in the evaluation of oxygen enrichment.

Operation of the furnace for these tests (other than duration of oxygen flow) was left to the discretion of its operators; it was to be favored in no way. Inspection of the second column shows that scrap-charging time was rapid. To be sure, one

TABLE 1—Effect of 27 Per Cent Oxygen Enrichment on 60 Per Cent Hot Metal Heats

Heat No.	Chg. Time, Hr		Melt Time, Hr	Working Additions		Chg. Tap, Hr	Tap, Hr	Production, Tons		Fuel, Gal. Per Ton	Oxygen		Metallic Consumption, Per Cent		
	Cold	Hot		Hot Metal	Ore			Total	Per Hr		Cu Ft Per Ton	Flow, Hr	Hot Metal	Cold Iron	Scrap
62050	0:35	1:40	4:40		2,000	5:55	6:45	130	10.3	10.2	698	1:48	58.2		34.7
62053	0:29	1:54	4:19			5:05	5:55	132*	20.7	19.3	842	2:00	60.8		32.2
62055	1:25	2:30	4:40		3,000	6:10	7:38	137	17.9	19.9	768	2:03	58.2		33.8
62058*	0:59	2:22	6:22	25,000		7:34	8:34	138	17.6	20.1	866	2:18	61.9		31.3
62060	1:07	2:47	7:05	12,000		7:34	8:34	138	16.4	22.1	832	2:23	60.1		33.0
Avg.	0:55	2:14	5:25			6:21	7:10	132	18.2	20.2	801	2:18	59.8		33.0
Alternated Non-oxygen Heats															
11 Heats	2:09	3:34	8:13			10:06	11:03	134	12.1	26.7			52.1	5.0	35.9
Diff.	1:14	1:20	2:48			3:45	—3:47		6.1	6.5					
Percentage Change						37.1	—34.2		50.4	24.3					

* About 14,000 lb of hot metal lost during charging.

advantage of oxygen enrichment is that faster melting permits charging to proceed without delay, yet it is certain that part of the average difference of 1 hr 14 min. between oxygen and non-oxygen heats is ascribable to the favoring of the former. Since scrap cannot be melted until it is in the furnace, charging time has an effect on heat time and part of the 50 pct greater rate of production shown for the oxygen heats is ascribable to faster charging. The psychologic factor was responsible also for part of the shortened refining time of these particular oxygen heats, as compared with that of the non-oxygen heats; this sort of thing disappears under routine practice and is mentioned only to discourage misplaced emphasis. Even so, the tonnage-rate and fuel gains (approximately 50 and 25 pct, respectively) were high compared with those cited for the 200-ton furnace (20 and 10 pct, respectively). This suggests a furnace factor, for which additional evidence was found and which is discussed later.

To return to the matter of fraction of scrap charged, in Table 2 are shown data on three different charges. Those for 100,000 lb of scrap are from Table 1; the others were obtained similarly. It is admitted that more data would increase certainty, yet these results are consistent with many others; the essential point is that oxygen enrichment tended to smooth out ordinary variations of melting time. A remarkable consistency of heat time had been noted for the first test furnace which was charged uniformly; here was evidence that, within limits, oxygen tends to maintain that consistency despite varia-

tion of scrap charged. In retrospect, this is not entirely inexplicable; a detailed heat balance will show that heat requirement per ton of steel produced is nearly independent of fraction of scrap charged. This results from the fact that increased fraction of hot metal charged is necessarily accompanied by increased fraction of ore and the ore reaction just about consumes the extra heat charged with the hot metal. The observed longer heat time with the higher scrap charges is therefore ascribable to (1) the longer time required for charging and (2) slower over-all rate of heating of a voluminous mass of scrap. Oxygen here is helpful in several ways; especially important is the fact that it compensates for the low air temperature resulting from the chilled furnace that inevitably accompanies charging. The high rate of melting permits continuous charging and the over-all effect is the tendency to melt in the same time elapsed from the start of charge. It follows, then, that oxygen does produce the greatest effect on the higher scrap charges. It must be emphasized, however, that this inherent advantage of oxygen is useful only if shop conditions permit rapid charging.

An extreme of charge variation was obtained by using oxygen on cold-charge furnaces tapping about 60 tons. The metallic charge consisted of scrap and about 10 pct pig iron. These furnaces normally produce at a rate of about 6 tons per hr. Results of the few heats made are summarized in Table 3. Enrichment varied from 23 to 27 pct. However, by selecting conditions that were best and worst by using one new and one old furnace, it was

TABLE 2—*Effect of Fraction of Scrap on 300,000-lb Metallic Charge Heats*

No. Heats	Scrap Charged, Lb	Cold Charge Time, Hr	Melt Time, Hr	Charge-Tap, Hr	Tap-Tap, Hr	Tons Per Hr	Fuel Per Ton, Gal	Oxygen Per Ton, Cu Ft
6	80,000	1:08	5:22	6:46	7:50	16.8	20.0	882
5	100,000	0:55	5:25	6:21	7:16	18.2	20.2	801
5	125,000	1:25	4:55	6:43	7:40	17.5	21.8	885
Avg			5:14	6:37	7:36	17.4	20.6	860

felt that sufficient information was obtained. Required was only enough to estimate probable behavior which, in this case, appears to have been about like that

charged was used also to obtain further information on the effect of degree of enrichment. It will be remembered that the enrichment of 27 pct chosen for the initial

TABLE 3—*Effect of Oxygen on All-cold-charge Heats*

Condition of Furnace	No. Heats	Tons Per Hr			Fuel, Gal Per Ton			Oxygen per Ton, Cu Ft
		With Oxygen	Normal	Gain, Per Cent	With Oxygen	Normal	Gain, Per Cent	
Old.....	10	6.9		17.0	33.0		14.3	1100
Old.....	28		5.9			38.5		
New.....	4	8.85		40.5	29.5		14.5	1200
New.....	16		6.3			34.5		

for the larger furnaces with scrap-hot metal charges—in other words, say about 25 pct increased tonnage and about 15 pct fuel saving.

tests on the 200-ton furnace proved to be about as effective as the richer mixtures. This value was substantiated on the 135-ton furnace, as is demonstrated by Fig 3,

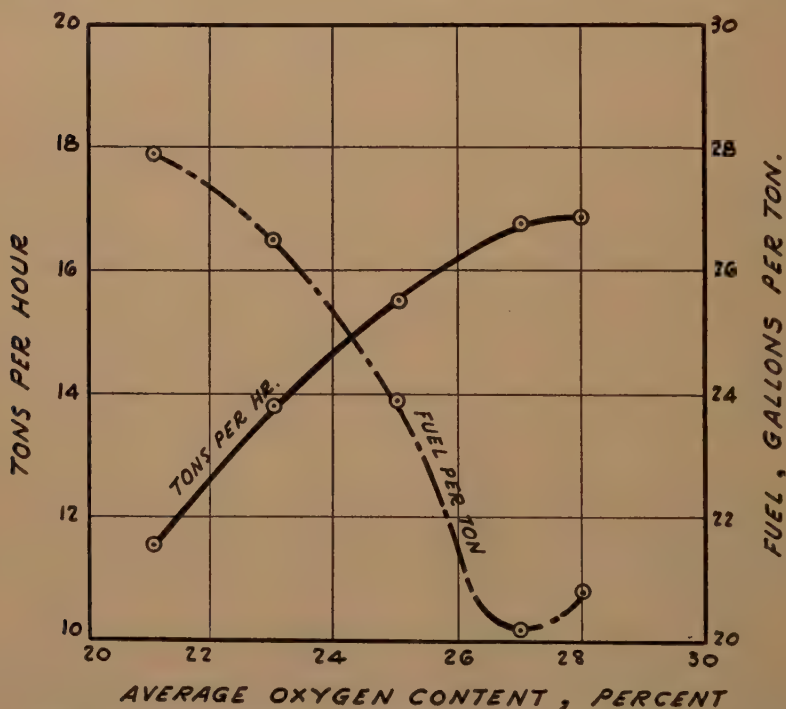


FIG 3—EFFECT OF DEGREE OF OXYGEN ENRICHMENT ON RATE OF PRODUCTION AND FUEL CONSUMPTION AS DERIVED FROM DATA ON 57 HEATS.

EFFECT OF DEGREE OF ENRICHMENT

The furnace used for investigation of the effect of variation of fraction of scrap

which is based upon 57 heats. The minimum in the fuel consumption curve indicated by the data must be real, since the

production curve reaches its maximum at an intermediate oxygen value; although more fuel can be burned at the higher degrees of enrichment, seemingly the extra

flow was at a rate of about 400 gphr and oxygen enrichment was to 25 pct. Hot metal in the charge was about 50 pct. Production data are summarized in Table 4.

TABLE 4—Summary of Production Data on a Routinely Operated Oxygen Furnace

Item	Oil Fired			Mixed Gas and Oil Fired		
	With Oxygen	Normal	Gain, Per Cent	With Oxygen	Normal	Gain, Per Cent
No. heats.....	149	28		96	31	
Cold-charge time, hr.-min.....	1:45	2:18		1:50	2:29	
Hot-charge time, hr.-min.....	2:55	3:55	24	3:00	3:53	13
Melt time, hr.-min.....	6:32	7:25	20	7:35	8:28	20
Charge to tap, hr.-min.....	7:47	9:05	12	7:35	8:28	10
Heat weight, tons.....	134	138	14	9:09	10:20	12
Tons per hr.....	134	138		130	133	
Oil, Gal per ton.....	15.3	13.6	13	13.2	11.4	16
Mixed gas, equiv. gal.....	21.8	23.8	8	15.3	19.3	
Total fuel, gal per ton.....	21.8	23.8	8	10.8	8.6	
Oxygen per ton, cu ft.....	674			26.1	27.9	7
Oxygen flow, hr.-min.....	2:16			609		
				2:26		

heat released was not transferred to the charge—at least in furnaces of the design and construction tested. It will be remembered that this is consistent with what was found for the first test furnace with enrichment to 33 pct oxygen.

EFFECT OF OXYGEN ON REFRACTORIES

Although nothing abnormal about roof wear had been noted for the test furnaces, it was recognized that the behavior might be different for a furnace on which oxygen was used for every heat. Insufficient oxygen was available to supply the 200-ton furnace used initially; consequently, the work was transferred to a smaller furnace. The one selected is of 600 sq ft-hearth area, taps about 135 tons, and was completely rebuilt, with basic ends, prior to the start of the oxygen campaign. Operation was with a minimum of special supervision; this was for the purpose of arriving at an estimate of what might be expected reasonably under routine conditions. In all, over 300 heats were made; for 177 of these, the fuel was oil, and oxygen was used on 149 of the 177 heats. (Either mixed gas or mixed gas and oil were used on the others; of these, oxygen was used on 96.) Fuel

It is interesting to note that the usual difference of results from liquid fuel and gas firing persisted with oxygen enrichment; in terms of percentages, there is little to choose between the two sets of data. The gains are relatively small compared with those found with the other 135-ton furnace, but are roughly in accord with those for the 200-ton furnace in the adjacent shop. Part of the difference from the neighboring furnace is probably ascribable to the fact that, principally because of supply, enrichment was limited to 25 pct, although the furnace and shop factors were undoubtedly operative also. However, it is the purpose of this section to discuss refractories.

In brief, all that can be stated is that no definite effect of oxygen enrichment was found. The roof was first patched after 119 heats and again after 195 heats. In terms of one 13.5-in. roof, knuckle to knuckle, exclusive of skewbacks, life was 177 heats. Oxygen enrichment was stopped before the end of the campaign; consequently, the aim of the test was not entirely fulfilled. To be certain, considerably more data would be needed, although as has been stated, nothing unusual was observed

about refractories on any of the oxygen furnaces.

DISCUSSION OF RESULTS

In all, more than 400 oxygen enriched heats were made in five different furnaces which ranged from older types in congested shops to newer designs in modern shops. Charges covered the range likely to be encountered; that is, from all-cold to over 60 pct hot metal. Information obtained on some items was necessarily incomplete; for example, it was not proved conclusively whether or not oxygen has an effect on furnace life, although indications were that any such effect at least is not harmful. Further, it is clear that the production of an all-oxygen shop would not necessarily be the rate for one furnace multiplied by the number of furnaces; however, before expanding this statement, it may be well to record several so-far unmentioned, or casually mentioned, observations:

1. A furnace "set" for 1 to 3 pct oxygen in the waste gas remains set upon enrichment of the combustion air.

2. Oxygen-enriched furnaces equipped with waste heat boilers produce less steam. The certain cause is the smaller volume of waste gas, owing to the smaller fraction of nitrogen; a possible cause is more efficient transfer of heat from flame to charge, which leaves less to be carried to the exhaust system.

3. Intimately connected with the foregoing is the fact that, for a given fuel flow, the flame is shorter with enrichment as a consequence of faster combustion. This changes the temperature pattern to the extent that the hottest zone is concentrated to a narrower range, with the result, in large furnaces at least, that the outgoing end is likely to be cooler than that of the same furnace without oxygen.

4. There exists a furnace factor which is intimately associated with thermal efficiency. The items lumped in thermal efficiency are well known, yet at first glance it

may not be clear that, in general, *as inherent furnace efficiency increases, the potential gain from oxygen enrichment necessarily decreases*. Thus, rate of production with oxygen might be increased by as much as 50 pct with one type of furnace and as little as 10 pct or less with another, despite constancy of items such as type of charge, charging time, and grade of steel made. (Data for the old and new furnaces given in Table 3 may appear to the contrary; however, attention is directed to the small number of heats. Even so, it is likely that a furnace may be so worn and clogged that oxygen enrichment is not capable of effecting complete rejuvenation. The general statement remains true, however.)

Returning to the matter of an all-oxygen shop, much more is involved than supplying an adequate amount of oxygen, assuming that an existing shop is being considered for conversion. If the potential gain—whatever it might be for a given type furnace—is to be achieved, there must be no charging delay, and especially no scrap-charging delay. Each increment of increased production requires a corresponding increase in the number of charging boxes handled per unit time; ordinarily this means increased probability of delay. From here on, speculation can proceed in either of two directions; that is, on production of the same ingot tonnage with a reduced number of furnaces or on production of increased tonnage. This discussion is confined to the latter. Then, in addition to more charging boxes to be handled per unit time, there are more ladles of hot metal, more molds, and so on. Many an existing shop could not maintain such accelerated tempo. Future shops, of course, could be suitably designed, but such is not a problem of the moment. Restricting consideration to existing shops, to repeat, each type of furnace and each shop evidently must be treated individually. It appears that there is no single answer to the question of how much open-hearth production of the coun-

try would be increased by the use of combustion oxygen; the amount is seemingly rather less than that which might be assumed by the unsuspecting reader of the popular press.

SUMMARY

1. In all, more than 400 heats were made with oxygen enrichment. Five different furnaces were used.

2. Furnace charges ranged from all-cold to those in which hot metal composed 60 pct of the total metallic charge.

3. Maximum rate of production was found to result from enrichment to the neighborhood of 27 pct average oxygen.

4. Oxygen consumption ranged from about 1200 cu ft per ton for cold charges to about half that for high-metal charges.

5. On specially supervised tests, production increases ranged from 20 to 50 pct; these were accompanied by fuel savings of 10 to 25 pct. However, gains were markedly less for unsupervised heats extending over nearly a furnace campaign.

6. Differences of production increase caused by oxygen enrichment are ascribable to furnace and shop factors.

7. It follows from item 6 that each type furnace and each shop must be considered individually.

8. It appears that over-all rate of routine production with oxygen would be less than might be indicated by results of tests conducted under special conditions.

REFERENCES

1. H. C. Bigge: U.S.P. 1,513,735. (1924)
2. F. W. Davis: The Use of Oxygen or Oxygenated Air in Metallurgical and Allied Processes. Rep. of Invest. 2502, Bur. of Mines, Washington, D.C., (1924).
3. AIME: Use of Oxygenated Air in Metallurgical Operations. *Abstracts of Symposium Papers*, N. Y. (1924).

DISCUSSION

(C. R. Taylor presiding)

C. R. TAYLOR—Thank you very much, Mr. Marsh, that was an excellent presentation.

I realize that this type of paper is one which has greater interest to operating men, perhaps, than to metallurgists, but I am sure we have enough operating men here to bring out some interesting points.

C. E. SIMS*—I am not an operating man, but I was very interested in the statement made by Mr. Marsh that the refractories did not seem to suffer because of the oxygen-enriched air.

I recall that about 20 years ago the popular topic on open hearth operation was insulation. When that was proposed, there were many dire predictions that if one attempted to insulate the furnace, the refractories would suffer terribly—the walls would burn down. Of course, that did not happen.

And the same thing now seems to be true of the oxygen-enriched air. The somewhat higher flame temperature does not appear to damage the refractories as long as there is something to absorb the heat. Apparently, the damage to refractories comes only when the whole furnace, bath and all, gets up to excessive temperatures. As long as there is cold metal there to absorb some of the heat, the extra flame temperature apparently can be handled without damaging the refractories.

Mr. Marsh brought out one other point which I think is extremely important in evaluating any of these factors. It is the virtual certainty that there will be an improvement in operating results, even in normal operations while a test is going on.

C. R. TAYLOR—Perhaps I could open up the meeting a bit by giving some of our own experiences at Middletown. We operated one furnace on oxygen to the flame, trying various burner types and designs, and came very much to the same conclusions to which Mr. Marsh has come. The entire scheduling of the heats is necessarily stepped up; the rate of melting the scrap is such that the additions of hot metal have to come a lot faster; and in general the heats are much more sensitive to charging delays.

MICHAEL TENENBAUM†—I do not think this paper should go by without Mr. Marsh's being

* Battelle Memorial Institute.

† Inland Steel Co.

complimented for a very excellent presentation and for a very fine manipulation of a very difficult subject.

I have just one question I would like to ask. We found in our experience that with use of oxygen-enriched air we had a considerable increase in temperature gradients from the top to the bottom of the solid material charged within the furnace. This was especially evident in ore heats. I would just like to know if you had a similar experience.

J. S. MARSH (author's reply)—I think it is true that there is a sharply increased temperature gradient. The top of the charge is hotter, and necessarily so. But owing to the fact that we cut off enrichment about the time of hot metal addition, the effect disappears. The behavior seems to be just about as usual from there on. Sometimes there is some indication—how good it is I do not know—that because of the faster melting one gets the illusion that such heats are a little bit hotter, but I do not think they really are. They seem to be the same as usual by the time the heat is melted.

C. R. TAYLOR—I think sometimes the efficiency of a silica roof has been somewhat underrated. We had occasion some years ago to install a silimanite roof. We were able to operate at about 200° higher roof temperature but found that we did so without increasing production. We attributed this effect to the relatively high reflectivity of a silica roof, which might account for its lack of damage with use of oxygen.

J. B. WAGSTAFF*—I would like to congratulate Mr. Marsh for his very excellent paper, but I would like to ask him one further question, and that relates to the curve he showed for the fuel consumption of the furnace.

Over in England, the works of Leckie and others have shown both on the actual operating open hearths and on a model furnace, that if you plot fuel consumption in whatever units you choose against output, you actually get a curve that goes through a minimum.

I am wondering whether the curve you showed for the use of oxygen—where you showed, I think, that the fuel decreased and then increased again—was in fact because you

were varying the rate of working. I wonder whether you have any data showing fuel consumption as a function of output for oxygen and the ordinary heats, because I feel without taking output into account, that the fuel consumption may be misleading.

J. S. MARSH—That is true. We have all kinds of numbers on just that sort of thing. I think it is the experience of everybody that the faster the rate of operation for a given furnace, the lower will be the fuel rate. I think that that factor was wiped out on these numbers because the furnace was working against itself on the oxygen vs. non-oxygen heats. On the non-oxygen heats it was working faster than usual, so its fuel rate was lower than usual. That was one of the reasons why we chose, in making these comparisons, to make the furnace work against itself rather than as it had been doing previously.

I think your point is certainly well taken—that that must be taken into account—but I contend that it was taken into account.

T. S. WASHBURN*—I, too, would like to compliment the author on his extremely excellent and pertinent paper. It was very comprehensive.

I do not know whether he brought in the point in connection with the effect of this combustion oxygen on the scrap and hot metal ratio; in other words, one expects an increase in scrap as a result of the faster melting and less oxidation of scrap. Did you find that? And was there any percentage determined on that ratio comparing your non-oxygen with your oxygen heats?

J. S. MARSH—That was one thing we expected, and I am glad you brought it out, because in attempting to save time I deleted something that should have been said.

The oxygen consumed for the best over-all results depended on the fraction of solid material in the charge. It ranged in these 400-odd heats from about 1200 cft for the all-cold charge down to about half of that for the scrap hot metal ones.

When it comes to the point about which you are talking, we had some indication that with the faster melting there was less oxidation;

* Hydrocarbon Research, Inc.

* Inland Steel Co.

heats were melting rather high and we had to up the ore charge a bit. On the whole, the difference was not as much as we expected to find. The results are not too clearcut, but I think it is true the faster melting heats do tend to melt higher on the same ore charge, if that is what you meant.

F. G. NORRIS*—That is right, about the effect of melting rate with the same ore charge. At first thought you could reason with some justification either to increase or to decrease the iron. You could say for more oxidizing conditions you have to charge a little more iron. But apparently that is not the case. The melt seems to be a function of the time of exposure. The faster melting time more than offsets the effect of the increased oxidizing atmosphere. So the tendency on these heats with oxygen for scrap melting is for the heat to melt a little higher for the same charge.

J. S. MARSH—I am glad to have that confirmation.

* Wheeling Steel Corp.

C. E. SIMS—Is it a more oxidizing atmosphere?

J. S. MARSH—No, I should say it is not.

C. R. TAYLOR—I can offer more confirmation. We also had higher melts when we first started using oxygen, simply because the scrap was exposed to the oxidizing flame for a short time.

Mr. Marsh mentioned an optimum density of the charge. There definitely is an optimum density. It is possible to get the charge density too high, resulting in a loss in heat time.

F. G. NORRIS—Just one correction. In speaking of more oxidizing conditions I had reference to jet melting. Of course, using burner oxygen all you are doing is burning more fuel. The use of a jet or lance to melt down scrap does increase the oxygen in the furnace atmosphere, but still does not increase the pig iron requirements.

The Role of Thermochemical Factors in Basic Open Hearth Production Rate

By T. E. BROWER* AND B. M. LARSEN,* MEMBERS AIME

(San Francisco Meeting, February 1949)

INTRODUCTION AND SUMMARY

By "thermochemical factors" we refer to those variables which affect the net heat which must be put into the bath in order to make a heat of steel from any given set of charge materials. This is admittedly only one phase of the production rate problem. The whole problem includes also consideration of rate of charging, flame radiation intensity, rate of optimum fuel input obtainable without undue damage to the furnace structure and any variations in conditions such as stirring, slag volume or viscosity which affect the rate at which heat can flow down and away from those exposed surfaces where the heat is first received from the flame.

Because a given type of charge in a shop is often considered as being nearly constant in both physical and chemical characteristics from one heat to another, and because such a state of affairs may be thought of as resulting in a reasonably constant net heat requirement, this requirement is usually neglected as an invariable, inevitable matter, about which nothing can be done. With normally variable charge, and variable percentages of limestone and cold pig, however, the net heat requirement can be subject to very appreciable change; it may also be affected by such things as the currently popular procedure of blowing oxygen into the bath. To bring the general problem of production

rate into better perspective, therefore, it seems worthwhile to try to evaluate the net bath heat requirement and the amount by which it may change through variation in different factors. Because our calculated values of net heat are admittedly uncertain, we have tried to check them in part by statistical data on actual production rates over rather large groups of commercial heats.

The results of calculation of net heat requirements in a wide range of actual commercial practices may first be summarized briefly. We find a wide range between the extremes of different practices, as would be expected, with duplex practice (essentially blown metal plus hot metal) having essentially a zero net heat requirement, an all-cold charge practice somewhat over 1 million Btu per ton of steel and a high hot metal practice about 0.75 million Btu per ton. Over the commercial range of scrap plus hot metal practice, increasing the percentage of hot metal from 40 to 78 pct, with other factors nearly constant, decreased the net heat by only some 5-10 pct. The net heat is increased by about 1.2 pct for each 1 pct of the metallic charge present as cold pig. Calculated values of oxygen supplied by air varied from about 25 up to 60 lb per ton of steel, and in a 60 pct hot metal practice, an increase from 32 to 52 lb oxygen from air decreased the calculated net heat from 0.88 to 0.74 million Btu per ton. Use of pure cold oxygen to substitute for about one half of the total charge ore (about 28 lb oxygen replacing 145 lb ore per ton of steel) decreased the

Manuscript received at the office of the Institute March 16, 1948. Issued as TP 2451 in METALS TECHNOLOGY, October 1948.

* Research Laboratory, United States Steel Corporation, Kearny, N. J.

calculated net heat from 0.79 to 0.53 million Btu per ton or about 33 pct. In a 40 pct hot metal practice, decreasing the limestone from 190 to 120 lb per ton also decreased the net heat by calculation from 0.96 to 0.79 million Btu per ton. For the net heat from charge to melt, upon which approximate values of net fuel efficiency may be based, a chart is given showing approximate net heat requirements based on carbon at melt and amounts of limestone and cold pig in the charge, assuming that total oxygen absorbed from air or gases is close to 40 lb per ton of steel.

Studies on production rate tend to fulfill the expectations based on these calculated net heat values. It is shown that in any reasonably well controlled practice, the time of heat will vary by 40–50 pct even for the same or similar grades of steel, and we estimate that about 35 to 50 pct of this variability is probably related to change in net heat requirement. Change in percentage of hot metal caused little effect on average production rate. Increasing limestone or cold pig in the charge increased the time of heat by about half of what would be expected from corresponding effects on net heat requirement, indicating a probable compensation caused by improved heat absorption from flame to bath or charge respectively. The substitution of light for heavy scrap and the occurrence of decreased feed ore requirements or of lower carbon at melt, variables which are probably all related to increased air oxidation, caused a decrease in time of heat of about what we should expect on the assumption that their effects are related essentially to change in net heat requirement.

HEAT BALANCE CALCULATIONS

The net heat requirement of the bath, which is defined as the net difference between the sum of all the various items of heat carried in as sensible heat or evolved by exothermic reactions, and of heat absorbed, requires a complete heat balance

calculation for that system which is bounded by the surfaces of charge and molten slag and metal. Since the method of calculation, as well as part of the data and calculations used here, have already been presented in some detail by Darken¹ in the book "Basic Open Hearth Steel-making," it is unnecessary to give details here, though some mention of the assumptions and uncertainties involved appears warranted.

The method involves the following imagined sequence of changes:

Hot metal is cooled to room temperature with its C, Si, Mn and P removed from solution, the net amount of ore to be reduced is decomposed into Fe and O₂, CaCO₃ in charge is dissociated into CaO and CO₂; all these various chemical reactions are completed at room temperature and the products formed are heated up to the various average temperatures at which they leave the bath. This cycle is thermally equivalent to the actual one in the furnace and permits the use of room temperature values for heats of reaction, these being in general most accurately known at this temperature level.

The heat balance includes the following main items:

Credits (or items of heat evolved or carried in to the bath):

1. Sensible heat in hot metal (or any other heated materials such as blown bessemer metal) entering the furnace.
2. Net heat of oxidation of C to CO and CO₂, Si to SiO₂, Mn to MnO, P to P₂O₅.
3. Heat of formation of slag compounds (mainly 2CaO.SiO₂ and 3CaO.P₂O₅).
4. Sensible heat in oxygen (O₂) absorbed into the bath from the hot gas space above it.
5. Credit for that part of the heat of combustion of CO and H₂ to CO₂ and H₂O, respectively, over the slag surface which is returned to the bath.

¹ Reference are at the end of the paper.

Debits (items of heat absorbed or carried out in products):

1. Sensible heat in steel and slag at tap.
2. Sensible heat in gases, CO, H₂, CO₂ and H₂O at the average temperature at which they leave the charge or slag surface.
3. Heat required to change the net amount of ore reduced to Fe and O₂ or to the FeO present in the slag, (this may become a credit if more iron is oxidized than reduced in the heat).
4. Decomposition of CaCO₃ to CaO and CO₂.
5. Reduction of CO₂ from limestone to CO by C in bath.

Since the larger items, specifically the heat content in iron, slag and steel and the heat derived from the main chemical reactions, are known to quite high accuracy, the net heat from such a balance should be approximately correct in spite of its being a net difference between larger sums. There are, however, several uncertain items, the main ones being probably as follows:

1. The average temperature at which oxygen enters (from gases), and CO₂, H₂O, H₂ and CO leave, the charge or slag surfaces.
2. The average extent to which CO is oxidized to CO₂ in slag or metal and to which CO₂ from limestone is reduced to CO before leaving the charge or bath.
3. The percentage of the heat of combustion of the residual CO and H₂ burned just above the bath which is reabsorbed into it before these gases mix with the combustion gases and pass out of the furnace.

We have assumed that all oxygen from air or combustion gases enters the bath at an average temperature of 2925°F and that the average temperature of gases leaving the bath is 2750°F. Carbon oxidized by FeO is assumed to form 10 pct CO₂ and 90 pct CO before leaving the slag surface; of all the CO₂ from limestone, two thirds is assumed to be reduced to CO in the bath; 20 pct of all water charged is assumed to be

reduced to H₂. Out of the total heat of combustion of residual CO and H₂ over the bath, 20 pct is assumed to be reabsorbed. Considering probable partial cancellation of positive and negative errors and the fact that most of the larger items are known rather accurately, we estimate a probable error of not more than 15 pct in this method. These assumptions imply that our understanding of this rather complex thermochemical process is not seriously in error. Some decrease in uncertainty might be obtained from extended sampling and analysis of gases leaving the bath in (1) the ore boil; (2) the lime boil; and (3) the refining periods. A little work along this line has been done but more extended research appears desirable since it would also tend to amplify our general knowledge of the process.

As an initial example of such net heat calculations we give (Table 1) three balances which include the approximate extremes in American open hearth practice. (The reader is again referred¹ to "Basic Open Hearth Steelmaking" for most of the details of thermal data, method for materials balances including an oxygen balance from all sources, and calculations of weights of various gases and slag formed). This tabulation indicates a net heat requirement of 770,000 Btu per ton of steel for high-iron practice with 78 pct hot metal, which increases to only 1,060,000 Btu per ton for an all-cold charge practice at 33 pct cold pig iron. The latter practice includes much smaller credits, such as no heat from hot metal and less heat from exothermic reactions, but it also has a smaller total of debit items because of smaller weights of slag and gases, less ore decomposed and the use of burnt lime in place of limestone.

In practice, the fuel consumption with an all-cold charge is frequently higher and production rate lower than in hot metal shops, but this difference is quite small in some cases. Besides the higher net heat require-

ment of the cold charge heat, it usually has the additional handicap of a relatively larger mass of scrap to be charged; if this is mostly light and miscellaneous scrap a longer charging period is (more or less) inevitable. On the other hand, the cold

Thus the fuel consumed, which is approximately one-half of that used in normal practice with scrap and hot metal, is entirely used up in maintaining the melting chamber at 2950–3000°F. In practice, the charge-to-tap time in duplex heats is usu-

TABLE 1—*Heat Balance for Three General Types of Charge*

	1	2	3
	Hot Metal 78 Pct Scrap 22 Pct	All-cold Charge 33 Pct Pig	Duplex Charge Liquid Metal 82 Pct Hot Metal 17 Pct
Million Btu Per Net Ton Steel in Bath			
<i>Credits (heat evolved):</i>			
1. Sensible heat in hot or blown metal.....	0.75		1.16
2. Heat of oxidation of C + O ₂ → CO and CO ₂ ...	0.28	0.15	0.06
Si → SiO ₂	0.14	0.11	0.06
Mn → MnO.....	0.09	0.05	0.06
P → P ₂ O ₅	0.06	0.02	0.02
3. Heat of Formation in Slag:			
2CaO.SiO ₂ and 3CaO.P ₂ O ₅	0.05	0.03	0.02
4. Sensible heat in O ₂ supplied from air.....	0.03	0.05	0.01
5. Heat of combustion of CO and H ₂ over slag at 20 pct efficiency.....	0.14	0.05	0.02
Total credits.....	1.54	0.46	1.41
<i>Debits (heat absorbed):</i>			
1. Heat in steel at tap.....	1.20	1.22	1.22
run-off slag.....	0.15		
tap slag.....	0.14	0.19	0.10
2. Heat in gases leaving bath.....	0.18	0.05	0.02
3. Heat of decomposition of ore and H ₂ O.....	0.49	0.06	0.09
4. Heat of decomposition of limestone.....	0.09		
5. Heat of reaction of CO ₂ from stone with carbon..	0.06		
Total debits.....	2.31	1.52	1.43
Net requirement from fuel.....	0.77	1.06	0.02

charge practice has an advantage in the high efficiency of heat absorption into cold scrap during charging and early melting periods. Thus, if the furnace is operated so as to give a high flame intensity with high input rate plus efficient burning of fuel in the melting period, and there are facilities for charging rapidly enough to keep pace with the maximum available heat absorption, a cold charge shop may obtain production rates practically as high as in good hot metal practice, with fuel consumption only some 15–25 pct greater.

The duplex practice shows a net heat requirement of only 20,000 Btu per ton, an amount well within the probable limits of error in the calculations so that we may consider that there is essentially no net heat absorbed into the bath in this case.

ally limited by the time needed to shape up the slag and adjust the final carbon content.

These examples in Table 1 represent extreme variations in practice which would naturally be expected to change the net heat requirement. The more important question is that of whether much variation in net heat is present in a given practice with reasonably constant charge and operating conditions. We know that time of heat does vary even under such conditions; this may be illustrated by the fairly typical frequency curve in Fig 1, which represents the variation in time for charge-to-tap for a group of 320 heats, all of 0.05–0.08 pct C made for the same grade of steel in a single shop under constant "practice control" and normally constant general shop practice. The spread here of from 9.5 to

14.5 hr, or 50 pct in charge-to-tap time, is no doubt caused partly by the various other furnace and operation conditions mentioned at the beginning of this paper;

any given shop, which changes many thermochemical items in the heat balance. Table 2 gives balances for three heats with 40, 60 and 78 pct hot metal, respectively.

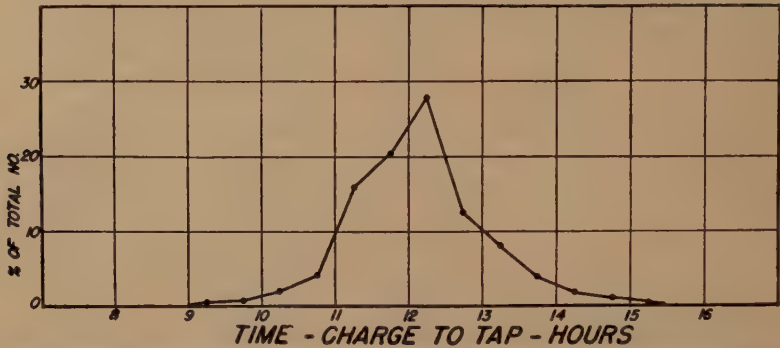


FIG 1—FREQUENCY DISTRIBUTION OF THE TIME FROM CHARGE TO TAP OF 320 HEATS OF 0.05 TO 0.08 PCT C STEEL MADE UNDER CONSTANT PRACTICE CONTROL.

the question is, does an appreciable part of such variability result normally from change in net heat requirement?

RELATION BETWEEN PROPORTION OF HOT METAL OR COLD PIG AND NET HEAT REQUIREMENT

Operating conditions commonly dictate a variation in proportion of hot metal in

These three heats, which cover about the whole commercial range of hot metal percentage, are nearly comparable in other respects, the only other significant difference being a larger amount of air oxidation in No. 1 (discussed in a later section). We have therefore made an approximate correction in the bottom line to the net heat to adjust all three to the same amount

TABLE 2—Heat Balances for Various Percentages of Hot Metal in Charge

	Percentage of Hot Metal		
	1 40 Pct	2 60 Pct	3 78 Pct
Million Btu Per Net Ton Steel			
<i>Credits (heat evolved):</i>			
1. Sensible heat in hot metal.....	0.40	0.59	0.75
2. Heat of oxidation C + O ₂ → CO and CO ₂	0.13	0.20	0.28
Si → SiO ₂	0.07	0.18	0.14
Mn → MnO.....	0.05	0.09	0.09
P → P ₂ O ₅	0.03	0.04	0.06
3. Heats of formation in slag.....	0.02	0.04	0.05
4. Sensible heat in O ₂ from air.....	0.04	0.03	0.03
5. Heat of combustion CO, H ₂ over slag.....	0.08	0.11	0.14
Total credits.....	0.82	1.28	1.54
<i>Debits (heat absorbed):</i>			
1. Heat in steel at tap.....	1.20	1.20	1.20
run-off slag.....	0.14	0.14	0.15
tap slag.....	0.18	0.16	0.14
2. Heat in gases leaving bath.....	0.10	0.15	0.18
3. Heat of decomposition of reduced ore and H ₂ O.....	0.01	0.30	0.49
4. Heat of decomposition of limestone.....	0.09	0.09	0.09
5. Heat of reaction CO ₂ from stone with C.....	0.05	0.05	0.05
Total debits.....	1.63	2.09	2.30
Net requirement from fuel.....	0.81	0.81	0.76
Net heat corrected approximately to constant air oxidation.....	0.85	0.81	0.77

of air oxidation. In all three cases, the limestone charge is the same, 116 lb per net ton of steel.

Generally speaking, the data indicate that difference in hot metal percentage has

regarded as a rough check on the indications of Table 2. If charging and handling of the larger scrap volume in the lower-iron practice is a limiting factor, production rate is usually slower than in high-iron

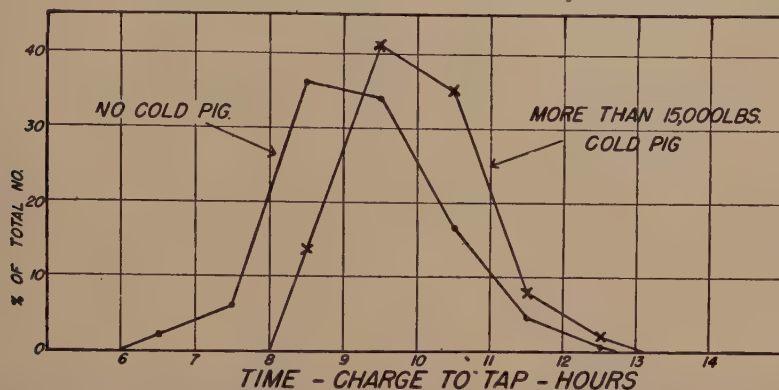


FIG 2—FREQUENCY DISTRIBUTION OF THE TIME FROM CHARGE TO TAP OF 135 HEATS WITH NO COLD IRON IN THE CHARGE AND 141 HEATS WITH 15,000 LB OR MORE OF COLD IRON.

a rather small effect on net heat requirement. All three uncorrected values are within 5 pct, and after correction within 10 pct. With more hot metal, both the sensible heat in hot metal and the heat of oxidation of C, Si, Mn and P become larger on the credit side; but the greater heat contents of slag and gases leaving the bath, together with the heat of decomposition of the larger ore charge (including its moisture content), almost neutralize the larger credits by increasing the debit side. As may be seen more clearly from later discussion, this is only true for increase of hot metal when certain other conditions are present. These are: (1) Presence of about the same percentages of C, Si and P in the hot metal; (2) flushing off all excess slag so that no heavier limestone charge is required for the higher-iron charge; (3) air oxidation remains about the same in amount; and (4) the composition of the charge ore remains about the same, particularly with respect to SiO_2 and moisture.

In general open hearth practice, the difference in speed and fuel consumption between 40-45 pct and 60-65 pct iron practices are usually small enough to be

heats. In some cases, however, with difficulties in excessive boils and increased slag volume related to the increased ore in charge, production rate may decrease with increasing hot metal percentage. In one plant study, three large comparable groups of heats with 60, 65 and 70 pct of hot metal, gave average charge-to-tap times of 9.72, 9.80 and 9.82 hr, respectively, all within 6 min., though the slight trend is opposite to that in Table 2.

From Table 2, it is evident that partial substitution of cold pig for hot metal increases the net heat requirement, because there will be essentially the same proportionate effects on other items such as heat in gases leaving bath, but proportionately smaller compensating increase in the sensible heat carried in by hot metal. This change will vary only a little with the temperature at which the substituted hot metal is delivered to the open hearth, so that the net effect will be rather close to 0.01 million, or 10,000 Btu per net ton steel for each 1 pct of metallic charge substituted by cold pig; (or roughly 1.2 pct of the usual net heat requirement).

Fig 2 shows the frequency distribution

of time of heat for 135 heats with no cold pig as against 141 heats with from 15,000 to 60,000 cold pig, (averaging about 25,000 lb and equal to about 15 pct of the average hot metal charged). There were no other appreciable statistical differences between the two groups. With no cold pig the average time of heat is 9 hr 9 min. compared to an average of 9 hr 54 min. for the group with 15 pct cold pig. Similar comparisons from other data gave similar results; for example, substitution of 13 pct cold pig increased the average time of heat by 25 min., and 28 pct cold pig by 49 min. In a group of medium carbon heats, substitution of about 15 pct cold pig increased the average time of heat from 11 hr 2 min. to 11 hr 48 min., or 46 min. In another group of low carbon heats, substitution of about 13 pct cold pig increased the average time from 12 hr 2 min. to 12 hr 36 min. or 34 min. Thus we have statistical comparisons from various shops which all agree to the extent of indicating an increase of about 2 to 3 min. in time of heat for each 1 pct of the metallic charge as cold pig.

This 2 to 3 min. represents about 0.45-0.65 pct of the usual time from charge to melt, so that the effect on production rate is less than the proportionate effect on net heat requirement, probably because of the fact that the cold pig is such an excellent absorber of lower temperature heat during melting. This comparison reveals nothing very new, but the fact that the effect here is about what might be expected gives us a confirmation of the role of net heat requirement in production rate in a simple case where secondary factors are unlikely to be significant.

RELATIVE OXIDATION BY AIR OR BY ORE

The open hearth process is in general an oxidation process. For a given amount of silicon, carbon, or other element, to be oxidized, a certain weight of oxygen must be supplied, and whatever part of this total is not absorbed from the air into slag and

melting scrap, must be supplied by charge or feed ore. The character of the scrap charge is probably the most significant factor affecting the amount of "air oxidation," during melting. Experience shows that "light" scrap generally absorbs more oxygen as it melts than "heavy" scrap. The amount of excess air supplied with the fuel, and the rate of melting are other probable factors.

Table 2 shows that with an increased supply of Si, Mn, and others, to be oxidized the credit heat items in the balance become larger, but if the oxygen comes from charge or feed ore, the heat required to decompose the ore neutralizes this gain so that there is no net reduction in heat requirement, and even with the added sensible heat in liquid iron in higher iron charges, the total net heat is only slightly less.

Air oxidation tends to remain approximately constant in amount through the usual range of hot metal percentage; at around 40 pct hot metal it is usually about equal to the total oxygen requirement, so no charge ore is then required. If now as we increase the hot metal, we could increase the amount of air oxidation in proportion to the increased oxygen requirement, then, with the heat of decomposition of ore remaining negligible on the debit side and the sensible heat in the preheated oxygen from air increasing on the credit side, the net heat requirement for 80 pct metal would decrease rapidly to only about 10-15 pct of the usual value. Actually, however, under the conditions existing in the melting chamber, it is difficult to get even a small increase in air oxidation, and charge ore must be added as the proportion of hot metal increases.

In practice, an extra high or low amount of air oxidation is usually accidental, and it is difficult to find examples of actual heats comparable enough in other respects to illustrate the effect of this variable alone. The three cases in Table 3 are actual heats which approximate this condition. All

three charges were close to 60 pct hot metal, with the same limestone charge, and with certain other differences, largely balanced out between credit and debit items so that the amount of air oxidation (by calculation of oxygen balances) is the chief variable.

Scrap classification as "light" or "heavy" is rather crude, but should conform roughly to the amount of surface area exposed to air oxidation. The large surface of light scrap favors increased rate of heat absorption and thus tends to increase production

TABLE 3—Sixty per cent Hot Metal Heats with Different Amounts of Oxidation by Air

	Oxygen from Air per Net Ton Steel		
	1 31.9 Lb	2 41.9 Lb	3 52.0 Lb
Million Btu per Net Ton Steel			
<i>Credits:</i>			
1. Sensible heat in hot metal.....	0.59	0.59	0.60
2. Heat of oxidation $C + O_2 \rightarrow CO$ and CO_2	0.23	0.20	0.23
Si $\rightarrow SiO_2$	0.22	0.18	0.12
Mn $\rightarrow MnO$	0.05	0.09	0.07
P $\rightarrow P_2O_5$	0.02	0.04	0.02
3. Heats of formation in slag.....	0.04	0.04	0.03
4. Sensible heat in O_2 from air.....	0.02	0.03	0.04
5. Heat of combustion CO, H_2 over slag.....	0.12	0.11	0.12
Total credits.....	1.29	1.28	1.23
<i>Debits:</i>			
1. Heat in steel at tap.....	1.20	1.20	1.20
run-off slag.....	0.11	0.14	0.07
tap slag.....	0.13	0.16	0.16
2. Heat in gases leaving bath.....	0.15	0.15	0.15
3. Heat of decomposition of reduced ore and H_2O	0.43	0.30	0.24
4. Heat of decomposition of limestone.....	0.09	0.09	0.09
5. Heat of reaction CO_2 from stone with C.....	0.06	0.06	0.06
Total debits.....	2.17	2.10	1.97
Net requirement from fuel.....	0.88	0.82	0.74

This variation was probably caused largely by the scrap charge; No. 1 had 100 pct heavy scrap, No. 2 a mixture of light and heavy, and No. 3, 100 pct of what was classified as light scrap. If we assume that these cases cover about the normal range of variation in air oxidation, this factor can alter the net heat requirement by about 20 pct.

PRODUCTION RATE WITH LIGHT OR HEAVY SCRAP

In ordinary open hearth records we get approximate indications of variable air oxidation from factors such as: (1) proportion of light and heavy scrap; (2) amount of extra feed ore required; or (3) carbon at melt. No simple relationship exists for any of these, but they should show a statistical trend with production rate to conform with the thermal effect of variable air oxidation.

rate directly by shortening the melting period rather than indirectly by increased rate of oxygen absorption. On the other hand, light scrap is usually slower to charge, requiring longer periods with doors open into the melting chamber, and this should tend to lessen production rate.

In one group of plant data the percentage of total scrap present in the form of light scrap was an outstanding variable with respect to time of heat; between extremes of 90–100 pct and 0–10 pct light scrap, there was about 60 min., or about 10 pct decrease in average time of heat for the light scrap charges. In 160 heats from another shop, there was a difference of about 25 min. in average time between groups averaging about 8 pct and 37 pct of light scrap respectively. In a group of 275 medium carbon heats, those averaging about 55 pct light scrap showed 25 min.

less than those averaging 19 pct light scrap. In another group of 310 low-carbon heats those averaging 66 pct light scrap had an average time of heat 15 min. shorter than

delay in charging is avoided. From other calculations on various light scrap heats we found that these heats do not always show a high proportion of air oxidation;

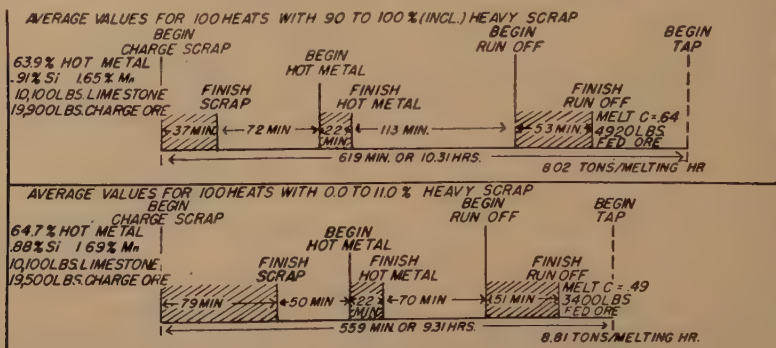


FIG 3—COMPARISON OF THE AVERAGE TIME OF SEPARATE STAGES OF THE HEAT FOR TWO GROUPS OF 0 TO 10 PCT AND 90 TO 100 PCT LIGHT SCRAP CHARGES.

those averaging 42 pct light scrap. In one group of heats there was no positive indication, the difference being only a few minutes in favor of the lighter scrap charge. In spite of this exception, however, the data as a whole are rather conclusive in their indication of around 50 to 60 min. shortening in charge-to-tap time between the extremes of light and heavy scrap charges.

Fig 3 shows average time of separate stages in heats (all close to 82–84 tons per heat) for two groups of 0–10 pct and 90–100 pct light scrap charges. Its significance is in the indication that the light scrap heats were 60 min. faster even though the charging period was more than twice as long.* We are inclined to believe that this results largely from the predominant effect of extra air oxidation, as indicated also by the difference in average feed ore requirement. From the standpoint of production rate, very light and even rusty light miscellaneous scrap is good charging stock if excessive

this may be because the scrap charge melts down so rapidly that there was not sufficient time for absorption of extra oxygen. However, the rapid melting rate in itself probably speeds up production rate directly, to make up for the lack of indirect effect by extra air oxidation. Incidentally, in the heats of Table 3 above, the charge-to-tap time of No. 1 was 12 hr 15 min. where that of No. 3 was 9 hr 25 min.

RELATION BETWEEN EXTRA FEED ORE AND CARBON AT MELT AND PRODUCTION RATE

Shop practice commonly aims at an adjustment of ore in the charge which gives at melt an excess of carbon of around 0.50 pct. When this condition is obtained it usually means that a moderate amount of feed ore, perhaps 10–15 thousand lb, is needed to complete the oxidation. If the carbon at melt is higher, more feed ore is needed; if lower, only a few thousand pounds or no feed ore at all, will be required. When carbon at melt and feed ore requirement are either unusually high or low, one or both of the following factors is normally responsible: 1. The ore charge was incorrectly adjusted to the oxygen requirements

* These heats were all made in furnaces fired with natural gas; foamy slags are more predominant in such practice and certain factors such as the time between hot metal and run-off may not be comparable to a practice using driven fuels. The comparison here is between two groups both under almost identical average practice conditions, however.

of the excess Si, C, Mn and P present in the heat. 2. The amount of air oxidation was above or below its average value.

The first condition has essentially no effect on the net heat requirement of the bath over the whole heat. If the ore charge is too small, melt carbon is high and extra feed ore is required; the melting period is shorter and the refining period is longer. Conversely, with too much charge ore and melt carbon and feed ore low, the melting period is long and the refining period short, but as regards any effect of net heat requirement, we should expect the total time of heat to be essentially the same in both cases. The second factor has a marked effect on net heat requirement, however, as shown in Table 3. Therefore, when an unusually low amount of feed ore and carbon at melt is, partly or wholly, the result of an abnormally high amount of air oxidation during melting, we should expect the total time of melting and finishing to be shorter, resulting in some increase in production rate.

Four groups of heats divided on the basis that the amount of feed ore was above or below average, showed an increase in average time of heat for the high feed ore subgroups of 18, 12, 10 and 0 min., respectively. Since the low feed ore subgroups did not have a longer average charge-to-tap time in any case, these results appear consistent with the considerations outlined above.

These results have helped to explain the rather puzzling fact that out of a number of comparisons of charge-to-tap time between groups of high and low melt carbon heats, some comparisons showed definitely faster production rate for lower melt carbon heats, with about an equal number showing a negligible or no difference. It seems probable that this difference in effect depends on whether the melt carbon variance is mainly caused by factors (2) or (1) above, respectively.

EFFECT OF OXYGEN BLOWING ON NET HEAT REQUIREMENT

In connection with the effect of variable air oxidation, it may be of interest to calculate the effect on net heat requirement of the currently popular innovation of blowing pure oxygen into the bath. In Table 4 the 60 pct hot metal heat in col. 1, with charge ore weight of 26,500 lb gave the oxygen balance shown in Table 3A in col. 1:

TABLE 3A—Oxygen Balance

	1	2
	Total Lb Oxygen Per Heat	
	Regular Practice	Gaseous O ₂ for Part of Ore
<i>Oxygen out:</i>		
Oxygen leaving bath in CO ₂	1,906	(Same as in regular practice)
Oxygen leaving bath in CO.....	6,040	
O ₂ in slags as SiO ₂ from Si.....	1,437	
O ₂ in slags as MnO from Mn.....	665	
O ₂ in slags as P ₂ O ₅ from P.....	418	
Total O ₂ out.....	10,486	10,486
<i>Oxygen in:</i>		
Ore reduced to Fe.....	2,370	304
Ore reduced to FeO in slags.....	811	664
In CO ₂ from limestone.....	3,057	3,057
In water reduced to H ₂	390	311
Total O ₂ in from charge.....	6,628	4,336
Oxygen from gases over bath.....	3,858	3,858
Oxygen from O ₂ gas blown in.....		2,292
Total O ₂ in.....	10,486	10,486

For comparison, we now assume that 12,000 lb of ore are omitted from this same charge, with a proportionate reduction in SiO₂ charged, giving a smaller run-off slag but the same weight of final slag and the same limestone consumption. Assuming also that replacement of the oxygen from this 12,000 lb of ore with pure cold oxygen injected somehow into the bath will leave the same amount of air oxidation, we find from the oxygen balance in Table 3A, col. 2 that about 2300 lb of oxygen will have to be effectively introduced into the bath during one or more blowing periods in the

heat (or about 325 ft³ of pure oxygen per ton of steel).

The heat balances for these two cases are given in col. 1 and 2 of Table 4. The credit items are unchanged but the 2300 lb

net heat requirement. This case may approximate somewhat to an approach to maximum use of oxygen, but this is uncertain, since we have still substituted for only about half the total ore charge.

TABLE 4—Heat Balances for Typical 60 pct Hot Metal Heat, Also with 12,000 lb Ore Substituted by Equivalent Cold Oxygen

	Million Btu Per Net Ton Steel in Bath	
	Regular Ore Practice	Part of Ore Substituted by 2300 Lb Cold O ₂
<i>Credits:</i>		
1. Sensible heat in hot metal.....	0.62	0.63
2. Heat of oxidation, C → CO ₂	0.05	0.06
C → CO.....	0.14	0.14
Si → SiO ₂	0.20	0.21
Mn → MnO.....	0.08	0.09
P → P ₂ O ₅	0.04	0.04
3. Heats of formation in slag 2CaO.SiO ₂ and 3CaO.P ₂ O ₅	0.05	0.05
4. Sensible heat in oxygen from air.....	0.03	0.03
5. Heat of comb. of H ₂ and CO over bath at 20 pct eff.....	0.12	0.11
Total credits.....	1.33	1.36
<i>Debits:</i>		
1. Sensible heat in steel.....	1.23	1.23
Sensible heat in run-off slag.....	0.14	0.10
Sensible heat in tap slag.....	0.16	0.16
2. Heat in gases leaving bath.....	0.16	0.14
3. Heat of decomp.-reduced ore and H ₂ O.....	0.30	0.11
4. Heat of decomp. of limestone.....	0.08	0.09
5. Heat of reaction CO ₂ and C → 2CO.....	0.05	0.06
Total debits.....	2.12	1.89
Net requirement from fuel.....	0.79	0.53
Wt. of steel in bath.....	86.0 net tons	83.5 net tons

gaseous oxygen substituted for 12,000 lb of ore (out of the original 26,000 lb) decreases the heat in slag and especially the heats of decomposition of ore and its included water content to reduce net heat per ton from 790,000 to 530,000 Btu, a reduction of 33 pct. Ore saved amounts to 6 tons, but there is a resultant loss of 2.5 tons of finished steel. For a probable oxygen consumption of 28–35 lb per ton we obtain a probable fuel saving of at least 20–30 pct and it would appear probable that rate of production would increase by about 30 pct or more. These gains would be balanced against the cost of oxygen plus the lower iron recovery from reduced ore and any increased labor and refractories costs incident to such treatment. We give this comparison merely to indicate the relationship between oxygen treatment and

PRODUCTION RATE VS. CHARGED LIMESTONE

Extra limestone in the charge causes a number of changes in the thermal balance; more slag is formed, more reaction between CO₂ from stone and carbon and less oxidation by ore occurs, besides the increased heat required to decompose the limestone. The net effect, being a little complex, can best be illustrated by heat balances of comparable heats varying in amount of charged stone per ton of steel. The four heats in Table 5 are not exactly comparable, but are nearly enough so that the amount of stone charged is by far the biggest variable. On the debit side, we have increasing heat to decompose stone, (item 4), more heat absorbed by the reaction CO₂ + C → 2CO during the lime boil, (item 5), increased heat content in slag

(item 1b), but less heat absorption by net ore reduced, (item 3; for heat 1 this is small, but this is because the amount of silicon charged was much lower, so that item 2b

charge of 82 and 105 lb per ton respectively, the average time of heat was about 54 min. longer in the high limestone group; the distribution here however was such as to make

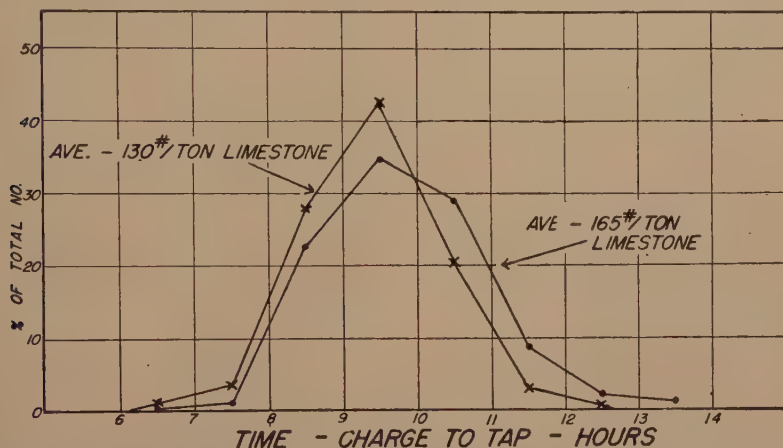


FIG 4—FREQUENCY DISTRIBUTION OF THE TIME FROM CHARGE TO TAP OF 350 HEATS DIVIDED INTO TWO NEARLY EQUAL GROUPS, WITH 130 AND 165 LB OF CHARGED LIMESTONE PER TON OF INGOTS, RESPECTIVELY.

on the credit side is also much smaller). On the credit side, since more carbon is oxidized by limestone, the amount remaining to be oxidized by air and ore is less and this credit item (2a) is less with larger stone charge. The total indicated effect on net heat requirement of about 20 pct is large enough so that it should have a noticeable effect on production rate.

It is difficult to find groups of heats differing in limestone charge without some other variable present to complicate the picture; but we finally found two statistical groups, comparison of which apparently shows a true effect of stone charge. The best of these was a group of 350 heats which divided almost equally into two subgroups with 107–135 lb and 157–178 lb respectively of charged limestone per ton ingots. The frequency curve of charge-to-tap time for each of these two subgroups is shown in Fig 4; the average time of heat was about 24 min. longer for the high lime group. In a similar comparison of heats between groups with an average stone

us suspect that the true effect of the stone charge variation was somewhat less, probably 30–40 min. Thus in these two instances, the probable effect on production rate is only about 5 pct, for differences in limestone charge which should affect the net heat requirement by about 8–10 pct, according to Table 5. However, such a qualitative check, which is about all that can be expected from such data, is enough to confirm the effect on production rate indicated by the thermal changes with higher stone charges.

Stirring produced by the lime boil after the ore boil has ended helps to speed up heat flow into the bath, and thus probably neutralizes part of the thermal effect of the heavier limestone charge. This is probably especially true in any comparison between limestone and all-burnt-lime charges. We have calculated the balance for a hypothetical heat with the same charge as in case 1 of Table 1 (78 pct hot metal), except that equivalent burnt lime was substituted for the limestone charge (which

was 117 lb per ton) and the weight of charge ore was increased enough to compensate for the oxidizing effect of the limestone, assuming that the amount of air oxidation would remain the same. Indicated net heat requirement was reduced from 0.76 million (Table 1) to 0.67 million

time of the latter was 20, 23 and 40 min. longer, respectively. A large part of this difference is probably related to an increased net heat requirement, which is difficult to estimate with any degree of accuracy from data available at present. Heats needing extra feed lime usually have

TABLE 5—40-44 pct Hot Metal Heats with Different Amounts of Charged Limestone

	Lb Limestone per Ton Steel			
	(1) 118 Lb	(2) 133 Lb	(3) 171 Lb	(4) 190 Lb
Million Btu per Net Ton Steel				
<i>Credits:</i>				
1. Sensible heat in hot metal.....	0.40	0.43	0.44	0.41
2a. Heat of oxidation $-C + O_2$ to CO and CO_2	0.13	0.13	0.11	0.10
2b. Si to SiO_2	0.07	0.14	0.13	0.15
2c. Mn to MnO	0.05	0.05	0.07	0.06
2d. P to P_2O_5	0.03	0.01	0.03	0.03
3. Heat of formation in slag.....	0.02	0.03	0.03	0.03
4. Sensible heat in oxygen from air.....	0.03	0.02	0.03	0.03
5. Heat of combustion CO , H_2 over slag.....	0.08	0.09	0.09	0.09
Total credits.....	0.81	0.90	0.93	0.90
<i>Debits:</i>				
1a. Heat in steel at tap.....	1.20	1.19	1.19	1.21
1b. tap slag.....	0.13	0.15	0.20	0.22
2. gases leaving bath.....	0.10	0.10	0.10	0.11
3. Heat to decompose reduced ore and H_2O	0.03	0.14	0.13	0.09
4. Heat to decompose limestone.....	0.09	0.10	0.13	0.14
5. Heat of reaction CO_2 from stone with C.....	0.05	0.06	0.08	0.09
Total debits.....	1.60	1.74	1.83	1.86
Net requirement from fuel.....	0.79	0.84	0.90	0.96

Btu per net ton. This indicated reduction of about 12 pct has not been reflected in equivalent gain in production rate in tests on burnt lime charges, though these tests may not have been complete enough to show accurately the true effect of burnt lime substitution. However, especially with low to medium limestone charges, stirring and resulting faster heat flow may very largely offset the increase in net heat requirement.

The production rate of heats with extra feed of burnt lime or limestone tends to be lower than that of heats requiring no such feeds during the finish melting or refining periods, independently of variations in charged limestone. In three groups of heats, comparison of those with no feed lime with those requiring some extra lime (averaging 22-2500 lb on heats of 130-145 tons), showed that the average charge-to-tap

a higher silicon charge and a larger slag volume, so that the net requirement probably averages 5 to 10 pct larger. Part of the decreased production rate on such heats may be related to delays in working S or P, or others, but the increased heat requirement of the larger slag volume is also involved.

Fig 5 is included merely to illustrate the cumulative effect of several of these variables in the charge on time of heat. Group A has a lower limestone charge with none or only a small amount of cold pig and no extra lime feed. Group B has a higher limestone charge, a larger average amount of cold pig, and required extra additions of lime. We have not attempted a complete statistical study such as would show the total effect of charge variables, but have done only enough to indicate that they are largely independent and thus may combine

to cause a rather wide variation in production rate on individual heats, as illustrated in Fig 5.

POSSIBILITIES IN CONTROLLING OR INCREASING PRODUCTION RATE

A few other possible variables influencing production rate through variation in net

decreasing the average time of heat, any improvement in control over its variability would help, in most shops, to lessen the frequent occurrence of "bunched-up" furnaces with so many heats ready to tap at so nearly the same time that normally adequate charging and pouring facilities are taxed beyond their capacity and poorer

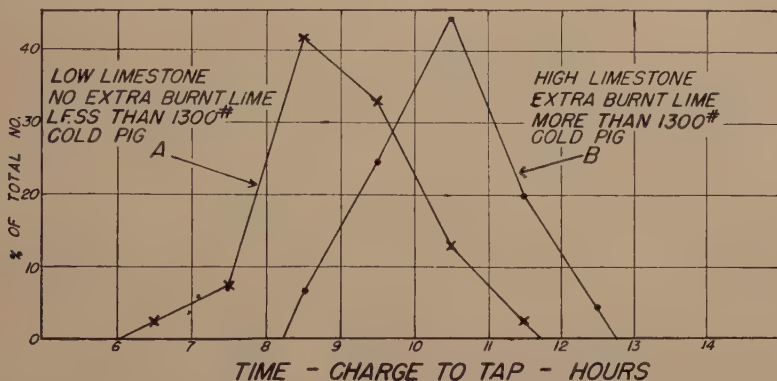


FIG 5—FREQUENCY CURVES SHOWING CUMULATIVE EFFECT OF THREE FACTORS, AS NOTED, ON TIME FROM CHARGE TO TAP.

heat requirement, such as hot metal temperature and total slag volume, probably have some small effect, but are difficult to trace from ordinary production or metallurgical records. Those discussed above represent the main variables of this class. As noted earlier, we have used statistical comparisons of actual data merely to indicate that variations in the net heat required do give approximately the expected effect on production rate. More exhaustive statistical work would show more exactly the cumulative effect of these "thermal variables," but even from our comparisons of simple frequency curves we can estimate that out of a usual 4 to 5 hr variation in charge-to-tap time in any large group of similar heats, about $1\frac{1}{2}$ to $2\frac{1}{2}$ hr, or something like 35-50 pct, at least, may be caused simply by variation in the net heat which must be poured into the bath to produce a batch of steel and slag ready for tap of block.

In addition to the obvious advantage of

practice as well as furnace delays may result. Many of the underlying causes are accidental and not entirely avoidable, but as soon as a furnace begins to get out of step with its ideal time schedule, this tendency can be offset by proper charge variation to gradually bring it back into line. For example, if it gets too fast, it can be fed with more cold pig and more heavy scrap until it is back on its regular schedule.

Some appreciable gain in average production rate may also be possible in certain shops by methods such as: 1. Cutting down still further the average amount of cold pig charged in hot metal shops. 2. Diverting more heavy scrap to cold charge and low-percentage-hot metal shops where blast furnace metal is more expensive, and using relatively more light scrap in "cheap hot metal" shops, or any other means that will increase air oxidation in the furnaces of such shops. 3. Further decreases in limestone charge in some shops to give slag of

minimum basicity ratio (2.0-2.5) in all heats where this is possible. 4. Cutting down SiO_2 and H_2O content of charge ores, 2475°F, which is about as high as we could normally hope to attain, the net heat requirement would be less by about 10 pct

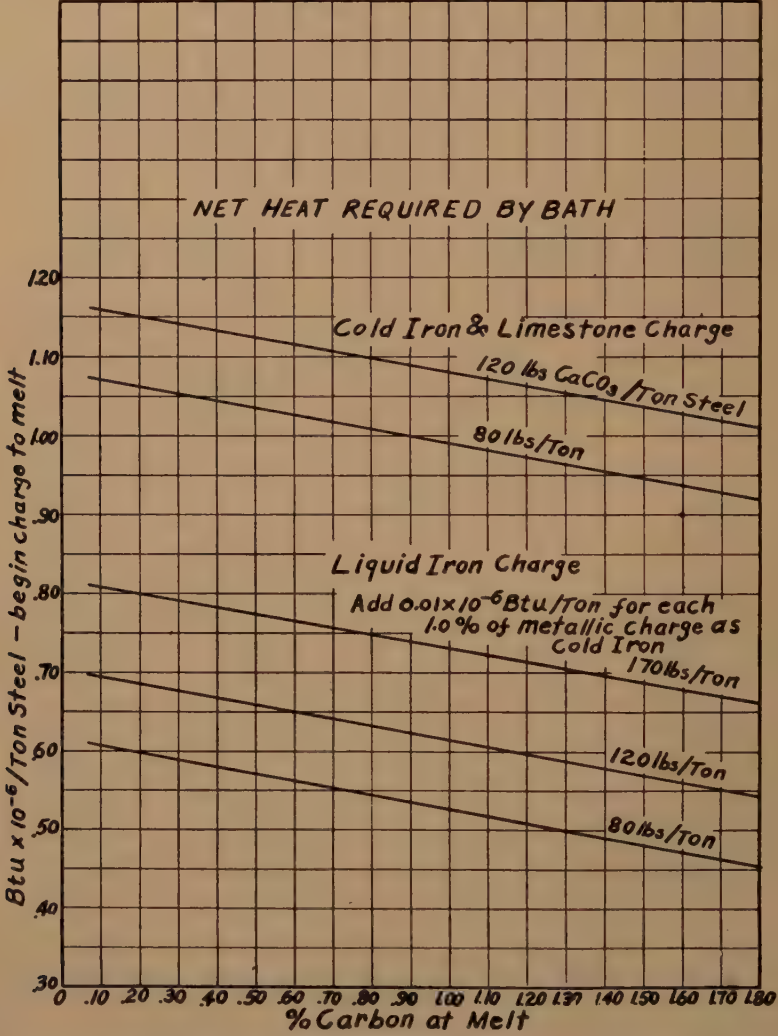


FIG 6—CHART OF APPROXIMATE NET HEAT REQUIREMENT OF BATH (NET USEFUL HEAT SUPPLIED BY FUEL) PER TON OF STEEL UP TO END OF MELTING PERIOD.

silicon content of iron and lower SiO_2 in heat 3 (with 78 pct hot metal) and by from other sources to give minimum slag volumes. about 3.5 pct in heat 1 (40 pct hot metal).

Some advantage is possible from higher temperature of the hot metal entering the furnace, but the effect is not very large. In Table 2, the hot metal temperature assumed was 2275°F; if this were increased to

NET HEAT REQUIREMENT FROM CHARGE TO MELT

From the point of view of fuel combustion and net furnace efficiency, the refining period of the heat is relatively unimportant

because the net heat in this period is usually only a small part of the total and is determined largely by metallurgical factors. Usually about 75 to 90 pct of the total net heat has been absorbed by the time the heat is melted and it is in this period that factors affecting furnace efficiency, such as rates of fuel and air input and flame intensity, have their main influence. It is therefore of occasional usefulness to the fuel engineer to be able to estimate the useful heat absorbed up to melt in a single heat, or at least in a small group of heats.

We have made calculation for a rather large number of actual heats (about 40-50) to obtain the net heat absorbed at melt, assuming that the bath temperature just after melt corresponds to a small, constant superheat (90°F) above the iron-carbon liquidus temperature for the given melt carbon. It was found that these values could be represented reasonably well in terms of: melt carbon, lb limestone per ton of steel, and per cent cold iron in metallic charge.

There was one other fairly important variable, namely, the amount of air oxidation. This value is difficult to calculate, whereas those above can all be obtained easily from ordinary open hearth records. By correcting the values to an average of 40 lb oxygen per ton steel absorbed from gases, the lines in Fig 6 were found to

represent the values of net heat reasonably well (to within 5-10 pct). For example, in a heat with 140 lb CaCO_3 per ton in charge, no cold pig, and 0.60-pct C at melt, net heat with normal air oxidation is about 0.70 million Btu per ton steel.

We are hesitant about presenting this chart because it is at best somewhat approximate and because values for any one heat may give still larger errors (10-20 pct) mainly because the air oxidation is much below or above the above average value. However, it does help to picture the main variables. Also, it is frequently useful in fuel efficiency calculations, since the approximate useful heat may be obtained easily from the open hearth heat records, and net furnace efficiency may be determined if fuel readings "at start charge" and "at melt" are available. The uncertainty in such calculations may be large for one single heat but is probably small enough for many practical purposes when using averages of groups of 5-10 heats. (The upper lines for all-cold charges would be some 10 pct lower with burnt lime charges; we did not happen to have enough good data for calculations under such conditions.

REFERENCE

1. "Basic Open Hearth Steelmaking." AIME, Physical Chem. of Steelmaking Comm. N. Y., 1944, Chap. XV, 456-65.

Structure, Segregation and Solidification of Semikilled Steel Ingots

BY MICHAEL TENENBAUM,* MEMBER, AIME

(Chicago Meeting Oct. 1947)

THE importance of semikilled steel as a high tonnage grade has long been recognized. The increasing severity of the applications for which semikilled steel is used makes it desirable to obtain further information regarding the features of open hearth practice and ingot structure that can affect steel performance in subsequent rolling and fabricating operations. Accordingly, an investigation is being carried out studying the structure of various types of semikilled steel ingots. This paper reviews some of the observations made and information gathered in this investigation.

By definition, semikilled steel may be considered to include all nonrimming steels in which the natural shrinkage occurring during ingot solidification is offset to an appreciable degree by gas formation. Accordingly, this type of steel includes the entire range intermediate between rimmed and fully killed steel. The resultant ingot structures range from those of steels that have been capped to suppress a weak rimming action to those steels that have been killed in the furnace or ladle to the extent that no mold deoxidizer is required.

A survey reported to the 1946 AIME Open Hearth Conference¹ reviewed the practices being used at 28 major plants for the deoxidation of semikilled steel. It was found that most plants divide the deoxidizing additions between the ladle and the mold—many of the plants adding only minor amounts of deoxidizer to the bath or

none at all. Silicon, aluminum and titanium were the only elements used for ladle and mold deoxidation. Mold deoxidizers were added as capping additions or as uniformly fed additions. Several practices were reported in which the steel was deoxidized in the ladle to the extent that little or no mold deoxidation was needed. No reference was made to grades capped by using special mold designs or special closures over the top of molds. Accordingly, specific examples of this type of practice will not be considered in this paper.

It appeared from this survey of deoxidation practice that semikilled steel can be divided into three types, namely, capped semikilled, in which aluminum is added near the end of pour or after shut-off, intermediate semikilled steels, in which aluminum is fed uniformly throughout the pour, and semikilled steels requiring no mold deoxidation.

In an attempt to cover the ingot structures obtained by the range of practices reported in the preceding survey, three series of experimental heats were made using increasing amounts of aluminum, silicon and titanium for ladle deoxidizers. The ladle deoxidizers were added as stick aluminum, 50 pct ferrosilicon and 20 pct ferrotitanium (4 pct carbon), respectively.

Two methods of studying ingot structures were used. Ingots were removed from production, burned longitudinally and machined to allow observation of the central pipe and coarse blowholes. During the machining operation much of the finely porous subsurface structure was obliterated. Accordingly, observations were also made

Manuscript received at the office of the Institute July 10, 1947. Issued as TP 2273 in METALS TECHNOLOGY, September 1947.

* Metallurgist, Inland Steel Co., East Chicago, Ind.

¹ References are at the end of the paper.

on smaller sections burned from the outer edges of the same split ingots. These sections were machined, polished, and etched, bringing out clearly the subsurface structure. To supplement the information obtained on the ingots, observations were also made of deep etched slab sections from all experimental heats.

The split ingot faces were also drilled intensively to provide samples for chemical analysis. The results of segregation studies based on these analyses and sulphur prints will be covered later.

REVIEW OF LITERATURE

While a considerable volume of material has been published regarding ingot structure, a very limited amount of information is available dealing directly with semikilled steel. Accordingly, many of the basic concepts regarding this type of steel have been derived by applying the fundamentals of solidification, segregation, and gas formation that have been developed in studies of rimmed or killed steels.

The comprehensive paper by Hultgren and Phragmen² includes an extensive bibliography that can be used for reference in any study of ingots in which gas is evolved. In the Second,³ Fourth,⁴ Fifth,⁵ and Sixth⁶ Reports on the Heterogeneity of Ingots, examples of several types of semikilled steel split ingots are presented. In the marginally deoxidized ingots of these reports it was shown that subsurface blowholes form on certain types of semikilled steels and that these blowholes can originate within the outer quarter inch of the ingot. The zone in which these holes existed was negatively segregated. The subsurface zone was located either throughout the length of the ingot or near the top, depending on the nature of the liquid steel deoxidation. Various top central and Λ segregate patterns on semikilled steel ingots were shown in the British reports.

The classic work of Hultgren and Phrag-

men² on rimmed steel ingot structure can be profitably applied to considerations of semikilled steels. This work set forth the fundamental factors governing gas formation and the mechanisms determining observed features of ingot solidification and segregation. Hultgren and Phragmen's clear demonstration of the primary roles of carbon and oxygen in gas evolution from rimming steel ingots can be applied with few modifications to the freezing of any ingot that tends to evolve observable amounts of gas during solidification. Following are some features of the Hultgren and Phragmen paper that can be applied to solidification of semikilled steels:

1. The gas evolved from rimming ingots is largely CO resulting from the carbon-oxygen reaction. The rate of gas evolution is necessarily affected by the carbon and the oxygen contents and the resultant gas pressure.

2. Gas bubbles that form during the solidification of the outer rim can be swept away by motion of the liquid. Moreover, bubbles can rise out of the seat in which they form simply by growing large enough to cause the gas to "float away."

3. Blowholes appear in the solidified ingot when the amount of gas formed is not great enough to result in the vigorous motion of the liquid metal needed to sweep gas from the original bubble seat. The exact shape of the residual blowhole depends considerably on the effectiveness of the sweeping action.

4. The reaction between the CO in gas bubbles and the carbon and oxygen of the surrounding liquid probably proceeds near equilibrium.

5. Two distinctly different mechanisms can affect the thickness of the skin between the outer surface and the subsurface blowholes. On low carbon heats vigorous gas evolution begins immediately with the result that the gas formed is swept away leaving a solid negatively segregated skin. On the higher carbon lower oxygen heats,

the rapid chilling of the skin completely suppresses the weak tendency toward gas formation. In the absence of gas formation, there is little or no disturbance of the normal freezing procedure and columnar dendrites are formed in the skin zone.

6. The casting rate can influence skin thickness. The exact nature of this effect depends on whether the skin is formed under conditions of rapid gas evolution at the freezing interface, or whether the skin solidifies under conditions favoring suppression of gas formation.

7. In ingots with varied rim hole depths, freezing can proceed more rapidly at one ingot level than at another. Symmetrical deformation lines that are evident in sulphur prints of split ingots were described as having resulted from differences in the freezing rate at various levels in the ingot.

All the top cast experimental ingots that were studied in the Hultgren and Phragmen paper weighed less than 1500 lb and were poured in big-end-up molds. Accordingly, the observations and interpretations made in their paper should be carefully considered before applying them to the large sized big-end-down ingots that prevail in the manufacture of semikilled steel.

In earlier papers on ingot structures,^{7,8,9,10,11,12} some features were cited that have apparent application to the following aspects of the solidification of semikilled steel:

(1) The possible entrapment of gases below the frozen top surface of an ingot,^{7,11} (2) the effect of aluminum deoxidation on gas evolution,⁸ (3) differences in the skin thickness and position of the blowholes at different ingot levels,⁹ (4) the effect of casting rate on skin thickness and nature of the skin, and the effect of oxygen content on the skin thickness.^{10,12}

THEORETICAL CONSIDERATIONS

Surveys of semikilled steel practices show that manganese, silicon, titanium and alu-

minum are the only elements used for bath, ladle, or mold deoxidation. These can be added as ferroalloys or as commercial forms of the individual deoxidizer.

The curves of Fig 1, taken largely from the work of Chipman,¹⁷ compare the deoxidizing power of the elements, manganese, silicon, titanium, aluminum and carbon at 2900°F. The solid lines in Fig 1 have been determined experimentally. The dotted lines have been calculated. Unpublished data obtained on low carbon steels containing aluminum and titanium verify roughly the approximate level of the titanium line.

Fig 1 indicates that it would not be practical to deoxidize semikilled steels using manganese as the sole deoxidizer since prohibitively large percentages would be required to suppress the carbon-oxygen reaction.

Somewhat the reverse situation appears to be true in the case of aluminum and titanium. With any significant residual percentage of either element in the steel, the deoxidation would be so complete that the primary gas forming reaction would be entirely suppressed, with the result that considerable piping would occur during freezing.

Silicon is peculiar in that its deoxidation curve closely approaches that of carbon in the analysis ranges normally encountered in semikilled steels. It is conceivable, therefore, that with closely controlled additions of silicon it would be possible to produce ingots in which only the initial gas formation would be suppressed. A large part of the natural shrinkage would be offset by later gas formation. On such ingots sufficient silicon should be added so that the residual oxygen content of the liquid steel in the mold is reduced to a value just below that required to react with carbon at the pressure existing in the top of the ingot. As shrinkage occurs in the ingot with a consequent reduction in pressure, some gas would be evolved. The de-

gree to which this latter process occurred would naturally be reflected in the size of the final pipe cavity.

In addition to the residual percentage of

controlled so as to yield exactly reproducible finishing bath and tapping conditions, it is generally not possible to obtain the desired ingot shrinkage characteristics with

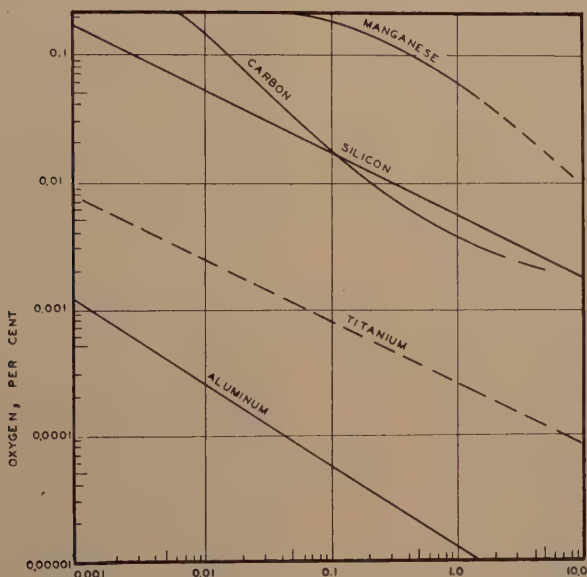


FIG 1—COMPARISON OF DEOXIDIZING POWERS OF CARBON, MANGANESE, SILICON, TITANIUM AND ALUMINUM AT 2900° F. (CHIPMAN).

deoxidizing element present in the liquid steel, certain operating variables would also affect the tendency toward gas evolution. The most obvious of these variables are the height of pour (head of metal), the rate of pour, and the temperature, each of which has a small but direct effect on the carbon-oxygen equilibrium.

In actual practice the delicate balance in liquid steel deoxidation that evidently is required for production of satisfactory semikilled steel ingots is usually obtained by using more than one deoxidizing addition. These deoxidizing additions are most often divided between the ladle and the mold—the bulk of the deoxidation being carried out in the ladle and only minor additions being made to the mold. The size of the mold addition is determined by the appearance of the steel in the mold. Because the open hearth process can not be

a single addition of ladle deoxidizer. The practice of making a small final deoxidizing addition based on the behavior of the liquid steel in the molds offers a simple method of adjusting for variations in both the physical condition of individual heats as well as for differences in the steel analysis.

SEMIKILLED STEEL OPEN HEARTH PRACTICE

A substantial proportion of semikilled steel tonnage reported in the AIME survey¹ is actually a form of capped steel. In this practice the steel is deoxidized very lightly in the ladle and the final gas formation suppressed by capping the ingot with aluminum. The main difference between the practices in the various plants is the type of ladle deoxidizer used. The three

types used were 50 pct ferrosilicon, aluminum, and 20 pct ferrotitanium.

In most studies of semikilled steel which have been published, it is pointed out that the ideal ingot structure is one in which all initial gas formation is suppressed and all shrinkage is offset by blowhole formation occurring later in the freezing process. To accomplish the marginal deoxidation needed for this practice it is necessary that an

three groups mentioned previously (see page 108), namely: 1. Capped semikilled steels. 2. Intermediate semikilled steels requiring small mold additions. 3. Semikilled steels requiring no mold deoxidation. Essential data on the experimental ingots used for this report are given in Table 1. All ingots were poured in $24\frac{1}{2} \times 43$ in. big-end-down molds. Ingot weights were all about 20,000 lb. With the exception of

TABLE 1—Data on Experimental Ingots

Ingot	A	B	C	D	E	F	G	H	I	J	K	L
Analysis, per cent												
Carbon.....	0.17	0.18	0.21	0.16	0.17	0.17	0.17	0.17	0.16	0.19	0.20	0.18
Manganese.....	0.43	0.42	0.39	0.43	0.45	0.45	0.40	0.47	0.38	0.41	0.48	0.40
Phosphorus.....	0.009	0.009	0.010	0.010	0.013	0.013	0.010	0.011	0.011	0.009	0.010	0.009
Sulphur.....	0.025	0.023	0.025	0.023	0.021	0.021	0.032	0.025	0.034	0.032	0.026	0.025
Silicon.....	0.01	0.01	0.01	0.01			0.11	0.10	0.04	0.01		
Titanium.....			0.003		0.010	0.010					0.006	0.006
Furnace additions, pounds per net ton												
Spiegel.....	7	7	7	7	7	7	7	7	7	7	7	7
Ladle Additions, pounds per net ton												
50 per cent Ferro- silicon.....	0	0	0	1.0	0	0	5.0	5.4	3.2	0	0	0
Shot Aluminum.....	0.4	0.4	0	0	0	0	0	0	0	1.6	0	0
20 per cent Ferro- titanium.....	0	0	1.0	0	11.7	11.7	0	0	0	0	8.5	12.5
Fed Aluminum, pounds per net ton.....	0	0	0.1	0	0.08	0	0	0	0.2	0	0	0
Capping aluminum, pounds per net ton.....	0.6	0.3	0.5	0.3	0	0.1	0	0	0	0	0.4	0.15
Capping time.....	After Shut Off	After Shut Off	Before Shut Off	Before Shut Off		After Shut Off					After Shut Off	After Shut Off
Pouring Temper- ature, Degrees Fahrenheit....	2950	2810	2920	2900	2890	2890	2880	2890	2860	2930	2910	2910

element be used whose deoxidizing power closely approaches that of carbon—for example, silicon. It has been explained^{13,14} that even when sufficient silicon is added to prevent carbon and oxygen from reacting during early solidification, the segregation of the gas forming elements during freezing and the reduced pressure resulting from shrinkage would be sufficient for the formation of the blowholes needed to offset pipe.

EXPERIMENTAL INGOTS

In this discussion, semikilled ingot structures have been divided into the

E and *F*, each ingot shown in Table 1 was taken from a separate heat of steel. Samples for chemical analysis were obtained from a dip test taken on the preceding ingot. These analyses checked closely the regular ladle analyses from the same heat. Temperatures were read with an optical pyrometer, using an 0.4 emissivity coefficient.

INGOT STRUCTURE

Capped Semikilled Steel

An example of the central structure resulting from the practice of capping semikilled steel is shown in ingot *A* which



FIG 2—STRUCTURE OF SPLIT INGOT A. LADLE DEOXIDATION: 0.4 POUNDS AL PER NET TON INGOTS. MOLD DEOXIDATION: CAPPED AFTER POUR WITH 0.6 POUNDS AL PER NET TON INGOTS. TEEMING TEMPERATURE: 2950°F. ORIGINAL MAGNIFICATION 0.1. REDUCED APPROXIMATELY ONE-FIFTH.



FIG 3—SUBSURFACE STRUCTURE OF INGOT A. ORIGINAL MAGNIFICATION 0.3. REDUCED APPROXIMATELY ONE-FIFTH.

has been split and photographed in Fig 2. The ingot was capped with 6 lb of aluminum about 15 sec after finish pour. Actual deoxidation was effective only within the

of the ingot is the only indication of actual shrinkage during solidification.

In machining the split surface of ingot *A*, the actual subsurface porosity has been

Yield Position, pct: *a*, 90; *b*, 81; *c*, 72; *d*, 63; *e*, 54; *f*, 45; *g*, 36; *h*, 27; *i*, 18; *j*, 9; *k*, 0



FIG 4—DEEP ETCHED SECTIONS OF SLABS ROLLED FROM INGOT ADJACENT TO *A*. ORIGINAL MAGNIFICATION 0.2. REDUCED APPROXIMATELY ONE-HALF. DEOXIDATION IDENTICAL TO INGOT *A*.

upper 5 in. of the ingot. This deoxidized zone appears as a solid bulged cap above the upper central blowhole area. The role of the cap in suppressing gas formation is evident. Despite the fact that the pouring temperature was well over 2900°F, no large central pipe cavity exists in ingot *A*, the shrinkage having been largely offset by the formation of blowholes. A narrow central parting zone in the top central part

partly filled. To show the subsurface structure, sections cut from the top, middle and bottom of one edge of the same ingot were polished and etched in ammonium persulphate. The smaller sections showing the subsurface structure are photographed in Fig 3. Near the bottom of ingot *A* there was apparently some suppression of gas formation. A relatively strong tendency toward gas formation is indicated by the

porous structure in the middle section. Some of the blowholes approach closely the outer ingot surface. The contracted and discontinuous sections of the blowholes indicate gas evolution at the middle ingot height during the freezing of the outer two inches. It is likely that formation of the inner row of subsurface blowholes is responsible for the early bulging of tops of semikilled steel ingots. The solid deoxidized cap of the split ingot appears as the solid section in Fig 3.

The structure of ingot *A* is reflected in deep etched sections of slabs rolled from an identically treated adjacent ingot. Deep etched slab sections from eleven consecutive yield positions* are shown in Fig 4. The shallow, grayish streaks that are especially prominent throughout the subsurface zone above the 27 pct yield position* indicate the location of partly welded subsurface blowholes. While no open pipe is evident, a sharp central segregate line appears at the 72 pct yield position.* The position of this segregate line corresponds to the location of the lower half of the central parting zone of ingot *A* (Fig 2). The discontinuities in the bottom section are the result of fishtail.

The ladle deoxidation used on ingot *B* was identical to that of ingot *A*. Ingot *B*, however, was poured at only 2810°F. (After pouring this heat, a skull of 20,000 lb

remained in the ladle). To cap this cold ingot, 3 lb of aluminum was added after pour. A photograph of the split ingot surface of ingot *B* is shown in Fig 5. The original bulged top of this ingot was flattened slightly during stripping. The photographed surface of the split ingot shows neither a pipe cavity nor a central parting zone. The small, off-centered pocket that is evident near the top of the ingot resulted from enlargement of a concentrated blowhole zone by the action of the burning torch. The location of the subsurface blowholes is shown in smaller sections beside the split ingot photograph. In general, the blowhole distribution is similar to that of ingot *A* (Fig 3). Again the middle section shows the greatest tendency toward gas formation. In several cases, adjacent channels exhibit common contraction patterns, a phenomenon associated with gas evolution during solidification of rimming steels. The general scabby appearance of the middle section is probably a reflection of the low pouring temperature.

Ingot *C* illustrates the structure resulting from a common departure from the recommended capping practice. In teeming this ingot, part of the capping aluminum was added well before completion of pour, and the balance was added just at shut-off. A total of 6 lb of aluminum was added to the mold. A photograph of the split ingot surface is shown in Fig 6. A striking result of early capping with excessive amounts of aluminum is the pronounced central pipe cavity. Paradoxically, a distinct row of blowholes exists in the outer rim. In this case it was possible to bring out the blowhole structure in the machined ingot. The blowhole structure again resulted in subsurface segregate streaks in the rolled slab of the type shown in Fig 4 for ingot *A*. This condition was particularly pronounced in the lower half of the ingot.

Not all subsurface blowholes result in segregate streaks or spots in the outer

* The yield position locates the deep etched section with reference to the percentage of original ingot weight rolled in slab product. The section from the bottom of the product is referred to as the 0 pct yield position and the section from the top of the product is the actual ingot to product yield, expressed in percentage. Thus, in the yield positions shown in Fig 4 for ingot *A*, the 0 pct section was obtained just above the butt crop. (The fishtail evident in the 0 pct section indicates that insufficient steel was cropped from the bottom of this ingot, a condition that ultimately led to the scrapping of the entire bottom slab). The 90 pct section was obtained just below the top crop. Of the original ingot weight 90 pct was rolled into slab product. The slab weight between the adjacent test sections was equivalent to 9 pct of the original ingot weight. Thus the yield positions shown in Fig 4 increase from 0 to 90 pct at increments of 9 pct.

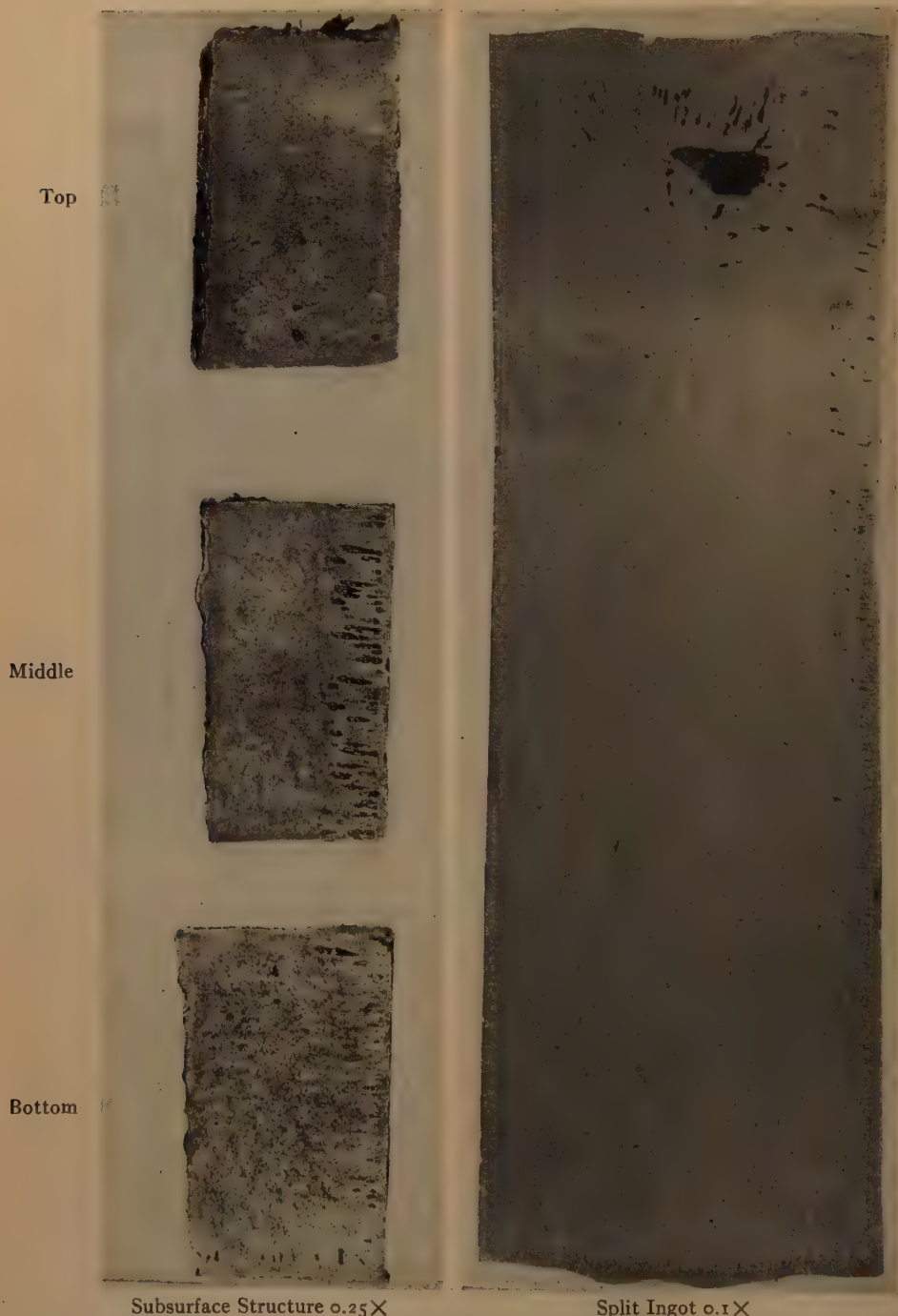


FIG 5—STRUCTURE OF SPLIT INGOT B. LADLE DEOXIDATION: 0.4 POUNDS AL PER NET TONS INGOTS. MOLD DEOXIDATION: CAPPED AFTER SHUT-OFF WITH 0.3 POUNDS AL PER NET TON INGOTS. TEEMING TEMPERATURE: 2810°F. ORIGINAL MAGNIFICATION REDUCED APPROXIMATELY ONE-FIFTH.

slab structure. Under ideal conditions, the blowholes weld completely, yielding a sound unsegregated subsurface structure. An example of this condition is shown in Fig 7 and 8. An excessive amount of aluminum was added early to ingot *D* and, as a result, severe shrinkage occurred. Fig 7 shows the original machined split ingot surface with the open pipe. The original porous subsurface structure is illustrated by sections burned from the edge at the top, middle, and bottom ingot positions. More complete sampling revealed a continuous row of blowholes from the middle to the bottom of the ingot. The blowholes changed gradually from the small rounded shape at the middle to the thin channels near the bottom. It is interesting to observe that in the bottom section of Ingot *D* there is some evidence of blowhole tracers between the main channel and the surface, indicating that gas evolution occurred during the freezing of the outer solid rim. For the most part, the outer rim thickness exceeded one quarter inch.

The macrostructure of slab sections rolled from an ingot adjacent to *D* is shown in Fig 8. The mold deoxidation on this ingot was identical to that of ingot *D*. The soundness of the deep etched subsurface structure is immediately apparent. The original blowholes have been welded completely during rolling. Only scattered evidence of the open pipe remains in the center of the top cut. Evidently, even the shrinkage cavity tended to weld in slabbing the ingot.

Intermediate Semikilled Steels

Intermediate between capped steels and those requiring no mold additions are steels deoxidized in the ladle to the extent that only minor quantities of aluminum are re-

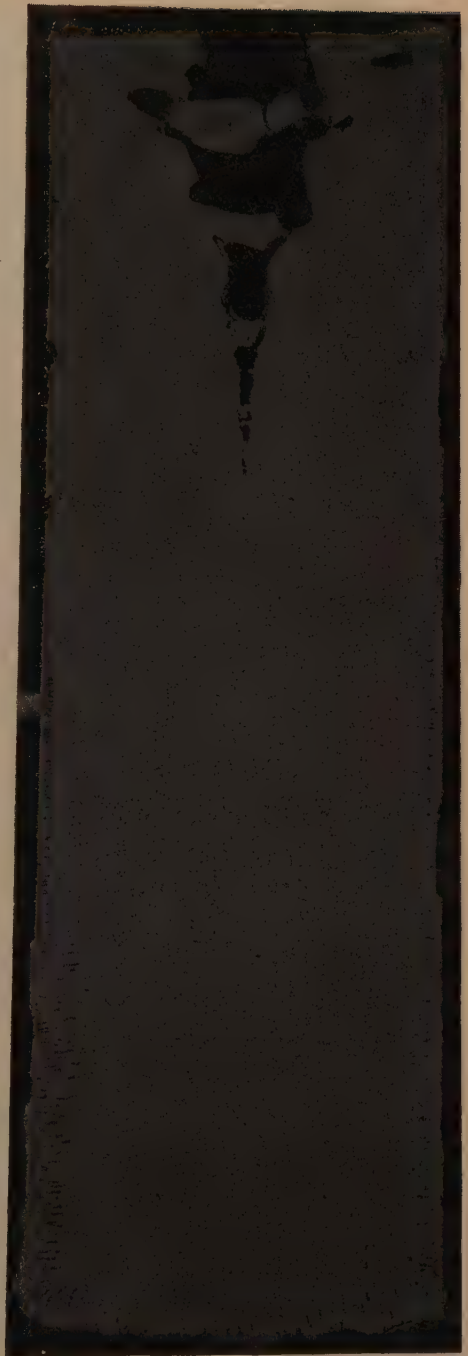
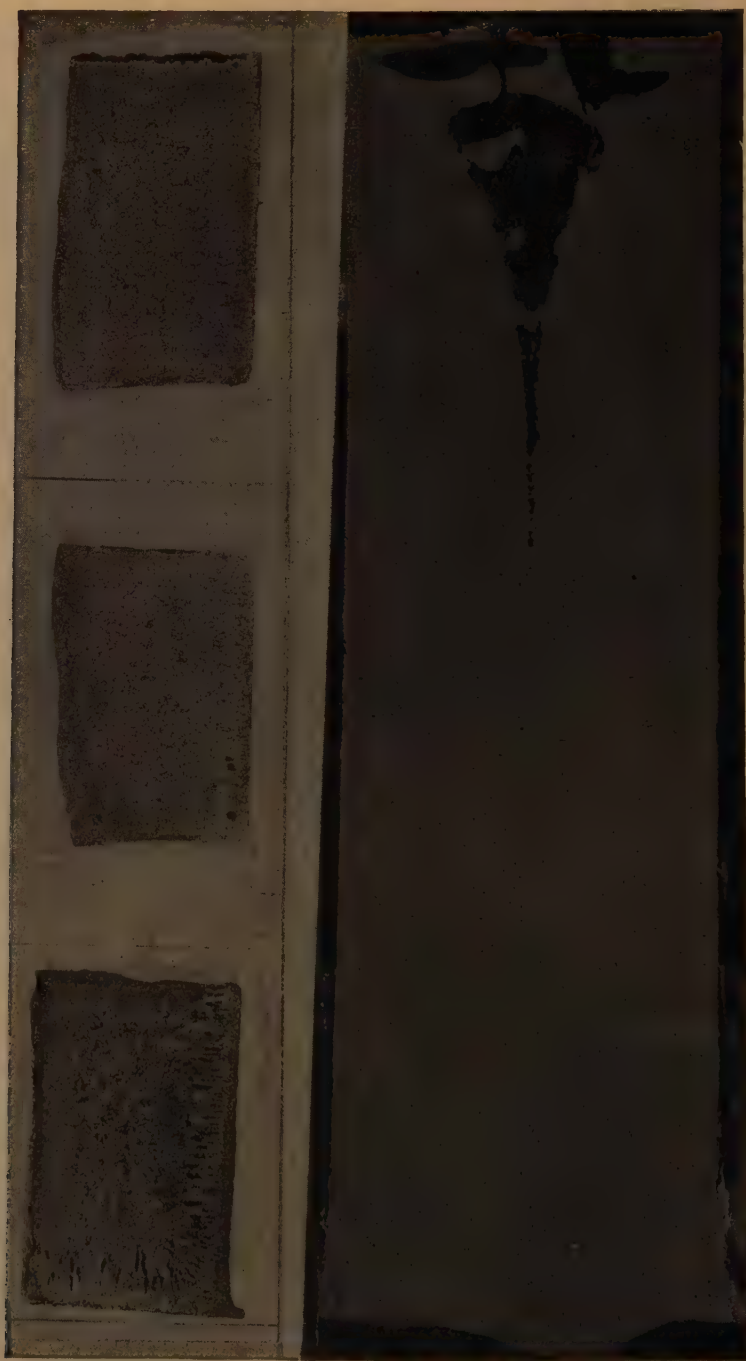


FIG 6—STRUCTURE OF SPLIT INGOT C. LADLE DEOXIDATION: 1.0 POUND FeTi PER NET TON INGOTS. MOLD DEOXIDATION: CAPPED JUST BEFORE SHUT-OFF WITH 0.6 POUND Al PER NET

TON INGOTS. ORIGINAL MAGNIFICATION O.I. REDUCED APPROXIMATELY ONE-FIFTH.



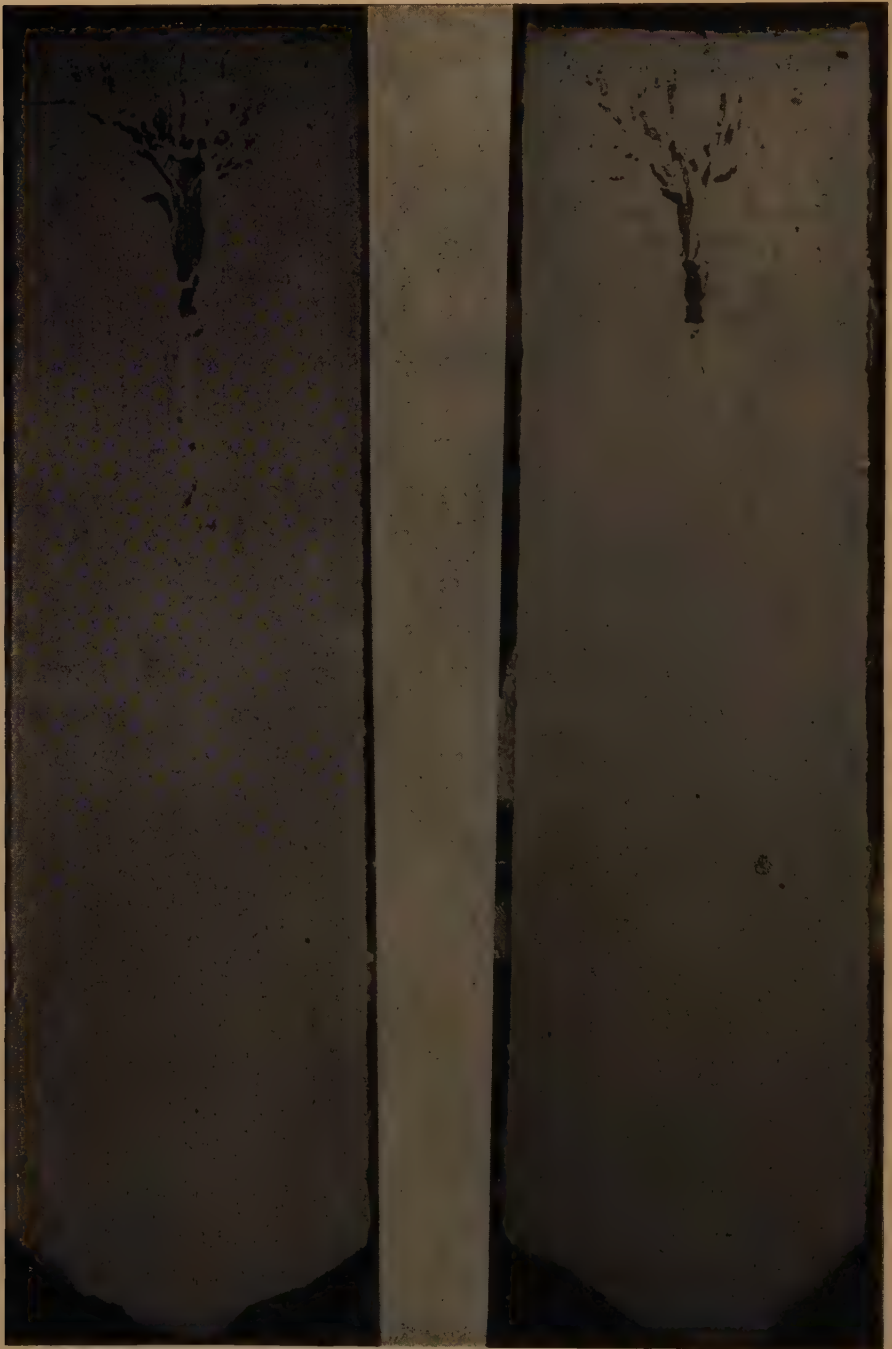
Subsurface Structure 0.25X

Split Ingot 0.1X

FIG 7—STRUCTURE OF SPLIT INGOT D. LADLE DEOXIDATION: 1.0 POUND 50 PER CENT FE-SI PER NET TON INGOTS. MOLD DEOXIDATION: CAPPED JUST BEFORE SHUT-OFF WITH 0.3 POUND AL PER NET TON INGOTS. ORIGINAL MAGNIFICATION REDUCED APPROXIMATELY ONE-FIFTH.



FIG 8—DEEP ETCHED SECTIONS OF SLABS ROLLED FROM INGOT ADJACENT TO D. ORIGINAL MAGNIFICATION 0.25. Reduced approximately one-third. DEOXIDATION IDENTICAL TO INGOT D.



Ingot E

Ingot F

FIG 9—STRUCTURE OF SPLIT INGOTS E AND F. LADLE DEOXIDATION: 11.7 POUND 20 PER CENT FE-TI PER NET TON INGOTS. MOLD DEOXIDATION: INGOT E: 0.08 POUND AL PER NET TON INGOTS ADDED DURING POUR. INGOT F: CAPPED AFTER SHUT-OFF WITH 0.10 POUND AL PER NET TON INGOTS. ORIGINAL MAGNIFICATION 0.1. REDUCED APPROXIMATELY ONE-FIFTH.

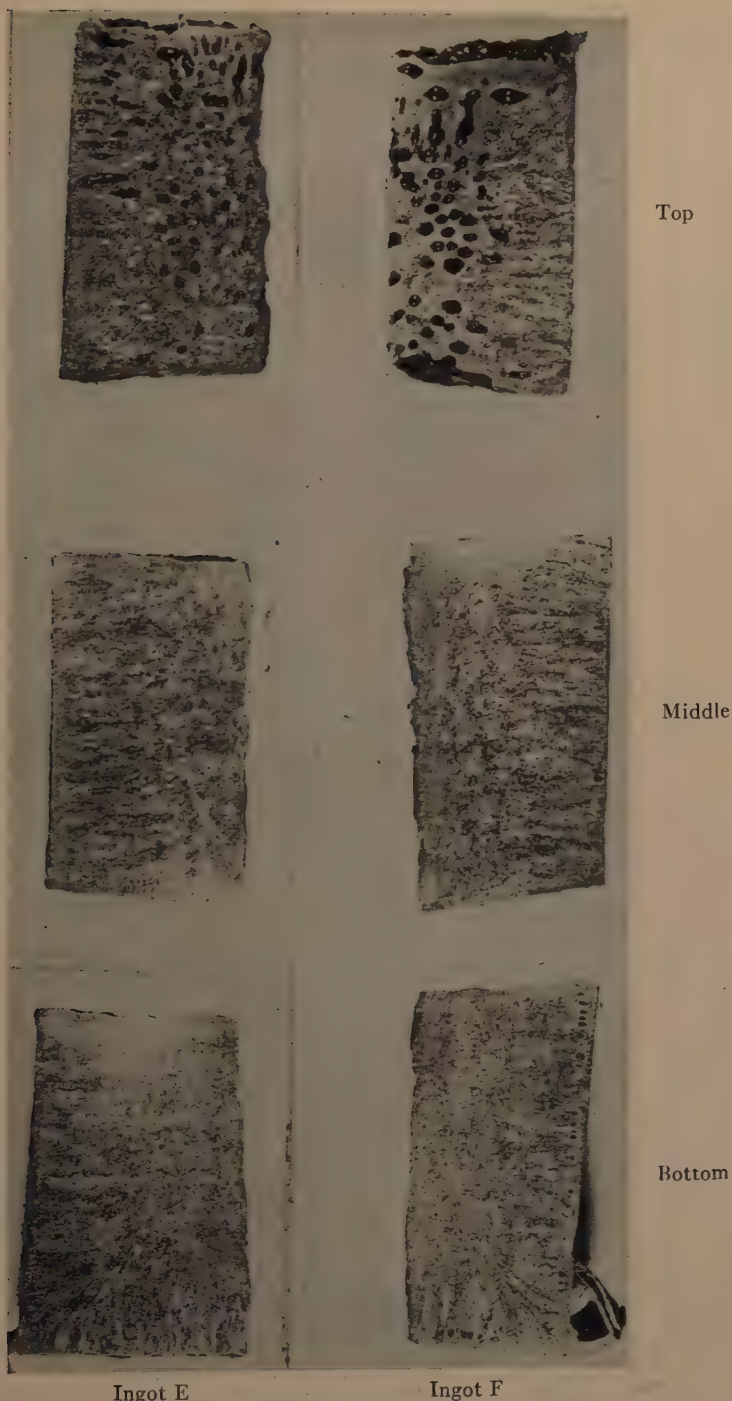


FIG 10—SUBSURFACE STRUCTURE OF INGOTS E AND F. ORIGINAL MAGNIFICATION 0.25. REDUCED APPROXIMATELY ONE-EIGHTH.

quired to suppress gas evolution during ingot solidification. Adjacent ingots of the intermediate type from the same heat are shown in Fig 9. Ingot *E* was deoxidized in the mold by feeding $\frac{3}{4}$ lb of aluminum, while ingot *F* was capped with 1 lb. The subsurface structure of these ingots is shown in Fig 10.

Since all of the aluminum was fed to ingot *E* before pour was complete, there is no evidence of upper crust deoxidation. The combined deoxidizing effects of the ladle and mold additions suppressed most of the gas formation and only a slight bulge can be observed in the ingot top. While no large pipe cavity is evident, there is a definite open zone in the upper central area that apparently is associated with the last phases of ingot solidification.

The subsurface structure of the main body of ingot *E* (Fig 10) appears absolutely sound. The only evident subsurface porosity exists in the top six inches of the ingot. When the porosity of the upper zone extends into the prime ingot yield, a serious checked and seamy condition can result in the rolled slab. An indication of such a seamy condition was observed in the top slab rolled from an ingot adjacent to *E* which was made with identical deoxidation practice. Surface defects of this type have been observed most frequently in conjunction with semikilled steels marginally deoxidized with silicon so that some subsurface gas formation occurs near the top of the ingot.

Because of the small capping addition, the upper crust of the intermediate semikilled steel ingot *F* is relatively shallow and somewhat porous. As shown in Fig 9, the upper central zone is similar to the previous ingot, showing considerable porosity and a narrow central cavity or parting zone. The slight tendency toward gas formation is reflected in a row of small pear-shaped subsurface holes in the middle and bottom section of Fig 9. These blowholes approach very closely the ingot surface.

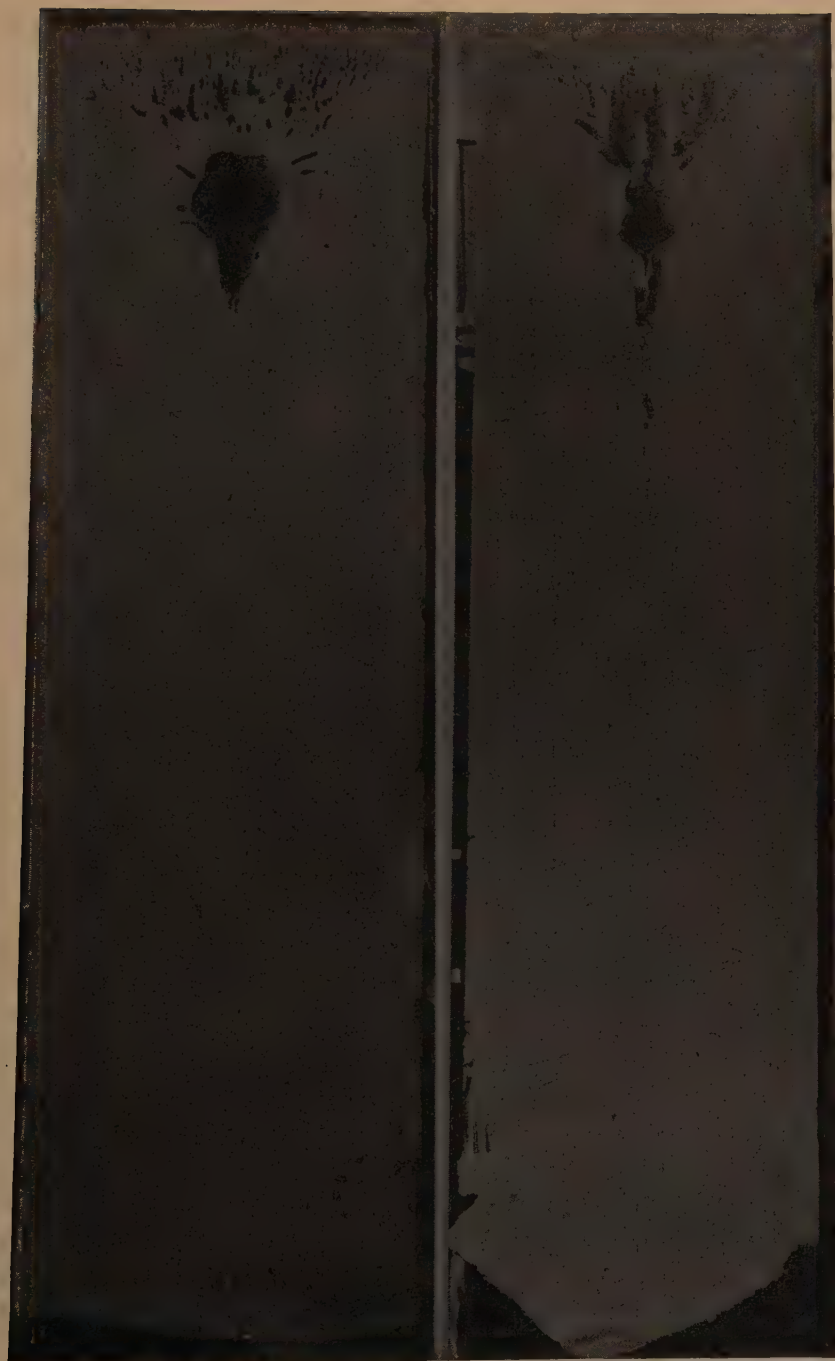
Semikilled Steels Requiring No Mold Deoxidation

It was attempted in this experimental program to make a group of heats where just enough deoxidizer was added to the ladle so that no mold additions would be required. It was found that this condition could be attained by adding $2\frac{1}{2}$ lb per net ton of silicon (added as 50 pct ferrosilicon) or by adding $1\frac{1}{2}$ lb per net ton of aluminum (added as stick aluminum). Residuals of 0.10 pct silicon or 0.020 pct aluminum were required to assure sufficient deoxidation to avoid mold additions.

With as much as 3.6 lb per net ton of titanium (added as 20 pct ferrotitanium), there was still considerable gas evolution in the mold. The residual titanium analysis on the heat with this large addition was only 0.011 pct. Because of the excessive additions required, no heats were made where titanium was the only deoxidizer used.

Fig 11 shows ingots from two heats that were deoxidized with silicon in the ladle to the extent that no mold additions were required. The silicon analysis of ingot *G* was 0.11 pct and that of ingot *H* was 0.10 pct. Both ingots have small shrinkage cavities, the main body of which extends down to about the 75 pct yield position. The balance of the shrinkage was offset by the blow-hole formation that is evident between the pipe cavity and the upper crust. Except for the very top of the ingot, there is no subsurface porosity visible either in the split ingots or the smaller sections. The bright blowholes that can be observed in ingot *H* were exposed during machining. The exceptionally clean surface of these holes indicates that they should weld easily during rolling. Some surface cracks appear in both ingots.

It was found in the study of more completely killed ingots that any decrease in ladle silicon deoxidation, while conducive to decreased shrinkage, would increase the



Ingot G

Ingot H

FIG 11—STRUCTURE OF SPLIT INGOTS G AND H. LADLE DEOXIDATION—INGOT G: 5.0 POUNDS 50 PER CENT FeSi PER NET TON INGOTS. INGOT H: 5.4 POUNDS 50 PER CENT FeSi PER TON INGOTS. MOLD DEOXIDATION: NONE. ORIGINAL MAGNIFICATION 6.1. REDUCED APPROXIMATELY ONE-FIFTH.



FIG 12—COMPARISON OF DEEP ETCHED SECTIONS OF TOP SLABS ROLLED FROM INGOTS G AND I. LADLE DEOXIDATION—INGOT G 5.0 POUND 50 PCT FESI PER NET TON INGOTS. INGOT I 3.2 POUND 50 PCT FESI PER NET TON INGOTS. MOLD DEOXIDATION—INGOT G NONE. INGOT I 0.25 POUND AL PER NET TON INGOTS ADDED DURING POUR. ORIGINAL MAGNIFICATION 0.25. REDUCED APPROXIMATELY ONE-THIRD.

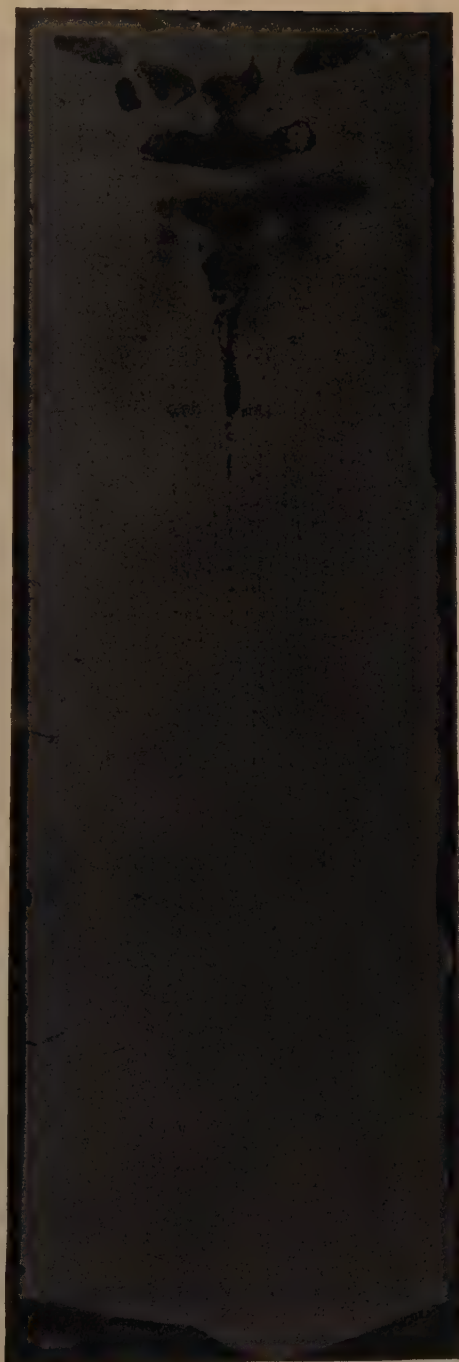
tendency toward subsurface blowhole formation in the top slabs. To illustrate this situation, Fig 12 compares top slabs rolled from ingot *G* with similar slabs from an ingot deoxidized with only 1.6 lb per net ton of silicon. As would be expected from the sound structure shown in the preceding figure, the slab surface from the heat of ingot *G* is reasonably sound. Only a few light seams appear on the edges of the slab. The comparison ingot (ingot *I*), with marginal silicon deoxidation, shows the characteristic seamy structure down to the 66 pct yield position.

With aluminum as the only ladle deoxidizer, a residual of about 0.020 pct was required to avoid the use of any mold additions. A ladle addition of about $1\frac{1}{2}$ lb of aluminum per net ton of ingots was required to obtain this residual analysis. This deoxidation was used on ingot *J*, the split section of which is shown in Fig 13. While this aluminum addition eliminated the subsurface ingot porosity, it also resulted in formation of an extensive shrinkage cavity. With the complete aluminum deoxidation there was apparently no central gas formation to offset the natural shrinkage and therefore ingot *J* should be regarded as fully killed. The fully killed appearance of ingot *J* is evident in Fig 13. It is interesting to observe that the shrinkage cavity is divided into several major zones, each separated from the adjacent one by a continuous bridge. In contrast to the silicon killed steel, the pipe cavity begins just below the upper ingot crust. The cavity extends down to the 70 pct ingot yield position. Associated with the fully killed structure are numerous cracks penetrating from the surface well into the ingot body.

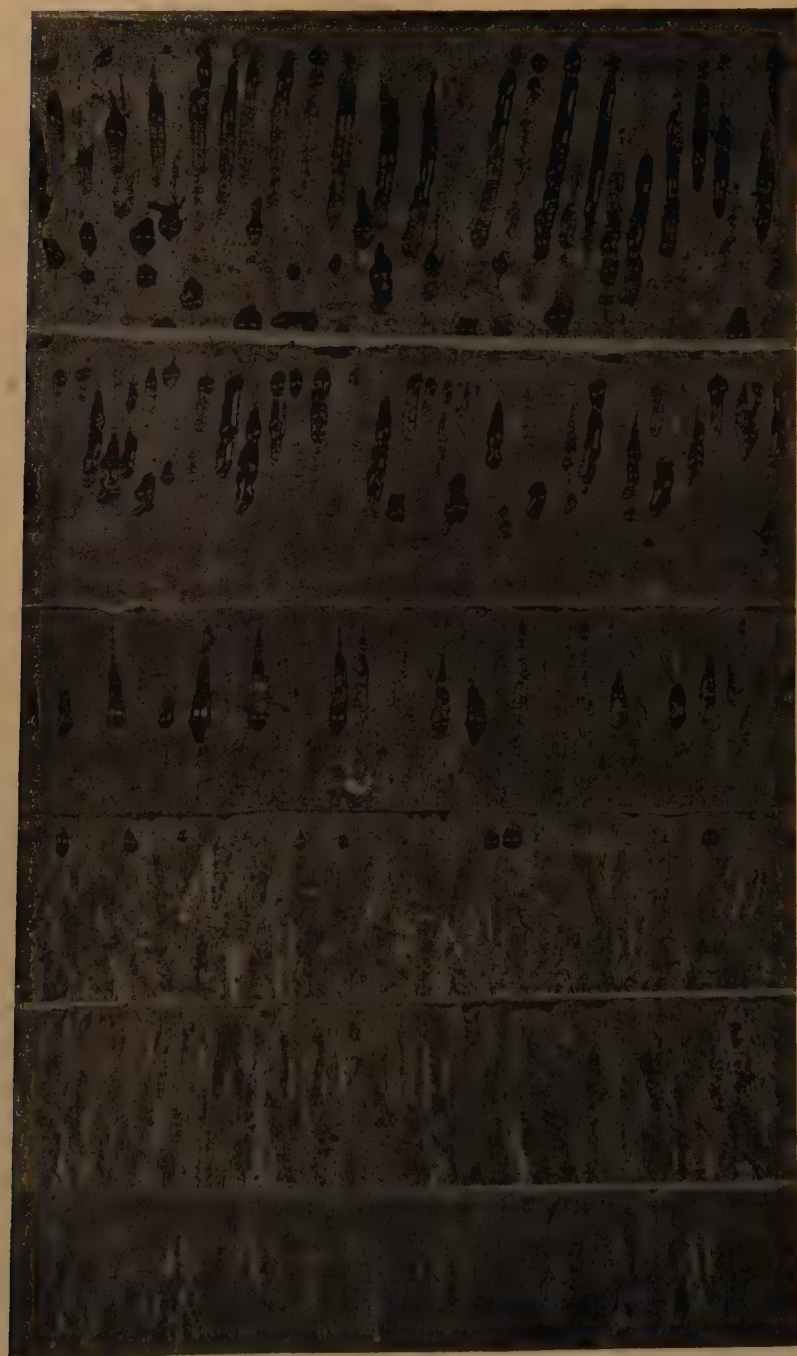
Total Oxygen Content of Liquid Semikilled Steel

On all experimental heats, samples for total oxygen analysis were obtained from

FIG 13—STRUCTURE OF SPLIT INGOT *J*. LADLE DEOXIDATION: 1.6 POUNDS AL PER NET



TON INGOTS. MOLD DEOXIDATION: NONE. ORIGINAL MAGNIFICATION 0.1. REDUCED APPROXIMATELY ONE-EIGHTH.



Total oxygen, per cent

0.010

0.011

0.016

0.022

0.030

0.042

FIG 14—EFFECT OF TOTAL OXYGEN CONTENT OF LIQUID STEEL ON FORMATION OF SUBSURFACE BLOWHOLES IN MIDDLE OF CAPPED INGOTS. ORIGINAL MAGNIFICATION 0.9. REDUCED APPROXIMATELY ONE-FIFTH.

the ingot preceding the one that was split for observation. To obtain the sample a standard bomb type mold was dipped into the liquid metal prior to making the capping additions. At least two such samples were obtained on each heat. To eliminate the use of mold additions, it was found necessary to reduce the total oxygen content of the liquid steel (0.16 to 0.20 pct carbon) during teeming to just under 0.015 pct. At 0.016 pct oxygen there was some small tendency toward gas formation (Fig 14). Where no additions were made to the ingot body, as on capped steels, a well defined row of subsurface blowholes appeared in edge sections. With increasing total oxygen content, there was a corresponding increase in the size of the subsurface blowholes. An interesting illustration of the effect of total oxygen content on subsurface porosity is shown in Fig 14. The edge sections shown were all cut from the middle height of capped ingots.

The carbon content of the ingots of Fig 14 averaged just under 0.20 pct. At 1 atm CO pressure, the liquid steel should be in equilibrium with about 0.010 pct oxygen. At the time that subsurface blowholes form, it is likely that the gas pressure is somewhat greater than 1 atm. The critical value of 0.015 pct oxygen obtained in actual operations probably approaches closely the equilibrium value.

The position of the blowholes relative to the outer ingot surface as shown in the middle height sections of Fig 14 is not readily explained. With increasing deoxidation, that is with lower oxygen content, there appears to be a general tendency for the subsurface blowholes to approach closer to the outer ingot surface. With only 0.016 pct total oxygen in the liquid steel, the entire blowhole zone exists in the outer quarter inch of the ingot. In contrast, a relatively substantial solid zone separates the outer surface from the subsurface blowholes of the ingot with 0.042 pct oxygen.

The work of Hultgren and Phragmen²

indicates that a solid outer skin can form either by complete suppression of gas formation or by the removal of evolved gas through vigorous rimming action. It also showed that in certain higher carbon rimming ingots, gas suppression occurred during skin formation near the bottom, while the gas was swept out in the upper part of the same ingot. Some evidence that both mechanisms are active in skin formation of this experimental series is presented in Fig 33 to 36.

It might be explained that the skin thickness at the midway ingot height can be associated with the extent of gas formation during the earliest stages of solidification. Such an explanation, however, ignores the possibility that with increased deoxidation all gas evolution will be suppressed by rapid chilling. On such ingots it would be expected that increased deoxidation would lead to increased skin thickness. The fact that this anticipated condition is apparently not realized in practice indicates that some factors that are very likely associated with metal movement during actual pouring may be significant during skin solidification:

Practical Aspects of Semikilled Steel Deoxidation Practice

In the manufacture of semikilled steel it is intended to produce an ingot from which a maximum yield of satisfactory product can be obtained. To assure maximum yield, it has been assumed that open hearth practices must be adjusted so as to produce an ingot in which the natural shrinkage on solidification is offset to an appreciable degree by gas formation.* By controlling the degree of deoxidation, the position of the blowholes resulting from such gas formation can be varied considerably. With little or no deoxidation, blowholes appear throughout the subsurface zone. Increased

* More recently there has been some evidence that maximum yields are also obtained by producing killed steels in which the pipe cavity welds on rolling.

deoxidation suppresses early gas formation up to the point where sound subsurface structure is obtained. Unfortunately, with the 24 by 43 in. mold section used in this investigation (and probably for any other mold section), the minimum ladle deoxidation required to insure sound subsurface structure also results in the formation of a definite pipe cavity. Where silicon is the main deoxidizer, the size of the pipe cavity associated with complete subsurface deoxidation is far smaller than with aluminum.

One factor, on which little direct data are available but which is necessarily of utmost importance in the production of capped semikilled steels, is the welding of blowholes on rolling. It has been observed among ingots from different heats with almost identical steel analysis (including oxygen content) that some roll into slabs with sound, completely welded subsurface structure, while others form slabs that are seamy, segregated and discontinuous along the outer surface. It appears likely that factors other than those controllable at the open hearth govern or at least exert considerable influence over the welding of the subsurface blowholes. An obvious suggestion for further investigation involves the heating of the ingot and its conversion into the slab form.

For the most part, the general porous structure that often occurs in the upper central part of the ingot welds completely on rolling. Fresh blowhole surfaces exposed on machining split ingots are clean, bright and free from inclusions. That such clean surfaces weld easily is to be expected. The welding of the more highly segregated pipe cavities again varies from heat to heat and is likely influenced by factors similar to those discussed in the preceding paragraph.

A feature of ingot structure not discussed previously is the tendency for the surface of certain ingots to crack or tear during rolling. In the analysis range studied, increased deoxidation is apparently conducive to poor blooming mill surface.

Surface cracking has been observed in varying degrees even before rolling several of the ingots. Examples of this condition were shown in Figs 11 and 13. In these ingots, the degree of deoxidation is indicated by the pipe cavity. Numerous cracks penetrate well into the ingot body. The exact cause for cracking in more highly deoxidized steels has not been established.

The production of ingots with little or no central pipe can be accomplished through a relatively wide range of liquid steel oxidation. Through much of this range, however, the upper part of the resultant ingots contains shallow subsurface blowholes that lead to poor slab surface. Only at the extremes in the oxidation range of semikilled steel is it practical to attempt production of ingots without pipe. Accordingly, it appears that one of the two following general deoxidation practices should be used in producing semikilled steel ingots.

PRACTICE NO. 1

Pour the liquid steel with a minimum bath and ladle deoxidation. Since this practice would encourage gas evolution the ingot would have to be capped. In capping, care should be taken to add the deoxidizer so as to obtain a continuous bulged upper crust. From observation of split ingot sections, it would appear that the following features of open hearth practice would be conducive to the best product performance from semikilled steels of the same general analysis: (1) Maximum steel oxidation to encourage gas evolution. (2) Long topping off period to encourage gas evolution in the upper part of the ingot. (3) Delayed capping to insure that excessive amounts of deoxidizer will not be taken into the body of the ingot before an adequate skin has formed. (4) Use of a minimum amount of deoxidizer in capping to avoid extensive deoxidation of the upper central part of the ingot (However, sufficient aluminum should be used to avoid eruptions through the top surface).

PRACTICE NO. 2

Pour the liquid steel with just sufficient deoxidation to suppress gas evolution during early solidification. The practice should be adjusted so that with controlled but marginal bath and ladle deoxidation and with carefully regulated mold additions, sufficient gas evolves during later stages of solidification to offset shrinkage.

In practice it has not been found possible to make ingots entirely free from pipe as well as subsurface porosity simply by regulating the ladle deoxidizing addition. Usually, the upper part of ingots made with bulged tops are susceptible to subsurface blowholes. When sufficient ladle deoxidizer is added to overcome this early gas formation, a small but definite pipe cavity appears between the 75 and 85 pct yield position.

The following features of open hearth practice would apparently contribute to better performance of the more highly deoxidized semikilled steels. (1) Sufficient residual deoxidizing element so that initial gas formation is almost entirely suppressed (apparently a residual silicon content just under 0.08 pct assures the marginal degree of deoxidation required for such steels.) (2) Rapid rate of pour to provide maximum head of metal to help suppress early gas formation. (3) Little or no topping off period to discourage subsurface gas formation near the top of the ingot. (4) The feeding of small amounts of aluminum to assist subsurface deoxidation and to obtain a small but definitely bulged continuous top surface.

For the production of semikilled steels that require little or no mold deoxidation (practice No. 2), the oxygen content of the liquid metal in the mold should be in the order of 0.015 pct. Referring to Fig 1 it appears that this general level of oxidation can be attained simply by aiming at a residual silicon between 0.05 and 0.10 pct. On the other hand, where aluminum is the only deoxidizer used, it would be necessary

to add exactly the amount needed to combine stoichiometrically with the excess oxygen. Since the crudeness of the open hearth process precludes the fulfillment of such an exacting requirement, it is obvious that deoxidation by a single ladle aluminum addition could not be expected to give satisfactory semikilled steel ingot structure.

Selection of Open Hearth Practice for the Manufacture of Semikilled Steel

From the information presented in this report, it is possible to make some generalizations regarding the selection of open hearth practice for the manufacture of semikilled steel.

For applications where maximum yield is desired without regard to any other ingot features, the aluminum capped semikilled steels of the type described under practice No. 1 appear the most desirable. To insure maximum yields, open hearth practice should be regulated to produce ingots with the solid bulged tops that indicate minimum pipe. The routine production of satisfactory capped ingots necessitates close supervision of open hearth pouring practice.

Even with closely supervised practice, it is likely that some ingots will be made in which fairly extensive piping occurs. To reduce losses on such ingots, precautions should be taken to avoid punching in the tops during stripping. By maintaining closed tops, oxidation of piped zones is minimized, and the surfaces of the cavity are more likely to weld on rolling.

In addition to their amenability to high ingot yields, capped semikilled steels are less prone to cracking and tearing during rolling than more fully deoxidized steels. Accordingly, in the critical carbon range where steels are particularly subject to cracking and tearing (approximately 0.15 pct carbon) the use of capped steels is indicated on applications requiring reasonable freedom from snakes and deep surface cracks.

When sound subsurface structure is re-

quired in the final product, it may be obtained by producing capped steel in which the subsurface blowholes weld or by deoxidizing the steel to the extent that no gas forms during the freezing of the subsurface zone. With current open hearth and blooming mill practice, there is no assurance that the product of any capped ingot will have a sound subsurface structure. Accordingly, it appears logical to use the more highly deoxidized type of semikilled steel. For the best results, additions would have to be adjusted to give just sufficient deoxidation to suppress subsurface gas formation. To minimize the size of the shrinkage cavity, silicon should be used as the primary ladle deoxidizer. With the silicon deoxidation practice, any pipe that formed would be small and exist entirely within the prime ingot yield. Since the part of the ingot over the shrinkage cavity welds readily into a sound unsegregated product, high yields should be readily attainable with this practice.

Where silicon is not desirable and aluminum is the primary ladle deoxidizer, ingots tend to form extensive pipe cavities. If enough aluminum is added to the ladle to avoid the use of mold deoxidizers, the ingots are essentially fully killed. On such aluminum killed steel ingots, the pipe cavity begins immediately below the upper crust and extends well into the ingot. To minimize oxidation of the shrinkage cavity, it is desirable to avoid erupted or punched tops. With the aluminum deoxidation practice, the yield of absolutely sound steel is necessarily limited by the position of the pipe cavity.

SEGREGATION AND SOLIDIFICATION OF SEMIKILLED STEEL INGOTS

The exposed face of each experimental ingot previously discussed was drilled intensively. The drillings were analyzed to determine the general macrosegregation pattern. To supplement data obtained by

chemical analysis, sulphur prints were made of each typical ingot structure.

All the drillings from the experimental ingots were analyzed chemically for carbon, manganese, phosphorus and sulphur. Silicon was determined on ingots to which significant percentages of that element were added. Most of the curves presented in this report are based on analyses of carbon and sulphur, since the relatively wide variation in the percentages of these two elements present in an ingot most clearly illustrates the segregation characteristics.

In the preceding section, semikilled steel ingots were classified according to the degree of ladle deoxidation as capped, intermediate, or requiring no mold deoxidation. This same classification is used in reviewing the segregation characteristics of the experimental ingots.

Segregation Data

In sampling the experimental ingots, drillings were obtained from at least five horizontal positions at about ten ingot heights. Usually, edge, midway and center samples were taken. Additional samples were taken in all areas that included sharp analysis changes. Examples of areas requiring more intensive sampling are the inside of subsurface blowhole zones, the central segregate areas and along Λ type segregate lines. To assist in locating the position of such supplementary samples, sulphur prints were made of all the ingots prior to drilling.

The analytical data for ingot *A* are shown in Fig 15. The analyses for carbon, sulphur, manganese, and phosphorus at various positions are shown in the indicated half-ingot sections. All edge and midway analyses shown in Fig 15 represent the average of the two samples from similar positions on either side of the center line. A total of 73 drillings was analyzed on this ingot.

To show more clearly the segregation pattern on all experimental ingots, iso-

analysis contours based on carbon and sulphur analyses were drawn in half ingot sections of the type shown in Fig 15. The contours for either of these elements were

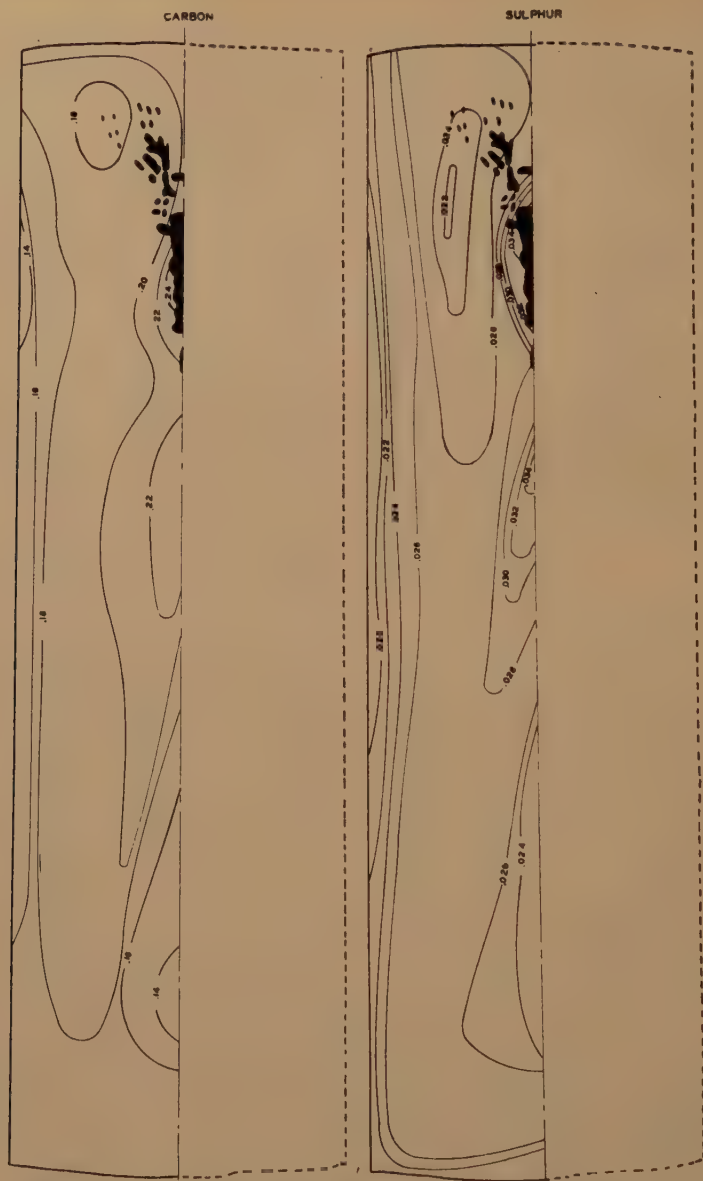
patterns for the two elements can be observed in some of the experimental ingots. Such differences, however, are usually localized in small areas. In general, the



FIG 15—DISTRIBUTION OF ANALYSES IN INGOT A.

drawn without referring to the curves obtained for the other element. For this reason, some difference between segregation

segregation patterns on any one ingot, as outlined by the contours, are strikingly similar for both carbon and sulphur.



CAPPED SEMIKILLED STEELS

The carbon and sulphur analysis shown in Fig 15 have been represented by iso-analysis contours in Fig 16. No attempt was made to draw contours for manganese or phosphorus since the variations in analysis were too small to illustrate segregation patterns. To avoid confusion the actual analytical data are not included in Fig 16.

Ingot A was poured at 2950°F (optical pyrometer E-o.4). The ingot was capped with 5 lb of aluminum 15 sec after pour was completed. Several characteristics of capped steels are evident in Fig 16. As would be expected from observations made in earlier studies, definite segregation takes place in the pseudo-rim zone. As a result of this action, the actual rim is negatively segregated. A definite sharp increase in carbon and sulphur content occurs just within the rim. The maximum positive segregation within the rim occurred just above the midway ingot height. Two other positive segregation zones existed in this ingot, one originating just below the upper central parting zone and one occurring on either side of this small cavity. It is interesting to observe that there is very little segregation in the upper central porous area itself, the analysis being very close to that of the steel originally poured from the ladle. The expected negative segregation cone exists in the lower central half of the ingot.

It is interesting to relate the quantitative analytical data of Fig 16 with the sulphur print of the same ingot in Fig 17. The rim is evident as the relatively light zone extending along the outer surface for practically the full length of the ingot. The location of the subsurface blowholes in the outer rim appears as dark streaks in the rim. The relatively unsegregated nature of the upper porous zone and the deoxidized cap are apparent in the sulphur print. The blackened section of the central parting zone as well as the dark streaks indicating the position of the subsurface holes are a result of an accelerated reaction of the sensitized paper with gas accumulated in



FIG 17—SULPHUR PRINT OF INGOT A. ORIGINAL MAGNIFICATION O.I. REDUCED APPROXIMATELY ONE-FIFTH.

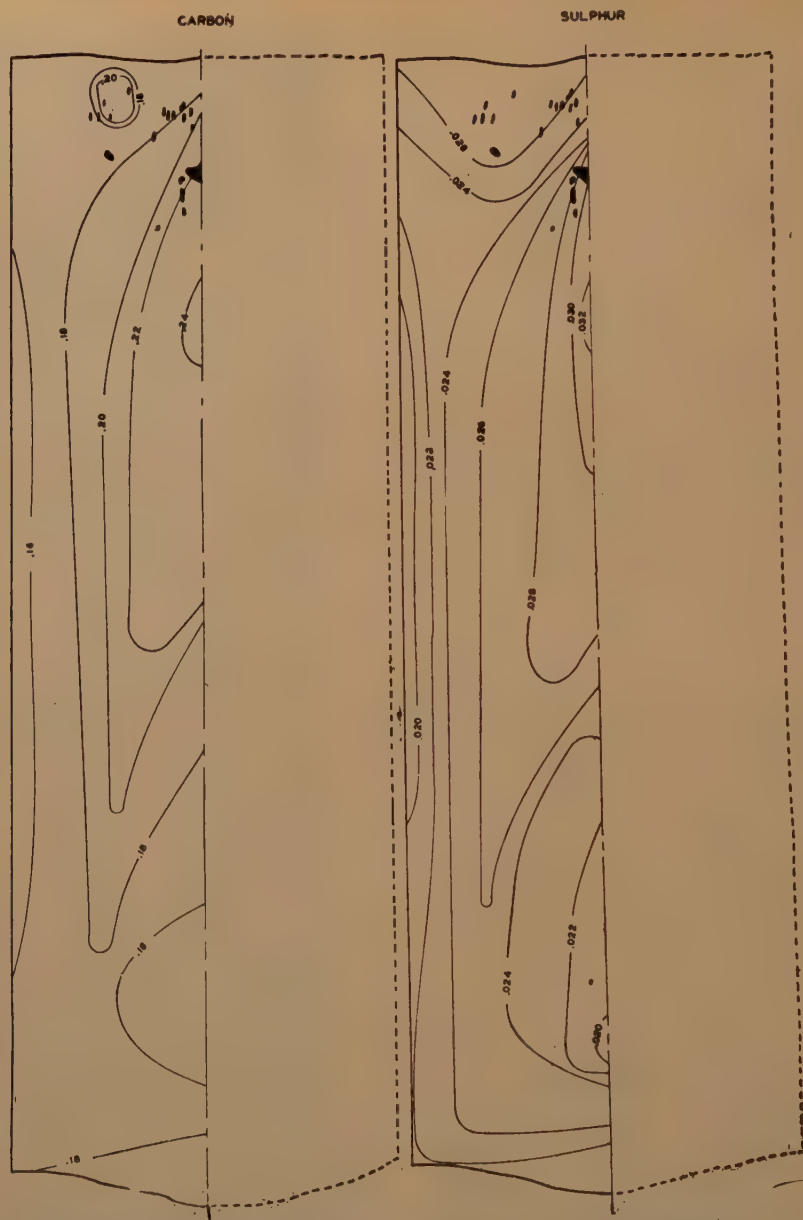


FIG 18—DISTRIBUTION OF CARBON AND SULPHUR IN INGOT B. LADLE DEOXIDATION: 0.4 POUNDS AL PER NET TON INGOTS. MOLD DEOXIDATION: CAPPED AFTER SHUT-OFF WITH 0.3 POUNDS AL PER NET TON INGOTS. TEEMING TEMPERATURE: 2810°F.

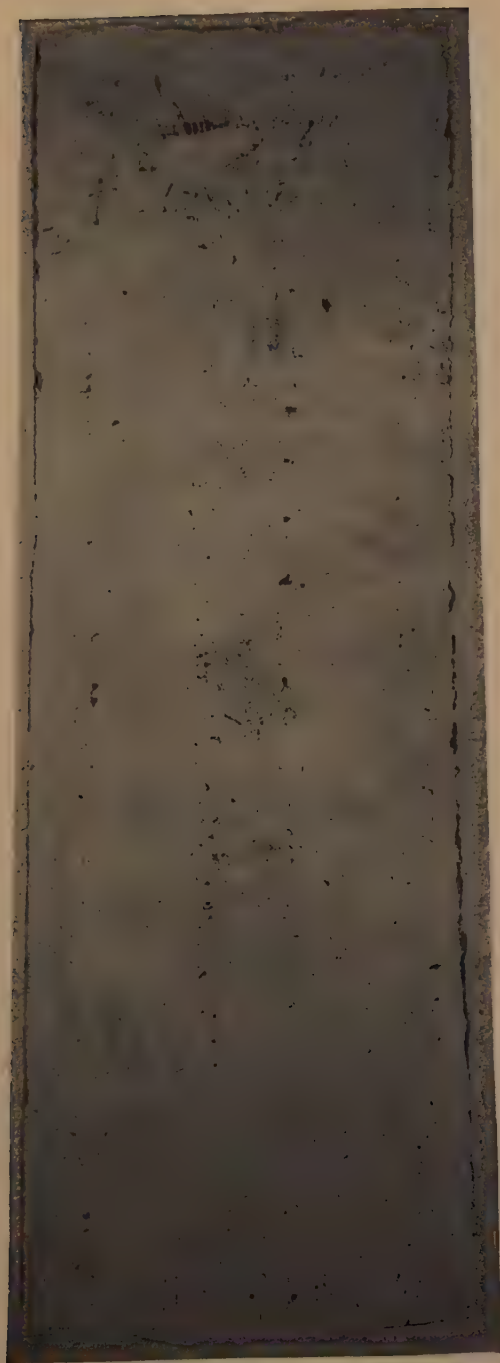


FIG 19—SULPHUR PRINT OF INGOT B. 0.1 X

voids during printing and does not necessarily reflect a high sulphur segregate area. One of the central areas of maximum positive segregation that was evident in Fig 16

direction of the contours emanating from these positive segregate areas are guided by the Λ segregate lines. The lower central negative segregate area is included within

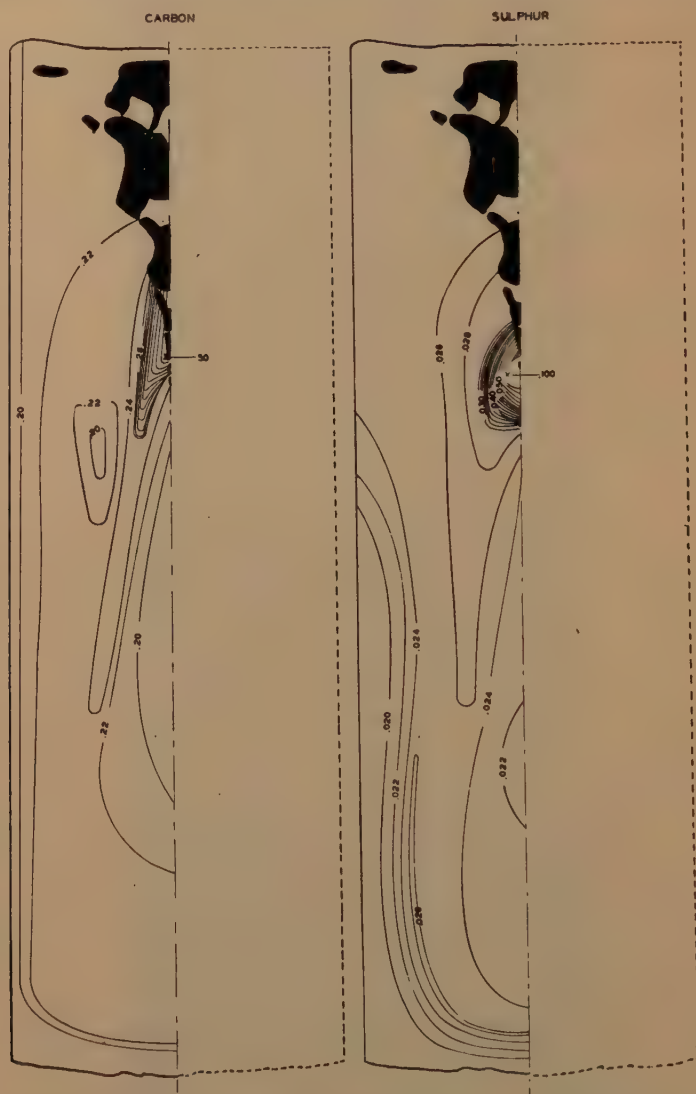


FIG 20—DISTRIBUTION OF CARBON AND SULPHUR IN INGOT C. LADLE DEOXIDATION: 1.0 POUND $FeTi$ PER NET TON INGOTS. MOLD DEOXIDATION: CAPPED JUST BEFORE SHUT-OFF WITH 0.6 POUNDS Al PER NET TON INGOTS.

coincides with the dark area surrounding the central void and the other corresponds to V segregate below the central zone. The

the legs of the inverted V. An interesting feature of Fig 17 is the series of parallel segregate streaks that apparently originate

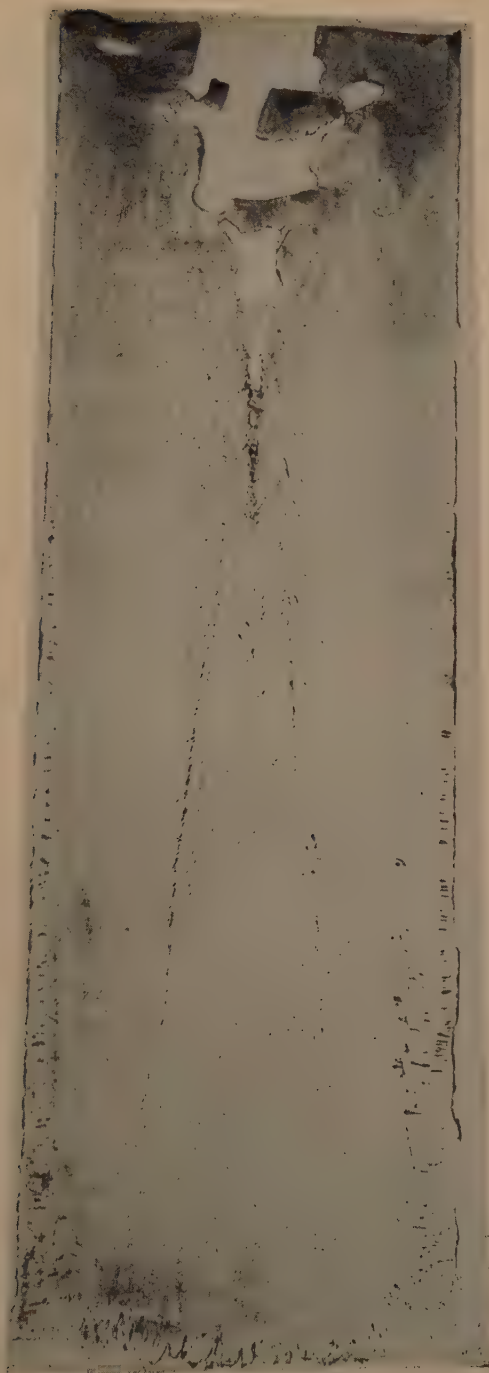


FIG 21—SULPHUR PRINT OF INGOT C. 0.1X

at the inner edge of the subsurface blowhole zone (Fig 32) and are directed toward the upper porous zone.* Despite fairly intensive sampling in these areas, no significant changes in chemical analysis were detected along these segregate lines.

Fig 18 shows carbon and sulphur segregation in ingot *B* which was poured at only 2810°F. Except for pouring temperature the general features of open hearth practice were the same for both ingots. Despite a difference of about 150°F in pouring temperature the overall segregation was practically the same in the two ingots. The highest carbon and sulphur analyses were encountered at about the same ingot position in both ingots. In the cold ingot, however, there was no apparent association with any central void. The slight segregation occurring during the freezing of the outer rim is brought out by the contours within this subsurface zone. Again very little segregation occurred in the top central porous zone. A lower central negative segregation zone and a Λ segregate are also indicated in Fig 18.

The sulphur print of ingot *B*, Fig 19, shows the same general characteristics as the contour drawing. The outer rim, the aluminum cap and the lower cone of nega-

tive segregation can be seen in Fig 19. This print differs from that of ingot *A* in that there is no distinct *V* segregate zone in the area of maximum segregation and no Λ segregate lines surrounding the cone of negative segregation. Positive central segregation appears to be included in a vertical band that starts at the top of the cone of negative segregation and terminates in the upper central blowhole zone. Inclined segregate streaks of the type mentioned in the discussion of ingot *A* can also be seen in Fig 19.

OVERDEOXIDIZED CAPPED STEELS

The section on ingot structure showed that early capping with excessive amounts of aluminum can result in complete deoxidation of a large zone in semikilled ingots. Such overdeoxidation is reflected in large shrinkage cavities in the final ingot. Segregation in two such overdeoxidized ingots is shown in Figs 20 and 22. Despite the similarity in practice, the two ingots differ considerably in the extent of segregation.

Segregation contours for ingots *C* and *D* are shown in Figs 20 and 22, respectively. In both ingots, subsurface contours outline the outer blowhole zone up to about the half ingot height. Above the point at which segregation contours intersect the surface, extensive gas formation was apparently suppressed. In both ingots there is practically no segregation surrounding the upper half of the large shrinkage cavity, the analysis throughout this area closely approaching that of the original liquid steel. This feature was checked by intensive sampling in this area. Negative segregation zones exist in the lower central part of both ingots. In ingot *C*, this lower central zone of negative segregation appears to terminate just within the leg of the Λ segregate.

The major difference between Figs 20 and 22 appears to be the degree of segregation, especially near the base of the pipe cavity. Analysis as high as 0.50 pct carbon

* Similar streaks are evident in examples 25, 27, 28 and 31 of the second report on the Heterogeneity of Steel Ingots.³ These same ingots also show the same type of rim and porous top central zone as occurs in ingot *A*. The British incidentally associate the occurrence of the oblique streaks with cold pouring temperatures, a feature not borne out in this study. They described the streaks as Λ segregate.

Hultgren¹⁰ suggested that parallel oblique segregate streaks may have resulted from gas evolution through a zone in the ingot that was in a pasty condition due to the existence of some solid dendrites. The gas passing through this pasty zone would force the solid crystals aside. The streaks then would be the result of the more segregated liquid flowing back into the path of the rising bubble. The inclination of such streaks would have been caused by the greater resistance of the solid crystals on the side of the bubble toward the mold wall.

Badenheuer's¹¹ excellent illustration of the association of the oblique segregate streaks with blowholes supports Hultgren's suggested mechanism.



FIG 22—DISTRIBUTION OF CARBON AND SULPHUR IN INGOT D. LADLE DEOXIDATION: 1.0 POUND 50 PER CENT FE-SI PER NET TON INGOTS. MOLD DEOXIDATION: CAPPED JUST BEFORE SHUT OFF WITH THREE POUNDS PER NET TON INGOTS.

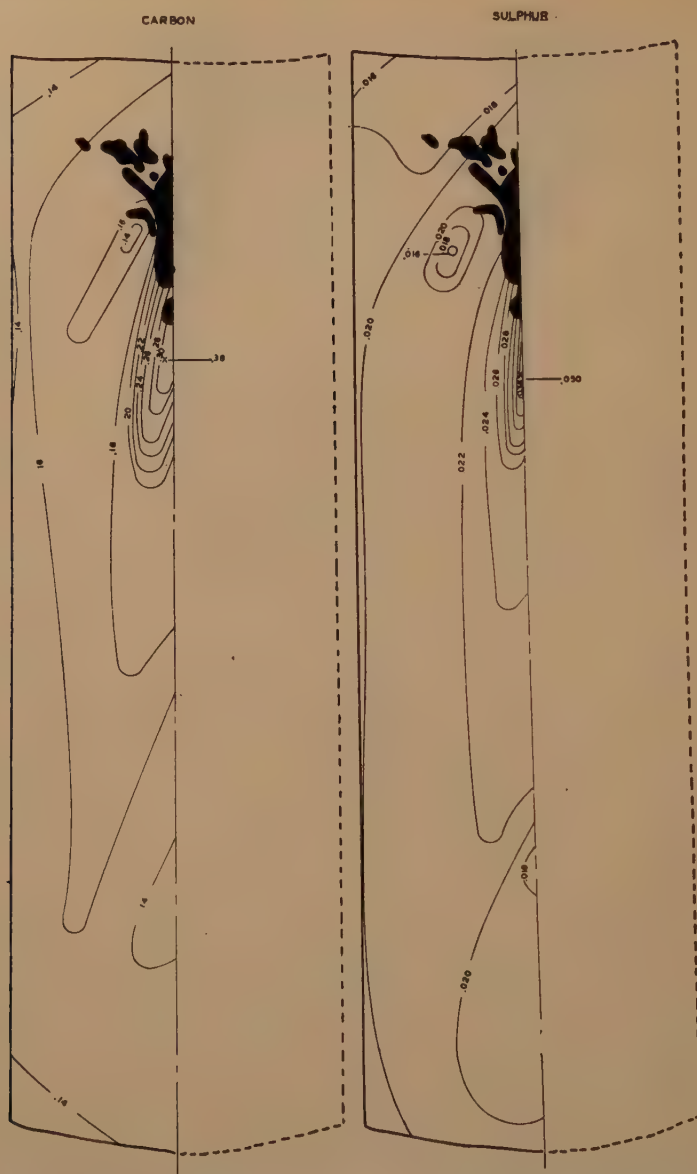


FIG 23—DISTRIBUTION OF CARBON AND SULPHUR IN INGOT E. LADLE DEOXIDATION: 11.7 POUNDS 20 PER CENT FE-TI PER NET TON INGOTS. MOLD DEOXIDATION: 0.08 POUNDS AL PER NET TON INGOTS ADDED DURING POUR.

and 0.100 pct sulphur were encountered in this zone on ingot *C*, whereas there was relatively little departure from the original liquid steel analysis in ingot *D*.

The sulphur print of ingot *C*, which is shown in Fig 21, merely confirms the data of Fig 20. Fig 21 shows clearly the subsurface blowholes in the rim up to just above the half ingot height, the absence of concentrated segregate areas immediately surrounding the upper part of the pipe cavity and the *V* segregate at the base of the pipe cavity. The location of the Δ segregate approximates that indicated in Fig 20. Because of general similarity between the two ingots no sulphur print is shown for ingot *D*.

In view of the fact that segregation in ingot *C* was so much more pronounced than in ingot *D*, reference is again made to Table 1 to observe any minor differences in open hearth practice that may have contributed to this situation. Ingot *C* contained slightly more carbon and sulphur than ingot *D*. The heat of ingot *C* was deoxidized in the ladle with 1.0 lb per net ton of 20 pct ferrotitanium while the ladle addition to the heat of ingot *D* was 1 lb per ton of 50 pct ferrosilicon.

The segregation differences between ingots *C* and *D* become more interesting when reference is made to the section on ingot structures, where it was shown that the subsurface blowholes in the unsegregated ingot *D* welded completely to form absolutely sound slabs while definite subsurface streaks were evident in the etched slab sections from ingot *C*.

INTERMEDIATE SEMIKILLED STEEL

Ingots *E* and *F* were adjacent ingots from a semikilled steel heat that had been deoxidized in the ladle to the extent that there was only a slight tendency toward gas evolution in pouring into molds. Gas evolution from ingot *E* was suppressed by feeding three-quarters pound (0.08 lb per net ton) of aluminum throughout the pour. The adjacent ingot *F* was capped with 1 lb of Al (0.1 lb per net ton).

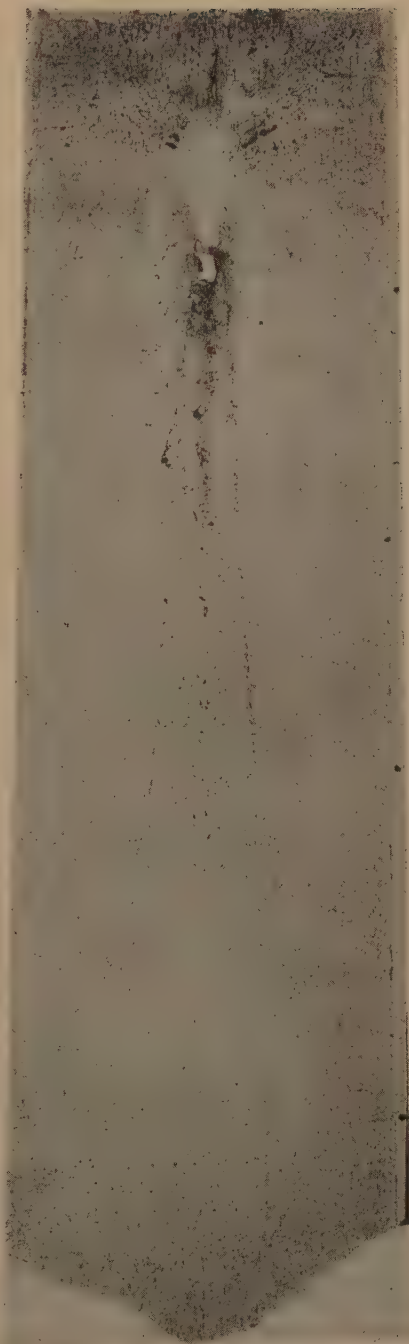


FIG 24—SULPHUR PRINT OF INGOT E. ORIGINAL MAGNIFICATION 0.1. REDUCED APPROXIMATELY ONE-EIGHTH.

Segregation curves for ingots *E* and *F* are shown in Fig 23 and 25. Since early gas evolution was entirely suppressed by aluminum added to ingot *E* during pour

mation. The central segregation characteristics of the two ingots are almost identical, even with respect to the absolute maximum and minimum analyses. Both ingots showed

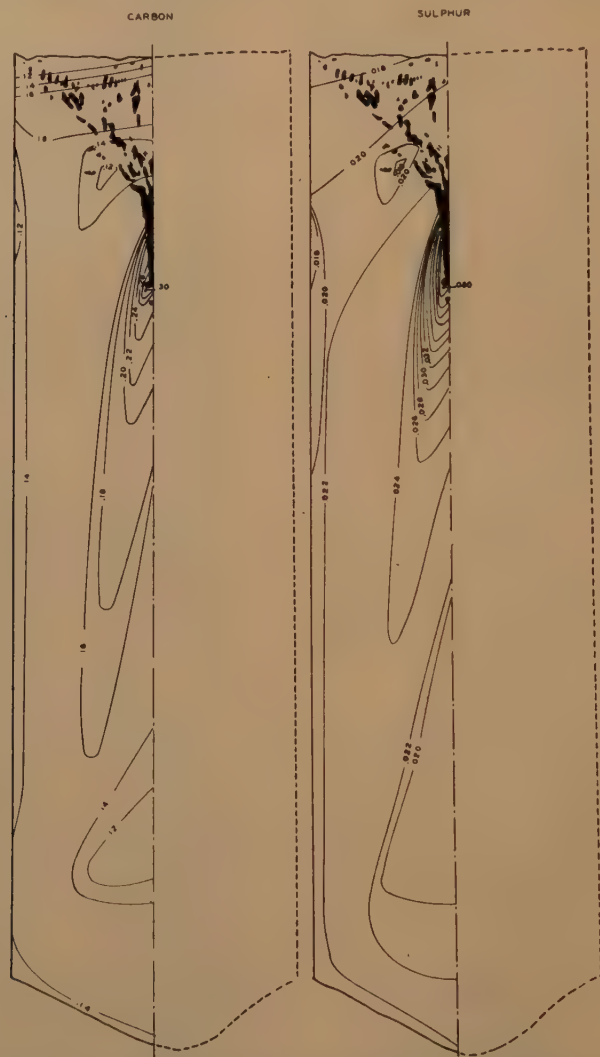


FIG 25—DISTRIBUTION OF CARBON AND SULPHUR IN INGOT F. LADLE DEOXIDATION: 11.7 POUNDS 20 PER CENT Fe-Ti PER NET TON INGOTS. MOLD DEOXIDATION: CAPPED AFTER POUR WITH 0.1 POUNDS AL PER NET TON INGOTS.

there is no evidence of any concentrated subsurface segregation. In contrast a small but definite negatively segregated outer rim was obtained in capped ingot *F* despite the very limited tendency toward gas for-

the usual absence of positive segregation surrounding the upper part of the central void, heavy segregate patterns below the central cavity, and the outline of the Δ segregate. The lower central negative segre-

gate pocket appears to be somewhat more extensive in ingot *F*. It is interesting to observe a small negative segregate pocket just to the side of the widest section of the open zone in both ingots. The carbon and sulphur analyses adjacent to both top surfaces were definitely lower than in the original liquid steel—this condition being especially pronounced in ingot *F*. The lower top surface analysis probably resulted from reaction with air rather than from any segregation process. The exact reason why more carbon and sulphur were eliminated near the surface of the capped ingot than from the adjacent ingot to which aluminum was fed is not immediately apparent.

The general segregation pattern of ingot *E* is also evident in the sulphur print of Fig 24. The only unusual feature of the print is the narrow area between the \wedge segregate lines. This feature, which was not brought out very clearly in the contour drawing, was very likely associated with the small size of the negative segregation zone in the lower central part of the ingot.

SEMIKILLED STEELS REQUIRING NO MOLD DEOXIDATION

In the previous section it was pointed out that there is a distinct difference in ingot structure of steels requiring no mold deoxidation depending on whether silicon or aluminum is used for ladle deoxidation. Segregation curves for the silicon deoxidized ingots *G* and *H*, are shown in Figs 26 and 28. The curves of Fig 30 illustrate the segregating characteristics of the aluminum deoxidized ingot *J*. (As previously explained, ingot *J* must actually be considered fully killed since it contains no definite blowhole areas.)

Certain general features appear common to all three of the more highly deoxidized ingots. None of the ingots gives any indication of subsurface segregation. There was relatively little segregation encountered in the area surrounding the upper part of the

pipe cavity in any of the ingots. The absence of marked segregation persisted in the upper central blowhole zone between the top surface and the shrinkage cavity in the silicon killed ingots, *G* and *H*. In ingot *J*, there was no definite segregation in the bridges separating the adjacent voids. Each ingot showed heavy positive segregation near the base of and just below the pipe cavity. The position of \wedge segregate lines in each ingot is indicated by the lower loops of the contour lines that originate in the heavily segregated zone near the base of the pipe. The outline of the \wedge segregate is shown clearly in ingots *G* and *J*. Each ingot shows the usual lower central negative segregate zone.

On each ingot in this group a negative segregation pocket originates just beyond the widest section of the pipe cavity. In ingots *G* and *H* the exact direction of this negative segregation zone could not be established by sampling for chemical analysis. In the aluminum killed ingot *J*, the negative segregate extended vertically downward from a point just beyond the large section of the shrinkage cavity.

The segregation characteristics of ingot *G*, Fig 26, were also evident in a sulphur print of the entire ingot that is not reproduced completely in this paper. Instead, a small section of the sulphur print surrounding the blowhole zone is shown in Fig 27. The enlarged section of the sulphur print brings out the heavy segregate below the cavity, the absence of segregate above the cavity, and the nature of the narrow negative segregate zone beside the cavity. Fig 27 is presented mainly to show that the shape of the latter segregate zone as determined from chemical analysis was apparently not a true indication of the segregation pattern. In the sulphur print this negative segregate appears as a narrow band extending vertically downward from just outside the widest section of the shrinkage cavity. This light band extended downward until it approached the leg of the \wedge segregate.

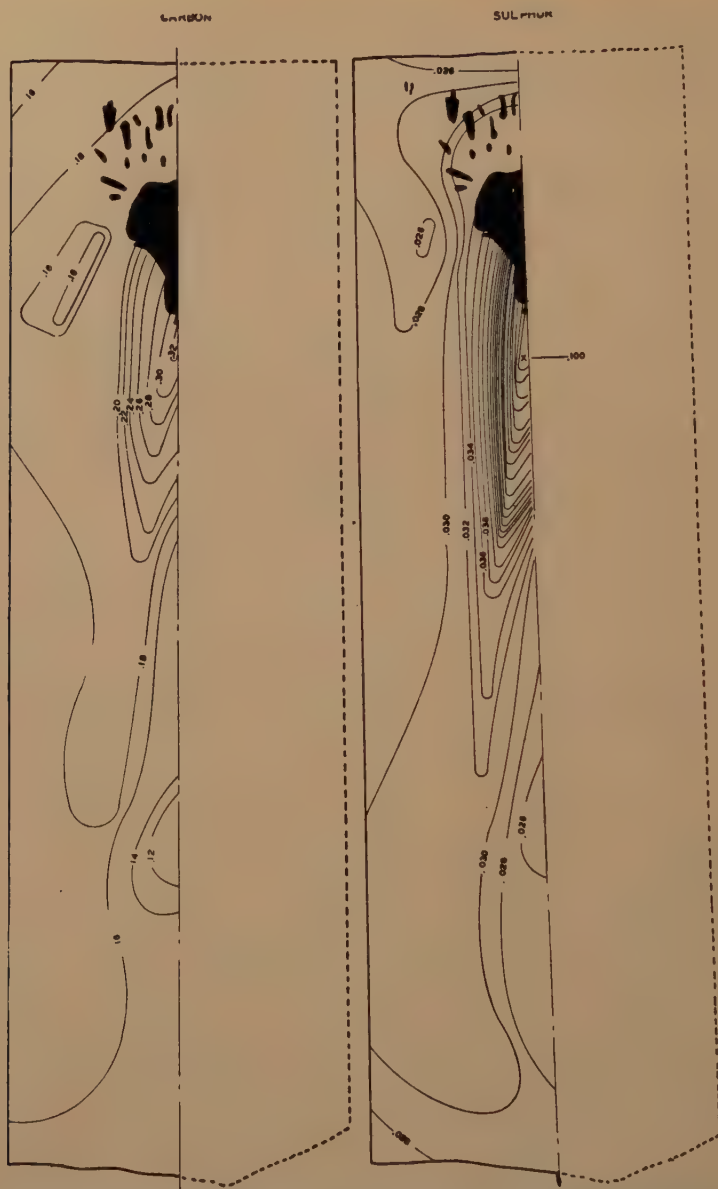


FIG 26—DISTRIBUTION OF CARBON AND SULPHUR IN INGOT G. LADLE DEOXIDATION: 5 POUNDS 50 PER CENT FE-SI PER NET TON INGOTS. MOLD DEOXIDATION: NONE.



FIG 27—SULPHUR PRINT OF AREA SURROUNDING SHRINKAGE CAVITY OF INGOT G. ORIGINAL MAGNIFICATION 0.5. REDUCED APPROXIMATELY ONE-EIGHTH.

A sulphur print of ingot *H*, shown in Fig 29, shows a light but definite \wedge segregate. The curves based on chemical analysis did not bring out this feature very clearly.

A sulphur print of ingot *J* is shown in Fig 31. An enlarged section of the area surrounding and just below the pipe cavity is also shown in the figure. The full ingot

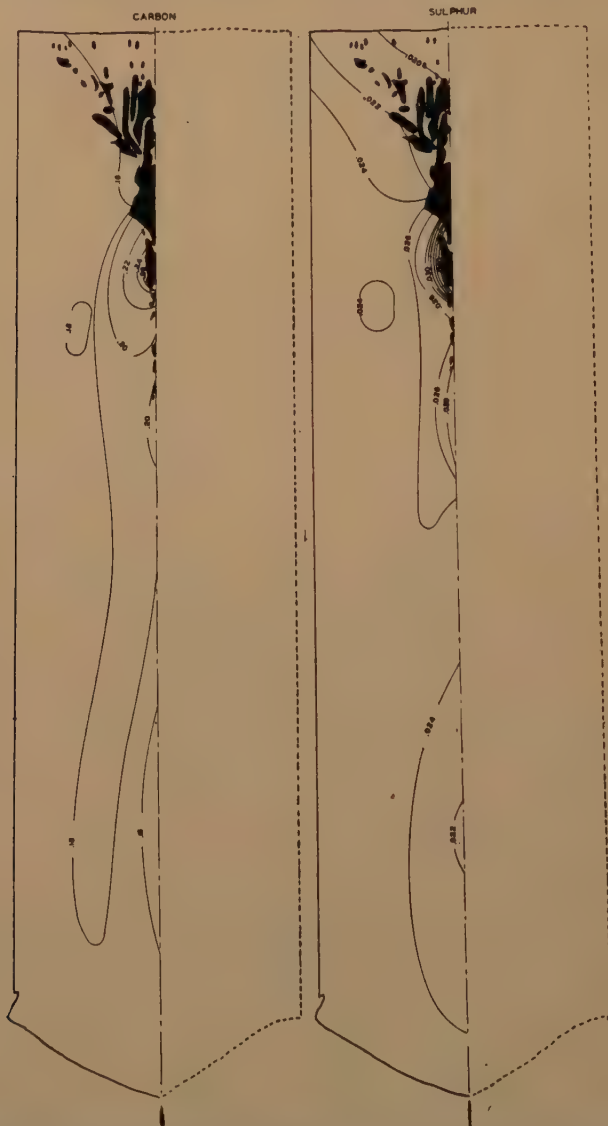


FIG 28—DISTRIBUTION OF CARBON AND SULPHUR IN INGOT *H*. LADLE DEOXIDATION: 5.4 POUNDS 50 PER CENT Fe-Si PER NET TON INGOTS. MOLD DEOXIDATION: NONE.

With this one exception, the general appearance of the sulphur print is in accord with the curves of Fig 28.

print shows the general distribution of the various segregate zones referred to in the discussion of Fig 30. The enlarged view

shows clearly the intersection of the \wedge segregate with the pipe cavity. The sulphur print also brings out the nature of the negative segregate bands that were suggested in the contour drawings. These bands originate at the edge of a cavity and extend continuously downward to the \wedge segregate line. It is also interesting to observe the coarse crystallites associated with the heavy V segregate below the pipe cavity.

Segregation of Elements Other than Carbon and Sulphur

There was no unusual nor unexpected segregation of manganese, phosphorus, or silicon. In general, these three elements segregated in the same direction but to a lesser degree than carbon and sulphur. On heats deoxidized with silicon to the extent that no mold deoxidizer was needed, there was a definite increase in silicon next to the upper surface. This high silicon was attributed to the entrapment of silica from the liquid scum during the topping-off period.

A rather interesting but logical variation in aluminum content was encountered in ingots to which that element was added. Near the top of capped ingots analyses were obtained varying from 0.10 to approximately 1.0 pct. On capped ingots with definite open pipe, the aluminum analysis of samples from the area surrounding the cavity was always over 0.015 pct. In most of the drillings from the zone surrounding the pipe cavity in capped ingots, the aluminum analysis was far greater than 0.015 pct indicating that steel product from this area might be fine grained as well as fully deoxidized. There was some evidence that even in capped steels with no excessive shrinkage cavity there was a tendency for aluminum to be drawn down into the body of the ingot. This effect, however, appeared to be restricted to an area just within the outer surfaces (Fig 36 and discussion). The total aluminum analysis in ingots to which aluminum was fed usually ranged from 0.005 to 0.020 pct.



FIG 29—SULPHUR PRINT OF INGOT H.
ORIGINAL MAGNIFICATION O.I. REDUCED APPROXIMATELY ONE-FIFTH.

DISCUSSION OF RESULTS

Most of the differences in segregation characteristics observed in the description of the individual ingots obviously resulted

tice. The latter features of segregation were apparently inherent in the mechanism of solidification. In this discussion, an attempt will be made to summarize the

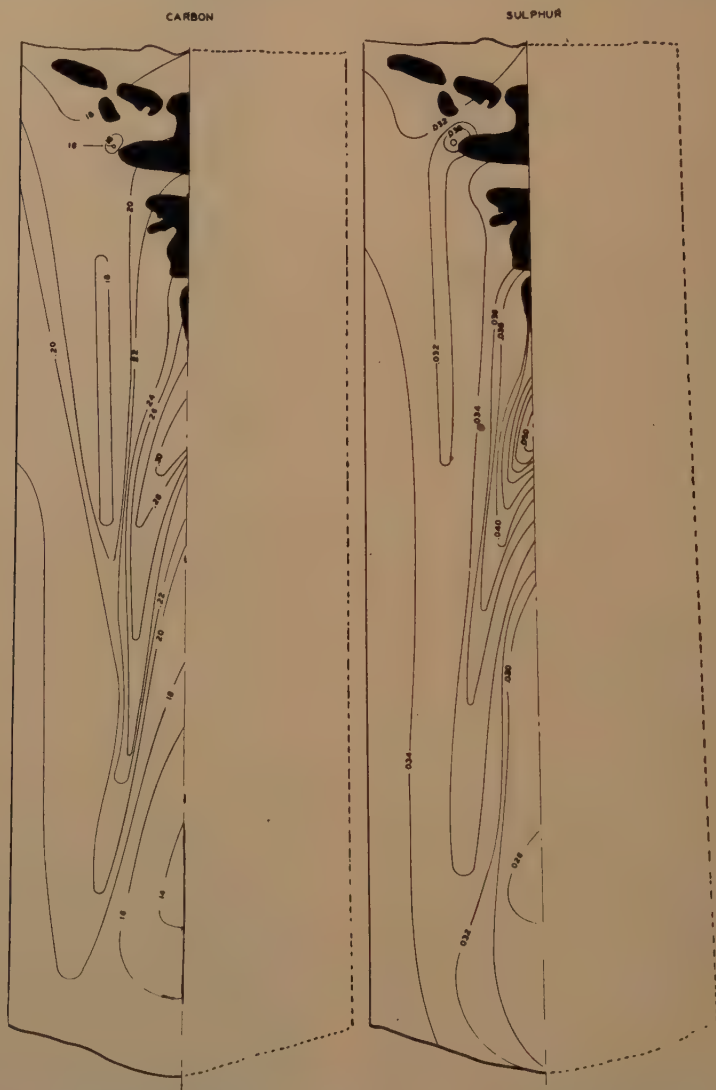


FIG 30—DISTRIBUTION OF CARBON AND SULPHUR IN INGOT J. LADLE DEOXIDATION: 1.6 POUNDS AL PER NET TON INGOTS. MOLD DEOXIDATION: NONE.

from variation in the deoxidation practice used in their manufacture. A few features, however, were observed commonly in ingots of widely varying deoxidation prac-

observations, to present a few additional illustrative sulphur prints and etched sections and to explain or, at least, speculate on the solidification mechanisms involved.



Full Ingot

Enlarged View of Below Pipe Cavity

FIG 31—SULPHUR PRINTS OF INGOT J. ORIGINAL MAGNIFICATION OF FULL INGOT 0.1, OF PIPE CAVITY 0.4. BOTH REDUCED APPROXIMATELY THREE-EIGHTHS.

Subsurface Solidification

Prominent among the features that depend on open hearth practice is the appearance of the rim on ingots that evolve noticeable amounts of gas in the mold and require capping. These subsurface blowhole zones

apparently demonstrate segregation characteristics similar to those encountered in rimmed steels, yielding a negatively segregated rim and a positively segregated zone just inside the subsurface blowhole zone. (Fig 16 to 25). This pattern persists as long

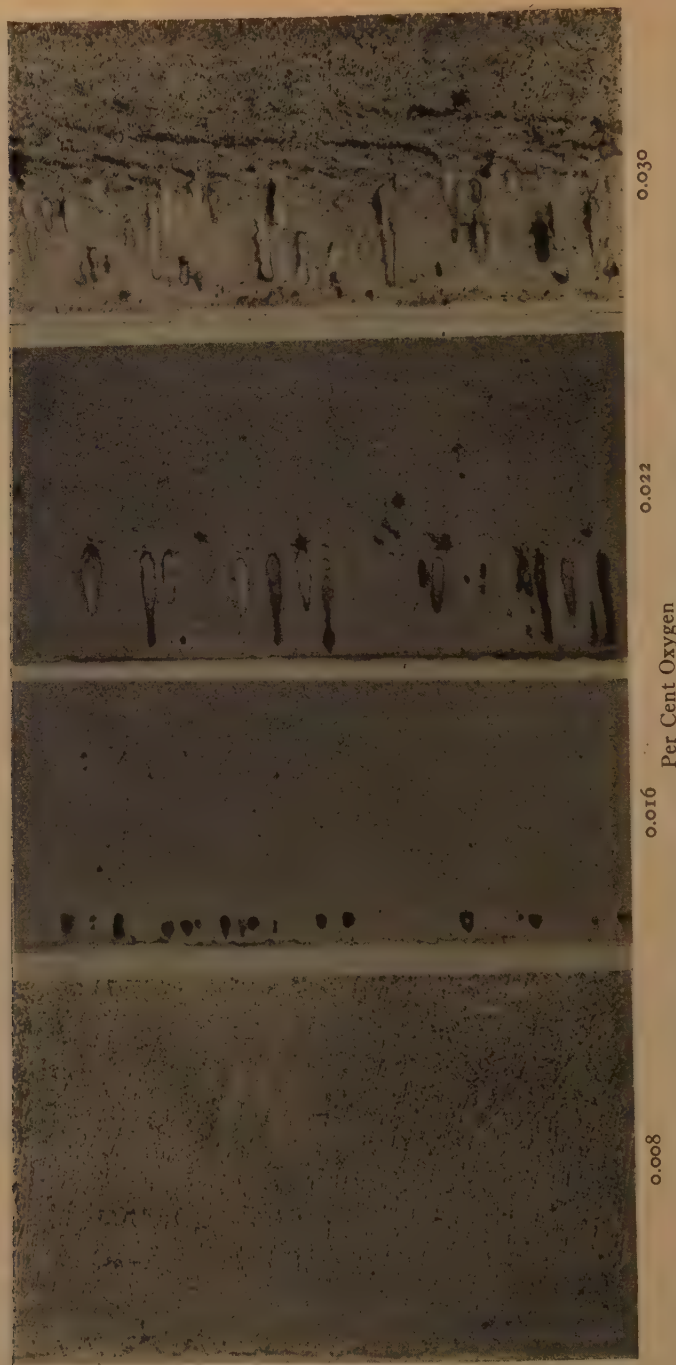


FIG 32—SULPHUR PRINTS OF EDGE SECTIONS FROM MIDDLE HEIGHT OF FOUR INGOTS WITH INCREASING OXYGEN CONTENT IN THE LIQUID STEEL. ORIGINAL MAGNIFICATION 0.1. REDUCED APPROXIMATELY ONE-HALF.

as a definite row of subsurface blowholes form (Fig 25). With increased deoxidation all gas evolution is suppressed and, as would be expected, this subsurface segregation pattern disappears.

The outer rim of capped semikilled ingots apparently freezes with considerable liquid movement and gas evolution; and it appears that the segregation pattern in the subsurface zone approaches that of rimmed steels. (Additional indications of the similarity to rim steels are presented in Figs 32 to 37 and Table 2.)

considerable segregation would be observed in all types of steel ingots. In the absence of any vigorous movement during solidification, however, there is nearly complete entrapment of the excess impurities that accumulate along the freezing interface between the adjacent solid crystals. Segregation under such conditions is largely on a micro-scale and is not detectable through the common sampling techniques. Where gas evolution causes rapid stirring, the extent to which the excess impurities that accumulate along the freezing interface are

TABLE 2—*Chemical Analysis at Four Positions Through Subsurface Blowhole Zone of Three Capped Ingots*
(Middle Ingot Height)

Original Liquid Steel Analysis, Pct					Position of Sample		Analysis, Pct			
Ingot	C	Mn	P	S	Description	Inches from Surface	C	Mn	P	S
1	0.18	0.42	0.009	0.023	In skin	5/16	0.15	0.43	0.009	0.021
					In blowholes	3/4	0.14	0.43	0.009	0.020
					Edge of blowholes	1 1/4	0.16	0.43	0.009	0.021
					Beyond blowholes	1 3/8	0.18	0.44	0.009	0.028
2	0.19	0.42	0.009	0.023	In skin	1/4	0.18	0.41	0.008	0.020
					In blowholes	3/4	0.17	0.42	0.008	0.022
					Edge of blowholes	1 1/4	0.21	0.45	0.009	0.032
					Beyond blowholes	1 3/4	0.21	0.44	0.009	0.032
3	0.16	0.41	0.009	0.029	In skin	3/8	0.11	0.41	0.008	0.023
					In blowholes	1 3/16	0.13	0.40	0.009	0.021
					Edge of blowholes	1 5/8	0.14	0.40	0.009	0.023
					Beyond blowholes	2 1/4	0.17	0.41	0.009	0.028

Segregation in various types of steels has been explained in several papers.^{2,13,18} The fundamental feature responsible for segregation during solidification of steel ingots is the greater solubility of the common impurities (elements other than iron) in the liquid than in the solid phase. Thus in the solidification of molten steel a solid freezes from the liquid that is lower in impurities than the original liquid, and a liquid phase containing the excess impurities accumulates along the freezing interface. The extent of segregation by this simple procedure depends on the exact phase relationship of the specific binary system involved and how closely equilibrium conditions are approached.

If no other considerations were involved,

entrapped is greatly reduced. Under such circumstances the degree of segregation of any element in the freezing zone approaches much more closely that which would be expected through consideration of the relative solubility in the solid and liquid phases.

As a result of the association of gas evolution with freezing, definite segregation occurs during the first stage of solidification yielding a narrow outer rim of lower analysis than the liquid metal and a high analysis area within the blowholes. To show more clearly the nature of subsurface segregation on capped steel supplementary drillings for chemical analysis were taken at four successive positions in and just beyond the outer rim at the middle height of three normal capped ingots. The analyses of the

samples are given in Table 2. The similarity in segregation pattern to that occurring in rimmed steel is immediately apparent in the table. Even in the sample closest to the ingot surface, the carbon and sulphur analyses were definitely below that of the original liquid. Approaching the edge of the blowhole zone the analysis of these two elements increases. Beyond the blowholes, the analysis is greater than the original liquids.

As might be expected, there was a definite tendency toward suppression of gas formation near the bottom of some of the experimental ingots. As a result, the tendency toward developing a negatively segregated rim in that part of the ingot was also suppressed (Figs 16, 17, 18, 25, 34, 35). The apparent suppression of gas formation in the bottom of ingots can obviously be associated with higher pressures existing in that region after the ingot is poured.

The sulphur prints of Fig 32 indicate some general differences in subsurface freezing pattern observed in ingots poured from liquid steel with increasing oxygen content. The oxygen determination was made on a bomb type sample dipped from the ingot preceding the one shown in Fig 32.

All sections of Fig 32 were obtained from the middle ingot height. The low oxygen completely deoxidized section of Fig 32 shows clearly a dendritic outline in the columnar zone. The ingot contained 0.033 pct aluminum. As would be expected, there is no indication of any blowhole or outer rim formation. In ingots with greater oxygen contents, the sulphur print shows the negatively segregated appearance of the rim. There is no indication of the dendritic pattern in any of the three more highly oxidized ingots. In ingots with a wide blowhole zone, an example of which is given in the 0.030 pct oxygen ingot, the difference in analysis between the subsurface zone and the balance of the ingot is clearly brought out by sulphur printing. The width of the subsurface blowhole zone in the ingot with 0.030 pct oxygen approximates that often

encountered at the midway height of capped steel ingots. (Incidentally, the 0.030 pct oxygen section clearly illustrates the origin of the oblique segregate streaks of the type mentioned earlier in connection with the description of ingot *A*.)

Figs 33, 34 and 35 are presented to show more clearly the nature of subsurface solidification in semikilled ingots. Fig 33 shows the subsurface freezing pattern at three positions in a capped ingot to which an excess of aluminum was added prior to completion of pour. As a result of the early aluminum addition, no blowholes exist beyond the relatively narrow zone in either the top or middle section. The line along which the steel was deoxidized is clearly evident in these two sections. In the top section blowholes began forming almost at the very surface and terminated at the inner edge of the shallow rim. A small V shape segregate streak appears attached to the inner end of the largest blowhole in the top section. Distinct columnar dendrites are evident toward the center of the ingot.

The middle section has a much wider negatively segregated zone than the top section. The outstanding feature of this rim is the refilled appearance of the rounded blowholes. This appearance, which is associated with local heavy aluminum deoxidation will be discussed in more detail later. The presence of arrow shaped blowhole contours between the refilled blowhole and the surface indicates that some gas was evolved during the early stages of freezing. The metal just inside the contours appears dendritic. Since the contours are located fairly close to the surface, it is likely that the gas evolution was associated with some movement in the liquid during the last stages of pouring the ingot.

The most prominent feature of the skin zone in the bottom section of ingot *C* is a number of nearly vertical lines that roughly parallel the ingot surface. These lines, which appeared characteristically in practically all ingots observed, could not be

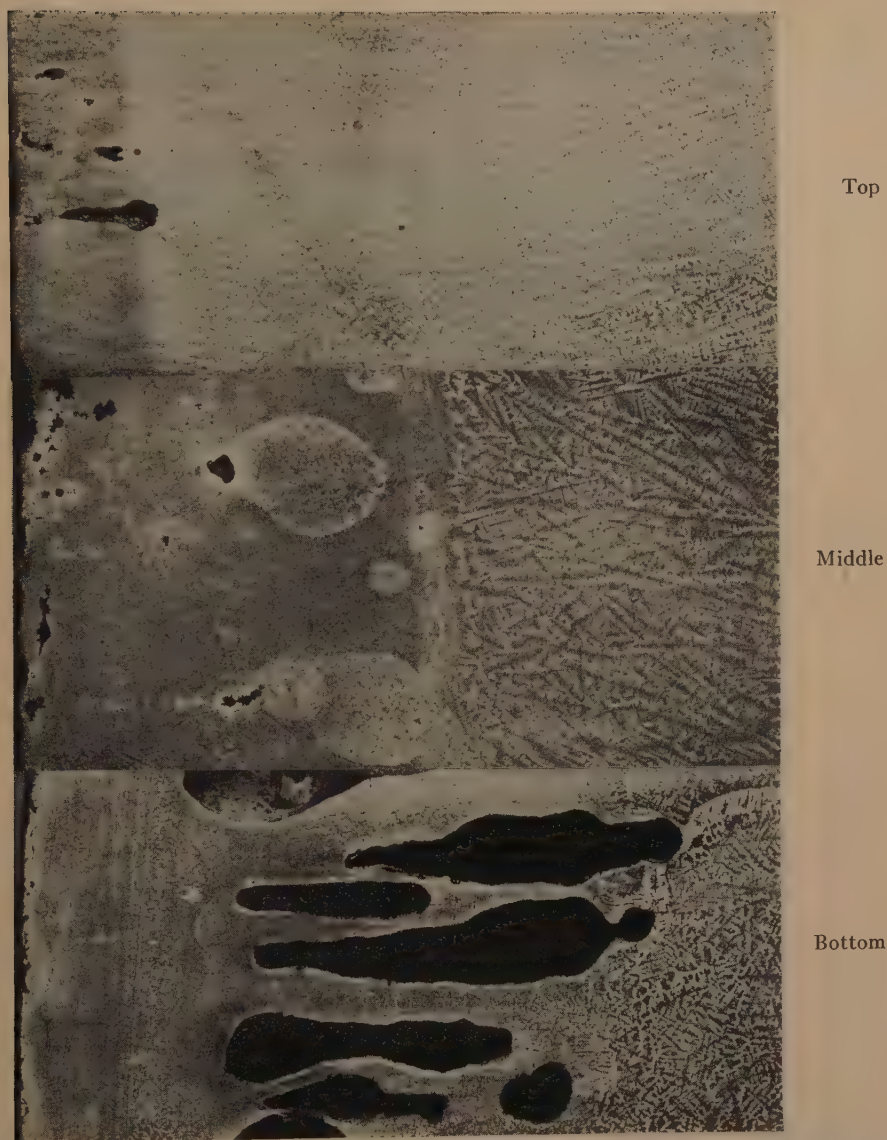


FIG 33—SUBSURFACE STRUCTURE AT TOP, MIDDLE, AND BOTTOM OF INGOT C. LIQUID METAL ANALYSIS IN PER CENT, CARBON 0.21, MANGANESE 0.39, PHOSPHORUS 0.010, SULPHUR 0.026. BOTTOM SKIN ANALYSIS IN PER CENT, CARBON 0.17, SULPHUR 0.020. ORIGINAL MAGNIFICATION 4. ETCHANT: STEAD'S REAGENT. REDUCED APPROXIMATELY ONE-THIRD.

resolved by sulphur printing. It appears likely that these lines are associated with surges in the flow of metal during pouring of the ingot. Between the lines and the

in Fig 33. The sample for analysis was obtained along a plane parallel to and about $\frac{3}{16}$ in. below the surface. The blowholes themselves are irregular in shape. Connect-

Middle



Bottom

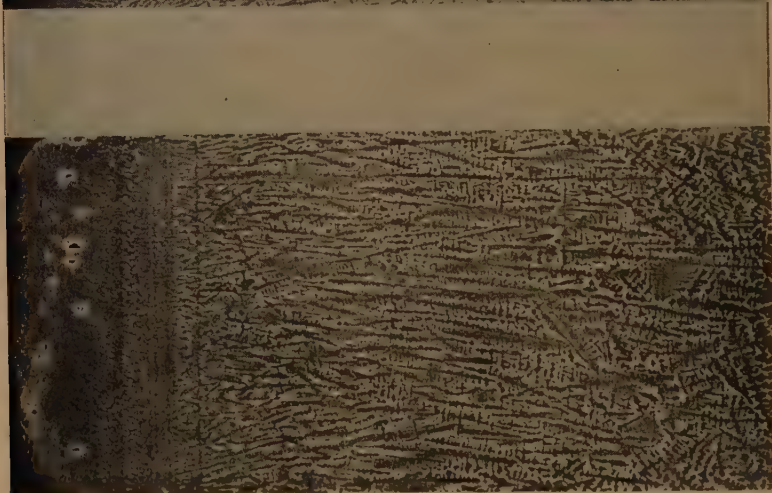


FIG 34—SUBSURFACE STRUCTURE AT MIDDLE AND BOTTOM OF INGOT K. LIQUID METAL ANALYSIS: IN PER CENT, CARBON 0.21, MANGANESE 0.48, PHOSPHORUS 0.010 SULPHUR, 0.026. BOTTOM SKIN ANALYSIS IN PER CENT, CARBON 0.19, SULPHUR 0.022. ORIGINAL MAGNIFICATION 4. REDUCED APPROXIMATELY ONE-THIRD. ETCHANT. STEAD'S REAGENT.

blowholes there is a faint suggestion of a contour representing some possible gas evolution. Since the only evidence of possible gas evolution is just beyond the skin zone it is surprising that the carbon and sulphur content of the skin was well below that of the original liquid. The analysis of the skin zone is shown below the bottom photograph

ing the inner edges of the two upper blowholes there is a clearly defined segregate band. The band projects into the body of the ingot from the upper blowhole. The general pattern of these bands indicates that the segregation is associated with sluggish gas movement from the inner blowhole zone.

As shown in Fig 34 blowhole formation in the bottom of ingot *K* appears to have been almost completely suppressed. There is again no clear evidence of gas evolution

position of the lines in the bottom section. Blowhole formation begins close to the outer ingot surface. Above and below the actual blowholes the dendritic skin struc-



Middle



Bottom

FIG 35—SUBSURFACE STRUCTURE AT MIDDLE AND BOTTOM OF INGOT L. LIQUID METAL ANALYSIS IN PER CENT CARBON 0.18, MANGANESE 0.40, PHOSPHOROUS 0.009, SULPHUR 0.025. BOTTOM SKIN ANALYSIS IN PER CENT CARBON 0.15, SULPHUR 0.020. ORIGINAL MAGNIFICATION 4. REDUCED APPROXIMATELY ONE-THIRD. ETCHANT: STEAD'S REAGENT.

in the outer skin zone and, as in ingot *C*, the skin analysis is somewhat below that of the original liquid metal. The bottom section also shows the vertical lines mentioned in the discussion of ingot *C*. Columnar dendrites penetrate a short distance into the ingot.

In the middle section the vertical lines are faintly visible and it is interesting to observe that their location is similar to the

ture appears columnar. The undisturbed dendritic appearance adjacent to the skin blowhole indicates that there is little actual gas evolution at that stage of freezing. Near the outer surface of the section there is a suggestion of several small arrow shaped blowhole contours indicating that gas was evolved during the earliest stages of solidification. An interesting example of a sloping segregate band emanating from a subsur-

face blowhole is evident in the middle section. The structure beyond the holes is dendritic.

Gas formation in the bottom section

phur content of the outer skin at the bottom of ingot *L* was below that of the liquid metal. If gas evolution were completely suppressed definite negative segregation



FIG 36—SULPHUR PRINTS OF SECTION THROUGH TOP EDGE OF TWO ALUMINUM CAPPED INGOTS. MAGNIFICATION 1.0. REDUCED APPROXIMATELY ONE-HALF.

ingot *L*, Fig 35, also appears to have been largely suppressed. The porous outer skin indicates some gas formation during pouring. A single vertical line appears in the section. A short section of columnar dendrites exists next to the skin followed by a zone in which the dendrites are oriented more or less at random. In the outer skin of the middle section is a row of small blowholes. A second group of larger irregular blowholes exists further into the ingot. At the blunt inner end of some of the blowholes in the outer row are segregate spots. A sloping segregate band connecting the two largest blowholes of the section, traces the path of some gas movement between the adjacent holes.

As in Ingots *C* and *K*, the carbon and sul-

phur should not occur in the skin. It appears that the observed segregation in the skin was obtained during pouring and any associated gas evolution was encouraged through the vigorous movement of liquid metal next to the freezing interface.

Further interesting observations regarding the subsurface zone of the top part of capped ingots can be made in connection with the sulphur prints shown in Fig 36. In this figure are presented sulphur prints of sections through the top edges of two capped ingots. The subsurface zone of the original unetched sections appeared surprisingly free from porosity. The left hand section of Fig 36 can be divided into three distinct zones—an outer light subsurface rim, a sound dark intermediate zone in

which definite dendrites can be observed, and a light inner zone that includes rounded groups of blowholes. Analysis along a plane about 3 in. below the upper surface of the left hand section revealed that in the light subsurface zone the aluminum content was only 0.012 pct. Two samples from the clearly dendritic intermediate zone analyzed 0.085 and 0.095 pct aluminum. Between the intermediate zone and the blowholes, 0.038 pct aluminum was obtained while a sample taken further into the ingot analyzed 0.023 pct aluminum. The position of these analyses is roughly indicated in the figure. The relatively high analyses obtained in the intermediate zone indicates that considerable aluminum is carried into the body of the ingot. The dendritic pattern apparently is restricted to the high aluminum zone, beginning just beyond the light outer rim and terminating at the rounded inner blowholes.

The right hand section of Fig 36 shows very clearly the line along which the aluminum addition stopped the rimming action. The rim, which appears as a light outer zone, varies in thickness from about $\frac{5}{8}$ in. at the bottom of the section to nothing at the intersection with the upper surface. The darker area within the rim near the top of the ingot again indicates the zone into which a significant percentage of the capping aluminum was carried. A very interesting feature in the rim zone of the right hand section is the light gray areas that have the same general shape and location as subsurface blowholes. The original unetched section was absolutely solid where these gray areas appear. It is assumed from their general appearance that these grayish areas were originally blowholes in which the included gas was either completely reduced by the capping aluminum additions or reabsorbed in the deoxidized metal. After deoxidation the remaining void was refilled with liquid. A dendritic pattern can be observed in the upper right hand corner of this section. Again this pat-

tern is associated with high aluminum analysis (0.050 pct). Next to the solid part of the rim the aluminum content was 0.018 pct. Just beyond this zone toward the center of the ingot, the aluminum content was 0.009 pct.

It required about 40 sec to pour the part of the ingot represented by the right hand section of Fig 36. During this period the evolution of gas must have been stimulated by the motion in the steel resulting from pouring. From the appearance of the bottom part of this section it seems that the action subsided before or at the time of capping. The motion in liquid steel that accompanies pouring very likely exerts a direct effect on subsurface gas evolution and segregation and, consequently, should be recognized as a major factor in developing the subsurface structure of capped steel ingots.

Both the refilled blowholes and the association of visible dendritic pattern with high aluminum content are demonstrated again in the sulphur printed section shown in Fig 37. This particular type of pattern was observed just above the visible subsurface blowholes on capped ingots with large shrinkage cavities (Ingots *C* and *D*). The example of Fig 37 was obtained from the midway height of ingot *C*. The left hand section, which was etched with ammonium persulphate, shows that the subsurface zone was, to a large extent, free from blowholes at this ingot height. The corresponding sulphur print of the right hand section shows that during the pour the usual negatively segregated rim, including subsurface blowholes, began to form. After the deoxidizing aluminum addition was made, the blowholes were refilled. The refilled blowholes and the high aluminum analysis indicate the completeness of the deoxidation. Associated with the high aluminum analysis is the previously mentioned dendritic pattern.

The process whereby a negatively segregated rim forms during subsurface solidification of capped steel ingots should

naturally tend to increase overall segregation as compared to steels freezing with no gas evolution. It also seems logical to expect that the blowholes that are present

capped semikilled steels show greater segregation

The effect of temperature on overall ingot segregation of killed steel is generally

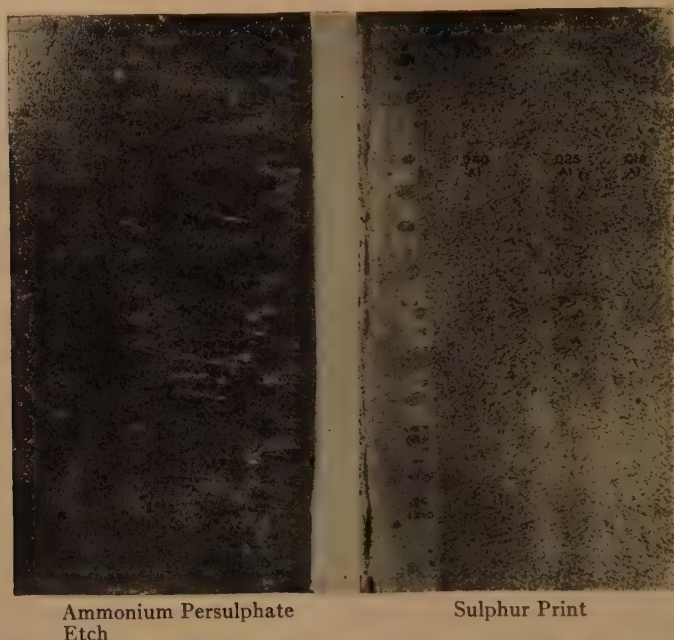


FIG 37--SUBSURFACE STRUCTURE AT MIDWAY HEIGHT OF INGOT C. ORIGINAL MAGNIFICATION 0.9. REDUCED APPROXIMATELY ONE-THIRD.

throughout a large fraction of the ingot subsurface area exert an insulating effect during freezing, thus reducing temperature gradients developed during solidification. As a result the extent of columnar freezing will be reduced.*

Both the negative segregation in the rim and the reduction in the extent of columnar freezing would contribute to increased overall segregation on capped semikilled steel. As a result it might be expected that capped steels segregate more than killed steel. In actual comparisons of the two types it is generally accepted that the

related to the extent of columnar freezing,¹³ increased temperature generally being associated with a deeper zone of columnar freezing. Any feature of ingot solidification which limits the extent of columnar freezing such as the insulating effect of subsurface blowholes on capped semikilled steels, could conceivably reduce the effect of temperature on overall segregation.* An indication that the effect of pouring temperature on overall segregation of capped semikilled steel is not as great as on fully killed steel was obtained in the segregation curves of

* Hultgren and Phragmen,³ (p 100), suggest that the heat insulating effect retards freezing at levels where rim holes exist. Thus they explain the formation of certain deformation lines as having been caused by the resultant difference in freezing rates at different ingot levels.

* The theory that pouring temperature has a reduced effect on segregation of capped steel ingots as compared to killed steel ingots can be inferred from the discussion of the heat of ingots 51 to 54 of the Fifth Heterogeneity Report.⁸ In that discussion it was pointed out that there was little difference in segregation between the first and last ingots of the experimental heats.

ingots *A* and *B*. (Fig 16 and 18). Despite a difference of 150°F in the pouring temperatures of these two ingots there was little observable difference in the overall segregation. The only marked difference between the two ingots is that the hot ingot (ingot *A*) had two areas in which the maximum carbon and sulphur analyses were obtained, one surrounding the central void and one just below the small cavity, whereas only one area of maximum segregation occurred in the cold ingot.

The interpretation of freezing patterns developed in sulphur prints is of interest. It was possible to bring out effectively large areas of negative segregation, localized zones of high sulphur, and zones of high aluminum content. With respect to finer details of solidification the sulphur print not only was inadequate but in some cases was confusing. For example, more sensitive etching techniques often show definite columnar dendrites in areas where there is no indication of this condition in the sulphur print. Aside from the general segregation pattern, the sulphur print gives very little information regarding the freezing in the blowhole zone.

A consistent association of dendritic patterns with high aluminum content was observed in the sulphur prints of several of the experimental ingots. Sims and Lillieqvist¹⁶ have predicted such a relationship in cast steel ingots. They attributed the dendritic freezing patterns (as those shown by sulphur printing) to variations in sulphide solubility caused indirectly by the addition of strong deoxidizers such as aluminum.

SOLIDIFICATION OF THE CENTRAL PART OF INGOT

Position of Maximum Segregation

The ingot height at which maximum segregation occurred was related, at least indirectly, to the method and extent of deoxidation. Table 3 compares the position of maximum segregation as estimated from

the segregation curves. The segregation position is given in terms of pct of the nominal ingot height.

TABLE 3—*Position of Maximum Ingot Segregation*

Ingot	Practice	Extent of Shrinkage Cavity	Maximum Segregation Position Per Cent Ingot Height
<i>A</i>	Capped	Very small	78 and 62
<i>B</i>	Capped	None	76
<i>C</i>	Capped	Wide Open	68
<i>D</i>	Capped	Wide open	62
<i>E</i>	Killed during pour	Small	70
<i>F</i>	Capped	Small	71
<i>G</i>	No mold deoxidization	Small	71
<i>H</i>	No mold deoxidization	Small	75
<i>J</i>	No mold deoxidization	Wide open	60

Position of maximum segregation:

Average for capped ingots with no definite pipe—

77 per cent

Average for ingots with small shrinkage cavities—

72 per cent

Average for ingots with wide open shrinkage

cavities—63 per cent

In the nine experimental ingots the position of maximum segregation varied from 60 to 78 pct of the ingot height. Apparently there is some elevation of the position of maximum segregation with decreasing size of the shrinkage cavity in the ingot. For the most part, the heavy positive segregation was localized in a fairly small area. There was very little positive central segregation above and below the range between 60 and 80 pct of the nominal ingot height.

Blowhole Formation in Interior of Ingot

Blowholes beyond the subsurface zone were largely limited to the top part of the ingot. In a few of the more highly oxidized ingots blowholes were observed in lower positions. In these cases the holes were commonly associated with inclined segregate streaks. For the most part the upper blowholes were elongated toward the center from the sides or the top of the ingot. In general, these elongated blowholes pointed toward the top position of maximum segre-

gation. There was very little positive segregation in the blowhole area.

These observations support the explanation of blowhole formation in the core zone of early capped ingots offered by Hultgren and Phragmen² (p 234). They attribute the central gas formation to the segregation of carbon and sulphur and to the reduced pressure resulting from natural shrinkage. The predominant occurrence of core blowholes in the top part of the ingot is likely the result of greater segregation of gas forming constituents as compared to the lower half of the ingot. This same segregation process provides the increased gas pressure that results in the formation of the blowholes that tend to reduce the size of shrinkage cavities. Since the upper blowholes form from a liquid phase that is relatively free from the interfering effects of any solid crystals, they tend to assume continuous elongated shapes in the direction of freezing.

In a number of ingots, sloping segregate lines were observed emanating from the inside of practically all blowholes (Fig 32, 0.030 pct oxygen section). If all the evolved gas represented by such streaks accumulated in a single zone in the ingot, some indication of large, compressed gas pockets should be evident in split ingot sections. The absence of such pockets suggests that much of the gas evolved from the highly segregated liquid just beyond the solid freezing wall is redissolved in unsegregated zones of relatively low CO pressure.

An interesting effect of low oxygen content on central blowhole formation was observed in the two ingots of Fig 11. These ingots contained 0.10 and 0.11 pct silicon at the time of pour. During the early stages in the solidification of these ingots the usual elongated top central blowholes began forming. In both ingots these blowholes terminate in a small but definite shrinkage cavity. Evidently, during the first part of freezing, sufficient oxygen was present to form some gas coincident with

the early reduction in pressure due to shrinkage. With continued pressure reduction, the limited supply of oxygen was not adequate for CO formation and as a result the shrinkage cavity formed.

Bridge Formation in Pipe Cavities

In all heavily piped ingots studied, it was found that bridges formed without regard to any features of teeming or steelmaking practices other than deoxidation. At least three distinct bridges formed in each heavily piped ingot (Figs 6, 7, 13). It is natural, therefore, to assume that such bridges may be present in all heavily piped ingots and that the exact nature of their formation is largely determined by the mold size and design. The bridges, for the most part, were free from any concentrated positive segregation. In several instances there was some indication of a slight negative segregation. The freedom of the bridges as well as the area surrounding the wide open sections of the pipe cavity from heavy segregation would indicate that the largest part of the surface of the cavity should be relatively free from oxides and high concentrations of metalloids. If precautions are taken to prevent oxidation (through eruptions and punched tops) of the inner surfaces of shrinkage cavities, the freedom from heavy segregation would favor welding in rolling.

Vertical Negative Segregate Bands.

The frequent association of vertical bands of negative segregate with successive pipe cavities (Fig 27, 30, 31) is not readily explained. In the absence of a better explanation, it is suggested that the streaks may have resulted from some motion of the liquid at the freezing interface at the time that the molten steel separated from the bridge. It is possible that just after the upper crust of a bridge solidifies a surface tension effect between the frozen metal and

the liquid below tends to retard the shrinkage process and thus tends to develop a negative pressure in the molten steel. A pause of this type in the shrinkage process is necessary to explain the fact that the thickness of the bridges often approaches two inches. When the tendency to contract becomes sufficiently great to cause the molten steel to separate from the solid bridge, the resultant pressure change sets up a physical motion in the liquid that sweeps the segregate away from the freezing interface. Such a process could conceivably be repeated below each bridge (Figs 30, 31). It is conceivable that the process by which the negative segregate bands were formed can exert considerable influence on the structure and segregation in fully killed hot topped ingots.

^ Segregate Lines

The vertical negative segregate bands appear to extend down to the ^ segregate lines, indicating that at the time of their formation the positive segregate had accumulated at the freezing interface. In most of the experimental ingots the lower central cone of negative segregation appears to begin just within the ^ segregate line. These two observations suggest the following mechanism for the formation of the inverted V.

It is generally accepted that the "cone" of negative segregation is formed as a result of free crystals settling to the bottom of the molten center of an ingot. It is conceivable, therefore, that ^ segregate lines merely represent the junction between the wall of metal freezing in from the outer surface and the accumulation of crystals building up in the form of the negative segregation cone. The ^ segregate lines, therefore, combine the highly segregated phase next to the solid metal freezing in from the mold wall and the less pure liquid displaced by the falling crystals. The fact that the ^ segregate lines terminate near the lowest part of the pipe cavity (enclosing the last

part of the ingot to freeze) is further indication that these lines represent the ingot depth at which there was a definite change in the mode of solidification. The continuity of the ^ segregate indicates that in many of these experimental open top ingots, freezing proceeded uniformly and often with relatively little physical motion in the liquid.

SUMMARY

This paper reports the results of an investigation of the structure and segregating characteristics of a series of experimental semikilled steel ingots. The experimental ingots were made with intentionally varied deoxidation under ordinary basic open hearth operating conditions.

By regulating the manner and extent of ladle and mold deoxidation, ingots were produced whose tendency toward gas formation ranged from a weak rimming action to a completely dead appearance. Throughout this entire range, the observed features of gas formation could be interpreted according to known equilibrium relationships between the specific deoxidizing element used, the carbon and oxygen contents and the pressures existing within the ingot.

The obvious features of semikilled ingot structure, such as pipe and subsurface blowholes, were primarily affected by the manner and extent of ladle and mold deoxidation. Increased ladle deoxidation reduced the tendency toward gas formation, thus reducing the extent of subsurface blowholes and increasing the tendency toward pipe.

In mold deoxidation, the timing of the addition was as important as its amount. The feeding of aluminum throughout the pour affected ingot structure much in the same manner as ladle deoxidation, an increase in the amount of the addition reducing the tendency toward gas formation. Capping with aluminum while a stream of metal is still entering the mold both deoxidized the liquid metal in the

body of an ingot and provided a cap to suppress gas evolution. Thus excessive capping additions made before shut-off were shown to result in heavily piped structure on ingots which also had definite subsurface blowhole zones. On almost all types of semikilled steel close control of mold deoxidation was a prime requisite for satisfactory ingot structure.

Many features of gas formation in capped semikilled steel ingots have been observed in varying degree in sluggish rimming steels. The rim that forms in capped steels is negatively segregated while positive segregate tends to accumulate just within this zone. The location, extent and type of subsurface blowholes vary both with change in deoxidation and ingot height. Solidification of the negatively segregated rim of capped steels differs from rimming steels in that a much greater proportion of the gas formed beyond the skin zone is retained in the form of subsurface blowholes.

In the experimental ingots, maximum positive segregation occurred in the top central position. The exact level at which maximum segregation occurred varied from 60 to 78 pct of the nominal ingot height, this position being highest in ingots with the smallest shrinkage cavity. There was very little positive segregation in the central zone above the position of maximum segregation.

In practically all experimental ingots, the existence of central blowholes was limited to the top part of the ingot. These central blowholes were usually elongated in the freezing direction; that is, they were directed from the surface and sides of the ingot toward the position of maximum segregation, indicating that the blowholes formed fairly continuously along with the wall of metal freezing in toward the center from the top and sides of the ingot.

All heavily piped ingots made in this study showed bridging. The bridges were essentially free from any heavy positive segregate. Also associated with the large

pipe in several of the ingots were narrow negative segregate bands that extended vertically from the edge of the cavity down to the Δ lines. A general mechanism was suggested that might explain the existence of such vertical negative segregate bands.

In most ingots, the Δ segregate lines were relatively straight and continuous and occurred in the same general position. It appeared that the Δ segregate line represented the junction between the outer wall of metal freezing in from the ingot surface and the interior zone that solidifies through a process involving the formation, settling and accumulation of free crystals.

The experimental ingots of this investigation covered a relatively narrow analysis range. In addition, a single mold size and pouring practice were used. These limitations should be recognized in applying the results of this study to any other set of operating conditions.

ACKNOWLEDGMENTS

The writer wishes to acknowledge the assistance received from personnel associated with open hearth and blooming mill operations at Inland Steel Co. He wishes to thank the management of Inland Steel Co. for permission to publish the data of this paper. He is grateful to A. P. Miller, General Superintendent, and J. H. Nead, Manager, Metallurgical and Inspection Department, who instigated the experimental program and who were instrumental in making the arrangements whereby the work could be carried out. He appreciates very much the aid in assembling data and the helpful suggestions regarding the preparation of the manuscript that he received from J. F. Woschitz, Supervisor, and J. W. Halley, Research Engineer. Chemical analyses were made under the supervision of C. O. Geyer, Chief Chemist and R. L. Harbaugh, Assistant Chief Chemist.

The writer is particularly grateful to T. S. Washburn, Assistant Manager, Metal-

lurgical and Inspection Department, for his advice regarding the development of the experimental program, his suggestions in conducting the work, and his invaluable helpful comments and criticism regarding the interpretation of the data and the preparation of the manuscript.

REFERENCES

1. M. Tenenbaum: Summary of Questionnaire on Deoxidation of Semikilled Steel. *Proc. AIME Open Hearth Conference* (1946) **29**, 222-226.
2. A. Hultgren and G. Phragmen: Solidification of Rimming Steel Ingots. *Trans. AIME* (1939) **135**, 133.
3. Committee of the Iron and Steel Institute. Second Report on the Heterogeneity of Steel Ingots. *Jnl. Iron and Steel Institute* (1928) **117**, 401.
4. Committee of the Iron and Steel Inst. Fourth Report on the Heterogeneity of Steel Ingots—British Iron and Steel Inst. (1932) Spec. Report **2**.
5. Committee of the Iron and Steel Inst. Fifth Report on the Heterogeneity of Steel Ingots. *Brit. Iron and Steel Inst.* (1933) Spec. Report **4**.
6. Committee of the Iron and Steel Inst. Sixth Report on the Heterogeneity of Steel Ingots. *Brit. Iron and Steel Inst.* (1935) Spec. Report **9**.
7. C. Walrand: Structure of Steel Castings. *Annal. Indust.* (1882) **14**, 234.
8. K. Styffe: Aluminum as a Refining Agent for Other Metals. *Jernkolorets Annal* (1892) **275**.
9. C. B. Wheeler: Report of Test of Metals. U. S. Gov. Print. Off. (1910).
10. W. Eicholz and J. Mehovar: Study of Properties of Steel Ingots. *Archiv Eisenhüttenwesen* (1932) **5**, 449.
11. F. Badenheuer: The Formation of Streaks in Silicon Steel Ingots. *Stahl und Eisen* (1934) **54**, 1073.
12. H. Schenck: Investigation in the Physical Chemistry of the Steelmaking Process. Berlin (1934).
13. B. M. Larsen: A Review of Factors Underlying Segregation in Steel Ingots. *Trans. AIME* (1945) **162**, 414.
14. Physical Chemistry of Steelmaking Committee. Basic Open Hearth Steelmaking. AIME (1944) **270**.
15. A. Hultgren: Crystallization and Segregation Phenomena in 1.10 Per Cent Carbon Steel Ingots. *Jnl. Iron and Steel Inst.* (1929) **11**, 120, 69.
16. C. E. Sims and G. A. Lillieqvist: Inclusions. Their Effect, Solubility and Control in Cast Steel. *Trans. AIME* (1932) **100**, 154.
17. John Chipman: Application of Thermodynamics to the Deoxidation of Liquid Steel. *Trans. ASM* (1934) **22**, 385.
18. John Chipman and Anson Hayes: Mechanism of Solidification and Segregation in a Low Carbon Rimming Steel Ingot. *Trans. AIME* (1939) **135**.

DISCUSSION

(H. B. Emerick presiding)

W. O. PHILBROOK*—We have no contributions of added information or criticism to offer, but since I have been given the first opportunity to discuss this paper I want very much to congratulate Mr. Tenenbaum and the members of the Inland Steel organization who worked with him for this very excellent paper, which extends the fine work they have done in the past on ingot structure and segregation of other types of steel into the important group of semikilled steels, and thus rounds out very nicely our picture of ingot solidification phenomena. I believe this paper is a most valuable contribution to the literature of steelmaking.

In reading the preprint, of course, I tried to analyze it from the standpoint of what it would mean to the steelmaker. It seems to me that it appears at first only to sharpen the "horns of the dilemma." The operator may produce steel by capping practice on the low side of the deoxidation range to avoid excessive pipe and segregation in the upper central portion of the ingot and hence obtain good billet yields, but at the expense of poor billet surface; or he may obtain good billet surface and low reconditioning costs by moderately strong ladle deoxidation practice, but with attendant piping of the ingots and perhaps lower yields, plus the added cost of the deoxidizers.

Perhaps Mr. Tenenbaum can tell us which is the worse of these two conditions from the overall standpoint of cost of production, yield of usable product and reconditioning costs, or does the balance change with various types of products and ingot sizes so that generalizations are not proper?

I was interested to note the extent to which the large pipe cavities of ingots fairly well deoxidized were welded in rolling to give apparently high yields of sound billets. I should like to ask if it would be safe to assume that pipe cavities of this size can consistently be welded to this same extent by rolling in normal commercial practice.

LEON NELSON†—Mr. Tenenbaum has certainly given us an excellent and detailed report

* Carnegie Institute of Technology.
† Republic Steel Co. Chicago.

on many phases of semikilled steelmaking. Really the only comment I have to offer is to state that I think trying to make semikilled steel so as to require no mold deoxidation is risky business if you wish to avoid low yield due to central piping.

This speaker favors the structure shown in the paper in Fig 2 and 5 (ingots *A* and *B*). To obtain best yield on semikilled ingots, it is essential that some gas evolution be prevented by the formation of a soundly deoxidized bridge across the top of the ingot. This sound bridge permits no oxidizing soaking pit atmosphere to reach any pipe cavity below. As a consequence any pipe cavity welds quite completely during rolling and results in maximum yield. As the report states, such an ingot is subject to some subsurface porosity but usually such blowholes are far enough below the surface so as not to be disturbed by proper soaking, pit heating, and rolling practice. Such an ingot is subject to more seaminess than a more fully deoxidized ingot but on the other hand is not nearly as subject to tearing as a more fully deoxidized ingot. Also as shown in Mr. Tenenbaum's paper, such an ingot (that is, one with a sound cap over the top) has appreciably less positive segregation along central axis below any pipe cavity.

A favored method for obtaining the desired condition (as shown in Fig 2 and 5) is to deoxidize with ferrosilicon in the ladle to such an extent that only a small amount of shot aluminum is needed to "cap off" properly in the mold. But ladle deoxidation should never be carried so far as to require no mold deoxidation. It is not too difficult to obtain this objective on the analysis considered in the report. But on high manganese-high sulphur analyses (where the large ladle additions have a definite deoxidizing effect), furnace oxidation must be carried to greater extremes and ladle deoxidation (by ferrosilicon, and the like) must be kept at a minimum—or even nil on some analyses.

It is noticed that a spiegel addition has been used on all ingots studied in the report. The speaker has always questioned the value of using a "spiegel wash" as a routine practice in making semikilled heats.

C. E. SIMS*—I was wondering if you had

* Battelle Memorial Institute.

found any way, other than the sulphur print, to show that there was segregation in those areas.

M. TENENBAUM (author's reply)—We have actually analyzed it by the inverted V segregated lines, and there was a distinct segregation there.

JOHN S. MARSH*—I should like to repeat what Mr. Philbrook said in complimenting Mr. Tenenbaum on his very fine job.

My question has been asked already: has any decision been reached on deoxidation practice which will give the greatest over-all ingot yield?

GILBERT SOLER†—I want to commend Mr. Tenenbaum on his very excellently prepared paper. It has quite a bit of data.

ROBERT K. KULP‡—I wish to join other discussers in congratulating Mr. Tenenbaum for the preparation of a thorough paper which covers some of the problems involved in the manufacture of semikilled steels.

A greater variety of practices are used for the production of semikilled steels than for any other class of steel. Variables must be held to a minimum in any experimental program, and the work involved in Tenenbaum's paper is extensive in spite of the fact that only one major variable, deoxidation practice, is considered. More emphasis might have been placed on the importance of several variables not included in the work. The following comments are offered as supplementary remarks to the general discussion on the factors involved in the manufacture of semikilled steels.

Tapping carbon and final analysis play an important role in determining deoxidation practice. With tapping carbons as low as 0.06 pct and final carbons as high as 0.30 pct, schedules requiring different amounts of deoxidizers must be established. In the practices described in the paper, ladle deoxidation included only single additions of either aluminum or ferrosilicon. Some plants use a combination of aluminum and ferrosilicon in the ladle and it would have been of interest to include such a practice. Mold size should be

* Bethlehem Steel Co.

† Atlas Steels Limited.

‡ Electro Metallurgical Co.

considered in developing deoxidation schedules; it can be broadly stated that as mold size increases, requirements for close control of ladle deoxidation decrease. Pouring rate is an important factor which affects surface quality. A slowing of the rate of rise of the metal in the molds normally results in an improvement in surface quality. One method of obtaining close control over metal entering the mold is to resort to bottom pouring by which practice rate of rise can be reduced to any desired figure.

Several of the ingot structures illustrated in the paper exhibited blowholes positioned fairly close to the ingot surface. Were these blowholes harmful to the surface quality of the rolled product or were such difficulties avoided by careful control in the soaking pits?

H. W. MCQUAID*—I might say something on the subject of semikilled practice especially as it applies to small ingots. There has been a lot of trouble lately in plants that are new in the semikilled and rimmed ingot field especially in the smaller ingots. Most of this trouble is due to too much furnace and ladle deoxidation resulting in deep pipe and tears. As Mr. Nelson said we get into trouble with tears with too much deoxidation so we cut down on our furnace and ladle deoxidation and the tears disappear and the first thing we know we get spongy ingots.

I would like to say that Mr. Kulp spoke of a lot of things which are especially interesting. One is the factor of rise of metal in the mold. I know directly from my experience in small molds, big end up, the rate of rise is a very critical factor as the heat in the mold affects gas formation.

It is hard in a discussion like this to separate semikilled from rimmed practice since they do overlap in some grades. There is no doubt but what the pouring floor practice is of the greatest importance with either grade—the principal requirement of the melter being to produce the desired analysis at the right temperature and open enough in the ladle so that the pourer can control the final deoxidation in the mold. The proper capping of a semikilled ingot can only be obtained when the man responsible for the capping has an open steel to work with and

knows what is required. It requires no little skill to produce sound semikilled ingots which are not spongy and which will roll without tearing in the blooming mill.

I would like to ask Mr. Tenenbaum what practice he would recommend on 14-in. and 18-in. ingots cast with the big end up. Would his practice vary if the end use were wire and not flat product?

I appreciate this paper very much and I know many of us will get a lot of good information from it. I think it is a real contribution to a much neglected section of steelmaking.

M. F. YAROTSKY*—The paper is a fundamental contribution to the steel industry and will materially assist us in resolving some of the confusion which exists in connection with the manufacture of this grade of steel. I have always believed that less control has been exercised in the manufacture of semikilled steel as compared to fully killed or rimmed steels. The apparent reason seems to be that it is an ordinary grade of steel made in large quantities and lends itself to a wide range of irregularities in practice. Also the ultimate quality of the semikilled ingot is more apt to be affected by the pouring pit practices.

I believe the author will agree that we must have diversified practice to produce satisfactorily the many varieties of semikilled steel in demand. The extent of oxidation, pouring temperatures, rate of pouring and other features of the steelmaking practices will vary, depending on the size of the ingot, the type of mill on which it is to be rolled and the type and shape of the product desired. It will range from open steel for small structural shapes and flat products to well deoxidized steel for heavy structural shapes and plates. We must also be aware that this type of steel is more sensitive to the effect of heating and rolling practices than either rimmed or fully killed steel.

In closing, I would like to compliment Mr. Tenenbaum and the Inland Steel organization for this excellent contribution. We are proud that it came from the Chicago District.

S. L. HOYT†—The discussions have repeatedly emphasized the importance of trying

* Consulting Engineer, Cleveland, Ohio.

* Carnegie-Illinois Steel Co., Chicago.
† Battelle Memorial Institute.

to make semikilled ingots uniform, with the yields secured. There can be no doubt about the importance of the yield because that affects the cost and also has an effect on the use to which the semikilled steel can be put. But the properties of the material are also important in their own right, regardless of the yield, or regardless of the process which you adopt in making the steel, and they, too, are bound to affect the general use of the product which you turn out.

When I was at A. O. Smith, we used large amounts of semikilled steel, and that led us into quite extensive investigations, not on the yield, of course, but on the properties of the steel. The more experience we had with the semikilled steel of the type we were using, the more respect we had for it.

That respect was engendered by two things: the small losses we had in fabrication and the quality of the product which we were able to turn out, when the steel was suitably made. When the steel was not suitably made with respect to the properties, our fabrication losses went up and the quality of the finished product suffered likewise—though I dare say the ingot yields were about the same in both cases and, from the paper, I presume the two would be judged to be equally satisfactory.

So in my discussion of this excellent paper I dislike accepting as the only criterion of success of semikilled practice, the ingot yield. The properties of the material are just as important; in fact, they are almost all-important when the steel gets into the hands of the fabricator.

There is one other point I should like to raise in connection with semikilled steel, and that is the deoxidizer used. I should like to ask if there is any difference in the properties of the steel and in the rolled surface conditions, with the use of silicon or aluminum to produce the desired ingot structure. Does the use of aluminum give as high a quality of surface as the silicon practice?

M. TENENBAUM—I would like to thank all of the discussers for their kind remarks regarding this paper. I appreciate them very much.

I think I will perhaps reverse the procedure in answering the questions and answer Dr. Hoyt's question first. I am very glad that someone did emphasize the point of view of the consumer because, after all, that is the person

for whom the steel is made, and it is his uses which we must consider first.

As John Marsh pointed out, we only produce the maximum yield of a quality that is acceptable to the consumer. It is my thought that the consumer should recognize both the limitations and the advantages of semikilled steel and thus allow himself to use the grades to the best advantage. With a knowledge of the properties of the semikilled steel, consumers are in a position to obtain a satisfactory product at a reasonably low cost.

Thus, if a consumer has use for a grade with no very severe properties desired other than it meet a rather wide tensile range, it usually is not necessary to provide a very expensive grade of steel. Thus he can obtain a grade that is perfectly satisfactory for his particular application at reasonable cost to himself.

In the manufacture of more completely deoxidized types of semikilled it is usually preferred to use silicon rather than aluminum for the primary ladle deoxidation. This preference is based on the fact that enough silicon may be added to suppress subsurface blowhole formation to the point where good surface quality is attainable. With controlled further deoxidation there can be some gas formation within the body of the ingot to compensate for some or all of the shrinkage.

Continuing and going backwards, I would like to support Mr. Yarotsky for his remarks on the effect of deoxidation on steel, and the effect of heating practice and rolling practice. He has pointed out that semikilled steels cannot be made by one single practice for all applications. I think our views coincide.

On the question of rolling and welding, I think welding during rolling is one of the very pertinent questions in the industry today. We are beginning to recognize more and more how much welding can be accomplished during the rolling process. I think the plants do some of it right along, whether they are doing it intentionally or unintentionally. Most plants are making grades in which they intend to accomplish some welding of pipe as well as subsurface blowholes during rolling.

Leon Nelson mentioned the undesirability of using no mold deoxidizers. The ingots of Fig 11 were made using no mold deoxidizers. In these ingots the pipe is away from the top surface and well down into the ingot. This practice is not

recommended when the overall deoxidation is marginal for the reasons given by Mr. Nelson. However, there appears to be some application

structure is concerned. Spiegel is a fairly innocuous furnace addition in its effect on gas-forming reactions. Thus its use is dictated



FIG 38—ETCHED SECTION FROM 12-IN. \times 12-IN. BLOOM ROLLED FROM INGOT TREATED WITH HYDROGEN—TOP CUT.

for grades made by a similar practice but which involve slightly more complete deoxidation.

Generally for the highest yields, some adjustment of oxidation is allowed for the mold addition. This not only completes deoxidation but allows for the variations from heat to heat which occur so characteristically in open hearth practice.

The question as to the use of spiegel does not seem to be very significant insofar as ingot

more by individual plant conditions than by any specific effect on ingot structure.

In answer to Mr. Sims' question as to evidence other than sulphur printing to establish the existence of inverted V segregate this was done by drilling around the indicated segregated position. When sufficient samples were taken the position of the segregate could be established by chemical analysis.

Mr. Yarotsky has answered John Marsh's

question as to the preferred practice. There is no preferred practice on semikilled steel as far as we can see. It depends considerably on the

was carefully controlled. The point that rate of pour may affect the position of blowholes is very well taken. We have had no direct experi-



FIG 39—ETCHED SECTION FROM 12-IN. \times 12-IN. BLOOM ROLLED FROM INGOT TREATED WITH HYDROGEN—BOTTOM CUT.

application. A more detailed discussion of this general subject is given on p. 127 of the text.

Mr. Kulp pointed out some of the limitations of this investigation. We intend to extend this investigation to other steel analyses, and hope to make further information available in the near future.

Mr. Kulp suggests that the rate of rise of metal in the mold definitely affects quality. This brings up a point that was not sufficiently stressed. On the ingots studied the rate of rise

ence with this variable, but there is some indirect evidence to indicate this is an important feature.

Mr. McQuaid's experiences with small ingots seem to parallel the results with larger sizes. It does not seem that any particular practice can be specified solely on the mold size and mold design. It is likely that the practice to be used would depend considerably on the end use.

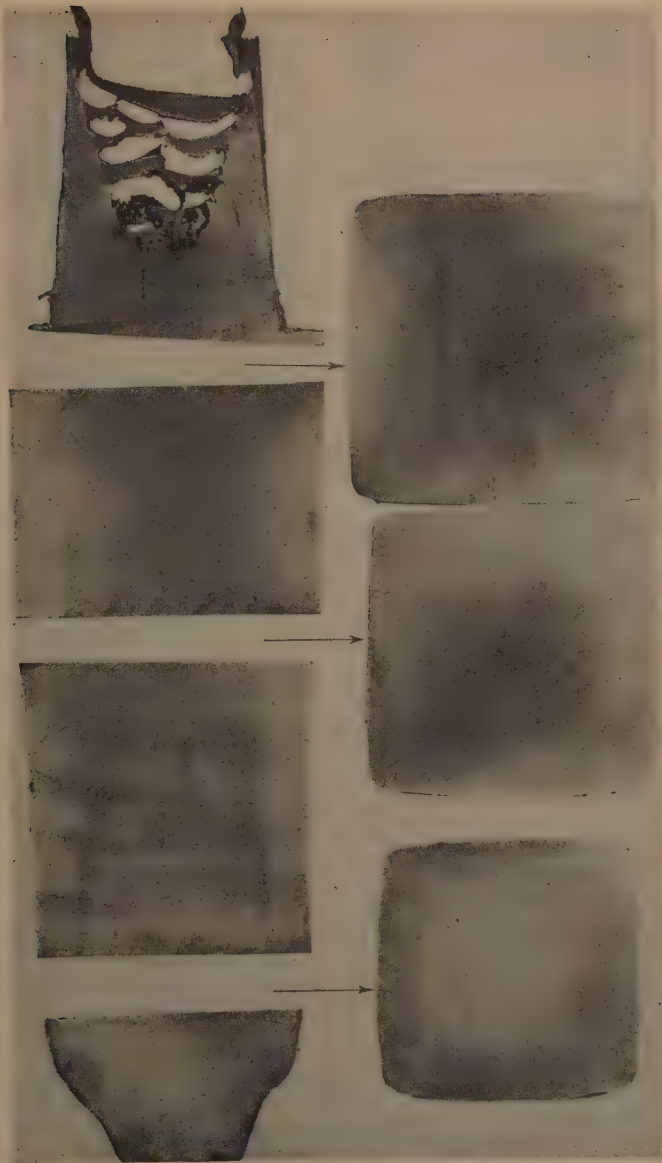


FIG 40—HEAT 7 \times 4320 INGOT NO. 1. 16 PCT HOT TOP EVACUATED.

*Further Discussion on Hydrogen in Killed Steels and Its Effect on Ingot Structure**

B. R. Queneau†—The origin and effect of hydrogen in liquid steel have been subjects of

considerable experimentation and discussion, but as yet our knowledge is incomplete. As part of a South Works investigation on flakes in steel, an ingot of SAE 4140 was treated with hydrogen. There were added to the ingot 130 cf of hydrogen by means of a lance as the metal

* This discussion on ingot structure was presented at the steelmaking session, Chicago, 1947.

† Carnegie-Illinois Steel Co., Chicago.

filled the mold. The ingot was rolled to 12 × 12-in. blooms and slowly cooled. Sections from these blooms were macroetched and compared with other ingots from the same heat.

etched more rapidly, whereas the untreated ingots do not show these defects. It is believed that hydrogen gas was liberated on solidification to form blowholes and that the last metal



FIG 41—HEAT 7 × 4320 INGOT NO. 2. 16 PCT HOT TOP H ADDED.

Fig 38 and 39 show the etched sections from the hydrogen treated ingot. The core of the top cut contains dark blotches where the steel

to freeze drained back into these gas cavities as the hydrogen was liberated. A microexamination of the dark blotches showed them to be

highly alloyed and the presence of numerous sulphide inclusions confirmed the belief that these areas were the last to freeze.

The two rings seen in the section of the bot-

As a result of this marked segregation occurring in a heat of killed alloy steel when treated with hydrogen gas in the mold, it was decided to make a fundamental study of hydrogen in

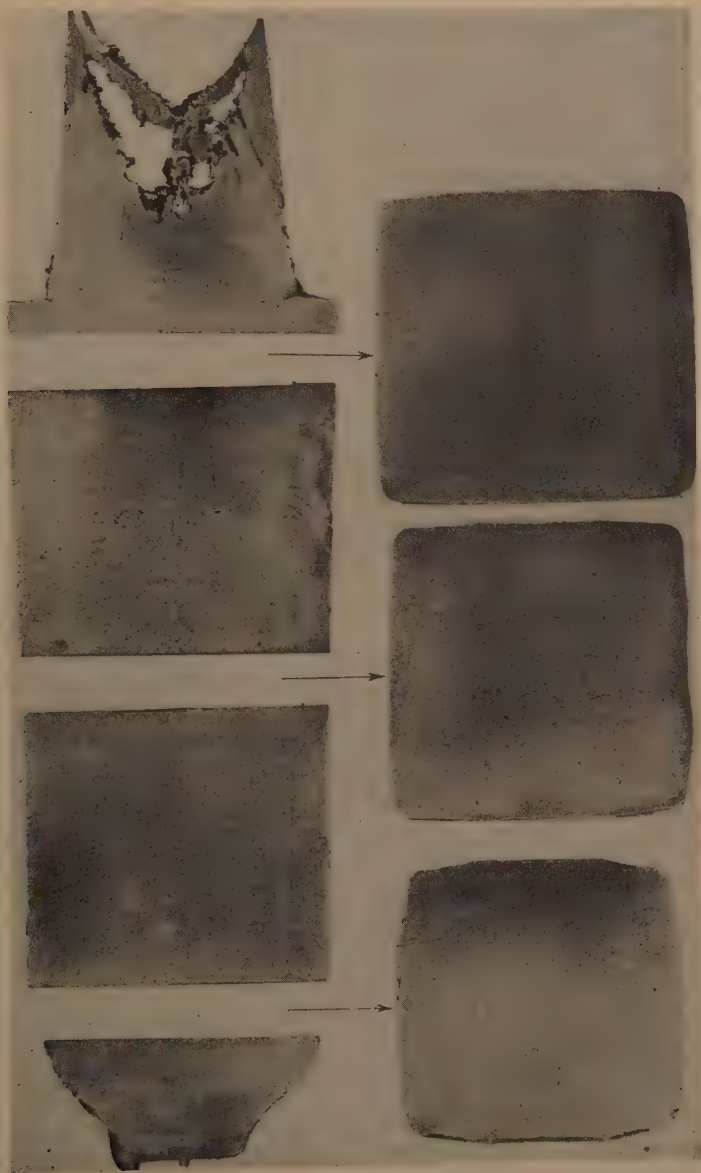


FIG 42—HEAT 7 X 4320 INGOT NO. 3. 16 PCT HOT TOP N ADDED.

tom of the ingot are mild steel and come from the lance which burned off while adding the hydrogen.

killed alloy steels. This investigation was divided in three parts: 1. The determination of the amount of hydrogen in molten steel as

affected by furnace practice and raw materials. 2. The methods of controlling the amount of hydrogen in the steel. 3. The effects of hydrogen on the steel quality.

To date, work has been completed on electric furnace steels. It has been found that (1) hydrogen in the steel increases with increase in the humidity of the furnace atmosphere and decreases with rise in the oxygen content of the bath. (2) Water vapor from additions during the reducing period seems to have greater effect than moisture in the charge or earlier additions. (3) A vigorous carbon boil or treatment of the bath with oxygen tends to reduce the amount of hydrogen in the molten metal.

In an effort to determine the effect of hydrogen on steel quality on electric furnace steels, a heat of NE 8740 was poured into 25-in. square molds with C & D hot tops. The various ingots were treated as follows:

No. 1—This ingot with a 16 pct hot top volume was continuously evacuated during its solidification. The evacuation was accomplished by placing a steel hood over the molten steel in the hot top and using a vacuum pump. Evacuation was continued for approximately $1\frac{3}{4}$ hr after pouring.

No. 2—Hydrogen was added to the steel throughout the teeming of the ingot. A $\frac{1}{4}$ -in. lance and a pressure of about 5 psi were used, the pressure being gradually increased as the ingot filled to 25 psi and a total of 35 cf was added

No. 3—Nitrogen was added to the steel throughout the teeming of the ingot in an effort to reduce the hydrogen content. The nitrogen was added in the same manner and approximately the same amount as the hydrogen.

Fig 40, 41 and 42 show the macroetched sections of these three ingots. No practical difference could be found between the evacuated, the hydrogen-treated or the nitrogen-treated ingots.

This heat of NE 8740 steel was made by standard South Works alloy steel practice using oxygen during the melt down period. The ingots are unusually sound, free of porosity or segregation and it is believed that this high quality is a direct result of the oxygen practice. The reason for the soundness of the hydrogen-treated ingot is apparently that there was insufficient pick-up of hydrogen to exceed the solubility at the freezing point and no hydrogen evolution occurred during solidification.

There is much further work to be done on the effect of hydrogen on steel quality but already we have good experimental data showing a marked decrease in flaking in alloy steels made with the oxygen practice, and the heat above indicates a marked decrease in segregation and increase in soundness in steel having low hydrogen content. Further experiments are planned to confirm these results.

The Origin of Silicate Inclusions in Basic Electric-arc-furnace Steel of Higher Carbon Contents

BY AXEL HULTGREN,* MEMBER AIME

(San Francisco Meeting, February 1949)

IN ingots of silicon-killed carbon steel made without addition of aluminum, transparent spherical or nearly spherical inclusions, up to about 0.15-mm diameter, are generally present. They may be glassy or crystallized, wholly or partially. In steels of high carbon contents they consist of silica,^{4,12} in steels of lower carbon contents and, in consequence, higher oxygen contents, of iron-manganese-silicate with higher iron and manganese contents the lower the carbon content.

Small silicate inclusions, about 0.01 mm or smaller, may occur, just as sulphide inclusions do, in portions that have been the last or nearly the last to freeze,^{10,12,17} this location being verified by primary etching.¹⁰ Hence, it may be concluded that they have separated from liquid steel that has become enriched in oxygen through segregation during freezing.

Silicate inclusions with a diameter larger than about 0.02 mm appear, at least in ingots of moderate size, to be distributed at random in relation to the primary structure and therefore may be assumed to have existed as droplets in the liquid steel before freezing started at the point in question. The average size of such large inclusions has been found to increase toward the axis¹⁷ and their amount to increase from the top downward in the axial region.^{2,10} It has been assumed

that this accumulation is a result of the droplets being brought down by the slowly settling metal crystals.²

It has been suggested that large silicate inclusions generally form,⁶ or may form,¹⁵ by coagulation of smaller ones, or by small drops being caught by larger ones during the rising of the latter.⁹ The occasional occurrence of a large inclusion surrounded by a swarm of small ones has been taken as a proof of this mechanism but, as suggested later, may be explained in another way. It has been pointed out that an inclusion droplet in the liquid steel may grow at the expense of an adjacent one, which implies diffusion of soluble inclusion-forming elements in the liquid steel.¹⁵ Further, it has been pointed out that, on cooling in ladle or mold, the metal-silicate equilibrium is displaced in the direction of separation of silicate. Thus inclusions may grow in size and amount.^{2,3,8,12,13,17,19,20}

The exposure of the liquid steel to the oxygen of the air during tapping and pouring, and the consequent reaction, has been mentioned as a source of the formation of inclusions^{19,20} but this possibility has not received particular attention. Further, the admixture of furnace slag during tapping¹ or of refractory material from various sources^{1,20} has been considered. The inclusions due to the latter may be recognized, however, through their resistance to hydrofluoric acid, imparted by the alumina content.

Silicate inclusions are often referred to as the natural and inevitable product of reaction on adding silicon or silicon

Reprinted from *Electric Furnace Steel Proceedings, AIME* (1946) 50, as translated by the author from *Jernkontorets Annaler* (1945) 129 (11), 633. Issued as TP 2418 in *METALS TECHNOLOGY*, August 1948.

* Professor of Metallography, Institute of Technology, Stockholm, Sweden.

⁴ References are at the end of the paper.

and manganese to the bath as deoxidizers.^{6,13,19,20} It is understood that under suitable conditions a certain amount of inclusions may be removed from the bath by rising, particularly when the

Kurlbaum pyrometer on a spoon sample and not corrected, was raised to about 1475°C and then allowed to drop to 1400° to 1390°C before tapping.

Still, the ingots cast from the ladle

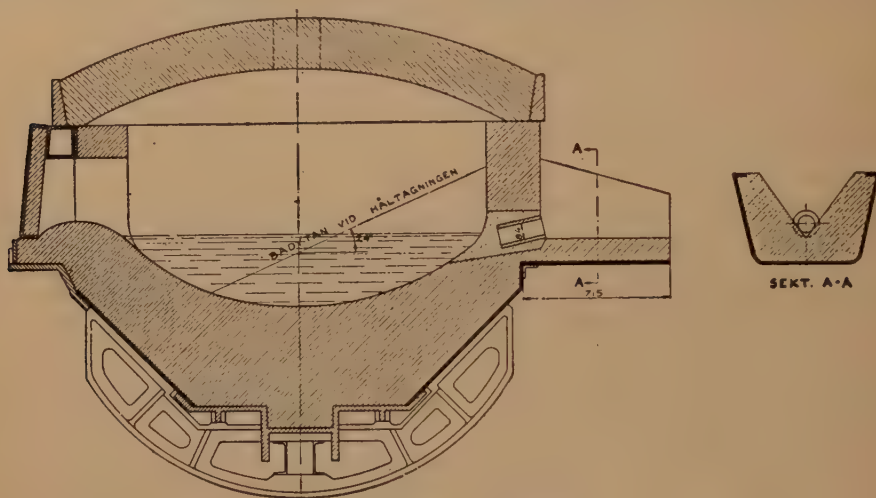


FIG 1—TAPPING ARRANGEMENT.

product is easily fusible, because it will then coaculate more readily.⁶ This question is discussed in succeeding paragraphs.

The idea that inclusions existing in the pig-iron charge may be preserved during the steel-melting process^{5,20} seems incompatible with the rapid reaction between liquid steel and dispersed slag demonstrated by Perrin.¹¹

EARLIER OBSERVATIONS AT SÖDERFORS STEEL WORKS

Steel samples taken from the furnace and cast in small test molds contained, or were free from, silicate inclusions, depending upon the moment of sampling. Within 10 or 15 min. after the silicon addition inclusions were present, later they were not. Only silicate inclusions larger than 0.01 mm were considered. The steel was 1.10 pct carbon steel, the furnace had two top electrodes and bottom electrode. Silicon addition was preceded by manganese addition. The temperature of the bath, as determined by a Holborn-

always contained silicate inclusions. At the time, the steel was tapped over an open spout in a broken stream, the tapping hole being pierced after the furnace had been tilted to let the slag come last.

Later, a refractory tapping tube was fitted to the spot (Fig 1) and a smooth, nonturbulent tapping stream was obtained. The amount of silicate inclusions appeared to decrease, probably owing to the contact area between steel and air on tapping, and therefore the amount of oxidation, being reduced. The fact that small test ingots poured with a restricted "strangled" stream from the ladle often showed up to 0.02 pct less carbon than the large ingots also seemed to indicate a reaction between steel and air.

SAMPLING AND METHODS OF INVESTIGATION

Several series of tests under varied conditions of tapping and pouring were carried out at Söderfors.

Samples were taken from the furnace with a slagged spoon and were cast in a

round mold (Fig 2). From the ladle samples were cast in a square mold (Fig 3). Further, samples were taken from furnace, ladle or mold by dipping a special sampling mold according to Kalling and Rudberg,¹⁶ so-called K-R samples.

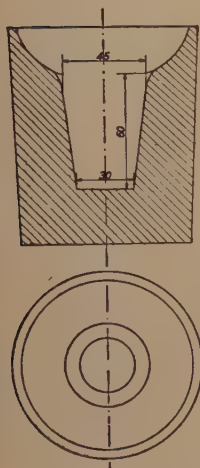


FIG 2—CIRCULAR
SAMPLE MOLD.

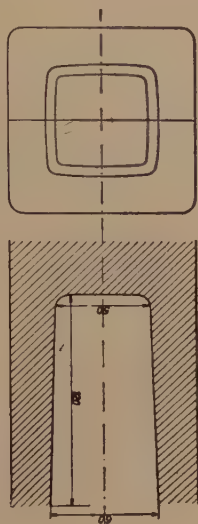


FIG 3—SQUARE
SAMPLE MOLD.

The sample ingots generally were cut in two lengthwise, one half was hardened and the longitudinal section was polished and examined in the microscope.

From ordinary ingots, generally 9 or 14 in. square, after annealing, transverse disks 12 mm thick were taken, often at two levels, $\frac{1}{3}$ and $\frac{2}{3}$ from the bottom. From each disk a rod was cut out from surface to center. The 12-mm wide section was used for investigation.

All inclusions larger than 0.01 mm were registered as to position, size, shape, color, degree of transparency and crystallization. From these data the number per unit area, average size and quantity of inclusions in percentage by volume were obtained. Generally, after a section had been examined it was reground to remove the inclusions counted and a new determination was made. This was often repeated.

EFFECT OF RESTRICTING THE POURING STREAM IN CASTING SMALL SAMPLE INGOTS

Sample ingots (Fig 3) were cast in succession from the ladle with full and with restricted stream, respectively. The steel had the following composition: C, 0.63 pct, Si, 0.72; Mn, 1.00; P, 0.007 and S 0.006. The nozzle diameter was 25 mm. Transverse sections, 50 mm from the bottom, were examined. The results are given in Table I.

TABLE I—Tests on Ingots of Figure 3

Position of Test	Ingot, poured with					
	Full Stream			Restricted Stream		
	n^a	d^b	Volume, Pct $\times 10^{-3}$	n^a	d^b	Volume, Pct $\times 10^{-3}$
Zone 0 to 1 mm from surface	5.0	66	1.7	47	92	31.3
Zone 1 to 3 mm from surface	2.5	42	0.4	52	254	265
Zone 3 to 7 mm from surface	1.5	68	0.5	18	104	15.8
Core 39 mm square.....	3.5	95	2.5	7	198	21.2
Total.....	1.8	82	1.3	19	170	54

^a Number of inclusions per 10 sq cm.

^b Average diameter, mm $\times 10^{-2}$.

A few inclusions with hard crystals (Fig 4) and opaque inclusions probably originating from refractory material were omitted. The transparent ones were generally round or rounded, of gray or yellow gray color in dark-field illumination. They were largely crystallized and often contained iron beads. Sometimes the matrix appeared to be eutectic. Various types of crystals were present, such as dark and light gray (light-field), more or less angular, elongated and rosette-like ones. Figs 5 to 15 show examples. Some inclusions showed a thin *border zone*, up to 0.002 mm thick, dark and transparent (Figs 6 and 8), others a *surrounding zone* in the metal, up to 0.02 mm thick containing dispersed small "satellite" inclusions, 0.001 to 0.004-mm diameter, and, within

a distance of about 0.012 mm, tiny particles 0.0001 to 0.0002-mm diameter (Figs 10 to 15). The satellite inclusions were also transparent and generally glassy.

Table 2 shows similar results obtained from another heat.

From the results recorded it may be concluded that the increase in amount of



FIG 4—INCLUSION WITH CRYSTALS IN RELIEF. $\times 1200$.

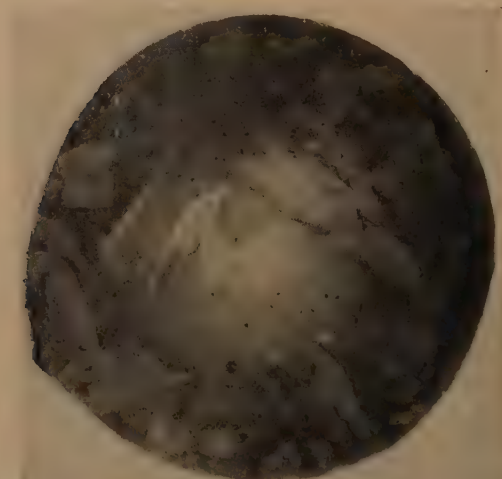


FIG 5—LIGHT GRAY CRYSTALS (PROBABLY FAYALITE) IN GLASSY GROUNDMASS.

When these inclusions showing surface phenomena were counted and measured the following results were obtained:

INCLUSIONS	NUMBER	DIAMETER, MM
With border.....	18	0.088
With surrounding zone.	14	0.271

inclusions caused by restricting the pouring stream is due to oxidation. Probably the surface of the metal stream is covered by a film of silicate rich in iron and manganese, which on mixing with the metal forms droplets. On account of their large size

they will probably rise quickly but many are caught by the rapidly freezing metal, particularly in the outer portions of the ingot. The flat inclusions (Fig 9) probably

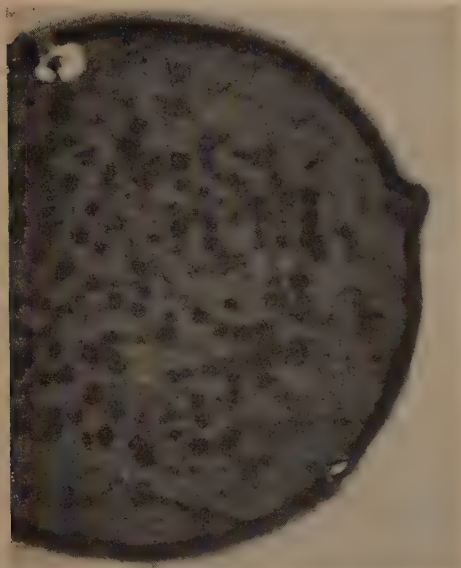


FIG 6—LIGHT GRAY (PROBABLY FAYALITE) AND DARK (PROBABLY CRISTOBALITE) CRYSTALS, IRON BEADS, BORDER ZONE.

owe their shape to the splashing movement of the liquid metal against the freezing front.

TABLE 2—Additional Tests on Ingots of Figure 3

Position of Test	Ingot, Poured with					
	Full Stream			Restricted Stream		
	n	d	Volume, Pct $\times 10^{-3}$	n	d	Volume, Pct $\times 10^{-3}$
Total.....	5.0	90	3.1	14	262	75

The iron-manganese silicate introduced into the steel in this way, not being in equilibrium with it, reacts with it. At the contact surface silicon in the steel will reduce iron and manganese from the silicate. The border probably is due to the increased silicon and decreased iron

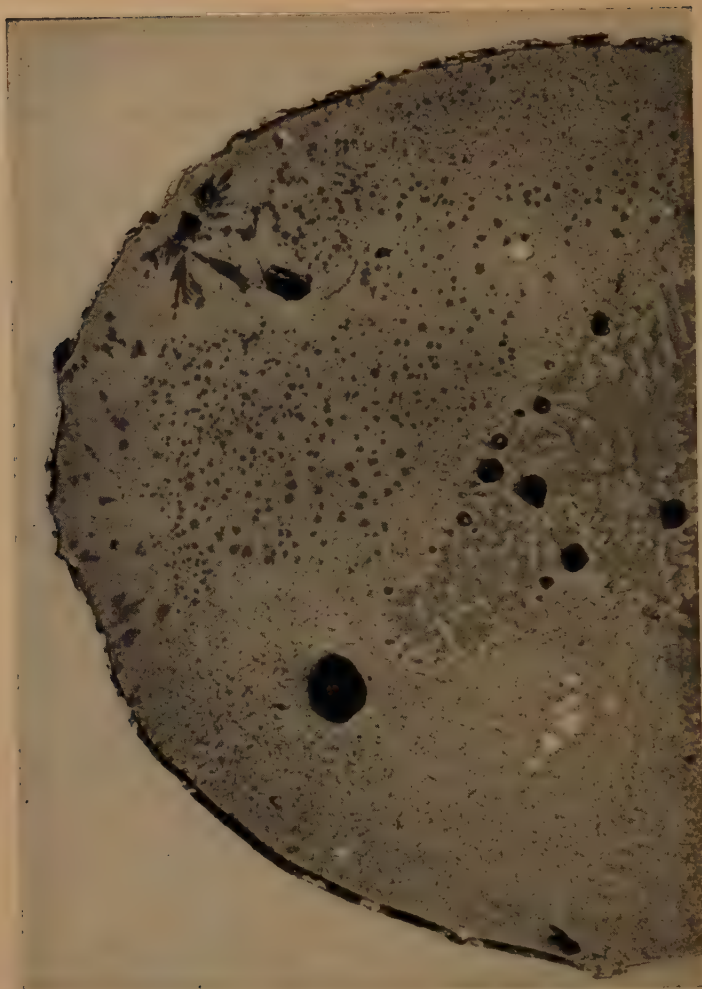
and manganese contents in the surface layer of the silicate droplet. In the surrounding metal zone the silicon content will thus decrease and the oxygen content will increase. In consequence, oxygen will diffuse into, and silicon from, the main mass of the metal. Where these diffusion currents meet, the small satellite inclusions are separated. The decrease in size of the main drop on reduction will probably influence the width of the surrounding zone. The fact that the inclusions with border were on the average smaller than those with surrounding zone may be due to the effect of the metal dominating in the former, and the silicate in the latter case.* These reactions may be assumed to stop when the steel freezes. The tiny oxide particles in the inner portion of the surrounding zone probably were precipitated from the solid metal during freezing or during cooling afterward. The ideas here put forward receive added support from results to be given in the following pages and are believed to have a bearing on cases described in the literature of larger inclusions surrounded by small ones.

TAPPING AND POURING TESTS ON A LARGE SCALE

Heats 6833-6836; 1.10 Per Cent Carbon and Silicon-manganese Steels

Four heats were made in a 3½-ton furnace, two of 1.10 pct carbon steel, and two of silicon-manganese steel. Compositions and tapping temperatures are given in Table 3. From each type of steel one heat was tapped as described in the foregoing pages, through a refractory tube (Fig 1), the slag coming last, and the other heat over a spout with a broken profile (Fig 22), in order to spread and impart a turbulent movement to the

* The average size of the sections is considered to be representative of the average size of the inclusions, although it is, of course, much smaller.

FIG 7—FAYALITE, CRISTOBALITE, IRON BEADS, BLOWHOLES. $\times 170$.TABLE 3—*Compositions and Tapping Temperatures*

Heat	Composition, Pct					Tapping Temperature, Deg C ^a	Tapping Procedure
	C	Si	Mn	P	S		
6833	0.66	0.70	0.99	0.011	0.006	1440	Through tube, metal first
6834	0.66	0.69	1.01	0.010	0.007	Fairly cold	Turbulent stream, some slag from the beginning
6836	1.12	0.26	0.34	0.010	0.007	1392	Same as heat 6833
6835	1.12	0.26	0.37	0.010	0.005	1388	Same as heat 6834

^a Uncorrected reading on bright metal surface in spoon.

TABLE 4—Inclusions in K-R Samples and Sample Ingots (Fig 2)

Heat	Steel	Tapping	Addition or Sample	Time			Inclusions Larger than 0.01 Mm																																																																																																																																																																																																																																																																																																																																																																																																																																																																
				Before Beginning of Tapping		During Tapping	After end of Tapping		Total			Transparent			Opaque																																																																																																																																																																																																																																																																																																																																																																																																																																																								
				Hr	Min.		Min.	Sec.	Pct $\times 10^{-3}$	n	d	Pct $\times 10^{-3}$	n	d	Pct $\times 10^{-3}$																																																																																																																																																																																																																																																																																																																																																																																																																																																								
6833	Si-Mn	Quiet stream	K-R 1 Mn added Pig iron added Si added K-R 2 K-R 3	1 1 30 27 15 4	I I 0	I 4	I 4	I 4	I 4	I 4	I 4	I 4	I 4	I 4	I 4	I 4	I 4	I 4	I 4	I 4	I 4	I 4	I 4	I 4	I 4	I 4	I 4	I 4	I 4	I 4	I 4	I 4	I 4	I 4	I 4	I 4	I 4	I 4	I 4	I 4	I 4	I 4	I 4	I 4	I 4	I 4	I 4	I 4	I 4	I 4	I 4	I 4	I 4	I 4	I 4	I 4	I 4	I 4	I 4	I 4	I 4	I 4	I 4	I 4	I 4	I 4	I 4	I 4	I 4	I 4	I 4	I 4	I 4	I 4	I 4	I 4	I 4	I 4	I 4	I 4	I 4	I 4	I 4	I 4	I 4	I 4	I 4	I 4	I 4	I 4	I 4	I 4	I 4	I 4	I 4	I 4	I 4	I 4	I 4	I 4	I 4	I 4	I 4	I 4	I 4	I 4	I 4	I 4	I 4	I 4	I 4	I 4	I 4	I 4	I 4	I 4	I 4	I 4	I 4	I 4	I 4	I 4	I 4	I 4	I 4	I 4	I 4	I 4	I 4	I 4	I 4	I 4	I 4	I 4	I 4	I 4	I 4	I 4	I 4	I 4	I 4	I 4	I 4	I 4	I 4	I 4	I 4	I 4	I 4	I 4	I 4	I 4	I 4	I 4	I 4	I 4	I 4	I 4	I 4	I 4	I 4	I 4	I 4	I 4	I 4	I 4	I 4	I 4	I 4	I 4	I 4	I 4	I 4	I 4	I 4	I 4	I 4	I 4	I 4	I 4	I 4	I 4	I 4	I 4	I 4	I 4	I 4	I 4	I 4	I 4	I 4	I 4	I 4	I 4	I 4	I 4	I 4	I 4	I 4	I 4	I 4	I 4	I 4	I 4	I 4	I 4	I 4	I 4	I 4	I 4	I 4	I 4	I 4	I 4	I 4	I 4	I 4	I 4	I 4	I 4	I 4	I 4	I 4	I 4	I 4	I 4	I 4	I 4	I 4	I 4	I 4	I 4	I 4	I 4	I 4	I 4	I 4	I 4	I 4	I 4	I 4	I 4	I 4	I 4	I 4	I 4	I 4	I 4	I 4	I 4	I 4	I 4	I 4	I 4	I 4	I 4	I 4	I 4	I 4	I 4	I 4	I 4	I 4	I 4	I 4	I 4	I 4	I 4	I 4	I 4	I 4	I 4	I 4	I 4	I 4	I 4	I 4	I 4	I 4	I 4	I 4	I 4	I 4	I 4	I 4	I 4	I 4	I 4	I 4	I 4	I 4	I 4	I 4	I 4	I 4	I 4	I 4	I 4	I 4	I 4	I 4	I 4	I 4	I 4	I 4	I 4	I 4	I 4	I 4	I 4	I 4	I 4	I 4	I 4	I 4	I 4	I 4	I 4	I 4	I 4	I 4	I 4	I 4	I 4	I 4	I 4	I 4	I 4	I 4	I 4	I 4	I 4	I 4	I 4	I 4	I 4	I 4	I 4	I 4	I 4	I 4	I 4	I 4	I 4	I 4	I 4	I 4	I 4	I 4	I 4	I 4	I 4	I 4	I 4	I 4	I 4	I 4	I 4	I 4	I 4	I 4	I 4	I 4	I 4	I 4	I 4	I 4	I 4	I 4	I 4	I 4	I 4	I 4	I 4	I 4	I 4	I 4	I 4	I 4	I 4	I 4	I 4	I 4	I 4	I 4	I 4	I 4	I 4	I 4	I 4	I 4	I 4	I 4	I 4	I 4	I 4	I 4	I 4	I 4	I 4	I 4	I 4	I 4	I 4	I 4	I 4	I 4	I 4	I 4	I 4	I 4	I 4	I 4	I 4	I 4	I 4	I 4	I 4	I 4	I 4	I 4	I 4	I 4	I 4	I 4	I 4	I 4	I 4	I 4	I 4	I 4	I 4	I 4	I 4	I 4	I 4	I 4	I 4	I 4	I 4	I 4	I 4	I 4	I 4	I 4	I 4	I 4	I 4	I 4	I 4	I 4	I 4	I 4	I 4	I

^a n, number per 10 sq cm.

^b d, average diameter, mm $\times 10^{-3}$

stream. In the latter case, some slag accompanied the metal from the beginning of tapping.

The ladle that was smeared with refrac-

No aluminum was added in ladle or molds. K-R samples and spoon-sample ingots (Fig 2) were taken from the furnace before and after additions. K-R samples

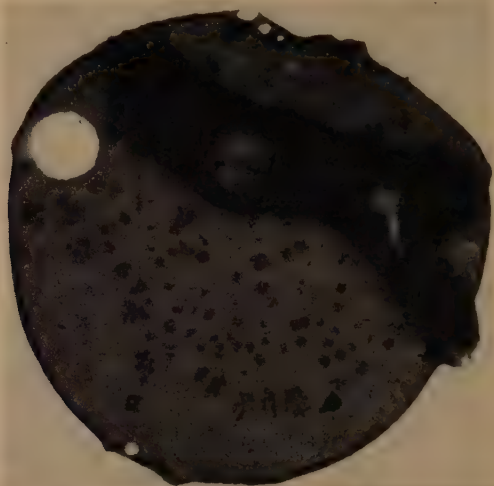


FIG 8—CRISTOBALITE ROSETTES, IRON BEADS, BORDER ZONE. $\times 500$.

tory mortar was well dried and preheated. The steel was held in the ladle for 4 to 6 min. and was poured through a 25-mm graphite nozzle. The following variables were represented in pouring:

- 9 and 14-in. square ingots.
- With and without after pouring.
- Full and restricted stream.
- Air blast directed on pouring stream.
- Pouring through funnel.
- Tarred and untarred molds.

were taken also from the ladle and in one case from a mold, always from a depth of about 15 cm below the surface. Sample ingots (Fig 3) were poured with full stream at three stages during the casting of the large ingots.

K-R Samples and Sample Ingots (Fig 2)

The K-R sampling was not entirely successful. Fig 23 shows that some of the K-R molds were not filled. Several of

TABLE 5—*Turbulent Tapping. Classification of Transparent Inclusions*

Heat	Steel	K-R Sample No.	Time after End of Tapping	Transparent Inclusions Larger than 0.01 Mm								
				Total		Per Cent			Average Diameter			
				<i>d</i>	Vol. Pct X 10 ⁻¹	Glassy	Semi- glassy	Non- glassy	Glassy	Semi- glassy	Non- glassy	
6834	Si-Mn	4	Min. Sec.	64	12.0	12	12	76	36	50	88	
		5	1 16	86	16.9	5	12	83	36	46	101	
		6	4 14	41	1.2	47	48	5	33	41	41	
6835	1.10 pct carbon	4	20	108	41	0.4	1.9	97.7	22	42	122	
		5	1 55	76	9.5	1.7	3.2	96.5	28	33	89	
		6	4 20	39	0.8	2.1	73.3	24.6	20	39	48	

the samples contain large cavities, apparently due to the outlet freezing prematurely. The varying locations of the

ingots (Fig 2) were solid. Two of the samples, taken before deoxidizing additions were made, contain blowholes.

The results of the examination of the sections are given in Table 4. A few large globules, exceeding 0.5 mm in diameter, have been omitted, on the consideration that drops of that size, had they been present before sampling, would have risen to the surface. They had probably been introduced in sampling, either from the basic slag cover--removed in preparation--or from oxidation of the metal. The opaque inclusions, which generally were few, probably originated in the refractory material. They will not be further considered here.

Table 4 shows that the metal in the furnace was free from inclusions before the additions were made, and contained only a small amount just before tapping, which was carried out 16 to 23 min. after the last silicon addition.

In the two heats that were tapped with a smooth stream, the steel showed in the ladle, immediately after tapping, an inclusion content of 2.4×10^{-3} , and 1.6×10^{-3} vol. pct, respectively. In the other two heats, tapped with a turbulent stream, the corresponding figures were 12.0×10^{-3} and 41×10^{-3} vol. pct. After 4 to 5 min. in the ladle, the latter figures had decreased to 1.2×10^{-3} and 0.8×10^{-3} vol. pct. Meanwhile, the average size of the drops decreased from 0.064 to 0.041 mm and from 0.108 to 0.039 mm.

It may be concluded that turbulence in the tapping stream causes oxidation of the metal to a far greater extent than smooth tapping does, with the result that larger and more numerous silicate inclusions are formed. These inclusions, however, will largely disappear during a few minutes in the ladle, partly by rising and partly by reduction and solution in the metal (see later). In consequence, the steel in all four heats showed about the



FIG 9—FLAT OR LENGTHENED INCLUSION 0.05 INCH FROM LATERAL SURFACE.

cavities is due to the mold, by oversight, having been held in different positions during freezing of the metal. The sample



FIG 10—"SURROUNDING ZONE," INCLUDING SILICATE GLOBULES AND PARTICLES. $\times 1500$.

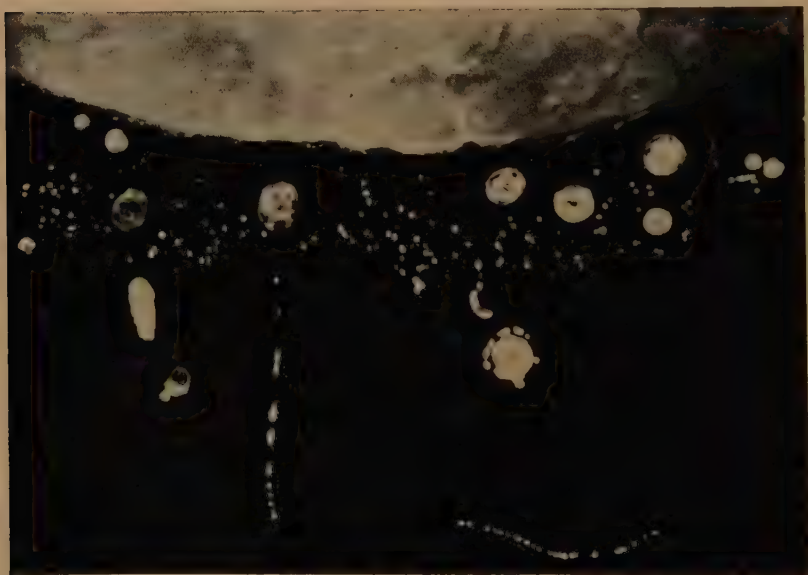


FIG 11—SAME AS FIG 10, DARK FIELD ILLUMINATION. $\times 1500$.

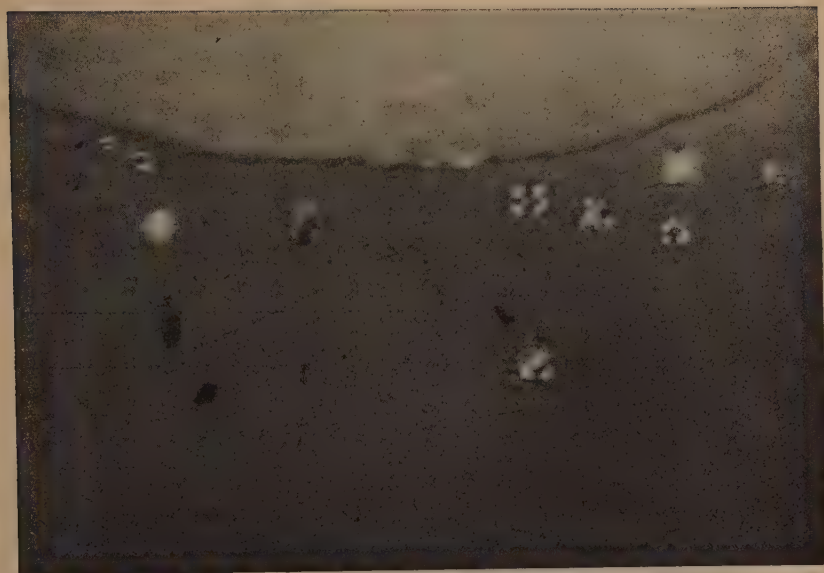


FIG 12—SAME AS FIG 10, POLARIZED LIGHT. $\times 1500$.

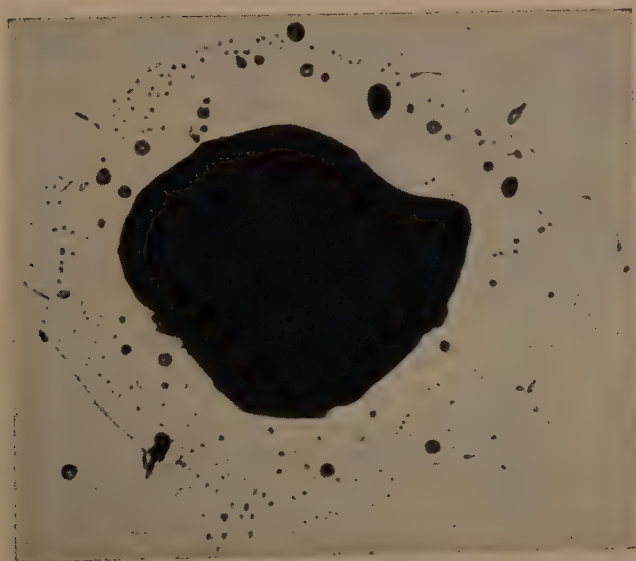


FIG 13—SURROUNDING ZONE. $\times 1500$.

same amount of inclusions in the ladle just before pouring.

Some transparent inclusions were wholly or largely *glassy* (Fig 16), showing in

Thus is confirmed what was suggested earlier in this paper—that the silica content of silicate inclusions formed by oxidation of the metal during tapping originally is

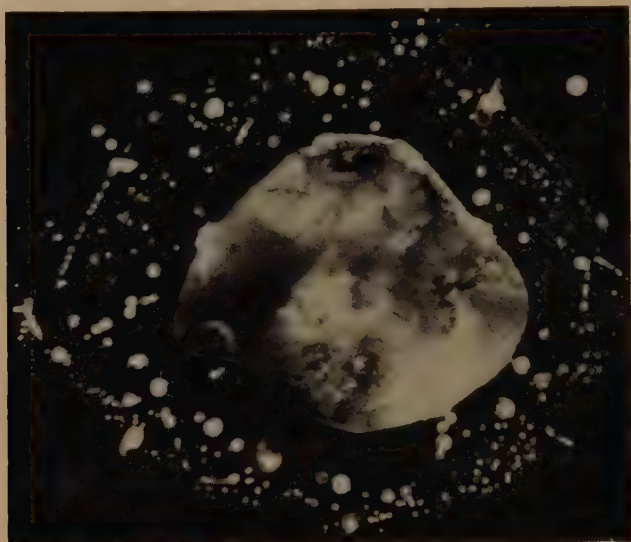


FIG 14—SAME AS FIG 13, DARK FIELD ILLUMINATION. $\times 1500$.

polarized light a dark cross (Figs 13, 15, 17). Others showed an imperfect cross, owing to the presence of a moderate amount of crystals. They will be called *semiglassy* (Figs 18 and 19). A third group of transparent inclusions lacked the cross (Figs 20 and 21) and are called *nonglassy*. Most of the latter showed a finely dotted structure; sometimes well-developed crystals were present. Transparent inclusions with crystals containing aluminum were not found.

On classification of the transparent inclusions in the ladle metal after turbulent tapping in these three groups, it is found (Table 5) that they changed with time. Their size and amount decreased and their composition was altered, as indicated by their increasing glassiness. This was most evident in the silicon-manganese steel but also visible in the carbon steel. Of all inclusions present at the same time the nonglassy ones were largest, the glassy ones smallest.

lower than the equilibrium value, and that during the ensuing chemical reaction it gradually increases, the tendency for crystallization thus diminishing. The velocity of this change will be greater in small than in large inclusion droplets and probably greater in the silicon-manganese than in the carbon steel.

It should be noted that the inclusions in these sample ingots rarely showed the reaction phenomenon referred to as border or surrounding zone. Two contributory causes thereof may be suggested: (1) the proportion of air to metal at the moment of oxidation was less in tapping than in pouring with a restricted stream and (2) the time for reaction was much longer in the ladle than in the cast sample ingots, which froze rapidly. It is to be expected that a so-called border will disappear with time by equalization. On the other hand, the small inclusions in a so-called surrounding zone may be gradually dissolved in the surrounding un-

saturated liquid metal, perhaps dissolved and reprecipitated on the large inclusion or possibly may join the latter through some coagulation process.

were not homogeneous in regard to distribution of inclusions. Thus results from the sample ingots (Fig 3) are probably more reliable.

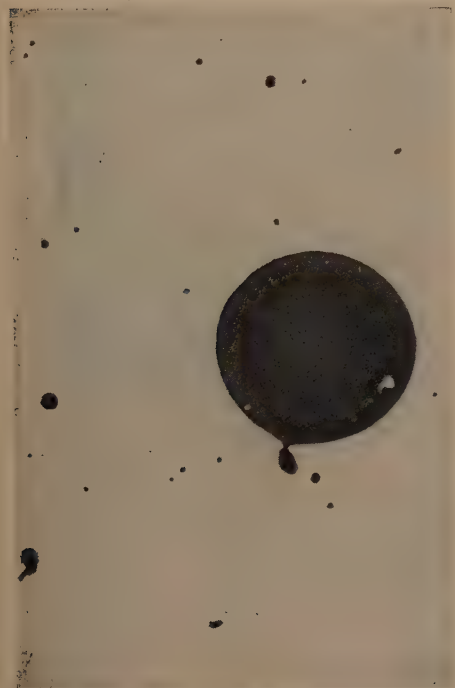


FIG 15—LARGE SILICATE GLOBULE TOGETHER WITH SWARM OF SMALLER ONES, 0.15 INCH FROM LATERAL SURFACE. $\times 500$.

Oxygen and Nitrogen Contents

Oxygen and nitrogen contents of steel samples obtained by the vacuum-fusion

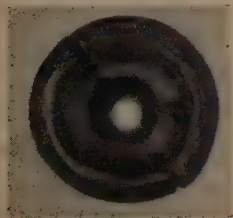


FIG 16—GLASSY INCLUSION. $\times 600$.

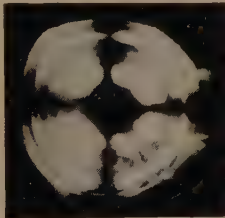


FIG 17—SAME AS FIG 16, POLARIZED LIGHT. $\times 600$.

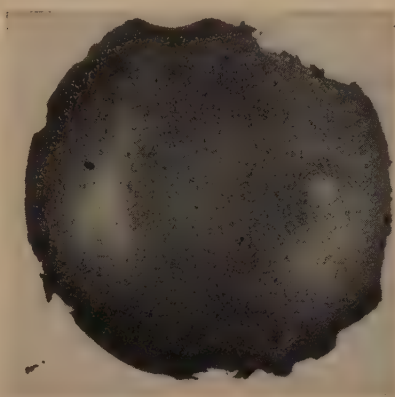


FIG 18—SEMIGLASSY INCLUSION. $\times 600$.

The oxygen content of the metal, at definite stages, is given for the four heats in Table 7.

Before tapping, the carbon steel was lower in oxygen than the silicon-manganese steel, probably an effect of the



FIG 19—SAME AS FIG 18, POLARIZED LIGHT. $\times 600$.

process are given in Table 6. Only one determination was made on each sample. As indicated above, the K-R samples

higher carbon content. On tapping, the oxygen rose, more on quiet tapping, unexpectedly. During about four minutes in the ladle it sank somewhat after turbulent tapping, but not after quiet tapping. In the sample ingots cast from the ladle,

oxygen was higher than before tapping and otherwise depended on composition and tapping procedure, being lower for turbulent tapping.

The only conceivable explanation appears to be that the white furnace slag on being mixed with the metal in the former case further reduces the dissolved oxygen

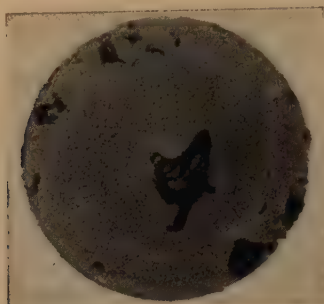


FIG 20—NONGLASSY INCLUSION. $\times 200$.

The expected correlation between oxygen and inclusion contents (Tables 6 and 4) was not realized. Allowing for some uncertainty in the oxygen determination for the K-R samples, it still seems probable that tapping the steel in a turbulent way, mixing it with slag, caused the oxygen content of the metal to increase less (about 70 pct) than quiet tapping, when the slag followed the metal (about 200 pct).



FIG 21—SAME AS FIG 20, POLARIZED LIGHT. $\times 200$.

content in a manner similar to the Perrin process for purifying liquid steel.¹¹ Simultaneously, other parts of the metal are brought in contact with the air and oxidized, with the result that a great many inclusions are formed. Part of the oxida-

TABLE 6—Oxygen and Nitrogen Contents

Heat	Steel	Tapping	Sample	Time	O. Pct	N, Pct
6833	Si-Mn	Quiet, metal first	K-R 2, furnace	14 min. before tapping	0.0035	0.0055
			K-R 3, furnace	5 min. before tapping	0.0018	0.0057
			K-R 5, ladle	1 min. after tapping	0.0054	0.0063
			Sample ingot Fig 3	After three 14-in. ingots	0.0033	0.0066
			Sample ingot Fig 3	After further four 9-in. ingots	0.0033	0.0068
6834	Si-Mn	Turbulent, slag from beginning	Sample ingot Fig 3	After further two 14-in. ingots	0.0033	0.0062
			K-R 4, ladle	14 sec. after tapping	0.0029	0.0063
			K-R 5, ladle	1 min. 16 sec. after tapping	0.0029	0.0053
			K-R 6, ladle	4 min. 14 sec. after tapping	0.0022	0.0055
			Sample ingot Fig 3	After three 14-in. ingots	0.0023	0.0059
6836	1.10 pct carbon	Quiet, metal first	Sample ingot Fig 3	After further one 14-in. ingot and two 9-in. ingots	0.0028	0.0054
			K-R 1, furnace	After further two 14-in. ingots	0.0025	0.0053
			K-R 2, furnace	17 min. before tapping	0.0010	0.0045
			K-R 3, ladle	6 min. before tapping	0.0013	0.0057
			K-R 4, ladle	45 sec. before end of tapping	0.0029	0.0060
6835	1.10 pct carbon	Turbulent, slag from beginning	K-R 5, ladle	1 min. 15 sec. after tapping	0.0036	0.0067
			Sample ingot Fig 3	4 min. 15 sec. after tapping	0.0038	0.0061
			Sample ingot Fig 3	After three 14-in. ingots	0.0027	0.0070
			Sample ingot Fig 3	After further five 9-in. ingots	0.0026	0.0073
			Sample ingot Fig 3	After further two 14-in. ingots	0.0024	0.0068
			K-R 2, furnace	18 min. before tapping	0.0012	0.0051
			K-R 3, furnace	7 min. before tapping	0.0014	0.0085
			K-R 4, ladle	20 sec. after tapping	0.0024	0.0073
			K-R 5, ladle	1 min. 55 sec. after tapping	0.0021	0.0073
			K-R 6, ladle	4 min. 40 sec. after tapping	0.0015	0.0051
			Sample ingot Fig 3	After three 14-in. ingots	0.0019	0.0070
			Sample ingot Fig 3	After further one 14-in. ingot and one 9-in. ingot	0.0016	0.0077
			Sample ingot Fig 3	After further two 14-in. ingots	0.0016	0.0075

tion product probably will react with the basic slag, the main part of which will rapidly rise out of the metal. A great many silicate droplets are left in the

contents of equilibrium with $(CO + CO_2)$ and with solid silica.

Considering the uncertainty of data for equilibrium conditions, particularly for

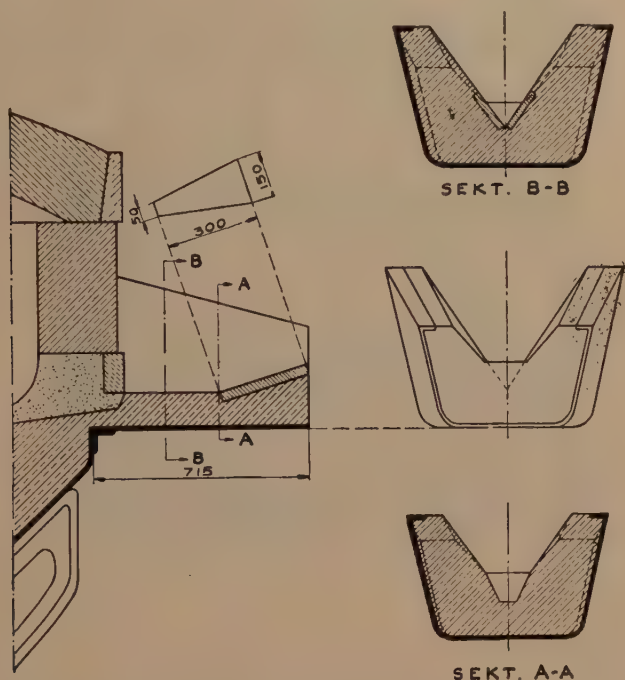


FIG 22—TAPPING SPOUT WITH BROKEN LONGITUDINAL SECTION.

metal as tapping is concluded. While the metal is in the ladle dissolved oxygen is equalized by diffusion and convection, the silicate droplets are gradually reduced and dissolved, the larger ones rising and leaving the metal at an appreciable rate.

Table 8 indicates the way in which the oxygen contents found compare with the

the silicate equilibrium and that of the oxygen determinations made, only tentative conclusions can be drawn from Table 8; as follows:

1. For both steels the furnace slag, reduced by coke additions, has brought the oxygen content of the metal *in the furnace* considerably below the value for

TABLE 7—Oxygen Content of Metal at Definite Stages

Steel.....	Oxygen, Pct			
	Si-Mn		1.10 Pct C	
	6833 Quiet	6834 Turbulent	6836 Quiet	6835 Turbulent
Tapping.....	0.0018		0.0013	0.0014
In furnace, 5 to 7 min. before tapping.....	0.0054	0.0029	0.0036	0.0021
In ladle, just after tapping.....		0.0022	0.0038	0.0015
In ladle, just before pouring.....		0.0025	0.0026	0.0017
In sample ingots, average.....	0.0033			

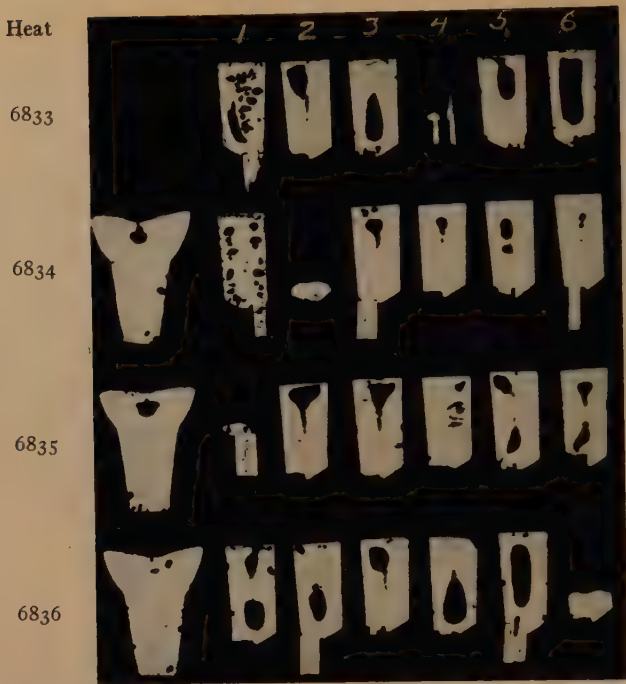


FIG 23—HEATS NO. 6833-36. SECTIONS OF SAMPLE INGOTS ACCORDING TO FIG 2 AND OF K-R SAMPLES.
 × 0.2.

TABLE 8—Dissolved Oxygen in Liquid Steel under Different Conditions, Compared with Oxygen Found by Analysis

	Steel with 0.65 Pct C	Steel with 1.10 Pct C
Dissolved O, 1500°–1600°C, 1 atm. equilibrium with (CO + CO ₂) (7) (18), approx. pct.....	0.0037	0.0021
	Steel with 0.70 pct Si 1.0 pct Mn	Steel with 0.25 pct Si 0.33 pct Mn
Dissolved O, equilibrium with silicate slag ^a 1600°C, approx. pct.....	0.0066	0.0120
1500–1525°C, approx. pct.....	0.0022	0.0039
O determined, furnace sample before tapping, pct.....	0.0018	0.0012
At approx. temperature, deg C: as read.....	1440	1390
as corrected.....	1590	1525
O determined after quiet tapping, ladle sample taken after time indicated, pct.....	1 min. 0.0054	1½ min. 0.0036 4¼ min. 0.0038
O determined after turbulent tapping, ladle sample taken after time indicated, pct.....	¾ min. 0.0029 1½ min. 0.0029 4¼ min. 0.0022	¾ min. 0.0024 2 min. 0.0021 4¾ min. 0.0015

^a Ref. 13, 300 (Fig 12) and 305 (Fig 18).

dissolved oxygen at gas equilibrium for one atmosphere pressure at existing carbon content and temperature, and also below the value for equilibrium with silicate slag

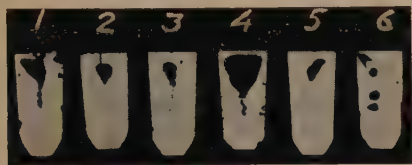


FIG 24—HEAT NO. 7320. SECTIONS OF CONSECUTIVE K-R SAMPLES. $\times 0.2$.

at existing temperature and contents of silicon and manganese. The latter is particularly evident for the carbon steel.

2. For both steels, tapping with *quiet stream* has caused an increase in the oxygen content to a value approximately corresponding to the silicate equilibrium and exceeding the value for gas equilibrium. The amount of inclusions in this case being moderate, the greater part of the oxygen was in solution.

3. On *turbulent* tapping the oxygen of the *silicon-manganese steel* was increased but still remained below the values for both equilibria. For the *carbon steel* the oxygen content was raised approximately to the value for gas equilibrium, which is less than that for silicate equilibrium. Since a large amount of inclusions was present in both cases, the dissolved oxygen content was probably low enough to favor the dissolution of the inclusions formed in the metal. While the metal remained in the ladle, the total oxygen fell almost to the value before tapping, very likely owing to the greater part of the inclusions rising from the steel, the dissolved oxygen rising meanwhile.

To indicate the deoxidizing power of the furnace slags, their FeO contents at tapping were as follows:

Steel	Si-Mn Steel		1.10 Pct Carbon Steel	
Heat.....	6833	6834	6836	6835
FeO, pct.....	0.29	0.37	0.22	0.29

Large Ingots

Data for large inclusions in the ingots of commercial size are given in Table 9. Samples were taken from two levels of each ingot. The total amount of large silicate inclusions is generally less than 0.5×10^{-3} vol. pct, of the same order as that of K-R samples taken from the ladle just before pouring began. There would appear to be no pronounced or definite effect of the intentional variations in tapping or pouring. Most of the oxidation products of restricting the pouring stream, for instance,—already referred to, have had time evidently to rise out of the metal, a result of the ingot size.

Heat 7320; Silicon-manganese Steels— Longer Stop in Ladle

The composition of the steel of heat 7320 was: C, 0.60 pct; Si, 0.85; Mn, 0.99; P, 0.013; S, 0.007; Cr, 0.28; W, 0.21. FeO in end slag was 0.59 pct. Temperature just before tapping was 1432°C (uncorrected), raised above the normal one—about 1420° —to compensate for the longer stop in the ladle. The metal was tapped quietly through a refractory tube. The stream being thinner than normal, tapping lasted for 2 min. 10 sec. The metal was held for 8 min. in the ladle. One K-R sample was taken from the furnace and five at intervals from the ladle. Sections are shown in Fig 24. Table 10 gives data on inclusions in the samples. Holding the metal for 6 min. brought the amount of inclusions down from a fairly high to a very low value. A few very large inclusions believed to be formed in sampling are not included. The results confirm the earlier results for quietly tapped heats, 6833 and 6836 (Table 4).

Two heats, Nos. 7703 and 7888, of silicon-manganese steel were made in the $3\frac{1}{2}$ -ton furnace with the object of testing the effects of using a Caspersson ladle and of surrounding the metal stream with nitrogen gas to prevent oxidation.

TABLE 9—Inclusions in Large Ingots

Inclusions Larger than 0.01 Mm																			
Heat	Steel	Tapping	Ingot No.	Pouring	Mold	Level from Bottom	Number of Examinations	Total						Transparent		Opaque			
								Pct $\times 10^{-3}$		n d ^b		Pct $\times 10^{-3}$		n d		Pct $\times 10^{-3}$		n d	
								n ^a											
6833	Si-Mn	Quiet stream	4	Restricted stream, no afterpouring	9-in. not tarred	$\frac{3}{4}$	2	3.0	0.4	2.442		0.3	0.636		0.06				
								4.3	0.4	4.338		0.3	2.939		0.13				
								5.2	0.8	5.048		0.7	1.241		0.15				
								6.0	0.4	3.528		0.1	1.544		0.2				
6	Normal, afterpouring	9-in. tarred	$\frac{3}{4}$	3	1.8	0.11	1.828		0.15	2.153		0.5							
					3.5	0.6	1.437		0.24	1.326		0.06							
					2.3	0.3	3.130		0.07	1.420		0							
					1.4	0.07	1.424		0.07	0		0							
7	Airblast toward stream, no afterpouring	9-in. not tarred	$\frac{3}{4}$	1	7.9	0.5	7.328		0.5	0.626		0.03							
					13.2	2.1	9.743		1.4	3.551		0.7							
					8.1	0.5	6.030		0.4	2.125		0.10							
					7.1	0.5	6.229		0.4	0.940		0.11							
6836	1.10 pct carbon	Quiet stream	4	Restricted stream, no afterpouring	9-in. not tarred	$\frac{3}{4}$	2	2.3	0.3	1.739		0.11	0.663		0.16				
								2.0	0.2	1.739		0.2	0.321		0.01				
								2.3	0.13	2.327		0.13	0		0				
								2.1	0.12	2.127		0.12	0		0				
6	Normal, no afterpouring	9-in. tarred	$\frac{3}{4}$	1	4.1	0.3	4.131		0.3	0		0							
					5.1	0.3	2.922		0.11	2.233		0.18							
					6.7	0.3	4.329		0.3	2.418		0.06							
					2.0	0.17	2.034		0.17	0		0							
7	Through funnel, no afterpouring	9-in. tarred	$\frac{3}{4}$	1	5.2	0.4	4.932		0.4	0.319		0.01							
					7.5	1.2	6.440		0.8	1.163		0.3							
					4.8	0.4	4.832		0.4	0		0							
					5.0	0.6	4.539		0.5	0.524		0.02							
8	Airblast towards stream, no afterpouring	9-in. not tarred	$\frac{3}{4}$	1	5.2	0.4	4.932		0.4	0.319		0.01							
					7.5	1.2	6.440		0.8	1.163		0.3							
					4.8	0.4	4.832		0.4	0		0							
					5.0	0.6	4.539		0.5	0.524		0.02							
6835	1.10 pct carbon	Turbulent stream	5	Normal, afterpouring	9-in. tarred	$\frac{3}{4}$	2	5.2	0.4	4.932		0.4	0.319		0.01				
								7.5	1.2	6.440		0.8	1.163		0.3				
								4.8	0.4	4.832		0.4	0		0				
								5.0	0.6	4.539		0.5	0.524		0.02				
6	Normal, no afterpouring	14-in. tarred	$\frac{3}{4}$	2	5.2	0.4	4.932		0.4	0.319		0.01							
					7.5	1.2	6.440		0.8	1.163		0.3							
					4.8	0.4	4.832		0.4	0		0							
					5.0	0.6	4.539		0.5	0.524		0.02							

^a n , number per 10 sq cm.
^b d , average diameter, mm $\times 10^{-1}$.

TABLE 10—Inclusions in K-R Samples, Heat 7320

Time before Tapping Started	Time after Tapping Ended	Inclusions Larger than 0.01 Mm								
		Total			Transparent			Opaque		
		n^a	d^b	Pct $\times 10^{-3}$	n	d	Pct $\times 10^{-3}$	n	d	Pct $\times 10^{-3}$
Min.	Sec.									
2	00	0		0	0		0	0		0
	Min. Sec.									
	0 20	8.6 ^c	67	3.1	6.1 ^c	60	1.7	2.5	81	1.3
	2 10	7.0	45	1.1	6.6	45	1.1	0.5	28	0
	4 20	2.7	80	1.3	2.0	82	1.1	0.7	74	0.3
	6 25	0.9 ^d	31	0.1	0.9 ^d	31	0.1	0		0
	8 15	1.5	41	0.2	0.5	31	0.0	1.0	45	0.2

^a n , number per 10 sq cm.^b d , average diameter, mm $\times 10^{-3}$.^c Not included: 0.5 1 167 54^d Not included: 4.0 540 90transparent, near top surface.
transparent, near top surface.*Heat 7703; Silicon-manganese Steel—
Caspersson Ladle*

The steel of heat 7703 had the following composition: C, 0.68 pct; Si, 0.65; Mn, 1.08; P, 0.015; S, 0.007. The Caspersson ladle attached to the furnace is shown in Fig 25, with the arrangement for nitrogen supply and the labyrinth seal between ladle and mold. The nozzle diameter was 30 mm. The nitrogen was deoxidized by passing it through three preheating tubes and one tube filled with charcoal, all tubes enclosed in a furnace and heated to about 850°C.

The furnace was tilted 4 min. before tapping. Three 14-in. ingots were cast and three K-R samples were taken. Results are given in Table 11.

The metal in the Caspersson ladle was low in inclusions and so were the ingots 3 and 4, cast without and with nitrogen protection, respectively. The K-R sample from mold 5 and ingot 7 cast with nitrogen were fairly high in silicate inclusions, however. Contributing causes thereof probably were: long time of pouring of ingot No. 7 (3 min., 45 sec) owing to cooling of the metal in the Caspersson ladle, which was insufficiently heat-insulated and probably too weak a nitrogen stream to prevent air from entering.

*Heat 7888; Silicon-manganese Steel—
Caspersson Ladle*

The composition of the steel in heat 7888 was: C, 0.59 pct; Si, 0.84; Mn, 1.02; P, 0.010; S, 0.007; FeO in end slag, 0.97.

TABLE 11—Inclusions in K-R Samples and 14-inch Ingots, Heat 7703

Sample	Remarks	Time before Tapping Started, Min.	Level from Bottom of Ingot	Inclusions Larger than 0.01 Mm								
				Total			Transparent			Opaque		
				n	d	Pct $\times 10^{-3}$	n	d	Pct $\times 10^{-3}$	n	d	Pct $\times 10^{-3}$
K-R 2	From Casp. ladle	2		0		0	0		0	0		0
K-R 3	From Casp. ladle	1		2.7	23	0.11	2.0	19	0.05	0.7	33	0.06
K-R 4	From mold No. 5			6.2	131	8.3	2.5	61	0.7	3.7	161	7.6
Ingot 3	Without nitrogen		$\frac{1}{8}$	4.0	29	0.26	3.5	30	0.25	0.5	19	0.01
Ingot 4	With nitrogen		$\frac{1}{8}$	4.0	19	0.11	4.0	19	0.11	0		0
Ingot 7	With nitrogen		$\frac{1}{8}$	9.5	47	1.6	3.5	48	0.6	6.0	46	1.0

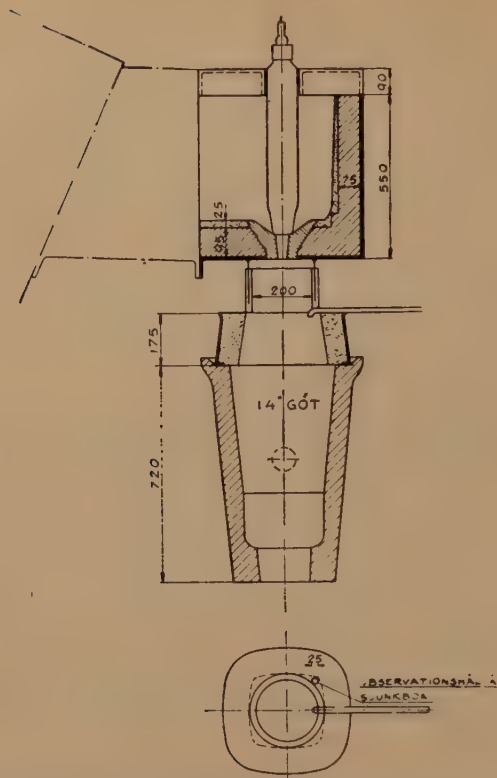


FIG 25—CASPERSSON LADLE WITH ARRANGEMENT FOR CASTING WITH NITROGEN PROTECTION (14-INCH MOLD).

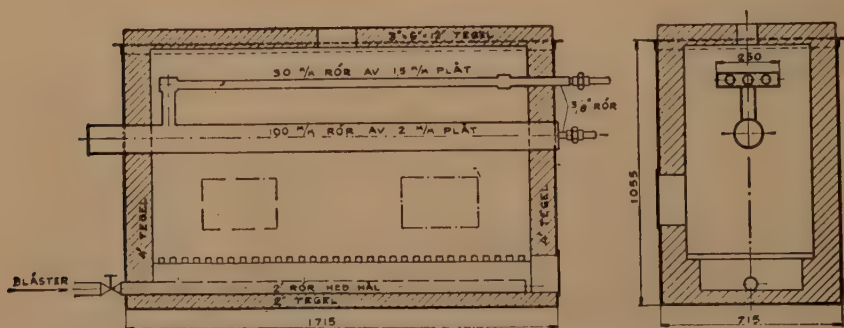


FIG 26—FURNACE FOR DEOXIDATION OF NITROGEN.

The inside dimensions of the Caspersson ladle were unaltered but a Sil-O-Cel layer 65 mm thick had been added to improve insulation (Fig 27).

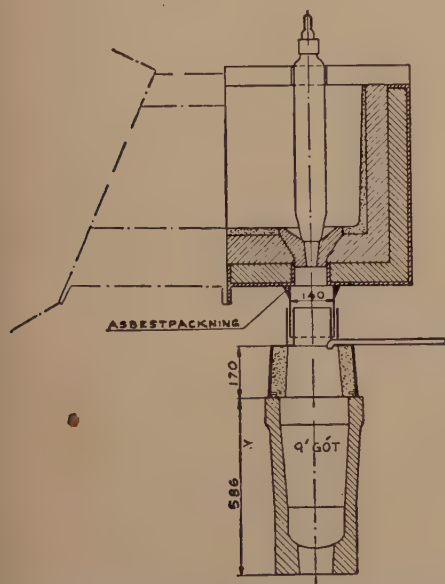


FIG 27—CASPERSSON LADLE WITH ARRANGEMENT FOR CASTING WITH NITROGEN PROTECTION (9-INCH MOLD).

Table 12 gives the results and shows that the ingot No. 4 cast in air, in regard to freedom from large inclusions, was comparable with the best ingots tapped and poured in the ordinary manner, and that ingots 5 and 8, cast with nitrogen protection, were purer than any other large ingot examined so far.

Heat 3269; Silicon-manganese Steel— 10-ton Furnace, Perrin Effect

The composition of the steel in heat 3269 was: C, 0.64 pct; Si, 0.73; Mn, 1.06; P, 0.016; S, 0.006; FeO of the end slag, 0.82.

This heat was made in the 10-ton furnace, in an attempt to utilize the reaction between furnace slag and steel in tapping (Perrin effect).

The metal charge was 5200 kg, the slag charge twice the ordinary one. The tapping hole was increased to 20 cm to enable tapping to be accelerated. Some slag was tapped first, then metal and slag together. The fall was about 2.5 meters.

The temperature 11 min. before tapping was 1450° (uncorrected). The metal was held 12 min. in the ladle. At intervals during pouring of 9-in. ingots sample ingots (Fig 3) were poured with full stream.

Results for 9-in. ingots and samples are given in Tables 13, 14 and 15. In Table 14 the transparent inclusions are classified; Table 15 gives oxygen and nitrogen contents.

The steel was almost free from inclusions before tapping, and contained 5.0×10^{-3} vol. pct transparent inclusions 1 min. after tapping (Table 13); as expected, a high value, but by far not as high as the one obtained from the 3½-ton furnace with the same steel composition. This is due probably to the tapping stream from the larger furnace being thick and fairly well collected.

TABLE 12—Inclusions in 9-inch Ingots, Heat 7888

Ingot No.	Remarks	Level from Bottom of Ingot	Examinations	Inclusions Larger than 0.01 Mm								
				Total			Transparent			Opaque		
				n	d	Pct $\times 10^{-3}$	n	d	Pct $\times 10^{-3}$	n	d	Pct $\times 10^{-3}$
4	Without nitrogen	1/8	3	1.1	54	0.3	0.5	45	0.09	0.5	72	0.2
5	With nitrogen	1/8	3	0.5	21	0.02	0.5	21	0.02	0		0
8	With nitrogen	1/8	2	0.8	18	0.02	0.8	18	0.02	0		0

In the ladle the amount of inclusions decreased (Table 14 K-R-2 to K-R-7), first rapidly, later slowly, and reached after 11 min. the value of 0.7×10^{-3} vol. pct. The purification in this case was

taken from the upper part of the liquid metal, which may be assumed to be richer in inclusions than the lower part. Furthermore, purification ought to continue in the ladle during pouring.

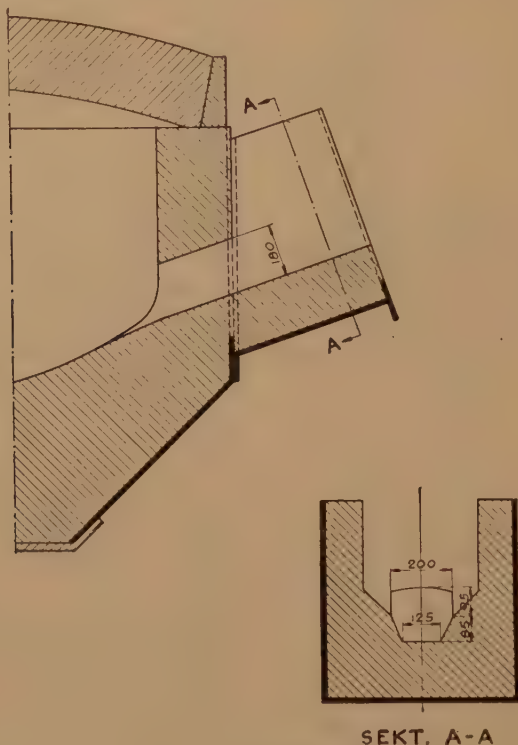


FIG 28—TAPPING SPOUT.

slower than in earlier comparable tests (heats 6834 and 6835, Table 4, and heat 7320, Table 10).

During the 12 min. in the ladle the character of the silicate droplets gradually changed, the resulting inclusions in the earlier stages being largely nonglassy; in the later stages semiglassy and glassy. At the same time, their size decreased somewhat. These results agree with the earlier ones (Table 5).

The inclusions content of the 9-in. ingots was somewhat smaller than that of the last K-R sample taken from the ladle, possibly because the K-R samples were

Considering further the 9-in. ingots, it is seen that ingot No. 11 was richer in inclusions than ingots Nos. 1 and 6; that glassy inclusions were absent in all three and that the proportion of nonglassy ones increased from ingot No. 1 to ingot No. 6. It is suggested that those inclusions originated largely in the pouring operation, probably because of decreasing speed and increasing dispersion of the pouring stream.

The oxygen contents from Table 15 may be compared with those of Table 7 for heat 6834, made in the $3\frac{1}{2}$ -ton furnace, as follows:

Oxygen	3½-ton Furnace	10-ton Furnace
Before tapping, pct.....	0.0018 (heat 6833)	0.0015
Immediately after tapping, pct.....	0.0029	0.0017
Before pouring, pct.....	0.0022	0.0015
In sample ingots (Fig 3) avg pct.....	0.0025	0.0027
In 9-in. ingot No. 6, pct		0.0022

fewer inclusions than the last K-R sample from the ladle.

The great scatter in oxygen values is connected probably with the deposit caused by the high manganese content of the steel.

Heat 8951; 1.10 Pct Carbon Steel—Ordinary Ladle—Nitrogen

For heat 3269 the metal evidently was only slightly oxidized in tapping, in agreement with what has already been said about the amount of inclusions. On pouring sample ingots (Fig 3) from the ladle there was, however, a considerable amount of oxidation, although they contained

The composition of the steel in heat 8951 was: C, 1.21 pct; Si, 0.20; Mn, 0.32; P, 0.010; S, 0.009. The temperature before tapping was 1395° (uncorr.). The furnace was tapped in the following way: first some slag, then metal in a smooth stream together with lags, followed by the remaining

TABLE 13—Inclusions in K-R Samples, Sample Ingots and 9-inch Ingots, Heat 3269

Sample	Time		Level from Bot- tom	Number of Ex- aminations	Inclusions Larger than 0.01 Mm								
	Before Tapping Started, Min.	After Tapping Ended, Min.			Total			Transparent			Opaque		
					n	d	Pct × 10 ⁻³	n	d	Pct × 10 ⁻³	n	d	Pct × 10 ⁻³
K-R 1.....	6			I	3.5	19	0.1	2.8	20	0.09	0.7	17	0.02
Sample ingot (Fig 2).....	2			I	0.3	20	0.01	0.3	20	0.01	0		0
K-R 2.....		I		I	39.2	43	5.9	35.1	43	5.0	4.1	52	0.9
K-R 4.....		4		I	22.7	38	2.5	18.2	32	1.6	4.5	50	0.9
K-R 5.....		6		I	24.8	28	1.5	22.3	28	1.4	2.5	26	0.1
K-R 6.....		7		I	17.6	27	1.1	15.8	27	1.0	1.8	31	0.1
K-R 7.....		11		I	17.1	22	0.7	17.0	22	0.7	0.1	19	0.04
9-in. ingot I..			1/8	2	3.8	26	0.2	3.8	26	0.2	0		0
9-in. ingot 6..			1/8	2	1.9	34	0.2	1.9	29	0.2	0		0
9-in. ingot 11.			1/8	2	5.7	33	0.5	5.7	30	0.5			
a Not included.....								1.5	306	11.2			

TABLE 14—Classification of Transparent Inclusions, Heat 3269

Sample	Time, Min.		Transparent Inclusions Larger than 0.01 Mm							
	Before Tapping	After Tapping	Total		Per Cent			Average Diameter		
			d	Vol Pct × 10 ⁻³	Glassy	Semi-glassy	Non-glassy	Glassy	Semi-glassy	Non-glassy
K-R 1.....	6		19	0.09	0	13	87		14	21
Sample ingot (Fig 2).....	2		20	0.009	100	0	0	20		
K-R 2.....		I	33	5.0	11	13	76	21	29	54
K-R 4.....		4	33	1.6	4	55	41	17	30	35
K-R 5.....		6	20	1.4	23	55	22	24	28	26
K-R 6.....		7	27	1.0	38	30	32	23	29	35
K-R 7.....		II	22	0.7	39	48	13	20	24	26
9-in. ingot I..			23	0.2	0	66	34		21	28
9-in. ingot 6..			29	0.2	0	20	80		21	35
9-in. ingot II..			28	0.5	0	23	77		28	28

slag. Some of the ingots, which were 9 in. square, were poured with nitrogen protection, a sand seal being applied below the ladle. The results are given in Table 16 (K-R samples and sample ingots) and Table 17 (9-in. ingots).

TABLE 15—Oxygen and Nitrogen Contents,
Heat 3269

Sample	Time	O, Pct	N, Pct
K-R 1.....	6 min. before tapping	0.0015	0.0077
Sample ingot (Fig 2)	2 min. before tapping	0.0015	0.0074
K-R 5.....	6 min. after tapping	0.0017	0.0079
K-R 6.....	7 min. after tapping	0.0014	0.0073
K-R 7.....	11 min. after tapping	0.0015	0.0070
Sample ingot A (Fig 3)	After ingot No. 1	0.0028 0.0028 0.0024	0.0081 0.0069 0.0074
Sample ingot B (Fig 3)	After ingot No. 6	0.0026 0.0028 0.0029	0.0071 0.0073 0.0074
Sample ingot C (Fig 3).....	After ingot No. 11	0.0024 0.0023 0.0034 0.0022	0.0073 0.0068 0.0053 0.0073
9-in. ingot No. 6		0.0020 (0.0003) 0.0023 0.0031 0.0019 0.0017	0.0077 0.0063 0.0077 0.0073 0.0084 0.0079

The furnace samples were not quite free from inclusions (Table 16). In the ladle the amount fell from 5.4×10^{-3} to 2.0×10^{-3} vol. pct in 7 min. The bottom sample taken after 8 min. showed 0.7×10^{-3} . Hence, the purification in the ladle was slow. (The values for K-R-3 and K-R-4 are doubtful, since only a small portion of the mold was filled.) As before, a marked glassiness characterized the inclusions in the later samples.

The amount of inclusions in the 9-in. ingots (Table 17) was moderate but not negligible (0.3 to 0.9×10^{-3} vol. pct). The repeated examinations of the same sample after regrading did not show good agreement. Evidently the total area examined should have been larger. No effect of the nitrogen protection is seen.

Either the metal was not sufficiently purified in the ladle or the arrangement for nitrogen supply was not leakproof. The conclusions drawn from the earlier tests using nitrogen in connection with the Caspersson ladle do not bear generalization.

Ingot No. 17, the last of the heat, was incompletely filled. It contained several blowholes and a number of very large silicate inclusions, partly globular, partly interdendritic, drawn into and between the steel crystals in the center of the ingot. A qualitative spectrographic analysis of the slag accumulated at the bottom of the pipe cavity gave the following composition: Ca (more than 10 pct), Mg, Al, Si, Fe (trace). Hence it would appear that both furnace slag (Ca, Mg) and refractory material (Al, Si) had taken part in its formation, probably also oxidation products of the steel (Si). Regardless of whether the great quantity of silicate inclusions is due to oxidation during the necessarily slow pouring at the end or a washing down of silicate drops earlier accumulated at the top of the ladle metal, the last ingot in the pouring series, even though it be filled completely, is likely to contain a large amount of inclusions.

Mechanism of Growth of Silicate Inclusions and of their Spontaneous Removal from Liquid Steel

As mentioned earlier, it has often been postulated that inclusions of larger size, during the time available in practice in the furnace, ladle and mold, are subject to rising in the liquid steel at a rate depending on their size and density, according to Stokes' law. A contributory factor, under favorable conditions considered to be important, would be the postulated growth in size by coagulation, the latter phenomenon being promoted by low viscosity of the silicate.

Herty and Fitterer⁴ produced test ingots 3 in. square with low carbon and

different silicon contents. They found that the silicate inclusions in the center of the ingot were considerably larger after small silicon addition than after large silicon addition. This was ascribed to the coagulation of small droplets in the former case, facilitated by the low viscosity of the silicate poor in silica. Near the surface the inclusions were small in both cases. This indicates that the large inclusions did not exist as such at the moment of casting.

caused by lowered solubility on cooling, or, in the case of constant temperature, by supersaturation. The growth of the separate drops would be favored by: (1) low rate of nucleation, (2) high oxygen and low silicon content in the metal, resulting in large decrease of solubility on cooling and steep concentration gradients. Possibly, in large ingots, small droplets are dissolved while large ones grow.

The coagulation hypothesis apparently

TABLE 16—*Inclusions in K-R Samples and Sample Ingots (Fig 2), Heat 8951*

Sample ^a	Time, Min.		Longitudinal Section, Area, Sq Cm	Examination	Transparent Inclusions Larger than 0.01 Mm			
	Before Tapping	After Tapping			n	d	Pct $\times 10^{-3}$	Glassy
K-R 1.....	12		10	1 2 Avg	1 1 1	49 20 35	0.2 0.03 0.1	
Sample ingot (Fig 2)	11		32	1 2 Avg	2 2 2	44 36 40	0.3 0.2 0.3	Most
K-R 2.....		1	20	1 2 Avg	13 20 16	78 54 66	6.2 4.5 5.4	Most
K-R 3.....		3	4.5	1 2 Avg	18 24 (21)	163 100 (132)	37 19 (28)	Most
K-R 4.....		5	6	1 2 Avg	16 33 (25)	98 32 (65)	12.4 2.6 (7.5)	Most
K-R 5.....		7	15	1 2 Avg	10 12 11	50 46 48	1.9 2.0 2.0	All
K-R 6.....		8	11	1 2 Avg	12 27 19	25 19 22	0.6 0.8 0.7	All

^a Samples K-R 2 to K-R 5 were taken about 15 cm beneath surface; sample K-R 6 near bottom of ladle.

The author has heard no explanation of the coagulation of inclusions in liquid steel convincingly demonstrating how it is that the droplets meet, at least not on the scale required to explain their regular increase in size toward the center of an ingot. It seems more likely that existing small droplets grow by continued separation from the metal, made possible by diffusion of silicon, oxygen, and manganese. The separation is believed to be

is strengthened by the occurrence of large inclusions surrounded by or adjacent to a swarm of small ones, an observation not seldom recorded. Still, the conclusion that the large inclusion is growing by coagulation of the small ones is doubtful. As demonstrated in the present investigation, it appears to be a common occurrence that silicate drops, newly formed by oxidation during tapping or pouring, and not being in equilibrium with the

TABLE 17—Inclusions in 9-inch Ingots, Heat 8951

Ingot No.	Time after Pouring Started		Casting Temperature, Deg C.	Nitrogen	Level from Bottom	Examination	Transparent Inclusions Larger than 0.01 Mm		
	Min.	Sec.					<i>n</i>	<i>d</i>	Pct $\times 10^{-3}$
2	1		1370°	without	1/4	1	4	42	0.6
						2	8	34	0.7
						3	15	33	1.3
						Avg	9	36	0.9
3	2	30		with	1/4	1	4	28	0.3
						2	15	31	1.2
						3	8	30	0.5
						Avg	9	30	0.7
7	15		1370°	without	1/4	1	2	30	0.2
						2	9	29	0.6
						3	8	34	0.7
						Avg	6	31	0.5
8	16			with	1/4	1	8	30	0.6
						2	8	27	0.5
						3	10	33	0.9
						Avg	9	30	0.6
13	19	30	1375°	with	1/4	1	6	27	0.2
						2	7	22	0.3
						3	6	36	0.6
						Avg	6	28	0.4
14	20	15		without	1/4	1	6	27	0.3
						2	13	29	0.8
						3	10	26	0.5
						Avg	10	27	0.6
16	21	15	1365°	without	1/4	1	3	37	0.3
						2	5	27	0.3
						3	6	36	0.3
						Avg	5	30	0.3

metal, react with the latter, causing a separation of smaller silicate droplets in the transition zone. The reaction droplets gradually disappear, probably by being redissolved in the steel. Only by arresting the process by the freezing of the steel is the configuration of inclusions described realized in the solid steel. The gradual change of nonglassy drops not in equilibrium with the steel to glassy drops in equilibrium as followed in some instances in the present investigation should be noted.

SUMMARY AND CONCLUSIONS

Two types of steel made in a basic-lined arc furnace were investigated, one a carbon steel with 1.10 pct C and the

other a spring steel with 0.65 pct C, 0.70 pct Si and 1.0 pct Mn.

The aim of the investigation was to determine: (1) the conditions for the formation of silicate inclusions in the molten steel, mainly during tapping and pouring, (2) in what manner the inclusions are affected by the stay in the ladle and (3) the value of certain measures for diminishing the amount of silicate inclusions in the steel.

With the metallurgical practice followed, the steel was practically free from inclusions and low in oxygen when tapped from the furnace. In the ladle, immediately after tapping, the steel contained spherical silicate drops in greater quantity the more turbulent the tapping

stream—from 1.4×10^{-3} to 41×10^{-3} vol. pct. The oxygen content also rose during tapping; curiously enough, less in a turbulent stream. In that case, it is suggested, the intimate admixture of the white furnace slag may have caused some deoxidation of the steel ("Perrin effect").

While in the ladle, the steel in a few minutes got rid of the greater part of its silicate contents as exemplified by the following figures:

VOLUME PER CENT		TIME, MIN.
FROM	TO	
12×10^{-3}	1.2×10^{-3}	4
41×10^{-3}	0.8×10^{-3}	4
2.4×10^{-3}	1.8×10^{-3}	3
1.4×10^{-3}	0.2×10^{-3}	$3\frac{1}{2}$
1.7×10^{-3}	0.1×10^{-3}	6
5.0×10^{-3}	0.7×10^{-3}	10
5.4×10^{-3}	0.7×10^{-3}	7

During the same time the average diameter of the inclusions (greater than 0.010 mm) decreased from 0.031–0.108 to 0.022–0.041 mm and their structure was altered: when just formed they were largely crystallized, after a few minutes they were more or less glassy.

It may be assumed that the oxidation of the tapping stream results in the formation of a silicate relatively rich in iron and manganese oxides. This will gradually dissolve to some extent in the unsaturated liquid steel and also through reaction with the silicon in the steel become successively poorer in iron and manganese oxides and richer in silica. Meanwhile the greater number of the larger inclusions obviously disappear from the steel by rising to the surface.

Two-inch test ingots were cast from the ladle using a normal and a restricted stream, respectively. The latter procedure caused an enormous increase in inclusions. Owing to the rapid freezing of the steel immediately after the formation of the inclusions, evidence of reaction between the latter and the steel was retained; for

instance, swarms of small drops around the larger ones. Such formations have been thought to indicate that large drops often are formed by coalescence of small ones, which seems a doubtful explanation.

In the ordinary ingots cast from the ladle (9 in. and 14 in. square) the contents of silicate inclusions were 0.1×10^{-3} to 0.9×10^{-3} , generally less than 0.5×10^{-3} vol. pct. Restricting the pouring stream or blowing air onto it had no appreciable effect on the amount of inclusions, presumably because most of the silicate drops formed had time to escape by rising. The last ingot poured seems likely to contain a large amount of silicate inclusions.

When using a so-called Caspersson ladle attached to the furnace and pouring through purified nitrogen, content of silicate inclusions as low as 0.02×10^{-3} vol. pct was obtained in the ingots.

The growth of silicate inclusions before freezing of the steel in the mold is considered to be due to precipitation from solution and diffusion in the liquid steel, generally not from coalescence of small drops.

ACKNOWLEDGMENTS

In the determination of the number, size, character, and distribution of inclusions in the steel, Messrs. K. G. Göthberg, P. C. Blomquist and A. Nilsson have assisted the author and deserve his thanks.

The resources and the experience of Söderfors Steel Works have been generously offered for the benefit of the investigation.

The investigation is part of a research program supported by Jernkontoret (The Swedish Ironmasters' Association) in Stockholm and has been carried out under the immediate guidance of a committee consisting of Messrs. B. Kalling, H. Kihlander, G. Phragmén, M. Tigerschiöld, and the author. To his fellow members of the

committee the author wishes to express his warm thanks for their pleasant and efficient cooperation.

REFERENCES

1. McCance: *Jnl. Iron and Steel Inst.* (1918) **97**, 239.
2. Dickenson: *Jnl. Iron and Steel Inst.* (1926) **113**, 177.
3. Wohrman: *Trans. Amer. Soc. Steel Treat.* (1928) **14**, 539.
4. Herty and Fitterer: *Min. and Met. Invest. Carnegie Inst. of Tech., Bull.* 36 (1928).
5. Herty and Gaines: *Trans. A.I.M.E.* (1929) **84**, 179, 195.
6. Herty and Fitterer: *U.S. Bur. Mines R.I.* 3081 (1931).
7. Vacher and Hamilton: *Trans. A.I.M.E.* (1931) **95**, 124.
8. Sims and Lillieqvist: *Trans. A.I.M.E.* (1932) **100**, 154.
9. Iron and Steel Inst., Spec. Rept. No. 2, 4th Rept. *Het. Steel Ing.* (1932) 62.
10. Hultgren and Phragmén: *Värml. Bergsmannafören Ann.* (1932) 116.
11. Perrin: *Rev. de Mét., Mem.* 30 (1933) **1**, 71.
12. Portevin and Perrin: *Rev. de Mét., Mem.* 30 (1933) **175**; *Trans. Iron and Steel Inst.* (1933) **127**, 153.
13. Körber and Ölsen: *Mitt. K.-W.-I. Eisenforsch.* (1933) **15**, 121, Abh. 242, 271.
14. Urban and Chipman: *Trans. Amer. Soc. for Metals* (1935) **23**, 93.
15. Portevin and Castro: *Jnl. Iron and Steel Inst.* (1935) **132**, 237.
16. Kalling and Rudberg: *Jernkontorets Ann.* (1936) **120** (3), 138.
17. Amberg and Hultgren: *Jernkontorets Ann.* (1936) **120** (7), 332.
18. Phragmén and Kalling: *Jernkontorets Ann.* (1939) **123** (5), 199.
19. Ranque: *Rev. de Mét., Mem.* 39 (1942) 331, 360; (1943) **40**, 25. *Stahl und Eisen* (1944) **64**, 459; **73**.
20. Wentrup and Linder: *Stahl und Eisen* (1943) **63** (48), 873.

A Method for Determining the Origin of Surface Defects in Rolled Steel Products

BY C. L. MEYETTE,* MEMBER AIME, AND V. E. ELLIOTT*

(New York Meeting, February, 1948)

THE conditioning of semifinished steel products such as billets, blooms, and slabs to remove surface defects before further processing to finished products is a necessary accompaniment to steel mill rolling operations. A knowledge of the kinds of defects which occur and of the conditions in melting, teeming, and rolling that may lead to their occurrence is favorable to the production of quality products.

Surface defects may be classed as either of mechanical origin such as those that occur in the heating and rolling operations and include breaks, tears, guide marks, mechanical laps and the like, or they may have been in the ingot before heating and rolling. Examples of the latter are ingot cracks, blow-holes, scabs, and inclusions which lead to the numerous known types of seams and surface flaws. Most of the common types of surface defects and methods for their identification by visual examination or by the aid of macro-etch tests are well known. The conditions which caused their formation are also appreciably understood and this knowledge has been instrumental in the establishment of methods for metallurgical control.

There are, however, defects of doubtful origin. In any endeavor to trace the causes for their occurrence, the question of first concern is:

Approved by the Publications Committee of the Carnegie-Illinois Steel Corporation, Pittsburgh, Pa., November 24, 1947. Manuscript received at the office of the Institute December 8, 1947. Issued as TP 2368 in METALS TECHNOLOGY, June 1948.

*Supervisor of Research and Metallographist, respectively, Carnegie-Illinois Steel Corporation, Gary, Indiana.

1. Whether they were formed in the rolling procedure. 2. Whether they existed in the ingot prior to rolling: In the case of semifinished products which are rerolled to finished products there is also the question of whether they were formed in the primary or in the secondary rolling.

In metallurgical laboratories where numerous or routine examinations of the quality of rolled products are made over the course of time, there will doubtless be many puzzling cases of defect origin. Microscopic examination of the defects may, however, reveal a characterizing condition that can be used to classify them broadly with respect to their origin: Such a condition has been observed and, after detailed investigation, is described here with the thought that it may offer a usable and relatively simple solution to a bothersome problem.

BASIS FOR CLASSIFYING

In this discussion the term "mechanical type defects" will be used to designate those that have occurred as a result of the rolling operations such as in rolling from the ingot to billets, blooms, or slabs or in rerolling to finished products. The term "steel type defects" will be used to designate those that were present in the ingot prior to primary rolling or that were in the semifinished product prior to secondary rolling to finished product.

The basis for distinguishing between the two types of defects lies in the relative degree of subscale formation surrounding them. Subscale is defined¹ as a zone of

¹ References are at the end of the paper.

oxide particles precipitated and dispersed within a metallic matrix which has occurred by diffusion of oxygen inward from the metallic surface. In the routine examination by means of the microscope of a large number of cases, it has been observed that the diffusion of oxygen from the scale formed within the defect during heating and rolling varies in degree, depending upon the time of contact between scale and metal. Where the defects were present prior to a heating operation, as in the case of steel type defects, the time of contact will be long depending upon the

drilled in various samples of carbon, alloy, and stainless steels.

2. To observe the extent of oxide diffusion adjacent to two kinds of defects which were produced artificially in the laboratory and which may be called synthetic, mechanical type and steel type defects.

3. To apply the method of examination to actual defects as observed on samples of rolled product processed in the mills.

Diffusion of Oxide from Scale-packed Holes

Samples from ten commercial grades of steel were obtained for this study. Eight

TABLE I—*Steels Tested*

AISI Grade	Billet Size in Inches (Section)	Chemical Composition								
		C	Mn	P	S	Si	Cr	Ni	Mo	Cu
C-1015	2 × 2	0.17	0.45	0.013	0.030	0.05	0.02	0.02	0.00	0.01
C-1045	2 × 2	0.45	0.75	0.015	0.032	0.23	0.02	0.02	0.00	0.01
C-1095	2 × 2	0.95	0.41	0.020	0.031	0.17	0.02	0.02	0.00	0.05
C-1112	2 × 2	0.14	1.01	0.019	0.115	0.06	0.02	0.02	0.00	0.01
A-2335	1½ × 1½	0.38	0.85	0.016	0.027	0.31	0.08	3.45	0.02	0.02
A-4068	1½ × 1½	0.68	0.86	0.018	0.031	0.26	0.02	0.01	0.25	0.01
A-4140	1½ × 1½	0.41	0.81	0.020	0.025	0.26	0.06	0.04	0.22	0.05
A-9260	1½ × 1½	0.61	0.75	0.026	0.029	2.08	0.03	0.02	0.00	0.03
403 (12 Cr)*	1½ × 1½	0.09	0.36	0.015	0.015	0.32	12.32	0.40	0.00	0.08
321 (18-8)*	1½ × 1½	0.07	0.60	0.018	0.010	0.45	18.90	8.84	0.00	0.06

* Electric furnace steel.

time required to bring the steel to rolling temperature, and the opportunity for oxide diffusion will be correspondingly great. Where the defects were formed during the rolling operation, as in the case of mechanical type defects, the time of contact between the metal and the scale formed within the defect will be short, depending only upon the time needed to roll and cool the steel. Since the average temperature is lower during rolling than during heating, the opportunity for oxide diffusion will be correspondingly small.

It will be convenient to illustrate the application of these effects to the determination of defect origin by dividing the subject into three parts:

1. To demonstrate the diffusion of oxide from scale-packed holes which were

of the grades were basic open hearth furnace steels chosen to represent rather wide variations in carbon, sulphur, silicon, nickel, chromium, and molybdenum. The other two were electric furnace, stainless steels. Samples of each grade were obtained in hot rolled billet form. Billet sizes and compositions are shown in Table I.

Using billet samples ½-in. in length, a ⅛-in. diam hole was drilled in each sample perpendicular to the billet surface. The hole was drilled to a depth of one inch and packed with scale which had been obtained by heating representative samples of the respective grades at 2150°F, removing the scale and grinding it to pass an 80-mesh sieve. The holes were then plugged with a steel rod and welded to exclude air during the subsequent heating operation. All

prepared samples were then heated in an electrically operated and controlled furnace for one hour at 2150°F and air cooled, after

tion. No etchants were used since oxide penetration was clearly revealed after the polishing operation.

Fig 1

Fig 2

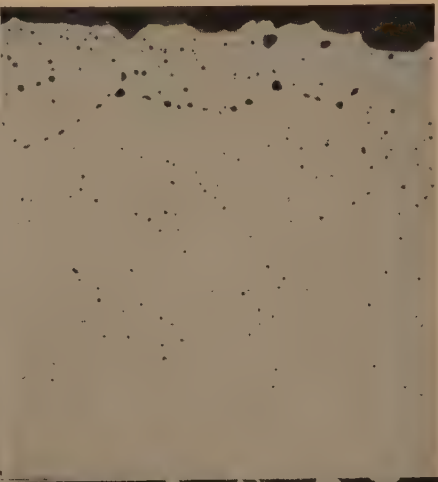


Fig 3

Fig 4

FIG 1—C-1112 STEEL.

FIG 2—C-1015 STEEL.

FIG 3—C-1045 STEEL.

FIG 4—C-1095 STEEL.

Micrographs showing the penetration of iron oxide from scale to metal in four AISI grades of carbon steel. Samples heated for 1 hr at 2150°F. Oxide-metal interface at top. Samples unetched. $\times 500$. Reduced one-fourth.

which a cross-section was cut through the scale packed portion of each hole. The section was mounted in bakelite, and polished by usual methods for microscopic examina-

The micrographs, Fig 1 to 10, illustrate the amount and type of oxide diffusion in the various grades of steel. It may be observed that considerable diffusion had

occurred in all of the grades with the exception of the 18-8 grade of stainless steel, Fig 10, in which there is only a small

random and extended to a greater depth in the plain carbon and AISI A-4068 grades than in the other alloy grades where

Fig 5

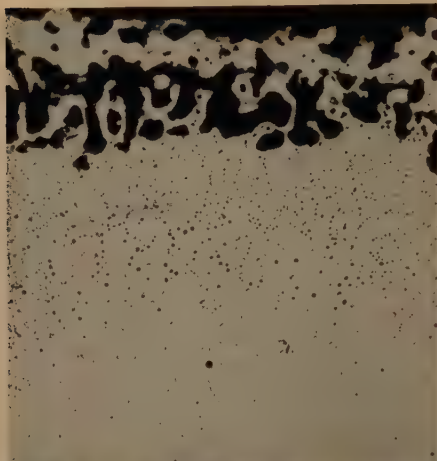


Fig 6



Fig 7



Fig 8

FIG 5—A-2335 STEEL.

FIG 6—A-4068 STEEL.

FIG 7—A-4140 STEEL.

FIG 8—A-9260 STEEL.

Micrographs showing the penetration of iron oxide from scale to metal in four AISI grades of alloy steel. Samples heated for 1 hr. at 2150°F. Oxide-metal interface at top. Samples unetched. X 500. Reduced one-fourth.

amount of oxide penetration. With this exception, the oxide appeared as a band of fine precipitate parallel to the edge of the exposed surface. The penetration was more

the penetration was more compact and showed evidence of outlining the grain boundaries. Variations in depth or character of the penetration are, however, of

less concern than evidence of penetration or lack of it in the various grades of steel selected for illustration. It may now be shown that evidence of oxide penetration

laboratory rolling mill. A photograph of the mill, a single pass hand mill of the screw-down type designed for experimental use, is shown in Fig 11. The samples were

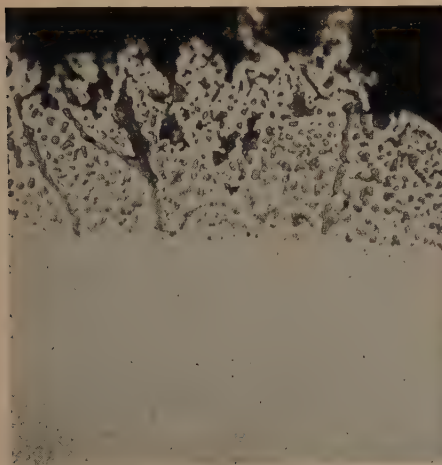


Fig 9

FIG 9—AISI 403 STEEL.



Fig 10

FIG 10—AISI 321 STEEL.

Micrographs showing the penetration of iron oxide from scale to metal in two grades of stainless steel. Samples heated for 1 hr at 2150°F. Oxide-metal interface at top. Samples unetched. $\times 500$. Reduced one-fourth.

from scale to surrounding metal is either lacking or is present in the metal adjacent to defects, depending upon whether they originated during or prior to the rolling process. Evidence will be shown first for flaws that were synthetically produced to simulate both mechanical type and steel type defects.

Diffusion of Scale from Synthetic Flaws

To produce mechanical type defects, billet samples 3-in. in length from each of the grades of steel shown in Table 1 were used. The samples were heated at either 2000 or 2150°F for periods of 1 or 3 hr, after which they were removed from the furnace and at once notched $\frac{1}{8}$ -in. deep on one surface along the center line in the direction of rolling, using a V shaped cutter and a sledge hammer. The billets were reduced 50 to 80 pct in section on a 6-in.

air cooled from the rolling temperature, with the exception that the high hardenability alloy grades were slow cooled. Sections for microscopic examination were taken in a manner to include a cross-section of the notch.

To produce steel type defects essentially the same procedure was followed, except that the samples were notched before instead of after heating at 2000 or 2150°F for periods of 1 or 3 hr. More explicitly, the samples were first preheated for a short time, removed from the furnace and at once notched in the same manner as above, returned to the furnace and heated at 2000 or 2150°F for periods of 1 or 3 hr and finally rolled and prepared for examination as before described.

It will be well to illustrate here the characteristic difference in oxide penetration observed for the two kinds of synthetic flaws, after which some illustrations will be

given to show the effects of temperature and time of heating. For example, micrographs showing the difference in iron oxide penetration around the two types of

all cases examined as will be shown in the succeeding representative illustrations.

To observe the effect of temperature, the above four illustrations, which are for

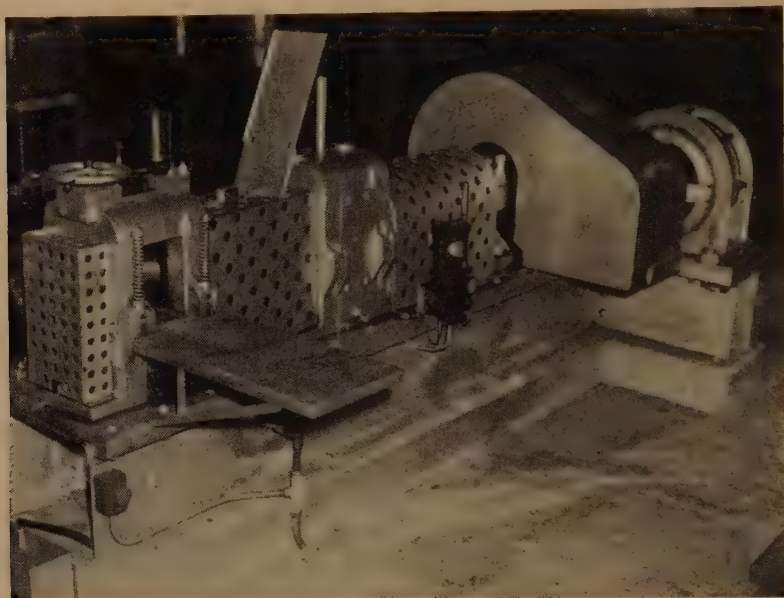


FIG 11—LABORATORY ROLLING MILL, EXIT SIDE.

synthetic defects produced in AISI C-1015 steel are shown in Fig 12, 13, 14, and 15. Fig 12 illustrates a characteristic mechanical type synthetic defect photographed at low magnification. Fig 13 shows the lowest portion of the same defect photographed at high magnification. In both illustrations there is essentially no evidence of oxide penetration.

Fig 14 illustrates a characteristic steel type synthetic defect photographed at low magnification and Fig 15 again shows the lowest portion of the same defect photographed at high magnification. In both illustrations, the penetration of oxide is in evidence, and the pronounced difference in the two types of defects becomes quite apparent upon comparison of the two photographs at high magnification. This characteristic difference has applied to

samples prepared by heating at 2150°F , may be compared with Fig 16, 17, 18, and 19, representing samples of the same grade of steel heated at a lower temperature, 2000°F . The latter figures are for steel type defects only and some penetration of oxide may be observed but the degree of penetration is noticeably less at the lower temperature. Similarly the degree of penetration is less for a shorter heating period, 1 hr as compared to 3 hr. This is best shown by a comparison of Fig 16 and 18. A similar comparison of the effects of temperature and time was made for all of the grades of steel examined and the observed differences were quite the same in each case where there was any evidence of oxide penetration. Further illustrations need not be given to show these effects and all remaining illustrations will be for

samples heated at 2150°F for 3 hr, the conditions that more nearly approach normal mill operating practices.

Although a complete study of synthetic

the characteristic difference in oxide penetration around the two types of defects, it is only necessary to show a few representative cases. For example, Fig 20, 21,

Fig 12

Fig 13

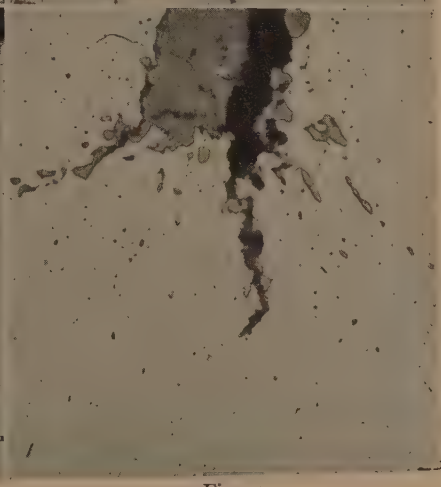
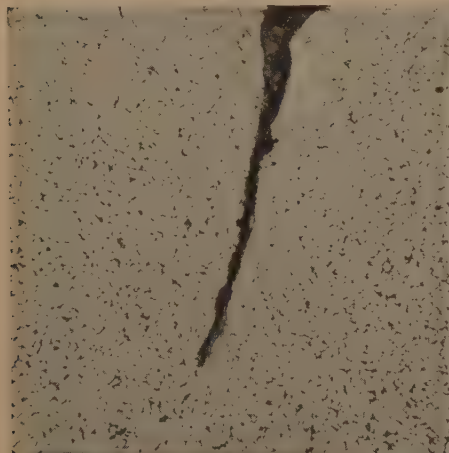


Fig 14

Fig 15

FIG 12—70 X. FIG 13—400 X. MECHANICAL TYPE SYNTHETIC DEFECT.
FIG 14—75 X. FIG 15—400 X. STEEL TYPE SYNTHETIC DEFECT.

Micrographs showing the difference in degree of iron oxide penetration within mechanical type and steel type synthetic surface defects in AISI C-1015 steel. Samples heated for 3 hr at 2150°F. Etched in nital. Reduced one-fourth.

defects of each type was made at different temperatures and heating times on the four carbon grades, four alloy grades, and two stainless grades of steel listed in Table 1 and many micrographs were made to illustrate

22, and 23 illustrate the two types of defects in a high carbon grade of plain carbon steel, the AISI 1095 grade. Figures are shown at low and high magnification. Penetration of oxide is quite evident in the

metal adjacent to the steel type defect as compared to little or no evidence of penetration adjacent to the mechanical type defect.

representing a high silicon grade, AISI A-9260 steel. Again, in both grades of steel, there is well defined evidence of oxide penetration adjacent to the steel type de-

Fig 16



Fig 17



Fig 18

Fig 19

FIG 16—THREE HOURS. 100 X.

FIG 17—THREE HOURS. 400 X.

FIG 18—ONE HOUR. 75 X.

FIG 19—ONE HOUR. 400 X.

Micrographs showing the difference in degree of iron oxide penetration within steel type synthetic surface defects in AISI C-1015 steel. Samples heated for 3 hr and 1 hr at 2000°F. Etched in nital. Reduced one-fourth.

Similarly two alloy grades are illustrated in Fig 24, 25, 26, and 27 which represent a chromium-molybdenum grade, AISI A-4140 steel, and in Fig 28, 29, 30, and 31

facts. In the silicon grade, A-9260, the penetrated oxide has assumed the form of a definite band surrounding the flaw. This is, perhaps, a true case of sub-scale formation

if, as suggested by Ward,² sub-scales are limited to the condition that there is a band of dispersed oxide separated from the outer scale by a layer of metal relatively

for sub-scale formation to steels containing a maximum of 3.25 pct silicon.

One grade of stainless steel, the 12 pct chromium grade, is illustrated in Fig 32, 33,

Fig 20

Fig 21

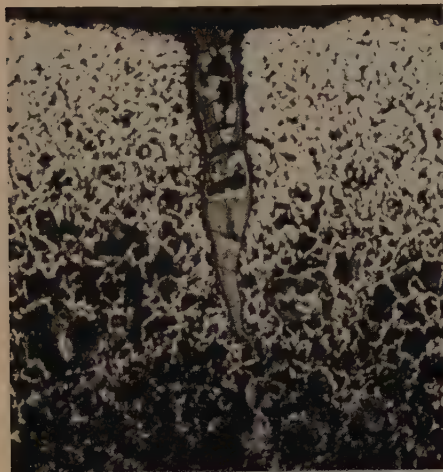


Fig 22

Fig 23

FIG 20—75 X. FIG 21—500 X. MECHANICAL TYPE SYNTHETIC DEFECT.
FIG 22—100 X. FIG 23—400 X. STEEL TYPE SYNTHETIC DEFECT.

Micrographs showing the difference in degree of iron oxide penetration within mechanical type and steel type synthetic surface defects in AISI C-1095 steel. Samples heated for 3 hr at 2150°F. Etched in picral. Reduced one-fourth.

free of oxides. He suggests further, that sub-scale formation of this nature is limited to steels containing 1.5 to 2.5 pct silicon, although Darken¹ limits the conditions

34, and 35 which show penetration of oxide adjacent to the steel type defect. This is in contrast to the 18-8 grade of stainless steel which, like the previous illustration

in Fig 10, showed no evidence of oxide penetration.

synthetically produced steel type defects. To illustrate the application of the method

Fig 24



Fig 25



Fig 26



Fig 27

FIG 24—100 X. FIG 25—500 X. MECHANICAL TYPE SYNTHETIC DEFECT.
FIG 26—100 X. FIG 27—500 X. STEEL TYPE SYNTHETIC DEFECT.

Micrographs showing the difference in degree of iron oxide penetration within mechanical type and steel type synthetic surface defects in AISI A-4140 steel. Samples heated for 3 hr at 2150°F. Etched in picral. Reduced one-fourth.

Defects in Rolled Steel Products

The preceding illustrations have all applied to laboratory examples in which oxide penetration was shown to occur adjacent to scale packed holes or to

of examination to actual cases, a number of billet samples representing several grades of steel were obtained from material that had been set aside for surface conditioning. Where surface defects were found, sections

containing them were cut from the billets and, without further treatment, the sec-

show an observed defect in AISI C-1060 steel that, in the absence of penetrated

Fig 28

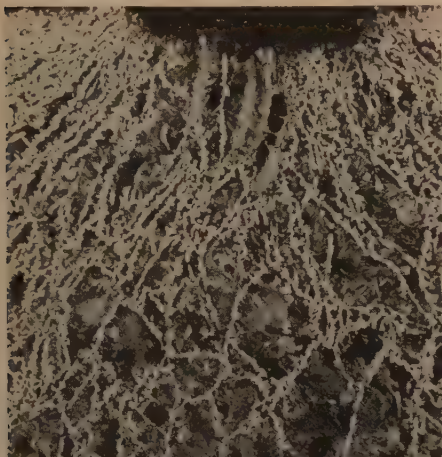


Fig 29

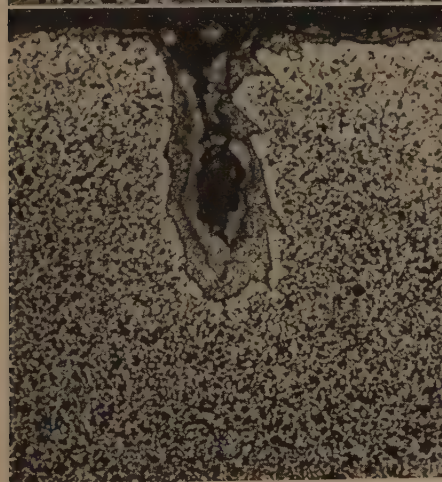


Fig 30



Fig 31

FIG 28—100 X. FIG 29—500 X. MECHANICAL TYPE SYNTHETIC DEFECT.
FIG 30—100 X. FIG 31—500 X. STEEL TYPE SYNTHETIC DEFECT.

Micrographs showing the difference in degree of iron oxide penetration within mechanical type and steel type synthetic surface defects in AISI A-9260 steel. Samples heated for 3 hr at 2150°F. Etched in picral. Reduced one-fourth.

tions were polished, etched, and examined under the microscope. Several examples of these are shown.

For example, two carbon grades are shown in Fig 36, 37, 38, and 39. The first two of these at low and high magnification

oxide, may be classed as a mechanical type defect. The latter two show a defect in a grade of similar composition, AISI C-1055 steel in which the pronounced evidence of penetrated oxide places this in the class of a steel type defect.

The remaining illustrations, Fig 40 through 43, are for samples selected from billets of an alloy grade of steel, the silicon grade A-9260. This grade again

The defect is shallow and shows the effect of a greater amount of reduction than noted in previous illustrations.

Micrographs pertaining to all of the

Fig 32



Fig 33

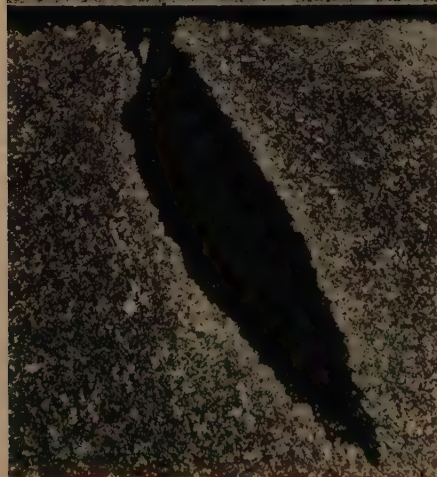


Fig 34

Fig 35

FIG 32—60 X. FIG 33—500 X. MECHANICAL TYPE SYNTHETIC DEFECT.
FIG 34—60 X. FIG 35—500 X. STEEL TYPE SYNTHETIC DEFECT.

Micrographs showing the difference in degree of iron oxide penetration within mechanical type and steel type synthetic surface defects in AISI 403 (12 Cr grade). Samples heated for 3 hr at 2150°F. Etched in Vilella's reagent. Reduced one-fourth.

shows the band of penetrated oxide adjacent to the steel type defect and no apparent evidence of penetration of oxide adjacent to the other type defect.

grades of steels observed in the course of this study would require a rather large number of illustrations and they are not all presented here. The examples shown for

rolled products are illustrations of flaws found in billet samples. The method should be readily applicable to the examination of defects in almost all grades of primary

secondary rolled products, although it will be well to consider a limitation of the method in this respect. In rerolled products surface defects which have occurred solely

Fig 36



Fig 37

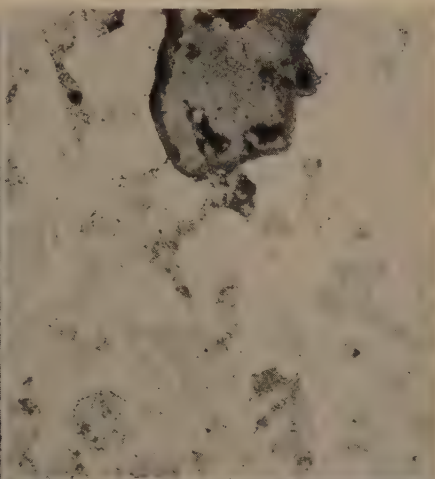


Fig 38

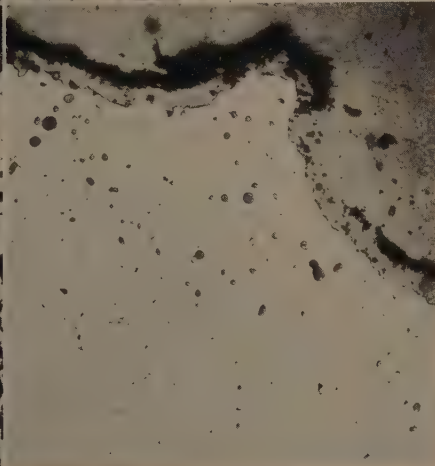


Fig 39

FIG 36—60 X. FIG 37—500 X. MECHANICAL TYPE ACTUAL DEFECT IN ROLLED C-1060 STEEL.
FIG 38—100 X. FIG 39—500 X. STEEL TYPE ACTUAL DEFECT IN ROLLED C-1055 STEEL.

Micrographs showing the difference in degree of iron oxide penetration within mechanical type and steel type actual surface defects in two AISI grades of carbon steel. Samples etched in picral. Reduced one-fourth.

rolled steel products, although there may be some grades like the 18-8 stainless steel that do not respond.

The method can be applied also to

as a result of the secondary rolling operation may be called mechanical type defects. Those which existed prior to the secondary rolling, whether they occurred as

mechanical type defects from the primary rolling or whether they carried through as existing defects from the ingot or from the heating operations for primary or second-

existed prior to the heating operation for either kind of rolling, except that it may usually be inferred that defects of the nature of those being considered generally

Fig 40

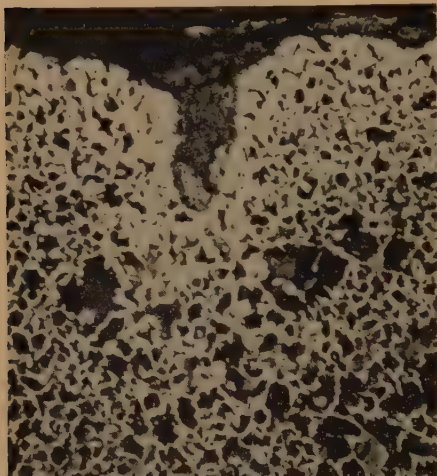


Fig 41

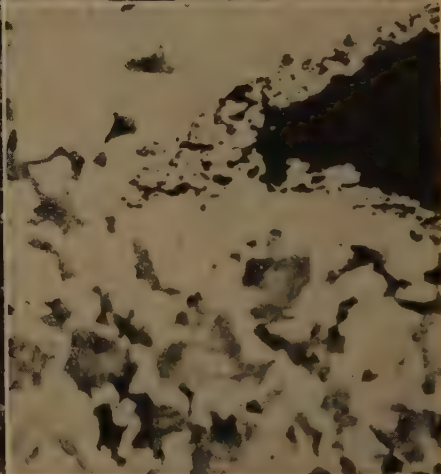


Fig 42

Fig 43

FIG 40—100 X. FIG 41—400 X. MECHANICAL TYPE ACTUAL DEFECT IN ROLLED A-9260 STEEL.
FIG 42—100 X. FIG 43—500 X. STEEL TYPE ACTUAL DEFECT IN ROLLED A-9260 STEEL.

Micrographs showing the difference in degree of iron oxide penetration within mechanical type and steel type actual surface defects in samples of AISI A-9260 steel. Samples etched in picral. Reduced one-fourth.

ary rolling, may be referred to as steel type defects. This means that the method is not usable for tracing the origin of the defects in either finished or semifinished products to conditions that may have

do not occur from the heating operations. Where, for example, the steel has been "burned" in the process of heating for rolling, such cases may be determined by visual inspection or other usual means.

Consideration has been given to the possibility that subscale formed on the surface metal as a normal result of scaling during the heating operation may become entrapped within a mechanical defect such as a lap and, as a result, the flaw may be misjudged as a steel type defect. This condition was not observed in the work on synthetic mechanical type defects, except in the case of the high silicon, A-9260 grade, where entrapped oxide was noted on the samples which had been notched prior to rolling. However, when the mechanical type defects were formed after the billets of A-9260 had been given two light passes through the rolls, no oxide penetration was found around the defects. This fact considered with the oxide penetration observed around steel type defects indicates that the action of the rolls in breaking and removing the scale on the surface will also remove the evidence of penetrated oxide unless it has occurred within an already existing flaw.

On the basis of the above observation it is conceivable in the case of rolled products of silicon steel, that if a mechanical defect were to occur early in the rolling process, such as in the initial passes of primary rolling, surface sub-scale might become entrapped and upon examination the flaw might have the aspects of a steel type defect. Judgment of origin would then be more a matter of degree of oxide penetration.

In studying the micrographs, attention is directed to the occurrence of metal decarburization adjacent to both types of defects. Generally the decarburization is less in the cases of mechanical type defects because of lower temperature and shorter time at temperature during rolling than during heating. Since, however, degree of decarburization is itself a function of temperature and is variable for the different grades of steel, it will be a less reliable guide to a determination of defect origin than will the occurrence of oxide penetration.

Although variations in operating condi-

tions such as time, temperature, furnace atmosphere, and amount of reduction in rolling must necessarily influence the degree of oxide penetration, it has not been the purpose here to explore these effects fully but rather to present a relatively simple method that may be applied as an aid in determining the origin of surface defects

SUMMARY

A method for determining the origin of surface defects in rolled steel products is described and illustrated. Defects which existed in the ingot prior to rolling are characterized by the penetration of oxide surrounding the flaw. These are classed as steel type defects. Defects which were formed in either the primary or secondary rolling operations do not show any appreciable penetration of oxide adjacent to the flaw. These are classed as mechanical type defects.

The method was applied to ten grades of steel and representative illustrations are presented to show diffusion of oxide from scale-packed holes in billet samples, from the two kinds of defects as produced artificially in the laboratory, and from actual defects as observed on samples of rolled billet product. The method was found applicable to all but one of the grades, the 18-8 grade of stainless steel. Certain limitations of the method are considered with respect to rerolled products and to silicon steels.

ACKNOWLEDGMENTS

The authors are indebted to Mr. A. N. Swanson, who contributed much to the early work on this problem, and to Mr. C. J. Hunter for his helpful suggestions in the preparation of this paper.

REFERENCES

1. L. S. Darken: Diffusion in Metal Accompanied by Phase Change. *Trans. AIME* (1942) **150**, 152.
2. R. Ward: Oxide-Metal Layers Formed on Commercial Iron-Silicon Alloys Exposed to High Temperatures. *Trans. AIME*, (1945) **162**, 141.

DISCUSSION

(C. Wells and M. Gensamer presiding)

C. E. SIMS*—It seems to me that the method described is an excellent one to determine the period in operation during which surface defects are produced. This is, of course, a necessary preliminary step to prevention.

N. C. FLICK*—The authors are to be congratulated for the practical approach to the problem of determining the origin of surface defects in semifinished steel. Almost invariably when a complaint is registered on steel quality, the open hearth places the blame on the rolling mill and the rolling mill in turn points an accusing finger at the open hearth. This paper should help settle this question of origin which comes up so often during the making, shaping, and treating of steel.

The shapes of the nonmetallic particles, particularly in the C-1015, A-9260, and 12 Cr steels, are particularly interesting in the light of the AIME Institute of Metals Lecture on grains, phases, and interfaces by Dr. Cyril Stanley Smith. Many of the specimens have not been etched. I would like to ask the authors to elaborate on their observations on the relation between the depth of oxide penetration and the depth of the decarburized zone.

C. L. MEYETTE (authors' reply)—In reply to Mr. Flick, the oxide penetration associated with the steel type defects was always accompanied by an area of decarburization. The decarburized zone in all the cases studied extended to a greater depth than the oxide penetration, although this difference in depth was not consistent and was found to vary even in defects observed on the same grade of steel and section.

F. G. NORRIS†—The authors have chosen a topic of considerable interest to those who are responsible for the control of quality in the manufacture of iron and steel products. The test which is proposed has the same relation to the improvement of quality that a post mortem examination has to the accurate diagnosis and cure of future patients.

Burning is a term that needs to be defined objectively. The definition needs to be explained to everybody and kept constantly in mind. Burning is frequently confused with overheating or general poor practice in some heating operation. Sometimes the simple statement of fact that steel has been burnt is regarded as an insult to the heater's knowledge, ability, skill, devotion to duty, and personal character. Such a display of emotion does not smooth the road to progress.

Under such pressure there is a tendency for burnt steel to go under cover and to reappear using an assumed name.

The tests proposed in this paper provide a means of describing exactly what is meant by burnt steel and other defects and also offer a standard for the classification of various conditions that are encountered.

All of our product is rolled from ingot to a slab 4 or 5 in. thick and then (usually without cooling) to strip on the order of one-tenth of an inch thick. The problem of sampling is more difficult than in the case of 4 × 4 billets. We usually sample the slab by burning off a chunk (it seems that it is always too heavy) and then resorting to the hacksaw. We would welcome any suggestions to improve this practice in either the hot or cold slabs or in the bar.

N. TINER*—The paper is an excellent contribution to the quality control in rolled steel products.

The presence of numerous oxide particles within the metallic matrix surrounding a defect which existed in the ingot before heating for rolling, and their absence within the metallic matrix surrounding a defect which formed during rolling were also observed by the writer in a number of instances in rail and structural steel products.

The above phenomena offer a relatively simple guide to determine whether a surface defect existed in the ingot prior to heating or formed during rolling. In certain cases, however, additional information may be required. We may, for example, have to know whether the flaw has resulted from blowholes or from ingot cracks or, in the case of mechanical flaws from breaks, guide marks, or laps.

If the blowholes produced by evolved gas

* Battelle Memorial Institute.

† Wheeling Steel Corporation.

* Palo Alto, California.

failing to escape during the solidification of the metal are near the ingot surface, they may be broken apart during rolling and form closed but not welded surface cracks. Unless the interface of the cavities contains a thick oxide film, the metallic matrix surrounding these cracks contains little or no oxide particles. According to the subscale formation method proposed by the authors, they should be classified as mechanical type defects.

In general, phosphorus and some sulphur are segregated near blowholes. If Stead's or Oberhoffer's reagent shows phosphorus segregation near a flaw under the microscope, one may infer that this flaw is due to a blowhole.

The metal decarburization is normally confined to a very thin layer on the surface of rolled products, and is characterized by the formation of a zone of free ferrite grains. If a flaw has resulted from overlapping during rolling, nearly always a uniform zone of free ferrite grains is observed around it. If the flaw has resulted from breaks, guide marks, or from the rupture of the blowholes near the surface during rolling, the free ferrite zone is not observed in the metallic matrix adjacent to the defect particularly at the bottom.

If a flaw has resulted from ingot cracks, a zone of free ferrite grains may be observed in the metallic matrix adjacent to the flaw. In such cases, numerous oxide particles are also present in the ferrite zone.

It is hoped that the foregoing remarks may be useful for determining the origin of surface defects in rolled steel products in connection with the subscale formation method proposed by the authors.

E. A. LORIA*—A method of determining the origin of surface defects in rolled steel products by the degree of oxide diffusion is a truly significant contribution. In a paper to be published shortly,³ the writer has also observed internal oxidation in cracks which occurred at or near the ingot surface in several large steel forging ingots made by the acid open hearth practice. These defects, classified by the authors as "steel type defects," are evident in trans-

verse macroetch tests as fine subsurface cracks and fully developed cracks which extend to the surface. Oxidized layers at both edges and the dispersion of fine particles beneath are seen microscopically in the latter type, the crack being rimmed by a decarburized layer (ferrite) containing the dot-like inclusions of oxide. In addition, the concentration of other fine precipitate particles—nonmetallic inclusions and carbides—partly oriented in streaks in the vicinity of such cracks is observed. Usually the cracks are not uncovered in the early processing of an ingot since they actually originate below the ingot surface and are detected only during forging, resulting in the formation of an oxide layer at the surface of the crack and some internal oxidation and decarburization.

In consideration of surface defects in rolled steel products, emphasis should be placed on hair seams which are the most common type of defect in semifinished steel. These fine cracks extend over a piece in the longitudinal direction and possess different lengths. Actually, one may distinguish between two types of seams: those originating at the steel plant which are the result of elongation and laying open of simultaneous blowholes and slag inclusions during the rolling of the ingot and those produced by faulty practices at the rolling mill. When viewed under the microscope, both types present themselves as cracks which are filled with scale. As a rule, the "steel type" hair seams are rimmed by ferrite that contains dot-like oxide inclusions. Sometimes the blowholes are not uncovered in the process of heating the ingot if they are seated so deeply that the overlying metal layer has not been burned away. In this case, they are uncovered only in rolling and then undergo very slight oxidation and, hence, the resulting hair seams are but slightly decarburized.

Since the segregation of sulphur and phosphorus are usually observed in blowholes, the use of Oberhoffer's reagent permits a rather accurate determination of the particular type to which the hair seam belongs. Zones rich in phosphorus are not attacked by Oberhoffer's reagent and hence remain bright. On the other hand, zones free from segregates can be etched, the ferrite assuming a dark brown color and the pearlite a light gray color. In his study of this problem, Oberhoffer stated that "after teeming the steel, as the temperature drops, the volume

* Mellon Institute of Industrial Research.

³ E. A. Loria and H. D. Shephard: Some Factors Affecting Subsurface Defects in Large Forging Steel Ingots. *Trans. Amer. Soc. for Metals* (1949) 41, 328-364.

of gas occluded in a blowhole decreases at a much faster rate than the volume of the blowhole itself. From this it is not difficult to understand that sulphur and phosphorus-rich metal is drawn into the voids." Thus sulphur and phosphorus segregates in hair seams or adjoining zones will indicate that the cracks are "steel type defects." Sulphur printing has fully confirmed this contention. Therefore, in addition to the degree of oxide penetration surrounding a defect, it appears that the relative depth of the decarburized layer adjoining a defect may also provide some indication of its origin, while the use of an etchant which will detect the presence of sulphur and phosphorus in areas adjacent to a defect will prove that such a defect occurred in the ingot before heating and rolling.

Additional evidence can be found which will more or less determine the origin of surface defects in semifinished steel. For example, hair seams produced at the rolling mill are found to be distributed according to definite relations along the length of billets. They occur on two, and sometimes on four, opposite sides of a billet and often differ from "steel type" hair seams by their greater length. Basically this type of defect is the result of roughness of the surface during the processing of the billet. On the other hand, lap seams, which are long cracks usually located over the entire length of a billet and originate from faulty rolling mill practice, do not differ from "mechanical type" hair seams in their outward appearance. Notwithstanding, on macroetching a transverse section of a test piece with lap seams, a characteristic fibrous structure may be observed if it is etched with Oberhoffer's reagent. The fibers are curved markedly around the seam toward the interior of the bar and run around the seam in the form of an arc. This fiber direction proves that such cracks are not "steel type defects" but the result of roughness produced in rolling. Microscopic examination of lap seams shows that the cracks are filled with scale; the rim of the cracks and also the surface of the bar are decarburized. In some cases there is merely a gradual transition from the weakly decarburized structure at the rim of the cracks to the normal structure which, no doubt, is attributable to the way the ingots and the billets were heated.

Finally, in the rolling of ingots and billets which have been insufficiently or unevenly soaked, high stresses are created which result in cracks preferentially located in areas of maximum weakness—such as inclusion segregates and zones rich in sulphur and phosphorus.² Acting as areas for stress concentration, such segregates lower the rupture stress of the steel and the magnitude of the lowering depends on the size and shape of the included particles. A high percentage of hair seams and cracks which are encountered after rolling is the result of rolled-out nonmetallic inclusions, and evidence of the origin of the defect can be found upon ordinary microexamination of the affected areas. Also, sulphur prints of transverse sections of forging ingots may reveal the segregation of inclusion stringers within the outer (chill) zone of forging ingots interspersed among an otherwise even distribution of minute sulphides. In general, it has been observed that where such stringer inclusions occur within a zone of relatively minute inclusions internal tears are most likely to occur on processing the ingot. The difference in conformation of the sulphides in the ingot subsurface is believed responsible for this "steel type defect" because the sulphide stringers are incapable of dispersion or diffusion within the otherwise minute, even distribution of globular sulphides and therefore act as points for stress concentration during hot working.

V. E. ELLIOTT (authors' reply)—Messrs. Loria's and Tiner's comments on the use of Oberhoffer's reagent for studying the segregation and flow lines adjacent to surface defects are interesting and in most cases substantiate the oxide penetration method. Blowholes opening up during rolling which had not been affected by the heating operation have not been observed by the authors, although under certain conditions of heating and working, such a possibility could occur. In this connection it would be well to reiterate that a deep acid etch test for internal quality usually accompanies the microscopic examination.

Oberhoffer's reagent has been used in an attempt to differentiate between the two possible sources of steel type defects on secondary mill products. However, possibly as a result of the large amount of reduction involved, the results have not been conclusive.

The Sampling and Analysis of Steel for Hydrogen

By G. DERGE,* MEMBER, W. PEIFER,* AND J. H. RICHARDS,† JUNIOR MEMBER AIME

(New York Meeting, February 1948)

INTRODUCTION

A WIDE variety of metallurgical defects in steel have commonly been attributed to the presence of excessive amounts of hydrogen. These defects include flakes in rails and forgings, cracks in welds, and blisters in enameled ware. They have been related to hydrogen largely by circumstantial evidence because the proper sampling and analysis of steel for hydrogen has been known to be difficult and because no general agreement has existed with regard to the relative suitability and accuracy of available methods. The need for a direct approach to these problems has been widely recognized.

This general situation has been well described in the publications of the British Committee on the Heterogeneity of Steel Ingots,¹ and current approaches to the problem were reviewed in a recent symposium of the AIME.¹² The plans described by the present authors at that meeting have now matured satisfactorily and will form the basis of this paper.

The principal object of this paper will be to describe the methods of sampling and analysis which have been developed and to illustrate the usefulness and limitations of these methods by citing their application to a specific problem. The first problem selected for investigation was the behavior of hydrogen in rail steel. This was chosen

because the occurrence of shatter cracks in rails has received a great deal of study over a long period of time. The defect can be controlled by the expensive procedure of slow cooling. However, it may be hoped that a better understanding of the factors influencing the hydrogen content of rails will lead to a more efficient control of this problem. Rails provide a good starting point for a more general study of hydrogen in steel because they provide a cross-section large enough to develop cracks, yet small enough for convenient handling and sampling. Rails were also selected because they are made from plain carbon steel and it was felt that the initial work should not be complicated by the effects introduced by alloying elements.

The considerations which determined the original planning of this study should be reviewed. The inherently complex nature of most hydrogen problems requires that a large amount of data must be collected for any particular case. This in turn means that any analytical procedure should be as rapid and simple as possible. The same objective of speed is indicated by the fact that it may finally become desirable to use hydrogen analysis in process control. It is also known that hydrogen is highly fugitive and that any procedure which facilitates early analysis of the sample without prolonged or irregular storage has distinct advantages.

The most important previously reported methods of analysis may be classified into three general groups: (1) Vacuum fusion, (2) Vacuum extraction (without melting), (3) Total combustion.

Manuscript received at the office of the Institute December 31, 1947. Issued as TP 2362 in METALS TECHNOLOGY, June 1948.

* Metals Research Laboratory, Carnegie Institute of Technology.

† Research and Development Division, Carnegie-Illinois Steel Corporation.

¹ References are at the end of the paper.

In selecting our procedure many considerations were weighed. The total combustion method was already under intensive development³ and offered little promise of meeting the requirements for speed and simplicity, even though it might provide a reference method of high precision. Many variations of vacuum extraction of hydrogen by heating without melting have been described^{1,12,4} and some of them have given usefully accurate results. Here again the combined objectives of speed and simplicity are difficult to attain and it would not appear likely that a sample with a one half inch cross-section could be analyzed in anything less than several hours. These systems range all the way from the extremely simple Toricellian vacuum⁵ to elaborate automatic equipment.⁴

Vacuum fusion was selected as the general method best suited to our purposes. Experience with oxygen analysis had demonstrated that the fusion method is capable of useful simplification under favorable circumstances⁶ and it seemed to be the only method capable of yielding a satisfactory analysis in less than an hour's time. It was recognized that many real or theoretical objections could be raised against the conventional vacuum fusion analysis for hydrogen. The most important of these are that the blanks are so high and erratic as to lower the accuracy beyond a useful limit; that the sample will lose its significance on account of hydrogen losses during the necessary outgassing and baking periods; that removal of the hydrogen may not be complete; that the hydrogen may react with the refractories or distilled metal films in the system; and that the hydrogen is only a few per cent of the total gas collected, but the pumps, calibrated reservoirs and manometers are normally designed for the oxygen (analyzed as CO_2) which constitutes about 95 pct of the gas volume; all of these factors would

contribute to inaccurate results. Nevertheless it was felt that the method held sufficient promise so that it should not be abandoned without careful investigation of the validity of these objections and the possibilities for overcoming them or minimizing their importance. These features will be pointed out throughout this paper.

Evidence has already been presented that hydrogen absorption by reaction with the various refractory oxide or graphite parts of the apparatus, or metal films on these parts is inconsequential.² This is confirmed by the internal consistency of the data to be presented.

In developing the program it was felt that methods of sampling could not be studied intensively until a suitable analytical procedure became available. However it is equally difficult to prove a procedure without known samples, and objections could be raised to any type of prepared sample considered. Although not entirely satisfactory, this situation was met in the beginning by analyzing known mixtures of gases in amounts and compositions comparable to those expected from steels. When it became possible to obtain satisfactory results on these gas mixtures, steel samples were used. These samples were made as nearly alike as possible by giving careful attention to the geometry of the section and to all the details of preparation and storage. A statistical analysis of a large number of such identical samples gives a good measure of the precision of the method. This accumulated background of information gradually developed an understanding of the variables involved in the proper preparation, storage and analysis of solid steel samples and it was finally possible to develop a satisfactory method for sampling open-hearth baths which will be described in a later paper. The important features of these procedures will now be described and supporting data will be presented.

APPARATUS AND TECHNIQUE FOR HYDROGEN ANALYSIS

The apparatus comprises two essential sections, an extraction system and an analytical system, as shown in Fig 1 and 2. The

begins to form on the mercury it can be removed readily by passing the mercury through a suction filter of the fritted-glass type. Just above the mercury level there is a water-cooled copper block surrounding

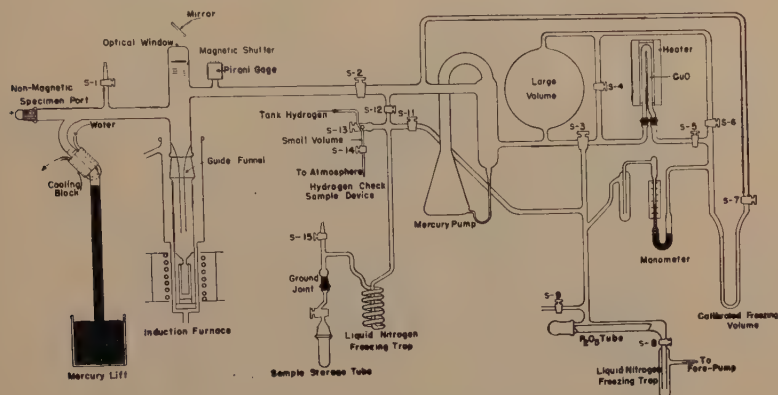


FIG 1—VACUUM FUSION APPARATUS FOR HYDROGEN.

entire vacuum system is made of Pyrex glass and fused silica. An important adjunct to the apparatus, the hydrogen sample tubes, will be described in a separate section. The system will be outlined with reference to Fig 1, starting from the mercury lift. This mercury lift rises to barometric height when the system is evacuated and permits the introduction of a magnetic specimen at any time without breaking the vacuum. More important, it makes it possible to start analyzing the specimen immediately after it has been introduced into the apparatus. The importance of this lies in its relation to the hydrogen lost from samples stored in a vacuum, which occurs in a conventional vacuum fusion apparatus during crucible degassing. The rate of loss of hydrogen from a sample stored in vacuum is shown in Fig 4. An important consideration in connection with the mercury lift is that of keeping the mercury clean. For this reason the specimens are inserted into the mercury with clean tongs and the mercury well is kept covered at other times. When a film

the tube. This cooling block condenses mercury vapor at a point where it will drain back into the lift. The cooling block is split and hinged so that one of the halves may be swung open to permit magnetic manipulation of the specimens up the tube. Just above this point are two glass semi-circular baffles which serve to deflect splashing mercury. If even a small drop of mercury falls into the hot fusion chamber, it generates a large volume of vapor with almost explosive violence. The ground joint cap at the top of the lift permits introducing non-magnetic samples into the system. This assembly is connected to the glass furnace head.

At the upper end of the furnace head is an optical window through which the temperature of the crucible is observed by means of an optical pyrometer. It was found that a 35°C correction for the mirror and window must be added to the observed temperature to obtain the true temperature of the crucible. The shutter of the baffle which is located below the window is operated externally by means of a magnet.

The shutter is closed, except during a temperature observation, to eliminate condensation of vapors on the window. The Pirani type vacuum gauge connected into

are water cooled. Cooling of the waxed joint prevents leaks at the joint caused by softening of the wax and also keeps the vapor pressure of the wax at a negligible

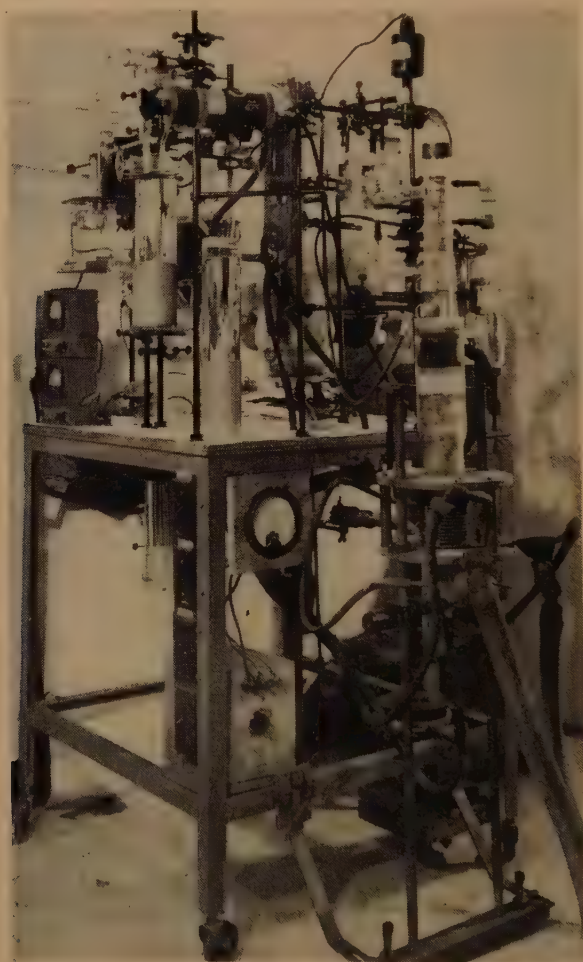


FIG 2—VACUUM FUSION APPARATUS FOR HYDROGEN.

the furnace head is used for detecting leaks in the extraction system. The lower end of the furnace head terminates in a ground joint into which the silica tube containing the crucible assembly is sealed with Picein wax. A special clamp holds the silica tube in place until the freshly waxed joint cools. The silica tube and the waxed connection

value. A glass funnel in the upper part of the tube directs the specimens into the graphite funnel of the crucible. A 6 KVA generator of about 50,000 cycles frequency energizes the induction coil.

A detailed sketch of the silica tube and crucible assembly is shown in Fig 3. Magnesia sand supports the alundum base and

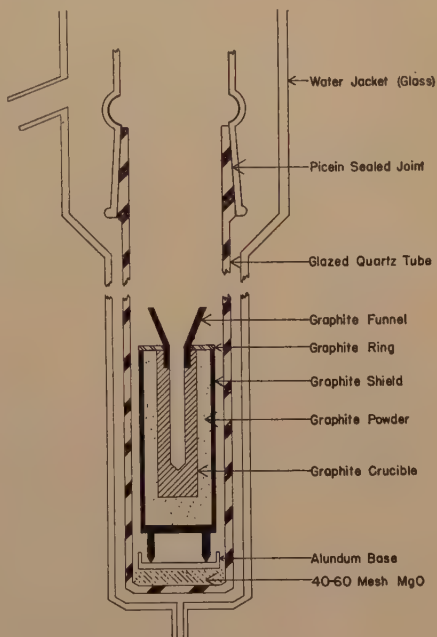
also provides sufficient freedom of movement to the base so that the crucible assembly can be adjusted with respect to the tube axis by tapping the side of the silica tube near the bottom. The crucible, ring cover, crucible funnel and shield are turned from graphite rods. The latter two items are slotted to reduce heating. Small legs, not shown in sketch, on the base of the shield are beneficial in reducing the blank. In this connection the ring is also of help as it prevents graphite powder from blowing out of the shield. The graphite powder is obtained from turnings passed through a 40-mesh and caught on an 80-mesh screen. Generally the graphite shield, funnel, ring and powder are used more than once. Any particles of iron adhering to the shield and funnel are removed by soaking in hydrochloric acid. The powder is freed of iron particles by combing with a magnet.

Degassing of the crucible to a very low blank requires from 4 to 6 hr at 2050°C . This is about as high a temperature as can generally be obtained in this furnace with the 6 KVA generator. If additional power is available, higher temperatures reduce the degassing time without any significant improvement in the blank.

The 2-stage mercury diffusion pump connected to the furnace head through stop-cock *S*₂ serves to evacuate the furnace and also serves as the gas circulating pump in the analytical system. This pump, when operating at the maximum pumping speed, will pump against a fore-pressure of about 4 mm of mercury. Increasing the heater input will permit the pump to work against about 6 mm of mercury with a sacrifice of some pumping speed. The pump heater input is indicated on a voltmeter across the heater and is controlled by a variable auto-transformer. A high speed fore-pump is used.

The parts of the apparatus considered up to this point comprise the extraction system.

The analytical system will be considered next. By way of introduction it may be stated that the hydrogen extracted from a sample is oxidized by copper oxide to water



FURNACE ASSEMBLY
FIG 3—DETAILED CROSS-SECTION OF CRUCIBLE ASSEMBLY.

vapor and determined by measuring the water vapor pressure in a calibrated volume. The copper oxide tube is heated in a split type combustion tube furnace, the temperature of which is maintained at 325°C by a controller operating from a chromel-alumel thermocouple inserted into the furnace. A special fuse, sealed in an evacuated glass tube with external leads, is located in the furnace with the copper oxide tube to protect the tube against failure of the temperature controlling equipment. This zinc fuse is connected in series with one side of the furnace power line. The copper oxide is prepared in the tube by oxidizing and reducing pure copper gauze that has been cleaned in nitric acid.

The hydrogen and oxygen gases used to prepare the copper oxide are passed through stopcocks S_3 and S_5 in Fig 1 by replacing the glass plugs with brass plugs

temperature changes the lower part of the manometer is immersed in water to prevent sudden changes in temperature. A vibrator is attached to the manometer to assure

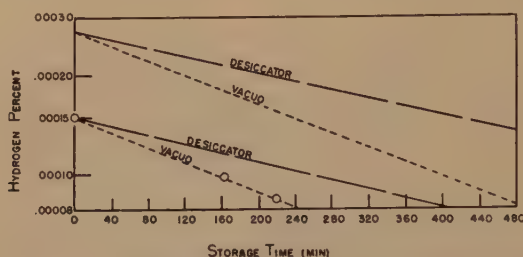


FIG 4—RATE OF HYDROGEN LOSS DURING STORAGE AT 27°C (VACUUM AND DESICCATOR) FOR CUT CUBES ($\frac{3}{8}$ -IN.) OF RAIL STEEL.

which permit a hose connection to be made to the tanks of gas. This makes it possible to confine the gases to the copper oxide tube and avoids passing large amounts of water vapor through the rest of the system. The oxidation-reduction cycle is repeated three or four times using commercial tank oxygen and hydrogen, finishing with an oxidation. Oxidizing and reducing temperatures are 325 and 225°C respectively. It is necessary to repeat the oxidation-reduction process occasionally to keep the copper oxide active.

The volume included between the mercury in the manometer and the freezing trap when S_5 , S_6 , S_7 are closed is calibrated. Water vapor pressure within this volume is indicated on the manometer.

The manometer is a combination oil (Amoil-S) and mercury manometer so constructed that it has the sensitivity of an oil manometer (approximately 10 times that of a mercury manometer) without the disadvantages. The scale of the manometer is readily moved to a zero position by a rack and pinion. It is necessary to protect the oil by mercury because water vapor is soluble in the oil. With this design, pressure measurements are made with the water vapor in contact with only the mercury. Because the manometer is sensitive to

hydrostatic equilibrium at the moment a reading is made.

A phosphorus pentoxide drying tube and a liquid nitrogen trap are placed in series with the fore-pump. The dehydrant keeps water out of the fore-pump, from whence it could get back into the system when the liquid nitrogen trap is not cooled. The dehydrant is held in a glass boat which is replaced through the ground glass cap. The liquid nitrogen trap keeps hydrocarbons originating in the fore-pump oil out of the system.

Stopcocks S_{13} and S_{14} provide a means for admitting a hydrogen check sample which is contained in the small volume between them. This sample is used to determine the efficiency of the copper oxide. Stopcock S_{13} has a hollow plug with a diagonal bore which is connected to a commercial tank of hydrogen. A quarter turn of the plug connects it with the small volume and S_{14} which discharges into the atmosphere.

Fig 1 also shows the ground joint connection by means of which the special hydrogen sample storage tubes are attached to the apparatus for evacuation. A helical liquid nitrogen trap is inserted in the vacuum line between the storage tube connection and the system.

Procedure

The procedure for determining hydrogen in steel may be conveniently described under the following operations: (1) sample preparation; (2) measurement of blanks; (3) determination of efficiency of the copper oxide; (4) extraction of the hydrogen from the metal; (5) measurement of the quantity of hydrogen extracted. Experimental evidence will be presented in a later section to substantiate the validity of this procedure.

Sample Preparation— $\frac{3}{8}$ -in. cubes of metal are cut from the massive piece by means of a metal band saw provided with an oil emulsion coolant. The coolant is removed from the freshly cut specimens with acetone before lightly filing the surfaces. After filing, the specimens are washed in reagent benzene followed by two washings in reagent acetone. This is followed by drying in a current of warm air and weighing. If the specimens are not introduced into the apparatus immediately, they are held in a phosphorus pentoxide desiccator for periods not exceeding 3 hr. The loss of hydrogen during this storage interval is accounted for by a method which will be described in a later section. In the event protracted storage is necessary the specimens are held in the storage tubes to be described.

Measurement of Blanks—Since the procedure has been developed specifically for hydrogen analysis, this is the only gas included in the blank measurement. The blank comes from two principal sources. These will be referred to as the "furnace blank," which includes all gases originating from the vacuum extraction part of the system, and the "copper oxide blank," which includes all gases originating in the analytical part of the system. The blanks from these two sources may be measured independently and adjusted for time to give a "total blank" for any particular analysis. In general, predetermined time

intervals are used for all analyses. These blanks are measured by a sequence of operations using half the time intervals required for a regular metal analysis. The total blank is measured first by collecting furnace gases for 15 min. while operating at 1500°C, and analyzing with a 10-min. period for circulation over the copper oxide. The 10-min. copper oxide blank is measured as above, except that the 15-min. collection of furnace gases is omitted by closing S_2 . The difference between the total blank and the copper oxide blank is the furnace blank. These blanks are determined each day and the analyses appropriately corrected.

Copper Oxide Efficiency—The efficiency of the copper oxide in converting hydrogen to water is determined each day as follows. Hydrogen is rapidly flushed through S_{13} and S_{14} for several minutes. S_{14} is then closed and S_{13} given a quarter turn to remove the hydrogen through S_{11} and the fore-pump. The small volume is then filled and emptied three times without flushing, following which it is again filled and the hydrogen pumped into the analytical system through S_{12} , at which time the apparatus is adjusted as it would be for collecting furnace gases except that S_2 is closed. After pumping for one minute S_6 and S_{12} are closed and the left arm of S_3 is opened to the fore-pump. The fore-pump removes from the system all of the hydrogen except that portion held in the calibrated volume. The pressure in this volume is measured on the manometer. Five minutes pumping clears the rest of the system of all the excess hydrogen, after which the analysis of the measured portion is carried out. The ratio of the original hydrogen gas pressure to the water vapor pressure gives an efficiency factor by which all subsequent analyses are multiplied.

Extraction of Hydrogen—After the above operations, the prepared steel sample is introduced into the lower end of the mercury lift from whence it floats to the top of the mercury. A magnet is used to

move the sample through the copper cooling block and the glass baffles into the horizontal part of the sample arm. At the time the sample is introduced into the sample arm, S_2 , S_3 (left), S_5 , S_7 and S_8 are open to permit pumping of the whole system. All other stopcocks are closed. After two minutes S_5 and S_7 are closed, S_6 and S_3 (right) opened, and the apparatus is now ready to collect furnace gases. The sample is then dropped into the crucible where it is degassed at a temperature of 1500°C for 30 min., after which S_2 is closed and the extraction phase is completed.

Measurement of Hydrogen: The furnace gases are next circulated for 20 min. through the copper oxide and the calibrated freezing volume, about which a dry-ice acetone mixture has been placed. This freezing mixture should be between -85 and -90°C . This temperature may be attained with the dry-ice acetone mixture, which is ordinarily about -78°C , by subjecting it to the reduced pressure of a water aspirator for 5 or 10 min. For circulation, S_3 and S_6 are closed in that order, and S_7 , S_5 and S_4 opened in that order. During this circulation the hydrogen is converted to water vapor and collected in the calibrated freezing volume. When this is completed, S_5 is closed and S_2 and S_3 (left) are opened. The analytical system is thus pumped free of nitrogen and carbon dioxide for 2 min., after which S_7 is closed. The manometer scale is adjusted to zero and the calibrated freezing volume thawed by surrounding it with a container of water at room temperature. The water vapor

$$\left(\begin{array}{c} \text{Water vapor} \\ \text{pressure} \end{array} \right) = \left(\begin{array}{c} \text{Manometer} \\ \text{reading} \end{array} \right) - \left[\left(\begin{array}{c} 20 \text{ min.} \\ \text{CuO blank} \end{array} \right) + \left(\begin{array}{c} 30 \text{ min.} \\ \text{Furnace blank} \end{array} \right) \right]$$

$$= 2.08 - [0.02 + 0.02] = 2.04$$

pressure is read on the manometer. Then S_4 is closed, S_5 and S_7 are opened to permit pumping the whole system in preparation for the next sample. The hydrogen content of the sample is calculated from the water vapor pressure reading, weight of sample, catalyst efficiency and the

volume calibration factor for the particular room temperature.

A sample data sheet and calculation follow:

Operation	Time	Manometer Reading (Cm)
Hydrogen Blanks		
Furnace blank collected (15 min.).....	9:00-9:15	
Furnace blank analyzed (10 min. circulation over CuO)	9:15-9:28	
Total blank = Furnace blank (15 min.) + CuO blank (10 min.).....	9:28	0.02
Analytical system evacuated	9:28-9:33	
CuO blank analyzed (Collected for 10 min.).....	9:33-9:46	0.01
CuO blank for 10 min.	9:46	
Furnace blank for 15 min. (Total blank - CuO blank).....		0.01
Analytical system evacuated.....	9:46-9:51	
Copper Oxide Efficiency		
Hydrogen check sample introduced.....	9:51-9:56	0.54
Hydrogen check sample analyzed (20 min. circulation over CuO).....	9:56-10:19	
Hydrogen recovered + CuO blank.....	10:19	0.52
CuO blank for 20 min.....		0.02
Hydrogen recovered.....		0.50
Analytical system and furnace evacuated.....	10:19-10:29	
CuO efficiency factor = 8%		
Analysis of Steel Sample		
Collection of gas from sample.....	10:29-10:59	
Gas analyzed.....	10:59-11:22	
Hydrogen from sample and blanks as water vapor....	11:22	2.08

Calculation of H in Specimen

Wt specimen = 9.800 g

Room temp = 20°C

Calibration factor for 20°C = $0.000780 \frac{\text{g pct}}{\text{cm}}$

$$\text{Pct Hydrogen} = \frac{(2.04) \left(\frac{54}{50} \right) (0.000780)}{9.800} = 0.000175$$

Evaluation of Method

An appraisal of the accuracy and precision of hydrogen values determined by this method may be made by evaluating the major stages of operation. These stages

may be considered as: (1) specimen preparation—this includes obtaining a representative specimen from the solid sample; (2) hydrogen extraction by vacuum fusion; (3) hydrogen analysis of the extracted gases. Experimental data will be presented for this purpose. In addition some independent evidence on accuracy and precision will be given.

Analysis—Even though the extraction stage precedes the analytical stage, it was necessary to evaluate the latter before it was possible to evaluate the extraction stage. The performance of the analytical system was determined by a series of analyses made on measured quantities of hydrogen and on mixtures of hydrogen and carbon monoxide (5 pct H and 95 pct CO by volume) as described in an earlier report.² In this additional work, the carbon monoxide was generated from formic and phosphoric acids and purified by passing through sulphuric acid, soda-lime and a

given in Table 1. The recovery in all instances is very satisfactory.

From a practical standpoint, it would require a longer period of circulation than is desirable to attain 100 pct recovery at all times, so that a circulation period of sufficient duration to obtain about 90 pct recovery is used, with the correction to 100 pct recovery being made by determining the efficiency of the hydrogen conversion to water. Thus the accuracy of the analysis is increased by the correction for the copper oxide efficiency as determined for the particular period of circulation used during analysis. There is no significant variation found for the copper oxide efficiency during the operation of the apparatus on any given day, so that an efficiency determined once each day is valid for the whole day. The quantity of hydrogen used for the regular check sample is comparable to the amount of hydrogen found in many samples of steel. The point as to whether the copper oxide efficiency (hydrogen recovery) is dependent on the quantity of hydrogen being used as a check sample was tested by using check samples of different volumes as shown in Table 2.

TABLE 1—*Analyses of Measured Quantities of Gases*

Run	Nominal Composition of Gas, Volume Pct Hydrogen*	Hydrogen Admitted, Millimols	Hydrogen Recovered as Water Vapor	
			Millimols	Pct of Hydrogen Admitted
1	100	0.0138	0.0126	92
2	100	0.0114	0.0112	98
3	100	0.00996	0.00956	96
4	100	0.00884	0.00888	100
5	11	0.0095	0.0092	97
6	12	0.0122	0.0121	99
7	5	0.0060	0.0060	100
8	5	0.0065	0.0065	100
				av. 98

* Balance of gas mixture is CO.

liquid nitrogen trap. The carbon monoxide contained an average of 0.64 pct hydrogen by volume as impurity. The analyses were suitably corrected for the hydrogen impurity in the carbon monoxide. The gases were measured and mixed in the collecting volume of the apparatus and then analyzed. Some typical results of the analyses are

TABLE 2—*Copper Oxide Efficiency and Volume of Hydrogen Check Sample*

CHECK SAMPLE VOLUME (N.T.P.)	AVERAGE RECOVERY, PCT
0.05 ml (regular).....	93
0.10.....	90
0.15.....	93

These results show that the copper oxide efficiency is independent of the amount of hydrogen analyzed.

Blanks

The subject of blanks is of sufficient interest and importance to be considered briefly. Making blank corrections is an accepted analytical procedure, provided the corrections are only a small percentage of the amount of the constituent for which the analysis is being made. A condensation of actual blank data is shown in Table 3.

Blanks are determined each day even though the day to day variation for a particular furnace set up only amounts to about 0.000001 pct hydrogen per 10g

It should be pointed out that all of the analyses in Table 4 for which no hydrogen was found for the second 30 min. extraction period did give the predetermined hydro-

TABLE 3—*Digest of Furnace and Copper Oxide Hydrogen Blanks*

Origin of Blank	Number of Determinations	Blank per Analysis, Percent Hydrogen per 10 g. Sample		
		Maximum	Minimum	Average
Furnace blank for empty crucibles.....	10	0.000005	0.000000	0.000002
Furnace blank for full crucibles.....	10	0.000006	0.000000	0.000002
Furnace blank for all crucibles.....	57	0.000009	0.000000	0.000002
Copper Oxide*.....	50	0.000009	0.000000	0.000001
Total (Furnace plus Copper Oxide).....	44	0.000018	0.000000	0.000003

* Blank from copper oxide is water.

sample. The average total blank correction with this apparatus for a 10g sample is 0.000003 pct hydrogen. The blanks are often only half this value and occasionally they are double this value. This correction amounts to less than 10 pct of the total hydrogen found in most samples and can be considered very satisfactory. Each of the maximum values shown in Table 3 occurred only once, while zero total blanks are often obtained. However, it so happened that the maximum values of 0.000009 pct hydrogen for both the copper oxide and furnace occurred on the same day thus resulting in the comparatively large maximum total blank (0.000018 pct) shown in the table.

These data show that the presence of steel in the crucible has no effect on the hydrogen blank.

Extraction of Hydrogen—Before the hydrogen in a sample can be determined it must be extracted from the sample. If the extraction process were incomplete, the hydrogen value would be low even though the analytical stage is satisfactory. Experience with the present method indicates that all the hydrogen which can be extracted from ordinary steels is removed in 30 min., and that no additional hydrogen is obtained by an additional 30 min. of extraction. This is shown in Table 4.

gen blank. This indicates the blank gas was evolved at a constant rate under the operating conditions. It indicates too, especially since the amount of blank gas is very small, considerable sensitivity and precision for the apparatus because negative values were never obtained. It should be under-

TABLE 4—*Quantities of Hydrogen Obtained by Degassing a Sample for 30 and 60 Min.*

Type Steel	Pct Hydrogen* Obtained at 1500°C	
	First 30 Min.	Second 30 Min.
Ingot iron.....	0.000029	0.000000
Ingot iron.....	0.000042	0.000000
B.O.H. 0.35 pct C, Al killed.....	0.000235	0.000000
B.O.H. 0.45 pct C, Al killed.....	0.000161	0.000002
B.O.H. 0.45 pct C, Al killed.....	0.000173	0.000006
B.O.H. 0.52 pct C.....	0.000017	0.000000
Ni, Cr, Mo.....	0.000030	0.000000
Rails 0.74 pct C.....	0.000016	0.000000
Rails 0.74 C.....	0.000056	0.000000
Rails 0.74 C.....	0.000087	0.000008
Rails 0.74 C.....	0.000066	0.000001
Rails 0.74 C.....	0.000066	0.000000
Rails 0.74 C.....	0.000021	0.000000
Rails 0.74 C.....	0.000035	0.000000
Rimming, 0.03 pct C.....	0.000062	0.000000
Bessemer.....	0.000041	0.000001

* Corrected for blank (0.000002 pct).

stood that these data do not define the shortest time in which all of the hydrogen can be extracted at this temperature.

The complete extraction of hydrogen from steel in 30 min. or less is not possible unless the steel is actually molten. Data have been obtained to illustrate this point.

The amount of hydrogen removed without fusion at several degassing temperatures on the same sample was determined in the present apparatus. Degassing was continued for 30 min. at each temperature. The lowest temperatures used are several hundred degrees higher than those used in many hot extraction methods, which results in a more rapid diffusion of hydrogen through the solid metal than is the case in the usual hot extraction procedure. The data are shown in Table 5.

TABLE 5—*Effect of Temperature on Quantity of Hydrogen Removed from Steel in Vacuo in Equivalent Times (30 Min.)*

Type Steel	Pct Hydrogen Obtained at the Indicated Temperatures			Total Hydrogen from Sample
	900°C (solid)	1100°C (solid)	1500°C (liquid)	
B.O.H. 0.52 pct C.....	0.000016	0.000012	0.000031	0.000059
B.O.H. 0.52 pct C.....			0.000062	0.000062
Bessemer.....	0.000001	0.000006	0.000035	0.000042
Bessemer.....		0.000019	0.000025	0.000044
Bessemer.....		0.000020	0.000031	0.000051
Bessemer.....			0.000041	0.000041

In no case was the bulk of the hydrogen removed in 30 min. by solid extraction, even at the comparatively high temperature of 1100°C. It is further evident that even one hour at temperatures in excess of those generally employed for solid extraction did not remove even half the hydrogen present. Therefore, solid extractions could not be developed into a rapid method.

It is interesting to note that the total hydrogen obtained by adding the several temperature fractions checks the hydrogen found by fusing a comparable sample in the apparatus at 1500°C. This is not in accord with results reported in the literature. For example, one investigator¹¹ found that the sum of his hydrogen fractions was considerably higher than the value found by a single temperature fusion.

The question has been raised as to

whether or not vacuum fusion of a steel in graphite removes all of the hydrogen. Direct evidence is difficult to obtain as there is no standard sample available which can be analyzed. An indirect approach was attempted, based on the known fact that gases can be removed from molten steel by bubbling another gas through the bath, that is, removal of nitrogen and hydrogen by rinsing with the carbon monoxide resulting from the carbon-iron oxide reactions in steelmaking.⁷ Experiments were carried

TABLE 6—*Effect of Induced Boil during Vacuum Fusion on Quantity of Hydrogen Extracted*

Steel	Pct Hydrogen Obtained at 1500°C		
	First 30 Min.	Second 30 Min.	Third 30 Min. with Boil
Dehydrogenized ingot iron*.....	0.000031		
Dehydrogenized ingot iron*.....	0.000031		
Dehydrogenized ingot iron*.....	0.000011		
Dehydrogenized ingot iron*.....	0.000012		
Dehydrogenized ingot iron*.....	0.000019		
Dehydrogenized ingot iron*.....	0.000020		
Av.....	0.000021		
B.O.H. 0.35 Pct C†	0.000235	0.000000	0.000035
B.O.H. 0.45 Pct C†	0.000161	0.000002	0.000021
B.O.H. 0.45 Pct C†	0.000173	0.000006	0.000026
Ni, Cr, Mo.....	0.000030	0.000000	0.000013
			av. 0.000024

* Prepared by holding the iron in a vacuum at 950°C for 60 hr.
† Al killed.

out in such a manner that, after extracting all the hydrogen possible with the usual procedure, each sample was again rinsed during a CO boil created by introducing ingot iron into the crucible. Gases pumped off during the boil were analyzed for hydrogen. The hydrogen content of the ingot iron was determined separately. The ingot iron was partially dehydrogenized by holding in vacuum for 60 hr at 950°C. These data are shown in Table 6. Two conclusions can be reached. After the normal

30-min. extraction period no significant additional hydrogen can be removed by an additional 30-min. treatment. Furthermore, the induced boil, with large amounts of additional CO gas, produced no hydrogen beyond that present in the ingot iron required to produce the boil. This is strong evidence that all of the hydrogen is re-

A typical analysis of the grade used is:

Element	C	Mn	P	S	Si
Pct.....	0.75	0.83	0.018	0.038	0.16

The study was confined to 131-lb rails because the defect is most prevalent in the

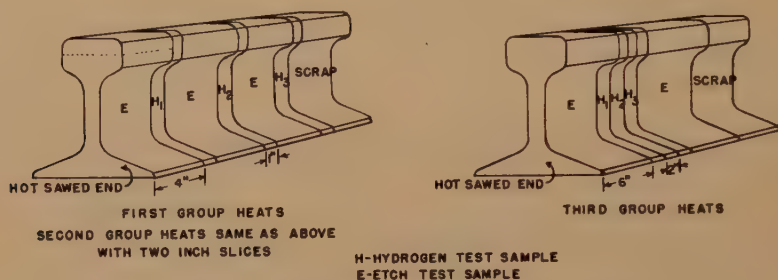


FIG 5—LOCATION OF HYDROGEN AND ETCH TEST SAMPLES IN RAIL.

moved by the standard 30-min. vacuum fusion treatment.

Further consideration will be given to the sampling and analytical techniques which have been developed and their precision and accuracy will be evaluated. The illustrative data which will be used for this purpose were obtained from a study of the behavior of hydrogen in rails. Therefore it will be necessary to digress and present the results of this project before the evaluation of procedures is completed.

HYDROGEN IN STEEL RAILS

The reasons for selecting rail steel as the most suitable material have already been given. The original plan was to analyze rails for hydrogen at stated intervals of time after rolling, and to correlate these analyses with susceptibility of the rails to flakes. It has been shown⁸ that large amounts of hydrogen added intentionally may produce flakes in such steels. But whether or not flakes result from the amounts encountered in normal commercial practice, and whether or not a critical or threshold amount is required is not known.

heavier sections. Crops from the rail rolled from the center portion of the ingot were taken at the hot saw for each heat, and test slices were removed from the crop as soon as it air cooled to room temperature. This cutting was done as shown in Fig 5. The samples marked *E* were sectioned through the head and examined for cracks on a predetermined schedule and the samples marked *H*₁, *H*₂, *H*₃ were analyzed for hydrogen on the same schedule. The first group of 9 heats came from Plant *A* and the *H* slices were 1-in. thick. The second group of 15 heats was sliced according to the same scheme except the thickness of the *H* slices was increased to 2 in. The third group of 7 heats came from Plant *B* and these were also cut with 2-in. *H* slices. At the designated time, specimens for hydrogen analysis were cut from the head of the *H* slice as $\frac{3}{8}$ -in. cubes at the positions indicated in Fig 6. By this scheme the four samples designated *A*₁, *A*₂, *C*₁, *C*₂ were symmetrical and were expected to have the same hydrogen content, and samples *B*₁, and *B*₂ were equivalent. The first hydrogen sample was always analyzed as soon as possible after rolling. The

corresponding *E* sample was sectioned and etched on the same day. The plane of the etched section was the same as the center

(2) Although it would be expected that the hydrogen diffusion process would continue until all the hydrogen had left the

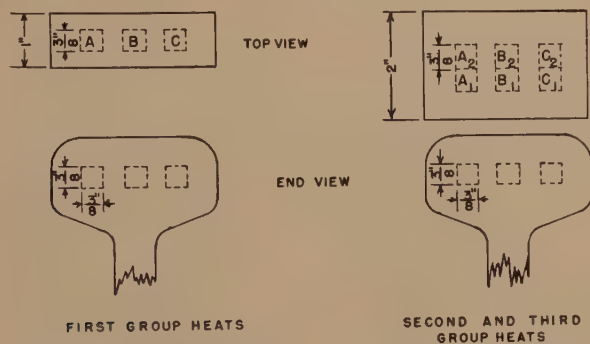


FIG 6—LOCATION OF HYDROGEN SPECIMENS IN RAIL SLICE.

of the cubes cut for hydrogen analyses, as shown in the *E* sample of Fig 5.

The hydrogen analyses of the rail slices made at various intervals of time after rolling have been plotted in Fig 7 to show

rails whatever their thickness, this is not the case. The hydrogen level for Plant *A* rail samples eventually reaches a constant value at about 0.00002 pct. For Plant *B* the constant hydrogen level is about

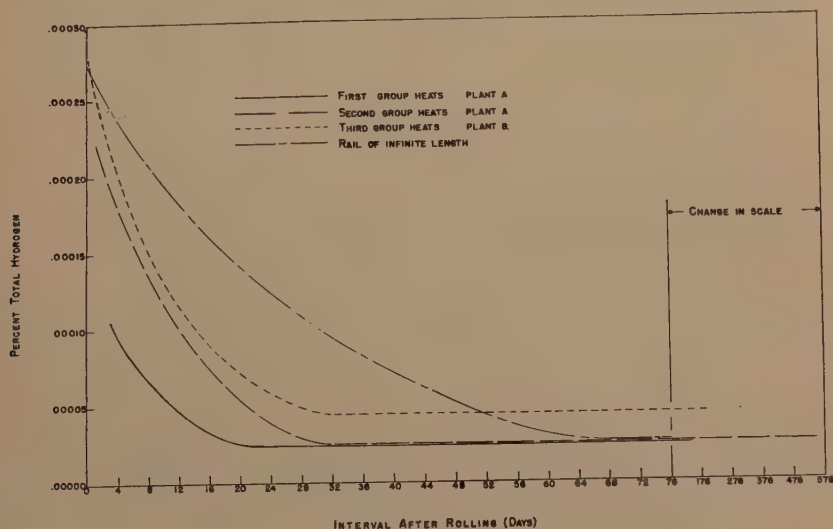


FIG 7—CHANGE OF HYDROGEN IN RAILS WITH TIME AFTER ROLLING.

the average variation of hydrogen with time for each of the three groups of heats. Examination shows several things:

(1) Hydrogen diffuses through rail steel at room temperature rapidly enough to decrease the hydrogen content appreciably in a few days.

0.00004 pct. It seems then that this constant level of residual hydrogen may be considered the zero level for diffusible hydrogen for this material. Independent work in England has led to a similar observation of a residual hydrogen content.^{9,10} The term "diffusible hydrogen"

is used in this paper to mean hydrogen which can be removed from steel, by a process that appears to be diffusion, in a practicably measurable length of time, as contrasted to the residual hydrogen which either does not diffuse from the steel at all or else does so at an extremely slow rate. The data shown in Fig 7 include a few samples which have been kept 540 days.

(3) It is interesting to note that the difference between the average hydrogen values for Plant *B* as compared to those for Plant *A*, for comparable test samples (2-in. slices), is about the same as is found for the difference (0.00002 pct) between the residual hydrogen for the two plants.

In the preceding discussion, zero time is considered as the time at which the rail reached room temperature and it is evident that the hydrogen content at this time is of special interest as the initial point of the curve. The shape of such curves makes their extrapolation inaccurate, but a method has been found for making such extrapolations from hydrogen analyses made at two different times. In the preferred method, the diffusible hydrogen, which is the analytical or total hydrogen minus the residual hydrogen, is plotted on a logarithmic scale against time on a linear scale. Such a plot should be linear if the process is controlled by Fick's diffusion law. Only the diffusible hydrogen is considered because the residual hydrogen does not appear to contribute to the concentration gradient controlling the process. Actually, the semilogarithmic plotting is useful even when the residual hydrogen is not known. This is especially true when analyses are available near zero time when the correction for residual hydrogen is relatively small. The correctness and convenience of such a plot are shown in Fig 8, which contains information deserving extensive discussion. It shows a comparison between the vacuum fusion method of hydrogen analysis described in this paper and the modified solid extraction method

which has been developed at Battelle Memorial Institute.⁴ The purposes of the comparison were served best by omitting the correction for residual hydrogen. In this comparison a rail crop was cut into 6 consecutive 2-in. slices which were distributed alternately to the two cooperating laboratories. The analyses obtained by vacuum fusion are shown by open circles, while those obtained at Battelle are shown by squares. It is evident that, if the best line is drawn through the four *B* points obtained by vacuum fusion on the tenth and nineteenth days after rolling, this line passes through the two *B* points obtained the day the rail was rolled. Analyses were made at only two times for the *A* specimens. One can observe the different hydrogen concentrations in the *A* and *B* locations and see that it is highest in the center of the rail. The dashed line is the average of all vacuum fusion analyses. Since the data could be treated in this way, and since the hydrogen content of the rail at any time would be established by a limited number of vacuum fusion analyses, it was possible to plan a comparison with the Battelle method without establishing a definite schedule of times at which the analyses must be made. It is observed that the points obtained at Battelle on the sixth and thirteenth days after rolling fall in the expected positions and establish a very good absolute agreement between the two independent methods. The Battelle analyses on the twenty-first day appear too low, but it should be remembered that the total amount of hydrogen present at this time is very small and that the logarithmic scale exaggerates differences which are actually very small.

The above example illustrates the value of the semilogarithmic plot without correcting for residual hydrogen, but the logical importance of the residual hydrogen concept must not be neglected. The use of the concept allows us to treat the time dependence of the hydrogen content of

steel by established diffusion theory. The recent British treatments of the subject^{9,10} have led to unnecessarily complex mathematical expressions whose physical sig-

content is plotted against time. The full interpretation of the "residual hydrogen" quantity and its part in the general hydrogen problem is not clear at this time. Data

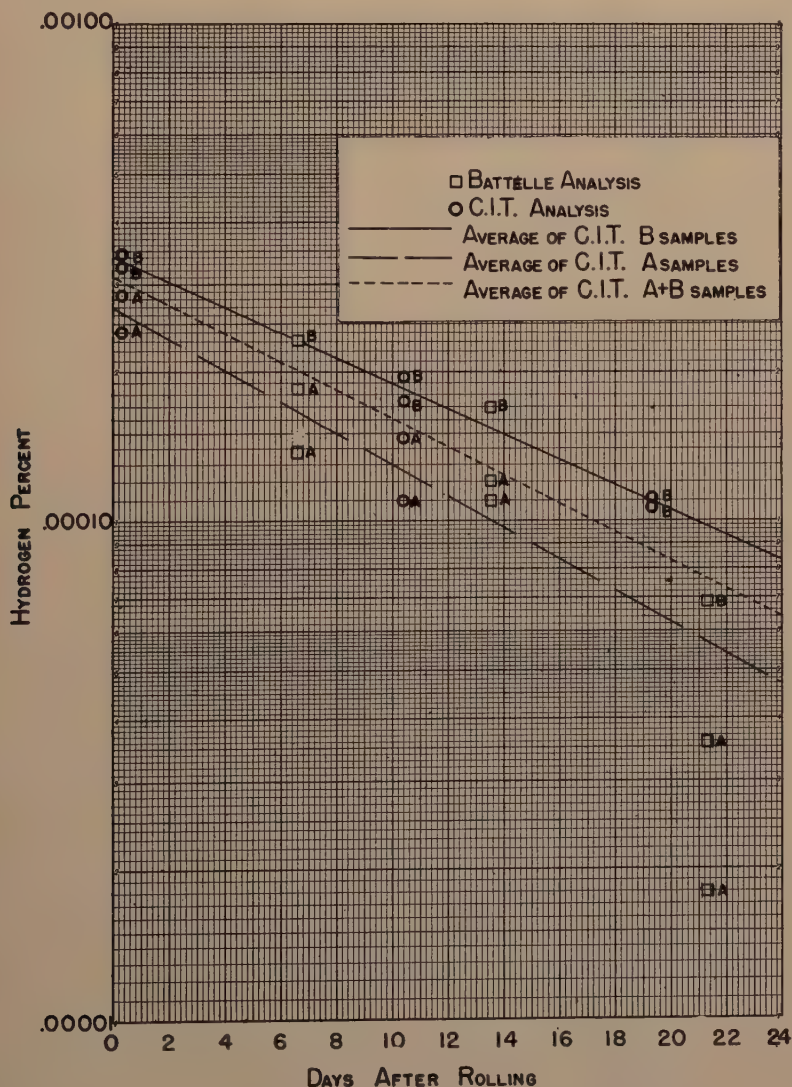


FIG 8—COMPARATIVE ANALYTICAL DATA ON RAIL SAMPLES.
Showing linear relation when plotted on semilogarithmic scale.

nificance is uncertain. If these data are reconsidered and corrected for residual hydrogen, they show the expected linear relation when the logarithm of hydrogen

to be presented in the section on *Sample Preparation* will show that this residual quantity is truly characteristic of the mass of metal considered and is not a surface

contaminant. However, if the above reasoning is correct, the residual hydrogen can be determined from a semilogarithmic plot of hydrogen analyses made at three

individual heats are considered, the first hydrogen analysis for each heat which flakes yielded a value above the 2σ limit. After longer storage the hydrogen content

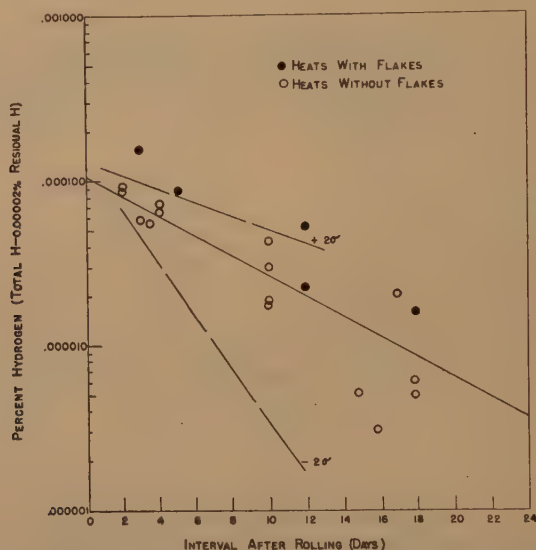


FIG 9—CHANGE IN HYDROGEN IN RAILS WITH TIME AFTER ROLLING.
Semilogarithmic plot. Group 1, one inch slices from plant A.

different times by finding what correction is required to make these points linear.

With this understanding of the loss of hydrogen from rails after rolling, and the semilogarithmic method of plotting, it is possible to consider the data in greater detail. Complete data for the diffusible hydrogen of all heats are plotted in Fig 9, 10, and 11 for Groups 1, 2, and 3 respectively. Analyses from heats which flaked are shown as solid circles. Since there is considerable scatter from heat to heat within each group of heats, and since only four of the 31 heats developed flakes, it is difficult to draw definite conclusions, but a relation between flakes and a high hydrogen content after rolling is indicated. In each group a solid line has been drawn to show the average trend, and the 2σ limits have been added on the basis of the data for the first 13 days, which are felt to be more significant than later points. When

of some of these heats fell below the 2σ limit, but all remained above the average of the group within the time limits included in Fig 9 and 10. It was not felt that further work on this program would be profitable because it is so difficult to find a heat which flakes.

Another series of experiments was made to establish the importance of temperature in the escape of hydrogen from a rail. For this purpose 2-in. rail slices from the same heat were kept in ovens at 108 and 203°C and water quenched at appropriate time intervals for sampling and analysis. A uniform procedure was adopted to evaluate the time at temperature. Heating curves were measured by imbedding a thermocouple in the center of the railhead and measuring the rate of heating in the oven. The time at temperature was taken as the time in the oven minus half the time required to bring the rail slice up to tempera-

ture ($1\frac{1}{4}$ hr at 203°C). The data are shown in Fig 12, where the curves for 23, 108, and 203°C are all adjusted to the same initial hydrogen value of 0.0003 pct. Curves for

hydrogen is accepted as a diffusion process, it should be possible to calculate the temperature coefficient for the process from these data and thus to calculate the rate

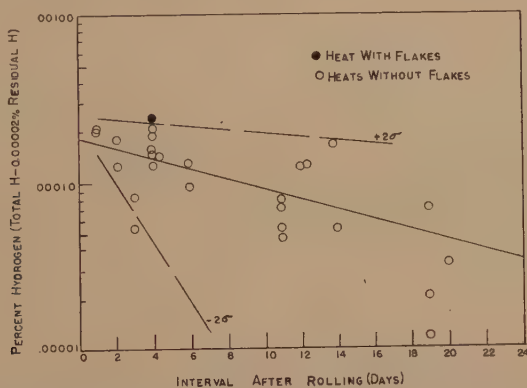


FIG 10—CHANGE IN HYDROGEN IN RAILS WITH TIME AFTER ROLLING. Semilogarithmic plot. Group 2, 2-in. slices from plant A.

commercial length rails are also included in this figure. Their calculation will be described later in the paper. The 23° curve is the average of all Group 3 heats and this value is chosen to represent average room temperature. It is clear from Fig 12 that

of hydrogen loss at any temperature below the eutectoid. The studies of Andrew and co-authors¹³ support these assumptions. A simple method for carrying out such calculations follows:

In Fig 12 the time intercepts for each of

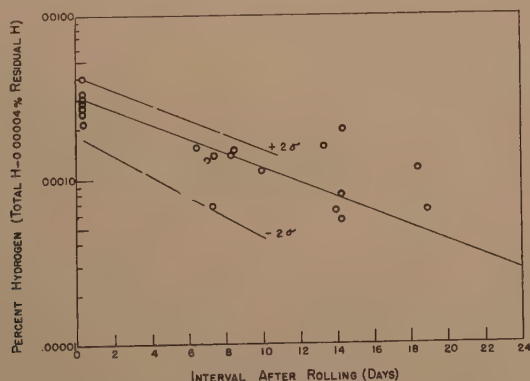


FIG 11—CHANGE IN HYDROGEN IN RAILS WITH TIME AFTER ROLLING. Semilogarithmic plot. Group 3, 2-in. slices from plant B.

the temperature coefficient for this process is so great that the same techniques could not be used to good advantage at higher temperatures because the time intervals would become too short to allow good measurement. However, if the escape of

the three temperatures are taken at any selected hydrogen level (0.00011 pct hydrogen level was used). This time is inversely proportional to the average rate of hydrogen evolution from the center of the rail heads for these temperatures. It has been

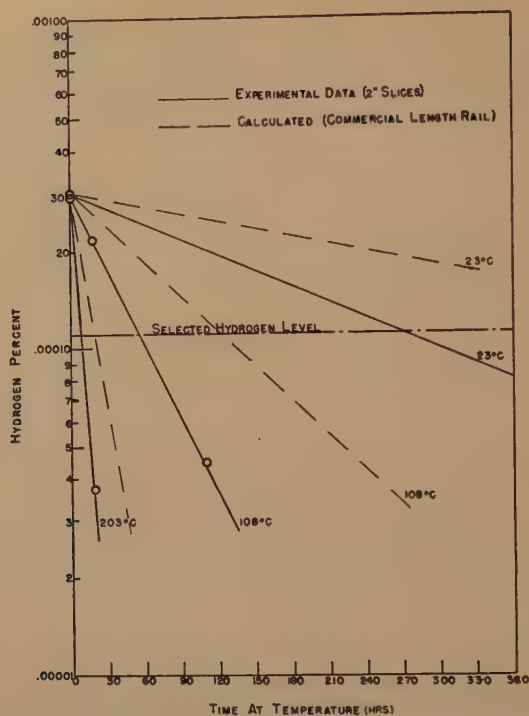
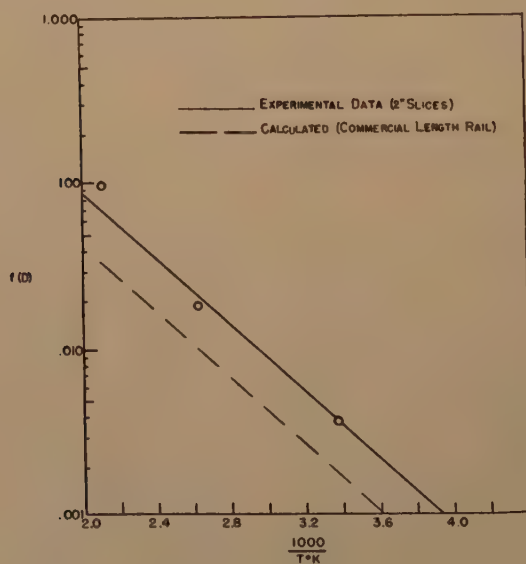


FIG 12—LOSS OF HYDROGEN FROM RAIL STEEL AT DIFFERENT TEMPERATURES.

FIG 13—RELATION OF $f(D)$ AND TEMPERATURE.

shown that the rate of hydrogen evolution is a diffusion process and it is therefore proportional to the diffusion constant, D , and the concentration gradient. For a selected concentration gradient such as we are considering, the rate of evolution is then proportional to D , or equal to a function of D , which will be designated $F(D)$. Also, the reciprocals of the time intercepts on Fig 12 are proportional to $F(D)$, or equal to a new function of D , $f(D)$. The value of the diffusion constant varies with the temperature in such a way that a linear relationship exists between $\log D$ and the reciprocal of the absolute temperature. Thus, a plot of the log of the reciprocal of the times taken from Fig 12, and the reciprocal of the absolute temperature would give a straight line. This line is shown in Fig 13. From Fig 13 the value of $f(D)$ for any temperature can be obtained. The reciprocal of this value inserted into Fig 12 at the selected hydrogen level gives the second point needed to draw in additional curves for other temperatures. (The point of convergence for the curves is the other point.)

EVALUATION OF THE PROCEDURE *Precision*

The data from the adjacent B_1 and B_2 specimens of the Group 2 heats provide a means of evaluating the precision of the procedure. It is felt that these specimens from the center of the rail head are the best duplicates available for this purpose, since any heterogeneity in the ingot should be largely eliminated by the processing required to form the rail. The results shown in Table 7 include effects of possible segregation as well as sampling and analytical errors. The statistical analysis¹⁴ of these twenty-seven pairs gives a standard deviation of ± 0.000019 pct for the total error of the hydrogen values. The probable error is ± 0.000013 pct.

No absolute standards are available for hydrogen in steel. Its fugitive behavior

makes it unlikely that any such samples will ever be available. It is therefore difficult to determine the accuracy of any analytical method. However, the comparative analyses of the rail heat shown in

TABLE 7—Data Showing Variation of Hydrogen between Adjacent Specimens in Rails (2-In. Slices) Used to Calculate Standard Deviation of the Total Error of the Hydrogen Values

Hydrogen Analyses on Pairs of Specimens in Pct		Difference in Percent Hydrogen (D)
Specimen B_1	Specimen B_2	
0.000135	0.000155	± 0.000020
0.000204	0.000199	0.000005
0.000144	0.000149	0.000005
0.000073	0.000072	0.000001
0.000211	0.000162	0.000049
0.000173	0.000126	0.000047
0.000088	0.000084	0.000004
0.000069	0.000075	0.000006
0.000102	0.000104	0.000002
0.000078	0.000114	0.000036
0.000034	0.000028	0.000006
0.000081	0.000068	0.000013
0.000107	0.000094	0.000013
0.000206	0.000206	0.000000
0.000007	0.000030	0.000023
0.000288	0.000218	0.000070
0.000013	0.000010	0.000003
0.000220	0.000232	0.000012
0.000014	0.000017	0.000003
0.000230	0.000206	0.000024
0.000006	0.000000	0.000006
0.000108	0.000122	0.000014
0.000185	0.000107	0.000078
0.000134	0.000157	0.000023
0.000158	0.000171	0.000013
0.000179	0.000171	0.000008
0.000092	0.000084	0.000008

$$B_1 - B_2 = +D \text{ and } B_2 - B_1 = -D$$

$$\frac{\sum (\bar{D} - Di)^2}{n} = \frac{200.96 \times 10^{-10}}{27} = 7.443 \times 10^{-10}$$

Standard deviation of difference

$$= \sigma_D = \sqrt{\frac{\sum (\bar{D} - Di)^2}{n}} = 27.28 \times 10^{-6}$$

Standard deviation of total error of hydrogen values
 $= \sigma_T$

$$\sigma_T = \frac{\sigma_D}{1.414} = \frac{27.28 \times 10^{-6}}{1.414} = \pm 0.000019 \text{ pct}$$

Probable total error of hydrogen values = $0.674\sigma_T$
 $= \pm 0.000013 \text{ pct}$

Fig 8, and similar results on other samples exchanged in the same program, indicate that the accuracy is good. These data will be the subject of a separate paper.

Sample Preparation

The accumulated data on rails make it possible to understand the importance of

well planned sampling procedures in work involving hydrogen and some important practices will be described.

It is apparent that no marked temperature rise should be permitted during the cutting of specimens to be used for hydrogen analysis. This condition is satisfactorily met by using a cutting machine with a coolant, as the following experiment shows. A length of rail head was cut longitudinally using a coolant on a metal band saw. The temperature was measured by means of a thermocouple placed in intimate contact with the rail head with the junction of the couple in the plane of the saw blade. The maximum temperature rise was 1.3°C for a new blade. For a new blade the cutting time and rise in temperature was a third of that found for a worn blade. There is no doubt that such cutting is safe in view of the fact that room temperature varies more than this.

Since hydrogen escapes from steel by a diffusion controlled process, it follows that even at room temperature, the smaller the specimen, the more rapid will be the hydrogen loss. The greater rate of hydrogen loss for the thinner rail slice is shown in Fig 7. Because of this, final cutting of the small analytical specimen should be as rapid as heating effects will permit, and the period of open storage of a cut specimen should be no longer than necessary. The hydrogen loss from a $\frac{3}{8}$ -in. cube of rail steel on storing in a desiccator is shown in Fig 4. It is apparent that the greater the initial hydrogen level in a specimen, the greater the hydrogen loss in a given interval of time. The curve for hydrogen loss in a desiccator in Fig 4 is taken from Fig 14. The data in Table 8 indicate that the hydrogen content of these small cubes reaches a constant residual value at the end of one day's storage.

For greater accuracy, then, it is necessary to take into account the hydrogen lost from the small cubical specimens between the time of removal from the massive

sample (taken as the midpoint of the cutting time) and the time of analysis. This is conveniently done by means of a curve, such as is shown in Fig 14, where the diffusible hydrogen concentration on a log scale is plotted as a function of time.

TABLE 8—*Loss of Hydrogen from Small Cubical Specimens*

Pct Hydrogen Present at Time of Removal from Rail	Length of Time Removed from Rail Before Analysis	Pct Hydrogen in Cubes by Analysis	Difference between Pairs, Pct
0.00016	24 hr	0.000042 0.000040	0.000002
0.00025	26 hr	0.000053 0.000050	0.000003
0.00027	3 days	0.000038 0.000039	0.000001
0.00014	6 days	0.000067 0.000061	0.000006
0.00021	21 days	0.000027 0.000051	0.000024
0.00034	23 days	0.000039 0.000045	0.000006
			av. 0.000009

Although Fig 14 shows two lines, both lines are a continuation of the same curve, segments of which have been displaced to provide for a greater range of hydrogen values in a compact form. A point on the curve corresponding to the diffusible hydrogen value, read on the appropriate scale, is extrapolated to the left a distance equivalent to the time interval being used for the adjustment. The hydrogen value read from the curve at this point plus the residual hydrogen is the adjusted total hydrogen value. The curve in Fig 14 is the average of analyses made at intervals of several hours on $\frac{3}{8}$ -in. cubes from three heats of rail steel. Similar hydrogen loss curves could be constructed for other materials. The maximum time interval for which the adjustment is normally made is about 3 hr. Longer extrapolations are not only subject to larger error, but are unnecessary with the availability of the hydrogen sample storage tubes to be described in the next section.

A number of pairs of specimens, assumed to be duplicates, were analyzed after various time intervals to compare the hydrogen

by analyzing, in pairs, cubes of the metal with and without the use of cleaning agents after filing. Great care was exercised in

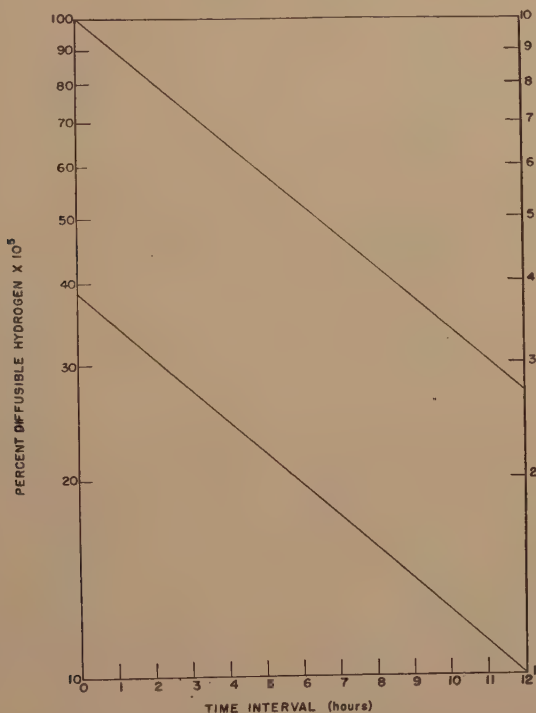


FIG 14—CORRECTION CHART.

Used for correcting $\frac{3}{8}$ -in. cubes for hydrogen loss between cutting time and analysis.

values obtained by analysis with those obtained from Fig 14. The hydrogen analysis of the second member of each pair extrapolated over the indicated time interval should check the analysis for the first member of the pair made at the beginning of the time interval. These results are shown in Table 9 which shows satisfactory agreement between extrapolated and analyzed values.

The possibility was considered of there being some absorption of the organic cleaning agents on the freshly filed steel surfaces of the specimens; which might thus account for the residual hydrogen found in various steels. The existence of such an effect in the case of rail steel and ingot iron was tested

handling these specimens so that no contamination should occur after filing, espe-

TABLE 9—Comparison of Actual with Extrapolated Hydrogen Values

Hydrogen in First Member of Pair Analyzed at Time of Cutting, Pct by Analysis	Time Interval Before Analysis of Second Member, Hr	Hydrogen in Second Member of Pair	
		Pct by Analysis	Pct Extrapolated
0.000106	3.0	0.000087	0.000105
0.000282	1.0	0.000266	0.000293
0.000172	1.1	0.000156	0.000172
0.000264	0.9	0.000252	0.000282

cially in the case of the specimens on which no cleaning agents were used. Specimens of low hydrogen content were used in order

to obtain the best possible duplicates. The data from these tests are in Table 10 and show that the method of cleaning described in this paper has no effect on the final hydrogen result. Even though regular shaped specimens may be cleaned by filing alone, the use of cleaning agents is a decided advantage because excessive and time consuming precautions against contaminations are necessary when agents are not used. However, it is important to insure that no solvent is carried into the crucible by specimens containing cracks or cavities.

TABLE 10—*Effect of Cleaning Agents on Hydrogen Analyses*

Material	Hydrogen Found, Pct		
	Regular Cleaning Procedure	No Cleaning Agents Used	Difference from Regular Procedure
Rail steel....	0.000061	0.000067	0.000006
	0.000080	0.000087	-0.000007
	0.000029	0.000027	-0.000002
Ingot iron....	0.000011	0.000012	0.000001
	0.000019	0.000020	0.000001
	0.000031	0.000031	0.000000
			av. 0.000007

In order to demonstrate further that this prescribed treatment does not introduce appreciable amounts of surface hydrogen into the analysis, a series of samples was analyzed in which the ratio of surface to mass was deliberately varied over a wide range. To increase the significance of the results, the ingot iron used for the purpose was partially dehydrogenized and homogenized by prolonged high temperature treatment in vacuum. Standard $\frac{3}{8}$ -in. cubes were cut from these bars and the remaining material was rolled into strips about 0.020-in. thick. Both cubes and strips were given an additional high temperature vacuum treatment to insure comparable surfaces. They were removed from the furnace and given the normal sample exposure to air, the strips were coiled for convenience in handling and

both cubes and strips were given the prescribed surface treatment with benzene and acetone. After storage in a desiccator for 14 days, they were analyzed with the results shown in Table 11. Even though the ratio of surface to mass was five times greater for the strips than for the cubes, the difference in hydrogen content of the two types of sample is well within experimental error and this could not be true if the hydrogen is present as surface hydrogen.

Studies of surface gases on silicon steels¹⁵ showed a high absorption of water on

TABLE 11—*Data Showing That Hydrogen Content Is Independent of Ratio of Surface to Mass*

Type of Sample	Analysis, Pct H	Area, cm ²	Weight, g	Area/Weight, cm ² /g
Strips.....	0.000012	80.7	14.95	5.81
Strips.....	0.000014	74.7	13.22	5.64
Strips.....	0.000020	75.5	15.73	4.80
$\frac{3}{8}$ -in. cubes..	0.000022	4.45	5.085	0.88
$\frac{3}{8}$ -in. cubes..	0.000022	9.20	10.84	0.85

exposure to air, but this is apparently a special case caused by the presence of silicon.

HYDROGEN SAMPLE STORAGE TUBES

It is now recognized that the fugitive nature of hydrogen in steel presents a problem in connection with the holding of a sample until a time when the analysis can be made. The loss of hydrogen can be serious in a matter of a few hours for small specimens removed from massive samples and also in the case of newly cast furnace samples of thin section.⁶ The obvious course of analyzing the specimen immediately is often neither possible nor practical, especially when the samples must be transported some distance to the laboratory for analysis or when the number of specimens removed from a massive sample excludes the possibility of analysis of all samples within a few hours or even in the

same day. It is apparent that some means is required to trap the escaping hydrogen in order to obtain an analytical hydrogen value which is truly representative of the

bead supports the copper receptacle and prevents contact with the dehydrant. Fresh dehydrant is placed in the tube each time it is used; also, the large ground joint

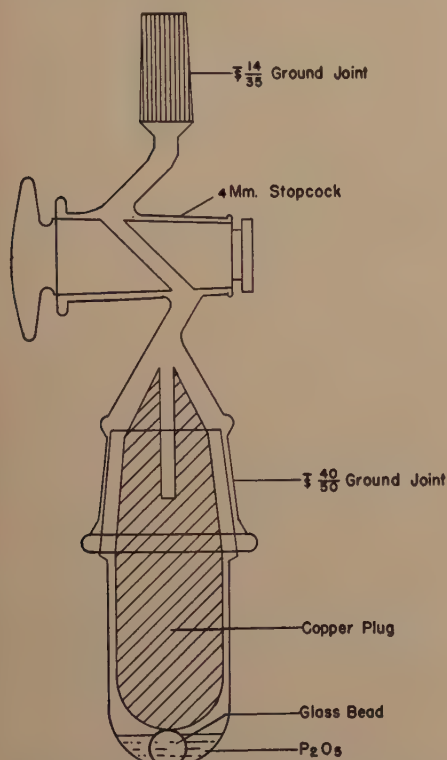


FIG 15—STORAGE TUBE FOR HYDROGEN TEST SAMPLES (TYPE 1).

source from which the sample was obtained. This has been accomplished by two types of sample storage tubes.

Type 1—The storage tube shown in Fig 15 consists of a copper receptacle stored over phosphorus pentoxide in a Pyrex container. The copper receptacle shown is slotted to take a thin chill cast sample; for cube shaped specimens, copper receptacles with a hole of the appropriate size drilled in the top are used. The copper receptacle absorbs the residual heat in the sample and reduces the volume of air in the tube. About 0.2 g of P_2O_5 and a large glass bead are located at the bottom of the tube; the

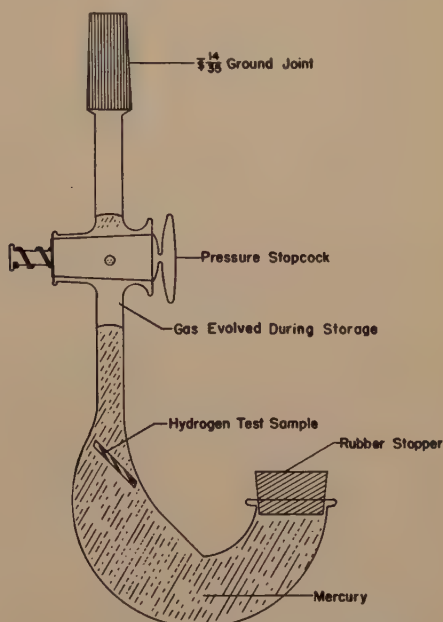


FIG 16—MERCURY IMMERSION TYPE HYDROGEN SAMPLE STORAGE TUBE (TYPE 2).

and stopcock are greased with just enough working-in of the grease to prevent the moisture in the atmosphere from leaking into the dehydrant. A small ground joint at the top of the storage tube serves to connect the tube to the hydrogen apparatus for the removal of the gas evolved during storage as shown in Fig 1. Six units are arranged in a small carrying case.

Type 2—The storage device in Fig 16 consists of a mercury trap which allows the gas evolved during storage to collect below a stopcock which can be connected to the hydrogen apparatus in the same manner as for *Type 1*. The mercury in this device must be kept clean, the method selected for the mercury lift being satisfactory, except that it may occasionally be necessary to degrease the mercury. The

mercury is raised just through the stopcock by application of a vacuum through a piece of rubber tubing. The rubber stoppers in the mouth of the tubes prevent loss of mercury in transit. These units are arranged in a small carrying case in such a manner that they can be used without removing them from the case.

Using the storage tubes is simple. With *Type 1* tube it is necessary only to remove the cap, place the sample in the copper receptacle, replace the cap with the stopcock open and, after turning the cap several times to obtain a tight joint, the stopcock is closed. The sample may then be held in the tube until the analysis can be made. For the *Type 2* tube the sample is pushed under the mercury, by means of a small rod with a flattened end, until it is beyond the bend in the tube. Samples cut from massive pieces are cleaned in the manner described under *Preparation of Specimen* before placing them in the tubes. At the time the analysis is made, the storage tube of either type is attached to the ground joint provided for that purpose on the hydrogen apparatus as shown in Fig 1. After the spiral freezing trap has been given a preliminary evacuation through *S11*, liquid nitrogen is placed around the trap, and the evacuation continued for several minutes through *S12* with *S2* and *S11* closed. The stopcock on the storage tube is then opened and the evacuation continued for several minutes after having set the apparatus for gas collection. For the tubes of *Type 2* the stopcock on the tube is opened only long enough to force any gas in the tube through the stopcock, *S12* and the stopcock on the tube are then closed and the gas analysed in the manner already described, *S15* is opened to release the vacuum so as to facilitate removal of the storage tube. The solid sample is then removed from the storage tube and prepared for analysis. The total hydrogen is, of course, the sum of the hydrogen in the gas sample and the solid sample.

It was found necessary to use phosphorus pentoxide in the *Type 1* storage tube to prevent rusting of samples. Samples in tubes containing moist air gave erroneously high and erratic hydrogen values.

The reliability of the storage tubes was decided on the basis of whether or not any significant gain or loss of hydrogen could result from holding samples in the tubes. Gain in hydrogen could occur only as the result of there being a water or hydrogen blank. Therefore, blank analyses were made on the air contained in the *Type 1* tubes after they had been opened to the atmosphere for about one minute, just as they would be when introducing a sample, and allowed to stand from one to seven days. With the present method of using the tubes, no hydrogen blank was found; only a small constant water blank equivalent to 0.000001 pct hydrogen per 10 g sample—Table 12, Part A.

Somewhat higher average water blanks were found with a shorter freezing trap and also with a solid CO_2 -acetone mixture as the coolant, as shown in Part B, Table 12. The necessity for preventing contact between the copper filler and dehydrant is indicated by the considerable hydrogen blank resulting after two days of direct contact. However, small amounts of the dehydrant spattered on the copper should be insignificant as the area of contact in the test just mentioned was much greater than would ever result with reasonable care in handling the tubes. The average blank for the *Type 2* tubes was the same as for the *Type 1* tubes, although greater variation from the average was found for the former than for the latter.

Some data have been obtained with rail steel specimens of known hydrogen content stored in *Type 1* tubes which indicate there is no loss of hydrogen in these tubes. These data are shown in Table 13. Each of the values given is the average of two analyses on specimens from the indicated locations in the rail head. The specimen location

notation conforms with that shown in Fig 6 except that the notations *AB* and *BC*, not shown in Fig 6, are used for specimens located between and adjacent to *A* and *B*

Further, the ability to detect the difference in hydrogen content between the *A* and *B* specimens has not been lost by holding the specimens in tubes. This is shown in Table

TABLE 12—*Storage Tube Blank Data*

Type Tube	Length of Freezing Trap (Cm)	Freezing Trap Coolant	Blank Equivalent in Pct Hydrogen per 10 g Sample					
			Water			Hydrogen		
			Max.	Min.	Av.	Max.	Min.	Av.
A—Present Method Used for Samples								
I	110	Liq. N	0.000001	0.000000	0.000001	0.000001	0.000000	0.000000
B—Other Methods Used								
I	110	Solid CO ₂	0.000005	0.000002	0.000003			
I	37	acetone	0.000005	0.000002	0.000004			
2	37	Liq. N	0.000007	0.000000	0.000004			"
C—Copper Filler and P ₂ O ₅ in Contact for Two Days								
I	110	Liq. N	0.000001	0.000001	0.000001	0.000013	0.000010	0.000011

and *B* and *C* respectively. Thus, we may expect the average of *A* and *B* specimens to be comparable to *AB* specimens. Like-

TABLE 13—*Comparison of Samples Held in Storage Tubes with Those Analyzed on Cutting*

Specimens Analyzed Immediately		Specimens Held in Tubes		
Location in Rail Head	Average Hydrogen Pct*	Location in Rail Head	Average Hydrogen Pct*	Time in Tubes (Days)
<i>A</i>	0.000342	<i>B</i>	0.000367	1
<i>A</i>	0.000128	<i>B</i>	0.000183	1
<i>A</i>	0.000319	<i>B</i>	0.000380	3
av. of <i>A</i> plus <i>B</i>	av. 0.000263		av. 0.000310	
av. of <i>A</i> plus <i>C</i>	0.000173	<i>AB</i>	0.000171	6
<i>AB</i>	0.000180	<i>BC</i>	0.000180	1
	0.000300†	<i>AB</i>	0.000418†	4

* Values adjusted for loss of hydrogen during cutting.

† Specimen not properly prepared before placing in tube.

wise the average of *B* and *C* would be comparable to *BC*.

This is shown in Table 13 to be the case.

13 where the average hydrogen value for the *B* specimens is 0.000047 pct higher than for the *A* specimens. This is a difference of about the same magnitude as that shown in Fig 8. It will be noted that the last item in Table 13 shows considerably poorer agreement because in this case the specimen was deliberately prepared improperly before placing it in the tube, in other words, the specimen was merely wiped dry after cutting. This points up the importance of great care in sample preparation.

EFFECT OF SIZE AND SHAPE ON THE LOSS OF HYDROGEN FROM A SOLID SAMPLE

Some means of predicting the influence of size and shape of the specimens on the rate of loss of hydrogen from steel would be of practical importance. Rigorous mathematical treatment to give a general solution of the problem of loss of hydrogen from finite solids of various sizes and shapes is extremely complex. Even if an exact mathematical treatment could be made, it would be less useful from a practical stand-

point than a simpler and readily applied though less rigorous method. Also, the results obtained by an exact treatment, except under exacting control, might be

and shape. The different shapes used were: $\frac{3}{8}$ -in. cubes, 1- and 2-in. rail slices and a $4 \times 4 \times 9$ -in. billet. The experimental diffusing times were taken from Fig 17 at

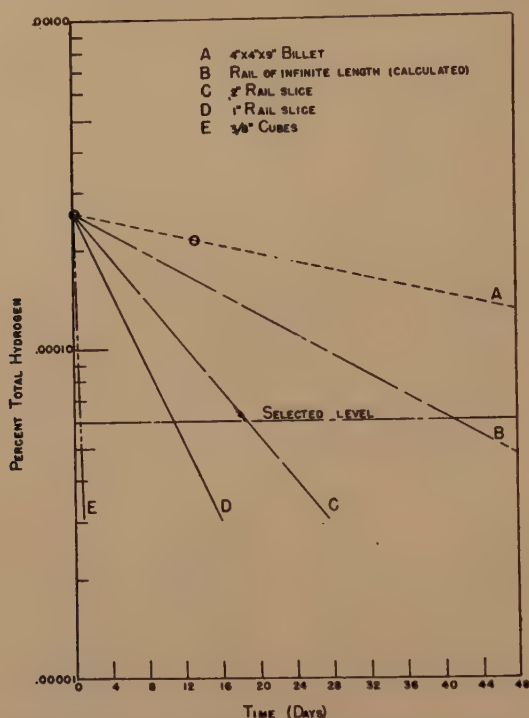


FIG 17—LOSS OF HYDROGEN FOR DIFFERENT SHAPES.

illusory because of the disturbing influence of various factors such as surface conditions, changes in atmospheric temperature and also the normal variation in composition of the diffusing medium which would affect the diffusion constant.

In this work the diffusing time for a given change in hydrogen content at the center of finite solids, is proportional to a shape factor (F_s); that is,

$$(\text{Diffusing time}) \propto F_s = \left(\frac{\text{Volume}}{\text{Surface area}} \right)^2$$

The usefulness of the relation was tested by plotting the shape factor against the experimentally determined diffusion times, in Fig 18, for four solids differing in size

the 0.00006 pct hydrogen level. The fact that the points plotted in Fig 18 fit a straight line indicates a linear relationship between diffusing time, for a given change in hydrogen content, and the shape factor. This relation was tested with the data given here and appears to be general. It was used, for example, in the present work on the diffusion of hydrogen from 2-in. rail slices which are of a size for convenient handling but too short to eliminate end effects. It was possible to reduce these data to equivalent data for a full length commercial rail, as shown in Fig 17. The shape factor was calculated for the head of a rail of infinite length by using the volume and surface area figures for a unit length without including the areas of the two ends in the

latter figure, on the principle that for a sufficiently long rail the volume to surface ratio is independent of the length. The diffusing time was then taken from Fig 18 and plotted in Fig 17. The curves for the rail of commercial length in Fig 7 and 12 were then taken from Fig 17.

SUMMARY

When a standard vacuum fusion equipment for the analysis of gases in steel is modified so samples can be analyzed immediately after introduction to the vacuum, so that hydrogen blank corrections are small, and so the gas reservoirs and pressure measurement are adjusted to the small amounts of hydrogen which are present, it is possible to analyze steel for hydrogen with a probable error of ± 0.00001 pct. If the results of such analyses are to carry significance, it is necessary to give careful attention to all details related to the preparation of the sample. The cutting of the sample must be rapid to avoid loss of hydrogen, and must be done with good tools to avoid heating. The time elapsed between cutting and analysis should be as short as possible but also a matter of record. The surface of the specimen must be free of oil or moisture. Samples can be stored in dry, closed containers so that the gas lost during storage can be collected and analyzed.

These procedures have been used to study the behavior of hydrogen in rail steel. It is observed that the initial hydrogen content of a rolled rail is about 0.0003 pct and that this decreases to a "residual" value of about 0.00003 pct in a period of about 60 days after which there are no further observable changes. If the gas which escapes during this 60 day period is considered separately as the "diffusible hydrogen" and treated in accordance with diffusion theory, it is possible to extend a limited number of analyses so as to describe the changes in hydrogen content of any size or shape of specimen at any tempera-

ture below the critical. Data from rail steels have been shown to conform to this interpretation.

In the group of heats studied, those heats

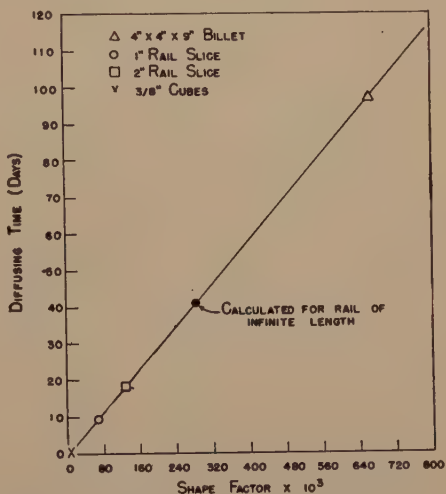


FIG 18—RELATION BETWEEN SHAPE FACTOR AND DIFFUSING TIME.

which flaked were also higher than average in hydrogen in the as rolled condition.

ACKNOWLEDGMENT

This paper presents research resulting from part of a project sponsored by the Carnegie-Illinois Steel Corporation, dealing with a study of certain aspects of steelmaking. The work involved a number of the personnel of the Operating and Research Department of that Corporation and of the Metals Research Laboratory of the Carnegie Institute of Technology. The authors appreciate the cooperation of this entire group and would like to acknowledge specifically the long range planning and interest of M. F. McConnell, M. W. Lightner and F. L. Toy; the arrangements for mill coordination by Shadburn Marshall, all of the Research and Development Division; the specific mill arrangements by H. B. Wishart at Gary Steel Works and Kenneth Vogel at Edgar Thompson Steel Works, all of the Carnegie-Illinois Steel

Corporation; the laboratory assistance of W. J. Best, D. Wineland, and E. Lloyd at Carnegie Institute of Technology; and the cooperation in exchange of samples by G. A. Moore, of Battelle Memorial Institute.

REFERENCES

1. Fourth Report of the Oxygen Subcommittee on the Heterogeneity of Steel Ingots: Iron and Steel Inst. (Brit.), July 1943.
2. G. Derge, W. Peifer and B. Alexander: Vacuum-fusion Analysis of Steel for Hydrogen, Symposium. *Trans. AIME* (1945) **162**, 361.
3. George A. Moore: Preliminary Experiments on the Total Combustion Method for the Analysis of Hydrogen in Steel, Symposium, *Ibid.*, 404.
4. C. Sims and G. A. Moore: Elec. Furn. Steel Conf., Pittsburgh Meeting, December 1947.
5. W. D. Brown: A Modified Vacuum Extraction Apparatus, Symposium, Ref. 2, 381.
6. G. Derge: Rapid Analysis of Oxygen in Molten Iron and Steel. *Trans. AIME*, (1943) **154**, 248.
7. W. Geller: Theory of Degassing of Metal Baths by Rinsing Gas, *Ztsch. für Metall.*, **35** (1943), 213.
8. R. E. Cramer: The Production of Flakes in Steel by Heating in Hydrogen, *Trans. A.S.M.*, **25** (1937), 927.
9. J. H. Andrew, H. Lee, A. K. Mallik, A. G. Quarrell: The Removal of Hydrogen from Steel; *Jnl. Iron and Steel Inst.*, (1946) **1**, 67.
10. C. Sykes, H. H. Burton, C. C. Gegg: Hydrogen in Steel Manufacture, *Jnl. Iron and Steel Inst.* (1947) **156**, Part 2, 155.
11. L. Reeve: Improvement in the Vacuum-fusion Method for Determination of Gases in Metals; *Trans. AIME* (1934) **113**, 99.
12. Symposium on Determination of Hydrogen in Steel, *Trans. AIME* (1945) **162**, 353-412.
13. J. H. Andrew, H. Lee, H. K. Lloyd, and N. Stephenson: Hydrogen and Transformation Characteristics in Steel, *Jnl. Iron and Steel Inst.*, **156** (1947) Part 2, 208.
14. L. Simon: Engineer's Manual of Statistical Methods, John Wiley & Son, Inc. (1941), 155.
15. L. Alexander, W. M. Murray, S. E. Q. Ashley: Determination of Oxygen in Steel by the Vacuum Fusion Method, *Ind. and Eng. Chem., Analytical Ed.*, **19** (1947) 417.

DISCUSSION

(J. G. Thompson and S. Marshall presiding)

L. S. DARKEN*—In general I was very favorably impressed by both the quality and

quantity of the work presented on the subject of hydrogen. There is a lot of information here that we have wanted for some time, and which will be very useful.

There is one point I would like to make. The authors belittle the extraction of hydrogen at lower temperatures and point out that at 900 to 1100°C very small amounts of hydrogen were extracted from the specimen. They say that the complete extraction of hydrogen from steel in 30 min. or less is not possible unless the steel is actually molten. In Table 5, they give data showing the very small amount of hydrogen they were able to extract at 900°C. Anybody looking at that table and reading that paragraph would be tempted to conclude that it would be foolish to attempt to extract hydrogen at lower temperatures. The authors even say that it is obvious that even less hydrogen may be extracted in a given time below 900 than at 900°C.

On the other hand, in a latter section of the paper, the authors emphasize the speed and care required to avoid loss of hydrogen from the specimen at room temperature. They give data at room temperature, and at 100 and 200°C, showing how very fast the hydrogen does escape. Their data for the rate of escape at 200°C shows about 90 pct evolved in a day. If this low temperature data were extrapolated a bit, we would conclude that at about 500 or 600°C, about 90 pct of the hydrogen would be evolved in a half hour or an hour. This is quite a contradiction to the authors' conclusion based on their data at 900°C and above.

I would like to suggest the possibility that this rapid evolution at low temperatures and the slow evolution they show at 900°C is related to the phase change of iron. The rapid evolution in the alpha iron range is in accord with my own experience and that of others, namely that in the alpha iron range the hydrogen can be extracted rather rapidly. The low rate found at 900°C may be much smaller than that at 600 or 700°C because the iron at 900°C is in the austenitic condition where the diffusivity is perhaps smaller.

G. A. MOORE*—Dr. Derge brought out the fact that time makes a lot of difference in the evolution rate and that the observed effects depend on whether you are looking at the be-

* U. S. Steel Research Laboratory.

* University of Pennsylvania.

ginning or the end of the process. No low temperature evolution which we have run has ever failed to leave some residual hydrogen in the sample; this is also true for aging experiments. However, no sample has failed to give off some hydrogen rapidly in the beginning of storage at room temperature.

I wish to show Dr. Darken some figures from the manuscript of a paper on comparative tests which Dr. Derge and I are hoping to finish in the very near future. In this test we measured the gas evolved at room temperature. We then followed the procedure recommended by the English, 2 hr extraction at 650°C, and completed the extraction at 1050°C. A slight residual correction was made for the final analysis.

METHOD	HYDROGEN (Wt. Pct)
Room Temp. (2 weeks).....	0.000463
650°C (2 hr).....	0.000651
1050°C (70 hr).....	0.00067
Calculated Residue.....	0.00007
Total analysis.....	0.000591

This result was checked by an independent run of the British method and by vacuum fusion tests. In the comparative tests we performed this particular procedure three times, always checking against the other methods, and got the same answer every time.

G. DERGE (authors' reply)—We wish to thank Dr. Darken for clarifying the influence of temperature on solid extraction. His observation of the importance of the critical temperature in this process is generally accepted as correct. However, there are some additional characteristics of the evolution process which

are important in analytical work. These features are demonstrated best in the work of Moore and Smith* which shows that in the alpha range there is an initial rapid evolution of hydrogen at any given temperature. This evolution appears to be complete, but, if the temperature is increased, another rapid evolution occurs. This behavior does not stop until the gamma range is reached. These observations do not encourage one to develop low temperature solid extraction methods.

Since preparing the original paper, we have had the additional experience of analyzing steel samples which had previously been analyzed by low temperature extraction. The vacuum fusion analysis of these samples showed more than 0.0001 pct additional hydrogen in many cases.

We also wish to thank Dr. Moore for the additional evidence he has provided in his discussion.

J. G. THOMPSON—The effects of hydrogen and methods of determination have been of extreme interest for a number of years, and have been highly controversial. It certainly seems from the papers presented this morning that we are making progress on the determination of hydrogen and on the understanding of how much hydrogen we have and, consequently, what its effects will be.

On the other hand, while we have made progress, we evidently have not reached the final and desirable state of knowing exactly where we stand.

* G. A. Moore and D. P. Smith: Occlusion and Evolution of Hydrogen by Pure Iron. *Trans. AIME* (1939) **135**, 225.

Apparatus for the Hot-extraction Analysis for Hydrogen in Steel

BY CLARENCE E. SIMS* AND GEORGE A. MOORE,† MEMBERS AIME

(New York Meeting, February 1948)

INTRODUCTION

IN previous publications of the writers⁴⁻⁷ it has been shown that vacuum extraction of steel can be carried as close to quantitative completion as desired provided the steel is in the austenitic state and sufficient time is allowed. For precise work, the method claims preference because the equipment for holding and heating the sample can be made simple, and because crucibles, boats, and other unnecessary materials can be eliminated and the blanks thus made very small.

It is well known that the evolution rate of hydrogen is smaller just above the transformation than immediately below, as would be expected from the increase in solubility when passing into the gamma state. Many attempts have been made to obtain analyses by extraction just below the transition, using times of approximately 2 hr. While it is true that the rate of evolution drops nearly to zero under these conditions, it has repeatedly been shown that the process is incomplete since on raising the temperature into the austenitic range, evolution will be resumed, usually after a considerable induction period.

The low-temperature evolution process appears to be useful in some cases for comparative tests where the residual error may be more or less constant between samples.

For general use, however, there is no guarantee that the error caused by incomplete extraction is constant; hence, the more laborious but more reliable high-temperature process must be used. At high temperature, an original flash evolution, similar to that at lower temperature, is first observed. After not more than an hour, the flash subsides and evolution settles down to a regular first-order reaction rate for which the half-life* is usually of the order of a few hours for the $\frac{5}{8}$ -in. diam cylinder at 1050°C. The regular evolution may be followed for whatever period appears justified, after which the residual gas may be estimated as equal to that which was evolved in the last observed half-life period. Tests have shown that the composition of the evolved gas does not vary greatly during the progress of evolution; therefore the residual gas may safely be taken to have the same composition as the portion col-

* A "first order" reaction is one in which the amount of reaction taking place at a given instant is directly proportional to the amount of a single reactant which still remains. This is the characteristic order of radioactive decomposition, photographic exposure, and many chemical decomposition processes. If the logarithms of the measured reaction rates are plotted against the times at which the rates are measured, a straight line results. This line slopes downward in such a way that the time necessary for the rate to fall from any value to a value just half as great is a constant, known as the "half-life of the reaction." While the reaction, therefore, never reaches a final termination, the amount of reaction yet to take place in all remaining infinite time is exactly the same as the amount which did take place in the last half-life period just prior to the final direct observation. The percentage of the process yet to be completed is thus 50, 25, 12.5, 6.3, 3.1, 1.6, 0.78, 0.39, 0.20, and 0.098 after 1 to 10 half-lives, respectively. A first-order process is technically complete after 5 half-lives, essentially complete after 7½, and scientifically finished after 10 periods.

Manuscript received at the office of the Institute December 26, 1947. Issued as TP 2369 in METALS TECHNOLOGY, June 1948.

* Assistant Director, Battelle Memorial Institute.

† Formerly Research Engineer, Battelle Memorial Institute; presently Assistant Professor of Metallurgy, University of Pennsylvania.

⁴⁻⁷ References are at the end of the paper.

lected. With the current practice of allowing 40 hr for evolution, about 5 half-lives are usually covered; hence, over 96 pct of the gas is collected and the residual correc-

equipment, one diffusion pump for preliminary exhaustion of the apparatus, and mechanical pumps to back this diffusion pump and to operate the Toepler pumps



FIG 1—HOT-EXTRACTION APPARATUS.

tion is usually within the limits of accuracy of the subsequent Orsat analysis.

The writers have made no attempt to justify this analytical method for routine commercial control or to adapt the method for such purposes, since they believe that some time must yet be spent on research analyses before sufficient quantitative information will be available to justify an attempt to apply routine controls to hydrogen in steel.

APPARATUS

The apparatus to be described was designed in June of 1944 and first operated in November of the same year.

A general view of the apparatus is shown in the photograph (Fig 1). The frame holds six evolution units which operate independently, together with one diffusion pump backed by a double-stage Toepler pump to collect the gas for transfer to the Orsat

and mercury seals. All operations are controlled by small solenoid needle valves mounted on the low vacuum and air manifolds in the lower part of the frame. The equipment is demountable in sections as: furnace units, pumping and measuring units, and connecting manifolds. All connections in the parts of the system carrying analytical gas are by welded glass seals which are placed in such a way that they can be easily cut open to remove units for repair if necessary. All closures in the analytical system are by means of mercury Y-seals, thus preventing all possibility of the stopcock leakage which so commonly acts as one source of large blanks.

All operations are controlled by switches and relays located on the larger of the two control panels. This equipment is also assembled in units on removable panels to allow removal for repairs when necessary. In general, the switches allow for manual

operation of the pumps and seals, while the automatic operation of the pumps is handled by relays; which are, in turn, locked to the 12-pt Micromax controller-recorder by

EVOLUTION UNIT

The evolution unit consists of a distorted T-shaped assembly of tubing between 25 and 32 mm in diam. The furnace

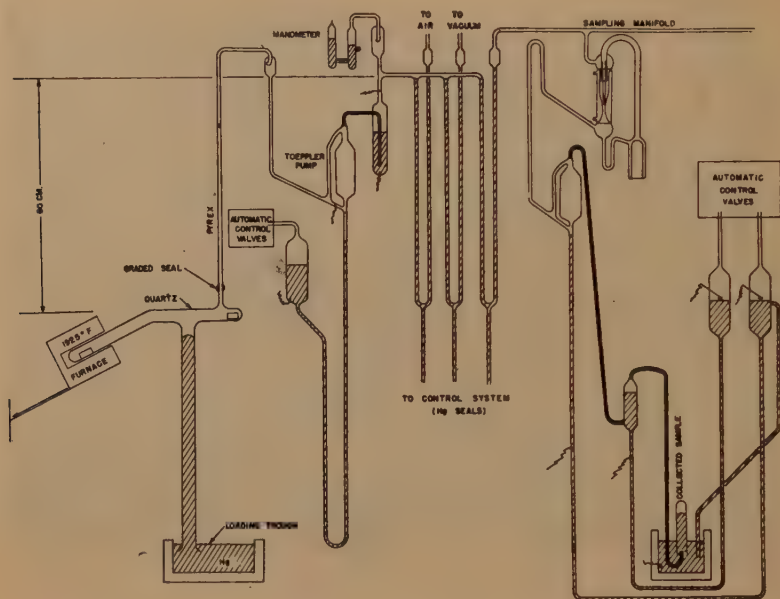


FIG 2—B.M.I. HOT-EXTRACTION GAS ANALYSIS APPARATUS.

a bank of synchronizing relays. The various switches and relays are interwired in such a way as to lock the operations and prevent almost all types of incorrect operation. The temperature control apparatus is located on the panel below the Micromax, and is of the type where variacs are switched between the high and low scales to allow for the time lapse between corrections on the multiple-station controller. The wiring system will not be described in detail in this report* since it should be modified to fit particular components available, but sufficient details of an evolution unit will be given to show the operation and permit duplication of the method. A simplified diagram is shown in Fig 2.

section and cold head are made from clear fused quartz which is sealed directly to the loading tube, or riser, made from an 82-cm length of Vycor glass. A short length of 10-mm quartz tubing is connected into the cold arm of the T, and terminates in a graded quartz-to-pyrex seal for connection to the pumping unit.

The evolution unit is mounted with the head in the vertical center of the apparatus and the loading tube projecting downward into a glass-lined mercury trough which rests on the bottom frame of the apparatus. The furnace arm of the T then slopes down at an angle (29°) which is just sufficient to allow a steel sample to slide down into the furnace without cracking the closed lower end of the tube. The furnace slides on a track inclined at the same angle which permits the furnace to be lowered at the end of

* Wiring diagrams are available at Battelle Memorial Institute to anyone wishing to duplicate the equipment.

a run and the sample to be retrieved with a magnet. The furnace itself is a simple wire-wound unit consisting of a single layer of Kanthal wire on an alumdum core, mounted between Transite end plates in a metal cylinder. Insulation is obtained by packing the space between core and shell with diatomaceous earth. Chromel windings may be used if the maximum temperature is restricted to about 1000°C instead of 1050°C.

Pumping and Measuring Unit

The gases evolved in the furnace are collected by an automatic Toepler pump and transferred to a bulb and attached manometer having a total volume of about 76 cc. The pump is of the Tamman style, with a by-pass inlet tube which restricts splashing under high inlet pressure to the few cubic centimeters of mercury in the by-pass. This type of pump does not require mounting on an angle and is, therefore, more easily supported than the sloping bulb type. The mercury for the stroke is supplied from a second bulb to which connection is made by a small-diameter U-tube running down to the base of the apparatus. This U-tube prevents blowing back into the supply bulb when air is admitted to the apparatus. The same provision is used on all pumps and on the mercury Y-seals between units and manifolds. The supply bulb is heated by a 100-w chromel and asbestos blanket which maintains the mercury at about 50 to 60°C and prevents condensation of traces of water vapor on the walls of the pump. It is found that heating the Toepler pumps is a considerable aid to smooth operation, even when the system may be presumed to be completely dry.

The Toepler pump discharges through a capillary outlet which is submerged about 18 cm in mercury in an outer tube about 14 mm in diam. On the up stroke, the mercury rises to fill this tube and to complete an electrical connection at the point where a wire lead is indicated in the diagram. This

connection trips the relay which operates a solenoid valve to connect the supply bulb to the operating vacuum line, thus returning the mercury in the pump to the supply bulb for the next stroke. At the same time, the mercury in the outlet seal drains back to a point level with the top of the pump, less whatever pressure has been accumulated in the measuring section. Thus no mercury is lost in the stroke and the pump never needs to be stopped to return mercury to the supply bulb.

In the measuring section, the collected gas is confined by five mercury surfaces, first in the outlet seal just described, secondly by the mercury in the manometer, and finally by the three columns of mercury in the three Y-seals. The volume on which the pressure is observed thus varies with the pressure. Calibration is therefore made by admitting successive known volumes of gas and observing the pressure after each addition and from these observations constructing a true pressure-volume curve which is appreciably nonlinear.

The measuring system is closed from the air, vacuum, and sampling manifolds by the three mercury Y-seals, each a little more than 76 cm in length. Details of the supply bulbs to these seals are not shown in the diagram. The tail of each seal goes down to the base of the apparatus and then returns to a mercury supply connected to a valve on the working vacuum line, for opening, and to a slow leak to the atmosphere, for closing. Since the mercury in the seals must move more than 76 cm and it is not safe to use a pressure of air above 1 atm to keep the seals closed, the supply bulbs are in the form of pressure amplifiers in which a sudden change of pressure first moves a portion of the mercury from one bulb to another and subsequently reacts directly on the remaining mercury to move the seal. A total motion of 92 cm is thus obtained from a 74-cm differential in the operating manifolds.

It may be obvious that the repeated

operation of the mercury seals, together with some splashing which occurs when the seals are opened with more than a few centimeters pressure differential, results in varying the quantity of mercury in the sealing system. Therefore it is arranged that there is a splash bulb between each seal and the manifold so that mercury splashed outward will return to the seal. On the inward side, the splashed mercury drains into the Toeppler pump. By placing the inner connection at a level of about 78 cm above the center line, the Toeppler, on manual operation, rises almost to the point where the mercury in the seals and pump will flow together. An aspirator bulb on the inlet to the air manifold gives a convenient means of momentarily increasing the apparent atmospheric pressure, which causes the Toeppler pump to overflow and refill the Y-seals to the original level at which the volume calibration was made. This operation is regularly performed at the start of every run.

Collecting System

One of the mercury Y-seals of each evolution unit connects to a sampling manifold which leads to a collecting pump. Since it is not desirable to use pressures above 1 atm for operation, this pump takes the form of a double-stage Toeppler. Two pumping bulbs are used of which the first is considerably larger than the second to allow for the different operating pressure. The pumping bulbs are supplied from two similar supply bulbs which are filled to the center line of the apparatus. The first-stage pumping bulb is, therefore, above its supply bulb and will collect from a manifold which goes down to infinitesimal pressure, while the second-stage pump bulb is below its supply and will deliver at more than 1 atm. A test tube originally filled with mercury is placed over the outlet of the second stage in the collecting trough at the bottom level and receives the gas for transfer to the Orsat equipment.

Since the sampling manifold has a considerable volume and is, in addition, directly connected to six splash bulbs of comparatively large volume, it has been found advisable to increase the pumping speed by the insertion of a two-stage diffusion pump between the sampling manifold and the Toeppler pump. This would not be essential with a smaller number of units.

In operation of the two-stage Toeppler pump, starting with both supply bulbs full, the first-stage pump chamber empty, and the second-stage chamber full, gas flows from the manifold to fill the first chamber. Air is admitted to the first supply bulb, allowing mercury to rise in the first pump bulb and push its contents through the capillary connection into the second-stage chamber, which is at about $\frac{1}{2}$ atm. Air is then admitted to the second supply bulb, increasing the pressure in the second pump bulb to $1\frac{1}{2}$ atm and forcing the gas out the discharge capillary to the test tube. The second supply bulb is then evacuated and the lost mercury is replaced by draining from the first stage. When the second supply bulb is refilled, the first supply bulb is evacuated, opening the first-stage pump bulb for the next cycle. The lost mercury is replaced from the discharge trough by way of the return tube which enters the first supply bulb at the level to which it is to be filled.

Orsat Analysis

The tube of collected gas is transferred to the inlet trough of the Orsat apparatus by means of a dipper. All gas samples are analyzed as the proportion of hydrogen in the collected gas cannot be predicted. At present standard Burrell equipment is in use and is sufficiently precise for ordinary problems. However, this equipment is the most important limitation in final accuracy; hence, a more precise version of the Orsat apparatus is being developed. The principal modifications found necessary in the more precise Orsat are substitution of a

25-cc and a 5-cc burette for the standard 100-cc unit and extension of the Petersen compensator to allow for changes in manifold temperature. The burettes are connected to a two-way stopcock so that either may be used at will. The compensator has a capillary extension to form a dummy manifold and small bulbs extending into the combustion furnaces and water absorption unit. An oil manometer has been substituted for the usual mercury manometer. Manifold tubing was reduced to 1 mm id and connected entirely by ground glass ball joints. The unit is operated dry and water determined by freezing in a U-tube immersed in dry ice mush. Motorized operation of the mercury leveling bulbs has been provided in order that a few cubic centimeters of gas may be passed through the reagents at a slow and uniform rate.

METHOD OF OPERATION

Samples

The preferred sample is approximately 50 g of steel in a single piece, with the preferred form being a cylinder $\frac{5}{8}$ in. in diam and $1\frac{1}{4}$ in. long. Most samples run have been of two origins. For sampling liquid steel from the furnace or ladle, a split copper mold is used which forms the sample cylinder below a conical head which weighs about 1 lb. A diagram of this mold is shown in Fig 3. The sample is separated from the head by a ceramic disk, or "Washburn Core" having a central hole about $\frac{3}{16}$ in. in diam. When removed from the mold, the sample is easily broken or cut from the head so that it can be placed in a storage tube. The liquid steel is normally transferred to the mold with a thoroughly heated and slagged spoon. Aluminum is added to the sample as quickly as possible after drawing from the furnace to prevent the sweeping action of CO evolution from carrying out the hydrogen. The time the sample cools in the chill mold is held as close as possible to 3 min. The apparent

loss of hydrogen in the sampling process is not over 0.01 relative volume or 0.00001 wt pct when the operation is correctly performed.

Other samples are taken by rough machining out of various solid bars or other specimens. It is preferred that the original piece be not held for any appreciable period in sections of less than 1-in. diam and that the machining be finished as quickly as possible once it has been started. If samples are stored over mercury within 1 hr of the start of machining, the loss of hydrogen does not appear to be a controlling error. Machined samples are washed with *carbon tetrachloride* before storing to remove hydrogen-bearing oils and dirt.

All samples are stored in glass tubes originally filled with mercury and inverted in troughs. This type of storage is essential, since in many cases it is observed that up to 50 pct of the hydrogen is evolved at room temperature in the few days which may elapse before analysis can be made. No ferritic sample has ever failed to evolve a measurable portion of hydrogen at room temperature.

While machined samples can be transferred directly from the storage tubes to the apparatus, cast samples require cleaning to remove surface oxide unless one is willing to allow a very large proportion of CO in the evolved gas and to allow for the conversion of a significant portion of the hydrogen content into water vapor. Cast samples are therefore stored for at least a week to allow room-temperature evolution to drop to a slow rate. The steel is then separated from the evolved gas in a mercury trough by pouring the gas upward into an Orsat tube through a funnel too small in diameter to pass the steel sample. The gas may be poured directly into the extraction apparatus if desired but is usually analyzed separately unless quite small in volume. The steel piece is then sandblasted and the dust removed with an air jet before the steel is introduced into the evolution appa-

ratus. A wash in carbon tetrachloride is used if any oil or grease is suspected on the sample.

Extraction

The extraction unit will have been blanked out previously overnight with the

pumped off with the unit Toeppler and its volume read on the manometer.

While the free gas is being pumped off, the steel sample is raised with a small electromagnet and balanced on the short horizontal section of the T-head between the loading tube and the sloping furnace

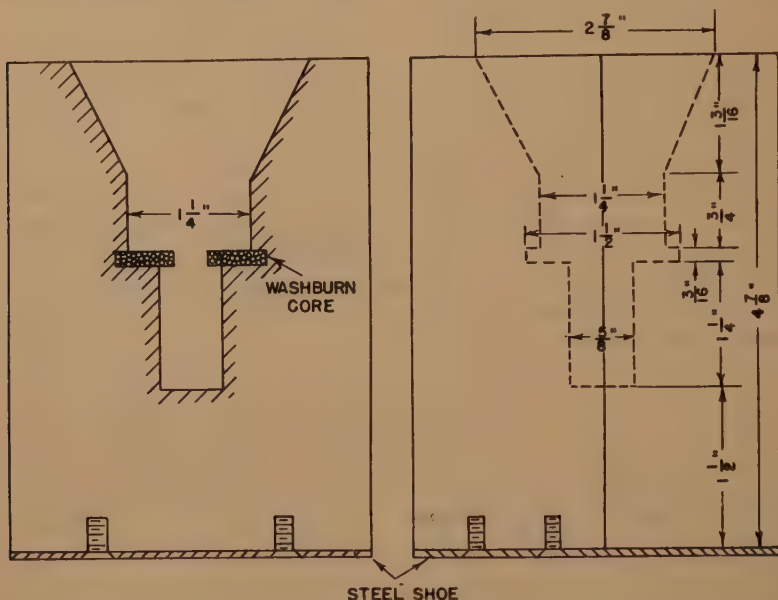


FIG 3—SPLIT COPPER MOLD FOR MAKING CAST STEEL SAMPLES FOR GAS ANALYSIS. Steel Guide on Back and Handles Not Illustrated.

furnace in place and at the temperature of the run, or will have been used for a previous analysis. Gas pressure in the extraction unit will be of the order of 10^{-5} mm, or low enough that it will not support a slow discharge from a 20,000-volt leak-testing coil. The Y-seals will be closed and filled to the proper level. The storage tube containing the sample, sometimes with gas evolved at room temperature, is transferred to the loading trough in a small dipper filled with mercury. The storage tube is then inverted under the funnel at the bottom of the mercury-filled riser, or loading tube. The sample and bubble of evolved gas rise to the top of the mercury column at the head of the T. The free gas is then

portion. At the time desired for the start of the run, the sample is easily shoved off with a small magnet and slides down the inclined tube into the hot zone of the furnace. Nonmagnetic samples are handled in the same manner by the expedient of first crimping them into a thin tube of ordinary steel which has previously been degassed in the same apparatus.

Extraction may be conducted at any temperature and for any time desired but has been mainly standardized at approximately 40 hr at 1050°C or 1925°F . This is the highest temperature at which good life can be obtained from the furnaces and quartz tubes.

During the extraction the manometer is

read from time to time and the results recorded to permit construction of an evolution curve. If the curve itself is a desired result, readings may be as frequent as desired. For checking the analytical evolution, about 10 to 12 readings, more or less logarithmically spaced, over the 40-hr period will be found sufficient since a high degree of accuracy is not necessary for a small correction.

At the end of the extraction run the furnace is turned down and slid to the lower end of its track. The gas sample is pumped out to the Orsat tube with the collecting pumps, which requires only 15 min. with the aid of the diffusion pump booster. The steel has meanwhile cooled and its magnetic properties have returned; hence the sample can be picked up with the electromagnet and worked up the sloping furnace tube to the T-head. The exhausted sample is stored in the cold portion of the head on the opposite side of the loading tube from the furnace section. The head on the present apparatus holds three exhausted samples. This is sufficient for one week of operation but can easily be enlarged if desired. The apparatus is ready for a new run after the furnace has been returned to working position and reheated to the correct temperature.

Samples are eventually removed by floating on the mercury in the loading tube and then admitting air to the unit, allowing the mercury to drop back to the trough level. The samples are retrieved from the lower end of the loading tube with a permanent magnet or with an iron wire hook. Since samples are not weighed until after removal from the apparatus, it is not desirable to accumulate them over too long a period before airing up the apparatus for their removal. It is important that the furnaces always be down and the evolution tubes cold before admitting air, since the films of evaporated metal which deposit on the quartz are damaging to the glass and may cause loss of analytical hydrogen by

conversion to water if they are allowed to become oxidized. In case of accidental oxidation of the film, the unit must be removed and cleaned with acid before the metal oxides have an opportunity to diffuse into the quartz glass.

Recording

Two types of recording manometers have been used. The first consisted of two fine chromel wires stretched in the arms of the manometers and wired as two arms of a Wheatstone bridge whose outbalance voltage was recorded by the Micromax. This manometer was quite accurate when new but within about 60 days serious contamination of the chromel surface appeared and the readings became erratic because of incomplete contact of the mercury with the wire.

A newer manometer is of the capacitive type in which the outside of the vacuum leg is plated with metal which acts as one plate of a condenser whose other plate is the mercury within the manometer tube.⁸ This condenser controls a radio frequency oscillator whose pitch thus varies directly with the pressure. As a transmitter to be read with a receiver or frequency meter, this system is highly stable and reliable. For automatic recording on the Micromax, the frequency is interpreted by a frequency-modulation receiver to give a millivolt output. This equipment is reliable for reasonably large pressure differences but is still undergoing development and therefore will not be further described at this time.

Direct checks of recorded pressures are made with millimeter scales mounted beside the manometers.

INTERPRETATION OF RESULTS

Pressure and volume readings from the evolution apparatus are used primarily in checking the completion of evolution and in measuring blanks which are too small to be read on the Orsat. Orsat readings are used for final analytical results. The ana-

lyzed volumes for gas removed at room temperature and for gas extracted at high temperature are added. A blank value may be subtracted when necessary but will normally be of the order of 10^{-4} cc or less and, hence, insignificant. If the hydrogen amounts to 0.10 relative volume or more (0.0001 wt pct), or the time has been short, or the rate of evolution unusually slow, an allowance for gas not extracted should be made equal to the amount extracted in the last observed half-life. This allowance is usually insignificant relative to Orsat errors when the hydrogen is low and the time of extraction long.

The weight of the sample of steel will have been determined after extraction and the theoretical volume calculated. The measured volumes of the collected gases are reduced to relative volumes and weight pct by the usual processes of arithmetic.

The evolved gases are principally CO, N₂, and hydrogen. The CO value does not represent the total oxygen in the steel as that portion killed with aluminum is not evolved. Iron oxide apparently is completely decomposed but the exact behavior of intermediate oxides has not been determined. The evolved nitrogen is a portion of the total, dependent on the amount of nitride-forming elements present and apparently also on the amount of oxygen. Iron nitride, if present, appears to be decomposed while aluminum nitride is stable at the temperature used except, possibly, in the presence of excess oxygen.

The evolved hydrogen appears to represent a total analysis except in cases where a large excess of oxygen is present and some hydrogen is lost by conversion to water. In these cases CO₂ also appears in the evolved gases and the water fraction can be roughly estimated from known equilibrium data. Checks have been made by use of a cold trap between the furnace and unit Toeppler pump and have shown that the water error, while detectable, is not significant in most cases. Water cannot be handled on the

standard Orsat but is being included on the special Orsat now being developed.

ACCURACY AND PRECISION

While the accuracy and precision of this method is being considered in a separate publication,¹ it may be said at this point that when good duplicate samples have been obtained, the tests run have given satisfactory evidence that the Orsat apparatus is, at present, the primary controlling factor. The standard Orsat apparatus allows a precision, probable error of ± 0.004 relative volume or ± 0.000044 wt pct on a 50-g steel sample.

Considerable difficulty is experienced in duplicating samples but in a large proportion of such cases it has been possible to establish that the samples were not entirely identical. The error in taking samples from liquid baths is larger than the precision of analysis under controlled conditions (about ± 0.01 relative volume) and may become very large with careless sampling. Within massive steel pieces, the distribution of hydrogen is highly nonuniform and samples separated by no more than their own dimensions will often show real differences several times the probable analytical error. The probable error in absolute accuracy, as judged by comparison with modified vacuum fusion, is not greater than the normal precision limit in duplication.

Several hundred samples have been run in the apparatus on various research programs and good correlation has been found between hydrogen content and history and various physical properties. While these correlations are far from perfect, it is believed that they are as good as can reasonably be expected in the light of the numerous other incompletely controlled variables which are unavoidably present in any work on commercial steel.

SUMMARY AND CONCLUSION

This paper is presented to show the general construction and operation of appa-

ratus developed at Battelle Memorial Institute for the quantitative hot extraction of hydrogen from steel for analytical purposes. Tests of the accuracy and precision of the method and descriptions of useful results obtained are to be found in other places.¹⁻³

Apparatus is described for conducting hot extraction of steel in a high vacuum up to 1050°C (1925°F) for periods of 40 hr or more. The system used is completely sealed in glass, has no stopcocks, and permits introduction of the sample after blanking out the apparatus. This method gives working blanks sufficiently small to be ignored. Except for loading samples, operation is entirely automatic. Periodic readings of the evolved gas are made, but equipment is under development for the automatic recording of such readings.

The accuracy of the results obtained is entirely controlled by errors in sampling methods and in analysis of the evolved gas, since the evolution apparatus is currently more precise than available associated equipment.

Evidence has been found that the method is essentially reliable in estimating the total hydrogen content of steel and that it can be operated regularly with sufficient precision for practical research problems. Several common sources of error have been evaluated and methods found either for their elimination or for calculation of their effect.

REFERENCES

1. Peifer, W., and G. A. Moore: Comparative Results of the Hot Extraction and Modified Vacuum Fusion Methods for Analysis of Hydrogen in Steel. (Not yet published.)
2. Sims, C. E., G. A. Moore, and D. W. Williams: The Effect of Hydrogen on the Ductility of Cast Steels. This volume, p. 283.
3. Sims, C. E., G. A. Moore, and D. W. Williams: A Quantitative Experimental Investigation of the Hydrogen and Nitrogen Contents of Steel during Commercial Melting. This volume, p. 260.
4. Moore, G. A., and D. P. Smith: Occlusion

and Evolution of Hydrogen by Pure Iron. *Trans. AIME* **135** (1939) 255-292.

5. Zapffe, C. A., and C. E. Sims: Hydrogen Embrittlement, Internal Stress, and Defects in Steel. *Trans. AIME* **145** (1941) 225-261.
6. Zapffe, C. A., and G. A. Moore: A Micrographic Study of the Cleavage of Hydrogenized Ferrite. *Trans. AIME* **154** (1943) 335-352.
7. Moore, G. A.: Preliminary Experiments on the Total Combustion Method for the Analysis of Hydrogen in Steel. *Trans. AIME* **162** (1945) 404-411.
8. Dayton, R. W. and Foley, G. M.: Capacitive Micrometer. *Electronics*, Sept. 1946.

DISCUSSION

(J. G. Thompson and S. Marshall presiding)

P. P. KING*—What precautions are taken after the sample is cast up until the time it arrives in the testing apparatus. How is the sample protected so that it does not lose gas?

G. A. MOORE (authors' reply)—The protection of the sample between casting and analysis has proven to be very critical. We have never encountered a sample which failed to show evolution of gas at room temperature between the time of preparation and the time of analysis. We collect this gas by using a carrier which consists of a trough and frame holding 12 short test tubes full of mercury, inverted so their ends are under mercury surface. All samples are put into individual test tubes as soon as they are prepared. They are held there until they are almost ready for analysis. Machined samples can go into the apparatus directly, together with the bubble of gas. Cast samples are separated from the bubble by pouring the gas through a funnel into another test tube, and then taking the sample out and cleaning it by sand blasting. We blow off the dust, but we do not ordinarily wash the sample. The gas which is evolved at room temperature will vary from perhaps 10 pct of the total to 50 pct—sometimes more.

J. C. LEWIS†—I would like to ask if there is any loss of hydrogen from the time when the sample is put in the apparatus until it is run. Obviously, from what you have said about evolution of gas at room temperature, such would occur, and I wonder if there is any blank

* Bethlehem Steel Co.

† Driver-Harris Company.

correction or any correction necessary if running of the sample is delayed for, say, 12 hr or so.

G. A. MOORE—If the sample sits under vacuum there is a very decided evolution in almost all cases. No correction is necessary, however, as the apparatus has already been blanked and exhausted and that gas which evolves into the apparatus is included in the analysis.

J. B. AUSTIN*—Were these determinations made by the warm extraction method, or by the combustion method?

G. A. MOORE—We have abandoned the combustion method because no one could supply us with refractories to hold the burning iron.

We usually make the distinction of calling our method a hot extraction. "Warm extraction" is used to apply to 6 hr at 650°C so we like a different word.

J. B. AUSTIN—The object of my question was to find out the status of the combustion method you described in 1945. Do you believe you are getting enough of the gas out to make your measurements reliable? Also, what is your time of extraction?

G. A. MOORE—The normal time of extraction is 40 hr. The normal elimination of hydrogen is 96 pct and up. We have applied a few tests to residual samples to see if we could find hydrogen that was not accounted for by the evolution law, and so far nothing has been found.

P. P. KING—Is there any possibility that the deoxidation of the sample, with aluminum causes any evolution of gas which might lend inaccuracies to the determination?

G. A. MOORE—We use considerably more aluminum than would be applied to the deoxidation of the ladle steel, and it is dead-killed immediately. If you allow the sample to cool without the aluminum it will boil and gas will be lost. We have found that by differences between samples.

In cases of direct pouring, we have never found that the aluminum had any effect on the

analysis. We have poured some steels which were high in silicon which could be cast without the aluminum, and poured others into molds containing aluminum and found the same analysis.

R. W. GURRY*—In work at our laboratory, we found that there is always a certain amount of adsorbed moisture carried into the apparatus with the sample. I would like to know what happens to that moisture. We have found that at elevated temperature the moisture is likely to show up as hydrogen.

Would you care to comment on this, Dr. Moore?

G. A. MOORE—When surface oxide which may be formed on the cast sample is eliminated, we have negligible moisture in the evolved gas. It is, of course, impossible to take a cast sample, clean it, and transfer it to the apparatus without exposing it to air. All I can say is, with careless handling and damp hands the error can be very large, but we have transferred very thoroughly aged samples and obtained nil hydrogen in the analysis. So, the error due to absorption of air on the surface is very small when the sample is handled with care.

R. W. GURRY—I would say further that in our laboratory we have found that if we expose an extracted sample to air even momentarily, the adsorption of moisture upon the steel is sufficient to again show up upon analysis to a considerable degree, and I think perhaps some such tests should be made.

G. A. MOORE—What is the surface to volume ratio or the general size of your sample?

R. W. GURRY—We have used cylinders of about $\frac{1}{2}$ -in. diam.

G. A. MOORE—We have not re-run exhausted samples in the same apparatus. Exhausted samples have been taken out and put in containers and re-run by combustion and have shown hydrogen out in decimal places beyond those of current interest. The specific test of taking the sample out for a specific time and putting it back has not been done for this apparatus. We have shown the effect for other methods.

* U. S. Steel Research Laboratory.

* U. S. Steel Corporation.

P. H. BRACE*—In the course of vacuum melting work with several different metals I have had the experience of melting under high-purity hydrogen at a pressure of a few centimeters of mercury and obtaining clean, clear fusions that would lie quietly in the furnace under a good vacuum, and, upon freezing, observing violent evolutions of gas, presumably hydrogen. In some cases it was necessary to follow the hydrogen-melt by two or three cycles of vacuum melting and freezing in order to obtain metal that would freeze in the furnace without some evidence of "blow."

Now, if there is so much difficulty in removing hydrogen from the molten metal is it certain that it can be reduced to a negligible amount by vacuum treatment in the solid state?

* Westinghouse Electric Corporation.

G. A. MOORE—The problem of evolution from a liquid state has worried everyone who has worked with hydrogen analysis. That is one of the reasons that we adopted this method. I believe that Dr. Derge will agree with me when I say that the evolution in the vacuum fusion method is complete only provided the sample is boiled in the apparatus. Apparently, if you boil under a high vacuum you overcome the surface tension or other factors which otherwise are holding the gas in the liquid.

In our case, the existence of the first order reaction is strong evidence that if you wait long enough you will get all the hydrogen out. We are, of course, dependent for proof on the fact that once the sample has been thoroughly exhausted by hot extraction it has been impossible to find any more hydrogen by other methods.

A Quantitative Experimental Investigation of the Hydrogen and Nitrogen Contents of Steel during Commercial Melting

By CLARENCE E. SIMS,* GEORGE A. MOORE,† MEMBERS AIME, AND DONALD W. WILLIAMS,*

(New York Meeting, February 1948)

INTRODUCTION

DURING the past several years the steel casting industry has made studies of heavy castings in which the test bar has been taken from heavy sections rather than from attached or separately cast coupons. It has been noted that the ductility properties of these heavy sections are often lower than those normally expected. Such lowered ductility is usually accompanied by a spotty test bar fracture and the ductility values often can be greatly improved if a low-temperature aging treatment is given to the casting. A loss of ductility of this type is considered "abnormal," since it is not accompanied by an increase of tensile strength or hardness, and "temporary" when the ductility can be restored by aging. The cure of such an abnormal condition represents a real improvement in the quality of the steel.

Some hundreds of previous investigations, largely qualitative in nature, have established beyond reasonable doubt that hydrogen is normally present in newly manufactured steel and that this gas, in small amounts, can cause a temporary ab-

normal loss of ductility. The commonly observed association of high gas content and low ductility has given strong evidence for the presumption that hydrogen, possibly assisted by other gases, is the primary cause of the low ductility observed. Accordingly, the Steel Founders' Society of America has, since Nov. 1, 1944, sponsored investigations at Battelle Memorial Institute whose primary objective is to obtain quantitative information on the relation of the amount of hydrogen and nitrogen in steel, together with associated methods of steelmaking and treatment, to low-ductility effects and porosity.

In order that these investigations might proceed on a quantitative basis, hydrogen analyses of a precision considerably higher than any previously reported in the literature were necessary. The method chosen was selected entirely on the basis that it had the highest probability of freedom from uncontrollable errors and will be described in detail in another publication.¹ Briefly, the method used consisted of the hot extraction of solid pieces of steel weighing from 45 to 50 g in a highly evacuated quartz tube maintained at 1050°C (1925°F) for a period of approximately 40 hr. The greatest precautions were taken to eliminate blanks and insure a sound gas-collection system. Vacuum and temperature conditions were maintained automatically. Mercury-filled risers were used for the introduction of samples in order that the system could be degassed thoroughly in

This article sets forth the results of research conducted by Battelle Memorial Institute and supported by the Steel Founders' Society of America. Copyright, 1947, by the Steel Founders' Society of America. Manuscript received at the office of the Institute Dec. 22, 1947. Issued as TP 2347 in METALS TECHNOLOGY, Feb. 1948 and in *Proc. Elec. Furn. Steel Conf.*, 1947.

* Assistant Director and Research Engineer, respectively, Battelle Memorial Institute, Columbus, Ohio.

† Formerly Research Engineer, Battelle Memorial Institute; presently Assistant Professor of Metallurgy, University of Pennsylvania.

¹ References are at the end of the paper.

advance and samples introduced without contamination of the system with air. From periodic records of the amount of gas evolved, an allowance, about 3 pct, was normally made for the residual hydrogen at the end of the extraction process. For the determination of the gas content of liquid steel, chill-cast cylinders of $\frac{5}{8}$ -in. diam and 1.25-in. length were made in copper molds. The mold provides a feeder head of about 1-lb capacity, separated from the sample by a pierced ceramic disk or "Washburn Core" in order that a rapidly cooled sound sample be obtained under all normal conditions. Samples were removed from the mold and broken or cut from the head and stored in closed tubes over mercury, pending analysis. The time before storage was generally approximately 3 min. and the time until the first appearance of a gas bubble usually about 10 min. The precaution of storing over mercury proved essential in all cases, not only of cast samples but of similar pieces turned or sawed from castings after additional treatment. Reported analyses include the hydrogen evolved both at room and elevated temperature, together with the small residual allowance previously mentioned.

In all discussions and plots in this work, hydrogen analyses are given in "relative volumes" (RV) in which one RV represents an amount of hydrogen which, when measured at 0°C (32°F) and standard atmospheric pressure, would occupy the same space as the amount of steel analyzed when in a form free of porosity. This unit is most convenient since it is the one most easily visualized, is independent of the system of measurement, and resulting figures are of convenient magnitude. Conversion factors for considering other reports are:

$$0.001 \text{ wt pct} = 0.874 \text{ RV}$$

$$1 \text{ RV} = 0.00114 \text{ wt pct}$$

$$1.0 \text{ cc per } 100 \text{ g} = 0.0786 \text{ RV}$$

$$1 \text{ RV} = 12.72 \text{ cc per } 100 \text{ g}$$

The precision of the analytical method used, when starting with actually identical solid samples, has been established to be the precision of the analysis of the evolved gas, which is ± 0.004 RV. The precision for liquid samples apparently is nearly as good under ideal sampling conditions, but for furnace samples taken with a slagged spoon and killed with aluminum and poured as rapidly as possible, an average error of ± 0.01 RV must be allowed. Checks of accuracy by comparison with other methods, which will be published elsewhere, indicate that the analyses obtained are probably within 0.01 RV of the truth.

The work to be presented here is in two sections. Section 1 will give a brief resume of some of the more impressive publications on the same subject which have come to the writers' attention during the period of the work. Section 2 will describe the behavior of twenty commercial heats of the four usual methods of making casting steels together with an analysis of the factors which affect the hydrogen content. Inasmuch as the complete details of these experiments can not be encompassed within the limits of a single paper, only the most instructive will be given in the paper proper while the more extensive details will be listed in an appendix which will be made available from Battelle Memorial Institute in the form of Recordak film.

Additional portions of the work, to be published at a later date, will show that the main adverse effects of hydrogen on ductility occur with amounts of hydrogen varying from 0.05 to 0.40 RV, with the effect varying with the structure and history of the steel. It will also be shown that a considerable portion of the hydrogen present in the ladle may be evolved during the casting process, and that the adverse effect of the remaining hydrogen apparently can be eliminated completely by aging for a sufficient time at a moderate temperature. The amounts of hydrogen found to be present in commercial steel melting are thus

coincident with the amounts of most interest with respect to ductility.

ACKNOWLEDGMENT

The writers wish to express their most sincere appreciation to the Technical Research Committee of the Steel Founders' Society of America, Charles W. Briggs, Technical Director, for the financial support of this work and for continuing advice and assistance in correlating the work with experience within the steel castings industry. Thanks are extended to The American Steel Foundries, The Bonny-Floyd Co., Buckeye Steel Castings Co., General Steel Castings Corp., National Malleable and Steel Castings Co., and The Ohio Steel Foundry Co. for their cooperation in collecting specimens for hydrogen analysis and for providing other essential data on the commercial heats. The writers wish to acknowledge the capable assistance of M. W. Mallett, C. L. Tyo, and Mrs. Martha E. Murphy of the Battelle Staff in connection with the analytical work on hydrogen.

SECTION I—ADDITIONS TO THE LITERATURE

Since the manifestations of hydrogen in steel have attracted very wide interest and led to a vast number of discussions in all quarters, the writers make no pretense of having examined all such efforts. The literature up to 1944 was examined in some detail in other publications of the writers.²⁻⁵ It is necessary here to examine only a few publications of special interest which have recently come to the writers' attention and to re-examine a few whose significance has only become apparent in the light of the experimental work.

In recent publications, the most generally accepted hypothesis for the behavior of hydrogen in steel has been outlined as follows: The hydrogen contained within a piece of steel is normally in three portions; (1) that in true solution in the lattice; (2) a portion in excess of that which can be in

true solution and which has precipitated and diffused into blowholes and other major openings; and (3) a portion which has been rapidly precipitated and has been unable to diffuse far from the point of precipitation. Of these, only the third portion is effective in altering such properties as the ductility; hence the effect of a specified amount of hydrogen will vary with the history of the steel. The adverse effect of the hydrogen arises from the fact that at low temperature the decomposition pressure of the solution reaches the same magnitude as the strength of the steel, thus forcing the precipitated gas into microscopic openings, within the grains, variously termed "rifts," "lattice dislocations," or "mosaic disjunctions." The combined effect of the interruption of the lattice structure and the triaxial tensile stresses set up to balance the gas pressure effectively prevent the normal deformation processes.

On the quantitative side, very little reliable information has appeared either on the amount of hydrogen associated with lowered ductility or porosity or on the amount normally present in commercial steel. From equilibrium measurements of the amount of hydrogen dissolved at one atmosphere pressure, it was known that the amount of hydrogen which might be contained in liquid steel just prior to freezing is about 2.2 RV and the amount in solid steel just after freezing about 1.0 RV. From numerous qualitative tests it could be presumed that the hydrogen content necessary to cause porosity might be of the same order. In austenite, the solubility decreases with temperature from 1.0 to 0.4 RV at the transformation, and there is evidence that steel saturated with hydrogen in this temperature range is subject to shatter cracking. The solubility in ferrite falls from 0.2 RV just below the transition to unmeasurable amounts below 350°C. Qualitative experiments have shown that steel saturated with hydrogen at and immediately below the transition showed markedly impaired

ductility. Actual analyses of hydrogen in either liquid or solid steel were apparently so variable as to shed practically no light on the amount normally present. The solubility of hydrogen in most alloying elements was known and there was some evidence that the solubility of hydrogen in alloy steels would usually be intermediate between that in pure iron and that in the alloying element. It was believed that the hydrogen content of steel during manufacture might be anything up to around one relative volume and it was known that some portion of the original content normally diffused away as the fresh steel aged. It was presumed that moisture in the furnace charge and moisture and hydrogen in the furnace gases were important sources of hydrogen and that the boil in the furnace and the rimming of ingots tended to reduce the amount of this gas.

In the light of the measurements on commercial steelmaking to be reported in this paper, it should be noted that Kobayashi⁶ found, by vacuum-extraction analysis, that the hydrogen content in the acid open hearth furnace decreased during the earlier portion of the oxidizing period but rose on killing and after tapping. No beneficial effect on hydrogen of oxidizing and boiling was found in the basic open hearth or arc furnaces although nitrogen decreased during the boil in each furnace. Hydrogen values at tap were 0.35 to 0.65 RV, which are somewhat higher than the writers' findings for current American practice. Kobayashi related the hydrogen content to an equilibrium involving the H_2 and H_2O content of the slag and the FeO content of the steel, but it does not appear that these analyses were certain enough to justify complete acceptance of such a relationship.

Chuiko⁷ found that, during rapid boiling, hydrogen was eliminated in proportion to the amount present, but that hydrogen was absorbed during a mild boil, i.e., when the carbon elimination rate was less than 0.1 pct per hr. In the acid furnace, meltdown

hydrogens from 0.9 to 1.5 RV were reduced to 0.55 to 0.7 RV at the end of boiling. In the basic furnace the corresponding analyses were 1.8 RV reduced to 0.45 RV. If these analyses, by vacuum fusion, are reliable, Russian steel contains a great deal more hydrogen than the current American product. Bulavkin and Katsen⁸ have compared Russian basic open hearths of different bath depths and found the boil three times as effective in the shallower furnaces. Both of these observations support a mechanistic control of hydrogen concentration in preference to the physiochemical viewpoint of Kobayashi.

Recent British experimenters use the chill-cast pencil sample, storage on dry ice, and warm extraction analysis as tested by Wells and Barraclough,⁹ who have established an accuracy of ± 0.05 RV. Sykes, Burton, and Gegg¹⁰ thus find the average content of open-hearth steels at tap to be 0.30 RV. Arc-furnace carbon steels average 0.32 RV, while steels in the 3-5 pct alloy range show 0.37 to 0.62 RV of hydrogen. Several "wild" heats of alloy steels gave hydrogen analyses from 0.7 to 1.3 RV. These investigators expected the hydrogen content to be lowered by boiling but did not detect the effect, apparently because they tried to correlate hydrogen with the length of the boil rather than with the intensity.

To further complicate the effect of alloy additions, Hung, Bever, and Floe¹¹ have found that the addition of silicon to molten iron *decreases the hydrogen solubility*, but Zapffe¹² brings out the counter point that the addition of silicon, manganese, or aluminum, by tending to react with the oxygen fraction of the atmospheric moisture, increases the effective solution potential of the nascent hydrogen and thus acts to *increase the actual amount of hydrogen dissolved*. It has been pointed out that all three of these elements so completely dissociate water vapor that there should be no practical difference in their effect observable in commercial practice.

Segregation of hydrogen during freezing was discussed by Larsen¹³ but was not detected by Sykes et al¹⁰ since no tests were made near the surface of their ingots.

followed from meltdown to ladle in seven-teen heats. Of these heats, six are acid arc, five basic arc, two acid open hearth, and four basic open hearth. Two additional

TABLE I—Summary of Hydrogen Content of Commercial Heats

Heat No.	Type	Active Period		Analyses				H ₂ Rise at Ladle
		Rate C Drop, Per Cent per Hr	Rate H ₂ Loss, RV per Hr	Hydrogen (RV)				
				Meltdown	Min.	Tap	Ladle	
Acid Arc Heats								
14	AAgB	1.03	0.73	0.27	0.10	0.25	0.24	
18	AA Mn Mo	0.54	0.23	0.28	0.16	0.26	0.27	0.01
22	AAgB	0.99	0.25	0.17	0.08	0.09	0.18†	0.09
27	AAgB	0.60	0.14	0.10	0.10	0.13	0.29	0.16
31	AAgB	0.32	0.24	0.25	0.14	0.14	0.30	0.16
41	AAIC	0.86	0.71	0.08	0.05	0.09	0.12†	0.04
41	AAIC	1.08	0.73	0.08	0.05	0.09	0.12†	0.04
Basic Arc Heats								
30	BAGB	0.20	0.10 gain	0.19	0.15	0.15	0.24	0.09
32	BAGB	0.43	0.09	0.18	0.15	0.24	0.29	0.05
33	BAGB				0.18	0.27	0.23	
35	BAIC	0.32	nil	0.28	0.28	0.29‡	0.42	0.13
36	BAIC	0.26	0.27	0.36	0.19	0.24	0.35	0.11
Acid Open Hearth Heats								
28	AOHgB	0.50	0.25	0.17	0.12	0.12	0.25	0.13
29	AOHhC	0.11	0.11	0.20	0.16	0.25	0.21	
Basic Open Hearth Heats								
23	BOHgB	0.32	0.04 gain	0.18	0.18	0.29	0.29	
23	BOHgB	0.60	0.40	0.18	0.18	0.29	0.29	
24	BOHgB	0.23	0.14	0.21	0.18	0.32	0.28	
25	BOHHT	0.64	0.14 gain	0.16	0.16	0.28	0.26	
39	BOHIC	0.28	0.28	0.18	0.18	0.31	0.32*	0.01
26	BOHgB						0.20	
38	BOHIC					0.30	0.29*	
40	BOHgB					0.31	0.25*	

* Via spoon.

† Via hand shank.

‡ This sample via wet hand shank.

§ Water leaking into furnace.

|| First heat on rebuilt furnace.

Type abbreviations:

AA = Acid arc furnace AOH = Acid open hearth
 BA = Basic arc furnace BOH = Basic open hearth
 gB = Grade B steel (plain 0.25 to 0.35 pct carbon steel)
 MnMo = Manganese-molybdenum alloy steel
 HT = Manganese-titanium high-tensile steel
 hC = High carbon, otherwise similar to Grade B
 IC = Low carbon, otherwise similar to Grade B

SECTION 2—HYDROGEN AND NITROGEN CONTENT OF STEEL IN COMMERCIAL PRACTICE

Experiments and Methods

The hydrogen and nitrogen content of commercial steels during melting has been

basic open hearth heats (38, 40) were sampled at tap and ladle and one at the ladle only (Heat 26).

In all cases of sampling from the furnace, about three pounds of metal were withdrawn in a well-slaggered spoon, the slag raked or dumped, the metal killed with

aluminum wire and poured into a copper chill mold. Time for this operation was normally 10 to 15 sec. The sample was cooled in the mold, cut from the head, and

clear example of the normal behavior is shown in Fig 1 for acid arc heat No. 18. During the active period the removal of carbon and nitrogen was approximately

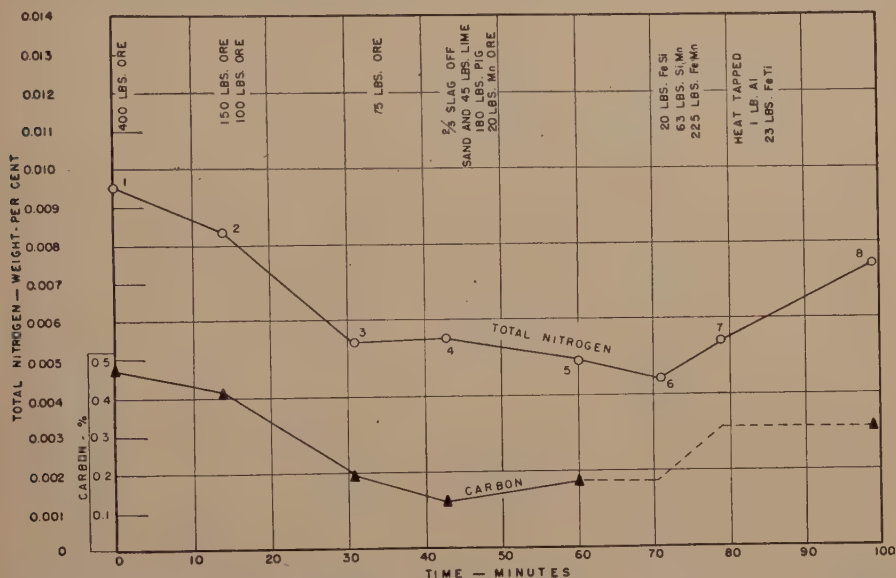


FIG 1—SIX-TON ACID ARC HEAT 18—MnMo STEEL. CHANGE OF TOTAL N_2 CONTENT WITH PROGRESS OF HEAT.

stored over mercury within 3 to 4 min. Ladle samples were normally poured directly into the chill mold from the smaller bottom pour ladles. In a few cases, which have been noted in the tables, a heated spoon was used with apparent success. Samples were poured from hand shanks when this practice was being used for the castings.

Graphs of furnace practice and analysis are given herein for the more illustrative heats. Data from all heats are summarized in Table 1 and Fig 15.

Nitrogen Variation

Total nitrogen analyses were made by the wet method on drillings from the head portion of each chill sample. In nearly all cases these were in the range of 0.005 to 0.01 wt pct and in this range followed very closely parallel with the carbon content. A

parallel. In the later period of the heat small unexplained variations were recorded while an important increase in nitrogen occurred with the alloy additions and on tapping.

When the original nitrogen at meltdown was abnormally high, as 0.015 pct in acid arc heat No. 31, there was a much more rapid loss of nitrogen in the first 15 min. of the boil (Fig 2) after which the behavior was as before. In open-hearth heats there was little variation in nitrogen, except for a rise on tapping. In a basic arc heat made by the double slag process the change of nitrogen was slow in agreement with the small carbon drop but showed definite drops at the completion of the formation of each slag. All nitrogen values are in fairly good agreement with the assumption that the nitrogen elimination runs roughly parallel to carbon removal. No cases were en-

countered where the nitrogen content was sufficient to lead to an expectation that it might cause a change in the physical properties of the steel.

were in each case subjected to a rather violent boil soon after melting. In each such case, a marked reduction of hydrogen occurred as illustrated by Tests 1 and 2 in

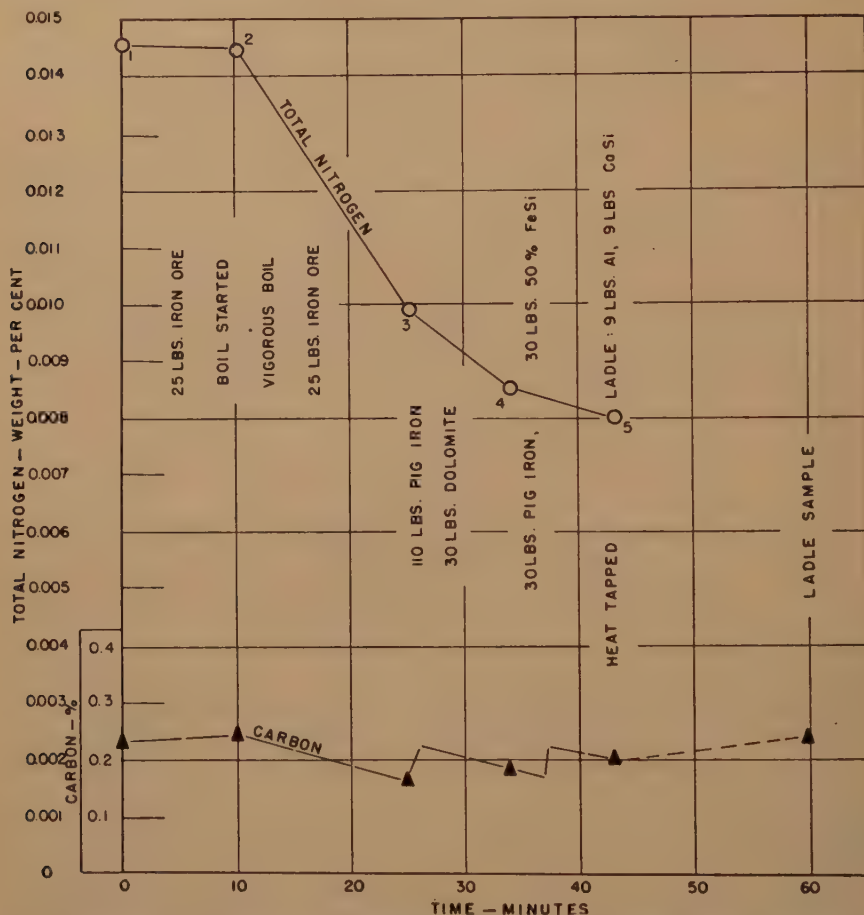


FIG 2—THREE-TON ACID ELECTRIC ARC FURNACE HEAT 31. CHANGE OF N_2 CONTENT WITH PROGRESS OF HEAT.

Hydrogen in the Acid Arc Furnace

A summary of the data on the hydrogen content of all of the commercial heats is given in Table 1. Of the six acid arc heats listed there, the four heats Nos. 14, 18, 22, and 31 may be considered normal practice where made. The typical features are shown in Fig 3, which represents the log of Heat 14. These heats melted high in carbon and

Fig 3. As the boil decreased the hydrogen content either rose or leveled off. This log shows a special increase with the alloy addition, which, however, was not generally confirmed by the other heats. This increase, together with other irregular increases shown in Fig 4 and 5 is more likely caused by moisture in certain additions than to a specific hydrogen content of any of the

additions. All of the acid arc heats except Heat 14 showed increases in the hydrogen content on transfer to the ladle. These, as listed in Table 1, may usually be correlated

effect of hydrogen from the air remains through the treatment.

In Fig 15 the rate of change of hydrogen and the rate of change of carbon are com-

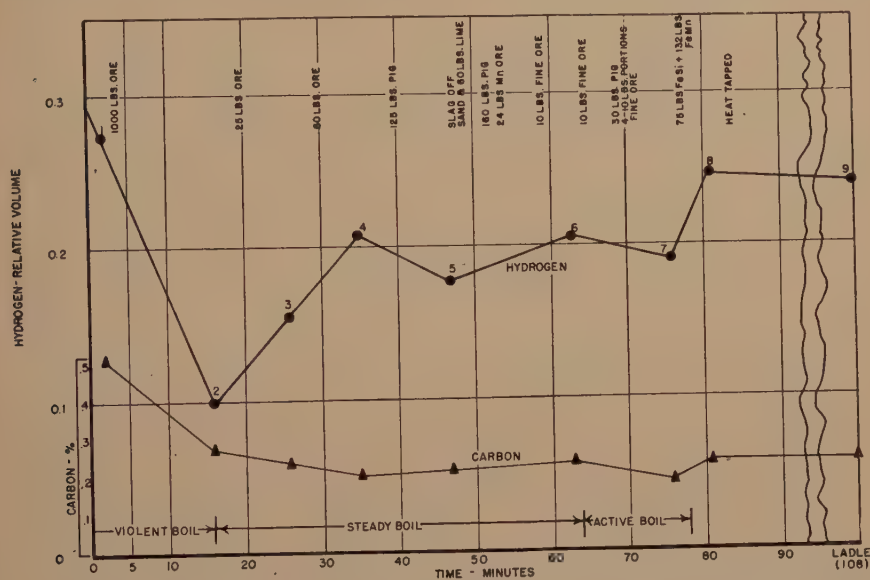


FIG 3—SIX-TON ACID ARC HEAT 14—GRADE B STEEL. CHANGE OF H_2 CONTENT WITH PROGRESS OF HEAT.

with the known presence of moisture in the ladle, and occur independently of the type of furnace.

Heat 27 was exceptional in that it melted soft and there was little boiling at the start. The heat was twice repigged during which period the hydrogen, low at meltdown, increased considerably. A good boil was obtained just prior to blocking and this boil brought the hydrogen back down at a rate comparable with the loss during the initial boil on the other heats. The log of this heat is shown in Fig 6.

In the case of the acid arc furnace, it has been found that there is a correlation between the atmospheric humidity and the hydrogen content of the steel. Pertinent data are shown in Table 2.

It is obvious that a high atmospheric humidity tends to increase the hydrogen absorbed during meltdown and that some

pared for the period of active boiling for each heat. Values for the acid arc heats are shown as solid triangles. It will be seen that

TABLE 2—Humidity at Time of Melting and H_2 Content of Steel, Acid Arc-furnace Heats

Heat No.	Month	Hu- midity, G per Cu M	Meltdown H_2		Tap H_2	
			Amt (RV)	Per Cent of Base	Amt (RV)	Per Cent of Base
14 (base)	May	10.0	0.27	100	0.24	100
18	Aug.	17.4	0.28	103	0.26	109
22	Oct.	6.4	0.17	63	0.09	37
27	Jan.	4.0	0.10	38	0.13	54
31	May	5.9	0.25	93	0.14	58
41	Apr.	6.0	0.08	30	0.09	33

there is a general trend toward increased hydrogen elimination as the violence of the boil increases, as indicated by more rapid

carbon removal. As the rate of boil is not the only factor affecting the hydrogen content, a precise relationship cannot be expected. The simultaneous absorption of

that a low-hydrogen steel could be produced on demand. On the basis of ductility studies to be described in a later paper, it was projected that a ladle hydrogen value

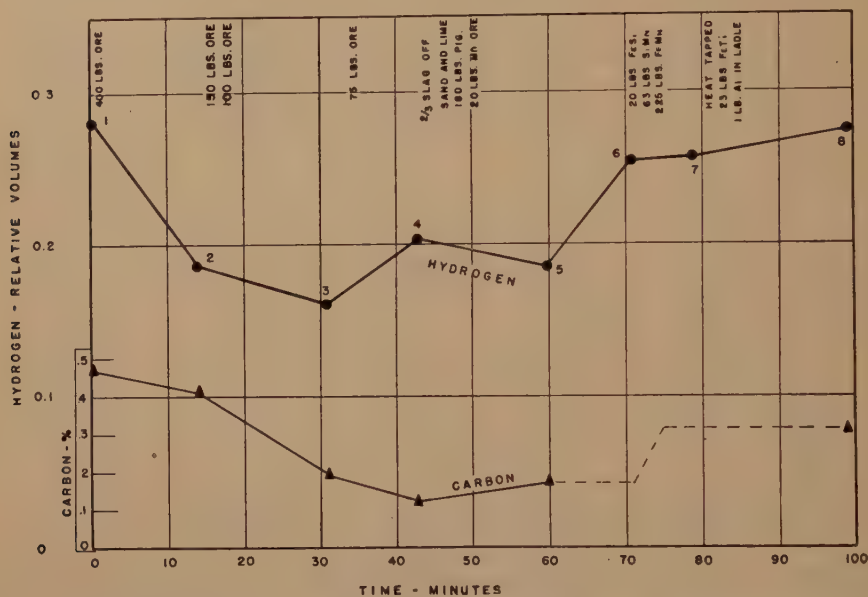


FIG 4—SIX-TON ACID ARC HEAT 18—MnMo STEEL. CHANGE OF H_2 CONTENT WITH PROGRESS OF HEAT.

hydrogen from atmospheric moisture has been noted. It may also be noted that heats such as Nos. 14 and 31 which started high in hydrogen show a comparatively high rate of hydrogen elimination during boiling, while heats such as Nos. 22 and 27 which started at lower levels show a lower rate of hydrogen loss at comparable boiling rates. The hydrogen elimination reaction during boiling thus appears as a normal type whose rate depends directly on the amount of hydrogen present as well as on the violence of boiling.

Special Practice for Low Hydrogen

After the study of sixteen commercial heats of the four usual types, it was desired to prove whether the principal factors controlling the hydrogen content had been determined by attempting to demonstrate

of 0.15 RV or less would not only be well below the normal commercial range but should give a noticeable improvement in ductility. Inspection of the data in Table 1 and Fig 15 showed that a carbon elimination rate of 1.0 pct per hr was obtainable in the acid arc furnace. It was estimated that with this boiling, the hydrogen elimination rate should vary between 0.70 and 0.25 RV per hr as the hydrogen decreased, and, therefore, that from a possible 0.30 RV at the start of boiling, 0.25 RV could be eliminated during 30 min. of sustained boiling. Such a practice should, therefore, leave an adequate margin for a certain inescapable pickup of hydrogen in the ladle.

To prepare such a heat, the following precautions were taken: To prepare an AX1024 steel after the specified boil, a melt-down carbon of about 0.75 pct was

desired. Allowing for meltdown losses, pig was charged to bring the carbon to 0.85 pct of which 0.69 pct actually survived at the time the boil was started. All charge mate-

at 1- to 2-min. intervals to a total addition of 785 lb of ore in a 12,000-lb heat. The desired carbon (0.24 pct) was passed 31 min. after the first addition with 740 lb of

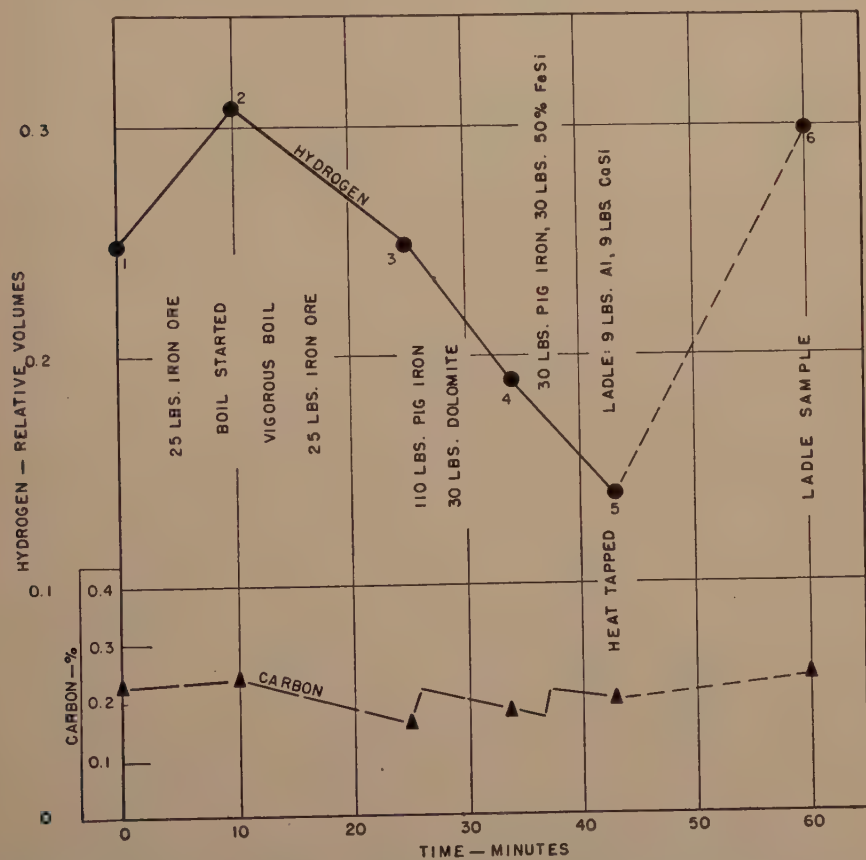


FIG 5—THREE-TON ACID ELECTRIC ARC FURNACE HEAT 31. CHANGE OF H_2 CONTENT WITH PROGRESS OF HEAT.

rials, as well as ore to be added later, were air dry. Lime and alloy additions were held at red heat until needed. A thoroughly dried, old ladle was used.

The results of this test, Heat 41, are shown in Fig 7. No ore was used in the charge or added until the heat had been melted and brought close to the desired reaction temperature. A first portion of 250 lb of ore was added to start the boil after which additions of 25 to 50 lb were made

ore in the furnace but because of analytical delays, the carbon undershot to 0.17 pct and repigging was necessary although not originally planned.

The apparent meltdown hydrogen was very low although it may be questionable whether a representative sample could be obtained from the completely inactive bath. The second analysis at 0.19 RV appears normal for the conditions of melting. During the boil the hydrogen fell

reasonably continuously and attained the desired value of 0.05 RV 34 min. after the first ore addition. This value could not be maintained when the boil tapered off;

final ladle value of 0.12 RV was, therefore, well within the range of the original aim.

In this test of special practice, both the minimum and final hydrogen contents in

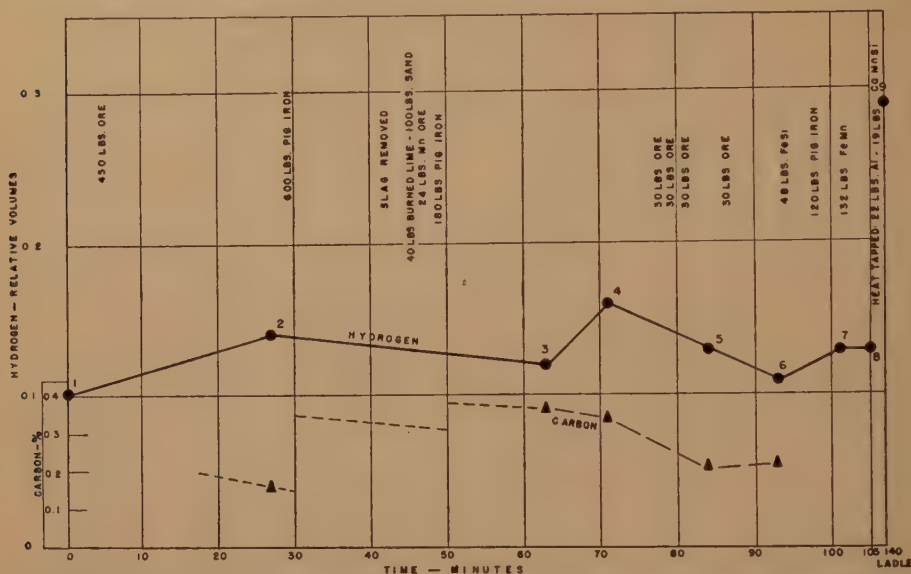


FIG 6—SIX-TON ACID ARC FURNACE HEAT 27. CHANGE OF H_2 CONTENT WITH PROGRESS OF HEAT.

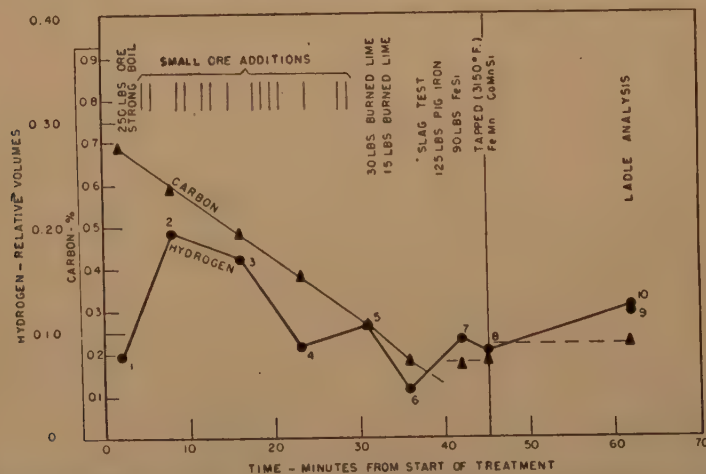


FIG 7—SPECIAL-PRACTICE SIX-TON ACID ARC HEAT 41. CHANGE OF HYDROGEN CONTENT WITH PROGRESS OF HEAT.

hence after repigging and blocking the hydrogen had risen to 0.08 to 0.09 RV. The hydrogen pickup in the well-dried ladle was no more than 0.04 RV, and the

the furnace and the hydrogen in the ladle were well below the best values attained in any standard practice. The resulting test bars were very low in hydrogen and had

excellent ductility which was not appreciably increased by aging. It may be concluded that in the acid arc furnace at least, low-hydrogen high-ductility steel can, in fact, be produced on demand.

eliminating carbon at the rate of 0.32 pct per hr was attained for 10 min., after which the carbon remained practically unchanged and the heat inactive. There was therefore no real opportunity for hydrogen elimina-

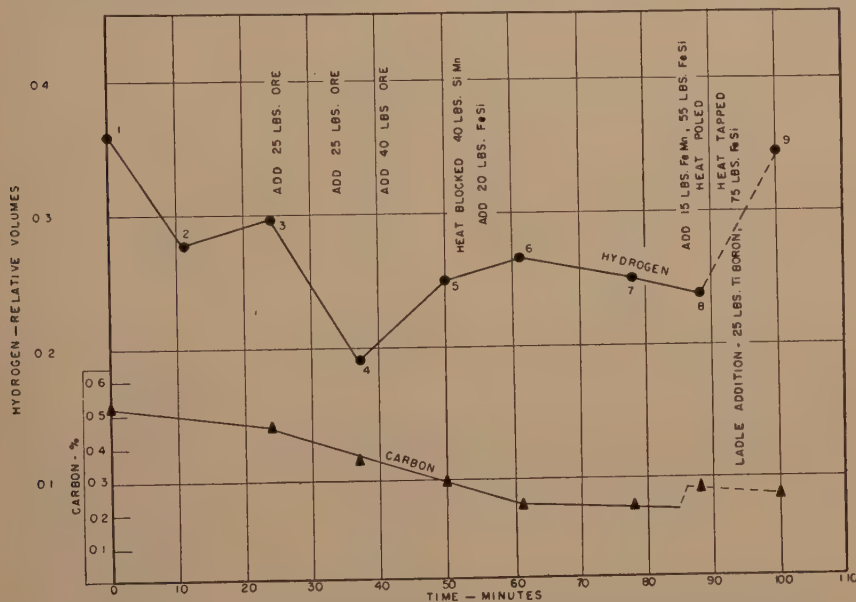


FIG 8—FIVE-TON BASIC ARC FURNACE HEAT 36. CHANGE OF H_2 CONTENT WITH PROGRESS OF HEAT.

Hydrogen in the Basic Arc Furnace

The five basic arc heats, Nos. 30, 32, 33, 35, and 36, are noticeably different from the acid arc heats in that no important over-all reduction of hydrogen was generally obtained during the molten period. Only one heat, No. 36, showed a good response to boiling. This heat is illustrated in Fig 8 and should be interpreted as showing the results of the best regular practice which is far better than average with respect to hydrogen control. Heats 30, 32, and 33 showed large but irrational changes in hydrogen and a general upward trend throughout the heat. Heat 32, typical of the group, is illustrated in Fig 9.

Heat 35 is the only example of true basic practice using the double-slag treatment (Fig 10). In this heat, a vigorous boil

tion. As a further abnormal and adverse factor, a furnace was used whose refractories were continually moistened by water leaking from the roof. An apparent equilibrium hydrogen value of 0.295 ± 0.01 RV was attained and held constant within the accuracy of analysis for almost 2 hr. The ladle used had been saturated with water to cool it for repairs; hence a ladle pickup of 0.13 RV of hydrogen occurred to give a final analysis of 0.42 RV, the highest so far found in commercial practice and a value which could be expected to do extensive harm to the physical properties of the steel.

Insufficient data were obtained to test the effect of humidity on the basic arc furnace.

The most important general difference between the basic and acid arc heats ap-

pears to lie in difference in practice where a much more violent boil is used in the acid furnace. There is actually only one overlapping of the rates of carbon elimination

per hr at a boil intensity giving 0.50 pct per hr carbon reduction. As shown in Fig 11, this heat compares favorably with the less violently boiled acid arc heats. As in nu-

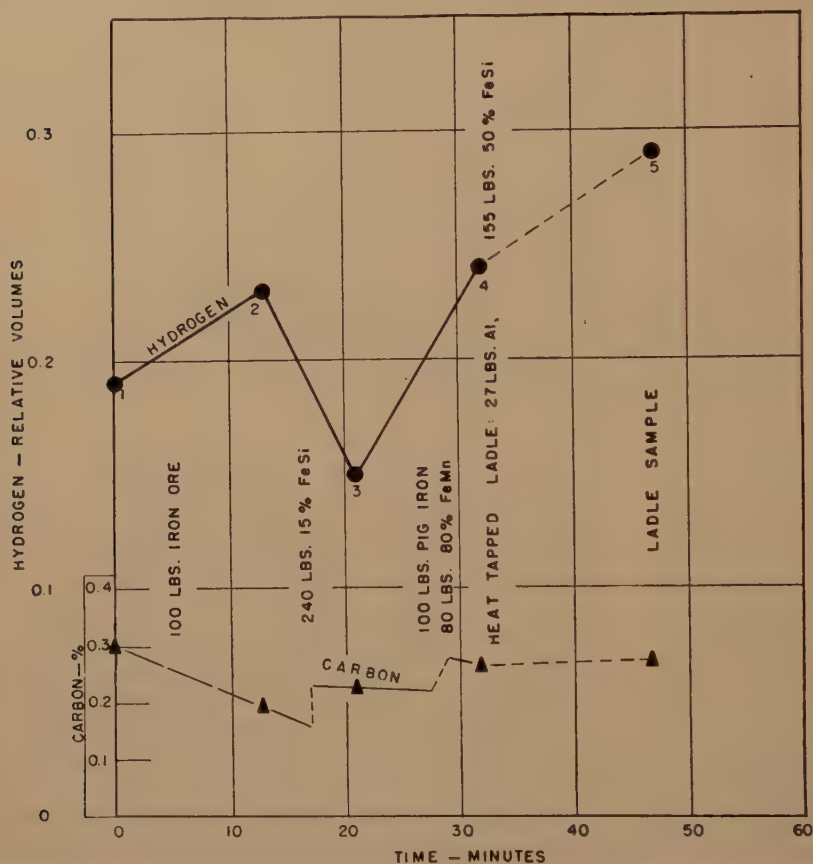


FIG 9—NINE-TON BASIC ARC FURNACE HEAT 32. CHANGE OF H_2 CONTENT WITH PROGRESS OF HEAT

in the eleven arc heats, at about 40 points per hr. This difference in rate of boil may easily be sufficient to account for all of the differences in hydrogen content in the two types of practice.

Hydrogen in the Acid Open Hearth

Both the two acid open hearth heats, Nos. 28 and 29, showed hydrogen elimination during the period of boiling. Heat 28, Grade B (plain 0.25 to 0.35 pct carbon steel), showed a hydrogen loss of 0.25 RV

merous other cases, the favorably low hydrogen at tap was spoiled by poor ladle practice.

Heat 29 (Fig 12), a 0.40 carbon steel, had very little boil and a maximum carbon loss rate of 0.11 pct per hr. There was a small hydrogen loss at the start and considerable increase later in the furnace period.

While the hydrogen content of the acid open hearth steel is high as compared with acid arc steel, the rate of hydrogen elimination apparently is entirely consistent with

the lower rate of boiling and does not indicate any special adverse condition.

Hydrogen in the Basic Open Hearth

Of the four basic open-hearth heats (Nos. 23, 24, 25, and 39) followed in detail, Heats

sistently in the range of 0.28 to 0.32 RV regardless of variations in practice and in humidity. Of the four types of furnace studied, the basic open hearth was thus the worst with regard to final hydrogen content.

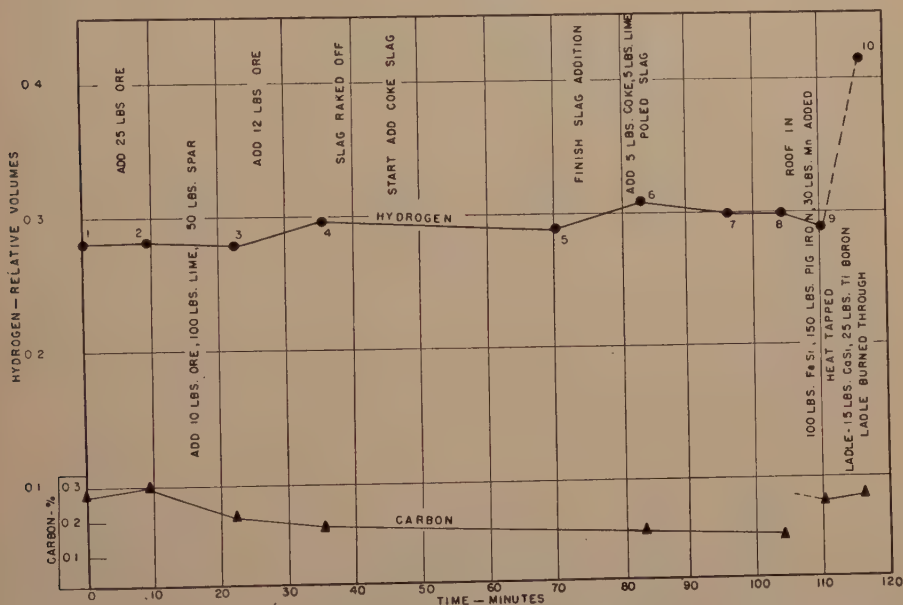


FIG 10—FIVE-TON BASIC ARC FURNACE HEAT 35—DOUBLE SLAG PRACTICE. CHANGE OF H_2 CONTENT WITH PROGRESS OF HEAT.

23, 24, and 39 showed some hydrogen elimination on boiling. Fig 13 for Heat 23 is typical. The amount of hydrogen reduction was insignificant as compared with the steady over-all rise which continued with the increasing temperature and continued exposure to an atmosphere high in hydrogen. Hydrogen reduction by boiling was not consistently observed in the basic open hearth as shown by the hydrogen gain in the early portion of the curve in Fig 13. Heat 25 (Fig 14) held a high carbon reduction rate longer than Heat 23, but no hydrogen reduction was observed at any stage.

Including the data on the heats not followed in detail, the tap hydrogen in the basic open hearth was found to remain con-

Overall Effect of Boiling

The comparative rates of carbon and hydrogen removal at times of maximum bath activity are shown for all of the commercial heats in Fig 15. As discussed under the acid arc, the dependence of the rate of hydrogen removal on the amount of hydrogen present and on the competing readsorption from hydrogen in the furnace atmosphere precludes the possibility of any legitimate single line to represent the average rate of hydrogen removal. The coherent band limits drawn include all heats except one basic open hearth and, with this exception, fail to indicate any specific tendency of one type of furnace to give high or low rates of hydrogen removal. The most important difference between furnaces shown

in this figure is the fact that the boil intensity in the acid arc is usually much greater than in the other types.

Considering heats such as Nos. 14, 31,

least 40 points per hr. Time in the inactive and blocked conditions must be minimized in contrast to the long inactive periods commonly encountered in the open hearth.

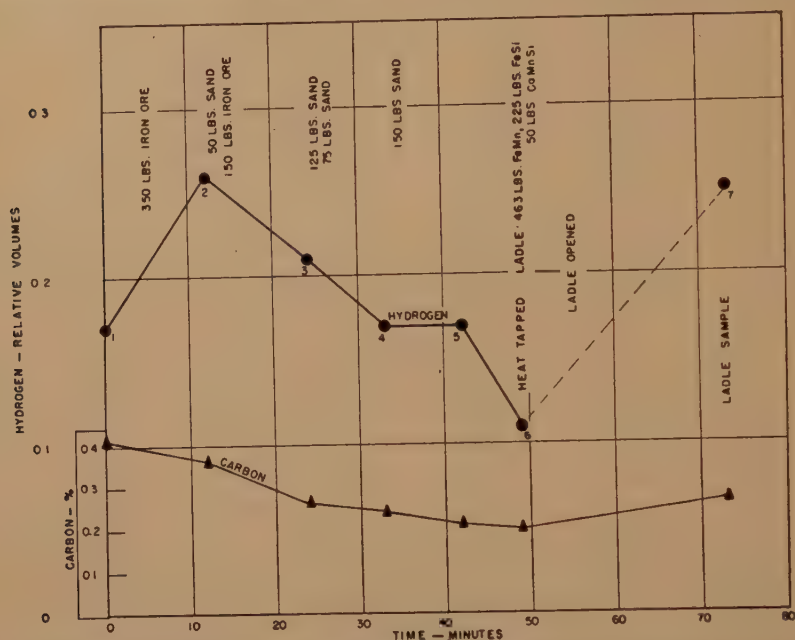


FIG 11—TWENTY-FIVE-TON ACID OPEN HEARTH HEAT 28. CHANGE OF H_2 CONTENT WITH PROGRESS OF HEAT.

and 36, where the original hydrogen (Table 1) was high, it is seen that hydrogen is slowly lost with a mild boil, and that the rate of hydrogen elimination increases regularly as the boil becomes more violent. On the other hand, with heats such as Nos. 22, 27, 30, and 32, where the melt-down hydrogen was less than 0.20 RV, hydrogen may actually be picked up at any time except when the boil is of sufficient violence to eliminate carbon at a rate of more than 40 points per hr.

The reduction of the final furnace hydrogen below 0.15 RV is a reasonable immediate objective for improved steelmaking practice. The attainment of this objective requires continued hydrogen reduction at the lower edge of the band in Fig 15; hence, continued carbon removal at a rate of at

least 40 points per hr. Time in the inactive and blocked conditions must be minimized in contrast to the long inactive periods commonly encountered in the open hearth. Since it has been demonstrated that a late boil can be just as effective as one at melt-down, the required conditions are quite attainable in the arc furnaces. In spite of difficulties in carbon estimation, blocking has been practically eliminated in some plants with no apparent harmful effects. In the open hearth, difficulties would be encountered in attaining temperatures necessary to maintain the rapid rate of boiling but new procedures such as the use of oxygen, already being considered on economic grounds, suggest that the difficulties are not insurmountable.

Effect of the Ladle

A most obvious and promising point for plant attack on the hydrogen problem lies in the reduction of the moisture content of

the ladles. Of nineteen heats investigated on this point, six reached tap with satisfactory hydrogen contents of 0.15 RV or less. The good record of all of these, except

beyond the point of immediate evaporation, the practice did not prove harmful. In contrast, some plants have allowed water to be used to the point where the refrac-

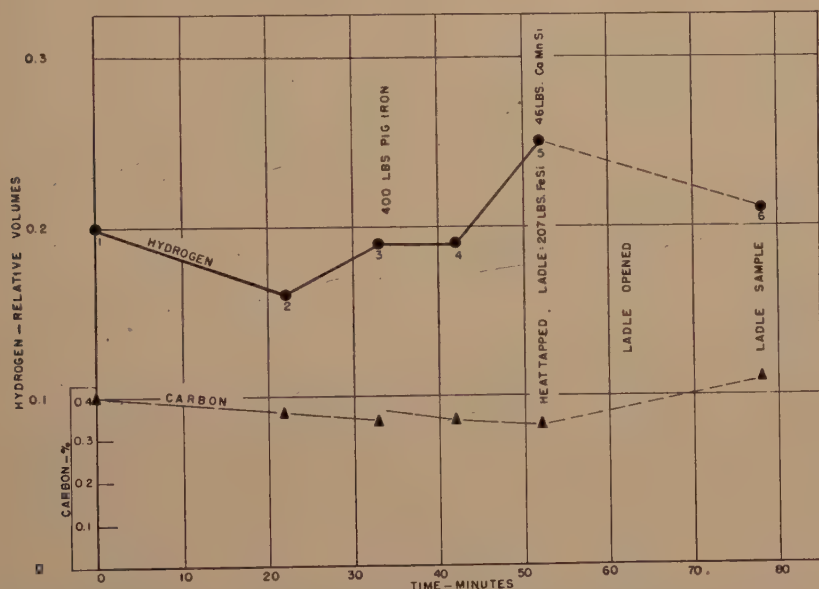


FIG 12—TWENTY-THREE-TON ACID OPEN HEARTH HEAT 29. CHANGE OF H_2 CONTENT WITH PROGRESS OF HEAT.

the one given special low hydrogen practice, was then spoiled by hydrogen pickup of 0.09 to 0.16 RV from the ladle. Five additional heats, to a total of 11 out of 19 also had noticeable hydrogen increase from the ladle, raising the final hydrogen in the extreme case to the very undesirable level of 0.42 RV.

Investigation has shown that a newly lined ladle, even when preheated in a normal manner, retains a large amount of moisture in its refractories. Much of this moisture is converted to hydrogen in the first heat poured in the ladle but a portion is also carried on in some cases to the second and possibly the third heat.

A second source of ladle moisture is the use of water for cooling prior to nozzle and stopper replacement. Where care was exercised to see that water was not used

tories are saturated and water may even stand in a pool in the bottom. Such cases were easily detected by the high hydrogen content of the resulting steel and included the highest value recorded.

The excessive use of water is subject to immediate control in any plant, and, whenever facilities permit air cooling, could be almost entirely eliminated. While the periodic use of new ladles is unavoidable, it should be practical in many cases to reserve these for heats which need to meet comparatively low specifications.

Other Controllable Factors

The previous literature contains numerous references to the adverse effect of such factors as high moisture in slag materials, rusty scrap, and high hydrogen in some alloy materials. While it is believed that

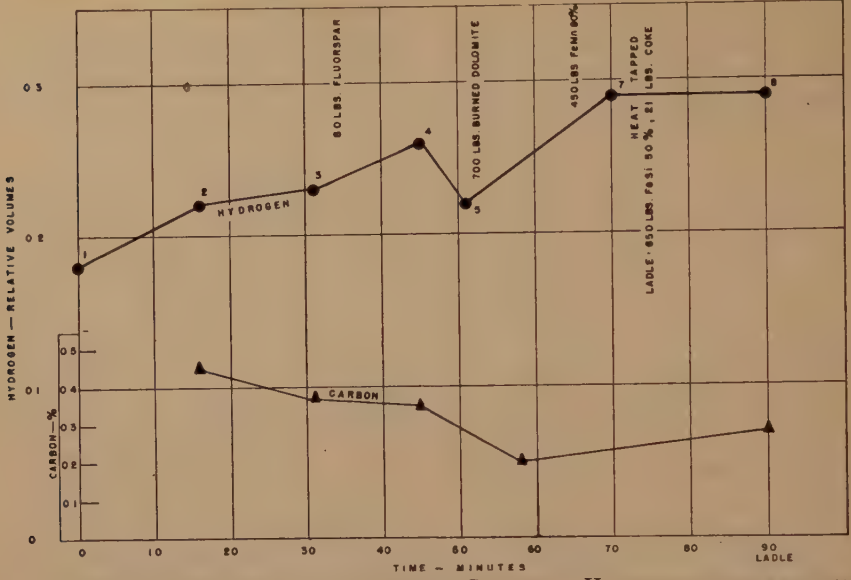


FIG 13—THIRTY-TON BASIC OPEN HEARTH HEAT 23. CHANGE OF H_2 CONTENT WITH PROGRESS OF HEAT.

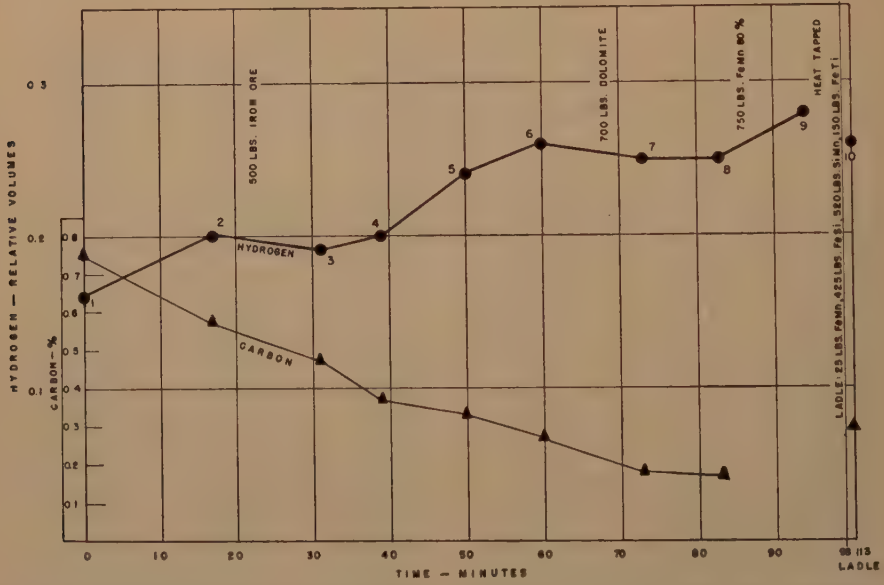


FIG 14—THIRTY-TON BASIC OPEN HEARTH HEAT 25. CHANGE OF H_2 CONTENT WITH PROGRESS OF HEAT.

the present investigation has detected these factors in some cases, the effects are usually small compared to the effects of boiling and ladle practice.

Apparently it would be proper to assume that a certain unavoidable concentration of hydrogen will be present at melt-down and that it is desirable to eliminate at least

half of this by furnace practice. Probably only the most elementary protection of charge materials could be economically justified. More care of addition materials

hydrogen can be reduced during steelmaking, with proportional benefit to ductility, by maintaining a strong boil, normally one of sufficient activity to reduce

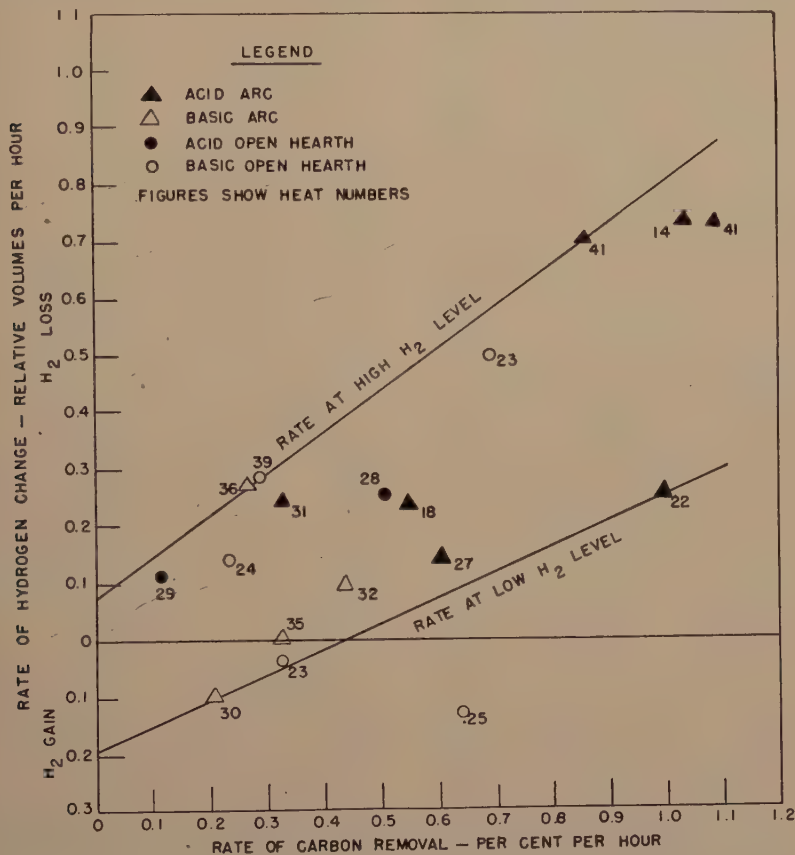


FIG 15—EFFECT OF RATE OF BOIL ON HYDROGEN CONTENT OF COMMERCIAL STEELS.

may be desirable, but probably may be limited to protection from rain, the preservation of lime in a freshly burned condition, and possible preheating of certain alloy materials used in higher alloy steels.

GENERAL CONCLUSIONS

1. Hydrogen to an amount of 0.30 RV or more is commonly present in steels of casting grades at the ladle, and a sufficient proportion of this hydrogen remains in test bars and castings to cause important reductions of their ductility. This quantity of

carbon at rates of 0.40 to 1.0 pct per hr. In this effort, the acid arc furnace seems most amenable to control while the basic open hearth furnace offers the greatest resistance to effective modification of practice.

2. To preserve the effect of hydrogen reduction during steelmaking, it is necessary to limit strictly the time spent in an inactive condition after boiling and to insure that the ladle refractories are thoroughly dry. Drying or preheating of furnace and ladle additions may give some additional benefit in certain cases.

REFERENCES

1. C. E. Sims, and G. A. Moore: Apparatus for the Hot-extraction Analysis for Hydrogen in Steel. This volume, p. 248.
2. C. E. Sims, and G. A. Moore: Low Ductility and Porosity of Cast Steels Due to Hydrogen and Nitrogen. Part I. Review of Literature, *Steel Founders' Soc. of Am., Res. Report No. 4*, Feb., 1945. Available on Recordak film Battelle Mem. Inst.
3. C. A. Zapffe, and C. E. Sims: Selected Bibliography on Hydrogen in Steel, U. S. Dept. Agr. Libr., Washington, D. C., Document No. 1255 obtainable as bibliofilm—500 references.
4. C. A. Zapffe, and C. E. Sims: Hydrogen Embrittlement, Internal Stress, and Defects in Steel, *Trans. AIME*, (1941) **145**, 225-261; disc. 161-71.
5. C. A. Zapffe, and G. A. Moore: A Micrographic Study of the Cleavage of Hydrogenized Ferrite, *Trans. AIME*, (1943) **154**, 335-352; disc. 352-359.
6. (a) S. Kobayashi: Hydrogen and Nitrogen in Steel, (1937) *Tetsu-to-Hagane*, **23**, 954-965; *Met. Abstr.* (in Metals and Alloys) (1938) **9**, 353. (b) S. Kobayashi: Hydrogen and Nitrogen in Steel During Manufacture. II. Mechanism of Hydrogen Intrusion into Molten Steel During Open-Hearth Refining, *Tetsu-to-Hagane* (1938) **24**, 227-234; *C.A.* **32**, 8331. (c) S. Kobayashi: Hydrogen in Steel, *Tetsu-to-Hagane* (1939) **25**, 745-773.
7. N. Chuiko: Theory of Hydrogen Elimination During Electric Steelmaking, *Teoriya i Prakt. Met.* 8/7 (1938) 48-55; *Met. Abstr.* (in Metals and Alloys) 10/3 (1939) 142.
8. A. Bulavkin, and L. G. Katsen: Effect of Bath Depth on the Degree of Gas Saturation of Molten Metal, *Stal* 10/11-12 (1940), 28-32; *Chem. Zentr.* (1942) **1**, 258.
9. J. E. Wells, and K. C. Barraclough: Determination of Hydrogen in Liquid Steel, *Jnl. Iron and Steel Inst.* 155/1 (Jan. 1947) 27-32.
10. C. Sykes, H. H. Burton, and C. C. Gegg: Hydrogen in Steel Manufacture, *Jnl. Iron and Steel Inst.* 156/2 (June 1947) 155-180.
11. Hung Liang, M. B. Bever, and C. F. Floe: The Solubility of Hydrogen in Molten Iron-silicon Alloys. TP 1975, *Metals Tech.* (Feb. 1946); *Trans. AIME* (1946) **167**, 395.
12. C. A. Zapffe: Concept of the Hydrogen Potential in Steam-Metal Reactions, *Trans. Am. Soc. Metals*, (1947).
13. B. M. Larsen: A Review of Factors Underlying Segregation in Steel Ingots, *Metals Tech.* (Sept. 1944) 13-34; *Trans.* (1945) **162**, 414.

DISCUSSION

(J. G. Thompson and S. Marshall presiding)

M. B. BEVER*—While the equilibrium solubilities of the common gases in iron and several

of its alloys have been determined with a fair degree of accuracy, knowledge of actual contents of steel in commercial melting has remained quite inadequate. The present paper is an important contribution to this subject.

When new data of great interest are reported, the question of units may appear trivial. Nonetheless, regret must be voiced at the authors' choice of "relative volumes" as units of gas content because they are limited to one particular system of reference. The density of iron or low-carbon steel differs by as much as 10 pct from the densities of some of the high-alloy steels. Certainly, any comprehensive discussion of gases in ferrous and nonferrous metals on the basis of "relative volumes" would be entirely artificial. These new units result in figures of smaller magnitude than do "cc per 100 g of metal"—certainly no gain in convenience.

In addition to the new data reported in this paper the authors' general comments are of interest. For example, the emphasis on moisture as a source of hydrogen seems well-founded. While such deoxidizing alloys as silicon are particularly effective in supplying hydrogen from moisture, iron itself acts similarly by combining with the oxygen in water vapor.

G. A. MOORE (authors' reply)—The problem of hydrogen analysis is complicated enough without getting into the problem of units. In going over something over 1000 papers which have been written on hydrogen in metals, I think you will find at least a dozen units of measurement. Sieverts used "cc per 100 g," and as far as I know that is the only series in which this unit has been used.

Weight per cent, of course, is the most general among analysts. In addition to these units, we have various papers in milligrams per hundred grams, in liters per pound, and almost every other combination of units that can be imagined.

The weight per cent value is, of course, most legitimate, but we find great difficulty in counting the number of zeros. Relative volume is a legitimate unit because it makes no difference whether we make our measurements in cc and in grams, or whether the values are read in cubic feet and pounds and converted into cubic feet of gas and cubic feet of steel; or read in any other system of measurement.

* Massachusetts Institute of Technology.

We would like to see the elimination of all except weight per cent and relative volume on the ground that such units as "cc per 100 g" are classed as illegitimate since they are not in comparable terms.

The effect of silicon, of iron, and so forth, in the reaction with moisture is very complicated. I will make just one point. In almost all of these cases where an alloying material is added, the potential of the material to decomposed water is already so high that the addition does not make much difference. Steels definitely all cause conversion of water vapor to hydrogen, especially in the commercial furnaces.

A. L. ASCR^{*}—The authors confirmed once more, and by more or less exact figures, that a strong oxidizing boil is an important factor in the process of eliminating hydrogen.

The main merit of this paper lies in the fact that investigations were made under commercial conditions requiring much labor and patience and the authors should be congratulated for this. The conclusions drawn are of a general nature and have been recognized for some time by many steelmakers dealing with quality steels.

However, the main recommendation that the rate of carbon boil should be of 0.4 to 1.0 pct per hr, still does not solve the problem of hydrogen in practice. As a matter of fact, the figures found by the authors seem to confirm this plainly. Four acid heats (14 and 22, 18 and 27) with the same rate of boiling, show as much as 100 pct difference in hydrogen contents at tapping time. It would be very interesting to know what hydrogen contents were found in the final products made from these heats.

In basic arc heats and basic open hearth heats, the figures found seem so confusing that it is hard to make any positive conclusion. It is regrettable that there were no heats made in a basic arc furnace, with the same rate of carbon boil as that of the heats made in the acid arc furnace. It is very probable that in this case, the basic arc furnace would have been treated more favorably by the authors particularly if the manganese contents during the boiling period had been low.

If the results are analyzed more closely, it can be noticed that the quantity of hydrogen varied in a matter of minutes although there

seemed to be no special factor which could cause such variations. Involuntarily two questions arise, namely whether the mechanism of absorption and elimination of hydrogen is really so flexible or whether we still did not reach the stage at which we can say that the percentage of hydrogen found is that which the metal really contains? If one of these questions were answered in a positive way, the struggle of the steelmakers with hydrogen could be considerably facilitated as we would know the essence of the behavior of hydrogen.

In the present investigations, the problem of sampling seems to cause some fears as far as the quantity of hydrogen retained in the samples is concerned. As mentioned by the authors, the sample taken out of the furnace contained about 3 lb of fluid metal. It was then killed in the spoon with aluminum and the whole sampling procedure lasted from 10 to 15 sec. It is a well known fact that the melting heat of aluminum is exceptionally high. In practice this means that the addition of aluminum in increased quantities chills the fluid metal very rapidly. When the metal is chilled, the evolution of hydrogen definitely occurs. Furthermore the process of casting the sample may be another factor which causes the elimination of hydrogen. It is a well known procedure practiced in some plants that in cases of unsound heats, the simple re-ladling eliminates hydrogen to the quantity sufficient to assure sound heats. As a matter of fact, the authors mentioned in this paper that a considerable portion of the hydrogen present in the ladle may be evolved during the casting process. Could it not then be partially eliminated from the spoon during the casting of the sample? The elimination of hydrogen in this way seems to be dependent on the degree of metal turbulence during casting which, in the case of hand spoon used, may in fact be different for each individual sample.

In addition to the previously mentioned chilling action of aluminum and possible evolution of hydrogen, another fact concerning the specific property of aluminum is known in practice: namely, that aluminum helps to eject the hydrogen from fluid steel.

It seems then that it would be desirable to find out whether there is any difference in hydrogen content in the samples taken directly

^{*} H. H. Robertson Company.

from the furnace by vacuum sampling and those taken by spoon sampling. This would reveal the influence of the sampling methods on the hydrogen contents in the samples. Furthermore, it would be desirable to ascertain whether there is any difference in hydrogen contents between rimmed samples, samples killed by aluminum, and those killed by any other deoxidizer such as silicon.

It is fully realized that relative errors should be taken into consideration in any investigation but when the variations obtained on samples taken 10 min. apart show a difference of 100 pct and more, a certain fear about the accuracy of the sampling seems to be justified. It is hoped that the authors will convince us that they chose the correct way of sampling.

Passing to the interpretation of the results, it can be noticed that all the heats showed an increase of hydrogen before tap, after they had been killed. Would this not indicate that the hydrogen content in fluid steel depends first of all on the quantity of dissolved FeO and that the relationship between H_2 , H_2O and FeO dissolved in steel plays an important part in the elimination or absorption of hydrogen? If this is the case, and in practice we have all indications that it is, then the quantity of FeO dissolved in steel depends not only on the carbon content but also on the temperature of the fluid bath and the quantity of such elements as Mn, particularly in basic processes.

In other words, when all the other conditions of the fluid bath are constant, the quantity of dissolved FeO in the fluid steel depends only on the temperature. The higher the temperature, the more FeO is dissolved and the less hydrogen is contained in the steel. It would be very desirable then that the graphs of furnace practice contain the temperature and the quantities of oxygen kept during the entire melting and the change in the quantity of manganese on all the heats investigated.

In our practice, we found the temperature factor so important that, in some cases, the simple overheating of the heat eliminated the hydrogen to the contents assuring a sound heat. Although somewhat contrary to the general belief, we definitely found that cold melted or cold worked out heats contained much more hydrogen than heats melted and worked out hot. Heat No. 41 shows tapping temperature at $3150^{\circ}F$, which should be considered as high.

This heat also shows the lowest hydrogen contents at the tap.

Finally, we do not quite agree that in order to obtain heats with a low hydrogen content, a strong oxidizing boil is required. The charge can be melted with a low hydrogen content and by the proper operation of the furnace, this low hydrogen content can be maintained. From an economical point of view, this factor is important as by eliminating the boiling period, a heat is shorter by at least one hour.

For instance, hot melting with lower initial carbon, which assures high residual oxygen contents, together with recarburizing the heat just before tap would give the same hydrogen contents as those found in the investigations, if not lower. In fact, the authors' own investigations seem to indicate that the acid heats melted to low initial carbon show lower initial hydrogen contents. This phenomenon would be more plainly visible if instead of melting to about 0.20 pct C, the heats were melted to about 0.1 pct C. One heat, No. 41, melted to 0.70 pct C, showed the lowest initial hydrogen but 6 min. later, the quantity of hydrogen found was almost 250 pct higher although a violent boil occurred at that time. It seems as though the figure of the initial hydrogen, in this particular case, could be questioned.

Another way of eliminating hydrogen in commercial conditions is to bubble the fluid steel with natural gases. Here too, the method seems more economical than boiling and it would be desirable to investigate its quantitative side.

All the above remarks should not be considered as a criticism of this work. We fully realize the difficulty of the problem involved. We mention some additional factors, which were not taken under consideration, for the purpose of pointing out the variety of methods which are used in practice to obtain steels containing the lowest possible quantity of hydrogen. We indeed would like to know which method is the most effective. This can certainly be found by the institution and authority which Dr. Sims represents and we strongly believe, knowing Dr. Sims from his previous works, that sooner or later he will give us a definite statement concerning the mechanism of the absorption and elimination of hydrogen and the most effective way of fighting against this cancer of steelmaking.

G. A. MOORE (authors' reply).—We are pleased that Mr. Ascik finds that the conclusions of this paper have been recognized for some time by many steelmakers, but feel that he thus places himself in a select minority which has so far been unsuccessful in selling these conclusions to the *average* steelmaker. It is true that all of our conclusions have been previously obtained by inference from other studies, but regrettable that even more direct quantitative evidence than was gathered for this paper is necessary before we have a right to expect these conclusions to be universally acceptable in the industry.

Mr. Ascik's remark to the effect that regulating the boil rate does not solve the problem emphasizes the first conclusion of the paper while ignoring the second. The heats 14, 18, 22 and 27 differ widely in duration of boil and time from boil to tap, as shown in part by the two for which logs are reproduced. They also represent a complete range of ladle conditions. The rates of removal of hydrogen shown in Fig 15 illustrate a spread at the same rates of boiling, but this is largely eliminated if the proportion of hydrogen eliminated is plotted as the vertical coordinate. We do not wish to imply, however, that the proportional elimination of hydrogen depends only on the rate of boil, since there is also the opposing rate of new hydrogen absorption which varies with the composition and the atmosphere. The point that we did not treat the basic furnaces favorably in the discussion is entirely ascribable to the fact that we did not find a basic furnace being operated in the high range of carbon elimination rates used in the arc furnaces. We would be very glad to have data on such heats. In fact data on many more heats are necessary before final conclusions may be drawn.

Data on the hydrogen contents of the end products from many of these heats are in the general report from which this paper was taken, and will appear in the forthcoming paper on hydrogen and ductility.

For several paragraphs Mr. Ascik anticipates another forthcoming report with Dr. Derge, which will cover in detail the accuracy and errors of the analytical methods. In essence, the ordinary error in sampling is not more than 0.01 relative volume under the technique ordinarily used in this work. This error probably is a loss in most cases. Mr.

Ascik's comments on all the things which could go wrong are well taken. We found that the accuracy of the sample varies considerably with the skill and interest of the melter whose furnace is being sampled. In one plant, duplicate samples checked to about 0.002 relative volumes, but in some other cases there were marked differences in the rate of pouring successive samples. Some logs taken under poorer conditions were remarkably uninformative and therefore do not appear in the paper. In the logs which are reproduced, we believe that the great majority of points are correct to 0.01 relative volume, but a small number may be in considerable error from undetected variation in procedure. No conclusions were drawn unless an effect was detected in several heats. Such sudden changes as the increases of hydrogen due to wet ladles and to blocking of the heat were detected on many occasions.

We agree with Mr. Ascik that more work is now needed on sampling methods than on further refinement of the analytical method. We must however take exception to certain of his specific statements. The addition of aluminum in amounts used for killing does not lower the temperature of steel, but rather raises it as a result of the high heat of combustion of the aluminum with the oxygen in the steel. Reladling and pouring often can cause hydrogen elimination provided that the heat is live, that is that it contains dissolved carbon monoxide in a quantity sufficient to exert an equilibrium pressure which is more than one atmosphere but less than enough to start bubble formation. The writer has seen no case of hydrogen elimination from an aluminum killed heat except for the possible example of a condition where atmospheric oxidation has progressed beyond the point of consuming all of the residual aluminum metal. The statement that aluminum helps to eject hydrogen from fluid steel in practice is directly contrary to all the analytical evidence collected on aluminum and silicon steels in this work. Data on the hydrogen contents of solid steels of these types will be included in the forthcoming paper previously mentioned.

It is probable that the reactions between Fe, FeO, H₂, H₂O, Mn, and others in the steel and slag play a part in the hydrogen problem as stated by Kobayashi (Ref. 6). Complete slag and metal analyses corresponding to every

hydrogen sample were obtained for heats 35 and 36 and shown in the original report, but as no relationships could be discovered, these are not included in the paper. It appears that the expected equilibrium is never obtained and the actual values found in ordinary furnaces depend on rate factors which are not closely related to the equilibrium conditions. We are unable to separate the effect on manganese as an element from the completely simultaneous effect of ending the boil. We did find in all cases where the temperature record was good that an increase of temperature invariably was accompanied by an increase in the dissolved hydrogen. This agrees both with the increasing solubility of hydrogen when applied at constant pressure and with the fact that water is more completely decomposed by iron as the temperature is raised. Mr. Ascik's finding that an increase of temperature eliminates hydrogen is inexplicable to us unless his heating induces a boil. His quotation of our heat No. 41 as supporting evidence is entirely inappropriate

since this is the heat that was specially processed by boiling continuously at 1.0 pct carbon loss per hr almost to the moment of tapping. Our hottest heat was No. 35, which burned completely through the bottom of the ladle about 2 min. after pouring. This heat had a ladle analysis of 0.42 relative volumes, the highest encountered. Fig 10 shows that this heat had practically no boil. It is quite possible that some of the initial hydrogen values are in the group of lowest accuracy as the heats often were not well mixed at this stage. No correlation was claimed between initial hydrogen and initial carbon and it does not appear that Mr. Ascik discovered one.

There is no doubt that bubbles of other gases, besides the carbon monoxide bubbles from natural boiling, are effective in helping to remove the hydrogen. Referring to gas sweeping treatments as artificial boiling gives a good implication of the effects to be expected. A separate investigation of this process has in fact been conducted and may form the subject of some future paper.

The Effect of Hydrogen on the Ductility of Cast Steels

By CLARENCE E. SIMS,* GEORGE A. MOORE,† MEMBERS AIME, AND DONALD W. WILLIAMS*

(San Francisco Meeting, February 1949)

INTRODUCTION

DURING the past several years, the steel casting industry has made studies of heavy castings in which the test bar has been taken from heavy sections rather than from attached or separately cast coupons. It has been noted that the ductility properties of these heavy sections are often lower than those normally expected. Such lowered ductility is usually accompanied by a spotty test bar fracture, and the ductility values can often be greatly improved if a low-temperature aging treatment is given to the casting. A loss of ductility of this type is considered "abnormal," since it is not accompanied by an increase of tensile strength or hardness, and "temporary" when the ductility can be restored by aging. The cure of such an abnormal condition represents a real improvement in the quality of the steel.

Several types of abnormal loss of ductility can be distinguished, of which those caused by excessive amounts of inclusions of undesirable type and those caused by unsuitable grain size and ingot structure are well known. The particular type of abnormal lowered ductility currently under consideration may be distinguished by the

fact that the low-temperature aging treatment necessary for its relief is insufficient to cause any visible change in the microstructure as ordinarily observed. As this aging will in fact eventually occur at room temperature, the phenomenon of present interest may be given the symptomatic definition, "Temporary Abnormal Low Ductility."

Some hundreds of previous investigations, largely qualitative in nature, have established, beyond reasonable doubt, that hydrogen is normally present in newly manufactured steel and that this gas, in small amounts, can cause a temporary abnormal loss of ductility. The commonly observed association of high gas content and low ductility has given strong evidence for the presumption that hydrogen, possibly assisted by other gases, is the primary cause of the low ductility observed. Accordingly, The Steel Founders' Society of America has, since Nov. 1, 1944, sponsored investigations at Battelle Memorial Institute whose primary objective is to obtain quantitative information on the relation of the amount of hydrogen and nitrogen in steel, together with associated methods of steelmaking and treatment, to low-ductility effects and porosity.

The interest of this investigation thus extends to permanent abnormal losses of ductility, such as are caused by the inclusions which sometimes result from special deoxidizing practices and possibly from metallic nitrides, but as these can be distinguished from the temporary effect of hydrogen, they have been excluded from the work reported here except when they

This article sets forth the results of research conducted by Battelle Memorial Institute and supported by the Steel Founders' Society of America. Copyright 1947, by the Steel Founders' Society of America.

Manuscript received at the office of the Institute May 26, 1948. Issued as TP 2454 in METALS TECHNOLOGY, October 1948.

* Assistant Director and Research Engineer respectively, Battelle Memorial Institute, Columbus, Ohio.

† Assistant Professor of Metallurgy, University of Pennsylvania; formerly Research Engineer, Battelle Memorial Institute.

appear as interfering factors. The nitrogen content of the commercial heats has been followed in detail, but since the nitrogen content has, in all cases, been small and has been shown to be unchanged on aging, the possible effect of nitrogen on ductility has been only incidentally considered. Aging as a means of obtaining lowered hydrogen content has been freely used throughout the work on ductility, but the quantitative investigation of the rate of progress of aging will be only briefly mentioned.

In order that these investigations might proceed on a quantitative basis, hydrogen analyses of a precision considerably higher than any previously reported in the literature were necessary. The method chosen was selected entirely on the basis that it had the highest probability of freedom from uncontrollable errors and has been described in detail in another publication.¹ Briefly, the method used consisted of the hot extraction of solid pieces of steel weighing from 45 to 50 g in a highly evacuated quartz tube maintained at 1050°C (1925°F) for a period of approximately 40 hr. The greatest precautions were taken to eliminate blanks and insure a sound gas collection system. Vacuum and temperature conditions were automatically maintained. Mercury-filled risers were used for the introduction of samples in order that the system could be thoroughly degassed in advance and samples introduced without contamination of the system with air. From periodic records of the amount of gas evolved, an allowance, about 3 pct, was normally made for the residual hydrogen at the end of the extraction process. For the determination of the gas content of liquid steel, chill-cast cylinders of 5/8-in. diam and 1.25-in. length were made in copper molds. The mold provides a feeder head of about 1-lb capacity, separated from the sample by a pierced ceramic disk or "Washburn Core" in order

that a rapidly cooled sound sample is obtained under all normal conditions. Samples were removed from the mold and broken or cut from the head and stored in closed tubes over mercury, pending analysis. The time before storage was generally approximately 3 min. and the time until the first appearance of a gas bubble usually about 10 min. The precaution of storing over mercury proved essential in all cases, not only of cast samples but of similar pieces turned or sawed from castings after additional treatment. Reported analyses include the hydrogen evolved both at room and elevated temperature, together with the small residual allowance previously mentioned.

In all discussions and plots in this work, hydrogen analyses are given in "relative volumes" (R.V.) in which one R.V. represents an amount of hydrogen which, when measured at 0°C (32°F) and standard atmospheric pressure, would occupy the same space as the amount of steel analyzed when in a form free of porosity. This unit is most convenient since it is the one most easily visualized, is independent of the system of measurement, and resulting figures are of convenient magnitude. Conversion factors for considering other reports are:

$$0.001 \text{ wt. pct} = 0.874 \text{ R.V.}$$

$$1 \text{ R.V.} = 0.00114 \text{ wt. pct}$$

$$1.0 \text{ cc per 100 g} = 0.0786 \text{ R.V.}$$

$$1 \text{ R.V.} = 12.72 \text{ cc per 100 g}$$

The precision of the analytical method used, when starting with actually identical solid samples, has been established to be the precision of the analysis of the evolved gas, which is ± 0.004 R.V. The precision for liquid samples apparently is nearly as good under ideal sampling conditions, but for furnace samples taken with a slagged spoon and killed with aluminum and poured as rapidly as possible, an average error of ± 0.01 R.V. must be allowed. Checks of accuracy by comparison with other methods, which will presently be published

¹ References are at the end of the paper.

elsewhere, indicate that the analyses obtained are probably within 0.01 R.V. of the truth.

The work to be presented here is in three sections. Section 1 will give a brief resume of the more impressive publications on the same subject which have come to the writers' attention during the period of the work. Section 2 will describe work leading to the deduction of the quantitative relationship between hydrogen content and ductility. Section 3 will give a brief introduction to the problem of determining the relationship between aging time and temperature and the change of hydrogen and ductility in various sizes and types of castings. Inasmuch as the complete details of these experiments can not be encompassed within the limits of a single paper, only the most instructive will be given in the paper proper while the more extensive details will be relegated to an appendix which will be made available from Battelle Memorial Institute in the form of Recordak film.

A portion of this work, previously presented at the Fifth Electric Furnace Conference,⁸ showed that the normal hydrogen content of commercial steel, as poured from the furnace, was in the range of 0.20 to 0.30 R.V. It will be shown in this paper that a portion of the hydrogen content of liquid steel may be lost during certain casting procedures, and also that the hydrogen concentration may sometimes be increased in certain portions of castings as a result of segregation. As it will also be shown that the range in which ductility losses are shown is mainly from 0.10 to 0.40 R.V., it may readily be seen that the amounts of hydrogen present during commercial steelmaking are coincident with the amounts of most interest with respect to ductility.

ACKNOWLEDGMENT

The writers wish to express their most sincere appreciation for financial support

of this work to the Technical Research Committee of the Steel Founders' Society of America, Charles W. Briggs, Technical Director, and for continuing advice and assistance in correlating the work with experience within the steel castings industry. Thanks are extended to: The American Steel Foundries, The Bonney-Floyd Co., Buckeye Steel Castings Co., General Steel Castings Corporation, National Malleable and Steel Castings Co., and The Ohio Steel Foundry Co. for their cooperation in collecting specimens for hydrogen analysis and for providing material for the ductility experiments. The writers wish to acknowledge the capable assistance of M. W. Mallett, C. L. Tyo, and Mrs. Martha E. Murphy of the Battelle staff in connection with the analytical work on hydrogen.

SECTION I—REVIEW OF RECENT LITERATURE

Since the manifestations of hydrogen in steel have attracted very wide interest and led to a vast number of discussions in all quarters, the writers make no pretense of having examined all such efforts. The literature up to 1944 was examined in some detail in other publications of the writers.²⁻⁶ It is necessary here to examine only a few publications of special interest which have recently come to the writers' attention and to re-examine a few whose significance has only become apparent in the light of the experimental work.

In recent publications, the most generally accepted hypothesis for the behavior of hydrogen in steel has been outlined as follows: The hydrogen contained within a piece of steel is normally in three portions, first, that in true solution in the lattice; second, a portion in excess of that which can be in true solution and which has precipitated and diffused into blowholes and other major openings; and third, a portion which has been rapidly precipitated and has been unable to diffuse far from the

point of precipitation. Of these, only the third portion is effective in altering such properties as the ductility; hence, the effect of a specified amount of hydrogen will vary with the history of the steel. The adverse effect of the hydrogen arises from the fact that at low temperature the decomposition pressure of the solution reaches the same magnitude as the strength of the steel, thus forcing the precipitated gas into microscopic openings, within the grains, variously termed "rifts," "lattice dislocations," or "mosaic disjunctions." The combined effect of the interruption of the lattice structure and the triaxial tensile stresses set up to balance the gas pressure effectively prevent the normal deformation processes.

On the quantitative side, very little reliable information has appeared either on the amount of hydrogen associated with lowered ductility or porosity or on the amount normally present in commercial steel. From equilibrium measurements of the amount of hydrogen dissolved at one atmosphere pressure, it was known that the amount of hydrogen which might be contained in liquid steel just prior to freezing is about 2.2 R.V. and the amount in solid steel just after freezing about 1.0 R.V. From numerous qualitative tests, it could be presumed that the hydrogen content necessary to cause porosity might be of the same order. In austenite, the solubility decreases with temperature from 1.0 R.V. to 0.4 R.V. at the transformation, and there is evidence that steel saturated with hydrogen in this temperature range is subject to shatter cracking. The solubility in ferrite falls from 0.2 R.V. just below the transition to unmeasurable amounts below 350°C. Qualitative experiments had shown that steel saturated with hydrogen at and immediately below the transition showed markedly impaired ductility. Actual analyses of hydrogen in either liquid or solid steel were apparently so variable as to shed practically no light on the amount normally

present. The solubility of hydrogen in most alloying elements was known, and there was some evidence that the solubility of hydrogen in alloy steels would usually be intermediate between that in pure iron and that in the alloying element. Alloying elements were also considered to affect hydrogen behavior by their effect on the austenitic field and the possibility was entertained that hydrogen might interact with inclusions and precipitated phases. It was believed that the hydrogen content of steel during manufacture might be anything up to around one relative volume and it was known that some portion of the original content normally diffused away as the fresh steel aged. It was presumed that moisture in the furnace charge and moisture and hydrogen in the furnace gases were important sources of hydrogen and that the boil in the furnace and the rimming of ingots tended to reduce the amount of this gas. In the work previously reported, the effect of moisture in the atmosphere and in the ladle was measured. The strong boil was found very beneficial in reducing hydrogen. The normal range of hydrogen in the commercial furnaces was found to be 0.20 to 0.30 R.V. in the absence of special precautions.

Recent British experimenters use the chill-cast pencil sample, storage on dry ice, and warm extraction analysis as tested by Wells and Barraclough⁷ who have established an accuracy of ± 0.05 R.V. Sykes, Burton, and Gegg⁸ thus find the average content of open hearth steels at tap to be 0.30 R.V. Arc-furnace carbon steels average 0.32 R.V., while steels in the 3-5 pct alloy range show 0.37 to 0.62 R.V. of hydrogen. Several "wild" heats of alloy steels gave hydrogen analyses from 0.7 to 1.3 R.V. These investigators expected the hydrogen content to be lowered by boiling, but did not detect the effect, apparently because they tried to correlate hydrogen with the length of the boil rather than with the intensity.

In the field of the effect of alloys, Hung, Beaver, and Floe⁹ find that the addition of silicon to iron decreases the hydrogen solubility. Miss Armbruster¹⁰ is apparently responsible for the observation that the effect of certain alloys on the solid solubility of hydrogen may be expressed by their effect on the proportion of retained austenite. This ties in exactly with the measurements of Andrew et al^{11b} that the rate of evolution of hydrogen from steel is very closely related to the changes in transformation temperature caused by the alloys present.

Segregation of hydrogen during freezing was discussed by Larsen¹² but was not detected by Sykes et al,⁸ because no tests were made near the surface of their ingots. Segregation during transformation in the last portion of austenite is noted by Andrew^{11a} but the concept of a "hydrogen-rich constituent" has been abandoned.^{11b}

Several new qualitative observations of the effect of hydrogen on ductility have appeared.¹³⁻¹⁵ Sykes⁸ and Andrew¹¹ give hydrogen analyses and ductility for the same samples. Sykes finds lowered ductility above 0.16 R.V. but finds the effect to vary erratically and with composition, heat treatment, and direction in the billet. Andrew finds embrittlement at 0.10 to 0.30 R.V. Neither finds a regular relationship of ductility to hydrogen, but it may be noted that if Andrew had eliminated the effects of composition and heat treatment from his data by plotting the true breaking strength on the reduced area as given in Ref. 11b, a quite regular loss of ductility from 0 to 0.30 R.V. of hydrogen would have appeared. Sykes finds that aging redistributes the hydrogen in less harmful form. Andrew notes that a portion of the hydrogen cannot be removed at low temperature and that the effect on ductility is greater in a heterogeneous than in a homogeneous structure. The current visualizations of the action of hydrogen held by Andrew and by Portevin¹⁶ are indistinguishable from the

mechanism outlined at the beginning of this section.

SECTION 2—EFFECT OF HYDROGEN ON THE DUCTILITY OF CAST STEEL

Outline of Experiments

While numerous prior experiments have demonstrated the existence of a connection between a temporary abnormal loss of ductility and the hydrogen content of steel, attempts to show this relation quantitatively have been greatly complicated not only by inaccuracies in measurement but by the interfering effect of permanent ductility changes associated with differences in structure, composition, or thermal history of the various specimens. It has been found that hydrogen is often highly segregated; hence, additional difficulty arises from the possibility of differences between the samples tested physically and adjacent portions of metal which may be analyzed. It must, therefore, be allowed that the true effect of hydrogen can only be seen in the average behavior of many samples and that individual tests may, in many cases, appear contrary to the general trend.

The tests covered in this section consist primarily of the preparation of samples of solid cast steel having different hydrogen contents, while being as nearly as possible similar in other respects, followed by simultaneous determination of the tensile properties and hydrogen analysis of closely adjacent portions. Impact tests were included in some cases. Such tests upon normalized samples permitted the plotting of correlation bands from which the average effect of hydrogen on ductility was determined. To establish the temporary nature of this ductility loss and to estimate the interfering effects of permanent abnormal ductility losses such as those resulting from inclusions, duplicates of the normalized samples were given arbitrary aging treatments similar to those used commercially, and tested in the same manner as the

normalized samples. An unforeseen result of these tests was that the average effect of the firmly held hydrogen retained after aging was found to be proportionally greater than that of the total hydrogen originally contained.

In the first series of specimens, from nine 4- \times 4 in. laboratory ingots of Grade B steel, hydrogen variation was obtained by variations in melting practice and by segregation of hydrogen in the ingot. The latter amounted to a ratio of about eight to one between samples from the center and corner positions. Heats 10 and 11 were melted under air, while the hydrogen contents of Heats 8, 9, 12, and 13 were modified by treatment with nitrogen, argon, ammonia, and dry hydrogen, respectively. Three additional heats, Numbers 15, 16, and 17, were treated respectively with dry hydrogen, wet hydrogen, and wet hydrogen followed by argon. The treatment of these last three heats caused an unplanned lowering of the carbon content and consequently a different range of ductility values.

A second series of specimens was obtained by taking samples from three positions within 6- \times 6- \times 12-in. sand-cast blocks, where the thermal gradients were less than those in the ingots. Heats 21, 25, 26, and 27 were, respectively, an aluminum-killed laboratory Grade B steel, a silicon-titanium high-tensile basic open hearth steel, a silicon-killed Grade B acid arc furnace steel. Heat 21 was compared as to hydrogen analysis only with Heat 20, a silicon-killed laboratory heat which developed too much porosity to allow tensile testing.

Further tests of correlation of ductility to hydrogen, in the aged condition only, were made on 4- \times 4-in. and 1- \times 1-in. keel block coupons from Heat 34, an aluminum-killed manganese-titanium high-tensile acid arc steel in which the hydrogen content was varied by aging for periods up to 256 hr at 400°F and to 19 months at room temperature.

Data on these fifteen heats not speci-

fically covered in the discussion to follow will be found tabulated in the Appendix.

Effect of Nitrogen

Twenty-seven normalized samples from three positions within the ingots of Heats 8 to 13 and 15 to 17 were analyzed for total nitrogen by the modified Kjeldahl method and for loosely combined nitrogen by hot extraction. While the free portion was often somewhat greater at the center of the ingots, this trend was not regular and the amount of free nitrogen was, in most cases, quite small as compared with the hydrogen present. The total nitrogen analyses, ranging from 0.005 to 0.012 wt pct, revealed no segregation. When these nitrogen analyses were plotted against ductility values, there was no evidence of any correlation.

Analyses on similar samples which had been aged for 25 hr at 700°F in the form of 1.5-in. square bars showed that the loss of nitrogen by aging was insignificantly small. Nitrogen analyses made in the other series of experiments likewise failed to show any important change upon aging.

It may, therefore, be concluded that nitrogen, in the amount present in these steels, plays no significant part in the temporary abnormal loss of ductility under consideration. This observation is not to be taken as contradicting the presumption that metallic nitrides may join with the other inclusions present to give permanent abnormal losses of ductility, or that larger amounts of nitrogen might be more significantly affected by aging at an elevated temperature.

Effect of Deoxidation Practice

It had been commonly observed within the industry that the use of some of the deoxidizing practices, especially those employing aluminum, often resulted in lower ductility. It was widely believed that these deoxidizers reduced the rate of aging of castings. While it was well known that

aluminum could increase the amount of harmful inclusions and cause the formation of the least desirable types, thus giving permanent abnormal losses of ductility, it was not inconceivable that the inclusions associated with special deoxidizers might affect the amount of hydrogen retained in the steel or influence its distribution.

To determine whether aluminum in fact affected the hydrogen content, three normalized and eleven aged bars were analyzed from each of Heats 20 and 21. Both melts had been treated with wet hydrogen to give essentially identical contents of 0.36 and 0.37 R.V. Heat 20 was incompletely killed with silicon only, while Heat 21 was additionally completely killed with aluminum. The average hydrogen contents of the solid samples were identical for the two steels, although the radial segregation was somewhat greater in the aluminum-treated heat in accord with the probability that freezing was quieter. The eleven pairs of aged samples all gave hydrogen analyses agreeing within the limit of error of analysis.

The same procedure was followed in examining sixteen sets of samples from each of Heats 25, 26, and 27, which were, respectively, silicon-titanium, silicon, and aluminum killed. At the ladle, the H_2 content of the silicon heat was lowered, and the aluminum-killed heat higher than Heat 25. The high original position of the aluminum-killed heat was preserved in the normalized samples, but the side and center bars of the silicon-killed heat were higher than those of the silicon-titanium steel, so that in this example the silicon-killed steel had the greatest radial segregation. Comparing three similar bars for each of thirteen aged conditions, the three heats occupied the high hydrogen position with essentially equal frequency.

From these tests, it may safely be concluded that the different deoxidation practices do not affect the amount of hydrogen retained in the cast steel, its segregation during freezing, or the rate of diffusion of

hydrogen on aging. This does not rule out, however, the possibility of secondary effects such as an influence of deoxidation products on the hydrogen segregation in localized areas.

Effect of Hydrogen on Tensile Properties of Steel Cast as Ingots

The nine chill-cast ingots from Heats 8-13 and 15-17 were first normalized by holding for 2 hr at 1650°F and cooling in still air. Sufficient lengths for tensile bars, impact and gas specimens, were cut from the upper portion of each ingot well below the unsound metal of the hot top. These sections were split longitudinally in nine equal sections (approximately 1.5 in. square), of which the single center section was designated *A* position, the four sections lying along the sides of the ingots *B*, and the four corners *C*. One section of each type from each ingot was machined to produce a standard tensile bar, three V-notch Charpy impact specimens, and one gas analysis sample. Tensile tests were conducted in a standardized manner at a controlled speed of 0.018 in. per min., and in all cases, completed within 4 hr of the time of machining. Gas analysis samples were stored over mercury at the time of the physical tests. In this series, the Charpy values were all relatively good and showed no appreciable variation between samples of varying hydrogen content.

For the samples from Heats 8-13, correlations were found between each of the tensile properties and the hydrogen content. The effect of hydrogen on the elongation is shown in Fig 1. An average elongation of 24 pct in 2 in. at zero hydrogen is reduced at the rate of 5 pct for each 0.10 R.V. of hydrogen until a minimum elongation of about 4 pct is established at about 0.40 R.V. and higher.

The effect of hydrogen on the reduction of area, shown in Fig 2, is similar to that on elongation. An average reduction of area of 32 pct at zero hydrogen is reduced approxi-

mately 5.5 pct for each 0.10 R.V. of hydrogen, and again the effect becomes maximum at about 0.40 R.V. A downward trend was

confidence can be placed in the observation. Tensile-strength values were more regular and indicated a continuous downward

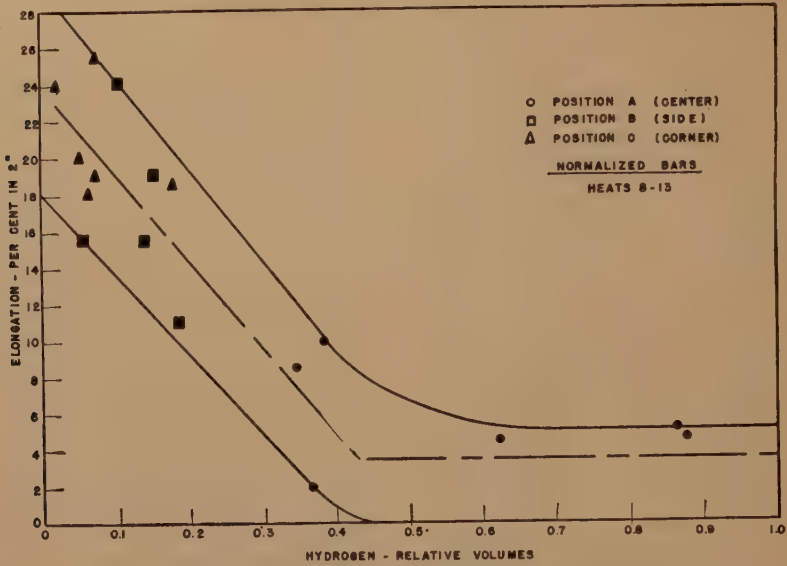


FIG 1—ELONGATION VS. HYDROGEN CONTENT.

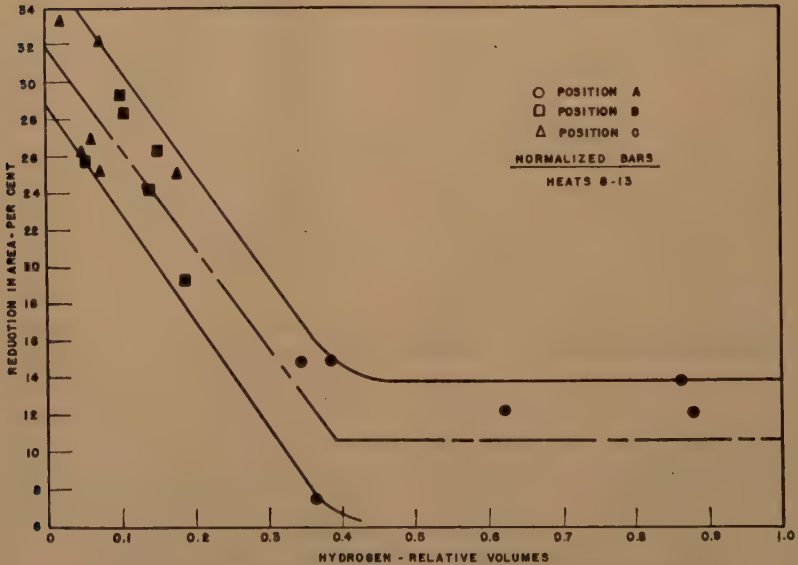


FIG 2—REDUCTION OF AREA VS. HYDROGEN CONTENT.

observable in the yield strength values, but the spread of the values was much larger than those for ductility and hence little

trend extending to a 45 pct loss from 80,000 psi at 1 R.V. As this trend includes the effect of differing cooling rates at the dif-

ferent sample positions, which is in the same sign on this property, the effect of hydrogen may be only a small part of the total.

percentage scatter here is only about half that of Fig 2, since effects due to variations in the cooling rate of the samples have been eliminated. The curve may be regarded as

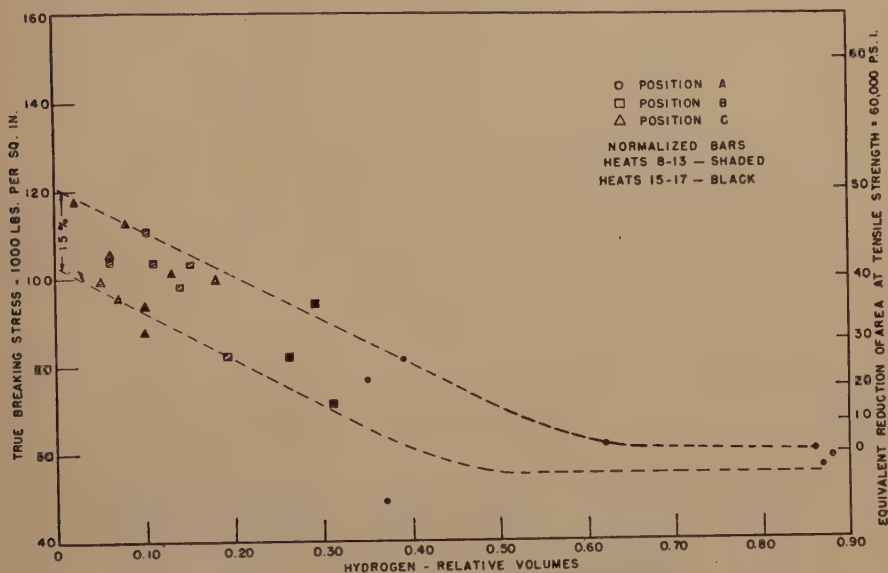


FIG 3—VARIATION OF TRUE BREAKING STRESS WITH HYDROGEN CONTENT.

In Heats 15-17, which had about 0.23 carbon instead of the 0.30 carbon of the heats above, elongation values were about 5 pct and reduction of area values about 10 pct above those in Fig 1 and 2, but, nevertheless, clearly showed the same trends. Slight downward trends of yield and tensile strength against hydrogen were detectable. In order to compare the ductility values of these heats with the previous group, it is necessary to have a measure of ductility relatively independent of carbon content. Most such measures which have been proposed are artificial in nature and of dubious significance, but it is quite commonly known that the true breaking stress, that is, maximum load divided by final reduced area, is nearly independent of ordinary variations of composition and heat treatment for a given class of steel. A plot of this quantity against hydrogen for all nine heats is shown in Fig 3. The

showing reduction of area corrected to an arbitrary tensile strength, as shown by the scale at the right of the plot, and on this basis it may be seen that hydrogen had an exactly equivalent effect on the heats of different carbon content.

By comparing Fig 3 with Fig 2, it may be seen, however, that the true breaking stress values indicate an adverse effect of hydrogen over and above the effect on ductility, since the effect of hydrogen continues in the range of 0.40 to 0.60 R.V., where ductility has already been reduced to a minimum value. A real effect of hydrogen on tensile strength must occur in this composition range. It is equally obvious that there was no continuing effect of hydrogen on tensile strength in the range of 0.60 to 1.0 R.V., since this would have appeared in the true breaking stress if real. It appears reasonable to conclude that of the 45 pct loss in tensile strength originally

correlated to hydrogen content, perhaps 10 to 20 pct may have been caused by hydrogen, while 20 to 35 pct was assignable to the lower cooling rate of central bars,

effects correlated to hydrogen were removed when the hydrogen was reduced.

The hydrogen contents of corresponding normalized and aged bars are compared in

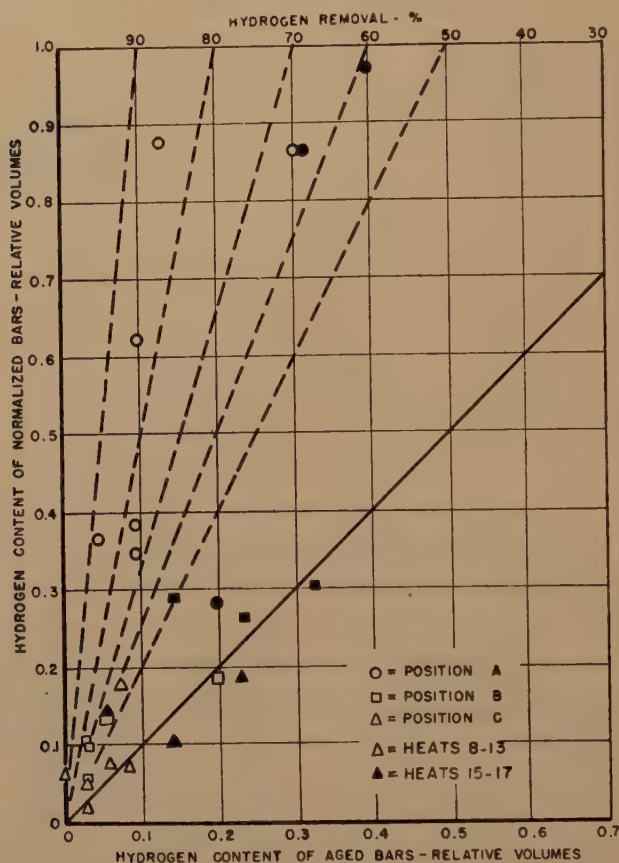


FIG 4—EFFECT OF AGING ON HYDROGEN CONTENT.

coincident with their higher hydrogen content.

Aging of Steel Cast as Ingots

Duplicates of the 27 bars whose properties have just been discussed were aged for 25 hr in the 1.5-in. square form at a temperature of 700°F. These are arbitrary conditions sometimes used commercially to reduce abnormal temporary losses of ductility. Gas analyses and tensile tests were made as before in order to determine if the

Fig 4. It may be seen that, with the exception of a few bars having relatively low original hydrogen content, all bars lost hydrogen on aging, but the amount lost varied from a few per cent to 85 pct with considerable dependence on the original hydrogen content.

As shown in Fig 5, aging almost always improved the elongation, and the improvement varied from 20 pct to 100 pct of the normalized values. For the 0.30 pct carbon steel, the final value seemed to reach a

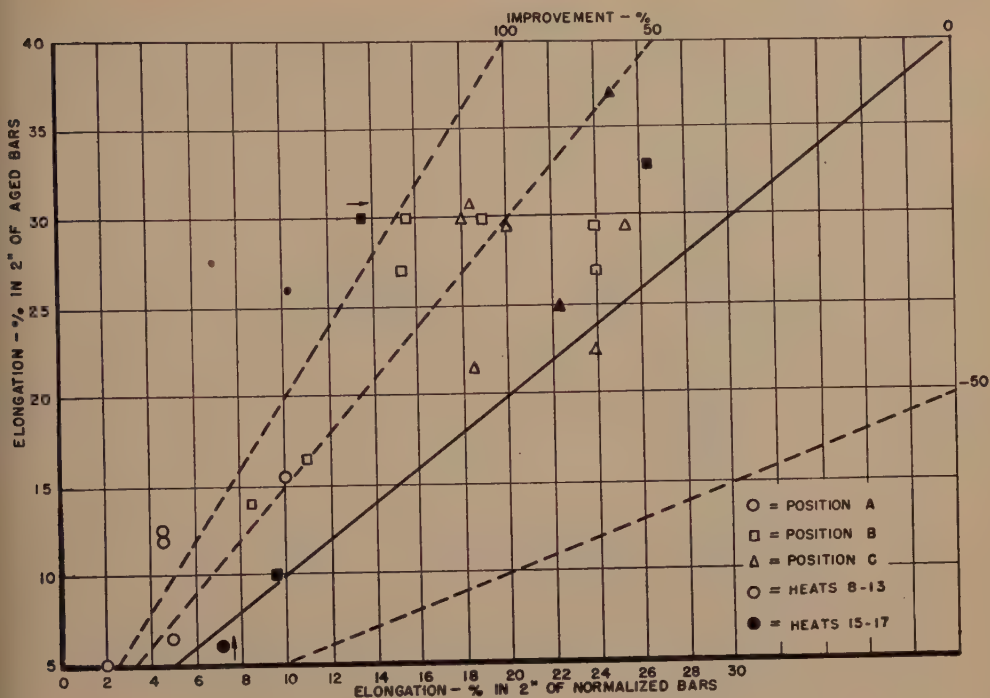


FIG 5—EFFECT OF AGING ON ELONGATION

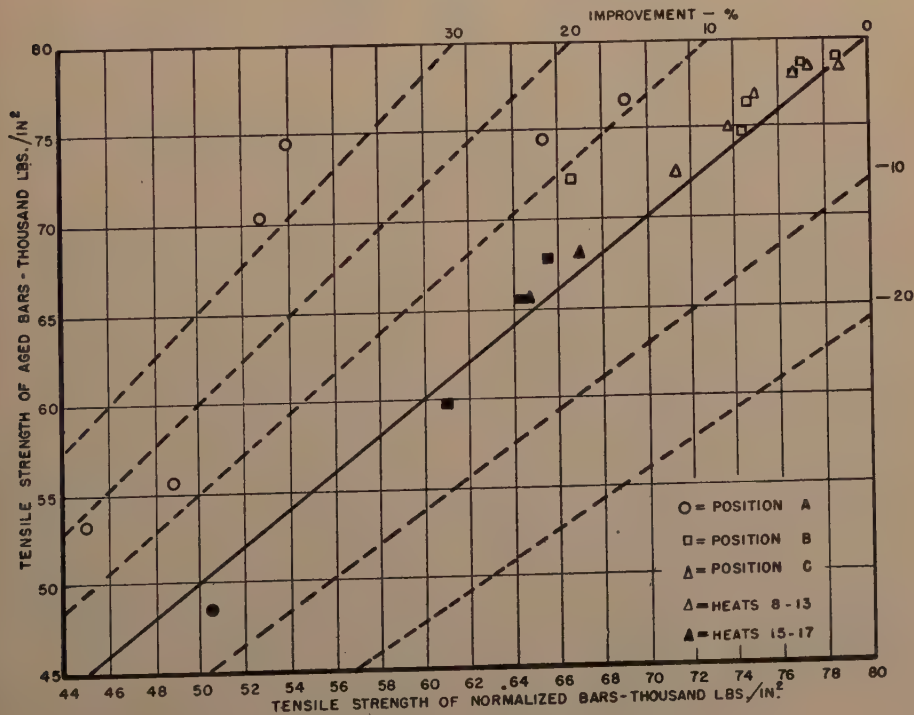


FIG 6—EFFECT OF AGING ON TENSILE STRENGTH.

limit of 30 pct elongation. The results on reduction of area were very similar to those on elongation and, therefore, are not illustrated. It may easily be seen that the over-

the tensile properties, but the uncontrolled losses of ductility due to permanent factors naturally assumed greater importance than in the normalized series. Such trends as

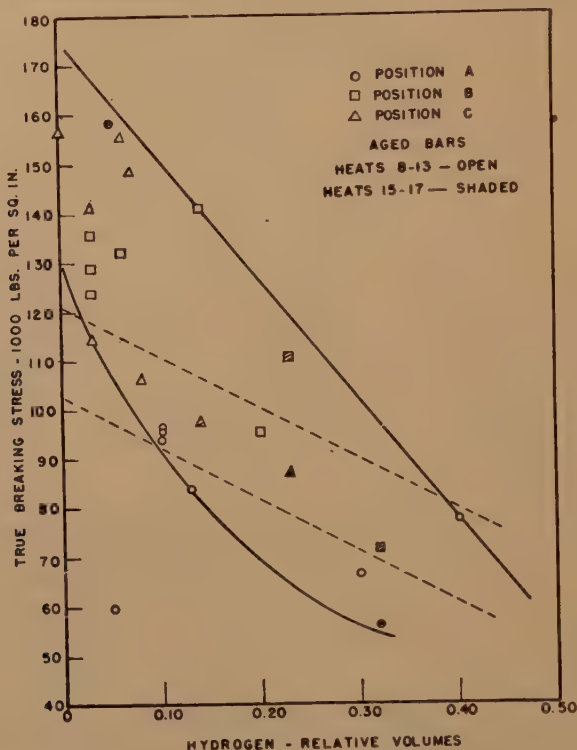


FIG 7—VARIATION OF TRUE BREAKING STRESS WITH HYDROGEN.

all effect of aging on hydrogen content and on ductility are very similar.

The improvement of yield strength on aging was not of particular importance. Aging had little effect on the tensile strength of bars cut from near the outside of the ingots, but Fig 6 shows that the tensile strength of the central bars increased from 10 to more than 30 pct in the 0.30 carbon steels, although it was not improved in the 0.23 carbon series. For the former, this supports the previous conclusion that at least a portion of the correlation between hydrogen and tensile strength was due to a real dependence.

After aging, some correlation remained between the residual hydrogen and each of

could be established indicated that the effect of a fixed quantity of hydrogen is greater when this hydrogen is the residue after aging, than when it is present in a normalized bar. Such regularity as remains in the values is best shown by the true breaking stress values in Fig 7, which may again be regarded as corrected ductilities. The dotted band shows the range occupied by the unaged samples. In spite of the increased spread, it may be seen that the properties of the aged bars change more rapidly with hydrogen than did those of the normalized samples, so that when the residual hydrogen is around 0.3 R.V., the aged bar can easily be inferior to a normalized bar with the same hydrogen content.

When the residual hydrogen is less than 0.10 R.V., however, the aged bar is usually much superior to a normalized bar of the same low hydrogen content.

four centrally located bars designated *A*, six bars along the sides and bottom designated *B*, and two bars from the lower corners designated *C*. Occasional duplicate

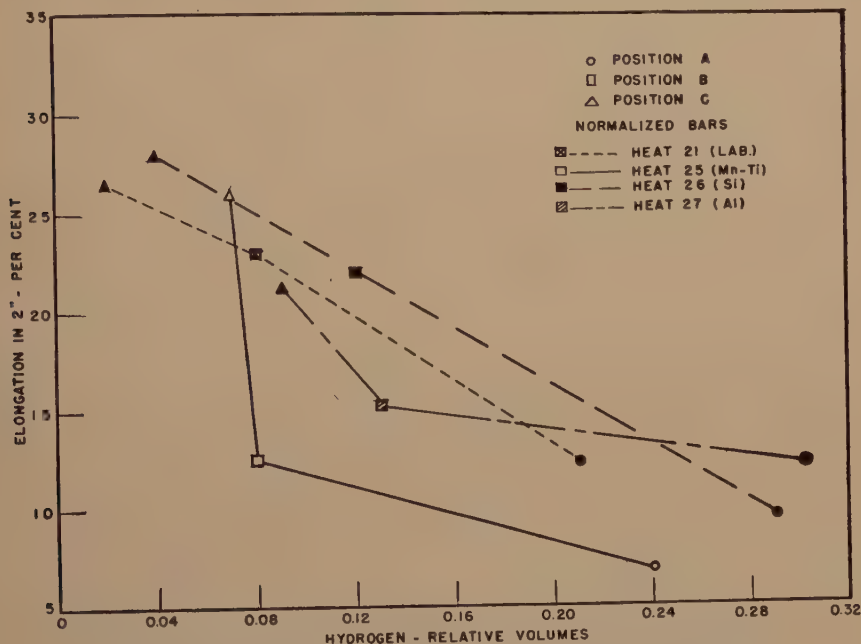


FIG 8—ELONGATION VS. HYDROGEN CONTENT. SAND-CAST BLOCKS.

Effect of Hydrogen on Properties of Steel in Sand-cast Blocks

Blocks, $6 \times 6 \times 12$ in., were cast in dry-sand molds from laboratory Heat 21 and commercial Heats 25, 26, and 27 as mentioned above. These were cast in the horizontal position under 9-in.-diam circular risers, so that the last metal to freeze was not included in the specimens as was the case in the ingot samples. Radial segregation of hydrogen and differences in cooling rates between samples were, therefore, much less than in the ingot samples.

After normalizing at 1650°F for 6 hr, each block was cut into 6-in. cubes which in turn were eventually subdivided into 16 horizontal bars 1.5 in. square by 6 in. long. The four bars at the top of the block, adjoining the riser, were discarded, leaving

tests showed that the bars in each group were similar in hydrogen content and properties but were not exact duplicates. One tensile and gas sample and impact samples were taken from each position in the normalized condition, while others were tested as aged 25 hr at 400°F in the 1.5-in. section, aged 96 hr in the 6-in. cube, both of these renormalized 1.5 hr at 1650°F in 1.5-in. section after aging, and renormalized 3 hr in $3 \times 3 \times 6$ in. section after aging. Special tests were made on a second block of Heat 27 to determine the agreement between similar samples and to determine the effect of renormalizing without intermediate aging.

The relationship of elongation to hydrogen content for normalized samples from the four blocks is shown in Fig 8. The observed lines for laboratory Heat 21 and

silicon Heat 26 are regular and parallel, showing elongation being lost at the rate of 7.5 pct for each 0.10 R.V. of hydrogen. The effect of unit hydrogen is thus 50 pct greater than in the ingot samples, but it appears reasonable that the slower cooled blocks may, in part, indicate the same phenomena which cause the unit effect of hydrogen to be much greater in aged than in normalized samples. The observations for the manganese-titanium heat, No. 25, are irregular, but if an average is taken, the trend is found at least as steep as for Heats 21 and 26. In the aluminum-killed heat, No. 27, the ductility available at zero hydrogen is apparently only about two-thirds that of the other heats, and the variation with hydrogen is much less. This heat contained numerous inclusions, mainly Type 3, which were apparently sufficient with other constitutional factors to account for a permanent loss of ductility of the magnitude observed. It appears that the temporary effect of hydrogen and the constant effect of constitutional factors acted as relatively independent limits on the ductility, which could not become high unless the specimen were relatively free of both types of limitation.

The change of reduction of area with hydrogen almost exactly confirms the observations for elongation. Heats 21 and 26 show regular lines which are almost parallel and indicate a reduction of area loss of about 7 pct for each 0.10 R.V. of hydrogen. As before, the slope is at least as great for manganese-titanium Heat 25, while aluminum-killed Heat 27 shows very little change with hydrogen content.

Heats 21 and 26 show no loss of yield strength with increasing hydrogen, while for Heats 25 and 27, the loss observed was so small that there is no certainty that it was real.

Heats 26 and 27 show a slight and uncertain decrease of tensile strength with increasing hydrogen, while Heats 21 and 25 show low tensile strengths in the central

bars which could possibly be due to structural differences rather than hydrogen. There was no definite change of impact values with changing hydrogen content in any of the four heats.

Aging of Steel from Sand-cast Blocks

Several samples from each position of each block were aged or aged and renormalized as described above. The loss of hydrogen in each case is shown in Fig 9 by plotting the analysis of the aged sample against that of the normalized sample from the same position. As in the ingot samples, the effectiveness of aging has been very erratic. Within the spread of observations, there is no evidence that the four heats aged at different rates, that renormalizing removed any additional hydrogen after aging, or that the arbitrary rule of 16 hr aging per inch of thickness favored either the large or small samples. Direct observations of renormalizing without aging, not plotted, showed some hydrogen loss at the high temperature when the original hydrogen was high.

The improvement in elongation on aging is shown in Fig 10 and makes a pattern very similar to that for hydrogen removal. Certain distinctions may be found, however, in the elongation pattern, notably that the improvement on the renormalized bars is not quite so good as on the aged bars without renormalizing, and especially that the improvement in aluminum-killed Heat 27 is only about half that of the other three heats.

The effect of aging on reduction of area was very similar to that on elongation, and again the renormalized bars showed a little less gain than those aged only, while the effect on Heat 27 was much less than on the others.

In contrast to the effect of aging at 700°F used for the ingot samples, aging at 400°F very seldom improved the yield strength of the block samples more than about 3 pct. On renormalizing, however,

improvements of 10 to 20 pct were common. The low-temperature aging had practically no effect on tensile strength, but when followed by renormalizing, many bars were

temperature treatment accomplishes only the elimination of a portion of the hydrogen content, while the higher temperature must also effect some slight rearrangement of the

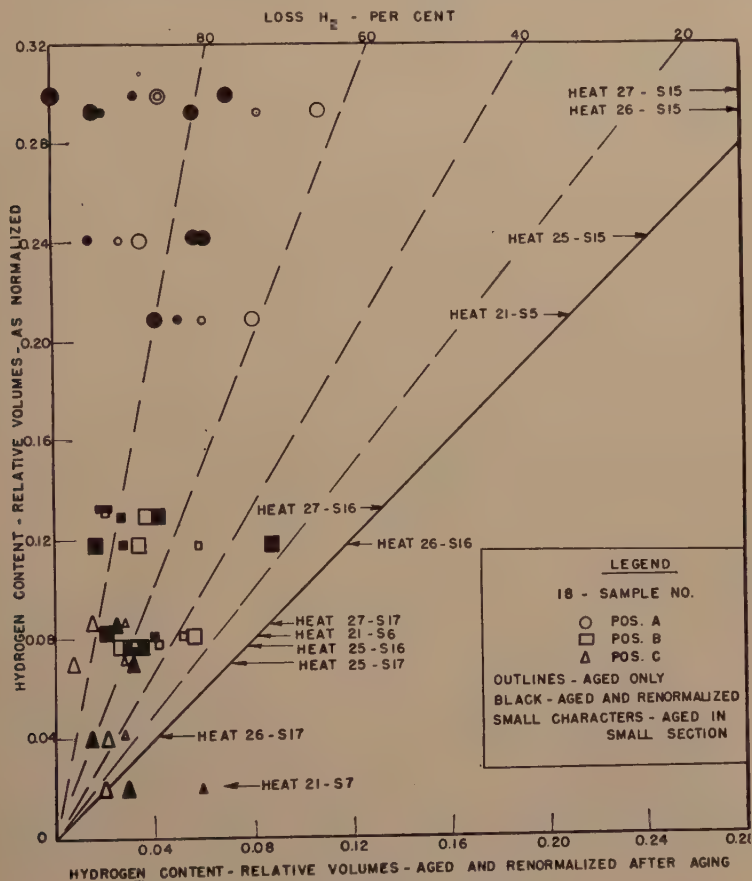


FIG 9—LOSS OF HYDROGEN AS A RESULT OF AGING.

improved 5 to 10 pct. The same effect was even more marked for the impact values. Most of these were improved less than 10 pct by aging alone, but a large proportion were improved 50 pct or more on renormalizing after aging.

The observations on yield, tensile, and impact strengths indicate quite clearly that the original aging test at 700°F contained the results of two actions which are separated by the use of lower temperature aging, followed by renormalizing. The low-

temperature treatment accomplishes only the elimination of a portion of the hydrogen content, while the higher temperature must also effect some slight rearrangement of the

Relation of Properties to Hydrogen after Aging

After aging, the increased relative importance of various factors having a permanent effect on ductility makes it difficult to observe a good correlation between hydrogen and the tensile properties. In most cases, however, a band of reasonable width

could be drawn about the original normalized ductilities which also included the ductility of samples renormalized after aging. Samples which were only aged,

two aged samples could not be included with the normalized group.

The bands for reduction of area are similar to those for elongation, except that a

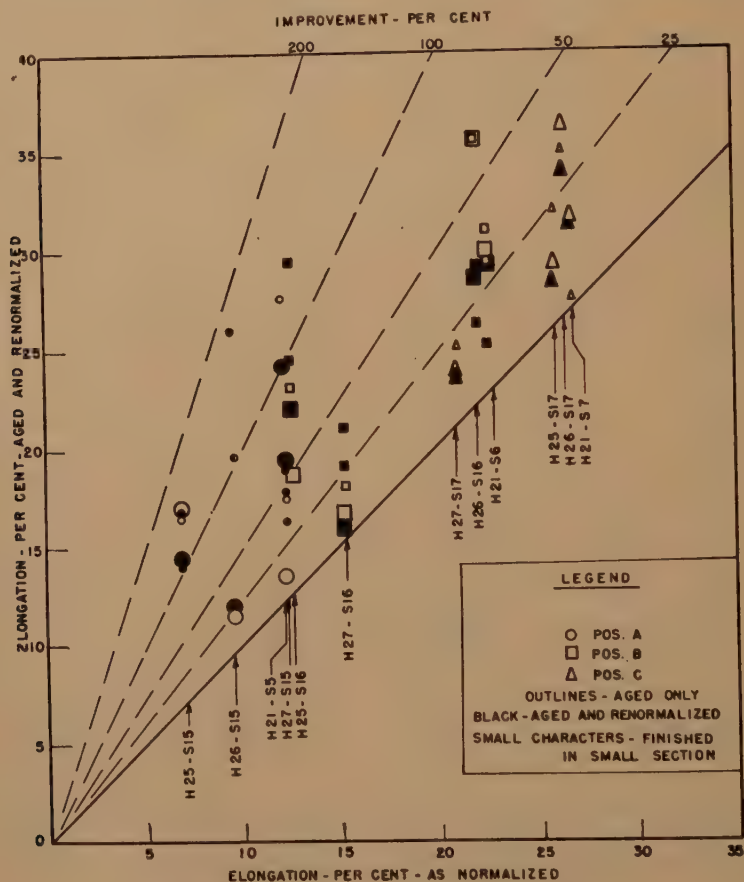


FIG 10—IMPROVEMENT OF ELONGATION BY AGING.

however, tended to fall outside these bands, being better at low hydrogen and worse at high hydrogen than the normalized groups. For elongation, Fig 11 shows the behavior of silicon Heat 26, which is typical. Laboratory Heat 21 gave almost identical results, while manganese-titanium Heat 25 was similar, except that there was stronger indication of an upward curvature when hydrogen was below about 0.06 R.V. Aluminum-killed Heat 27 gave a narrow and more nearly horizontal band and only

distinct upward curvature can be observed below 0.04 to 0.06 R.V. in each case. Results for the silicon heat are shown as Fig 12. Heat 25 again shows a greater change with hydrogen, and Heat 27 a very small change.

Yield, tensile, and impact strengths show no positive correlation with hydrogen after aging, but in each case, the values for samples which have been aged at 400°F remained close to those for the normalized samples. On renormalizing after aging, the

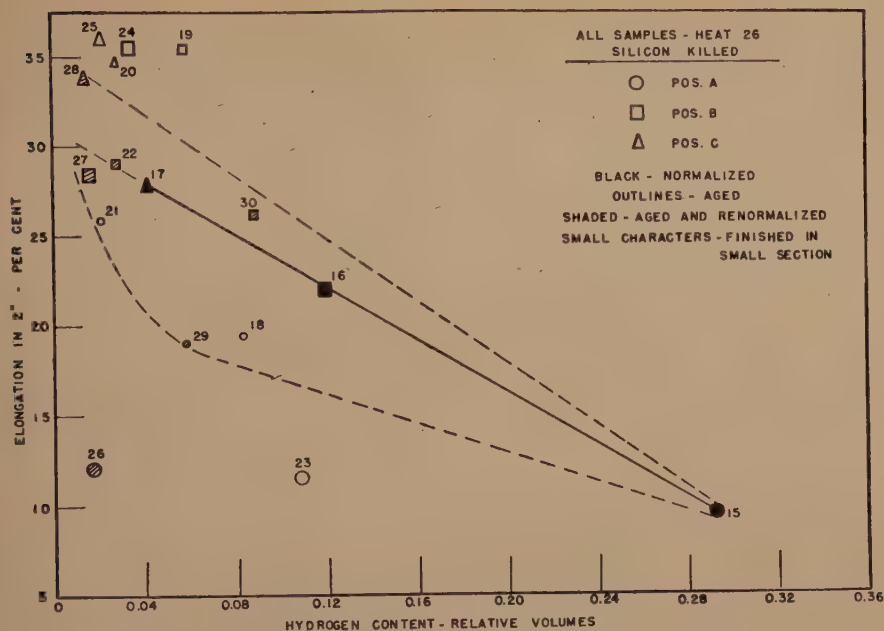


FIG 11—HYDROGEN CONTENT VS. ELONGATION IN HEAT 26.

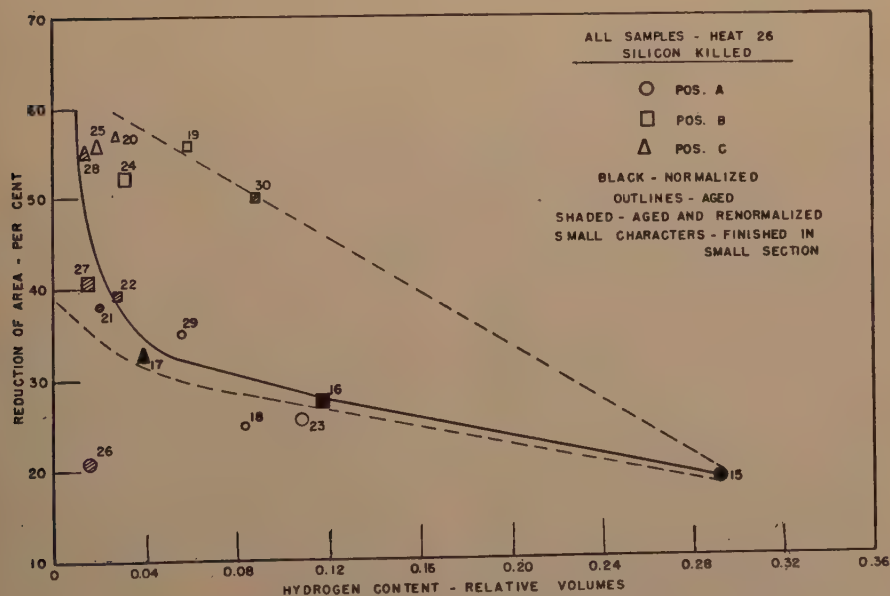


FIG 12—HYDROGEN CONTENT VS. REDUCTION OF AREA IN HEAT 26.

values of these properties nearly always fell distinctly above the range of the normalized or aged samples.

To determine the nature of the effect of

normalizing is a normal heat-treating effect, although it produces a combination of properties which could not be obtained before aging.

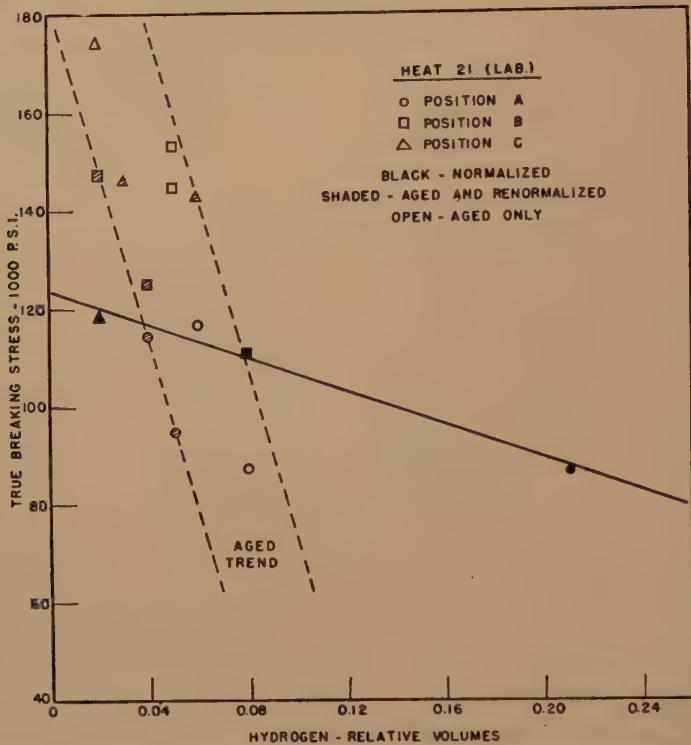


FIG 13—EFFECT OF AGING AND RENORMALIZING ON VARIATION OF TRUE BREAKING STRESS WITH HYDROGEN

renormalizing, the true breaking stress has been plotted against hydrogen analysis for the samples of Heat 21 in Fig 13. Silicon Heat 21 gives the most clear-cut results, but the observations are similar for each heat. The original normalized samples fall in a narrow band of moderate slope, while both the aged and aged and renormalized samples fall in another band of much greater slope. Since the true breaking stress is not affected by ordinary changes in structure which occur on normal heat treatment, but is affected by factors which abnormally lower ductility, and since it is not affected here by renormalizing after aging, it may, therefore, be seen that the effect of re-

Relation of Ductility to Hydrogen Changed by Aging

Thirty 4-in. square keel bars were aged at 400°F for various times up to 256 hr after which tensile tests and hydrogen analyses were made for the central portion of each bar. The correlation of hydrogen content and ductility for such samples is shown in Fig 14, where each observation is the average of three bars. It is seen that there is very little improvement in ductility until the hydrogen has been reduced to 0.10 R.V. after which the elongation increases rapidly on further reduction to 0.04 R.V.

In this series of tests, the use of triplicate samples not only gave much more reliable results, but also yielded interesting information on the inherent variability of the

variations occurred in yield and tensile strengths, there was no consistent change of these properties on aging.

Another set of 4-in. coupons were aged

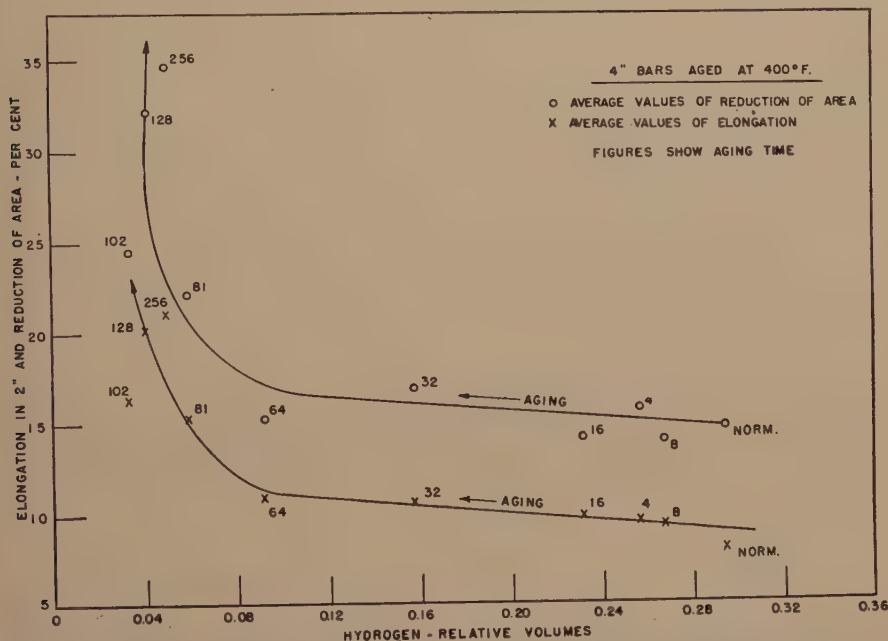


FIG 14—CORRELATION OF ELONGATION AND REDUCTION OF AREA TO HYDROGEN CONTENT ON AGING.

hydrogen effect. Both hydrogen content and ductility of the triplicates were in good agreement before aging, but during the early stages spread farther and farther apart. Late in the process, the values returned to consistent agreement. During the period of divergent values, the correlation of hydrogen to ductility was quite poor for individual samples, although the averages remained in a narrow band. It could clearly be seen that aging was not only progressing at differing rates in the various bars, but that the effectiveness of hydrogen in reducing ductility varied between bars according to random factors controlling its distribution.

The use of triplicate samples permitted the calculation of the normal range of error for the various observations, and by this test it was possible to show that while

at room temperature for periods up to 18½ months or 555 days. The variation in hydrogen content and tensile ductility with the log of time are plotted in Fig 15. The data plotted are the averages of triplicate tests. No hydrogen was lost for the first 60 days but by 555 days it had been lowered from 0.30 R.V. to 0.13 R.V. By extrapolation of the curve, it is estimated that it would require about 1200 days or over 3 yr to complete the aging, or to lower the hydrogen to the end point of 0.04 R.V. obtained at 400°F.

No perceptible improvement in ductility was obtained by aging for 18½ months. As shown in Fig 14, however, the ductility did not increase even at 400°F until the hydrogen content fell below 0.10 R.V. It might logically be anticipated, therefore, that after some 700 days or 2 yr, when the

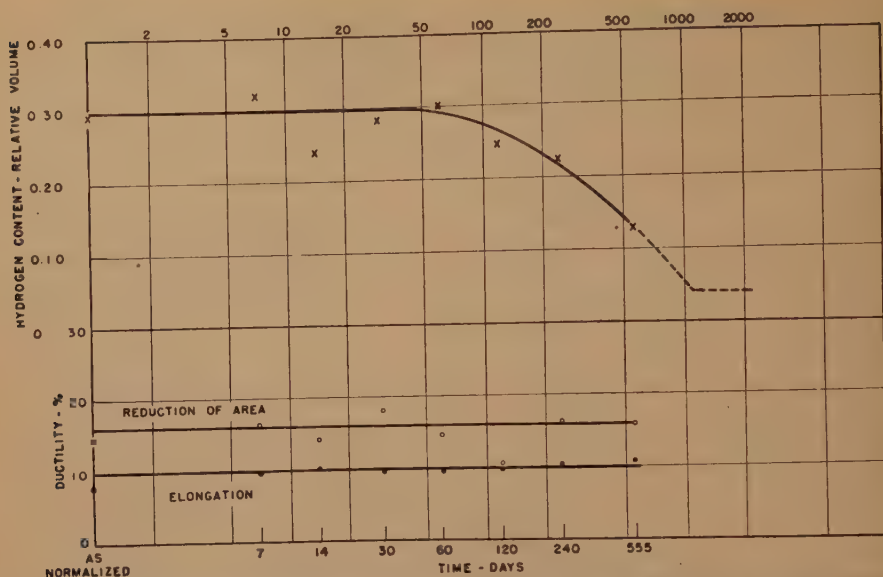


FIG 15—CHANGE IN HYDROGEN CONTENT AND DUCTILITY WITH TIME FOR CENTER OF 4-IN. COUPONS AGED AT ROOM TEMPERATURE. DATA PLOTTED ARE AVERAGES OF THREE TESTS.

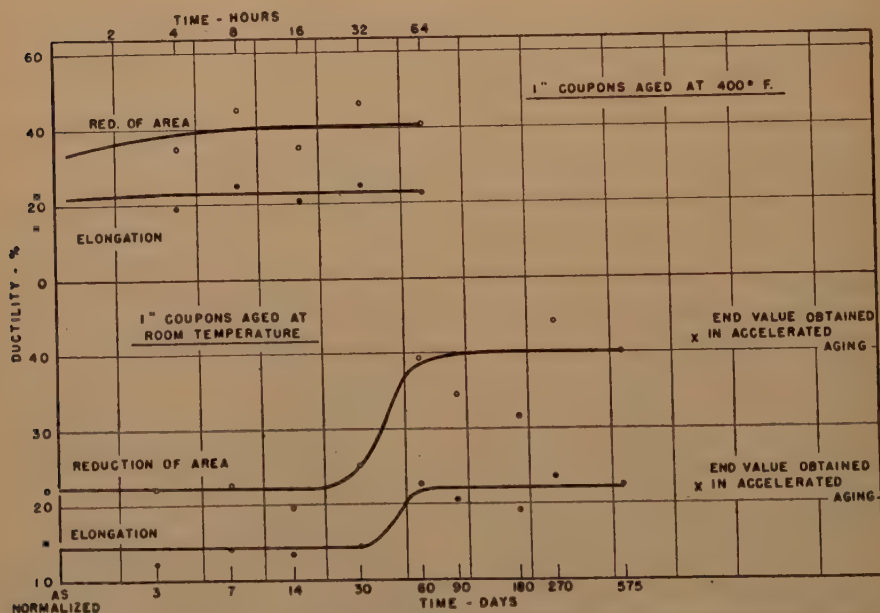


FIG 16—CHANGE IN DUCTILITY WITH TIME FOR 1-IN. COUPONS AGED AT ROOM TEMPERATURE AND AT 400°F. VALUES PLOTTED ARE AVERAGES OF THREE TESTS.

hydrogen has fallen below 0.10 R.V., the ductility would improve as it did in accelerated aging.

One-inch coupons from the same heat as the 4-in. coupons were aged both at 400°F and at room temperature. The effect of these aging treatments on the tensile ductility is shown in Fig 16. At 400°F there was an almost immediate improvement in ductility and after 6 to 8 hr an end value was reached which was not increased by a 64-hr treatment.

Aging at room temperature produced no change for 30 days, but by 60 days, practically full recovery of loss of ductility due to hydrogen was obtained. Equal improvement in ductility was ultimately attained at both temperatures.

The hydrogen content was lowered to an apparently irreducible minimum of 0.03 R.V. by both treatments. This took place in 15 to 20 hr at 400°F but required 180 days at room temperature.

Interpretation of Data on Ductility

All of the observations of the effect of hydrogen on the ductility of steel which have been reported in this section are in agreement with the mechanistic theory which has been stated in Part 1 and in Section 1 of this part. Before the quantitative observations can be properly interpreted, however, it is necessary to emphasize that the theory, itself, predicts variations in the quantitative effect, although this prediction has not generally been appreciated. At ordinary temperatures, all of the hydrogen affecting ductility has been considered as located in discreet pools centering on disturbed spots such as inclusions or small holes, but including an additional region where the continuity of the lattice is temporarily interrupted and the pressure of the contained molecular hydrogen is balanced by highly localized multidimensional tensile stresses in the surrounding metallic crystal. Common observations of flakes and

similar imperfections have shown that such pools are of visible size, and that in many cases a single such pool is sufficient to give a brittle fracture of a specimen of ordinary size. Since fracture will normally follow the rule of the weakest link in the chain, it will naturally seek out the most completely damaged spots in the material to be broken; hence, ductility will normally be determined by the size and hydrogen concentration of a few of the largest pools and will normally be almost entirely independent of the existence of smaller pools or pools with lower hydrogen concentrations.

On aging or slow cooling, the mechanics of hydrogen diffusion at low temperature assume importance. If, as at high temperature, hydrogen atoms were diffusing in solution, the rate would be proportional to the concentration of hydrogen, and the higher concentrations would disappear first. However, in the low-temperature range, where the hydrogen is diffusing as molecules, the controlling factors are mainly mechanical and the dependence on concentration may be of no importance. It appears only reasonable to assume that the same structural factors which were originally responsible for the local segregations continue to operate, so that the points of greatest original concentration retain their hydrogen content most permanently. This is, in fact, the only reasonable explanation of the repeated observation that a portion of the hydrogen is trapped at low temperature and is never entirely lost on any aging treatment.

Fig 17 has been constructed to best represent the data on ductility from all of the experiments reported here. Bands have been drawn to represent the trend lines for elongation for each of the 14 heats, putting them all on the same scale by representing the elongation of a normalized bar having no original hydrogen as 100 pct. Reduction of area data would have given a similar figure except that there would have been greater upward concavity at low hydrogen

and more difficulty would be found in extrapolating observations to zero hydrogen.

It will be seen that the efficiency of the hydrogen in reducing ductility varies con-

than that of the normal steel, and it could be lower with both hydrogen and inclusion factors than with either alone, but the loss does not appear to continue indefinitely.

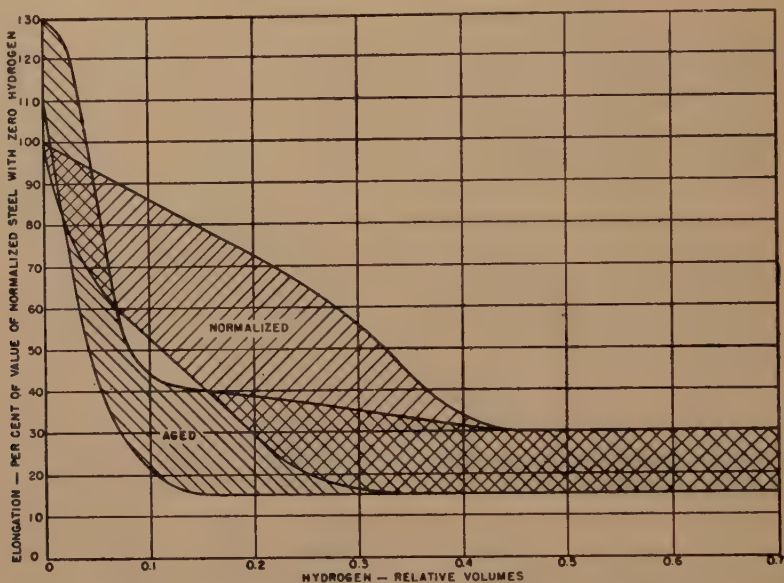


FIG 17—INFLUENCE OF HYDROGEN ON DUCTILITY (SCHEMATIC).

siderably both with the nature of the steel and with heat treatment. A steel of normal quality, such as the laboratory steels or the usual silicon-killed commercial grade, cooled at a rate sufficient to retain most of its original hydrogen content, as were the 4-in. ingots, tends to follow nearly a straight line in the middle of the normalized band. Ductility is reduced to about 20 pct of the original value by 0.40 R.V. of hydrogen.

With a steel whose composition gives permanent abnormal losses of ductility, such as one of the commercial steels killed with aluminum, the *proportional* effect of hydrogen is much less than on a normal type. Such a steel follows the upper portion of the normalized band, and 30 pct or more of originally lower ductility may survive above 0.4 R.V. of hydrogen. The absolute ductility value may, of course, be lower

There is some evidence that the increased number of inclusions may increase the number of hydrogen spots and thus lower the efficiency of the hydrogen by lowering the concentration per spot.

In samples where part of the hydrogen has been removed by aging, very little improvement of ductility occurs until the hydrogen is less than 0.10 R.V.; hence, the proportional effect of hydrogen is about four times as great as in normalized samples. This is reasonable only on the basis that the first hydrogen to diffuse out was so located as to have little or no effect on the ductility, with the remainder located in the critical spots which would fail in a brittle manner.

Steels which have high original ductility, or which have been cooled somewhat slowly, tend to follow the lower portion of the normalized band, with the ductility

being reduced to 12–20 pct of the original by 0.25 to 0.30 R.V. of hydrogen. A curvature of the same sign as that of aged samples tends to appear in these cases. The fact that hydrogen may be 50 pct more effective in reducing ductility in such steels is reasonable if it may be believed that there are fewer locations for hydrogen segregation in the high-ductility steels, and that a portion of the less effective hydrogen may be lost on slower cooling.

Interpretation of Data on Strength

Correlations were found between yield, tensile, and impact strengths and the hydrogen content, but these were, in part, a result of the coincidence that high-hydrogen specimens were often from interior locations which of necessity had slightly lower cooling rates. When hydrogen was changed by aging, changes of the strength properties could not be detected with certainty. On renormalizing after aging, strength properties increased to values higher than were obtainable before aging, while ductility decreased in an amount exactly appropriate to normal structural rearrangement. It appears that while hydrogen has no direct effect on yield strength and impact values, it does have a small effect on structure, for instance, the establishment of a rift system, and that the structure obtained in the absence of hydrogen has better strength properties.

A small effect of hydrogen on tensile strength, other than the structural effect, apparently remains for high hydrogen contents. This is best shown by the fact that the true breaking stress continues to decline after minimum ductility has been established, and that a small increase sometimes occurs on aging. This effect apparently is caused indirectly by the loss of ductility, since the full potential strength of the steel often cannot be realized when it fails prematurely from excessive brittleness. The limiting case would be reached

when the hydrogen embrittlement actually took the form of cracks, after which the cracked area obviously would carry no load. According to the data recorded in the literature, cracking may usually be expected to start in the range of 0.60 to 1.0 R.V. of hydrogen.

SECTION 3—NATURE OF AGING

In the previous section, aging was considered only in the form of an arbitrary treatment which normally increased ductility and reduced hydrogen. With the arbitrary time of 16 hr per in. of thickness, the actual effectiveness of any given aging test was largely unpredictable. This section is introductory to actual measurements of the effect of variations in time and temperature and the true dependence of aging on thickness of section and will not attempt quantitative answers to these questions since the measurements are still in the preliminary stages.

The progress of aging with time sheds some additional light on the nature of hydrogen embrittlement and the recovery of steel after embrittlement. Fig 18 shows a typical series of measurements representing hydrogen content and ductility at the center of aging 4-in. bars. Observations are the average of three tests. The hydrogen analysis curve remains very close to a first-order reaction, that is, with the rate of evolution proportional to the hydrogen concentration with possibly a small delay while waiting for evolution from the inner layers, but the hydrogen evolution suddenly stops after a little over 100 hr with about 0.04 R.V. remaining permanently in the specimen. Ductility shows a slight improvement on first heating to the aging temperature, which may be presumed to be a result of readjustment of structure or of the stress pattern. There was little further change of ductility until the hydrogen fell to about 0.10 R.V. at about 60 hr. At this point, the ductility increased rapidly as the hydrogen was falling to its final limiting value, fol-

lowed by a small slow increase of ductility which could again be associated with changes in structure and stress distribution. Further analysis of the magnitude of these

ment should, therefore, be of considerable interest since it shows that a recovery of ductility at least to the value characteristics of steel without hydrogen, and possibly to

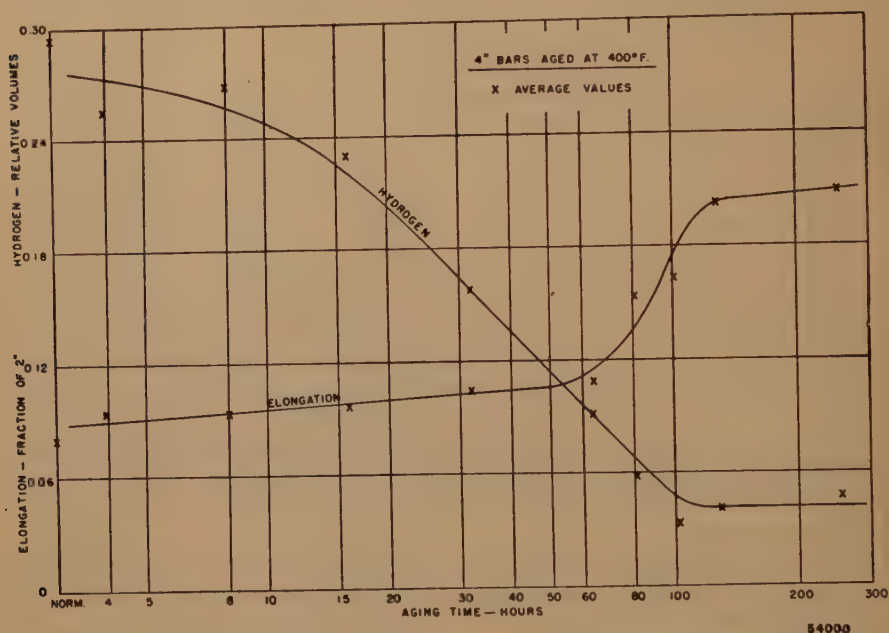


FIG 18—COMPARATIVE CHANGE OF HYDROGEN AND DUCTILITY ON AGING.

changes shows the change of ductility directly associated with the removal of the critical portion of hydrogen is at least three or four times the total change which can be associated with structural readjustment and stress relief.

The progress of aging with time should also be considered in the light of hydrogen-ductility relationship shown in Fig 14 and in the schematic form of the "aged" band of Fig 17. Since there have been numerous indications in the literature¹⁻⁴ that a portion of the hydrogen was irremovable at moderate temperature, aging has been regarded with some suspicion of being only a partial cure for lowered ductility caused by hydrogen. Comparison of this effect with permanent abnormal losses of ductility, for example from inclusions, has also supported this suspicion. The present experi-

even a greater value, can occur with a reasonable aging treatment. This is found to be true in spite of the fact that some of the hydrogen is not eliminated.

The data are not sufficiently comprehensive to be used in formulating any general laws regarding the time-temperature-size-relationships in aging. In the time-size relation, however, there is some indication that, with increasing size, the time required for aging will increase directly with increase in volume and inversely with increase in surface area. Thus, for most compact shapes, time will increase as the $\frac{3}{2}$ power of the diameter or thickness. The fact that larger sections are apt to contain higher hydrogen concentrations may upset this somewhat.

Results from only two temperatures are available, but they are fairly consistent in

showing that 1 hr at 400°F is equivalent to 10 days at room temperature or 70°F. This is a rate ratio of 240 to 1 for the two temperatures.

GENERAL CONCLUSIONS

In the light of the extensive information available in the literature and of the now generally accepted theory for the mechanism of hydrogen embrittlement, it may reasonably be concluded from the data presented in this report that:

1. The ability of hydrogen to cause a temporary abnormal loss of ductility has been definitely and repeatedly demonstrated, and that hydrogen is the only material whose concentration is changed by aging and, hence, the only primary cause of this particular type of ductility loss. This loss of ductility may be accompanied by a limited loss of tensile strength which is probably best regarded as an indirect effect of hydrogen acting through its effect on ductility.

2. The direct embrittlement caused by hydrogen is accompanied by changes in structure or in stress distribution which are apparently directly caused by hydrogen and which cannot be removed while the hydrogen remains present. The embrittling effect of these changes are a minor portion of the total temporary embrittlement.

3. This temporary abnormal loss of ductility is distinct from, and operates relatively independently of, other mechanisms causing permanent abnormal losses of ductility; an example of which is the effect of film forming or eutectic inclusions.

4. Hydrogen in amounts of 0.10 to 0.40 R.V. is sufficient to reduce ductility to a lower limiting value of 15 to 30 pct of the ductility possible in the hydrogen-free steel. The exact amount of hydrogen necessary to accomplish this damage in specific cases depends on the ductility originally available, on the number of sites for easy precipitation of embrittling pools of fluid hydrogen, which are in turn dependent on

the cleanliness and thermal history of the specimen and on the degree of segregation of hydrogen within the specimen. In general, the effect of a given amount of hydrogen is least when it can be evenly distributed over many sites, greatest when it is most highly segregated in a few locations, any one of which may be the site of brittle failure.

5. The abnormal loss of ductility caused by hydrogen can be completely eliminated by aging at a moderate temperature for sufficient time to remove all but a small residue of hydrogen, but the time necessary for completion of aging depends on several factors whose quantitative influence has not yet been determined.

REFERENCES

1. C. E. Sims and G. A. Moore: Apparatus for the Hot Extraction Analysis for Hydrogen in Steel. *AIME Met. Tech.* June, 1948. TP 2369. This volume, p. 248.
2. C. E. Sims and G. A. Moore: Low Ductility and Porosity of Cast Steels Due to Hydrogen and Nitrogen. Part I. Review of Literature. Steel Founders' Soc. of America, Res. Report No. 4, Feb., 1945. Available on Recordak film from Battelle Memorial Inst.
3. C. A. Zapffe and C. E. Sims: Selected Bibliography on Hydrogen Steel. U. S. Dept. Agr. Library, Washington, D. C., Document No. 1255 obtainable as bibliography—500 references.
4. C. A. Zapffe and C. E. Sims: Hydrogen Embrittlement, Internal Stress, and Defects in Steel, *Trans. AIME* (1941) **145**, 225-261; disc. 161-171.
5. C. A. Zapffe and G. A. Moore: A Micrographic Study of the Cleavage of Hydrogenized Ferrite, *Trans. AIME* (1943) **154**, 335-352; disc. 352-359.
6. C. E. Sims, G. A. Moore, and D. W. Williams: A Quantitative Experimental Investigation of the Hydrogen and Nitrogen Contents of Steel during Commercial Melting. *Proc. 5th Elec. Fur. Conf. AIME Met. Tech.* Feb. 1948. This volume, p. 260.
7. J. E. Wells and K. C. Barraclough: Determination of Hydrogen in Liquid Steel, *Jnl. Iron and Steel Inst.* **155/1**, 27-32 (Jan. 1947).
8. C. Sykes, H. H. Burton, and C. C. Gegg: Hydrogen in Steel Manufacture, *Jnl. Iron and Steel Inst.* **156/2**, 155-180 (June 1947).
9. Hung Liang, M. B. Bever, and C. F. Floe: The Solubility of Hydrogen in Molten Iron-silicon Alloys. TP 1975, *Metals Tech.* (Feb. 1946); *Trans. AIME* (1946) **167**, 395.

10. Miss Marion H. Armbruster: The Solubility of Hydrogen at Low Pressures in Iron, Nickel, and Certain Steels at 400°C. to 600°C., *Jnl. Am. Chem. Soc.* **65/6**, 1043-1054 (June 1943).
11. (a) J. H. Andrew, H. Lee, A. K. Mallik, and A. G. Quarrell: The Removal of Hydrogen from Steel. *Trans. Iron and Steel Inst.* (1946) **153**, 67.
 (b) J. H. Andrew, H. Lee, H. K. Lloyd, and N. Stephenson: Hydrogen and Transformation Characteristics in Steel. *Jnl. Iron and Steel Inst.* (June 1947) **156/2**, 208-253.
12. B. M. Larsen: A Review of Factors Underlying Segregation in Steel Ingots. *AIME Met. Tech.* Sept. 1944, 13-34. *Trans.* (1945) **162**.
13. G. E. Doan, R. D. Stout, L. J. McGeady, C. P. Sun, and J. F. Libsch: Effect of Welding on Ductility and Notch Sensitivity of Navy Steels. Final Report, Navy Contract NObs-31220 (1721), June 30, 1946, from Lehigh Univ., Bethlehem, Pa.
14. M. R. Gross, W. R. Angell, and G. D. Marshall, Jr.: Effect of "Fisheyes" on Impact Strength of High Tensile Manganese-Titanium Steel Plate, *Met. Prog.* (June 1946) **49/6**, 1173-1180.
15. Alan E. Flanigan: An Investigation of the Influence of Hydrogen on the Ductility of Arc Welds in Mild Steel. Welding Res. Council, *Jnl. Am. Welding Soc.* Supplement 12 No. 4 (April 1947), 193-2145.
16. A. Portevin: Hydrogen in Metals. *Met. Prog.* (Dec. 1946) **50/6**, 1206-1208.

Kinetics of the Transfer of Sulphur Across a Slag-metal Interface

By LO-CHING CHANG* JUNIOR MEMBER AIME AND KENNETH M. GOLDMANT†

(New York Meeting, February 1948)

INTRODUCTION

THE kinetics and mechanism of transfer of a constituent across a slag-metal interface are fundamentally important because many metallurgical processes involve the existence of a slag phase and a metal phase. Industrial processes seldom proceed to equilibrium, and information of the rates and modes of reactions are therefore often of greater practical importance than equilibrium data. A study of the kinetics of sulphur transfer across a slag-metal interface under reducing conditions will contribute a great deal toward a better understanding of desulphurization in the blast furnace process. The general principles existing in the transfer of a constituent, such as sulphur, across a slag-metal interface can be extended to similar transfer phenomena in other metallurgical processes. The present paper will demonstrate how such studies will lead to fruitful results from both the practical and theoretical standpoints.

EXPERIMENTAL METHOD

The apparatus used was simple. A graphite crucible $1\frac{5}{8}$ -in. id, a wall $\frac{1}{8}$ -in. thick, and a depth of 4 in., was packed in an outer fused silica tube with powdered magnesia. The crucible assembly was rotated at a speed of 235 rpm inside an in-

duction coil. A charge of 250 g of Armco ingot iron was introduced into the graphite crucible and melted by induction heating. The melt was held at a desired temperature

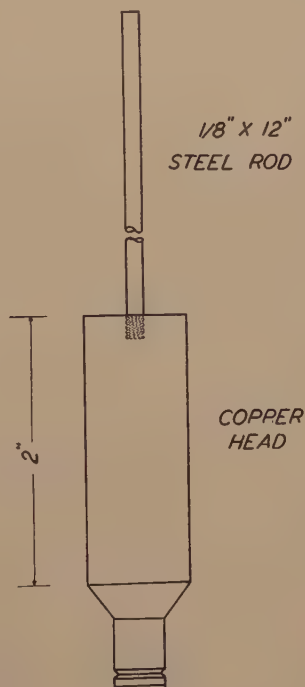


FIG 1—SLAG SAMPLER.

for 3-5 min., after which 7.5 g of granular ferrous sulphide was added and the bath was held for another 3-5 min. A metal sample was then taken by means of a fused silica tube and a rubber suction bulb. Immediately after the metal sample was taken, 30 g of a prefused and crushed slag were introduced. The slag reached the temperature of the furnace in 1 to $1\frac{1}{2}$ min. Slag

Manuscript received at the office of the Institute July 27, 1947; revision received January 12, 1948. Issued as TP 2367 in METALS TECHNOLOGY, June 1948.

* Formerly, Staff Member, Metals Research Laboratory, Carnegie Institute of Technology, now at Massachusetts Institute of Technology.

† Research Assistant, Metals Research Laboratory, Carnegie Institute of Technology.

samples were taken at regular time intervals with a copper sampler (Fig 1). After the last slag sample was obtained, the final metal sample was taken through the slag.

100°C lower than the wall temperature which was measured with an optical pyrometer. This difference was found to decrease to about 30°C after 90 min. The

TABLE 1a—*Chemical Compositions of Slags*

Slag No.	Approx. Chemical Composition Per cent by Weight			CaO SiO ₂	Chemical Analysis of Slag, Per Cent by Weight					
					Initial			Final*		
	Al ₂ O ₃	CaO	SiO ₂		Al ₂ O ₃	CaO	SiO ₂	Al ₂ O ₃	CaO	SiO ₂
1530	15	30	55	0.55	15.95	31.72	53.46	17.11	31.55	52.26
1535	15	35	50	0.70	16.09	37.46	47.57	16.08	36.52	46.55
1040	10	40	50	0.80	11.21	42.23	47.16			
1540	15	40	45	0.89	15.14	41.84	43.02	17.72	41.92	40.65
1545	15	45	40	1.12	16.29	46.66	37.24	15.00	47.15	35.69
2340	23	40	37	1.08	23.40	40.31	35.66	23.92	39.84	37.31
1550	15	50	35	1.43	15.97	51.70	32.66			
2838	28	38	34	1.12	28.01	38.22	33.92	27.14	38.40	33.85

* The final slags also contained small percentages of iron and up to 1.9 pct sulphur.

Temperature readings were obtained with a Leeds and Northrop optical pyrometer sighted on the hot graphite surface instantaneously left bare by the melt caused by the presence of a slight eccentricity of the rotating crucible set-up. The optical pyrometer was calibrated against a secondary standard platinum platinum-rhodium thermocouple.

region directly above the slag, however, was at the same temperature as the crucible wall throughout an experiment, because it received heat by radiation from the wall. Apparently the slag layer was very close to the hottest part of the crucible, and therefore it is safe to assume that the temperature of the slag was very close to that of the wall.

TABLE 1b—*Carbon and Silicon Content of Solidified Ingots from Various Heats*

Heat No.	Per Cent C	Per Cent Si
ST11	4.90	0.05
13	4.78	0.02
15	4.85	0.03
16	3.88	0.03
18	4.76	0.04
19	4.49	0.01
21	4.27	<0.01
23	5.12	0.02
24	4.64	0.01
35	4.50	0.01

Temperature checks were made to determine whether or not there was a temperature gradient between the crucible wall and the bath. Temperature measurements taken in the bath with a calibrated Pt-Pt 10 pct Rh thermocouple showed that at the start of a run the bath temperature, although uniform throughout, was about

TABLE 1c—*Carbon Content of Iron Melt (No Slag Cover)*

Heat No. ST-42	
TIME (MIN.)	PER CENT C IN IRON
0	*
1	3.89
3	4.20
4	4.17
5	5.01

* Zero time is the time at which the iron was observed to be molten.

The experimental conditions were planned to reduce the number of variables in the study to a minimum. Rotation of the crucible was intended to minimize inhomogeneity in the metal phase and the slag phase, as well as to maintain a uniform temperature in the bath. A comparatively large amount of metal was used relative to the slag so that the concentration of sulphur in the metal phase would not change very appreciably as a result of the transfer of sulphur from metal to slag. The loss of

TABLE 2—Data on Sulphur Transfer Experiments
 A. Slag 1530—15.95 pct Al_2O_3 , 31.72 pct CaO, 53.46 pct SiO_2 by weight

Time Minutes	Heat Number and Temperature							
	ST-11 1540°C		ST-12 1540°C		ST-13 1540°C		Average 1540°C	
	C_m^*	C_s^*	C_m	C_s	C_m	C_s	C_m	C_s
0		0.024		0.024		0.024		0.024
2		0.020		0.002		0.040		0.051
4		0.087		0.153		0.108		0.116
8		0.136		0.125		0.164		0.142
14		0.179		0.154		0.193		0.175
22		0.231		0.200		0.248		0.226
32		0.275		0.255		0.337		0.289
42		0.333		0.314		0.339		0.329
52		0.393		0.320		0.378		0.367
53		0.358		0.352		0.371		0.360

* C_m Chemically analyzed concentration of sulphur in metal, wt pct.
 C_s Chemically analyzed concentration of sulphur in slag, wt pct.

B. Slag 1535—16.09 pct Al_2O_3 , 37.46 pct CaO, 47.57 pct SiO_2 by weight

Time Min- utes	Heat Number and Temperature											
	ST-16 1525°C		ST-17 1525°C		Average 1525°C		ST-15 1540°C		ST-18 1504°C		Average 1540°C	
	C_m	C_s	C_m	C_s	C_m	C_s	C_m	C_s	C_m	C_s	C_m	C_s
0	0.992	0.020	0.902	0.020	0.947	0.020	0.972	0.020	0.945	0.020	0.959	0.020
2								0.108		0.168		0.138
4								0.126		0.181		0.154
8		0.173		0.175		0.174		0.162				0.102
14		0.226		0.222		0.224		0.243		0.356		0.300
22		0.285		0.328		0.307		0.390		0.461		0.426
32		0.369		0.352		0.361		0.452				0.452
42								0.471				0.471
47	0.795	0.497		0.366		0.366	0.832	0.547				0.547
52				0.422		0.422						
57			0.820	0.442		0.442						
67												

C. Slag 1040—11.21 pct Al_2O_3 , 42.23 pct CaO, 47.16 pct SiO_2 by weight

Heat Number and Temperature

Time Minutes	ST-10 1540°C	
	C_m	C_s
0		0.025
2		0.050
4		0.155
8		0.261
14		0.380
22		0.585
32		0.635
42		0.696
52		0.750
53		0.829

sulphur to the crucible and to the surroundings was found to range from 0 to 16 pct of the original sulphur addition. These figures were obtained from sulphur balances. A minimum amount of slag (about 0.4 g) was taken in each sampling to keep the weight of the slag practically con-

stant throughout the run. Speed of rotation (235 rpm) and temperature of the bath were held reasonably constant. Synthetic slag powders were prepared from chemically pure oxide components by weighing out the proper amount of each constituent and then mixing, fusing and crushing.

TABLE 2—(Continued)
D. Slag 1540—15.14 pct Al_2O_3 , 41.84 pct CaO, 43.02 pct SiO_2 by weight

Time Minutes	Heat Number and Temperature									
	ST-21 1520°C		ST-19 1540°C		ST-20 1540°C		ST-22 1540°C		Average 1540°C	
	C_m	C_s	C_m	C_s	C_m	C_s	C_m	C_s	C_m	C_s
0	0.929	0.020	0.918	0.020	0.905	0.020	0.992	0.020	0.938	0.020
2		0.078		0.050		0.144				0.097
4		0.132		0.18		0.186		0.211		0.192
6		0.327		0.23		0.296		0.272		0.266
14		0.425		0.30		0.400		0.409		0.370
22		0.520		0.68		0.507		0.633		0.607
32		0.633		0.75		0.756		0.767		0.758
42		0.751		0.99		0.852		1.02		0.953
52		0.748		1.08		0.978		0.877		0.978
62		0.894		1.22		0.915		1.08		1.11
72	0.770	0.873	0.721	1.14	0.740	1.10	0.764	1.08		1.15
82		0.922		1.29		1.04		1.13		1.19
87.5				1.19						1.07
85						1.07				1.15
92								1.15		1.27
102								1.27		1.25
103								1.25		

E. Slag 1545—16.29 pct Al_2O_3 , 46.66 pct CaO, 37.24 pct SiO_2 by weight

Time Minutes	Heat Number and Temperature							
	ST-23 1525°C		ST-24 1540°C		ST-26 1547°C		ST-25 1560°C	
	C_m	C_s	C_m	C_s	C_m	C_s	C_m	C_s
0	0.942	0.02	0.892	0.02	0.952	0.02	0.888	0.02
2		0.14		0.27		0.29		0.27
4		0.18		0.36		0.30		0.40
8		0.43		0.56		0.63		0.70
14		0.82		0.95		1.02		1.15
22		1.20		1.28		1.40		1.50
27						1.58		
32		1.29		1.55				1.83
37						1.81		
42				1.74				
43.5		1.56					0.664	2.02
52		1.79		1.91		2.12		2.09
62		1.81						2.19
63				1.85				
67						2.17		
72		1.76		1.99				
73.5								2.30
82		1.91		2.03		2.26		
83				2.05		2.30		
84	0.714	1.87	0.694		0.673			

Eight slag compositions were selected for study. The chemical compositions of these slags are shown in Table 1a. The percentages of carbon and silicon in the solidified metal ingots are given in Table 1b, and the

carbon content of the iron directly after melting is given in Table 1c.

DATA AND REPRODUCIBILITY

The experimental data of twenty-five runs are recorded in Table 2.

TABLE 2—(Continued)
F. Slag 1550—15.97 pct Al_2O_3 , 51.70 pct CaO , 32.66 pct SiO_2 by weight

Time Minutes	Heat Number and Temperature					
	ST-34 1547°C		ST-35 1565°C		ST-36 1580°C	
	C_m	C_s	C_m	C_s	C_m	C_s
0	0.912	0.040	0.884	0.040	0.885	0.040
4						0.15
6		0.180				
6.5				0.508		
8				0.683		0.835
9						
12		0.710				
14				1.53		1.53
20		1.420				
22				1.95		2.08
30		1.99				
32				2.23		2.37
40		2.14				
42						2.61
50		2.32				
52				2.36		2.87
60		2.54		2.69		2.90
62						
70		2.64				
72				3.17		3.25
80		2.83				
82			0.761	2.85	0.880	3.38
90	0.656	3.25				

G. Slag 2340—23.40 pct Al_2O_3 , 40.31 pct CaO , 35.66 pct SiO_2 by weight

Time Minutes	Heat number and Temperature					
	ST-31 1406°C		ST-32 1553°C		ST-33 1553°C	
	C_m	C_s	C_m	C_s	C_m	C_s
0	1.025	0.045		0.045	0.874	0.045
2				0.227		0.140
4		0.089		0.260		0.280
8		0.160		0.371		0.310
14		0.244		0.465		0.420
22		0.256		0.597		0.650
32		0.264		0.740		0.820
42						0.950
43		0.240				
52		0.250				1.05
55				0.990		
62				1.05		1.10
63		0.261				
72				1.12		1.17
73		0.302				
82		0.299		1.17		
82.5	0.710				0.770	1.17
92			0.734	1.24		

TABLE 2—(Continued)
H. Slag 28.38—28.01 pct Al_2O_3 , 38.22 pct CaO , 33.92 pct SiO_2 by weight

Time Minutes	Heat Number and Temperature					
	ST-37 1576°C		ST-39 1576°C		ST-38* 1582°C	
	C_m	C_s	C_m	C_s	C_m	C_s
0	0.860	0.020	0.918	0.020	0.870	0.020
2		0.022		0.030		0.060
2.5						0.065
4		0.170		0.110		0.185
8		0.345		0.270		0.360
14		0.470		0.450		0.470
22				0.640		
23		0.745		0.812		0.630
32						0.780
33		0.910		1.04		0.860
42		1.07		1.18		0.920
43		1.17		1.24		1.13
52		1.26		1.34		1.08
53		1.33	0.784	1.46	0.770	
62						
63		1.42				
72						
73						
82						
83	0.710					

* ST-38, crucible stationary

For each slag composition at a given temperature and at each sampling time, the chemically analyzed sulphur concentrations from the parallel runs were averaged, and the percentage deviation of each individual sulphur concentration from this average was calculated and listed according to sulphur ranges. A total of 110 such quantities was thus obtained for a statistical analysis. The results are shown in Table 3.

TABLE 3—Standard Variation of Sulphur in Slag for Various Composition Ranges

PER CENT S	STANDARD VARIATION (PER CENT OF SULPHUR PRESENT)
0.00-0.20	26.3
0.21-0.40	8.6
0.41-0.80	7.3
0.81-1.0	2.2
1.1-2.0	1.8
above 2.0	3.1

The table indicates that there is inherent in the experimental methods an absolute error of 0.05 to 0.1 pct S in the slag, which becomes large in percentage at low sulphur ranges. Much of this may be attributable to limited sensitivity of the analytical methods employed. Other factors con-

tributing to this variation may be (1) errors in temperature and time measurements, and (2) slag inhomogeneity.

INTERPRETATION OF DATA

The rate curves for the eight slags at various temperature levels are given in Fig 2, 3, 4, and 5. (For parallel runs the average is plotted). The same rate curves for five slags at 1540°C are reproduced in Fig 6 for purposes of comparison. It is apparent from the rate curves that the rate of transfer of sulphur from metal to slag increases with increasing basicity of the slag.

Assuming that the rate of transfer of sulphur from metal to slag is proportional to the concentration of sulphur in the metal phase and that from slag to metal is proportional to the concentration of sulphur in the slag phase, we may write the following equation for the net transfer of sulphur from metal to slag:

$$\frac{dW}{dt} = \frac{dC_s S}{dt} = AK_m C_m - AK_s C_s$$

or

$$\frac{dC_s}{dt} = \frac{A}{S} (K_m C_m - K_s C_s) \quad [1]$$

where $\frac{dW}{dt}$ = net rate of transfer of sulphur

from metal to slag in grams
per minute

S = weight of slag, in grams,
= 30

A = interfacial area between slag
and metal, in sq cm = 16

C_s, C_m = concentration of sulphur in
slag and metal respectively,
in weight per cent

K_s, K_m = coefficient of transfer of sul-
phur from slag to metal and

from metal to slag, respec-
tively, in grams per min. per
sq cm per unit concentration.

Actual measurements of A , the inter-
facial area between slag and metal, in
nineteen experiments, showed that there
was some variation in area from one experi-
ment to another, but since this variation
did not follow any particular trend and was
well within the experimental error involved
in measuring, the area was assumed to be
constant. The weight of the slag, S ,
although it varied by about 15 pct during
an experiment, and C_m , the sulphur concen-
tration in the metal, which also varied
up to 25 pct, were assumed to be constant

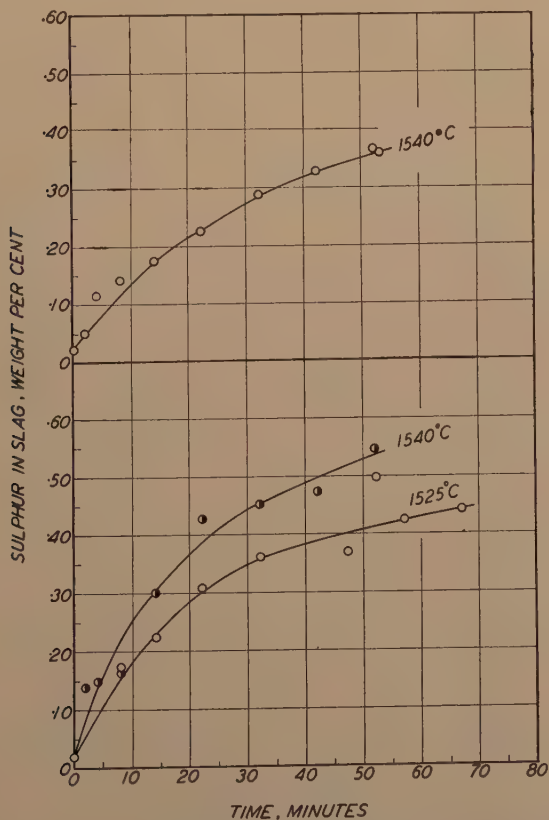


FIG 2—RATE CURVES.

Upper: Slag containing 15 pct Al_2O_3 , 30 pct CaO and 55 pct SiO_2 by weight.
Lower: Slag containing 15 pct Al_2O_3 , 35 pct CaO and 50 pct SiO_2 by weight.

in order to simplify the mathematical calculations. (These variations should be very small at the beginning of the run and become progressively larger during the course of the run.) If these assumptions are reasonable, then it follows that the plot of $\frac{dC_s}{dt}$, the slope of the rate curves, versus C_s , the concentration of sulphur in the slag, should be a straight line with a slope equal to $-\frac{A}{S} K_s$ and an intercept on the ordinate

equal to $\frac{A}{S} \cdot K_m C_m$, if K_m and K_s are also constant for a given slag at a given temperature. The $\frac{dC_s}{dt} - C_s$ plots for five slags at 1540°C are shown in Fig 7. The same plots for slags at various temperature levels are shown in Fig 8. The experimental points seem to follow a straight-line relationship as predicted, except a few nearing the end of a run. This deviation from straight-line

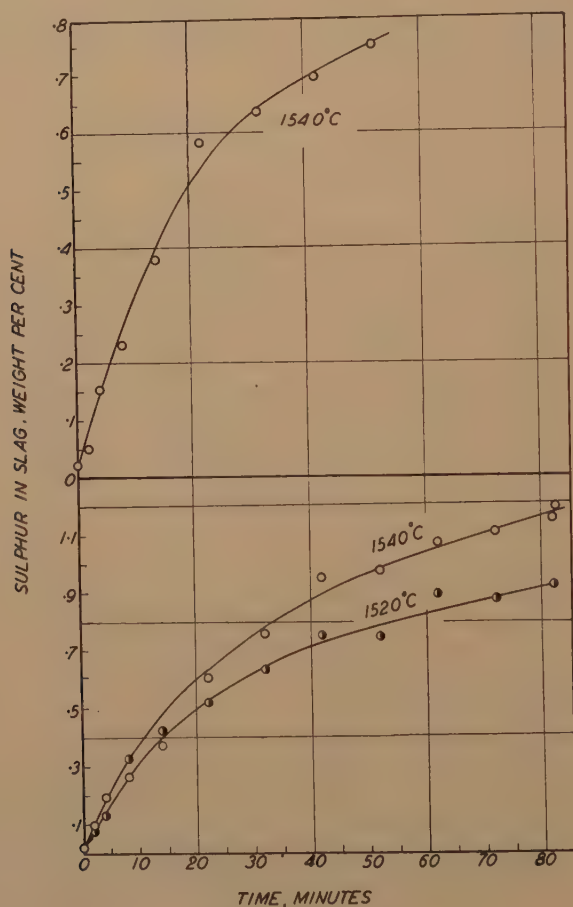


FIG 3—RATE CURVES.

Upper: Slag containing 10 pct Al_2O_3 , 40 pct CaO and 50 pct SiO_2 by weight.
Lower: Slag containing 15 pct Al_2O_3 , 40 pct CaO and 45 pct SiO_2 by weight.

relationship will be discussed in a later section.

From the slopes and the intercepts of these straight-line plots the K_s and K_m values are calculated and given in Table 4. In evaluating K_m the initial concentration of sulphur in metal (C_m at zero time) was used in all cases. (The initial concentration of sulphur in metal as chemically analyzed varied from 0.86 pct to 1.02 pct and averaged 0.93 pct. For experiments where the C_m value is not available the average value of 0.93 pct was used in the calculation.)

TABLE 4— K_s and K_m Values

Slag Designation	T°C	K_s	K_m
1530	1540	0.077	0.031
1535	1525	0.088	0.042
	1540	0.096	0.054
2838	1576	0.054	0.090
	1582	0.055	0.080
1040	1540	0.088	0.076
1540	1520	0.079	0.075
	1540	0.090	0.096
2040	1406	0.062	0.030
	1553	0.070	0.094
1545	1525	0.071	0.151
	1540	0.077	0.183
	1547	0.084	0.196
	1560	0.090	0.229
1550	1547	0.086	0.257
	1565	0.095	0.300
	1580	0.103	0.341

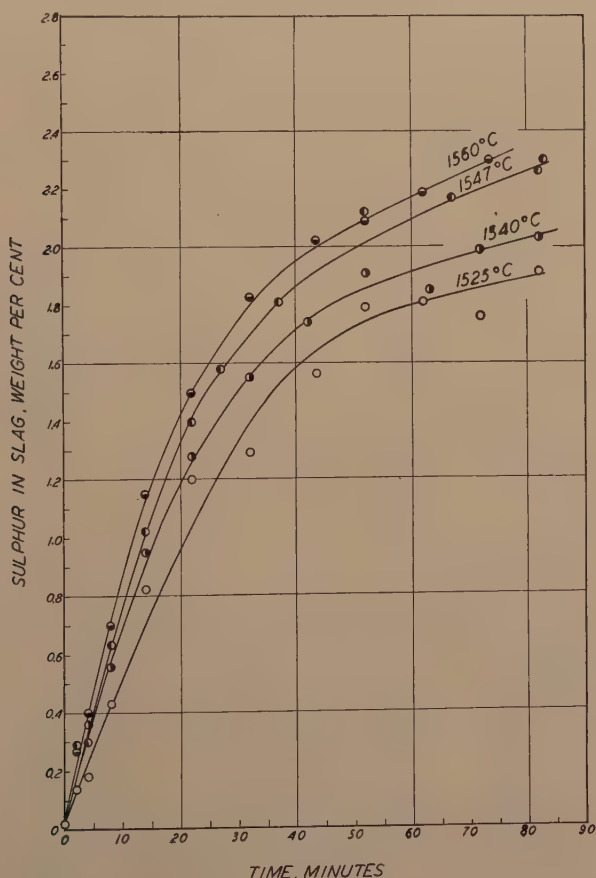


FIG 4—RATE CURVES.

Slag containing 15 pct Al_2O_3 , 45 pct CaO and 40 pct SiO_2 by weight.

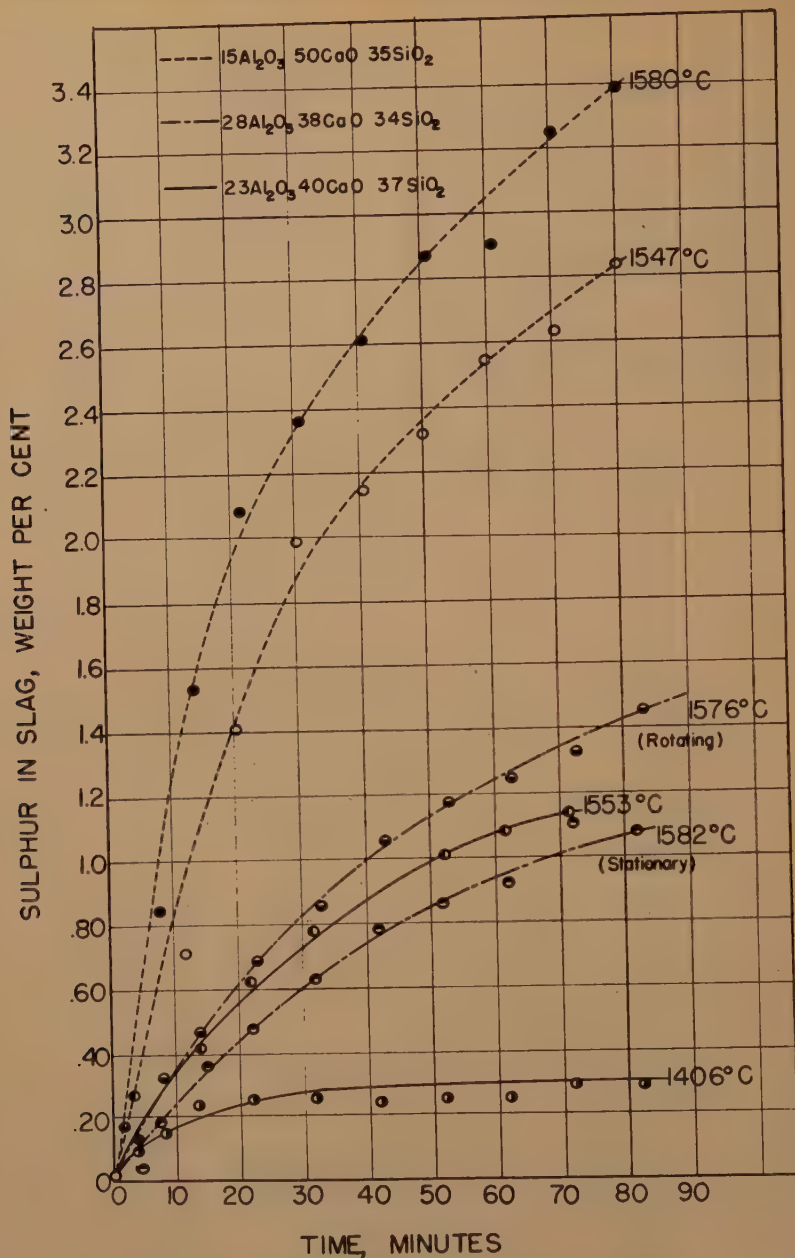


FIG 5—RATE CURVES.

Slags containing: 23 pct Al₂O₃, 40 pct CaO, 37 pct SiO₂
 15 pct Al₂O₃, 50 pct CaO, 35 pct SiO₂
 28 pct Al₂O₃, 38 pct CaO, 34 pct SiO₂

Expressing the coefficients of transfer in terms of Arrhenius' equation, we have:

$$K_s = K_s^0 e^{\frac{-Q_s}{RT}} \quad [2]$$

$$K_m = K_m^0 e^{\frac{-Q_m}{RT}} \quad [3]$$

where K_s^0 , K_m^0 = constants independent of temperature

Q_s , Q_m = activation energies for the transfer of sulphur from slag to metal and from metal to slag, respectively, in cal per mol.

R = gas constant = 1.987 cal per mol per degree K

T = absolute temperature in degrees K.

Taking logarithms of Eq 2 and 3, we have:

$$\log K_s = \log K_s^0 - \frac{Q_s}{2.303RT} \quad [4]$$

$$\log K_m = \log K_m^0 - \frac{Q_m}{2.303RT} \quad [5]$$

The plots of $\log K_s$'s and of $\log K_m$'s against $\frac{1}{T}$ are shown in Fig 9 and 10. The

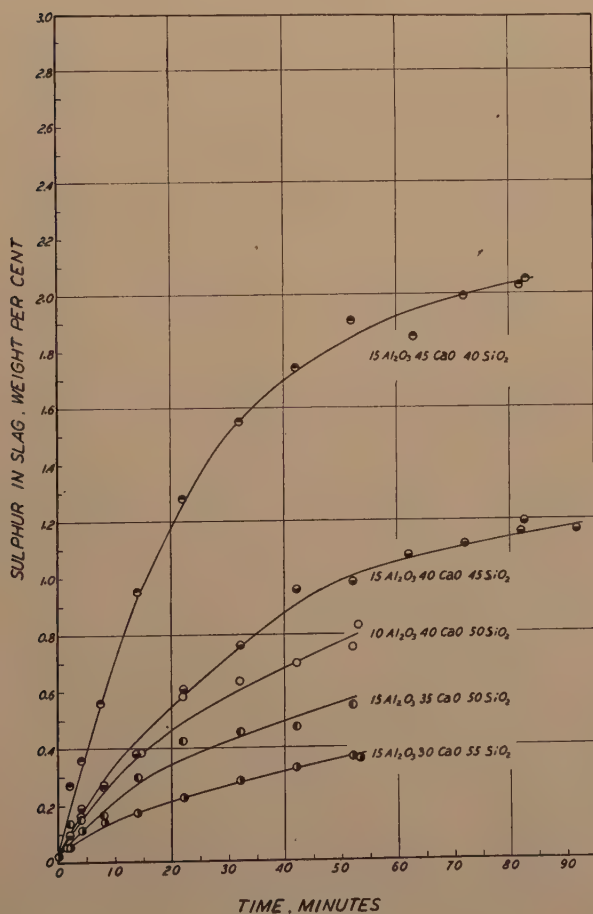


FIG 6—RATE CURVES FOR FIVE SLAGS AT 1540°C.

straight-line relationship is again followed. From the slopes of these straight lines, Q_s and Q_m may be calculated. It is interesting to note that the activation energies remain practically constant with respect to changes in the slag composition. The calculated

activation energies are:

$$Q_s = 39,000 \text{ cal per mol}$$

$$Q_m = 79,000 \text{ cal per mol}$$

The activation energy required for the transfer of sulphur from metal to slag

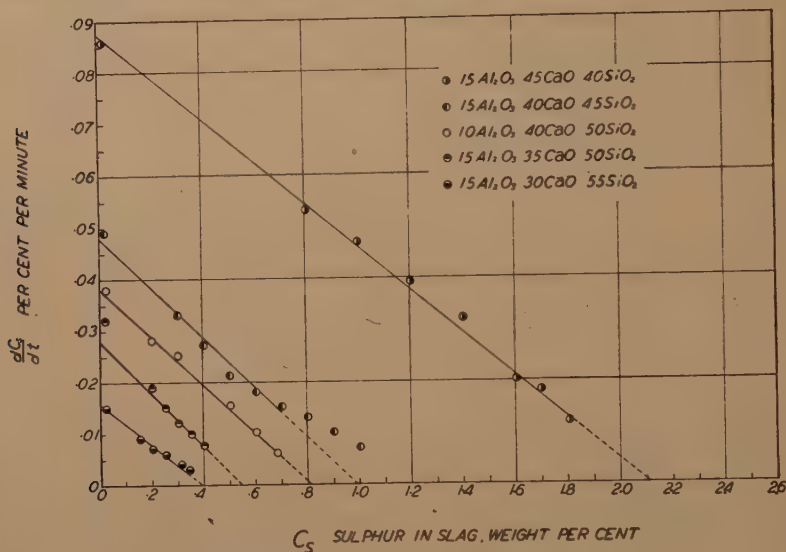


Fig 7— $\frac{dC_s}{dt}$ VERSUS C_s PLOTS FOR FIVE SLAGS AT 1540°C.

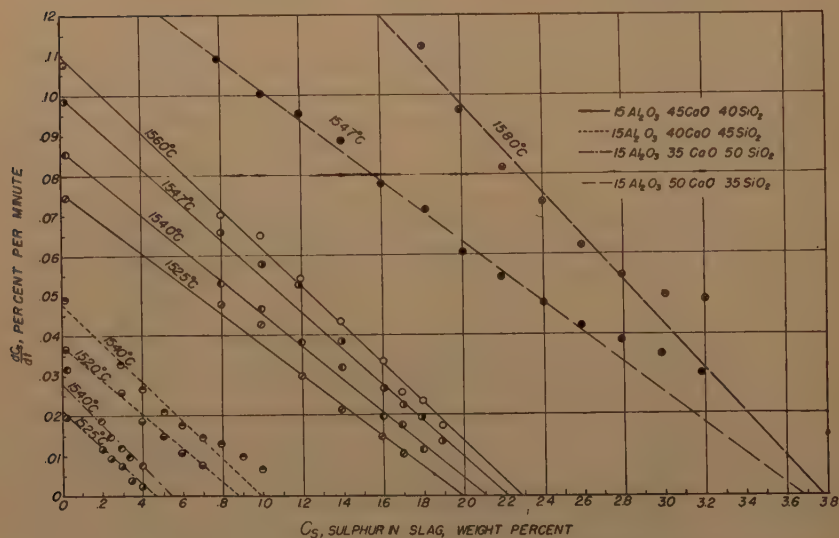


Fig 8— $\frac{dC_s}{dt}$ VERSUS C_s PLOTS FOR FOUR SLAGS AT VARIOUS TEMPERATURE LEVELS.

doubles that required for the reverse process, that is, the transfer of sulphur from slag to metal.

The K_s and K_m values for the five slag compositions studied at 1540°C are plotted against the CaO/SiO₂ ratios in Fig 11, showing that K_s remains practically constant while K_m increases very rapidly with increasing CaO/SiO₂ ratio of the slag.

Transfer Experiments with the More Basic Slags

A few runs were made with a slag of the nominal composition 15 pct Al₂O₃, 50 pct

CaO and 35 pct SiO₂ by weight. Considerable experimental difficulties were encountered in sampling. The experimental data are shown in Table 2, Sec. F. The calculated transfer coefficients are as follows:

Slag 1550, Containing nominally 15 pct Al₂O₃, 50 pct CaO and 35 pct SiO₂ by weight

Run No.....	ST-34	ST-35	ST-36
Temp °C.....	1547	1565	1580
K_s	0.086	0.095	0.103
K_m	0.257	0.300	0.341

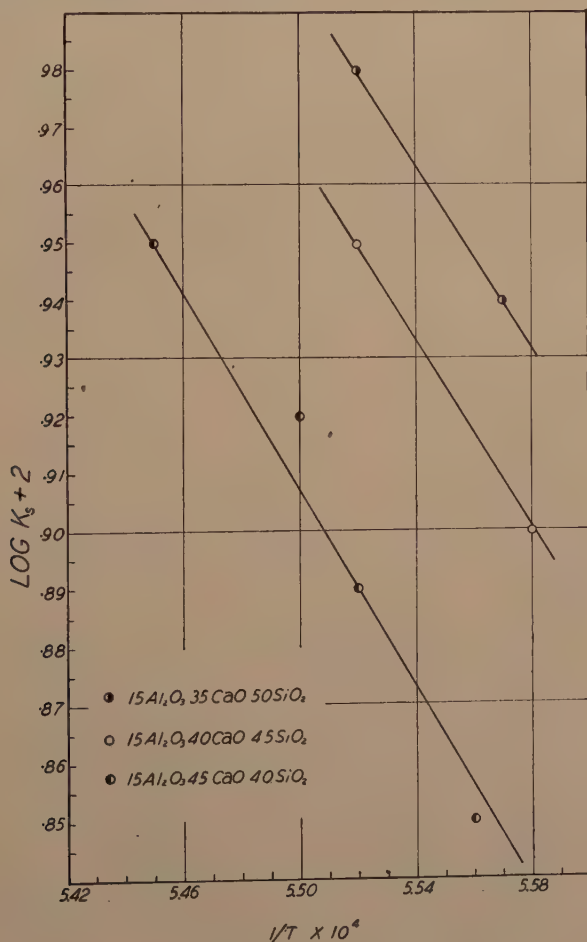


FIG 9—LOG K_s VERSUS $\frac{1}{T}$ PLOTS FOR THREE SLAGS.

The slag was analyzed chemically to give 15.97 pct Al_2O_3 , 51.70 pct CaO and 32.66 pct SiO_2 by weight. According to the ternary diagram of the system $\text{CaO-Al}_2\text{O}_3\text{-SiO}_2$, this slag has a melting point of about 1650°C , which is above the operating temperature of all three runs. The slag, however, was observed to be molten in all the runs. Apparently its melting point was lowered by the sulphur. Although the K_s and K_m values obtained seem to fit well in Fig 9 and Fig 11, they are not included in the plots.

Transfer Experiments with High Alumina Slags

A few runs were also carried out to determine the transfer coefficients of slags con-

taining alumina up to 30 pct by weight. The experimental data are given in Table 2, Sec. G and H, from which the following transfer coefficients are obtained:

Slag 2340, Containing 23.40 pct Al_2O_3 ,
40.31 pct CaO and 35.66 pct SiO_2 (as
chemically analyzed)

Run No.	ST-31*	ST-32, 33
Temp $^\circ\text{C}$	1406	1553
K_s	0.062	0.070
K_m	0.030	0.094

Slag 2838, Containing 28.01 pct Al_2O_3 ,
38.22 pct CaO and 33.92 pct SiO_2 (as
chemically analyzed)

Run No.	ST-37, 39	ST-38†
Temp $^\circ\text{C}$	1576	1582
K_s	0.054	0.055
K_m	0.090	0.080

* ST-31, operating temperature below melting point of slag, which is about 1440°C .
† ST-38, stationary crucible.

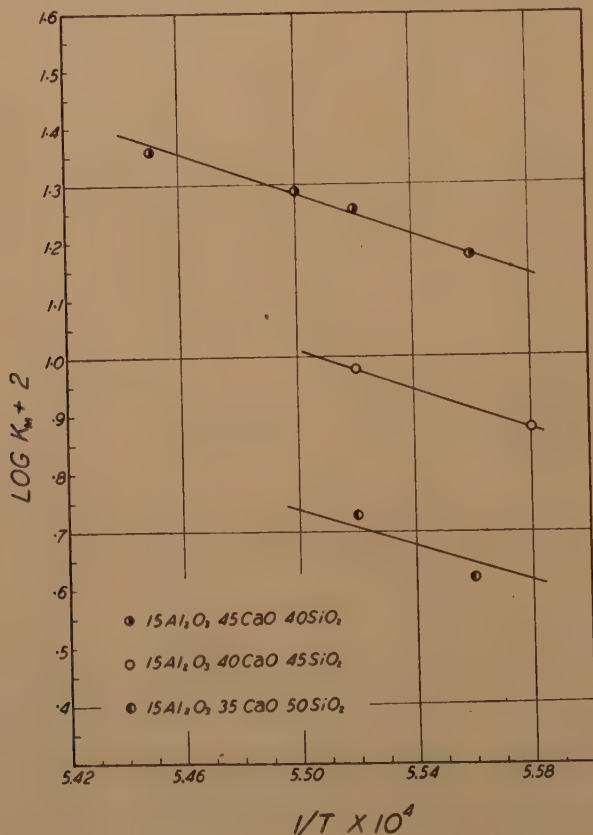


FIG 10— $\text{LOG } K_m$ VERSUS $\frac{1}{T}$ PLOTS FOR THREE SLAGS.

The effect of alumina in slag on the sulphur transfer coefficients may be seen from Table 5, which shows that for a given

TABLE 5—*Effect of Alumina in Slag on the Sulphur Transfer Coefficients*

Slag Designation	Chemical Composition, Per Cent by Weight			Temp °C	K_s	K_m
	Al ₂ O ₃	CaO	SiO ₂			
1040	11.21	42.23	47.16	1540	0.088	0.076
1540	15.14	41.84	43.02	1540	0.079	0.096
2340	23.40	40.31	35.66	1553	0.070	0.094
2838	28.01	38.22	33.92	1576	0.054	0.090

CaO concentration of the slag the sulphur transfer coefficients are only slightly affected when SiO₂ is replaced by Al₂O₃.

It will be noted that run ST-38 was carried out in a stationary crucible while runs ST-37 and ST-39 were made in crucibles rotated at a speed of 235 rpm, other experimental conditions being maintained the same. This will demonstrate whether

rotation of the crucible exerts a change in the magnitude to the sulphur transfer coefficients. The results are: $K_s = 0.055$, $K_m = 0.080$ from run ST-38 with stationary crucible at 1582°C, as compared with $K_s = 0.055$, $K_m = 0.090$ from runs ST-37 and ST-38 with rotating crucible at 1576°C, for the same slag of the composition 28.01 pct Al₂O₃, 38.22 pct CaO and 33.92 pct SiO₂ by weight. The data seem to show that rotating the crucible will exert an influence on the shape of the slag-metal interface only, but not the transfer coefficients. This may not hold true for very viscous slags.

DISCUSSION OF RESULTS

Practical Considerations

It is the accumulated experience of blast-furnace operators that a basic slag and high operating temperature are the necessities of good desulphurization in the blast-furnace. The present paper explains

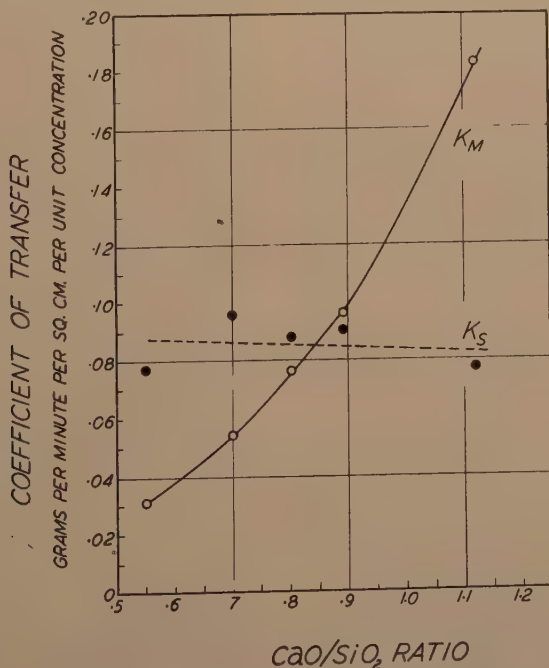


FIG 11—COEFFICIENTS OF TRANSFER VERSUS CaO/SiO₂ WEIGHT RATIO FOR FIVE SLAGS AT 1540°C.

why it is so. To elaborate the point further, the following items will be discussed: the slag phase, the metal phase, the temperature factor, and the distribution ratio.

The Slag Phase

1. **SLAG BASICITY:** The present work shows that the net rate of transfer of sulphur from metal to slag increases very rapidly with increasing basicity of the slag, at least within the range of compositions studied; hence a basic slag seems to be the primary requisite of good desulphurization in the blast-furnace. Since blast-furnace slags are a mixture of a number of oxide components, the correlation between slag composition and slag basicity is fundamentally important. Unfortunately no such work is available. It appears then that a direct determination of the net rate of sulphur transfer as influenced by changes of slag composition will be more practicable and straightforward. A review of literature reveals that the work of Holbrook and Joseph¹ on the relative desulphurization power of blast furnace slags is the only systematic presentation that is available to date.

2. **EFFECT OF SLAG COMPOSITION ON THE ACTIVITY COEFFICIENT OF SULPHUR IN SLAG AND METAL:** In rate studies where concentrations of the reacting phases vary over a wide range it will be preferable to use activities instead of concentrations. Thus Eq 1 may be rewritten:

$$\frac{dW}{dt} = A(k_m\alpha_m - k_s\alpha_s) \quad [6]$$

$$\text{or} \quad \frac{dW}{dt} = A(k_m\gamma_m C_m - k_s\gamma_s C_s) \quad [7]$$

where k_m, k_s = coefficient of transfer of sulphur from metal to slag and from slag to metal, respectively, expressed in g per min. per sq cm per

unit activity (instead of per unit concentration).

α_m, α_s = activities of sulphur in metal and slag, respectively.

γ_m, γ_s = activity coefficients of sulphur in metal and slag, respectively.

From Eq 1 and 7, it follows

$$\begin{aligned} K_m &= k_m\gamma_m & [8] \\ K_s &= k_s\gamma_s & [9] \end{aligned}$$

Since K_s does not change markedly with changes in slag composition (see Fig 11), it may be reasonable to assume that within the range of compositions studied the effect of the change of slag composition on the activity coefficient of sulphur in slag is relatively small. For a given slag at a given temperature, the plot of $\frac{dC_s}{dt}$ versus C_s will be a straight line if γ_s does not change with C_s . However, it will be noted from Fig 7 and 8 that in a few cases the experimental points at higher sulphur concentrations deviate from a straight line. It is possible that at higher concentrations of sulphur the activity coefficient of sulphur in slag decreases. The present data do not permit a quantitative evaluation of this effect. An independent determination of the effect of slag composition and of sulphur concentration on the activity coefficient of sulphur in slag, especially at high sulphur concentrations, is needed.

The Metal Phase

From Eq 8 we see that K_m is actually a product of two terms, k_m and γ_m . In this study the chemical composition of the metal phase was assumed to be constant. Therefore, the change of K_m with slag composition (see Fig 11) reflects actually a similar change of k_m because γ_m is now constant.

It will be fruitful to determine systematically the effect of change in composition of the metal on the activity coefficient

¹ References are at the end of this paper.

of sulphur in the metal phase. Such work is yet to be done.

The effect of carbon dissolved in iron on the activity coefficient of sulphur in iron has not been quantitatively established. It can be reasonably concluded, however, from the studies of Görrissen and of Darken and Larsen that the activity coefficient of sulphur in molten iron is increased by the presence of carbon.^{2,3} Thus for a given slag at a given temperature the higher the concentration of carbon is, the better will be the desulphurization of the metal.

The authors do not intend to discuss here the effect of other foreign elements dissolved in iron on the activity coefficient of sulphur in iron. An independent determination of this effect is needed.

The Temperature Factor

Since both K_m and K_s are sensitive to temperature, it is essential to maintain the highest possible temperature in the blast-furnace where most of the sulphur transfer is taking place. It will also be noted that K_m is more temperature sensitive than K_s . The effect of temperature on K_m may be attributed to a combination of several factors: the effect on the rate coefficient k_m , and the effect on the solubility of foreign elements dissolved in iron, notably carbon, which in turn will change the activity coefficient of sulphur in iron. In so far as the rate coefficient k_m and carbon solubility are concerned, both are contributing in the same direction. This shows again the advantage of maintaining the highest possible temperature where most of the sulphur transfer is taking place in order to get good desulphurization in the blast-furnace.

The Distribution Ratio

At equilibrium, $K_m C_m = K_s C_s$, the distribution ratio C_s/C_m of sulphur between slag and metal is simply the ratio K_m/K_s . A difference in the temperature coefficient between K_m and K_s predicts a change of

the distribution ratio with change of temperature; a rise in temperature will give rise to a higher distribution ratio. This applies to cases where the metal phase is saturated with carbon.³

It will be noted that a closer approximation of the distribution ratio of sulphur between slag and metal can be obtained from Fig 7 by extrapolation to zero rates of transfer ($dC_s/dt = 0$). The results for the five slags are given in Table 6.

TABLE 6—Distribution Ratio of Sulphur between Slag and Metal at 1540°C.

Slag Designation	C_s^*	C_m^*	C_m^*	C_s^*/C_m^*	R value at 1500°C (Holbrook and Joseph)
1545	2.11	0.64	0.69	3.3	3.5
1540	0.99	0.82	0.75	1.2	1.4
1040	0.82	0.83		0.99	0.9
1535	0.54	0.89	0.83	0.61	0.6
1530	0.40	0.88		0.45	

* C_s^* = Equilibrium concentration of sulphur in slag, extrapolated from Fig 7, in wt pct.

C_m^* = Equilibrium concentration of sulphur in metal, calculated from a sulphur balance, assuming no loss, in wt pct.

C_m = Chemically analyzed concentration of sulphur in metal at end of run (see Table 2), in wt pct.

It can be seen from Table 6 that the distribution ratios so obtained are very close to the R values of Holbrook and Joseph.¹ Unfortunately the comparison cannot be carried out far enough to the basic range where Holbrook and Joseph found the R value to decrease with increase in basicity of the slag. Furthermore, the extrapolation to zero rates of transfer is correct only when the plot of dC_s/dt vs. C_s remains a straight line throughout the transfer process. It is possible that such a plot will deviate from a straight line relationship near the equilibrium point. These ought to be interesting problems for future study.

Possible Mechanism of Transfer of Sulphur across the Slag-metal Interface

Color of Slags Containing Sulphur

During the course of sulphur transfer experiments, it was observed that the

color of the slag (as quenched on a copper sampler) changes from near colorless, through green, yellow, orange, brown to black. In the field of colored glasses ferrous sulphide is known as strong color producer. Colors that have been attributed to this compound include yellow, orange, brown, blue and black. Martin, Glockler and Wood,⁴ investigating the form of sulphur in blast-furnace slags by quenching molten slags to which ferrous sulphide, manganous sulphide and calcium sulphide were added separately, reported the following:

"When ferrous sulphide was added the color of the slag changed rapidly as the sulphide addition increased. The amount of ferrous sulphide required to form a colloid was approximately 0.03 pct. Slags containing about 0.4 pct or more sulphur were virtually opaque. Slags containing approximately 0.25 pct or less sulphur as calcium sulphide were colorless but contained a colloidal phase. Further additions of calcium sulphide produced slags whose color varied from light yellow to deep orange. Slags to which manganous sulphide has been added ranged in color from light yellow to dark brown and in sulphide sulphur content from 0.12 to 1.33 pct. All specimens contained a colloidal phase."

From these observations, then, it appears that the change in the color of the slags investigated in the present paper was caused by the presence of ferrous sulphide in the slag. This points to the probable mechanism of sulphur transfer as being a direct transfer of ferrous sulphide. It must be remembered, however, that what is observed on quenched slags may not hold true for molten slags.

Order of Reaction

The present study seems to indicate that the transfer of sulphur from slag to metal and from metal to slag under existing experimental conditions may be interpreted as first order reactions. But a first-order

reaction may not necessarily be a unimolecular one. There are reactions of various kinds which satisfy the first order equations, but actually involve more than one molecule; such processes are sometimes called pseudo-unimolecular reactions.

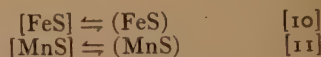
*Evidence Gained from Work with Radioactive Tracers**

A few experiments were made in this laboratory to determine if there are other elements that go with sulphur during the course of the sulphur transfer. The experimental data seem to indicate that iron, for one, goes together with sulphur from metal to slag at the early part of the transfer process. The increase in iron content of the slag seems to correlate fairly well with the gradual darkening in color of the slag.

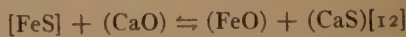
Possible Controlling Reactions of Transfer

It now seems proper to discuss the possible mechanisms of sulphur transfer across the slag-metal interface. Two lines of thought may be offered:

(1) The transfer is controlled by diffusion of sulphides across the slag-metal interface.



(2) The transfer is controlled by an interface reaction.



Grant and Chipman⁵ recently concluded from studies on open-hearth slags that Eq 12 is not the controlling reaction. Although the present work on blast-furnace slags seems also to be in favor of the first mechanism, metallurgists should be mindful of many other possibilities. It is our opinion that much work has yet to be done in order to establish beyond question the real mechanism of transfer of sulphur across the slag-metal interface.

* Experiments of this nature are still being carried on in this laboratory. Results will be reported in a separate paper.

SUMMARY

The kinetics of the transfer of sulphur across the slag-metal interface under the existing experimental conditions may be interpreted as reactions of the first order.

The net rate of transfer of sulphur from metal to slag increases very rapidly with increasing basicity of the slag. This rate may be mathematically expressed by two transfer coefficients: K_s , the coefficient of transfer of sulphur from slag to metal, and K_m , that from metal to slag. The experimental data showed that K_s does not change appreciably with changes in slag composition, while K_m increases very rapidly with increasing basicity of the slag.

Both transfer coefficients are temperature sensitive. K_m is more temperature sensitive than K_s . K_s is increased by about 6 pct for a 10° rise in temperature, while K_m is increased by about 12 pct for the same temperature rise. This can also be expressed mathematically in terms of the Arrhenius equation. The calculated energy of activation for the transfer of sulphur from slag to metal is 39,000 cal per mol and that for the transfer of sulphur from metal to slag is 79,000 per mol.

ACKNOWLEDGMENT

This work was part of a research program sponsored by the Office of Naval Research in the Metals Research Laboratory at the Carnegie Institute of Technology, under contract N6ori-47, Task Order 4. The authors wish to acknowledge the assistance of other members of the project, particularly Martha Helzel for supervision of the analytical work, and W. O. Philbrook and G. Derge for direction of the research.

REFERENCES

1. W. F. Holbrook and T. L. Joseph: Relative Desulphurizing Power of Blast-Furnace Slags, *Trans. AIME* (1936) **120**, 99-117.
2. L. S. Darken and B. M. Larsen: Distribution of Manganese and of Sulphur Between Slag and Metal in the Open-Hearth Furnace, *Trans. AIME* (1942) **150**, 87-109.
3. Johann Görrissen: Desulphurization by Manganese and Lime, *Archiv für das Eisenhüttenwesen* (1942) **15**, 347-350.
4. A. E. Martin, G. Glocker and C. E. Wood: Form of Sulphur Occurrence in Blast-Furnace Slag, U.S. Bur. Min. *Rep. of Invest. No. 3552* (1941).
5. N. J. Grant and J. Chipman: Sulphur Equilibria Between Liquid Iron and Slags, *Trans. AIME* (1946) **167**, 134-149.

DISCUSSION

(John Chipman and C. R. Taylor presiding)

Y. E. LEBEDEF*—I would like to ask Dr. Chang a question. Did you determine in what form your sulphur went into that slag? Was it iron sulphide or what? I am just curious about it; I am not an iron man.

LO-CHING CHANG (authors' reply)—We did some research on this. We are not sure which form sulphur goes from slag to metal. We used some radioactive iron in the metal and determined the rate of transfer of iron from metal to slag by measuring the radioactivity of the slag phase. There seems to be some correlation between the rate of increase of iron concentration and that of sulphur concentration in the slag at the beginning of transfer.

It seems to me that FeS is one of the constituents going across the interface, but I cannot say FeS is the only one.

Y. E. LEBEDEF*—Dr. Chang, is iron sulphide in this slag?

LO-CHING CHANG—When the thing goes to slag it probably disassociates into ions, or it may exchange with lime or magnesium oxide. I do not know precisely.

Y. E. LEBEDEF*—And your analysis did not indicate the iron, as you just stated yourself. That is the initial slag analysis, not the final.

LO-CHING CHANG—The iron is about $\frac{1}{10}$ of 1 pct.

Y. E. LEBEDEF*—Even at the end of your experiment?

LO-CHING CHANG—Yes.

C. R. TAYLOR—That is, even with 2 pct sulphur in the slag the iron is $\frac{1}{10}$ of 1 pct or less. I think that is right.

* American Smelting and Refining Co.

J. M. GAINES*—I would like to ask Dr. Chang one question. Dr. Feild and Dr. Joseph brought me up to believe that the transfer of sulphur as it takes place in the blast furnace was intimately connected with the viscosity of the slag. Would Dr. Chang comment as to what relation his work shows exists with respect to the viscosity, if any?

LO-CHING CHANG—All the slag compositions we have studied are quite fluid at the temperatures of experiment. We did not do any study on very viscous slags. Obviously, it is not easy to perform the experiment. I would think that in a blast furnace the sulphur equilibrium is hardly reached, and the desulphurization process probably occurs mostly when the metal droplets go through the slag. A more fluid slag would mix better let us say, so the sulphur concentration at the slag-metal interface on the slag side would not build up very much; therefore there would be a higher rate of transfer. For very viscous slag compositions one must go to high temperatures to insure a good, fluid slag.

T. L. JOSEPH†—I have been very much interested in this paper, and I think it gives us some new concepts, or something new to think about, in the transfer of sulphur across the interface.

I was particularly interested in the observation that the substitution of alumina for silica did not seem to change the rate of sulphur transfer from metal to slag.

A number of years ago, with Mr. Holbrook in the Bureau of Mines, I attempted to study the rate of transfer of sulphur from metal to slag in the range of composition ordinarily found in the blast furnace practice. We found that when alumina was substituted for silica, there was more rapid transfer of sulphur from metal to slag. This does not seem to be borne out by Dr. Chang's experimental data.

I am wondering just what might be responsible for the difference in results. I would like to have Dr. Chang comment on this, if he will, please.

LO-CHING CHANG—I am fairly well acquainted with Professor Joseph's paper pub-

lished a long time ago, and I think those slag compositions cover a very much wider range than ours. The variation of alumina in our experiments was from 10 to 30 pct. The accuracy of determination of the constant K_m is very much impaired by experimental difficulties; the errors may fall within ± 10 to 20 pct.

What we said is approximately true—that replacing of silica by alumina does not very appreciably affect the sulphur transfer coefficients. But there may be a slight effect which we were not able to detect. As a matter of fact, in the experiment with 28 pct alumina, the rate of transfer seems to be lower, but not enough so to show a very definite trend. Perhaps more investigations using still higher alumina compositions would tell the story. We can say there is some effect, but the effect may not be very great.

T. L. JOSEPH—I might add that this is a very important consideration in that our future supply of iron is ultimately going to come from taconite. Taconite is very deficient in alumina. Some modifications in practice may be necessary to compensate for a deficiency of alumina in the slag.

However, if a lower alumina slag will desulphurize just as well as a higher alumina slag—for example, if a slag with 10 pct will do just as well as one with 15 pct—then we need not be as much concerned with the practical implications of these results.

I hope in your future work you will have a chance to study this phase of desulphurization more thoroughly.

C. E. SIMS—It occurred to me that the slags with which Dr. Chang is working are considerably more basic than the average blast furnace slag, and inasmuch as alumina is an amphoteric material, it may be that in a distinctly basic slag it will act entirely as an acid and have very little effect, whereas in a more nearly neutral slag it could have a greater effect. Would you care to comment on that?

LO-CHING CHANG—What Dr. Sims said is quite true. Aluminum ions may have two coordination numbers, 4 and 6, with oxygen ions. In acid slags alumina will act as a base. As the basicity of the slag increases, an increasing proportion of the alumina will act as an acid.

* Linde Air Products.

† School of Mines, University of Minnesota.

Y. E. LEBEDEF—I noticed in the smelting of nonferrous metal that if we use a high lime slag—let us say lead sulphates containing tin oxide—in a reverberatory type furnace, they usually produce a metal lower in sulphur than the others.

JOHN CHIPMAN—I want to thank Mr. Lebedeff for bringing a little nonferrous information into these iron meetings. There is much that steel metallurgists can learn from other metallurgists and I think the reverse holds true.

Some Correlations between Variables Affecting Sulphur in Blast Furnace Iron

BY T. E. BROWER* AND B. M. LARSEN,* MEMBER AIME

(San Francisco Meeting, February 1949)

INTRODUCTION

THIS discussion is based on statistical manipulation and evaluation of operating data from several commercial blast furnaces which include rather wide variations in practice. We are concerned here mainly with the effect of manganese on sulphur elimination under operating conditions in commercial blast furnaces, but this effect can be outlined more clearly by including certain other variables such as silicon in iron and slag basicity, which are all in part interrelated.

Real progress in understanding all of the smelting-zone reactions in this process requires more laboratory studies of slag-metal melts similar to those in the blast furnace, with careful control of oxygen pressure. Such experimental work is very difficult, however, and in the meantime, with the present scarcity of more fundamental data, such statistical trends and correlations as can be obtained from commercial furnace operating records may help in choosing laboratory test conditions as well as adding to our knowledge of operating procedures.

We do not know just why the furnace data are apparently so irregular that statistical treatment of large numbers is needed to obtain accurate trends. It is partly caused, no doubt, by the many simultaneous variables present, but there are perhaps also such factors as: (1) the con-

tinual swings up and down so characteristic of the process; (2) difficulty of accurate sampling of co-existing phases, as well as (3) the presence of both equilibrium and rate factors as a result of the fast driving of the process.

In desulphurization, for example, the flow of thin layers of slag and metal over solid coke surfaces, plus the contact between droplets of iron falling through the slag layer in the hearth, would lead one to expect a close approach to equilibrium. On the other hand, most of the critical part of sulphur removal may occur in a short time and distance below the tuyeres with perhaps an accompanying decrease in oxygen pressure and the concurrent reduction of much of the silicon and manganese, so its degree of approach to equilibrium may be quite variable.

PROBABLE CHEMISTRY OF DESULPHURIZATION

Since there is little evidence that sulphur atoms in the iron solution are associated to any appreciable extent in molecules such as MnS , the transfer from slag to metal and back again can be written:*



hence the following reactions seem most probable in the slag phase,



and,



Manuscript received at the office of the Institute April 15, 1948; revision received July 22, 1948. Issued as TP 2465 in METALS TECHNOLOGY September 1948.

* Research Laboratory, United States Steel Corporation, Kearny, N. J.

* Parentheses are used here for substances in slag, brackets for solutes in solution in iron, when not otherwise indicated.

We should thus expect that free, or active, (CaO) and (MnO) plus a low concentration of active FeO in the slag would favor holding more sulphur in the slag, leaving less in the iron. These reactions have all been studied in the laboratory^{1,2} and the results have been shown by Darken and Larsen³ to apply quite well to the distribution of sulphur between slag and metal in the open hearth furnace, where the distribution ratio of sulphur in slag to that in metal, or

$$\frac{(S)}{[S]}$$

expresses the equilibrium. This ratio varies between about 2 and 14 in commercial open hearth operations. In the blast furnace it varies from about 15 to above 100. Assuming the probable reactions above, the following factors would seem to favor low [S] or high (S)/[S] values:

1. High basicity in slag, or high CaO or MgO.
2. High temperature, or high silicon in iron.
3. Low FeO in slag.
4. High MnO/FeO ratio in slag or high manganese in iron.

The true activity of (CaO), and (MgO) can be approximated only crudely with our scanty knowledge of the constitution of liquid blast furnace slag at 2700-2850°F. We have used the ratio

$$\frac{(CaO) + (MgO)}{(SiO_2)}$$

with all terms calculated to mols per 100 g slag, as an approximate measure of slag basicity. With few available data on furnace temperatures, it was assumed that [Si] values give a poor but approximate indication of smelting temperatures. The true activity of either MnO or FeO in blast furnace slag is probably small and quite impossible to approximate at present; the [Mn] values serve, however, as an approxi-

mate measure of the effective (MnO)/(FeO) ratio.

In general, even though most of the factors involved are difficult or impossible to evaluate in the blast furnace system it seems more than probable that the basic reactions and effects present are the same as in desulphurization in the open hearth bath. Thus, although we can not hope, with present available data, to evaluate anything quantitatively, the above background of theory may serve as an approximate qualitative guide to what may be expected in the way of correlations between factors in blast furnace operating data.

When the slag-metal system of the open hearth and the blast furnace are compared, the latter offers both advantages and disadvantages in the elimination of sulphur. Probable disadvantages are:

1. Much lower concentrations of free CaO and MnO
2. Lower temperature levels
3. Faster driving rates to limit time for reaction.

Probable advantages are:

1. Much smaller activity of FeO in slag, or lower oxygen pressures in the system,
2. A probable higher level of activity of sulphur in the carbon-saturated iron, perhaps by a factor of 5 to 10, helping to make FeS escape into the slag.
3. Higher values of manganese in the iron.

Since in the blast furnace, the (S)/[S] ratios are much higher it is evident that the advantages outweigh the disadvantages. Several conditions make the blast furnace problem more complex, however. The activity of sulphur in the metal is much more difficult to estimate in carbon-saturated iron than in the nearly pure iron solution of the open hearth steel bath. In the open hearth, temperature seems to have only a small effect, but in the blast furnace, in addition to the fact that it is not measured, smelting zone temperature has a large effect, probably by increasing the free CaO

^{1,2} References are at the end of the paper.

and MnO present in the liquid slag through dissociation of silicate molecules, as well as by accelerating the approach to low oxygen pressure and the rates of reaction in general.

BLAST FURNACE DATA USED

Large groups of operating data from three different practices were available as well as smaller groups or averages from a few others. Most of the work was done with data on about 1300 casts from each of two furnaces in one shop making basic iron and including about nine months of operation to cover seasonal variations; these data included: 1. On each cast: Silicon, manganese and sulphur in iron, average blast temperature, average moisture in air to blowers. 2. Daily averages of CaO, MgO, Al_2O_3 , SiO_2 , FeO, MnO, and S in slags, and other general data usually recorded in operating records, such as coke consumption, wind blown, and others.

On these data, representing what may be called practice X, simple frequency curve correlations were first tried between nearly all the possible pairs of variables; then, after selecting the significant variables affecting [S] or (S)/[S] values, trend curves and multiple correlation calculations were made.

In this basic iron practice X, the MgO in slag varied from 4 to 7 pct and manganese in iron from 1.5 to 2.5 pct. Contrasting with this was a group of less extensive data on a second practice Y, (about 1200 casts tabulated) in which the MgO in slag was 8 to 12 pct, and the manganese in iron about 0.30 to 0.50 pct. The same data on the composition of iron and of slag were included for practice Y but they did not include air humidity, blast temperature or certain other furnace variables such as tons iron per cast or pounds coke per ton iron. About 1200 casts were also tabulated on a third practice Z with only 1-3 pct MgO in slag and about 0.40-0.75 pct Mn in iron. Practice X, on which most of the work was done,

represents a practice common to many furnaces for basic iron.

QUALITATIVE CORRELATIONS WITH SULPHUR IN IRON

Simple frequency curve pairs were made of sulphur in iron in groups above and below the mean of all variables tabulated on all three practices X, Y, and Z.

In none of these practices was there any significant correlation between Al_2O_3 content in slag and the [S] values, thus indicating that (Al_2O_3) can be omitted from any ratio used as an approximate measure of slag basicity. In both the X and the Y practices, increase of either CaO or MgO in slag was related to lower [S], and increase of (SiO_2), to higher [S]. If the data were restricted so that, approximately, one mol of (MgO) was substituted for one mol of (CaO), increasing (MgO) in practice X (over the range 4-7 pct (MgO)) gave a good correlation with lower [S]; but in practice Y range of (MgO) 8 to 12 pct gave a fair correlation with higher [S], indicating that around 7-10 pct (MgO) is the optimum range. This was about the only marked difference between the three practices with respect to the factors affecting removal of sulphur. In nearly all other respects, the various furnace practices were similar as regards the qualitative direction of the various correlating factors.

The general similarity in effect of one mol of MgO with one mol of CaO over a moderately wide range seems to justify the use of the ratio

$$\frac{(\text{mols CaO}) + (\text{mols MgO})}{(\text{mols SiO}_2)}$$

as an approximate measure of basicity or activity of free bases.

In practice X, for which the data were most complete, the following factors appeared to give a "fair to good" correlation with *decreasing* [S] values, (that is, something like 10 to 20 pct difference or shift between the main portions of cumulative

frequency curves for groups above and below the mean values):

1. Higher moisture content in air blown (range—3 to 10 grains per ft³).

nance temperature, but the surprising aspect is that the correlation is opposite to that expected since lower blast temperature correlates quite definitely with lower [S]

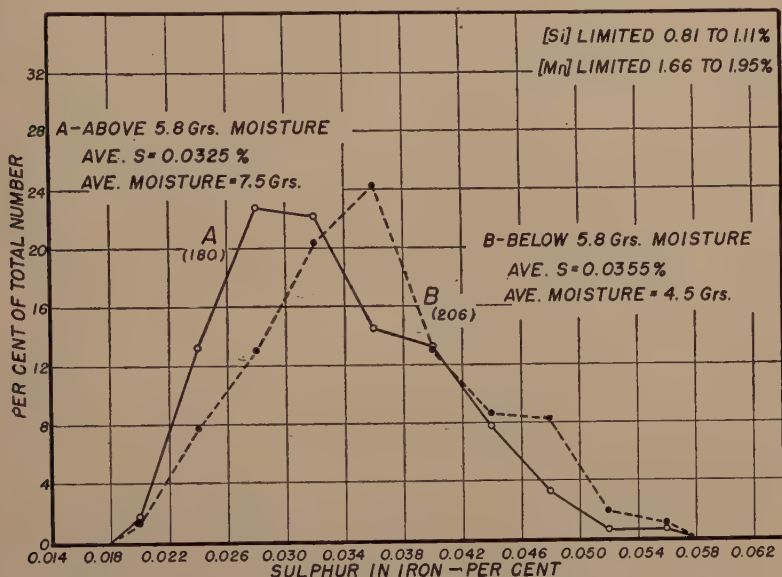


FIG 1—FREQUENCY CURVES OF SULPHUR IN IRON FOR GROUPS ABOVE AND BELOW THE MEAN MOISTURE CONTENT OF AIR BLOWN—TYPICAL BASIC IRON PRACTICE.

2. Lower blast temperature (range—mainly 1100 to 1500°F)

3. Higher silicon in iron (range—mainly 0.5 to 1.4 pct)

4. Higher coke per ton iron.

5. Lower tonnage of iron per cast.

6. Higher manganese in iron (range—mainly 1.40 to 2.20 pct).

7. Higher slag basicity ratio (range—mainly 1.45 to 1.75).

Except for items 1 and 2, these are all about as expected from the various considerations outlined above. Items 3 and 4 are probably secondary effects related to the primary factor of higher smelting or hearth zone temperature for which no direct measurements were available. Item 5 is a secondary effect, perhaps related mainly to available reaction time. Items 6 and 7 are probably primary factors similar to smelting or hearth zone temperature. Item 2 is probably a secondary effect related to fur-

values, also with higher [Mn] and [Si] values. The reason seems, however, fairly obvious, namely, that the blast temperature is the main control variable used to regulate silicon and sulphur contents in the iron. Thus, when the furnace starts to swing toward lower [Si] and higher [S], the blast temperature is raised, and vice versa, so that it always tends to be out of phase with its true effect on iron composition.

Item 1 (higher moisture content in air blown) is also surprising in its effect of lowering [S], especially since we also confirmed a definite correlation between higher moisture and lower [Si] and [Mn] values. The direct correlation between all moisture and all [S] values is small, but when [Si] and [Mn] are restricted to small ranges near their most frequent values, the correlation between higher moisture and lower [S] becomes more pronounced; this is shown in the frequency curves of Fig 1, showing

frequencies for [S] values in groups above and below the mean moisture level of 5.8 grains per ft³ of air, where the casts

It is worth noting here that the correlations with the last three factors are exactly what would be expected on the basis of the above

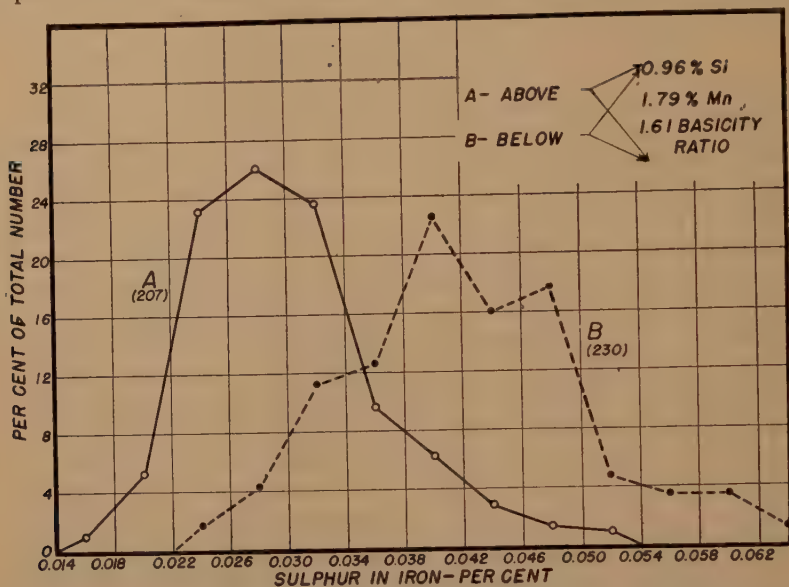
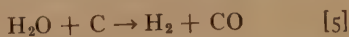


FIG 2—FREQUENCY CURVES OF SULPHUR IN IRON FOR GROUPS ABOVE AND BELOW THE MEAN OF THREE COMBINED VARIABLES; SILICON, MANGANESE IN IRON AND BASICITY RATIO.

selected were restricted to those with [Si] values between 0.81 and 1.11 pct and [Mn] values between 1.66 and 1.95 pct. Apparently, in addition to the indirect effect of reaction between moisture and coke,



to cause a lowering of hearth temperature with resultant decrease in [Si] and [Mn] and a consequent indirect tendency to raise the [S] values, there also seems to be a direct effect of the increased hydrogen content in tuyere zone gases toward lowering [S] values.

This results in four probable primary factors related to transfer of sulphur iron to slag, as follows:

Higher H₂O in blast.

Higher temperature in bosh and hearth zones indicated best by silicon level in iron.

Higher manganese in iron.

Higher slag basicity.

theory on desulphurization reactions and mechanisms.

INTERDEPENDENCE OF VARIABLES

The extent of interdependence of variables can be shown qualitatively, or even roughly quantitatively, by combining variables in simple frequency curves. For example, on these same data for practice X, we find that by selecting [S] values only on those casts with both [Si] and slag basicity low, or both high, the resultant shift between curves is very nearly the sum of the shifts for each variable alone, indicating that silicon in iron and basicity ratio in slag are essentially independent with respect to their effect on [S]. Similarly, the effect of [Si] and [Mn] combined is only 50 to 60 pct of the sum of the individual effects on [S], [Mn] and slag basicity are some 65-75 pct additive; and combining [Si], [Mn] and slag basicity gives a large total effect on [S] (Fig 2) which is about 60-70 pct of the sum

of the individual effects of the three variables. Moisture in blast appears as largely independent of the latter three variables in its effect on [S].

Such interrelationships may also be indicated by direct correlations between the apparently independent variables. In this same *X* practice, for example, higher [Mn] has a significant correlation with higher [Si], also with higher slag basicity, whereas there was only a negligible correlation between [Si] and slag basicity.

In most furnace practices, manganese in iron depends mainly on the total manganese in the burden, but also depends in part on furnace temperature and slag basicity, since high values of either seem to improve the recovery of manganese in iron. Slag basicity is determined almost entirely by the composition of the burden. Moisture in blast is an independent variable, but may be related to [Mn] and [Si] through its effects on hearth temperature unless compensated for by control of blast temperature.

Values of [Si] depend largely on the furnace temperature gradient in smelting and hearth zones, but may also be affected in part by slag composition. In practice *X*, with an intermediate MgO in slag (4–7 pct), [Si] was essentially independent of slag basicity; in practice *Y* with MgO in slag from 8 to 12 pct, [Si] *decreased* with higher slag basicity; in practice *Z*, with MgO in slag only 1 to 3 pct, [Si] *increased* with higher slag basicity. A plausible explanation for these different correlations could be suggested but would be uncertain in the absence of direct measurements of temperature in the smelting or hearth zones. Indeed, it is this lack of direct temperature data which is our present great handicap to an adequate clarification of most commercial furnace data.

QUANTITATIVE CORRELATION COEFFICIENTS

The data having been analyzed qualitatively to determine the three or four factors

which affect [S] values more or less directly, a fair picture of the interrelationships between these variables results, and the individual effects may be measured more quantitatively. The frequency curve pairs of Fig 3 and 4 show the effect of [Mn] and slag basicity respectively, on [S]. These are presumably close to the true individual effects, since in each case the indirect effect of the principal associated variables have been largely eliminated by holding these variables within restricted ranges. In Fig 3, for example, silicon in iron and slag basicity would both tend to be higher in the group with [Mn] above its mean, so that the apparent shift using all data would be greater than the true effect of [Mn] alone. Here the selection is limited to casts with [Si] between 0.81 and 1.11 pct, and slag basicity ratio between 1.56 and 1.66 and about 350 casts still remain—enough for a reliable correlation.

Correlation coefficients may be estimated from such frequency curves, though with considerable uncertainty, because the curves and arrangement of data do not reveal the distribution of the independent variable above and below its mean value. By first restricting the associated variables as in Fig 3 and 4, tabulating [S] values for small increments of the variable in question and plotting the average [S] in each increment against the respective means of the other variable, one gets simple trend curves but with secondary effects largely eliminated by the initial restrictions. Where the associated secondary relationships are known fairly well, such a method is simpler than most of the methods for so-called "multiple correlation." Such curves from our data on practice *X*, for [S] vs. moisture in blast, [Si], [Mn] and slag basicity ratio are shown in Fig 5, 6, 7 and 8, respectively. Although the points in Fig 7 suggest a slightly curvilinear relationship between [Mn] and [S], it is seen to be the greatest single factor, in this furnace practice.

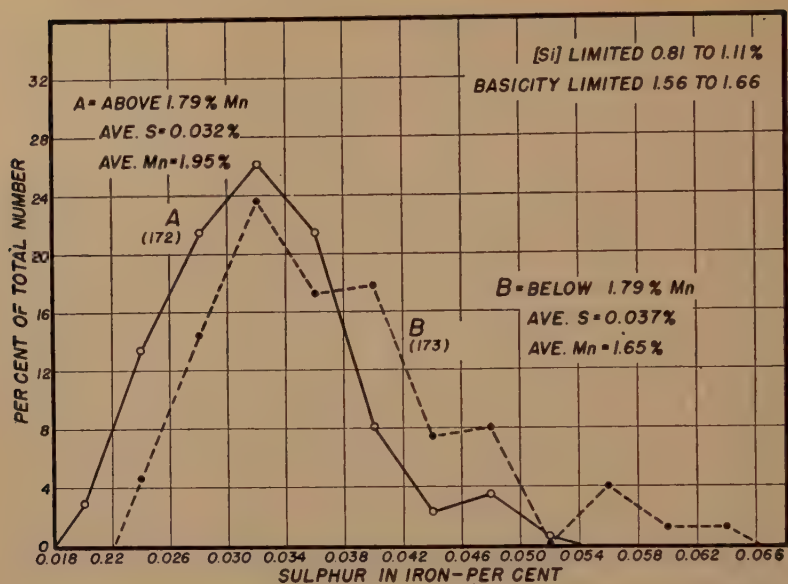


FIG 3—FREQUENCY CURVES OF SULPHUR IN IRON FOR GROUPS ABOVE AND BELOW THE MEAN MANGANESE IN IRON.

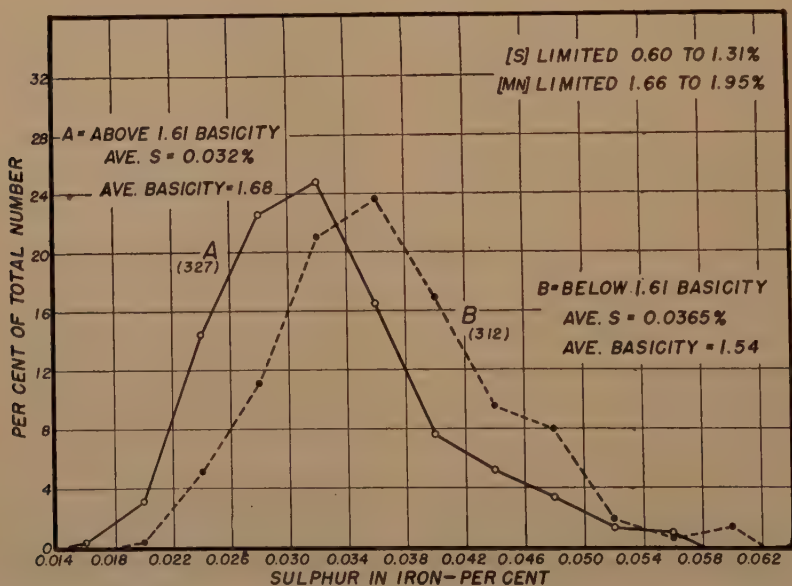


FIG 4—FREQUENCY CURVES OF SULPHUR IN IRON FOR GROUPS ABOVE AND BELOW THE MEAN BASICITY RATIO.

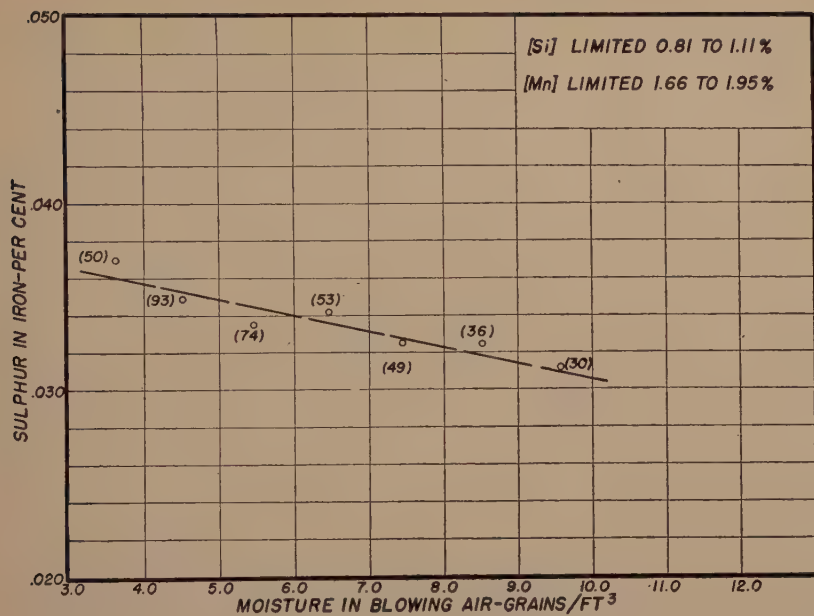


FIG 5—TREND CURVE OF THE SULPHUR IN IRON AGAINST MOISTURE CONTENT OF THE AIR BLOWN.

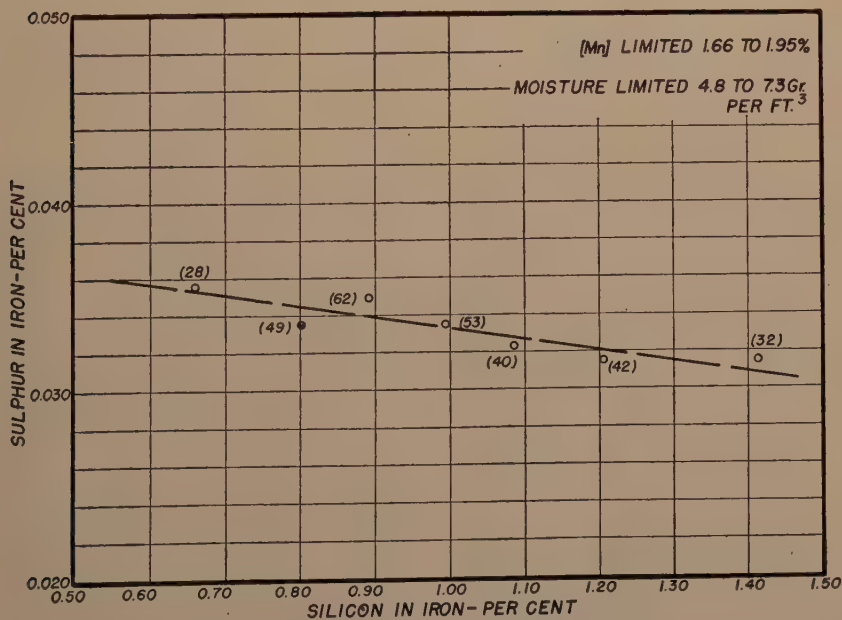


FIG 6—TREND CURVE OF THE SULPHUR IN IRON AGAINST SILICON IN IRON.

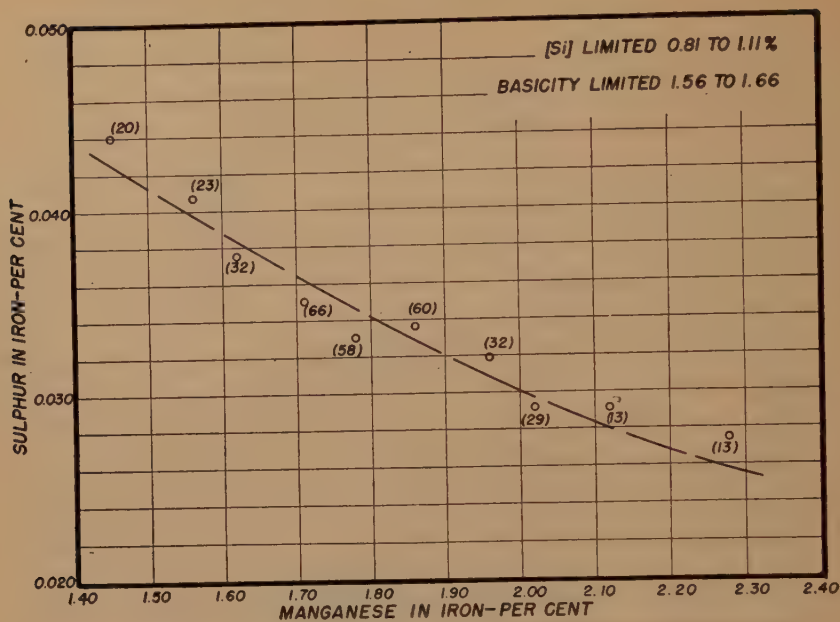


FIG 7—TREND CURVE OF THE SULPHUR IN IRON AGAINST MANGANESE IN IRON.

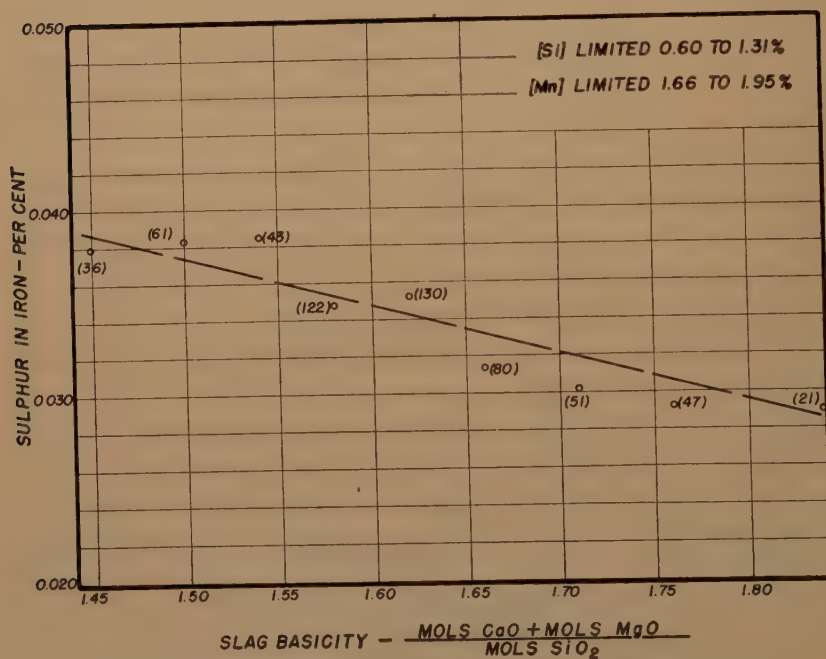


FIG 8—TREND CURVE OF THE SULPHUR IN IRON AGAINST BASICITY RATIO.

In Fig 9, a similar trend curve for [Mn] against [S] from practice Y indicates essentially the same degree of correlation at a

even with the help of punch card and machine methods is very laborious and time-consuming. We obtained the following

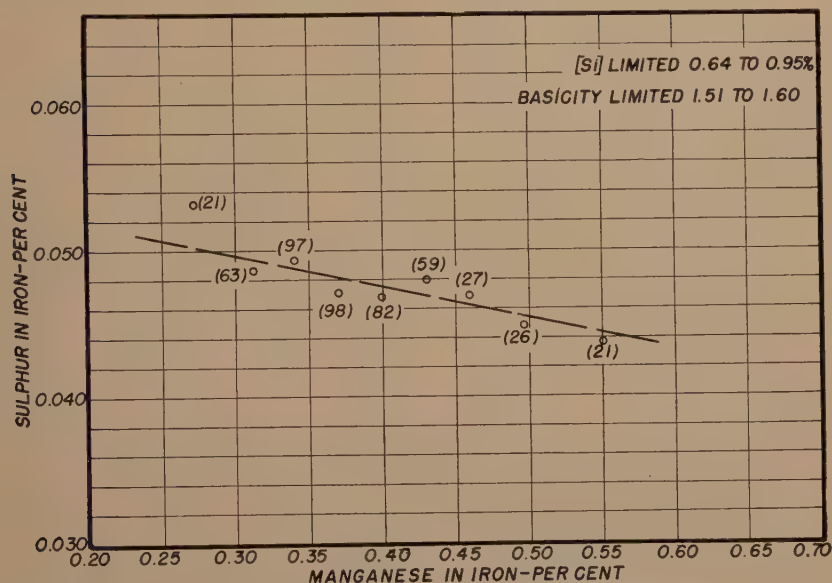


FIG 9—TREND CURVE OF THE SULPHUR IN IRON AGAINST MANGANESE IN IRON—IRON WITH LOWER RANGE OF MANGANESE CONTENTS.

much lower [Mn] range. A similar effect was obtained in a third practice Z, which was on blowing iron with a higher [Si] range.

As a further check on the curves in Fig 5 to 8, inclusive, selected data from 1300 casts from practice X were also put on punch cards, with squares and cross-products obtained by machine methods. These data were used to obtain the multiple coordinate equation by the method of orthogonal coordinates in linear regression given by Davis⁴ and worked out for such cases by W. O. Clinedinst⁵ of National Tube Co.

This method of multiple correlation,

equation from these data from practice X:

$$[S] = +0.1137 - 0.0067 [Si] - 0.018 [Mn] - 0.0224 (\text{Basicity Ratio}) - 0.00107 (\text{grains H}_2\text{O}) + 0.00023 (\text{Al}_2\text{O}_3).$$

The negligible coefficient for Al_2O_3 in slag shows that it may be neglected, in agreement with the similar indications from frequency curves on three different practices.⁶

The coefficients in this equation may be compared with the slopes of the simple trend curves (with restriction of associated variables) in Fig 5, 6, 7 and 8, as follows:

	Linear Regression Coefficients			
	[Si]	[Mn]	(Basicity Ratio)	Grains H_2O in Blast
From Orthogonal Coordinates Equation.....	0.0067	0.0181	0.0224	0.00107
Trend Curve Slopes.....	0.0060	0.0187	0.0203	0.00092

The agreement here suggests that where the interrelationships are fairly well known and sufficiently large groups of data are available, the simpler and somewhat easier method of trend curves with interrelated variables held nearly constant (or an equivalent mathematical method) may be used to advantage.

These results in general indicate that normal changes in these variables had effects roughly as follows on the sulphur content of the iron:

50 points rise in [Mn] (about 1.7 to 2.2 pct)—9 points drop in [S]

50 points rise in [Si] (about 0.7 to 1.2 pct)—3 points drop in [S]

Basicity Ratio in Slag from 1.4 to 1.7—6 points drop in [S]

H₂O in blast from 4 to 9 grains per ft³—5 points drop in [S]

Thus in this particular practice, manganese in iron is the largest single factor affecting residual sulphur in the iron, actually causing nearly as much effect as the other three factors combined. It should be emphasized that this would not necessarily be true in other furnace practices. In practice X, [Mn] appears to be predominant mainly because the furnace temperature was not so variable, whereas [Mn] varied rather widely, from about 1.3 to 2.5 pct. In the low-manganese basic practice Y and the blowing iron practice Z [Si] or furnace temperature and slag basicity were the main variables affecting [S]. Comparing low and high [Mn] practices as follows:

	Practice X, Per Cent	Practice Y, Per Cent
Mean [Mn].....	1.78	0.38
Mean [S].....	0.034	0.047

shows an effect on [S] which is largely the effect of the respective [Mn] levels. Such a difference, however, could no doubt be eliminated by operating practice Y with a much higher furnace temperature, with a slag composition such as would have a

higher free-running temperature and greater effective basicity.

SULPHUR BURDEN AND (S)/[S] RATIO

Such comparisons as these between different furnace practices are usually neither accurate nor satisfactory, mainly because of differences in total sulphur in the burden. The equation above for practice X accounts for only 40 to 50 pct of the total variation in sulphur. The largest single remaining variable is the sulphur content in coke, which largely determines the sulphur burden (90 pct of total sulphur from coke); in this case the sulphur content in coke happened to vary over a rather wide range. Again, in the above comparison between low and high-manganese practices, the differences in mean [S] levels would have been much larger but for the fact that the increase from X to Y in slag volume was greater than the corresponding increase in sulphur from coke so that sulphur contents in slag are much lower in Y than in X practice, (means of 1.1 and 2.0 pct, respectively).

Such differences in burdening and weight of slag per ton of iron can be eliminated by employing, instead of sulphur in iron, the ratio (S)/[S] between slag and metal, if we assume that the simple distribution law holds over the usual range of variation in commercial practice; (this is merely the assumption that if total sulphur charged is doubled, the percentage in both slag and metal will also be doubled, so that the ratio (S)/[S] remains constant).

In practices X and Y, we had daily averages of sulphur content in slag so that the average ratio (S)/[S] could be obtained over each 24 hr period. The frequency curves in Fig 10 show that [Mn], with [Si] and slag basicity restricted has an effect on the ratio (S)/[S] which is essentially the same as the corresponding effect on sulphur in iron. Simple trend curves as in Fig 5 to 9 can also be obtained for (S)/[S] as the dependent variable. Such points from three different practices, all on

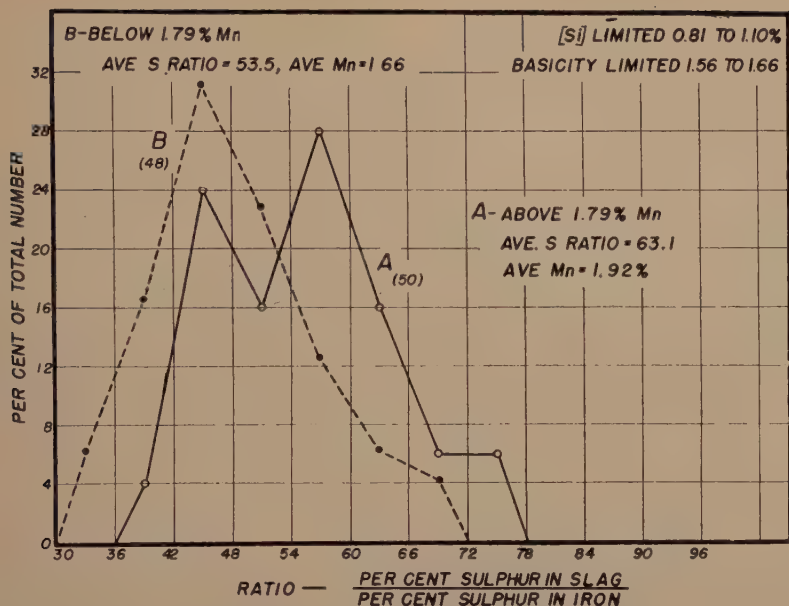


FIG 10—FREQUENCY CURVE OF THE RATIO OF SULPHUR IN SLAG TO SULPHUR IN IRON FOR GROUPS ABOVE AND BELOW THE MEAN MANGANESE IN IRON.

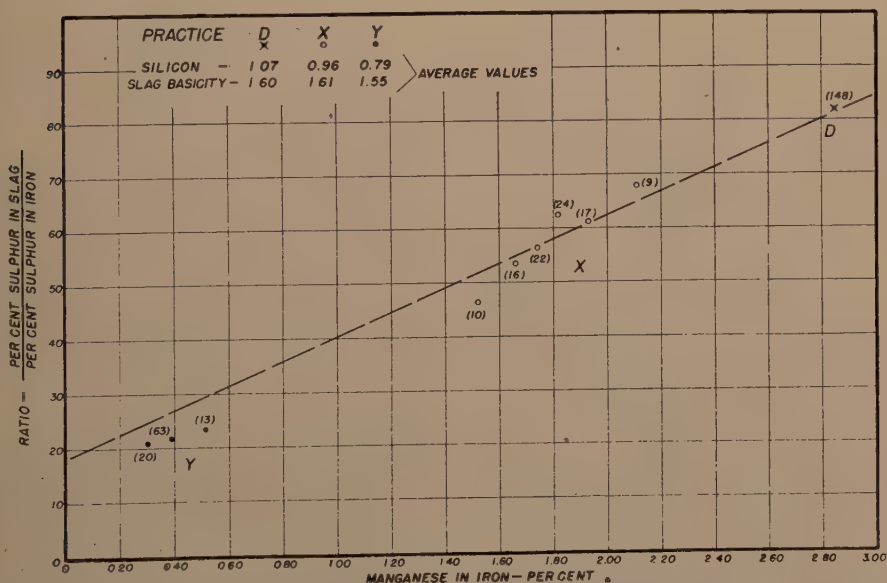


FIG 11—TREND CURVE OF MANGANESE IN IRON AGAINST RATIO OF SULPHUR IN SLAG TO SULPHUR IN IRON—WIDE RANGE OF MANGANESE CONTENTS OF IRON.

basic iron and with [Mn] as the main variable, have been plotted together in Fig 11. In addition to averaged points (numbers averaged shown in parentheses as in all other figures) from the *X* and *Y* practices, the point *D* represents a monthly average from a third practice with sulphur and manganese both high in the burden; (the respective mean [S] values for practices *X* and *D* were 0.034 and 0.029 pct). The average values of the other main variables, [Si] and slag basicity, are given in Fig 11 and are fairly close together; some effect of temperature and slag basicity may remain, however, and the trend curve as drawn may have a slope somewhat steeper than the individual effect of [Mn] on the (S)/[S] ratio. Again it should be remembered that a marked increase in smelting temperature, giving normally a higher [Si] level and higher effective slag basicity, can substitute largely and perhaps entirely, for this dominant effect of [Mn]. This was illustrated in our data on the blowing-iron practice *Z*, where a mean [Si] of 1.40 pct gave a mean (S)/[S] ratio of .70 with a mean [Mn] of only 0.55 pct. As noted above, the present difficulty in a more complete evaluation of these effects lies chiefly in the lack of direct measurements of furnace temperature in hearth and bosh zones.

SUMMARY

As regards the transfer of sulphur from iron to slag, the Al_2O_3 content in slag has a negligible effect, over the usual ranges in commercial practice. The ratio

$$\frac{(\text{Mols CaO}) + (\text{mols MgO})}{(\text{mols SiO}_2)}$$

appears to be a reasonably satisfactory, even if approximate, measure of slag basic-

ity at least over an MgO range of about 4 to 10 pct.

In addition to the factors of [Si] content (or furnace temperature, probably) and slag basicity, manganese in iron has a large effect on both [S] and the (S)/[S] ratio. Under certain conditions [Mn] may be the main determining factor.

Moisture content in air blown appears to have a direct positive effect on desulphurization in addition to its indirect negative effect through lowering of hearth zone temperature. Further evidence is needed, but the combination of positive and negative effects may explain why this has not been previously noted.

REFERENCES

1. P. Bardenheuer and W. Geller: Fundamentals of the Desulphurization of Iron and Steel. Mitt. K. W. Inst. für Eisenforsch. (1934) **16**, No. 7, 77-91.
2. O. Meyer and F. Schulte: The Equilibrium in the Reaction $\text{FeS} + \text{Mn} \rightleftharpoons \text{MnS} + \text{Fe}$ at High Temperature: *Archiv Eisenhüttenwesen* (1934-5) **8**, 187-195.
3. L. S. Darken and B. M. Larsen: Distribution of Manganese and Sulphur between Slag and Metal in the Open Hearth Furnace. *Trans. AIME* (1942) **150**, 87-112.
4. H. T. Davis: The Analysis of Economic Time Series. (1941) Principia Press, Inc.,
5. Unpublished manuscript.
6. Regression coefficients (by the Doolittle method as well as by that of orthogonal coordinates) which tend to be proportional to the relative importance of the respective factors, are as follows:

$y = [\text{S}]$	Regression Coefficients	
	Original of Doolittle Method	Final of Orthogonal Method
$x_1 = [\text{Si}]$	$\beta_1 = -0.218$	$\alpha_1 = -0.181$
$x_2 = [\text{Mn}]$	$\beta_2 = -0.421$	$\alpha_2 = -0.422$
$x_3 = \text{Slag Basicity Ratio}$	$\beta_3 = -0.215$	$\alpha_3 = -0.203$
$x_4 = \text{Grains H}_2\text{O per ft}^3$	$\beta_4 = -0.203$	$\alpha_4 = -0.201$
$x_5 = \text{Al}_2\text{O}_3 \text{ in slag}$	$\beta_5 = +0.022$	$\alpha_5 = +0.027$

Tracer Study of Sulphur in the Coke Oven

BY S. E. EATON,* R. W. HYDE,* MEMBER, AND B. S. OLD,* MEMBER AIME

(San Francisco Meeting, February 1949)

INTRODUCTION

ONE of the most important problems facing the steel industry at the present time is that of maintaining at a minimum the sulphur content of many grades of steel where sulphur is known to have harmful effects on both quality and yield. The present outlook in this struggle to reduce the amount of sulphur in steel is rather gloomy since the sulphur content of the raw materials available in the United States is gradually rising, with little relief in sight.

A flow sheet of sulphur in the steel process is shown in Fig 1. The values used here were obtained by averaging coke oven and blast furnace data at No. 5 furnace in Cleveland and are considered typical for high top pressure practice. The sulphur evolved in the blast furnace top gas was obtained by difference and since the amount is relatively small, little significance should be attached to this particular value. From Fig 1 it is apparent, however, that coals used in the production of metallurgical coke represent by far the largest single source of sulphur in steel-making. As an indication of the decrease in quality of these coals as regards sulphur content the weighed average annual sulphur analysis of the coals supplied to two different steel plants, since 1925, is plotted in Fig 2.¹ The sharp rise since 1940 is strikingly apparent.

Another indication of this trend is found in estimates of coking coal reserves. Thus

Manuscript received at the office of the Institute May 19, 1948. Issued as TP 2453 in METALS TECHNOLOGY, October 1948.

* Chemical Research Laboratory, Arthur D. Little, Inc., Cambridge, Massachusetts.

in the case of Pittsburgh seam coals available in Allegheny, Fayette, Greene, Washington, and Westmoreland Counties in Pa. as of Jan. 1937 only 25 pct of the coal reserves would contain less than 1.50 pct sulphur after washing.^{2,3} Many of these lower sulphur reserves have been seriously depleted in recent years because of accelerated war demands. Still another demonstration of the increasing sulphur content of coals on a country-wide basis is found in a report by the Bureau of Mines⁴ which shows a steady increase in the sulphur content of coke made in the United States. It should be noted that this increase continues in spite of the wider use of coal washing in recent years.

Sulphur occurs in coal in three forms, pyritic (FeS_2), organic sulphur, and a small amount of sulphate sulphur (CaSO_4). The sulphur is subsequently found in the coke in combination with carbonaceous material of unknown composition and as calcium and iron sulphides. In considering the general problem of sulphur elimination, the Republic Steel Corp. was interested in determining which, if either, of the two major forms of sulphur in coal contributes the greater portion of sulphur to the coke. Since the ratio of pyritic to organic sulphur varies widely in different coals, it was thought that if it could be shown definitely that the major part of the sulphur occurring in coke originates from one of the two major forms of sulphur in the coal, it would then be possible to select with confidence coal which, although high in total sulphur, would yield coke of fairly low sulphur content. Using the new

"tracer" or "tagged atom" technique it appeared possible to determine quantitatively what percentage of the various forms of sulphur found in coal persist through the coking operation.

carbonization, 25-50 pct of the sulphur content of the original coal passes off in the gas, the balance remaining in the coke. Early investigators considered only the total sulphur in this connection. However,

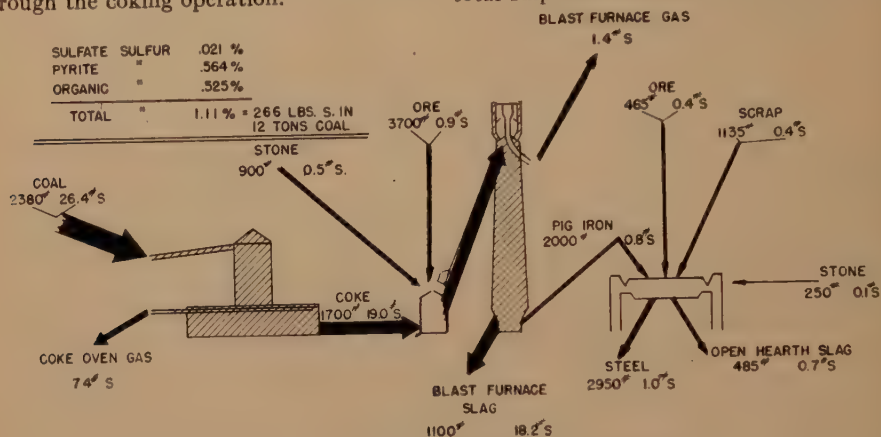


FIG 1—FLOW OF SULPHUR IN BASIC STEEL PROCESS.

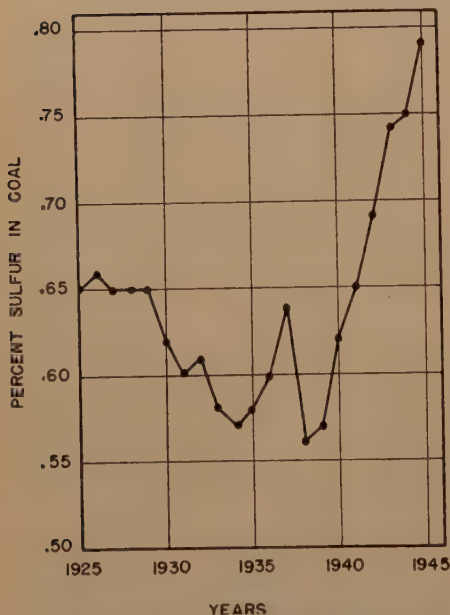


FIG 2—TREND OF SULPHUR CONTENT IN COKING COAL.

Considerable work has been done previously on the behavior of sulphur in the coking of the coal, and it is well known that, depending on the conditions of

this problem has been approached recently from the standpoint of the behavior of the individual forms in which the sulphur is present in coal. The results of two statistical studies involving forms of sulphur vary somewhat. Lowry⁶ found that the ratio of sulphur of pyritic origin to sulphur of organic origin in the coke was the same as the ratio of pyritic to organic sulphur in the original coal, whereas Thiessen⁶ showed that the pyritic to organic sulphur ratio in the coal was altered during coking and that 62 pct of the pyritic sulphur and 45 pct of the organic sulphur remained in the coke. Powell⁷ in his small-scale laboratory investigations found that the total sulphur of the coal is the most important factor affecting the sulphur content of the coke. The source of this difference between Thiessen and Lowry may be in the nature of the coal used or in the different operating conditions of the small-scale coke oven. This problem seemed to be very well suited for positive solution employing the new "tagged atom" technique under typical full-scale coking conditions at Republic.

Radioactive tracers represent a powerful new tool for studying chemical and physical problems in research and industry. By the tracer technique radioactive atoms can be followed through complicated chemical reactions with instruments which detect the radiations emitted. The use of a radioactive element for tracing purposes is based on the fact that it is identical in chemical behavior with the nonradioactive form of the same element. The radioactivity of any particular element is completely unaffected by temperature, pressure or chemical reactions. Therefore atoms, such as sulphur, from a particular source may be marked or tagged radioactively, mixed with other nonradioactive sulphur atoms of identical chemical nature and by the use of detecting instruments the amount of marked sulphur can be quantitatively measured in the mixture. Thus the two major forms of sulphur may be traced through the coking process in a manner impossible by chemical means.

The exact composition of organic sulphur compounds in coal is unknown. However, it appears that they are uniformly distributed throughout the coal structure. On the other hand, pyrites is a definite compound occurring in coal as particles from microscopic size up to large pieces. For this reason it was decided to study the action of iron pyrite sulphur during carbonization rather than to attempt to work with sulphur in the form of organic sulphur compounds.

The general line of attack was to synthesize iron pyrite from radioactive sulphur, mix this material thoroughly with 12 tons of coal, the normal charge to one coke oven, and trace the pyritic sulphur by taking samples of gas and coke, as well as the original coal. It was assumed, and this is believed to be a reasonable assumption, that the added radioactive pyrites behaved identically with the pyrites naturally occurring in the coal. Since the sulphate sulphur content in the

coal used was fairly small, the action of organic sulphur in the coking operation could be estimated fairly accurately by difference.

Calculations indicated that, in order to obtain accurate radioactive readings in the sulphur extracted from samples of coal, gas and coke, it would be necessary to add to the 12 tons of coal about 2.3 lb of radioactive FeS_2 prepared from sulphur obtained from the Atomic Energy Commission. This amount increased the sulphur content of the coal from the original value of 1.06 to about 1.065 pct which, it is believed, would not introduce an appreciable error by increase of the sulphur content.

The activity of the radioactive sulphur obtained from the Atomic Energy Commission was about 40 microcuries per g when received. Radioactive sulphur 35 has a half life of 87.1 days and emits a beta ray, the energy of which is 0.17 Mev. This beta radiation emitted by the sulphur 35 is so weak that ordinary clothing or the outer layer of the skin is sufficient to stop it completely and prevent any dangerous action on the body. Dr. Robley D. Evans, an authority on health hazards associated with radioactivity, gave assurance before the tests were made that there was even less danger in this experiment from radioactivity of the sulphur than there would be from chemical poisoning from the hydrogen sulphide formed in the coking operation.

Because of the very low penetrating power of this beta radiation it was impossible to detect the presence of the active sulphur with a very sensitive Geiger-Mueller counter once the radioactive material had been mixed with the coal, the beta radiations being absorbed completely by the coal. As a matter of fact, in order to overcome this absorption of the beta rays by other material and to permit measurement of the activity, the sulphur had to be extracted from all

samples of coal, coke and gas. During each phase of the experiment, precaution, as outlined by Dr. Evans, was taken to protect all personnel from any dangers resulting from radioactivity.

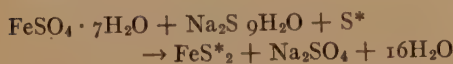
DESCRIPTION OF THE EXPERIMENT

Preparation of Radioactive Pyrite

The first step in the experiment was the preparation of radioactive iron pyrite from sulphur obtained from the Atomic Energy Commission. The active sulphur obtained weighed 2000 g and contained about 80 millicuries of sulphur 35 and about 150 millicuries of "carrier free" phosphorus 32 as a minute chemical impurity which later was eliminated in the synthesis of the pyrites.

With a few minor changes, the hydrothermal synthesis as described by E. J. Allen and coworkers⁸ was used. The yield obtained by this method varied between 90 and 100 pct based on the iron available for reaction.

The overall reaction in this synthesis is as follows, where S* indicates radioactive sulphur:



Actually, the reaction is believed to occur in two steps, the immediate reaction of sodium sulphide with iron sulphate to form ferrous sulphide and sodium sulphate proceeds easily, while the bomb reaction, the addition of the elemental sulphur to form iron pyrite, proceeds much more slowly. Since pyrite forms preferentially at high pH, excess sodium sulphide was used to give the desired alkaline medium. All the sulphur in the iron pyrite does not originate from the elemental radioactive sulphur added to the charge. Actually only about 43 pct of the sulphur in the iron pyrite comes from the radioactive sulphur, the remainder being inactive sulphur from the $\text{Na}_2\text{S} \cdot 9\text{H}_2\text{O}$. The symmetry of the

FeS_2 molecule causes both sulphur atoms to be identical in chemical behavior.

The prepared pyrite was studied under the microscope and by X ray diffraction and no impurities were detected. A slight trace of marcasite, but no trace of free iron or amorphous FeS_2 , was found. The product gave a good pyrite pattern and it was concluded that the FeS_2 was largely in the crystalline pyrite form which is the same form believed to be present in coal.⁹ Chemical analysis showed the dry pyrites to be about 97.5 pct purity with 0.87 pct moisture. The radioactive phosphorous which had been present as an impurity in the original active sulphur was practically eliminated in the synthesis of the iron pyrite. P^{32} emits a beta ray, 1.71 Mev and has a half life of only 14.3 days. In the several months' time which elapsed after synthesis only the weak beta radiations of sulphur could be detected in the final sample measurements.

Coal Mixing and Sampling

In order to facilitate handling and insure thorough mixing, 1050 g (2.315 lb) of the prepared iron pyrite was premixed with 300 lb of Republic's normal coal mixture.

On July 8, 1947, the coke oven experiment proper was started. Twelve tons of coal, the normal charge to one oven, was dumped from a hopper car onto the top platform at the end of the ovens. The coal mixture in use that day was as follows:

	Pct
Freeport (Russelton, Pa.).....	9.4
Clyde.....	9.4
Lower Elkhorn (from stock pile).....	58.6
Low volatile (Pocahontas).....	22.6

The coal was then shoveled down a chute into a clean, 4-cu yd cement mixer truck. The premix was first added and the mixer run while the raw coal was being added to insure adequate mixing. During the mixing operations all personnel handling either the pyrite or the premix were equipped with dust masks to minimize the possibility of inhaling the active

material. About 50 lb of dry ice (CO_2) was added to each load to lower the explosion hazard of the finely divided coal in the mixer. After all the raw coal was added,

a small calculated correction was applied later to the coal activity readings.

After mixing, each load was dumped into the waste coal elevator bin and a

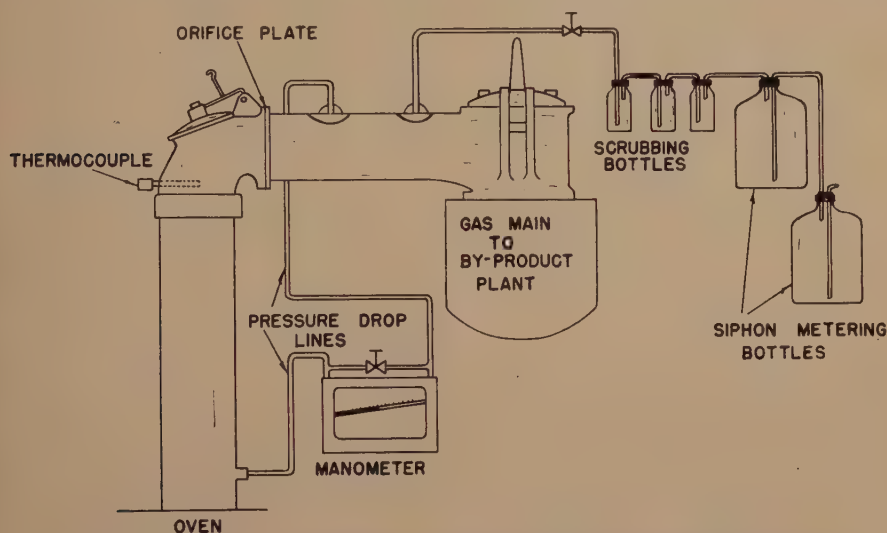


FIG 3—GAS SAMPLING AND METERING APPARATUS FOR SULPHUR TRACER EXPERIMENT.

mixing was continued for at least 20 min. The mixer truck was weighed on large platform scales to determine the amount of coal added. A gross sample was taken from each load as described below. This procedure was repeated three times in order to mix the entire twelve tons of coal in three batches as follows:

TABLE 1—*Mixing and Sampling Data*

	Weight of Coal	Weight of Premix	Sample Weight	Net Weight
1st load.....	9400	97	411	9086
2nd load.....	8003	97	274	8726
3rd load.....	6103	97	274	5926
Unmixed coal.....	450			450
Total.....	24,856	291	959	24,188

About 450 lb of coal were left in the waste coal elevator bin to make up for the rather large portion of the mixed coal taken for a sample. By oversight this raw coal was charged to the oven without any premix being added to it. To overcome this error

shovelful of the mixed coal taken from the stream every 20 sec to obtain a truly representative sample from each mixer load. The weight of sample taken from each load is shown in Table 1. A final 100-lb composite sample was made by mixing the three gross samples in proportion to the weight of the coal in each load. The 100-lb composite sample was then run through a Jones splitter to obtain a representative sample which was used for all subsequent coal analyses.

The coal after sampling was loaded on the waste coal elevator and reloaded back into the hopper car preparatory to charging the oven.

Gas Metering and Sampling Apparatus

The upcomer and gooseneck from the oven had previously been adapted for metering, sampling and taking gas temperatures as shown in Fig 3. A $4\frac{1}{2}$ in. diam orifice plate was inserted between the upcomer and gooseneck in order to

create a pressure drop for the purpose of measuring the flow of gas. The pressure drop lines were connected to a manometer capable of reading directly to an accuracy of 0.02 in. of differential water pressure.

Gas samples were taken from a $\frac{3}{8}$ -in. pipe line and passed through an absorption train by means of two 5-gal calibrated siphon bottles. The absorption train consisted of three 16-oz gas scrubbing bottles, each being about half full of the standard ammoniacal cadmium chloride solution used in the plant laboratory for H_2S determinations. After taking a gas sample, the first two scrubbing bottles of the absorption train were combined to make up a single sample. The third bottle was used in the train to determine whether any H_2S was passing the first two bottles. No cadmium sulphide precipitate was ever noticed in the third bottle indicating complete removal of H_2S from the gas in the first two scrubbers.

The Coking Run

At 2:00 A.M. EST July 9, 1947, the 24,188 lb of mixed coal was charged to No. 56 oven which at the time was operating on approximately a 16-hr coking schedule with a 2450°F flue temperature and producing about 10,500 cu ft of coke oven gas per ton of coal. The covers and vents were closed at 2:05 A.M. and the run started.

During the coking period, gas samples were taken as often as possible; 20 to 30 min. were required per sample and several times it was necessary to clean the sampling line which had become plugged with tar. A volume of 1.32 cu ft of gas was taken for each of 21 samples. The pressure drop readings across the orifice were taken as well as gas temperature readings. However, during run the temperature readings were suspected to be in error and when the thermocouple was removed for inspection it was found to have been damaged.

At 5:35 P.M. the coke was pushed and appeared quite normal to most of the

Republic personnel present, although the foreman thought it looked "green." This means that the coke looked as though it had not been completely carbonized. Immediately after pushing it was quenched with additional water to make sure it would not catch fire before it could be weighed and sampled.

Coke Sampling

After standing for about 11 hr, the coke was weighed and a sample taken immediately for moisture determination. The coke weighed 23,100 lb and contained 17.65 pct moisture. This unusually high moisture resulted from the large amount of extra water which was used in quenching the coke and from the fact that it rained during the night.

In order to obtain a representative sample, the coke was sampled from the conveyor belt. The coke dock and belt were first cleaned and the coke dumped on the dock which feeds the belt. A gross coke sample of 598 lb was taken by stopping and completely clearing a section of the belt every 20 sec for a total of 9 samples. In this way, a representative sample of fine as well as coarse material was obtained. The gross coke sample was then crushed by hand and run through a riffler to obtain a sample which was used for all subsequent coke analysis.

ANALYTICAL WORK

Coal and Coke Analyses

The samples of coal and resulting coke were analyzed at Republic's laboratory for moisture, volatile matter, ash and total sulphur by the standard methods employed by many steel companies. The peroxide fusion method was employed by Republic in the determination of total sulphur. Since the main interest here is sulphur, the total sulphur determinations were repeated by the Eschka method at Arthur D. Little, Inc. and later by the Bureau of Mines and both results checked closely

with Republic's determinations. The results are shown in Table 2.

Volatile matter in coke generally runs about 1.0 pct at Republic. The high percentage of volatile matter in the coke indicates that the coking of this coal may have been incomplete.

Gas Analysis

During the coking run known volumes of gas were scrubbed with ammoniacal cadmium chloride to precipitate the sulphur as cadmium sulphide. These cadmium sulphide gas samples were purified by evolving the H_2S into fresh ammoniacal

TABLE 2—*Coal and Coke Analyses*

	Coal Mixture			Coke		
	Republic, Pct	A.D.L., Pct	Bureau of Mines, Pct	Republic, Pct	A.D.L., Pct	Bureau of Mines, Pct
Moisture.....	3.95	Dry Basis		17.65	Dry Basis	
Volatile matter.....	28.75			2.89		
Ash.....	8.73			11.71		
Total sulphur.....	1.09	1.07	1.06	0.90	0.91	0.91

TABLE 3—*Forms of Sulphur in Coal and Coke*

Coal	Pct	Lb	Coke	Pct	Lb
Sulphate Sulphur.....	0.06	14	Calcium Sulphide Sulphur....	0.04 ± 0.02	8
Pyritic Sulphur.....	0.45	104	Iron Sulphide Sulphur.....	0.08 ± 0.01	15
Organic Sulphur.....	0.55	128	Carbonaceous Sulphur.....	0.79 ± 0.02	150
Total Sulphur.....	1.06	246	Total Sulphur.....	0.91 ± 0.01	173

The coal and coke samples were also analyzed by the Bureau of Mines to determine the forms of sulphur present. In the case of coal, the forms of sulphur, sulphate, pyritic and organic were determined by the method approved by the Bureau of Mines as developed by Powell and Parr.¹⁰

The coke was analyzed by Republic, Arthur D. Little, Inc., and the Bureau of Mines for calcium and iron sulphide according to a method described by the Chemists Committee of the U. S. Steel Corp.¹¹ The sulphur in combination with carbonaceous matter in the coke was obtained by difference. The results obtained by the three laboratories were averaged and are presented in Table 3. All values checked within limits shown.

The data of Table 3 are expressed as per cent sulphur, based on dry coal and coke and pounds of sulphur for the whole run are as follows:

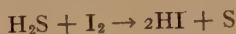
cadmium chloride to obtain a new cadmium sulphide precipitate free of tar. This fresh precipitate was then dried to constant weight, weighed and calculated as elemental sulphur. The residue from each gas sample was treated to extract the remaining sulphur. This value was added to the cadmium sulphide sulphur to obtain the total sulphur content of each gas sample. This addition was a small one and raised the sulphur values by about an average of 5.5 pct.

Preparation of Samples for Activity Measurements

The initial radioactive sulphur used in this experiment had a relatively low specific activity of 40 microcuries per g. Because of the large dilution of this radioactive sulphur with inactive sulphur from the 12 tons of coal, the activity was reduced still further. In the above analyses,

sulphur was recovered as barium sulphate and cadmium sulphide, and the diluting effect of the other atoms of these molecules further reduced the specific radioactivity of the sulphur. In order to obtain higher activity readings on our measuring instrument and thus greater accuracy, a method was devised to obtain pure elemental sulphur from these sulphur compounds. All samples were reduced to elemental sulphur before activity measurement.

In the case of the gas samples, the sulphur was simply evolved from CdS as H_2S into hydriodic acid-iodine solution where it was precipitated as sulphur, according to the following reaction:



Preparations of barium sulphate samples from the coal and coke by the Eschka fusion method were repeated using 40 g of coal and coke to obtain enough sulphur for the activity measurements. The sulphate obtained was then reduced and precipitated as cadmium sulphide,¹² and converted to elemental sulphur by evolving H_2S into iodine solution.

Using large samples of coke in order to yield enough sulphur for activity measurements the water soluble sulphide (CaS) and the acid soluble sulphides (CaS and FeS) were separately extracted from the coke and reduced to elemental sulphur. This was done to determine the distribution of sulphur of pyritic origin in the calcium sulphide, iron sulphide and the carbonaceous sulphur of the coke.

Radioactive Standards

The per cent of sulphur which was of pyritic origin in the sulphur samples from the gas and coke was calculated from the radioactivity of these samples, the radioactivity of the coal sulphur samples (0.22 units) and the per cent pyritic in coal sulphur (42 pct) as follows:

$$\frac{\text{Per cent pyritic in sample sulphur} = \text{activity of sample sulphur}}{0.22} \times 42 \text{ pct.}$$

This calculation is based on the fact that measured activity is directly proportional to the per cent radioactive sulphur present. To illustrate this, a series of sulphur standards containing known amounts of radioactive pyritic sulphur was prepared. The standards contained percentages of from 0.1 to 1.0 pct radioactive sulphur in total sulphur. The radioactive sulphur in these standards was obtained by reducing the sulphur from a sample of the original active pyrities first to sulphide¹³ and then to elemental sulphur by evolving into iodine solution. The standards were made up by diluting this active sulphur with chemically pure flowers of sulphur powder and melting the mixture to insure intimate mixing of the active with the inactive sulphur.

An examination of Fig 4 indicates that the percentage of radioactive sulphur and therefore the percentage of pyritic sulphur in the sulphur of each sample are directly proportional to the activity reading, which is the normal and expected behavior at this level of radioactivity.

Activity Readings

Activity is measured in terms of the number of atomic disintegrations per unit time. No correction has to be made in the case of these samples for the decrease in activity with respect to time, since all the samples contained active sulphur of the same age from the same original batch. Therefore the readings could simply be compared with one another provided the readings were taken at the same time. The elemental sulphur samples and the standards to be counted were each placed in a stainless steel cup, the inside dimensions of which were 0.00197 in. (0.5 mm) deep by 0.707 in. in diam. The powder surface was "doctored" off level with the cup edges to produce a uniform surface.

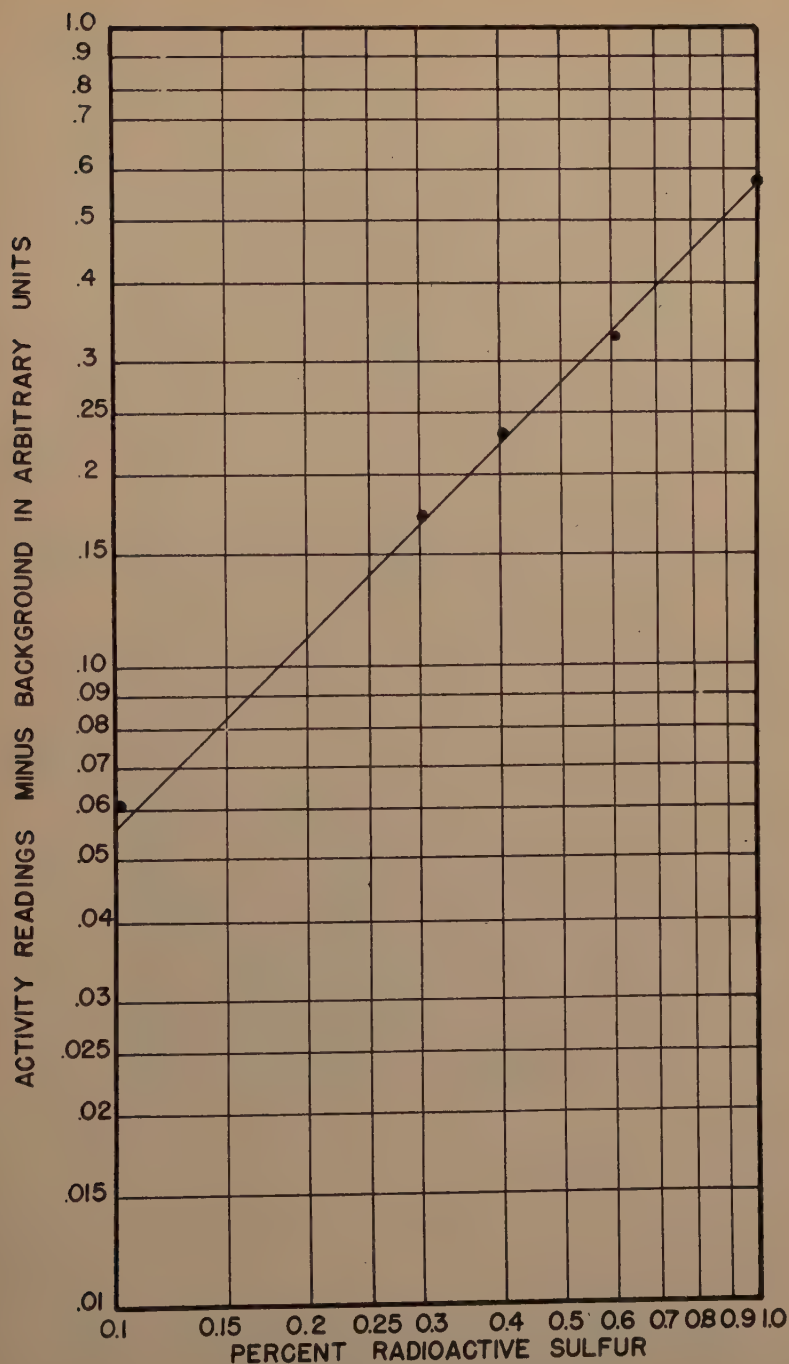


FIG 4—Activity Calibration Curve.

This surface was kept at a fixed distance (about 0.12 in.) from the counter window during all measurements.

All the activity measurements were made on "infinitely thick" samples. For every beta radiating material there is a definite thickness of sample above which the number of radiations emitted per unit area of sample surface is constant. This is because of the internal self-absorption of the material used. Thus, regardless of how thick the sample is, as long as it is equal to or greater than this definite thickness, the same reading will be obtained by a counter held near the sample surface. "Infinite thickness" for the sulphur 35 powder used in this work is less than 0.2 mm and since the thickness of sample in all readings was 0.5 mm, no correction for thickness had to be applied.

In making the activity measurements, all the standards and samples were counted the same day because of the decrease in activity which takes place with time. Readings were made in a constant temperature humidity room. The standards were counted first and after the background reading was subtracted a calibration curve was obtained as shown in Fig 4. The activity of the coal, coke and gas sulphur samples were then measured and the instrument checked periodically with a standard. Readings on each sample were obtained by averaging instantaneous readings taken every 5 sec for a total of 25 readings. The coal and coke samples were remixed and recounted three times respectively as a precaution but the readings all checked very closely (± 0.01 unit), the average being recorded in Table 4. The background reading, or reading obtained with no sample present, was measured frequently and always remained about 0.02 units on the scale used throughout this paper. The activity of the total sulphur in the coal before addition of any radioactive pyrites was found to be the same as the background. This value was

subtracted from all readings to obtain the activity of the sample itself.

A portable Instrument Development Laboratories Count Rate Meter, Model 2610, employing a Victoreen bell-type Geiger-Mueller counter with a thin mica window as shown in Fig 5 was used for all measurements. Its readings indicate the relative specific activity of radioactive samples.

TABLE 4—Radioactivity and Pyritic Sulphur Content of All Sulphur Samples

	Activity Readings	Percentage of the Total Sulphur Which Is of Pyritic Origin
Coal charge to oven.	0.22 ± 0.01 units	42
Coke.....	0.21 ± 0.01 units	40
Total sulphides (Fe and Ca) from coke	0.32	62
CaS from coke.....	0.13	25
Gas sample 1.....	0.18	35
Gas sample 2.....	0.14	27
Gas sample 3.....	0.14	27
Gas sample 4.....	0.17	33
Gas sample 5.....	0.20	39
Gas sample 6.....		
Gas sample 7.....	0.21	40
Gas sample 8.....	0.22	42
Gas sample 9.....	0.22	42
Gas sample 10.....	0.23	44
Gas sample 11.....	0.23	44
Gas sample 12.....	0.24	46
Gas sample 13.....	0.24	46
Gas sample 14.....	0.24	46
Gas sample 15.....	0.24	46
Gas sample 16.....	0.25	48
Gas sample 17.....	0.27	52
Gas sample 18.....	0.24	46
Gas sample 19.....	0.19	37
Gas sample 20.....	0.19	37
Gas sample 21.....	0.18	35
Combined activity of all the above gas samples (calc.)*...	0.21	40
Combined acid insoluble residues from all gas samples.....	0.26	50

* Obtained from Table 5 by comparing total per cent pyritic sulphur in gas, 40 pct, with per cent pyritic in the coal, 42 pct, above, and calculating activity by proportion.

Table 4 shows the average activity reading in arbitrary units for each sample (0.1 unit = roughly 330 counts per min. getting through the counter window). The background readings (about 66 counts per min.) have been subtracted. In the case of coal the recorded activity reading is the average of two separately analyzed

samples of coal; in the case of coke three individual samples were analyzed and the average activity of these three recorded in the table. The individual coal and coke

of dry coal. The coal mixture used in this experiment yields an average 10,700 cu ft of gas at 60°F and 14.7 psi per ton of dry coal coked. This figure was obtained

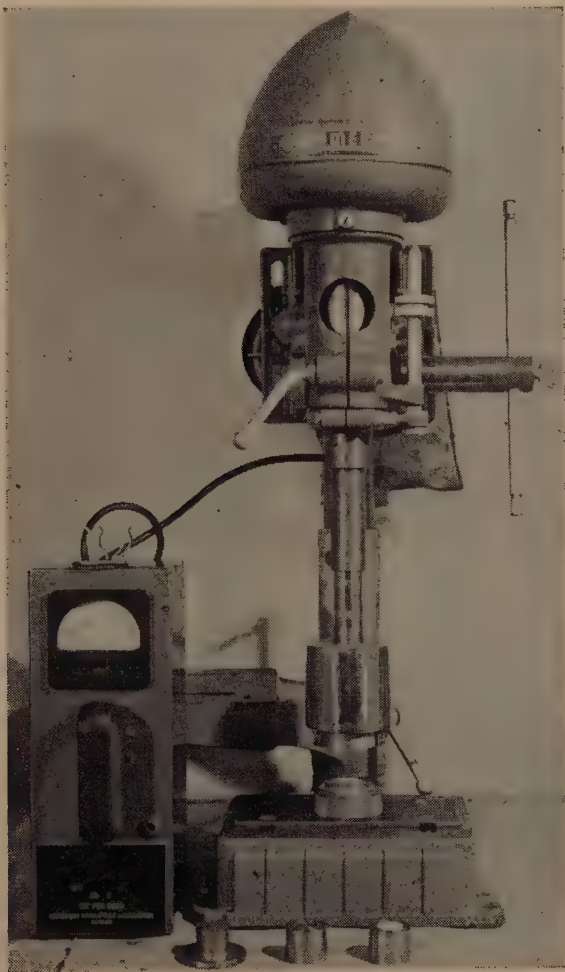


FIG 5—COUNTING APPARATUS.

readings were within ± 0.01 of the average recorded. All other readings were on individual samples.

CALCULATION OF RESULTS

The 24,188 lb of coal at 3.95 pct moisture charged to the oven yielded 23,100 lb of coke at 17.65 pct moisture. One ton of dry coke was obtained for every 1.22 tons

from Republic's coke plant superintendent and is the average gas produced per ton of this coal mixture for all the ovens. On this basis it is calculated that 130,000 cu ft of gas was evolved in the present run measured at 60°F, 14.7 psi.

The rate of gas evolution during coking of the charge is calculated from the pressure drop readings recorded during the

coking period and the average gas evolution per ton of coal, using Eq 4 and 5 below, which are derived as follows:

$$V_0^2 - V_p^2 = K(\Delta P), \quad [1]$$

where V_0 = velocity gas through orifice in ft per sec (calculated at 60°F)

V_p = velocity gas through pipe in ft per sec (calculated at 60°F)

ΔP = pressure drop in inches H_2O .

The orifice and pipe velocities are inversely proportioned to the area A_0 (orifice

The calculated gas evolution curve is plotted in Fig 6. From the determination of sulphur in the gas samples, the total sulphur grain loading in the gas was calculated for each sample taken during the coking run, as shown in Fig 7. The percentages of pyritic sulphur in the gas samples, Table 4 and Fig 8, were determined from the activity measurements according to the equation given on p. 350. From these percentages the pyritic, and organic plus sulphate sulphur grain loading

TABLE 5—Rate of Evolution of Organic and Pyritic Sulphur

Period (Hr)	Cu Ft Oven Gas Per Hr	Lb Pyritic Sulphur Evolved Per Hr	Lb of Organic and Sulphate Sulphur Evolved per Hr	Lb of Total Sulphur Evolved Per Hr
1	12,000	2.1	3.8	5.9
2	9,300	1.0	2.5	3.4
3	9,450	1.0	2.8	3.8
4	10,050	1.7	3.4	5.1
5	10,100	2.2	3.4	5.5
6	9,900	2.2	3.1	5.3
7	9,650	2.1	2.9	5.0
8	9,350	2.0	2.6	4.6
9	9,000	1.9	2.2	4.1
10	8,550	1.8	2.1	3.9
11	8,050	1.8	2.0	3.8
12	7,100	1.7	1.6	3.4
13	5,350	1.1	1.3	2.4
14	5,200	0.9	1.3	2.2
15	4,750	0.5	1.0	1.5
1st half of 16	2,070 cf per 0.5 hr	0.2 lb per 0.5 hr	0.3 lb per 0.5 hr	0.5 lb per 0.5 hr
Total	129,870	24.	36.	60.

area) and A_p (pipe area) and the ratio of the velocities, C , is constant, thus

$$C = \frac{V_0}{V_p} = \frac{A_p}{A_0}$$

$$[C^2 - 1]V_p^2 = K\Delta P,$$

$$\text{Let } \frac{K}{[C^2 - 1]} = K' \quad [2]$$

$$\text{Then } V_p^2 = K'\Delta P \quad [3]$$

The constant K' can be calculated by substitution of average values for V_p and ΔP . The general form for velocity is, then:

$$V_p = \sqrt{K'\Delta P}; \quad [4]$$

or, with K' evaluated,

$$V_p = \sqrt{4.92\Delta P} \quad [5]$$

To reconvert V_p to vol. per hr,

3320 V_p = vol. gas in cu ft per hr at 60°F.

of the gas was also calculated as shown in Fig 9 and 10. The rate of evolution of organic and pyritic sulphur in lb per hr from coal was determined from Fig 6, 7, and 8, and is shown in Fig 11 and in Table 5.

The total sulphur balance on the run is shown in Table 6 as follows:

TABLE 6—Total Sulphur Balance on the Run

	Lb of Sulphur	Per Cent
Coal.....	246.0	100
Coke.....	173.0	70.3
Gas.....	60.4	24.5
Total.....	233.4	94.8

Of the total sulphur charged in the coal 70.3 pct was retained in the coke while

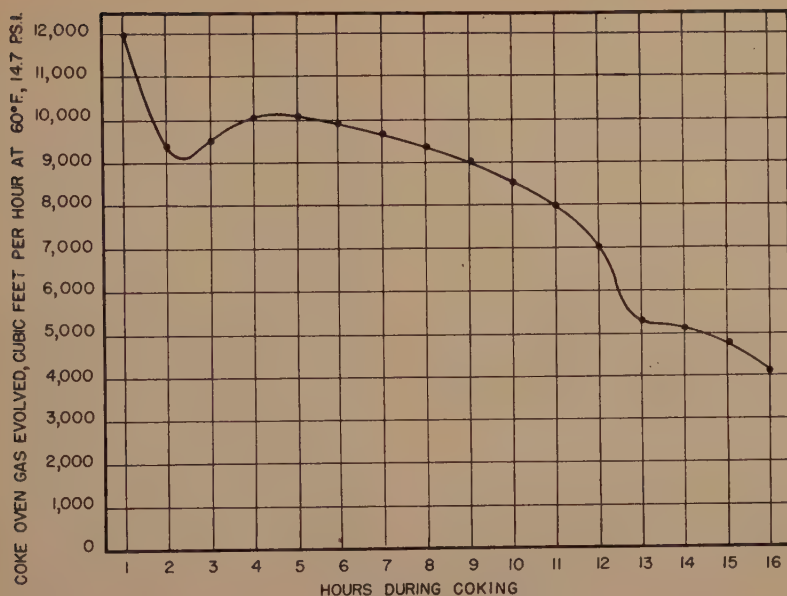


FIG 6—COKE OVEN GAS EVOLUTION DURING COKING OF 12 TONS OF COAL.

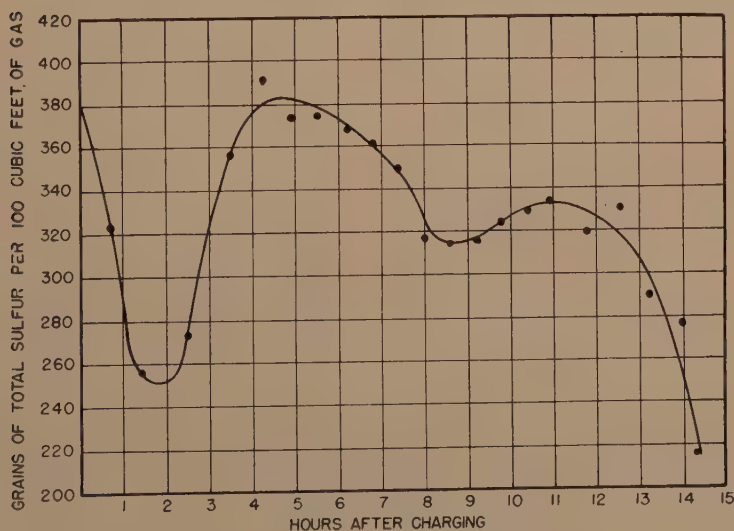


FIG 7—TOTAL SULPHUR CONTENT OF THE GAS.

24.5 pct was evolved in the gas; 5.2 pct (13 lb) was unaccounted for.

The average radioactivity readings for the coal and coke sulphur samples were 0.22 ± 0.01 for the coal and 0.21 ± 0.01 for the coke. This coal reading is corrected for the 450 lb of unmixed coal that was not

represented in the sample. Of the total sulphur in the coal 42 pct is pyritic by chemical analysis. Therefore, by comparing the activity readings, 40 pct \pm 2 pct of the total sulphur in the resulting coke originated from the pyritic sulphur of the coal. The various origins of sulphur in the

coal, coke and gas, which were calculated from the activity measurements, are expressed in Table 7 in per cent of the total sulphur present in each case which originated from sulphate, pyritic or organic sulphur in the coal.

TABLE 7—*Origins of Sulphur in Coal, Coke and Gas, Calculated from Activity Measurements*

	Sulphate Origin, Per Cent	Pyritic Origin, Per Cent	Organic (and Sulphate*) Origin, Per Cent	Total, Per Cent
Coal....	6	42	52	100
Coke....	*	40 ± 2	60 ± 2*	100
Gas....		40 ± 2	60 ± 2*	100

Table 8 shows how the three forms of sulphur in the coal were distributed in the coke and gas, and the amount of each that was accounted for in pounds for the whole run. Where pyritic or organic sulphur

TABLE 8—*Showing Distribution in Coke and Gas of Sulphur in Coal*

Form	Pyritic Sulphur, Lb	Organic (and Sulphate*) Sulphur, Lb	Total Sulphur, Lb
Coal.....	104.0	142.0	246.0
Coke.....	69.0 ± 3	104.0 ± 5*	173.0
Gas.....	24.2 ± 1	36.2 ± 2*	60.4
Total sulphur, coke + gas.....	93.2 ± 4	140.2 ± 6*	233.4
Per cent accounted for.....	90	99	95

content of the coke or gas is listed it refers to sulphur of the coke or gas originating from the pyritic or organic sulphur of coal.

It can be seen from Table 8 that 66 pct

* Sulphur in coke and gas originating from sulphate sulphur could not be determined accurately without running a similar experiment in which the sulphate sulphur was tagged and traced. The sulphur of both the coke and gas originating from the sulphate and organic sulphur of the coal is obtained together by difference between total and pyritic sulphur and is presented in Tables 7 and 8 under organic sulphur.

of the pyritic and 70 pct of total sulphur of the coal remains in the coke, which is an insignificant difference.

It should be pointed out that the per cent radioactive sulphur in the total coal sulphur, which can be obtained from Fig 4 using the coal sulphur activity reading, is somewhat lower than that which material balance calculations, based on the weight of active and inactive sulphur, indicate it should be. Thus from the 0.22 activity reading of the total coal sulphur, the per cent radioactive sulphur present in the total coal sulphur sample should be 0.39 pct according to Fig 4. Since 1.12 lb of radioactive sulphur was actually added to make a total of 246 lb of sulphur in the coal charged to the oven, the per cent radioactive sulphur is calculated to be 0.45 pct. This moderate difference does not affect the conclusions of the test but it is interesting theoretically to consider the possible causes.

An error in obtaining a representative sample of radioactive sulphur from the synthesized pyrites or an error in the actual dilution of this active sulphur to make up the standards used in Fig 4 is possible although the dilution in preparing the standards was repeated with practically identical results. Loss of the finely powdered (minus 100 mesh) active pyrites as it was being premixed is also possible. That about one third of the apparent loss of radioactive pyrites had already occurred by the time the premixing had been completed was indicated by radioactivity measurements on a premix total sulphur sample. The activity of the premix sulphur was too high for direct measurement so inactive sulphur was added in the proportion of 246 parts inactive sulphur to 1.12 parts premix sulphur to give the same dilution calculated to be present in the coal charged to the oven. The activity readings of these diluted premix sulphur samples was 0.24 corresponding to 0.43 pct radio sulphur and indicated that about

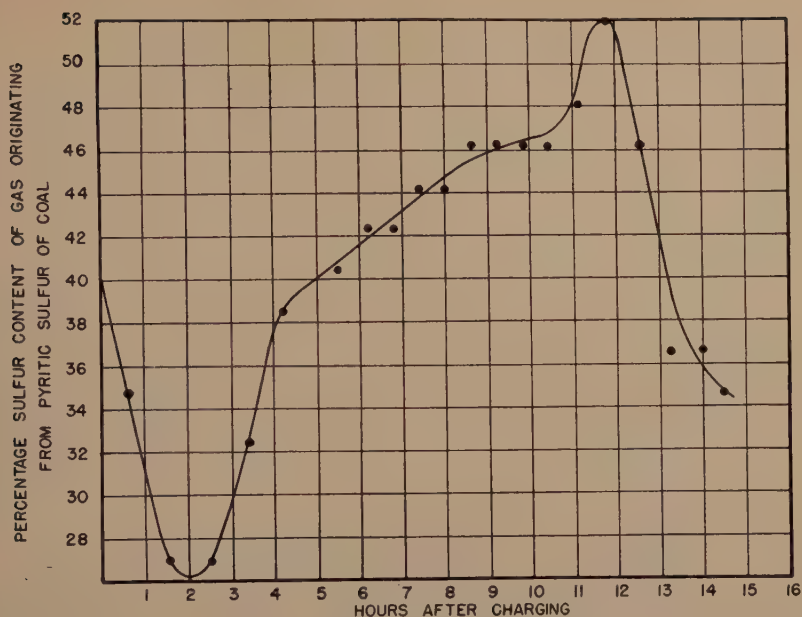


FIG 8—PERCENTAGE OF SULPHUR CONTENT OF COKE OVEN GAS ORIGINATING FROM THE PYRITIC SULPHUR OF THE COAL.

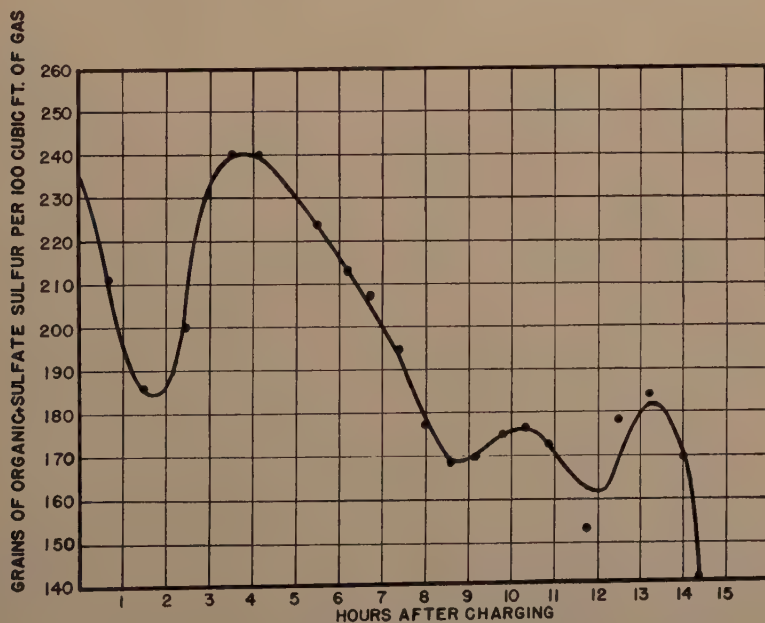


FIG 9—SULPHUR CONTENT OF THE GAS ORIGINATING FROM THE ORGANIC AND SULPHATE SULPHUR OF THE COAL.

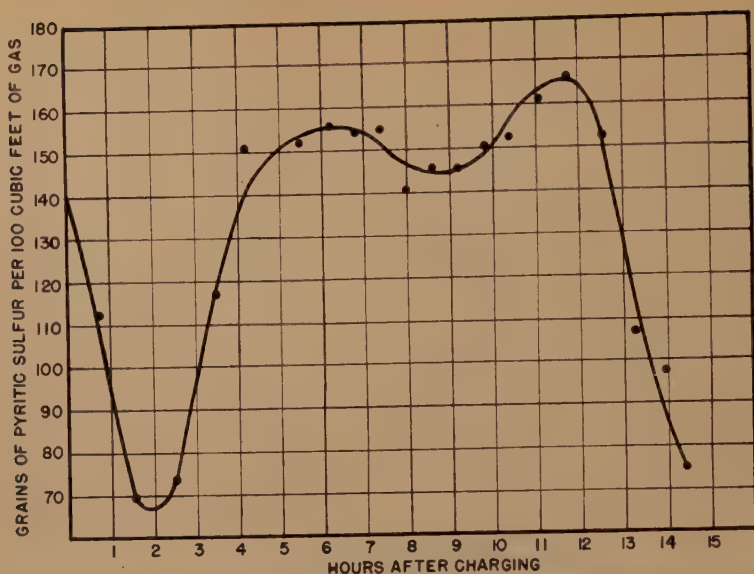


FIG 10—SULPHUR CONTENT OF GAS ORIGINATING FROM THE PYRITIC SULPHUR OF THE COAL.

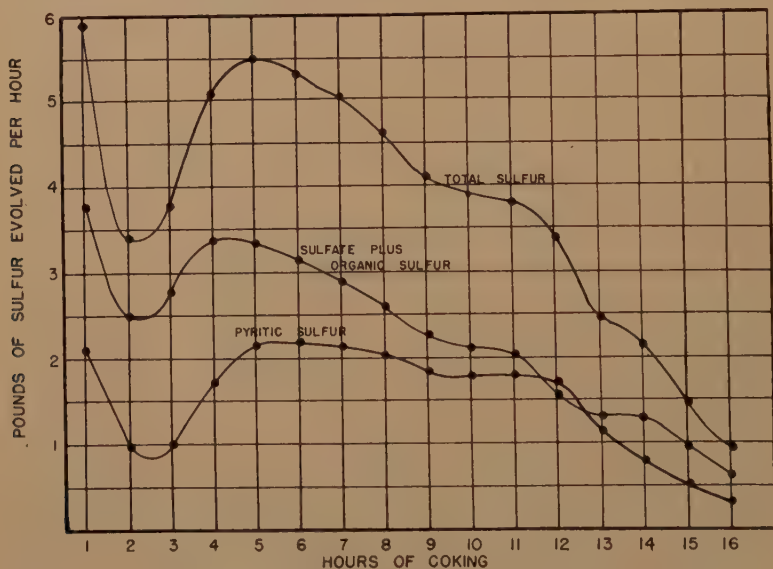


FIG 11—RATE OF SULPHUR EVOLUTION FROM COAL DURING COKING.

one-third of the apparent loss of radioactive sulphur had occurred in premixing.

It is also possible that the method of analysis of coal for total sulphur gives results which are slightly low. This would account for the difference discussed. Some evidence for this is found in the above

dilution of the weighed premix radioactive sulphur with an amount of inactive sulphur based on chemical analysis of the coal. The activity of the resulting diluted sulphur is slightly higher than that of the coal sulphur, possibly indicating that a greater dilution occurred in the coal, that

is the coal actually contained more sulphur than the chemical analysis showed.

Fortunately, the explanation of this difference is not necessary for correct interpretation of the coke oven experiment. It is only necessary to consider one is starting with coal containing sulphur with a measured activity of 0.22 and a known pyritic sulphur content. The linear relationship existing between activity readings and radioactive sulphur contents allows one to calculate the per cent pyritic sulphur in any sulphur sample by comparing its activity with that of the coal sulphur, which is the procedure used in this work.

DISCUSSION OF RESULTS

It is well known that coal contains sulphur as FeS_2 , as CaSO_4 and as organic compounds, the nature of which is not definitely known. After coking, the sulphur that remains in the coke is present as FeS , CaS , and as sulphur combined with carbon. The sulphur passing off in the gas is largely H_2S , with some gaseous organic sulphur.

Of the total sulphur charged to the oven in the coal 95 pct was accounted for in the coke and gas. Most of the sulphur unaccounted for is believed to have been lost in the gas, since the gas sampling system removed all the H_2S but probably only part of the organic sulphur compounds present in the gas. Although sulphur in the acid-insoluble tar residue in the gas scrubbing bottles was determined and added to the total sulphur determinations of each sample, it is doubtful whether an aliquot portion of tar for each sample was obtained. Radioactivity measurement on the combined insoluble residues of the 21 gas samples indicated that 50.0 pct of the sulphur present in these residues came from the pyritic sulphur of the coal, which is higher than the 40 pct for the bulk of the gas sulphur. The tar may thus account not only for the small loss of total sulphur

but also for part of the discrepancy that exists in the pyritic sulphur balance shown in Table 8.

From Fig 6 it can be seen that upon charging the oven there was initially a large evolution of gas. It is believed that when coal is charged to the hot oven the large initial evolution is caused by the more volatile constituents and by rapid coking of the coal adjacent to the hot walls of the oven. The cooling effect of the cold charge plus the large initial gas evolution has a tendency to reduce the temperature of the oven walls and the rate of evolution decreases until enough heat has been supplied to the walls to bring the temperature back up and increase again the coking rate through the charge. Once the charge has been coked through, gas evolution starts to drop off after the more volatile materials have passed off. Further gas evolution probably results from a gradual increase in the temperature of the whole charge.

From Fig 11 showing the rate of pyritic and organic sulphur evolution, and from Fig 8 and 10 showing the pyritic sulphur content of the gas, it can be seen that the organic sulphur compounds were slightly more volatile. At any rate, organic sulphur was evolved more rapidly during the first part of the carbonization period. The pyritic sulphur evolution after the initial dip remained more constant until late in the coking run. Since the rate of organic sulphur evolution was dropping steadily after the 4th hour, the percentage of the sulphur which was pyritic in the gas increased as shown in Fig 8.

It is interesting to note from Table 3 that the FeS content of the coke was much lower than would correspond to reduction of the FeS_2 to FeS , the reaction stopping there. On the other hand, radioactivity measurements indicated that 40 pct of the sulphur in coke was of pyritic origin, more than was represented by the FeS present. This apparently means that the

pyrites of the coal used in this run decomposed to FeS and some of the FeS further decomposed, but part of this sulphur remained in the coke and did not escape in the gas.

From Table 4 it will be noticed that the activity of the water soluble sulphur of the coke, believed to be calcium sulphide, measured 0.13. This activity indicates that the calcium sulphide sulphur did not all come from calcium sulphate which was completely non-radioactive, but part of it, approximately 25 pct or 2 lb, came from the original pyritic sulphur, either directly or through the medium of carbonaceous sulphur in coke which had also become radioactive.

From the activity of the total coal sulphur, 0.22, and the known pyritic content (42 pct of the sulphur) of the coal, one can calculate the activity of the total pyritic sulphur in the coal to be about 0.49. However, the measured activity of the combined iron and calcium sulphides from coke (0.32) is lower than the activity calculated from the above individual calcium and iron sulphide activities. The calculated total sulphide activity is 0.36. If one assumes that the calcium sulphide sulphur content of the coke of Table 4 is correct at 0.04 pct the above discrepancy would indicate that part (about 18 pct, or about 3 lb) of the sulphur of the residual FeS in the coke must have come from organic or sulphate sulphur in the coal because of its low activity. However, the experimental error of the calcium sulphide determination is so large that this finding cannot be considered conclusive.

The most important consideration in regard to this experiment is the relative action of the two forms of sulphur, organic and pyritic in the carbonization of coal. Although the individual pyritic and organic rates of evolution vary considerably, final results show about the same proportion of pyritic sulphur in the gas and coke as in the coal (Table 8). This apparently means

that at the temperatures attained in coking the pyritic, organic and sulphate sulphur compounds of the present coal mixture are all at least partially decomposed and some of the pyritic sulphur liberated seems to distribute itself in each of the forms of sulphur remaining in the coke. The final overall results of this experiment as regards the origin of sulphur in the gas and in the sulphur compounds of the coke is shown schematically in Fig 12.

SUMMARY

A study has been completed using radioactive tracers to determine the principal sources of sulphur in coke. It is generally recognized that sulphur exists in coal as pyritic, organic and sulphate sulphur. Since the sulphate sulphur content of most coals is very small, the experiment was designed to indicate how much pyritic and, by difference, how much organic and sulphate sulphur remain in the coke after carbonization. It was hoped that the results would then serve as a guide in the selective purchasing of coal to produce a low sulphur coke.

Briefly, the principle used was to prepare from radioactive sulphur a small amount of iron pyrites which was then mixed thoroughly with the coal charge to one full-scale coke oven and the mixture coked under normal conditions. The course of the pyritic sulphur was then traced in order to determine the quantity evolved in the gas and the quantity remaining in the coke.

The results which are illustrated schematically in Fig 12 indicate that on a typical full-scale 16-hr coking run at the Republic Steel Corporation, sulphur remains in the coke without regard to the form originally present in the coal. Thus with this typical coal mixture neither of the two main forms of sulphur is preferentially removed during coking. It seems reasonable, therefore, that with present coking

techniques, there would be no advantage in choosing coal for its high or low pyritic or organic sulphur content. In order to produce low sulphur coke, coals low in

portion of pyritic sulphur would produce lower sulphur coke. However, radioactive measurements show definitely that a considerable part of the pyritic sulphur re-

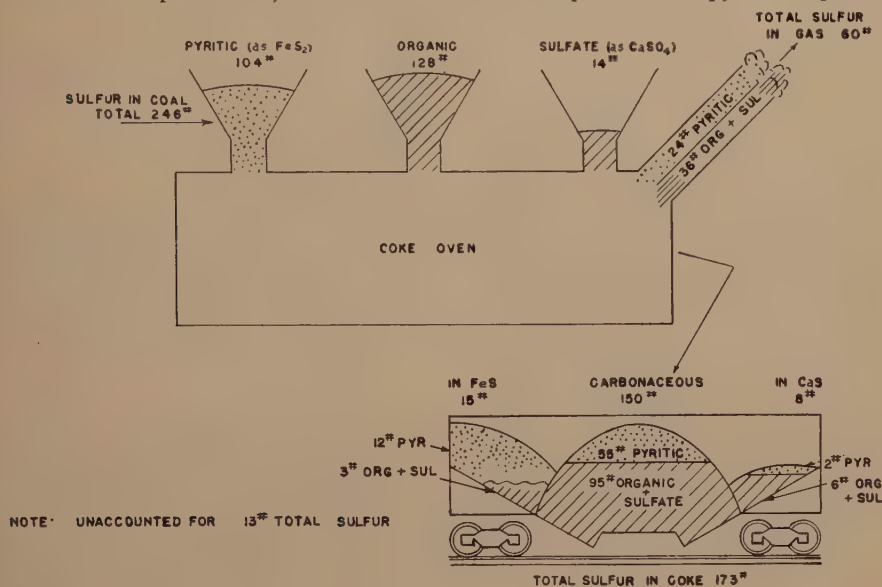


FIG 12—FLOW OF SULPHUR IN COKE OVEN.

total sulphur must be used. The effect obtained with a high sulphate sulphur coal cannot be judged accurately from the present experiment.

There have been observed in this experiment variations in the evolution rate of the two main forms of sulphur but the total amount of each form evolved is in proportion to its original concentration in the coal. The difference in evolution rate suggests the possibility of using a slightly shorter coking period as far as sulphur is concerned if coal of low pyritic sulphur were used.

Chemical analysis alone could not have determined from this experiment how much of the pyritic sulphur escaped in the gas and how much remained in the coke. In fact, the low FeS content of the coke might have been interpreted to indicate that more pyritic sulphur was evolved than organic sulphur and this might have led one to believe that coal with a high pro-

portion of pyritic sulphur would produce lower sulphur coke. However, radioactive measurements show definitely that a considerable part of the pyritic sulphur re-

1. In general, there is no satisfactory way, using present coking methods, to reduce the sulphur content of coke by choosing coal of high or low pyritic or organic sulphur. The results of the experiment indicate that the pyritic and organic sulphur appear in coke in proportion to their concentration in the coal.

2. In view of the large initial evolution of organic sulphur observed in the experiment, coals containing large amounts of organic sulphur and small amounts of pyritic might be coked for a slightly shorter time to produce coke containing a given percentage of sulphur. Coals high in pyritic sulphur would have to be coked for a slightly longer period of time to obtain the same results.

It must be clearly understood that the

observations made here represent results obtained from one coking run using one set of conditions and one coal mixture. A duplicate experiment has since been run on a small movable wall test oven using the same coal mixture with identical results with respect to total sulphur. How the nature of the sulphur compounds in other coal mixtures would change the picture is not known. Coking at a different temperature or with a different moisture content coal could also change somewhat the results obtained.

As far as is known this experiment is the largest scale tracer study ever undertaken, and is the first utilization of tracers in investigating the complicated reactions in the coking process. It shows the value of the use of radioactive isotopes in the study of process metallurgy and it is hoped that it will stimulate further research in this field in which so much remains unknown.

ACKNOWLEDGMENTS

The authors are indebted to the late Mr. J. H. Slater and Dr. Earle C. Smith of the Republic Steel Corporation, Professors Robley D. Evans and John W. Irvine, Jr. of the Massachusetts Institute of Technology for their part in sponsoring and guiding the study.

We are further indebted to the following Republic Steel personnel for their assistance in the performance of the experiment: Messrs. C. Heinz, Supt. Cleveland Coke Ovens, O. L. Henry (now of Koppers Co.), C. H. Flickinger, Chief Chemist Cleveland

District, R. L. Horn, and the operating personnel of the Cleveland Coke Plant.

We appreciate the assistance given us in analyses of samples by the United States Bureau of Mines.

We are also grateful to Mr. H. H. Lowry of the Carnegie Institute of Technology and Mr. F. M. Becker of the United States Steel Corporation for furnishing us data on sulphur in coking coals.

Finally, we acknowledge the participation of the following personnel at Arthur D. Little, Inc. who assisted in preparation of the pyrites and in obtaining and analyzing the samples: M. H. Rood, E. A. Rietzel, J. L. Utter, A. R. Almeida, and E. L. Pepper.

REFERENCES

1. H. H. Lowry: Private Communication (Coal Research Lab., Carnegie Inst. of Tech.).
2. D. H. Davis and John Griffin: *Trans. AIME* (1944) **157**, 22.
3. F. M. Becker: Reserves and Future of Coking Coals in United States. AIME, Blast Furnace, Coke Oven and Raw Materials Comm., Apr. 1947.
4. W. Seymore: U.S. Bur. Mines, R.I. 3907, June 1946.
5. Lowry, Landon and Naugle: *Trans. AIME* (1942), **149**, 297-330.
6. Thiessen: *Ind. Eng. Chem.* **27**, 473-478 (1935).
7. A. R. Powell: *Jnl. Ind. Eng. Chem.* **13**, 33-35 (1921).
8. F. J. Allen: *Am. Jnl. Sci.* (4) **33**, 161-912.
9. W. H. Newhouse: *Jnl. Geol.* **35**, 73-83 (1927).
10. A. R. Powell and S. W. Parr: U.S. Bur. Mines TP 254 (1921).
11. Sampling and Analysis of Coal, Coke and By-products: Carnegie Steel Co., 3rd ed., 77-80 (1929).
12. H. N. Furman: *Scott's Standard Methods of Chemical Analysis*, **1**, 5th ed., 913.
13. Treadwell and Hall: *Analytical Chemistry*, 8th ed., **2**, Quantitative Analysis, 336.

Anisothermal Formation of Bainite and Proeutectoid Constituents in Steels

BY LEONARD D. JAFFE,* JUNIOR MEMBER AIME

(New York Meeting, February 1948)

IN recent years, the advantages of tempered martensite as a microstructure for steel parts have been well established. For parts that must not fracture brittly when loaded at high rates, at low temperatures, or under conditions of combined stress, tempered martensite is especially desirable.

One of the factors that determine whether a steel part will have a martensitic structure after heat treatment is the hardenability of the steel. Despite the large amount of recent research, there are still many unsettled basic questions concerning hardenability and its relation to chemical composition, and, indeed, considerable disagreement among investigators in the field. Much of the uncertainty that beclouds the existing knowledge of hardenability arises from the fact that hardenability is still a wholly empirical concept, and has not been quantitatively related to the more fundamental knowledge of isothermal decomposition of austenite. Hardenability is, essentially, a measure of the time required for small percentages of austenite to decompose, *during continuous cooling*, to pearlite, bainite, proeutectoid ferrite, or proeutectoid carbide. In the practical heat-treat-

ment of steel, also, the decomposition of austenite is usually not isothermal but rather during cooling, or, in general, is not at a single constant temperature. Thus, both hardenability and practical heat treatment involve *anisothermal* decomposition of austenite.

In a previous publication¹ the author and his collaborators outlined the principles that govern the relations between isothermal and anisothermal decomposition of austenite, and reviewed the experimental information available in 1945. To avoid repetition, familiarity with that article (Paper 1) will be assumed, and attention given primarily to work carried out or published since 1945.

The method generally employed was explained in Paper 1: anisothermal transformation is studied through investigation of the effect of holding austenite at one temperature upon its subsequent decomposition at another temperature. Both temperatures are below the stability range of the austenite. This paper is confined to studies in which only a small amount of transformation occurred at the first temperature. This is the only case of importance in practical heat treatment when an essentially martensitic structure is sought.

MATERIALS AND PROCEDURE

It was necessary to use different steels for the studies involving proeutectoid ferrite and for those involving proeutectoid carbide, because the two constituents have not been found to form in the same steel. Several steels were tried and rejected

The statements and opinions in this article are those of the author and do not necessarily express the views of the Ordnance Department. This work forms a portion of a thesis submitted in partial fulfillment of the requirements for the degree of Doctor of Science at Harvard University.

Published by permission of the War Department, USA.

Manuscript received at the office of the Institute June 30, 1947; revision received September 3, 1947. Issued as TP 2290 in METALS TECHNOLOGY, December 1947.

* Watertown Arsenal Laboratory, Watertown, Mass.

¹ References are at the end of the paper.

because of excessive banding. Two which were only slightly banded and which started to transform in both the proeutectoid and bainite ranges in convenient lengths of time were finally selected.

A suitable hypoeutectoid steel was found in the form of a large forged block of the following composition:

C	Mn	S	P	Si	Ni	Cr	Mo	V	Cu	Al	N	B
0.30	0.69	0.051	0.029	0.22	2.83	0.85	0.30	<0.01	0.12	0.005	0.005	0.0004

This steel will be referred to as 4330, even though it is somewhat outside the specification limits for SAE 4330. Specimens $\frac{5}{8} \times \frac{5}{16} \times 0.040 \pm 0.005$ in. were cut from the block. They were then electroplated with approximately 0.003 in. of nickel on each surface, to reduce subsequent decarburization during heat treatment.

A hypereutectoid steel of the following composition was selected:

C	Mn	S	P	Si	Ni	Cr	Mo	V	Cu	Al	N	B
0.97	0.72	0.020	0.012	0.32	1.54	0.80	0.26	0.027	0.06	0.025	0.005	0.0006

From a $\frac{1}{16}$ -in. bar of this steel, which will be referred to as 43100, discs 0.040 ± 0.005 -in. thick were machined and cut in half along a diameter. The specimens were then plated with 0.003 in. of nickel.

For studies of anisothermal decomposition, the specimen was austenitized in purified nitrogen, transferred to a metal bath at the first transformation temperature and kept there for the desired time, transferred to a metal bath at the second transformation temperature and kept there for the desired time, and finally quenched in cold water. For studies of isothermal transformation, the second bath was omitted and the specimen was quenched in water directly from the first bath. For determination of martensite-start temperatures, the Greninger-Troiano technique² was used.

All furnaces were controlled to $\pm 3^\circ\text{C}$. Times in the furnaces were controlled manually to ± 1 second for times up to 10 min. and to ± 1 min. for times over 1 hr, with intermediate accuracy for intermediate times. Previous work indicated that approximately 2 sec after immersion were required for specimens to reach essen-

tially the temperature of the metal bath. Less than 1 sec was required to transfer specimens from furnace to furnace or quench. These times were generally negligible. As a check, anisothermal runs were made in which the time in the first bath was only 2 to 5 sec.

It was decided to base all computations upon the time necessary for the formation of 1 pct of transformation product.* The

times necessary for the formation of smaller percentages were too sensitive to segregation effects. With larger percentages, composition changes in the bulk of the untransformed austenite would be likely to arise from diffusion of carbon to or from the transformation product. To aid in estimating the time at which 1 pct transformation had occurred, standard drawings were made showing typical forms and distributions of the various transformation products. In these drawings the transformation products occupied 1 pct of the area. The microstructure observed in each specimen was compared with the appropriate drawing. All comparisons were made by the

* Since the density of austenite is practically equal to that of any of the transformation products, the formation of 1 pct transformation product was considered equivalent to transformation of 1 pct austenite.

same observer. Either the entire polished surface (excluding decarburized edges) or about ten representative areas were ex-

work. The times for 1 pct isothermal transformation, with which the anisothermal data are to be compared, are listed in

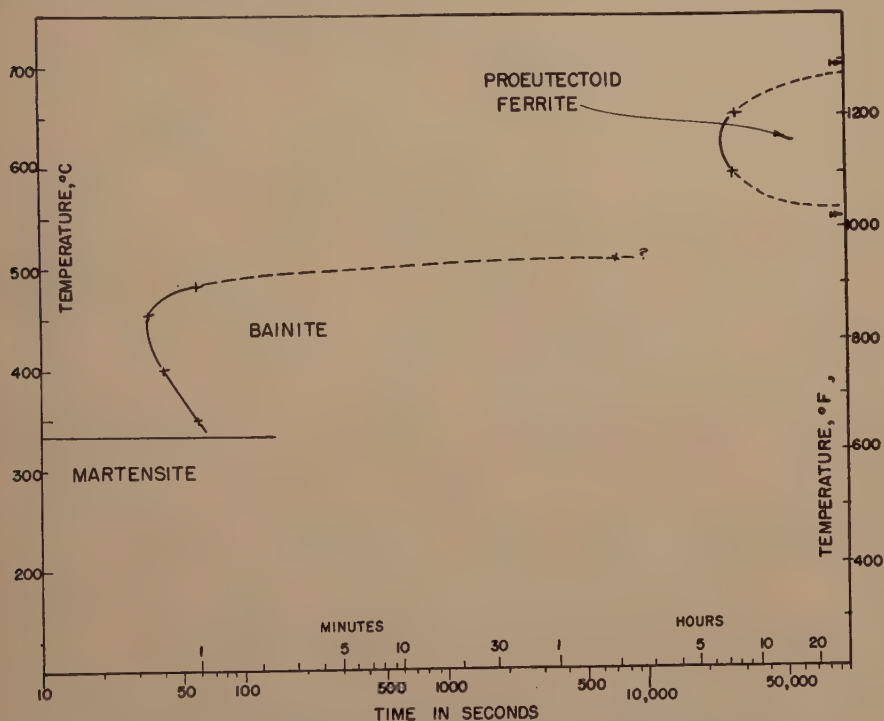


FIG 1—ISOTHERMAL TRANSFORMATION DIAGRAM. 4330 STEEL.
Austenitized 15 minutes at 1095°C. Times shown are for 1 per cent transformation.

amined. The accuracy of this method, while not great, appeared to be sufficient in view of the variability arising from segregation and other factors. The method had the advantage of rapidity, which was needed because more than 1200 specimens were studied. The precision of the times determined for 1 pct transformation is believed to be about 5 pct.

AUSTENITIZING AND ISOTHERMAL TRANSFORMATION

For the 4330 steel, 15 min. at 1095°C was found to give a grain size of ASTM 1-3 with occasional larger grains, and no undissolved carbides. This austenitizing treatment was selected for the remainder of the

Table 1. Fig 1 shows the corresponding isothermal transformation diagram.

An austenitizing treatment of 15 min.

TABLE 1—Time Required for Isothermal Decomposition of 1 Per Cent Austenite—4330 Steel

Austenitized 15 minutes at 1095°C

Temperature, °C	Time	Product
700	Over 24 hr	Ferrite
650	460 min	Ferrite
593	450 min	Ferrite
550	Over 24 hr	Ferrite
510	Approx. 120 min	Bainite
483	60 sec	Bainite
455	34 sec	Bainite
400	41 sec	Bainite
350	60 sec	Bainite
335	(Ms on cooling)	Martensite

at 1150°C was standardized for the 43100 steel. This produced a grain size of ASTM 2-4, with a few larger grains (ASTM 1), and no undissolved carbides. Table 2 gives the times required for 1 pct isothermal

that, for the 4330 steel studied, holding in the ferrite range accelerates subsequent formation of small percentages of bainite, and accelerates it so greatly that the reactions are not additive.

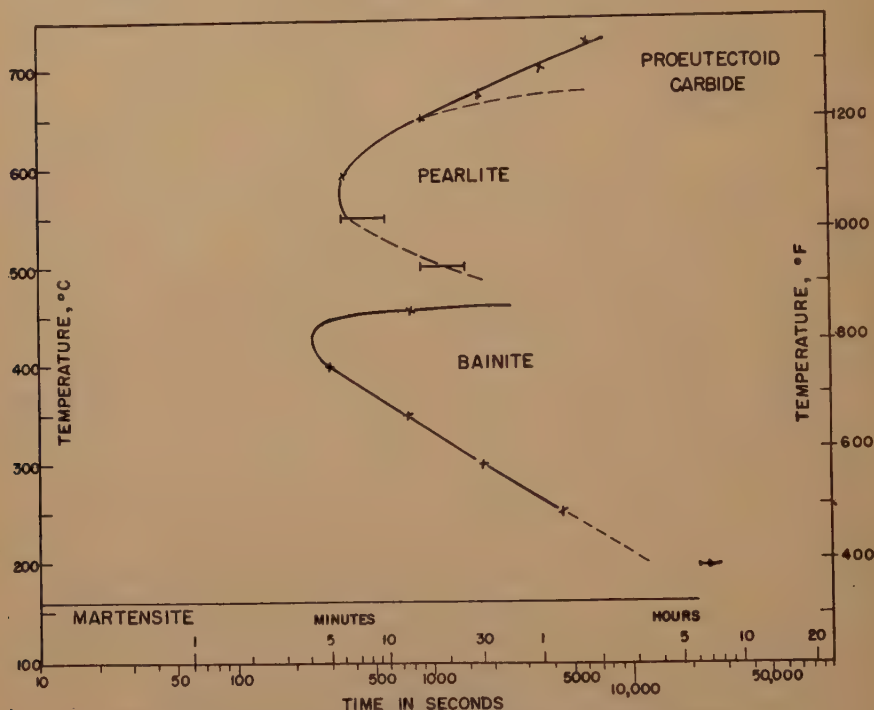


FIG 2—ISOTHERMAL TRANSFORMATION DIAGRAM. 43100 STEEL. Austenitized 15 minutes at 1150°C. Times shown are for 1 per cent transformation.

transformation. Fig 2 shows the isothermal transformation diagram.

FERRITE-BAINITE REACTION

In Table 3 are summarized the findings, in the present investigation, concerning the effect of holding austenite in the ferrite range upon the subsequent time required for formation of 1 pct bainite.* It is clear

* In interpreting the tables, it should be remembered that the "fractional time" is defined as the actual time that a steel is held at constant temperature divided by the time for 1 pct isothermal transformation at that temperature. A reaction is considered additive (for small amounts of transformation) if 1 pct transformation occurs when and only when the fractional time, added or integrated over the various temperatures of anisothermal reaction, is equal to one.

TABLE 2—Time Required for Isothermal Decomposition of 1 Pct Austenite—43100 Steel
Austenitized 15 minutes at 1150°C

Temperature, °C	Time Minutes	Product
725	105	Carbide
700	60	Carbide
675	29	Carbide
650	15	Carbide & Pearlite
593	6	Pearlite
550	6-10	Pearlite
510	15-25	Pearlite
455	13	Bainite
400	5	Bainite
350	12½	Bainite
300	30	Bainite
250	74	Bainite
200	Over 360	Bainite
160	(Ms on cooling)	Martensite

This result is in accord with those of Hollomon, Jaffe and Norton¹ for their samples austenitized at 925°C and of Grange.³ The acceleration found is more marked

1095°C and by Manning and Lorig⁴ for their samples held in the ferrite range at 620°C. It is in contradiction to the results obtained by Manning and Lorig for their

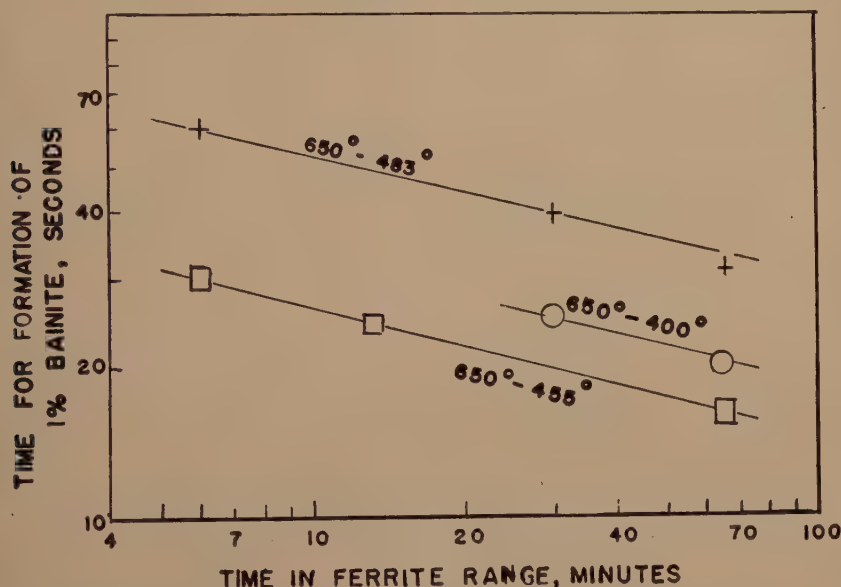


FIG 3—EFFECT OF HOLDING IN FERRITE RANGE UPON TIME FOR SUBSEQUENT FORMATION OF ONE PER CENT BAINITE. LOGARITHMIC SCALE. 4330 STEEL.

than that reported by Hollomon, Jaffe and Norton for their samples austenitized at

samples held at 760- and 700°C. Hollomon, Jaffe and Norton used the steel employed in the present work, and their austenitizing temperature of 1095°C coincides with that of this investigation. It seems unlikely, therefore, that the difference in results is attributable to a real difference in behavior of the steel. The same is true of the divergency between the findings of Manning and Lorig and those reported herein, for the steels and transformation temperatures employed are rather similar. It appears possible that the differing conclusions arise from less rigorous experimental techniques used in the earlier studies, such as consideration of the time for appearance of the first trace of bainite rather than 1 pct, and, in some cases, failure to run tests in duplicate.

The results given in Table 3 are plotted on a logarithmic scale in Fig 3. It will be

TABLE 3—Effect of Holding Austenite in Ferrite Range upon Time for Formation of 1 Pct Bainite—4330 Steel

Ferrite Range			Bainite Range			Sum of Fractional Times
°C	Minutes Held	Fractional Time	°C	Seconds for 1 pct Bainite	Fractional Time	
650	0	0	483	60	1	1
650	1/2	0.0002	483	63	1.05	1.05
650	6	0.01	483	60	1.00	1.01
650	30	0.07	483	40	0.67	0.74
650	65	0.14	483	32	0.53	0.68
650	0	0	455	34	1	1
650	1/2	0.0002	455	32	0.94	0.94
650	6	0.01	455	30	0.88	0.89
650	13	0.03	455	24	0.71	0.74
650	65	0.14	455	16	0.47	0.61
650	0	0	400	41	1	1
650	30	0.07	400	25	0.61	0.68
650	65	0.14	400	20	0.49	0.63
593	0	0	455	34	1	1
593	1/2	0.0002	455	34	1.00	1.00
593	150	0.33	455	17	0.50	0.83

seen that straight lines are obtained, and that the lines for the various temperatures of bainite formation are parallel. This indicates that the time held in the ferrite range, t_f , and the time for formation of 1 pct bainite in the bainite range, t_b , are related by an equation of the form $t_b/t_{ob} = \sqrt[n]{t_{of}/t_f}$ where t_{ob} and t_{of} are constants dependent upon the temperatures used and n is approximately 4.1. Too much significance should not be attributed to this equation, since no theoretical justification has been found for it, and the equation breaks down at values of t_f and t_b approaching those necessary for 1 pct transformation under isothermal conditions. Nevertheless, the equation should prove useful for practical computations.

For a fixed time of hold at 650°C, Fig 3 indicates that the times required for 1 pct transformation to bainite at 483, 455, and 400°C, are in the ratio 1.6:0.8:1. The times for 1 pct isothermal transformation at these same temperatures (Table 1) are in the ratio 1.5:0.8:1. The agreement is close enough to suggest that holding in the ferrite range accelerates formation of small amounts of bainite by a percentage which is independent of the temperature at which the bainite forms.

The time in the ferrite range required to accelerate the bainite reaction (at 455°C) to a given extent is three times as great for a ferrite-range temperature of 593°C as for a temperature of 650°C. The time for isothermal formation of 1 pct ferrite at 593°C is practically equal to that at 650°C. Thus, the acceleration produced by holding in the ferrite range does not depend solely upon the fractional time in this range. It will be necessary to obtain further information concerning the dependence of the acceleration upon the temperature of holding in the ferrite range before quantitative consideration of the ferrite-bainite effect under conditions of continuous cooling becomes possible.

That holding austenite in the ferrite

range would accelerate its subsequent transformation to bainite is certainly to be anticipated, as was pointed out in Paper 1. Why the acceleration of the bainite reaction should be greater than that corresponding to additivity is not evident. The explanation may lie in the differing kinetics of the ferrite and bainite reactions. Thus suppose that the rate of nucleation is smaller, compared to the rate of growth, for the bainite reaction than for the ferrite reaction. Then the presence of a few nuclei would accelerate the bainite reaction more than it would accelerate the ferrite reaction.

BAINITE-BAINITE REACTION

Table 4 shows, for the 4330 steel, the newly observed effects of holding austenite

TABLE 4—Effect of Holding Austenite at One Temperature in Bainite Range upon Time at a Lower Temperature for Formation of 1 Per Cent Bainite (Total)—4330 Steel

First Temperature			Second Temperature			Sum of Fractional Times
°C	Seconds Held	Fractional Time	°C	Seconds for 1 pct Bainite	Fractional Time	
483	0	0	455	34	1	1
483	20	0.33	455	26	0.76	1.09
483	40	0.67	455	18	0.53	1.20
483	0	0	400	41	1	1
483	20	0.33	400	39	0.95	1.28
483	40	0.67	400	30	0.73	1.30
455	0	0	400	41	1	1
455	10	0.29	400	35	0.85	1.14
455	20	0.59	400	21	0.51	1.10

at one temperature in the bainite range upon the subsequent time required at a lower temperature for formation of a total of 1 pct bainite. The results are plotted in Fig 4. As the table demonstrates, holding at the higher temperature slows to some extent the subsequent reaction at the lower temperature, so that the times are not additive. The greater the difference between the first and second temperatures the greater is the retardation of the reaction. In none of the cases examined, however, was

the retardation great enough to increase the time at the second temperature over that required under isothermal conditions. With greater differences between the first and

times are additive within the limits of experimental error.

Holding austenite of the 43100 steel at one temperature in the bainite range was

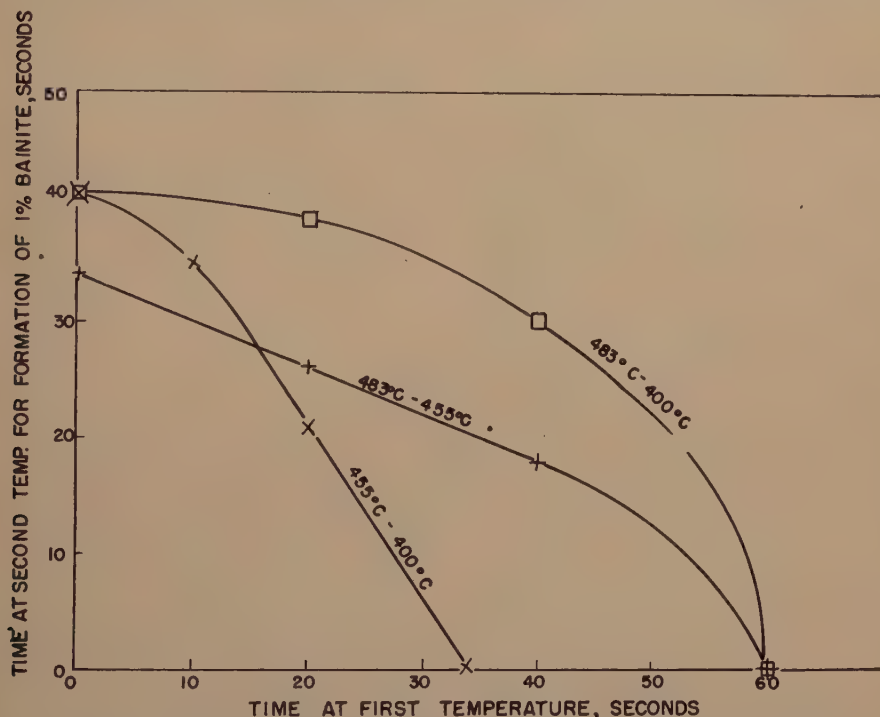


FIG 4—EFFECT OF HOLDING AT ONE TEMPERATURE IN BAINITE RANGE UPON TIME AT A LOWER TEMPERATURE FOR FORMATION OF ONE PER CENT BAINITE (TOTAL). 4330 STEEL.

second temperatures, this might very well occur. In previous work on an 0.30 pct carbon steel by Manning and Lorig,⁴ the accuracy was not sufficient to determine whether the reaction was additive or a slight retardation occurred.

The results of the converse experiment on the 4330 steel—holding austenite at one temperature in the bainite range and determining the subsequent time required at a higher temperature for formation of 1 pct bainite—are presented in Table 5 and Fig 5. For a first temperature of 455°C and a second temperature of 483°C, a slight retardation appears to have taken place. For the other temperature combinations, the

TABLE 5—Effect of Holding Austenite at One Temperature in Bainite Range upon Time at a Higher Temperature for Formation of 1 Per Cent Bainite (Total)—4330 Steel

First Temperature			Second Temperature			Sum of Fractional Times
°C	Seconds Held	Fractional Time	°C	Seconds for 1 pct Bainite	Fractional Time	
455	0	0	483	60	1	1
455	10	0.29	483	54	0.99	1.19
455	20	0.59	483	33	0.55	1.14
400	0	0	483	60	1	1
400	15	0.37	483	37	0.62	0.99
400	0	0	455	34	1	1
400	30	0.73	455	less than 8	less than 0.24	less than 0.97

found to retard markedly the subsequent transformation to bainite at a lower temperature. As Table 6 indicates, holding the steel at 455°C, for less than 1/4 the time

Table 7 shows that, under the converse conditions, holding the 43100 austenite at a low temperature in the bainite range greatly accelerated subsequent bainite formation

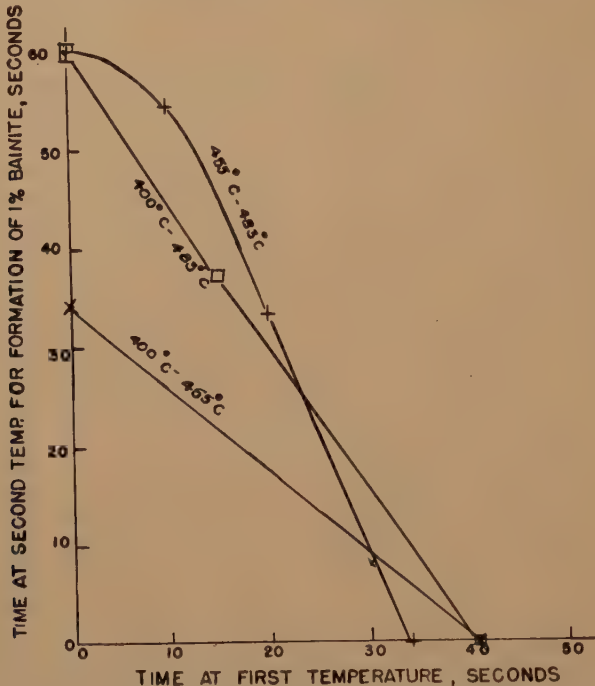


FIG 5—EFFECT OF HOLDING AT ONE TEMPERATURE IN BAINITE RANGE UPON TIME AT A HIGHER TEMPERATURE FOR FORMATION OF ONE PER CENT BAINITE (TOTAL). 4330 STEEL.

necessary to produce 1 pct bainite isothermally, more than doubled the time required to obtain 1 pct bainite at 250°C.

TABLE 6—Effect of Holding Austenite at One Temperature in Bainite Range upon Time at a Lower Temperature for Formation of 1 Per Cent Bainite (Total)—43100 Steel

First Temperature			Second Temperature			Sum of Fractional Times
°C	Time Held	Fractional Time	°C	Minutes for 1 pct Bainite	Fractional Time	
455	0	0	250	74	1	1
455	5 sec	0.006	250	more than 70	more than 0.95	more than 0.95
455	3 min	0.23	250	150	2.02	2.25

at a higher temperature. The time required at the second temperature for 1 pct transformation was considerably less than that

TABLE 7—Effect of Holding Austenite at One Temperature in Bainite Range upon Time at a Higher Temperature for Formation of 1 Pct Bainite (Total)—43100 Steel

First Temperature			Second Temperature			Sum of Fractional Times
°C	Time Held	Fractional Time	°C	Minutes for 1 pct Bainite	Fractional Time	
250	0	0	455	13	1	1
250	15 min	0.20	455	5	0.38	0.50
250	30 min	0.41	455	2 1/2	0.10	0.60
250	60 min	0.81	455	much less than 2	much less than 0.15	less than 0.85

corresponding to additivity. The times are given graphically in Fig 6.

The data of Lange and Mathieu⁵ on a hypereutectoid steel, discussed in Paper 1, concur with those of the present study.

It is somewhat surprising that less than 1 pct transformation is apparently sufficient to enrich the remaining austenite in carbon to a significant extent. It must be postulated that the enrichment is localized

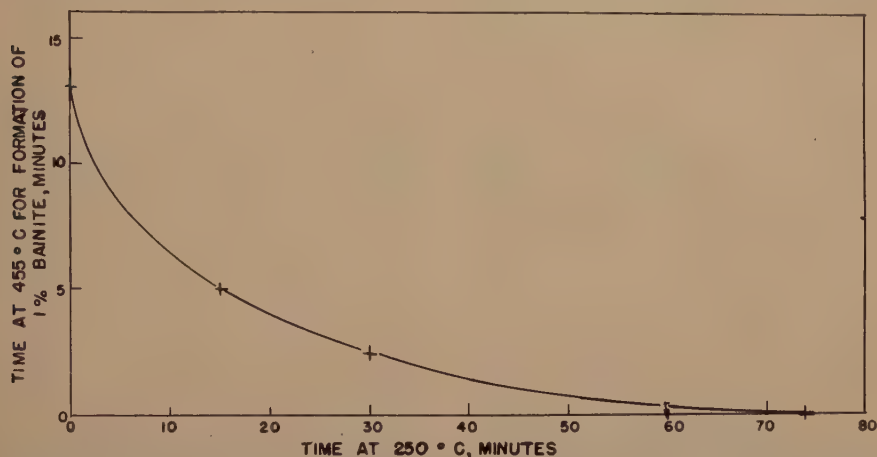


FIG 6—EFFECT OF HOLDING AT ONE TEMPERATURE IN BAINITE RANGE UPON TIME AT A HIGHER TEMPERATURE FOR FORMATION OF ONE PER CENT BAINITE (TOTAL). 43100 STEEL.

The results obtained for the bainite reaction are in accord with the theory outlined in Paper 1. This theory is based upon the view of Zener⁶ that the reaction is accompanied by diffusion of carbon from the growing bainite to the remaining austenite. The amount of this diffusion is greater the higher the temperature. The resulting carbon enrichment of the austenite impedes its subsequent transformation to bainite.

The more marked accelerations and retardations observed in the 43100 steel as compared with the 4330 steel evidently arise from greater changes in the carbon content of the undecomposed austenite. Greater changes in carbon content during the bainite reaction in the 43100 steel may be attributed either directly to the higher carbon content of this steel or, more probably, to the greater difference between the first and second transformation temperatures employed in the experiments on the 43100 steel.

in the neighborhood of the newly formed bainite, and does not extend very far into the austenite matrix.

BAINITE-FERRITE REACTION

There seems to have been no previous work concerning the effect of holding in the bainite range, for times insufficient to cause much bainite formation, upon the time required for initiation of the proeutectoid ferrite reaction. The new studies are summarized in Table 8. This table indicates that, although holding in the bainite range speeds up ferrite formation, the effect is less than that corresponding to additivity. Such a small effect is somewhat surprising. A possible explanation is that the rate of nucleation may be greater, compared to the rate of growth, for the ferrite reaction than for the bainite reaction. The presence of a few nuclei would then accelerate the ferrite reaction less than it would accelerate the bainite reaction. No measurements have been made of the nucleation and

growth rates of the bainite and proeutectoid ferrite transformations. It is well known, however, that growing ferrite crystals are commonly observed in all sizes, whereas bainite usually appears either as fairly large needles or not at all. This substantiates the idea that the ratio of the rate of growth to the rate of nucleation is higher for bainite than for proeutectoid ferrite formation.

It might be suggested that the divergence arises from the use of 1 pct ferrite as the basis for calculation of the fractional times, rather than 1 pct total transformation product (ferrite plus bainite). In all but one of the time-temperature combinations listed in Table 8, however, use of 1 pct

TABLE 8—*Effect of Holding Austenite in Bainite Range upon Time for Formation of 1 Per Cent Ferrite—4330 Steel*

Bainite Range			Ferrite Range			Sum of Fractional Times
°C	Sec-onds Held	Frac-tional Time	°C	Minutes for 1 pct Ferrite	Frac-tional Time	
455	0	0	650	460	1	1
455	15	0.44	650	more than 300	more than 0.65	more than 1.09
455	25	0.74	650	180	0.39	1.13
455	0	0	593	450	1	1
455	25	0.74	593	more than 300	more than 0.67	more than 1.41
400	0	0	650	460	1	1
400	30	0.73	650	190	0.41	1.14

total product would make no difference whatsoever in the times listed, because only very small percentages of bainite were present in the specimens containing 1 pct ferrite. Throughout the anisothermal studies, it was generally found that, except for specimens held at the first temperature almost long enough to transform 1 pct isothermally, very little of the first product could be detected in samples containing 1 pct of the second product. In the isothermal studies, too, no transformation product could be detected except at times almost long enough to form 1 pct product.

This observation indicates that the various reactions start slowly and continue with increasing rapidity (for small percentages of transformation), as is usual for reactions proceeding by nucleation and growth.^{7,8}

FERRITE-FERRITE REACTION

In Paper 1, data of Grange and Kiefer⁹ on initiation of the proeutectoid ferrite reaction in SAE 4340 during continuous cooling were compared with values calculated from isothermal data on the assumption of additivity. The agreement, though by no means perfect, was sufficiently good to suggest that the proeutectoid ferrite reaction is approximately additive, at least for small percentages of ferrite.

Manning and Lorig⁴ have recently made direct measurements of the effect of holding at one temperature in the ferrite range upon the time required for the appearance of a small percentage of ferrite at a lower temperature. For the four tests made, the reaction was additive.

In view of these determinations, it was not considered necessary to devote much effort at this time to further anisothermal studies of the ferrite reaction. Only a limited number of specimens were employed and because of the scatter of the data, the only definite conclusion drawn was that none of the new observations was inconsistent with the assumption of additivity.

It thus appears, at least over the ranges so far examined, that the carbon and alloy concentrations during the formation of ferrite are not sufficiently modified by changes in temperature to prevent additivity of the reaction.

CARBIDE-CARBIDE REACTION

No data have been found in the literature that are indicative of the relations between isothermal and anisothermal formation of proeutectoid carbide. The results of the new studies are summarized in Table 9. For the specimens held first at 700°C, and

then at 725°C, the times for formation of 1 pct carbide are additive. For specimens given the converse treatment, the data are

TABLE 9—*Effect of Holding Austenite at One Temperature in Proeutectoid Carbide Range upon Time at a Second Temperature for Formation of 1 Per Cent Carbide (Total)—43100 Steel*

First Temperature			Second Temperature			Sum of Fractional Times
°C	Minutes Held	Fractional Time	°C	Minutes for 1 pct Carbide	Fractional Time	
700	0	0	725	105	1	1
700	35	0.58	725	44	0.42	1.00
725	0	0	700	60	1	1
725	20	0.19	700	more than 50	more than 0.83	more than 1.02

not conclusive, but are not inconsistent with additivity.

In the proeutectoid carbide reaction, as in the ferrite reaction, the carbon and alloy concentrations are apparently not sufficiently affected by changes in temperature to prevent additivity, under the conditions investigated.

CARBIDE-BAINITE REACTION

Table 10 indicates the effect of holding in the proeutectoid carbide range upon the subsequent time required for 1 pct transformation to bainite. These results, although not as complete as might be desired, show that the times for the carbide and bainite reactions are certainly not additive. Holding in the carbide range apparently retards the transformation to bainite. This agrees with conclusions drawn in Paper I from data of Lange and Mathieu.⁵

Why formation of small amounts of carbide should delay the bainite reaction is easily understood. The proeutectoid carbide would nucleate at the most severe discontinuities in the austenite. The newly formed carbide would then "cover up" these severe discontinuities and make them unavailable for nucleation of the bainite

transformation, thus retarding the latter. Since bainite appears to originate from nuclei having the ferrite lattice structure

TABLE 10—*Effect of Holding Austenite in Proeutectoid Carbide Range upon Time for Formation of 1 Per Cent Bainite—43100 Steel*

Carbide Range			Bainite Range			Sum of Fractional Times
°C	Minutes Held	Fractional Time	°C	Minutes for 1 pct Bainite	Fractional Time	
700	0	0	250	74	1	1
700	30	0.50	250	82	1.11	1.61

(possibly somewhat modified), the proeutectoid carbide would not itself serve to nucleate bainite.

BAINITE-CARBIDE REACTION

Nothing appears to have been known of the effect upon the proeutectoid carbide reaction of holding in the bainite range for times insufficient for appreciable bainite formation. The results obtained in this investigation are given in Table 11. Holding

TABLE 11—*Effect of Holding Austenite in Bainite Range upon Time for Formation of 1 Per Cent Proeutectoid Carbide—43100 Steel*

Bainite Range			Carbide Range			Sum of Fractional Times
°C	Minutes Held	Fractional Time	°C	Minutes for 1 Pct Ferrite	Fractional Time	
455	0	0	700	60	1	1
455	1	0.08	700	less than 60	less than 1.00	less than 1.08
455	5	0.38	700	100	1.67	2.05
250	0	0	700	60	1	1
250	15	0.20	700	less than 45	less than 0.75	less than 0.95
250	60	0.81	700	75	1.25	2.06

in the bainite range, for moderate fractions of the time necessary to produce 1 pct bainite isothermally, retarded the proeutectoid carbide reaction to a considerable extent.

Holding in the bainite range for shorter times did not retard the carbide reaction appreciably, and perhaps accelerated it.

The observed retardations are attributable to utilization by bainite of the sites of most ready nucleation, making them unavailable to the proeutectoid carbide reaction. This phenomenon has been discussed in the preceding section. It is true that carbide particles must form rapidly from the bainite, especially on reheating to the higher temperatures of the proeutectoid carbide range, and it may be asked why these particles do not nucleate precipitation of proeutectoid carbide from the austenite. The orientation, with respect to the austenite, of carbides precipitated from the bainite would be expected to differ from that of proeutectoid carbide, because of the different mechanism of formation. If the orientations differ, it is to be anticipated that the carbide particles formed from the bainite would not nucleate the proeutectoid reaction.

The observed lack of retardation of the proeutectoid carbide transformation after short times of holding in the bainite range might possibly indicate that the number of bainite nuclei formed during these times was too small to reduce significantly the number of sites of most ready nucleation. An acceleration of the proeutectoid carbide reaction cannot be explained in this way.

IMMEDIATE APPLICATIONS

Even without additional research, practical applications of some of the results may be suggested. Thus, the observed additivity of the proeutectoid reactions should provide a sound basis for predicting quantitatively, from isothermal data, the conditions for 1 pct transformation of austenite by these reactions under any conditions of temperature and time, including continuous cooling. Detailed methods for carrying out the computation have been published previously.^{4,10,11}

The results of the present investigation

may also be applied to the practice of delayed quenching of steel parts. This practice, intended to reduce quench-cracking and distortion, consists of slowly cooling the part from the austenitizing temperature to some lower temperature before quenching in a liquid medium. The slow cooling is ordinarily done in air, and may extend down to 550–700°C. It has now been found that holding austenite in the proeutectoid ferrite range accelerates its subsequent transformation to bainite (at least up to 1 pct transformation), whereas holding austenite in the proeutectoid carbide range retards its subsequent transformation to bainite. Slowly cooling an austenitized hypoeutectoid steel into the proeutectoid ferrite range before quenching therefore involves not only the risk of increasing the percentage of ferrite in the as-quenched microstructure, but also the risk of increasing the percentage of bainite. Effectively, a quench delayed below the A_{cs} temperature reduces the bainitic hardenability of a hypoeutectoid steel (hardenability with respect to bainite formation¹²). On the other hand, slowly cooling an austenitized hypereutectoid steel into the proeutectoid carbide range before quenching tends to decrease the percentage of bainite in the as-quenched microstructure. Effectively, a quench delayed below the A_{cm} temperature raises the bainitic hardenability of a hypereutectoid steel. This effect may be very useful.

An interesting discrepancy in our knowledge of austenite decomposition has been that increases in molybdenum content and in austenitic grain size raise the bainitic hardenability of hypoeutectoid steels, whereas they have little effect on the time for isothermal bainite formation. Since the present study demonstrates that holding austenite in the ferrite range considerably accelerates its subsequent transformation to bainite, the following explanation, previously suggested^{1,12} by the author and his coworkers, may be considered established:

An increase in molybdenum content or austenitic grain size retards the proeutectoid ferrite reaction. For a fixed cooling rate, this decreases the fractional time spent in the ferrite range. This decrease in turn increases the time required for formation of 1 pct bainite, and thus increases the bainitic hardenability.

CONCLUSIONS

As a result of the studies described above, it is concluded that:

1. The proeutectoid ferrite and carbide transformations are each approximately additive, at least up to 1 pct transformation.

2. The bainite transformation is not additive, reaction at a high temperature tending to retard subsequent reaction at a low temperature, and reaction at a low temperature tending in general to accelerate subsequent reaction at a high temperature. The deviations from additivity increase with increasing difference between the temperatures involved, and perhaps with increasing carbon content of the steel. These deviations accord with theory based upon the variation with transformation temperature of the carbon content of the austenite adjacent to newly formed bainite.

3. Holding austenite in the ferrite range (for times insufficient to produce 1 pct ferrite) accelerates the bainite reaction by an amount significantly greater than that corresponding to additivity. It is suggested that the acceleration beyond additivity arises from a smaller ratio of the rate of nucleation to the rate of growth in the bainite transformation than in the ferrite transformation. Over a considerable range, the time for formation of 1 pct bainite varies inversely as the n -th root of the time of prior holding in the ferrite range, where n is approximately 4.1. The fractional acceleration of the bainite reaction appears to be independent of the temperature of bainite formation, but not of the temperature of holding in the ferrite range.

4. Holding austenite in the bainite range

for a time insufficient to produce 1 pct bainite accelerates subsequent transformation to ferrite, but not as much as would be expected on the basis of additivity. The divergency is attributed to a difference between the two reactions in the ratio of the rate of nucleation to the rate of growth.

5. Holding in the proeutectoid carbide range retards subsequent transformation to bainite, and holding in the bainite range appears to retard subsequent transformation to proeutectoid carbide (when less than 1 pct decomposition occurs by the first reaction). This agrees with the hypothesis that the first constituent to form occupies the sites of most ready nucleation, making them unavailable for nucleation of the second constituent.

6. Among the immediate applications of the results are:

a. The conditions for 1 pct transformation of austenite by the *proeutectoid reactions* under any conditions of temperature and time, including continuous cooling, can now be calculated from isothermal data.

b. It is predicted that delaying the quench of a hypoeutectoid steel until it is below the A_{e3} temperature will effectively decrease its bainitic hardenability. It is predicted that delaying the quench of a hypereutectoid steel until it is below the A_{cm} temperature will effectively increase its bainitic hardenability.

c. A cause is established for the increase in bainitic hardenability observed to result from increasing the molybdenum content or austenitic grain size of a hypoeutectoid steel. It is now clear that, for a fixed rate of cooling, increases in molybdenum content and grain size reduce the fractional time in the proeutectoid ferrite range, and this reduction in turn increases the time necessary for subsequent formation of small percentages of bainite.

7. Additional research will be necessary before hardenability and the decomposition of austenite during practical heat treatment can be predicted quantitatively, under

general conditions from data on isothermal decomposition of austenite.

ACKNOWLEDGMENTS

The author wishes to thank for their assistance Mr. W. P. Clancy, Dr. J. N. Hobstetter, Dr. J. H. Hollomon, Miss Rose Karol, Miss Mary Norton, Dr. E. L. Reed, and Mr. W. R. Yankee.

REFERENCES

1. J. H. Hollomon, L. D. Jaffe, and M. R. Norton: Anisothermal Decomposition of Austenite, *Trans. AIME* (1946) **167**, 419-441. *Metals Tech.*, Aug. 1946. T.P. 2008.
2. A. B. Greninger and A. R. Troiano: Kinetics of the Austenite to Martensite Transformation in Steel, *Trans. ASM* (1940) **28**, 537-574.
3. R. A. Grange: Discussion to Ref. 1. *Trans. AIME* (1946) **167**, 440-441.
4. G. K. Manning and C. H. Lorig: Relationship between Transformation at Constant Temperature and Transformation during Cooling, *Trans. AIME* (1946) **167**, 442-466. *Metals Tech.*, June 1946. T.P. 2014.
5. H. Lange and K. Mathieu: The Course of the Austenite Transformation in the Supercooled State for Iron-nickel-carbon Alloys (in German). *Mitt. K.-W.-Inst. Eisenforschung* (1938) **20**, 125-134.
6. C. Zener: Kinetics of the Decomposition of Austenite. *Trans. AIME* (1946) **167**, 550-598. *Metals Tech.*, Jan. 1946. T.P. 1925.
7. M. Avrami: Kinetics of Phase Change—I. General Theory. *Jnl. Chem. Phys.* (1939) **7**, 1103-1112.
8. M. Avrami: Kinetics of Phase Change—II. Transformation-time Relations for Random Distribution of Nuclei. *Jnl. Chem. Phys.* (1940) **8**, 212-224.
9. R. A. Grange and J. M. Kiefer: Transformation of Austenite on Continuous Cooling and Its Relation to Transformation at Constant Temperature, *Trans. ASM* (1941) **29**, 85-116.
10. E. Scheil: Initiation Time of the Austenite Transformation (in German). *Arch. Eisenhüttenw.* (1935) **8**, 565-567.
11. S. Steinberg: Relationship between Rate of Cooling, Rate of Transformation, Undercooling of Austenite, and Critical Rate of Quenching (in Russian). *Metallurg* (1938) **13**, No. 1, 7-12.
12. J. H. Hollomon and L. D. Jaffe: The Hardenability Concept. *Trans. AIME* (1946) **167**, 601-616. *Metals Tech.*, Jan. 1946, T.P. 1926.

DISCUSSION

(B. R. Queneau presiding)

R. A. GRANGE*—Of the several conclusions drawn by Mr. Jaffe, we subscribe most whole-

heartedly to the last, in which he states that additional research will be necessary before hardenability and decomposition of austenite during many practical heat treatments can be predicted quantitatively. Mr. Jaffe mentions discrepancies which exist in published data relative to the effect of holding an austenitized steel at one temperature upon subsequent isothermal transformation at another temperature, but feels that his choice of the time for 1 pct of transformation product at each of the two temperatures, rather than some smaller percentage such as others have chosen, resulted in accurate and reliable results which can be interpreted quantitatively. In our experience, segregation in steel affects the time for 1 pct transformation just as it does the time for any smaller percentage; we suggest, therefore, that while Mr. Jaffe's data are most interesting and valuable in revealing trends, the more quantitative aspects of his observations may need confirmation before they can be reliably applied to precise calculation of cooling transformation behavior from isothermal data. In particular, other grades of steel, and even other conditions of austenitizing for the particular alloy type of steel he used, should be investigated before applying the fractional time data given in the paper to steel in general.

Mr. Jaffe mentions that a discussion* by this writer confirms his own conclusion that holding in the ferrite range accelerates subsequent transformation to bainite to such an extent that the two reactions are not additive. Actually, in our discussion we stated that the reactions seemed to be *approximately* additive, meaning only that we observed an increase in the percentage of bainite in a sample prequenched in the ferrite range, as compared to a corresponding specimen not prequenched; we have no data which indicate definitely that proeutectoid ferrite and bainite reactions either are, or are not, exactly additive.

It is stated in the paper that molybdenum has very little effect on the time required for isothermal bainite formation. Recently we investigated this question using a series of similar steels with varying molybdenum content and concluded that, in this series at least, molybdenum decidedly increased the time required to initiate isothermal transformation of austenite to bainite.

* United States Steel Corporation.

* Refers to ref. 3 of the paper.

In discussing application of his results to heat treating, Mr. Jaffe suggests that the hardenability of hypereutectoid steel can be increased by delaying the quench until austenite has cooled somewhat below the A_{cm} temperature. If such a treatment permits the formation of even a trace of proeutectoid carbide network, the advantage of greater hardenability may be more than offset by the harmful effect of the carbide network on mechanical properties. Most hypereutectoid steel is austenitized in commercial practice in such a way that considerable carbide remains undissolved, in which case the austenite may not be hypereutectoid in composition; we wonder if, in Mr. Jaffe's opinion, a hypereutectoid steel austenitized in this way would have greater hardenability as a result of a delayed quench.

B. H. ALEXANDER*—I should like to mention some work that is being done on a related problem by Mr. Dube at Carnegie Institute of Technology. Preliminary measurements of the rates of nucleation and growth of hypoeutectoid ferrite indicate that the ratio of N/G is lower the higher the temperature of the reaction.

If the same behavior is assumed in the bainite region, the author's suggested explanation (on the basis of nucleation and growth) of the effect of holding in the ferrite region on the bainite reaction (or vice versa) would be inadequate. However, it seems more probable that the reverse is true and that the ratio of N/G for bainite decreases with decreasing temperature so as to become lower than the corresponding ratio for ferrite. This is in accordance with the author's explanation, but suggests that the acceleration of the bainite reaction would depend not only on the temperature of holding in the ferrite range but also on the temperature of bainite formation.

W. F. HESS†—I was not quite clear—I did not read the paper ahead of time—as to whether holding a steel in the range where it takes a long time to transform the bainite made a difference in the subsequent transformation at elevated temperature. In other words, just how long a time, in proportion to the time necessary to initiate transformation at the low bainite range, was used in these tests or experiments?

Also you did not mention this morning whether you have investigated the effect of holding a relatively long time in the temperature where it takes a still longer time to start transformation, and what effect does that have on subsequent transformation to a pearlite, say, or an elevated temperature transformation product?

E. A. LORIA*—Dr. Jaffe has presented a very interesting paper concerning anisothermal decomposition of austenite in two steels. It is not only timely but reveals new and useful information on a rather complex subject and points the way for further work. The obvious inadequacy and uncertainty of our knowledge of the transformation of austenite in alloy steels and the pressing need for more descriptive fact on which to base further attempts at quantitative theoretical attack make this a valuable contribution.

The present knowledge of incubation, where incubation is understood to mean the process occurring during the period before which the subcritical reaction is detectable, is scant. There are three possible explanations as to the nature of incubation. One is that nothing is happening during incubation. Another more plausible one is that nucleation and growth processes are occurring, but on such a small scale as to be undetectable. The third is that some unknown type of behavior is being exhibited. The effect of incubation on the rate of reaction can be studied either by choosing an incubation temperature which is greater than the reaction temperature, or vice versa.

The principal references to incubation in the literature are to be found in connection with the attempts of various investigators to ascertain the relation between the isothermal TTT diagram and the cooling rate or continuous cooling diagram. These have been very adequately covered in a previous publication¹ by the author and his collaborators. However, some aspects of Krainer's work¹³ on incubation within the pearlite range merits further attention. He showed that reaction begins when $\Sigma[t_i/t_b] = 1$, where t_i = incubation time and t_b = the time for the beginning of the reaction.

* Mellon Institute of Industrial Research.

¹³ H. Krainer: The Conditions for Through-hardening of Steel. *Archiv Eisenhüttenwesen* (1936) 9, 619-622.

* Carnegie Institute of Technology.

† Rensselaer Polytechnic Institute.

That is, if the specimen is incubated for a time equal to half the time for the beginning of reaction at one temperature and then quenched to another and held there for an equal fraction of reaction time, the reaction will begin. From nine of such duplex treatments using various time fractions, Krainer found that the average $\Sigma[t_i/t_b] = 0.96$, with limits of 0.7 and 1.2 which were considered to be within experimental error. Also, Steinberg¹¹ has suggested the use of the same type of treatments in determining the position of the cooling rate curve. But rather than using only two treatments, he felt that the cooling curve could be split into an infinite number of such fractional steps and predicted that reaction would begin

on cooling when $\int_0^t \frac{dt_i}{t_b} = 1$. Substantially the

same mathematical representation has been suggested recently by Manning and Lorig.⁴

One of the more important conclusions derived from this investigation is that, at certain incubation temperatures in the bainite transformation range, the author has found an unusual type of behavior in the effect of incubation time at constant temperature. In general, the data show that for short incubation times the time for beginning of reaction decreases, and that longer incubation times produce an even greater decrease in the reaction time. For example, the marked effect of holding austenite at low temperature in the bainite range upon time for formation of 1 pct bainite and shifting of the nose of 1 pct bainite curve to the left in 43100 steel is to be noted. It would be of interest to know if the plateau is shifted upward and to the left by such incubation treatments. More data in the range from 250 to 300°C would have to be obtained in order to determine the extent of the shift in the upper limit of bainite formation. The effect of incubation in the bainite region of 4330 steel upon time at a lower temperature for 1 pct bainite follows a similar trend in that it moves the bainite nose to the left (shorter time intervals) but here again more experimental data are necessary though it is realized that the incubation time interval is very short.

For the case where reaction temperature is greater than incubation temperature, the ideal behavior is believed to be exemplified by Fig 6 portraying the effect of holding at one tem-

perature in bainite range upon time at a higher temperature for formation of 1 pct bainite in 43100 steel. The hyperbolic curve shows that with increasing incubation time the reaction rate increases, seemingly toward a maximum at the time for the beginning of the reaction at the incubation temperature. This acceleration of the bainite reaction may be explained on the basis of nucleation and growth theory. At lower temperatures (in the vicinity of the bainite nose), nucleation rates are higher, so that, if nucleation and growth are occurring on a minute scale during incubation, nuclei will form quickly at the low incubation temperature and serve as nuclei at the higher reaction temperature, thus increasing the reaction rate at the latter temperature. It is interesting to note that Krainer may have unknowingly obtained the same type of behavior as is here explained for the case where incubation temperature exceeds reaction temperature. As explained above, he was trying to show that reaction begins on cooling when $\Sigma[t_i/t_b] = 1$. He used two-step treatments in which he held the specimens for a certain fraction of reaction at one temperature and quenched to another, observing the actual beginning of reaction at the latter and then calculating his $\Sigma[t_i/t_b]$. Thus the fact that Krainer's data show a decreasing value of $\Sigma[t_i/t_b]$ for increasing incubation times is in complete agreement with the results here obtained.

The writer would like to have seen more complete diagrams for Fig 1 and 2 in order that the extent of the proeutectoid constituents over the temperature range from A_{c1} to M_s could be ascertained. For example, is it possible that the TTT diagram for 4330 steel has two ferrite regions preceding the pearlite and bainite regions? Hultgren¹⁴ has shown this for a steel of similar composition which he designated as NiCrMo 34723. Hultgren stated that in steels of sufficient and suitable alloy contents there is a distinct break between the zero curve of the propearlitic ferrite and probainitic ferrite and that possibly, owing to insufficient accuracy in the determinations, no such break can be found with certainty for most of the alloy steels investigated.

Also, in the TTT diagrams presented, it is

¹⁴ A. Hultgren: Isothermal Transformation of Austenite. *Trans. ASM* (1947) **39**, 915-1005.

interesting to note that a dotted line is drawn for the plateau of the bainite region in 4330 steel and a solid line for 43100 steel. The writer believes that no connecting (solid) line should be drawn in the temperature range 485 to 525°C for 4330 steel and 450 to 475°C for 43100 steel. It is frequently observed in *TTT* diagrams of the type shown that a connecting (nearly horizontal) line is drawn but this can hardly be termed a correct procedure because in such a narrow temperature range alloy segregation and banding which may occur in any of the small specimens produce microstructures which resemble those obtained for either of the temperature end points.

The observations noted above point to the necessity of recording the microstructural changes that accompany isothermal transformation in alloy steels. In view of the known inadequacy of the present nomenclature for the decomposition products of austenite and the variations in microstructures observed it is necessary to resort to micrographs in order to classify some of the microstructures encountered in alloy steels. Typical micrographs of the bainite-bainite and the ferrite-bainite reactions for 4330 steel and the carbide-bainite reaction for 43100 steel would be appreciated.

Both steels under consideration were austenitized at very high temperatures (much higher than austenitizing temperatures used in commercial heat treating practice) in order to dissolve austenite heterogeneities and approach austenite homogeneity. In spite of this it is to be noted that the pearlite nose of the higher carbon 43100 steel has shifted markedly to the left compared to the 4330 steel. What explanation can the author give for this result if any undissolved carbides which would enhance nucleation of the pearlite reaction were supposedly eliminated by the high temperature austenitizing treatment? Perhaps the initial precipitate of proeutectoid carbides at temperatures below A_{c1} and proceeding more rapidly the lower the temperature nucleates the subsequent pearlite reaction to a greater degree in this steel.

The practical applications to be found in the results relate to the increased reaction rate due to relatively long incubation treatments. For example, in the spheroidization of steels, the annealing cycle might be reduced if the piece were quenched to a temperature at or near the

pearlite nose and held only long enough to insure that no reaction takes place before reheating to the spheroidizing temperature for the initiation of the transformation product desired. A properly selected incubation treatment should materially reduce the reaction time. Does the author believe that, working with steels of high hardenability which would permit greater time latitude in incubation treatments, it would be possible to secure a minimum in the t_s vs. t_h curve indicating the optimum condition for beginning of reaction at the second temperature? Also, it would be of interest to speculate if longer incubation then causes a reversal in that the reaction time increases and returns to the reaction time interval necessary to transform an unincubated specimen isothermally.

L. D. JAFFE (author's reply)—I agree wholeheartedly with Mr. Grange that it would be very desirable to carry on further work using different steels and different austenitizing temperatures, and hope it will be possible to do so.

I greatly regret having misquoted Mr. Grange when referring to some of his previous work. His comment on the effect of molybdenum upon the time required for isothermal bainite formation is most interesting. I hope the results of his investigation of this effect will be published soon.

Mr. Grange asks whether a delayed quench would increase the hardenability of a hypereutectoid steel if the austenitizing temperature were so low that carbides were initially out of solution. Experimental work on that question is needed. The results of this paper are likely not to be applicable; in particular, attention would have to be given to the effects of holding in the range where pearlite is the first product to form. This range was not studied in the present paper.

I agree with Mr. Grange that if a hypereutectoid steel is austenitized at a high temperature and then delay-quenched, it is necessary to consider the effect on the mechanical properties of possible submicroscopic traces of carbide that might form as a grain-boundary network. The mechanical properties of steel given such heat treatments form a separate problem, which should be investigated.

I would like to thank Mr. Alexander for his information regarding the nucleation and growth of proeutectoid ferrite. It may well be that future studies will reveal that the acceleration of the bainite reaction by holding in the ferrite range depends on the temperature of bainite formation.

Dr. Hess asks about the times of holding in the bainite range. As indicated in the paper, the times were always less than the time necessary for 1 pct transformation. The amount of transformation for reactions occurring by nucleation and growth initially varies as the cube or the fourth power of the time. For times significantly shorter than that needed for 1 pct transformation, the percent transformation was therefore very small indeed; in general, at the first temperature of holding, there was no visible transformation at all.

Dr. Hess also asks about the effect on transformation at a high temperature of holding for a long time in the bainite range where still longer time is required for transformation to start. In the steels used in this work, visible bainite formation occurred in a matter of seconds or minutes at all temperatures (Tables 1-2). While I have not studied steels where the times required for bainite formation are longer, there seems no reason to think that treatments mentioned by Dr. Hess would have different effects upon subsequent high-temperature transformation than the treatments reported in the paper. That is, they would be expected to accelerate formation of high-temperature bainite and of proeutectoid ferrite and to retard formation of proeutectoid carbide. The effect of small amounts of bainite on subsequent pearlite formation has not been investigated.

The mathematical expressions of Krainer, of Steinberg, and of Manning and Lorig, referred to by Mr. Loria, are all based upon the assumption of additivity. As shown in this paper, though such an assumption may be made for the proeutectoid reactions, it is not in general permissible.

Mr. Loria asks whether holding in the bainite range has the effect of shifting the curve, for 1 pct bainite formation at higher temperatures, to the left and upward. Tables 5 and 7, Fig 5-6 show that the curve is shifted to the left. There are no data as to an upward shift, and no reason to expect one.

Variation of nucleation rate with temperature is suggested by Mr. Loria as an explanation of the non-additivity observed in the bainite range. I do not see how this explanation accounts for the observation that holding at a high temperature in the bainite range can actually increase the time necessary to form 1 pct bainite at a lower temperature (Table 6).

Mr. Loria suggests that ferrite formation may isothermally precede bainite formation. I do not think the ferrite often observed to form in the bainite range *precedes* bainite; I think it *is* bainite. In other words, freshly formed bainite is simply ferrite supersaturated with carbon.^{6,15-17}

I agree that micrographs are needed to identify the microstructures discussed. In accordance with Mr. Loria's request, micrographs of the bainite and proeutectoid constituents observed in the steels studied are given as Fig 7-10. These micrographs were prepared by Miss Mary Norton. The percentage of transformation product visible in each figure is not necessarily equal to the average found throughout the specimen.

It may be mentioned that two to five specimens, heat treated separately but supposedly identically, were in general examined for each heat treatment used.

Mr. Loria asks why the pearlite nose of the high carbon 43100 steel was to the left (at shorter times) than the pearlite nose of the lower carbon 4330 steel. Despite popular opinion to the contrary, it is well established that an increase in carbon content accelerates the pearlite reaction, moving the pearlite nose to the left.^{10,18-20}

Mr. Loria asks whether annealing could be speeded by quickly cooling the steel to the pearlite nose, holding it there for a short time, and then reheating it to a temperature higher in the pearlite range. That procedure seems perfectly feasible. However, further work is needed before quantitative data can be provided. As indicated in a previous paper by the author,¹⁷ it is likely that the pearlite reaction is additive, but the evidence is not conclusive.

Finally, Mr. Loria would like to know whether a long "incubation" period may have an effect, on subsequent transformation at

¹⁵⁻¹⁷ References are at the end of the discussion.



FIG 7—MICROSTRUCTURE OF 4330 STEEL AUSTENITIZED 15 MIN. AT 1095°C , QUENCHED INTO METAL BATH AT 650°C , HELD $7\frac{1}{2}$ HR, AND WATER-QUENCHED. WHITE ANGULAR AREAS OF FERRITE ARE VISIBLE AGAINST BACKGROUND OF MARTENSITE. MAGNIFICATION: $\times 1000$. OBJECTIVE: 60 APO, 0.95 N. A. ETCHANT: 1 PCT NITAL. REDUCED APPROXIMATELY ONE THIRD.

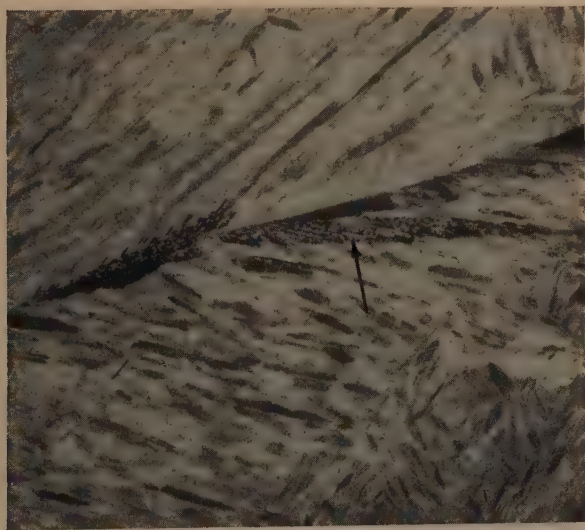


FIG 8—MICROSTRUCTURE OF 4330 STEEL AUSTENITIZED 15 MIN. AT 1095°C , QUENCHED INTO METAL BATH AT 455°C , HELD 33 SEC, AND WATER-QUENCHED. AREAS OF BAINITE ARE VISIBLE AGAINST BACKGROUND OF MARTENSITE. BLACK ARROW INDICATES TYPICAL BAINITE AREA. MAGNIFICATION: $\times 1000$. OBJECTIVE 60 APO, 0.95 N. A. ETCHANT: 1 PCT NITAL. REDUCED APPROXIMATELY ONE THIRD.



FIG 9—MICROSTRUCTURE OF 43100 STEEL AUSTENITIZED 15 MIN. AT 1150°C , QUENCHED INTO METAL BATH AT 725°C , HELD 2 HR, AND WATER-QUENCHED. WHITE PROEUTECTOID CARBIDE IS VISIBLE AS A NETWORK AGAINST BACKGROUND OF HIGH-CARBON MARTENSITE. MAGNIFICATION: $\times 1000$. OBJECTIVE: 60 APO, 0.95 N. A. ETCHANT: 1 PCT NITAL. REDUCED APPROXIMATELY ONE THIRD.

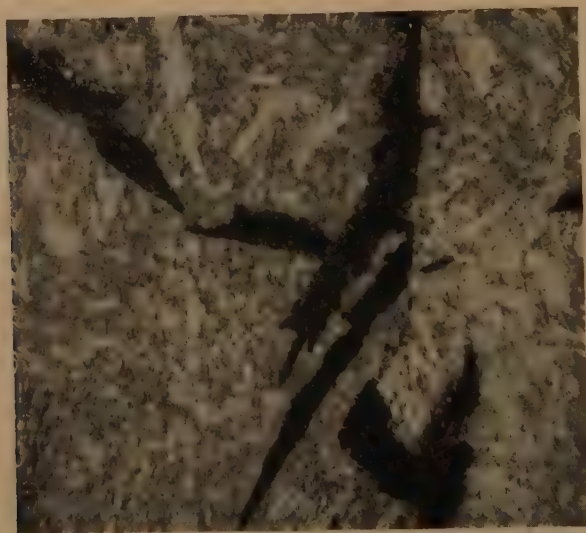


FIG 10—MICROSTRUCTURE OF 43100 STEEL AUSTENITIZED 15 MIN. AT 1150°C , QUENCHED INTO METAL BATH AT 455°C , HELD 13 MIN., AND WATER-QUENCHED. DARK AREAS OF BAINITE VISIBLE AGAINST BACKGROUND OF HIGH-CARBON MARTENSITE. MAGNIFICATION: $\times 1000$. OBJECTIVE: 60 APO, 0.95 N. A. ETCHANT: 1 PCT NITAL. REDUCED APPROXIMATELY ONE THIRD.

other temperatures, opposite to that of a short period. Holds at a temperature long enough to produce considerable transformation of austenite may have an effect opposite to short holds, because they may considerably change the composition of the remaining austenite. Thus, it has been found that precipitation of large amounts of proeutectoid ferrite retards the bainite reaction,²¹ whereas, as shown in this paper, short holds in the ferrite range accelerate bainite formation. Precipitation of large amounts of proeutectoid ferrite necessarily enriches the remaining austenite in carbon, thus slowing its transformation to bainite.

REFERENCES

15. E. S. Davenport and E. C. Bain: Transformation of Austenite at Constant Subcritical Temperatures. *Trans. AIME* (1930) **90**, 117-154.
16. F. Wever and H. Lange: The Transformation Kinetics of Austenite. I. Magnetic Investigations of Austenite Decomposition, (in German), *Mitt. K.-W. Inst. Eisenforsch. Dusseldorf* (1932) **14**, 71-83.
17. H. Jolivet and A. Portevin: Kinetics of Austenite Decomposition in the Upper Region of the Intermediate Domain (in French), *Compt. rend.* (1939) **209**, 556-558. Also; *Genie Civil.* (1939) **115**, 464-465.
18. T. Sato: On the Critical Points of Pure Carbon Steels (in English), *Tech. Reports Tohoku Imp. Univ.* (1929) **8**, 27-52.
19. F. Wever, A. Rose, and H. Lange: The Influence of Cooling Velocity on the Transformations of Steels (in German), *Mitt. K.-W. Inst. Eisenforsch. Dusseldorf* (1937) **19**, 289-298; (1938) **20**, 55-65.
20. T. Lyman and A. R. Troiano: Influence of Carbon Content upon the Transformations in 3 per cent Chromium Steel. *Trans. A.S.M.* (1945) **37**, 402-448.
21. C. A. Liedholm and W. C. Coons: Effect of Cooling Transformation upon Subsequent Isothermal Reactions. *Metal Progress* (1946) **46**, 104-107.

Austenite Transformation Above and Within the Martensite Range

BY ROBERT T. HOWARD, JR.* AND MORRIS COHEN,† MEMBER AIME

(Chicago Meeting, October 1947)

THE purpose of this paper is to direct attention to the lower part of the austenite transformation diagram, or TTT curves, where considerable uncertainty still exists as to the blending of the bainite and martensite reactions. The dissimilarities between these two low temperature transformations have been summarized recently by Troiano and Greninger.¹ Of particular importance to the present work is the fact that martensite formation, unlike bainite formation, is not suppressed by the fastest quenching rates attainable. However, most of the investigations in this direction have been concerned primarily with the start of the martensite transformation (M_s) during cooling, rather than with the quantitative aspects of the subsequent reaction on either further cooling or isothermal holding.

Several years ago, Cohen² suggested a form of transformation diagram which reconciled, at least schematically, the isothermal characteristics of the bainite transformation with the insuppressible nature of the martensite transformation. In essence, the diagram consisted of a family of horizontal lines (representing the progress of the austenite-martensite

reaction during quenching) which were interrupted in point of time by the bainite family of C-curves extending down from higher temperatures. This picture received later support by metallographic³ and dilatometric^{4,5} studies, but the techniques employed were not sufficiently critical to substantiate some of the details.

Elmendorf⁶ and Grange and Steward⁷ have shown that the Greninger-Troiano metallographic technique⁸ may be used not only for M_s determinations, but for studying the course of further austenite decomposition. In fact, the latter investigators have observed the amount of martensite formed as a function of temperature below M_s in fourteen commercial steels.

In the present paper, the Greninger-Troiano technique has been combined with the lineal method of Howard and Cohen⁹ to provide a unique, quantitative treatment of the austenite-martensite reaction. Furthermore, isothermal transformations have been similarly measured on holding at temperatures above and below M_s , thus permitting a fairly detailed presentation of the lower part of the conventional austenite transformation diagram.

EXPERIMENTAL DETAILS

Materials

The steels, listed in Table I, were selected for study because they exhibit a satisfactory range of M_s temperatures and have not received as much attention as the lower carbon grades. They were prepared as 30 lb induction furnace heats in the laboratories of the Vanadium-Alloys

This paper is based on a portion of a thesis submitted by Robert T. Howard to the Department of Metallurgy at the Massachusetts Institute of Technology in partial fulfillment of the requirements for the degree of Doctor of Science. Manuscript received at the office of the Institute July 7, 1947. Issued as TP 2283 in METALS TECHNOLOGY, September 1947.

* Republic Steel Corporation Fellow, Massachusetts Institute of Technology, Cambridge, Massachusetts.

† Professor of Physical Metallurgy, Massachusetts Institute of Technology, Cambridge, Massachusetts.

¹ References are at the end of the paper.

Steel Co. Ferrosilicon was used for deoxidation. The ingots were hot rolled to $\frac{3}{32}$ in. and centerless ground to 0.250 in. The rods were received in the spheroidized condition.

TABLE 1—Compositions of Steels Investigated

Designation, Per Cent C	Per Cent					
	C	Ni	Si	Mn	S	P
0.75	0.75		0.27	0.50	0.020	0.007
1.12	1.13		0.24	0.59	0.018	0.006
1.35	1.35		0.28	0.52	0.017	0.006
1.1-3.5 pct Ni	1.12	3.56	0.28	0.55	0.014	0.007
1.1-5 pct Ni	1.12	5.36	0.24	0.51	0.016	0.009

Specimens

The center of the ground stock was machined out with a No. 36 drill (approximately $\frac{1}{10}$ in. diam) and the resulting "tubes" were sectioned into $\frac{3}{32}$ in. lengths. This produced suitably small specimens, free from decarburization and pipe segregation, in a form that could be easily wired to a holder for heat treatment purposes. The steels were identified by longitudinal grooves that were cut along the rods before the sectioning.

Austenitizing

The specimens were austenitized in a vertical resistance-wound furnace, so arranged as to permit rapid removal of the specimens for quenching to lower temperatures. Decarburization was minimized by a prepurified nitrogen atmosphere which was further "cleansed" by the presence of a block of graphite in the hot zone of the furnace.

An austenitizing temperature of $955 \pm 2^\circ\text{C}$ ($1750 \pm 4^\circ\text{F}$) was selected after a series of runs to determine an optimum treatment for dissolving all carbides without undue grain coarsening in the five steels. Since austenitizing times of 15 to 60 min. caused little difference in the amount of retained austenite (after quench-

ing to room temperature in 10 pct NaOH brine*) a standard soaking period of 30 min. was adopted. Table 2 indicates the

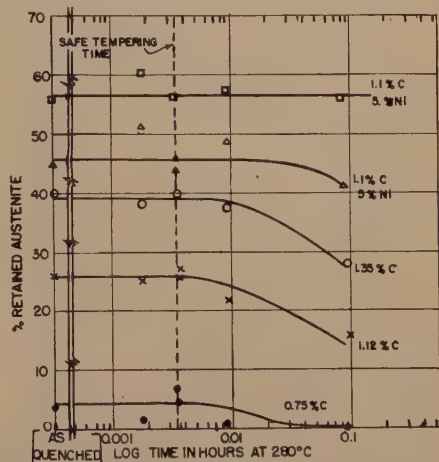


FIG 1—EFFECT OF TEMPERING AT 280°C (535°F) AFTER BRINE QUENCHING FROM 955°C (1750°F).

TABLE 2—Austenite Retained after Quenching from Standard Austenitizing Treatment of 30 Minutes at 955°C (1750°F)

Steel Per Cent C	Per Cent	
	Brine Quench	Oil Quench
0.75	2-5	7
1.12	24-27	30
1.35	39-41	45
1.1-3.5 pct Ni	44-46	54
1.1-5 pct Ni	54-56	68

range of austenite contents retained under the above conditions.

Quenching

The hot-quenching practice was conventional, using lead-base alloy baths controlled to $\pm 2^\circ\text{C}$ ($\pm 4^\circ\text{F}$) in the range of 80 – 300°C (175 – 570°F). Generally, the hot-quenched specimens were held for 36 sec (to insure reaching the bath temperature) before being transferred to the

* The term "brine" as used hereinafter signifies an aqueous solution of 10 pct sodium hydroxide.

tempering bath (see below). In some cases, this time was reduced to 5 sec. No isothermal transformation was observed during these periods. Holding times up to

mine the extent of undesired austenite decomposition. Fig 1 shows that, for brine-quenched specimens at least, no appreciable conversion of the retained austenite occurs

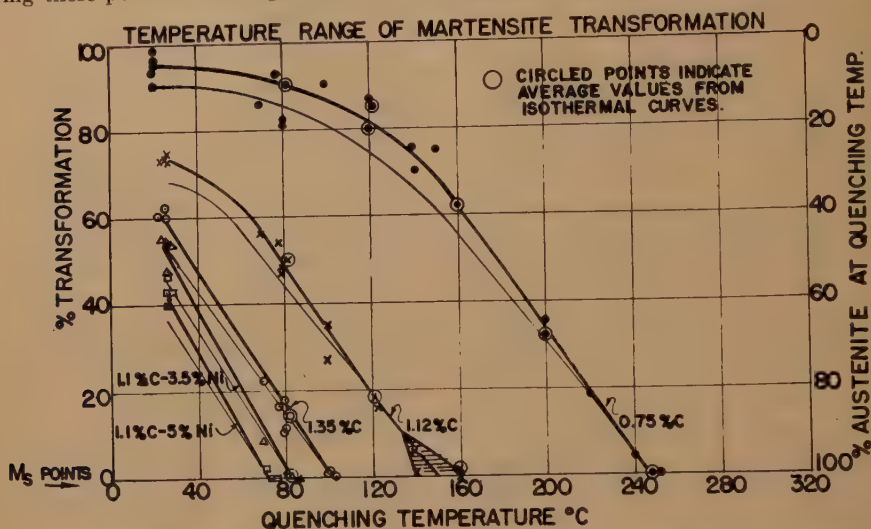


FIG 2—RELATIONSHIP BETWEEN PERCENTAGE MARTENSITE TRANSFORMATION AND QUENCHING-BATH TEMPERATURE. AUSTENITIZING TEMPERATURE = 955°C (1750°F). HEAVILY RULED CURVES OBTAINED WITH BRINE FOR ROOM TEMPERATURE QUENCHING BATH AND MOLTEN LEAD ALLOYS FOR HIGHER TEMPERATURE QUENCHING BATHS. LIGHTLY RULED CURVES SHOW CALCULATED COURSE OF MARTENSITE FORMATION WHEN QUENCHING RATE CORRESPONDS TO OIL INSTEAD OF BRINE AT ROOM TEMPERATURE. ALL PLOTTED POINTS APPLY TO HEAVILY RULED CURVES.

100 hr were studied in the isothermal runs. Room-temperature quenching was conducted in 10 pct NaOH brine which, as will be mentioned later, seemed to match the quenching effect of the metal baths at the higher temperatures. A few room-temperature quenching experiments were carried out in oil for comparison purposes (Table 2).

Tempering

In accordance with the Greninger-Troiano technique, the quenched specimens were tempered to darken the transformation product formed on cooling to the bath temperature and, in the isothermal runs, on holding at the bath temperature. It was found that satisfactory tempering could be attained in these steels at 280°C (535°F), and a series of time variations at this temperature was investigated in order to deter-

mine the extent of undesired austenite decomposition. Fig 1 shows that, for brine-quenched specimens at least, no appreciable conversion of the retained austenite occurs

Measurements

Following heat treatment, one face of each "doughnut" specimen was carefully ground to remove $\frac{1}{32}$ in., and then was metallographically polished and etched with nital. The etching was adjusted by trial and error to yield maximum contrast between the dark (tempered) reaction products and the untransformed matrix. Usually, best results were obtained with 1 pct nital for the high austenite structures, 3 pct nital for the medium austenite, and 6 pct nital for structures approaching complete transformation.

The relative amounts of reaction product and untransformed matrix were determined quantitatively by lineal analysis. The authors have discussed this method and its precision in considerable detail elsewhere.⁹ By this procedure, the course of martensite formation during cooling and of bainite formation during isothermal holding was measured. In the specimens containing both martensite and bainite, no attempt was made to distinguish between the two products during the lineal analysis—in other words, the total transformation (S) was evaluated. The amount of martensite (P) formed on the cooling to the holding temperature was determined separately on specimens that were similarly quenched but held for only 36 sec. By subtracting P from S , the percentage of isothermal transformation was obtained.

EXPERIMENTAL RESULTS

Martensite Range

The percentage* of martensite as a function of quenching bath temperature is plotted for the five steels in Fig 2. Encircled points were averaged from isothermal studies below M_s , and include all the determinations made up to the holding time where isothermal transformation was found to set in. Two of the curves, 0.75 pct carbon and 1.12 pct carbon, in Fig 2 are essentially straight down to the temperature where approximately 60 pct of martensite has formed, and then bend off as the rate of transformation with respect to dropping temperature diminishes. The other three curves do not show this tapering off, presumably because the transformation has not progressed far enough by the time room temperature is reached. In the three plain carbon steels, about $\frac{3}{4}$ pct martensite forms per °C over the linear portion of the curves, while in the nickel steels, this value increases to approximately 1 pct martensite per °C despite the lower M_s temperatures.

* Percentages are on a volume basis.

The curves in Fig 2 fit an empirical equation of the type:

$$P = 100 - k[T - (M_s - M_s^\circ)]^c$$

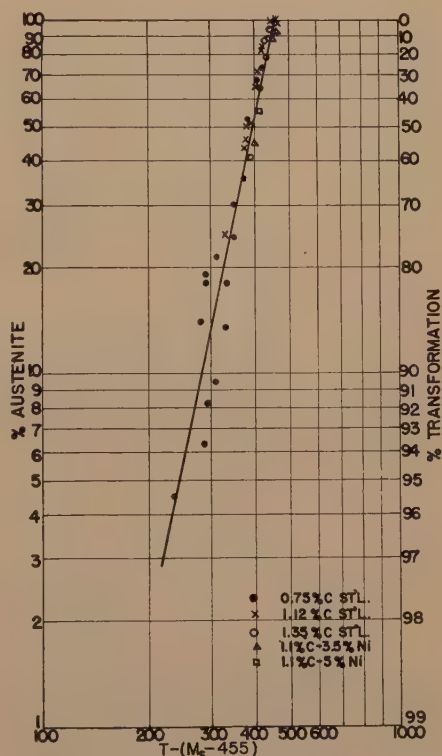


FIG 3—DATA OF FIG 2 PLOTTED AS LOG PERCENTAGE AUSTENITE [$\log(100 - P)$] AND LOG PERCENTAGE TRANSFORMATION [$\log P$] VS $\log [T - (M_s - 455)]$. SYMBOLS ARE DEFINED IN TEXT. STRAIGHT-LINE RELATIONSHIP LEADS TO FOLLOWING EQUATION FOR PERCENT MARTENSITE AS A FUNCTION OF ABSOLUTE TEMPERATURE: $P = 100 - 2.2 \times 10^{-11} [T - 455]^{4.75}$.

where P is the pct martensite, k and c are constants, T is the absolute temperature of the quenching bath, M_s is the M_s (absolute) temperature of the steel in question, and M_s° is the M_s (absolute) temperature of a standard composition used for reference purposes. In the present case, M_s° is taken as 455°K (182°C - 360°F), which is M_s for a 1 pct carbon steel.

Fig 3 shows $\log(100 - P)$ and $\log P$

plotted against $\log [T - (M_s - 455)]$, using the data given in Fig 2 for the five steels. From the straight line thus derived, the two constants may be evaluated:

the constants: $k = 8.0 \times 10^{-9}$ and $c = 3.8$. These constants define the lightly ruled curves in Fig 2, which intersect the previously discussed curves at M_s but which

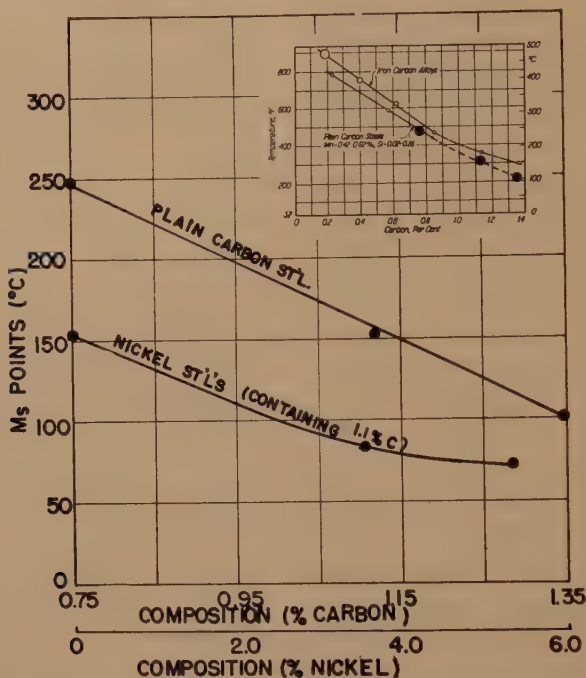


FIG 4—VARIATION OF M_s AS A FUNCTION OF CARBON CONTENT IN RANGE OF 0.75 TO 1.35 PCT AND OF NICKEL CONTENT IN RANGE OF 0 TO 5 PCT AT 1.1 PCT CARBON LEVEL. M_s POINTS ARE DETERMINED BY EXTRAPOLATION OF MARTENSITE CURVES IN FIG 2 TO 0 PCT TRANSFORMATION. INSET SHOWS PRESENT DATA (SOLID CURVES) SUPERIMPOSED UPON SUMMARIZED DATA OF GRENINGER¹¹ (OPEN CIRCLES).

$k = 2.2 \times 10^{-11}$ and $c = 4.75$. It is interesting to note that the room temperature points obtained with brine quenching fit the same equation as the higher temperature points obtained with metal-bath quenching. Substituting $T = 298^\circ \text{K}$ ($25^\circ \text{C} - 77^\circ \text{F}$) in the equation yields retained austenite contents of 3.9, 19, 39, 49 and 55 pct for the five steels listed in Table 2, where the experimentally determined values may be compared.

When these steels are oil quenched to room temperature, more austenite is retained than on brine quenching, as indicated in Table 2. These values also fall on a straight line in a log-log plot, and lead to

indicate less martensite formation below M_s .^{*} Evidently, even though M_s is not affected by quenching rate, the extent of the transformation at any temperature below M_s is dependent on the quenching rate. It may be worth emphasizing that this dependence is not in the nature of suppression: in fact, the austenite-martensite reaction proceeds faster with respect to dropping temperature, the faster the rate of cooling.

* The lightly ruled curves represent the amount of martensite formed as a function of quenching bath temperature, wherein the quenching baths hypothetically match the oil quench at room temperature.

M_s Temperatures

The linear portion of the curves in Fig 2 can be readily extrapolated back to zero transformation, thus providing a convenient determination of M_s . The experimental points bunched at the extrapolated value in each case testifies to the validity of the extrapolation. Only in the 1.12 pct C steel is there any uncertainty (note the spread of values), and this is attributable to segregations. In other words, it appears that the austenite-martensite reaction in these high carbon steels does not set in slowly at M_s as found in the lower carbon grades,⁷ but gets underway suddenly at its maximum rate. McReynolds¹⁰ has also observed very sharp M_s points by following changes in electrical resistance during the quenching of wires.

The M_s temperatures are plotted as a function of carbon and nickel contents in Fig 4, and these are the values used in the previous section dealing with the equation of the martensite reaction. Over the carbon range studied, M_s is lowered by 250°C (450°F) per 1 pct carbon. As shown in the inset of Fig 4, these determinations overlap, and constitute a logical extension of the lower carbon values of Greninger.¹¹

At a carbon level of 1.1 pct, the effect of nickel on M_s is not linear, although it may be substantially so up to 3.5 pct nickel. In the latter range, M_s is lowered by 20°C (36°F) per 1 pct nickel, and by 7°C (13°F) in the range of 3.5 to 5 pct nickel. This compares with a uniform lowering of 20°C (36°F) per 1 pct nickel up to 14 pct nickel in medium carbon steels.¹²

Isothermal Transformation Curves

Specimens for isothermal studies were hot quenched to temperatures in the range of 80 to 300°C (175 to 570°F) and held for varying periods up to 100 hr. Before returning to room temperature, each specimen was given the standard temper for

darkening the transformation products. The extent of transformation was measured by lineal analysis in each case, and the results were plotted in the form of isothermal

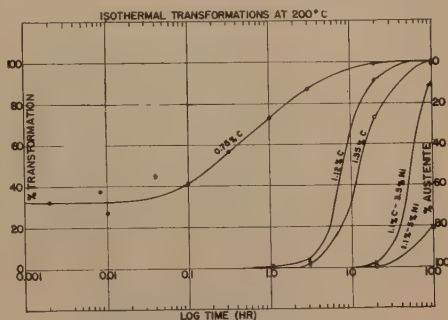


FIG 5—ISOTHERMAL TRANSFORMATION CURVES FOR FIVE STEELS HOT QUENCHED TO 200°C (390°F) AND HELD FOR 100 HRS. THIS TEMPERATURE IS BELOW M_s FOR THE 0.75 PCT CARBON STEEL BUT ABOVE FOR THE OTHERS.

reaction curves. Typical examples are given in Fig 5 for the five steels at 200°C (390°F), and in Fig 6 for the 1.12 pct carbon steel at six temperatures. Actually, all five steels were investigated at all six temperatures.

When the holding temperature is above M_s , the isothermal transformation starts from zero after an appreciable incubation period, and progresses in a normal manner at a rate that decreases with decreasing temperature, with increasing carbon content and with increasing nickel content.

When the holding temperature is below M_s , the isothermal transformation again exhibits an incubation period, but it does not start from zero since some martensite forms during the cooling between M_s and the holding temperature. Thus the isothermal transformation is superimposed upon an existing amount of martensite, whose pct is indicated either by the initial horizontal portion of the isothermal curves in Figs 5 and 6 or by the martensite reaction curves in Fig 2. It will be shown later that, at temperatures not too far below M_s , the entré of the isothermal reaction is speeded up by the presence of martensite, but the

later stages of transformation are not so affected.

Whether the holding temperature is above or below M_s , the isothermal reaction

martensite reaction at M_s . The martensite range is depicted as a family of horizontal lines spaced with respect to temperature according to the amount of martensite

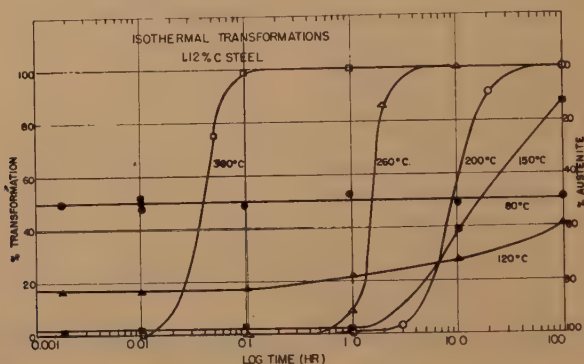


FIG 6—ISOTHERMAL TRANSFORMATION CURVES FOR THE 1.12 PCT CARBON STEEL HOT QUENCHED TO THE INDICATED TEMPERATURES AND HELD FOR 100 HR. 300, 260 AND 200°C CURVES ARE ABOVE M_s FOR THIS STEEL, OTHERS ARE BELOW.

product is bainite. No evidence of isothermal martensite formation was found. Fig 7 illustrates the coexistence of martensite and bainite in the 1.12 pct carbon steel after quenching below M_s to 120°C (250°F) and prolonged holding for 100 hr.

Austenite Transformation Diagrams

By picking off the time-temperature combinations for various percentages of transformation from the smoothed martensite curves in Fig 2 and from the smoothed isothermal curves typified by Figs 5 and 6, it is possible to construct the austenite transformation diagrams shown in Figs 8-12. These diagrams, though quite similar in principle, demonstrate clearly the depressing effect of increasing carbon and nickel on the martensite range and the retarding effect on the bainite reaction.

The bainite curves exhibit the characteristic downward slope toward longer times, since all the temperatures studied here lie below the nose of the bainite or pearlite C-curves. However, this normal course is interrupted by the onset of the

formed on the cooling temperature. These lines remain horizontal in point of time until the first traces of isothermal reaction are observed, and then bend upward to meet the corresponding bainite curves extending down from the higher temperatures. In the two nickel steels (Figs 11 and 12), the bainite transformation is so slow at temperatures below M_s that the martensite and bainite families do not intersect within the 100 hr period studied. The anticipated blending of the two sets of lines undoubtedly occurs off the diagram.

The locus of points at which the isothermal transformation sets in below M_s is represented by the dotted curves in Figs 8-10. Their C-shaped nature signifies that the beginning of bainite formation, which requires longer and longer times as the temperature is lowered above M_s , actually requires somewhat less time as the temperature is lowered below M_s . This speeding-up effect is noticed for about 20-30°C (35-55°F) and then a reversal occurs at still lower temperatures. The bottom part of this new C-curve flattens out within a limited range of temperatures, and hence

the stimulating influence of martensite on the bainite formation rapidly fades out. In fact, even at the nose temperature, the acceleration is observed only during the

mal shape of the bainite curves extending down from above M_s . These trends were indicated earlier² by other data.^{3,8}

The speeding up of the beginning of iso-

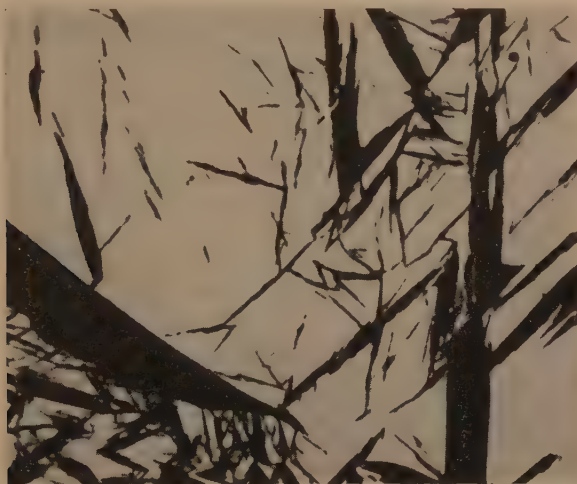


FIG 7—MARTENSITE AND BAINITE IN 1.12 PCT CARBON STEEL. MARTENSITE FORMED ON HOT QUENCHING TO 120°C (250°F), AND BAINITE FORMED SUBSEQUENTLY ON HOLDING AT 120°C FOR 100 HR. NITAL ETCH. 1500X.

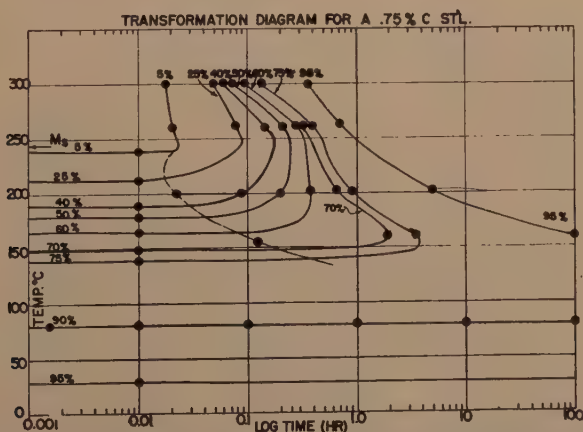


FIG 8—AUSTENITE TRANSFORMATION DIAGRAM FOR 0.75 PCT CARBON STEEL. HORIZONTAL LINES REPRESENT FORMATION OF MARTENSITE ON COOLING; CURVED LINES SHOW FORMATION OF BAINITE ON ISOTHERMAL HOLDING. DOTTED LINE INDICATES BEGINNING OF ISOTHERMAL TRANSFORMATION ON HOLDING BELOW M_s .

first part of the isothermal transformation. The latter part seems to take place at a rate more or less predictable from the nor-

mal shape of the bainite curves extending down from above M_s . These trends were indicated earlier² by other data.^{3,8}

The speeding up of the beginning of iso-

speed steel.⁵ Both bainite and martensite enjoy the same lattice relationships relative to the austenite matrix.¹³ However, this may be only a secondary factor since much

little effect. Since decreasing temperature produces more martensite but lower diffusion rates, the C-curve behavior might well be expected.

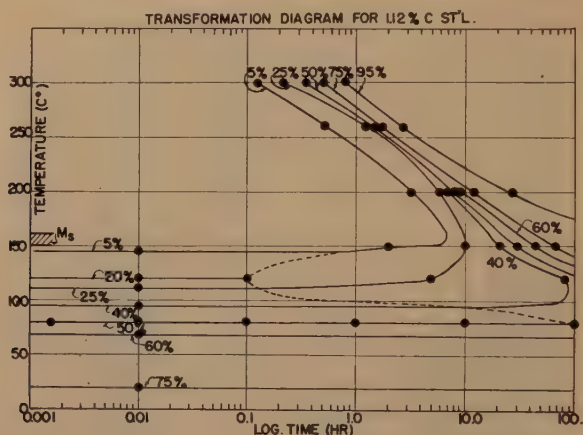


FIG 9—AUSTENITE TRANSFORMATION DIAGRAM FOR 1.12 PCT CARBON STEEL. SEE CAPTION OF FIG 8.

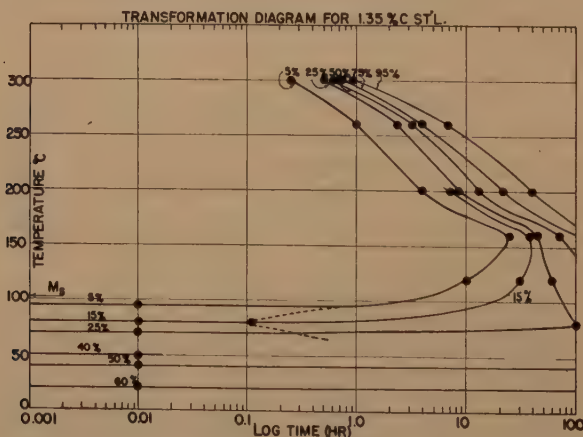


FIG 10—AUSTENITE TRANSFORMATION DIAGRAM FOR 1.35 PCT CARBON STEEL. SEE CAPTION OF FIG 8.

of the premature bainite forms "in the clear" away from the martensite plates. Possibly, deformation of the austenite by the martensite reaction stimulates the subsequent bainite transformation. In any case, the reaction temperature is an important consideration because if it is too low, even large amounts of martensite have

The 5 pct curve for the 1.35 pct carbon steel exhibits an interesting anomaly in that it bends back to shorter times just above M_s . No martensite is present to account for this accelerated effect. A new transformation product is found in this range (see below), and seems to account for the observed change in kinetics.

Microstructures

With the exception of the new structure in the 1.35 pct carbon steel mentioned above, the same types of transformation products appear in all five steels. In general,

higher-temperature form of bainite. It is partly massive or arborescent¹⁴ and partly plate-like. With decreasing temperature (Figs 14 and 15) the massive variety gradually disappears in favor of the plate type, and the latter becomes more acicular.

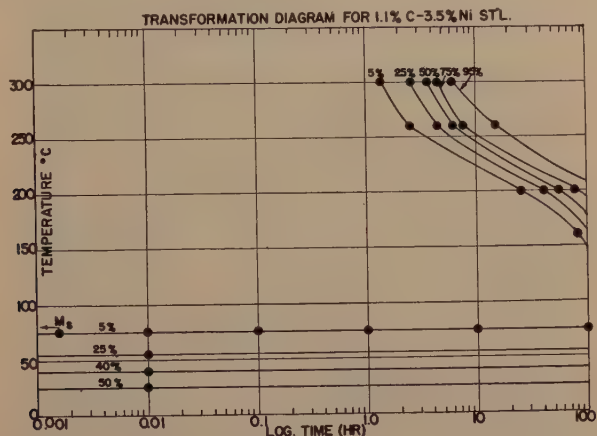


FIG 11—AUSTENITE TRANSFORMATION DIAGRAM FOR 1.1 PCT CARBON—3.5 PCT NICKEL STEEL. SEE CAPTION OF FIG 8.

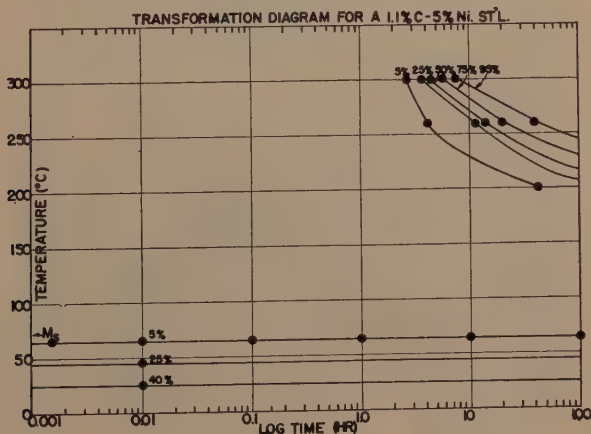


FIG 12—AUSTENITE TRANSFORMATION DIAGRAM FOR 1.1 PCT CARBON—5 PCT NICKEL STEEL. SEE CAPTION OF FIG 8.

a given type of bainite occurs at lower temperatures, the higher the carbon and nickel contents. The series of micrographs in Figs 13-18, taken from the 1.35 pct carbon steel, serves to illustrate the microstructures observed. Fig 13 shows the

At 160°C (320°F), which is still well above M_s for this steel, the new product is found (Fig 16). It consists of long, thin plates or needles which do not fit in with the foregoing progression of bainitic structures. However, on further reaction at this

temperature, the new product does not form exclusively, but gives way to the heavy type of plate shown in Fig 15. At 120°C (250°F) (Fig 17) the thin product is

The acicular structure is even coarser than the heavy bainite plates. An example of coexisting martensite and bainite produced by holding below M_s is given in Fig 7.

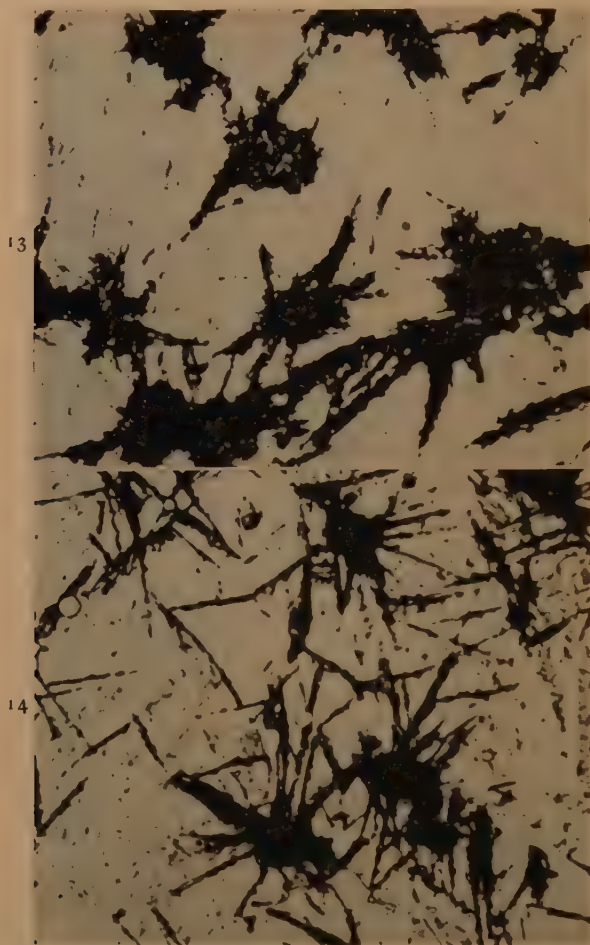


FIG 13—ISOTHERMAL TRANSFORMATION PRODUCT IN 1.35 PCT CARBON STEEL AFTER ONE-HALF HOUR AT 300°C (570°F). NITAL ETCH. 1500X.

FIG 14—ISOTHERMAL TRANSFORMATION PRODUCT IN 1.35 PCT CARBON STEEL AFTER ONE HOUR AT 260°C (500°F). NITAL ETCH. 1500X.

more in evidence and here the reaction has gone sufficiently far to generate some of the heavy plates.

By way of comparison, Fig 18 shows the nature of the martensite found in this steel.

The new product was found only in the 1.35 pct carbon steel, and its formation coincides with the change in kinetics between 160°C (320°F) and M_s . It has the shape of cementite plates,¹⁵ but the dark-

etching characteristics of bainite. Its origin is possibly related to the high carbon content of the steel.

respect to dropping temperature has been determined, and a single empirical equation has been fitted to the five curves. Increasing

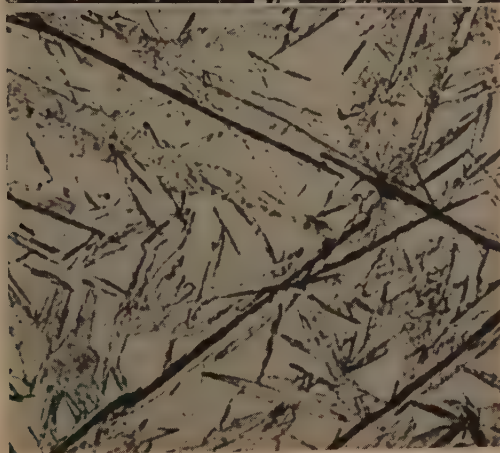
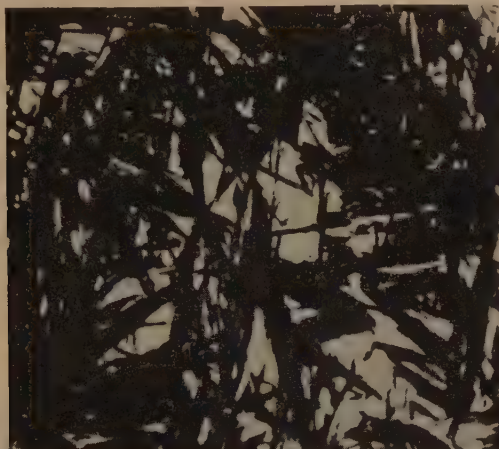


FIG 15—ISOTHERMAL TRANSFORMATION PRODUCT IN 1.35 PCT CARBON STEEL AFTER 20-HR AT 200°C (390°F). NITAL ETCH. 1500X.

FIG 16—ISOTHERMAL TRANSFORMATION PRODUCT IN 1.35 PCT CARBON STEEL AFTER 20 HR AT 160°C (320°F). NOTE CHANGE IN CHARACTER OF THE PLATES AS COMPARED TO FIG 15. NITAL ETCH. 1500X.

CONCLUSIONS

1. The transformation of austenite into martensite and bainite has been studied quantitatively by lineal analysis in a series of five high carbon and nickel steels.

2. The rate of martensite formation with

carbon or nickel lowers M_s and increases the amount of austenite retained at room temperature.

3. Increasing the quenching rate, while not affecting M_s , increases the rate of martensite formation with respect to dropping temperature, and therefore de-

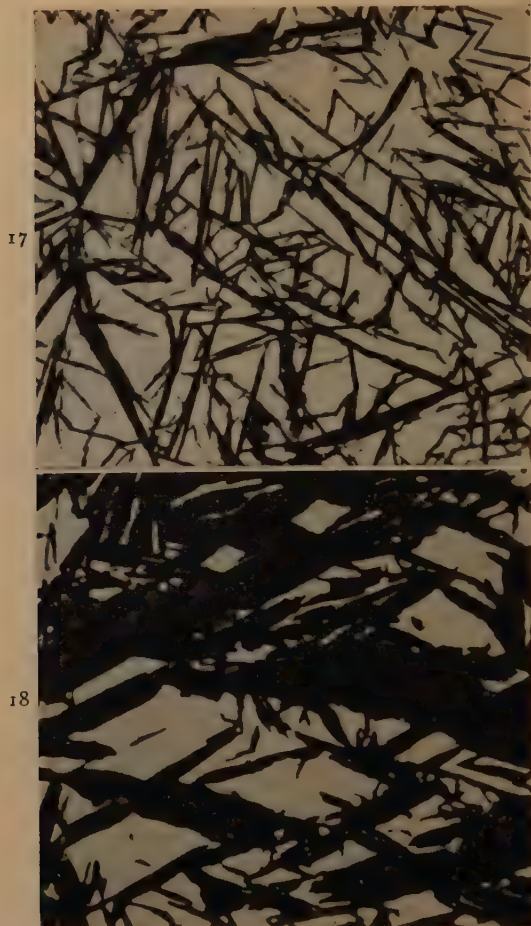


FIG 17—ISOTHERMAL TRANSFORMATION PRODUCT IN 1.35 PCT CARBON STEEL AFTER 100 HR AT 120°C (250°F). NITAL ETCH. $1500\times$.

FIG 18—MARTENSITE (TEMPERED) IN 1.35 PCT CARBON STEEL, BRINE QUENCHED TO ROOM TEMPERATURE. ABOUT 40 PCT RETAINED AUSTENITE IN SPECIMEN. NITAL ETCH. $1500\times$.

creases the amount of austenite retained at room temperature.

4. Isothermal transformation of austenite into bainite occurs above and below M_s with an incubation period in both cases. In general, the rate of bainite formation decreases with decreasing temperature in the range studied, except just below M_s where the existing martensite hastens the onset of the isothermal transformation.

5. The low temperature part of the austenite transformation diagram has been established, with detailed blending of the martensite and bainite regions.

6. In the 1.35 pct carbon steel, an anomalous change in the beginning of isothermal transformation occurs between 160°C (320°F) and M_s . This behavior coincides with the formation of a very thin plate-like product that does not belong in the bainite sequence.

ACKNOWLEDGMENTS

The authors are indebted to the Republic Steel Corp. for a grant under which part of this work was conducted. They also appreciate the cooperation of Dr. George A. Roberts of the Vanadium-Alloys Steel Co., through whose courtesy the steels were furnished.

REFERENCES

1. A. R. Troiano and A. B. Greninger: The Martensite Transformation, *Metal Progress* (Aug. 1946) **50** No. 2, 303.
2. M. Cohen: Discussion to ref. 8.
3. E. R. Saunders and J. T. Kahles: A Study of Martensite Formation by a Photometric Method. *ASM Trans.* (1942) **30**, 1139.
4. R. A. Flinn, E. Cook and J. A. Fellows: A Quantitative Study of Austenite Transformation. *ASM Trans.* (1943) **31**, 41.
5. P. Gordon, M. Cohen and R. S. Rose: The Kinetics of Austenite Decomposition in High Speed Steel. *ASM Trans.* (1943) **31**, 161.
6. H. J. Elmsendorf: The Effect of Varying Amounts of Martensite upon the Isothermal Transformation of Austenite Remaining after Controlled Quenching. *ASM Trans.* (1944) **33**, 236.
7. R. A. Grange and H. M. Stewart: The Temperature Range of Martensite Formation. *Metals Tech.* (June, 1946) **13**, 4, TP 1996. *AIME Trans.* (1946) **167**, 467.
8. A. B. Greninger and A. R. Troiano: Kinetics of the Austenite to Martensite Transformation in Steel. *ASM Trans.* (1940) **28**, 537.
9. R. T. Howard and M. Cohen: Quantitative Metallography by Point Counting and Lineal Analysis. *Metals Tech.* (1947) Aug., TP 2215. *AIME Trans.* **172**, 413.
10. A. W. McReynolds: Electrical Observations of the Austenite-Martensite Transformation in Steel. *Jnl. Appl. Phys.* (Oct. 1946) **17**, 823.
11. A. B. Greninger: The Martensite Thermal Arrest in Iron-Carbon Alloys and Plain Carbon Steels. *ASM Trans.* (1942) **30**, 1.
12. H. H. Chiswick and A. B. Greninger: Influence of Nickel, Molybdenum, Cobalt and Silicon on the Kinetics and Ar¹ Temperatures of the Austenite to Martensite Transformations in Steels. *ASM Trans.* (1944) **32**, 483.
13. G. V. Smith and R. F. Mehl: Lattice Relationships in Decomposition of Austenite to Pearlite, Bainite and Martensite. *AIME Trans.* (1942) **150**, 211.
14. H. Jolivet: Transformation of Austenite on Cooling; Morphology and Genesis of the Aggregate Formed. *Jnl. Iron and Steel Inst.* (1939) **140**, 95P.
15. T. Lyman and A. R. Troiano: Isothermal Transformation of Austenite in One Per Cent Carbon High-Chromium Steels. *Trans. AIME* (1945) **162**, 196.

DISCUSSION

(S. Epstein presiding)

R. A. GRANGE*—In thoroughly exploring the lower portion of the isothermal transformation diagram the authors have performed a service that is as valuable as it is difficult. Working principally with medium carbon steels, we have repeatedly tried to fill in this portion of the diagram with only moderate success; the combination of the lineal measuring method of Howard and Cohen⁹ and selection of high-carbon steels seem to have resulted in accurate and reliable data.

The authors find that curves representing martensite formation as a function of temperature are straight lines from M_s to about 50 pct martensite, whereas other such published curves^{6,7} taper off as M_s is approached. In our experience, the shape of this curve is appreciably influenced, particularly just below M_s , by the presence of segregation (banding); the more severe the segregation, the more gradually the curve tapers off. In a recent study of the effect of carbon on martensite formation in two low-alloy steels, we also observed that martensite seemed to form more abruptly (curve tapered off less) the higher the carbon content. These two factors may explain why the authors, who used samples of high-carbon steel from small induction furnace heats in which segregation was further minimized by the method of sampling, obtained curves that are straight lines between M_s and about 50 pct martensite.

Messrs. Howard and Cohen find that increasing the cooling rate increases the amount of martensite formed on quenching to a temperature below M_s . This means that the location of the lines on their austenite transformation diagram showing how bainite blends into martensite are influenced by cooling rate and hence do not, strictly speaking, belong on an *isothermal* transformation diagram; furthermore, such data should seemingly not be applied quantitatively to pieces of steel appreciably larger in cross-section than the small specimens used in this investigation.

It is surprising to find in Howard and Cohen's work that quenching to room temperature in brine matched the quenching

* U. S. Steel Corporation, Research Laboratory.

effect of hot lead-alloy baths, whereas quenching in oil to room temperature did not; we would have anticipated the reverse, inasmuch as we have found a hot-lead quench to be approximately equivalent to an oil quench. However, this statement is based on measurements of center cooling rates in much larger pieces than those used by the authors.

It is interesting to note that while nickel and carbon lowered M_s , as shown by the authors' Fig 4, neither element apparently widened the temperature range of martensite formation, since the slope of the curves of Fig 2 does not increase with increasing carbon or nickel. This does not agree with data published by Grange and Stewart⁷ which indicate that carbon widened the temperature range of martensite formation.

We were puzzled by the authors' statement that "no evidence of isothermal martensite formation was found." Does this mean that the authors believe there might be such a constituent as "isothermal martensite?" If so, we would like to ask them how they would distinguish it from bainite.

P. K. КОН*—The authors are to be congratulated for developing an exact technique to analyze the most important transformation in metals. The results produced and the conclusions drawn are most revealing and interesting.

I have no comment to make on this paper, but would like to ask one question. I wonder whether the authors have attempted to measure the microhardness of the transformation products at the various stages of the transformation. The microhardness measurement will indicate what proportion of the resultant hardness of white martensite is due to the internal stresses. If the required hardness of a tool steel can be attained by isothermal transformation below the M_s temperature and thus accompanied with little internal stresses, distortion of tools during heat treating could be avoided, and the wearing of cutting point of tools due to possible fracture by triaxial stresses may also be reduced.

S. EPSTEIN†—The martensite transformation starts at a higher temperature and does

not tend to finish until a considerably lower temperature is reached. Thus in a rather low carbon steel of say 0.2 pct carbon, the martensite transformation starts at the high temperature of about 800°F. When is it finished? Is the transformation completed upon cooling to room temperature? I am thinking of dilatation. Would it be your guess that on cooling all of the expansion which accompanies martensite formation in low carbon steel is finished well above room temperature, at say 300°F, or do you think there is still some expansion going on until room temperature is reached?

D. N. ROSENBLATT*—I would like to ask the authors one question in connection with the micrograph they have in the paper, Fig 7. They explain that the martensite seems to stimulate the subsequent bainite transformation, yet the micrograph shows areas, other than martensite-austenite interfaces, where bainite has nucleated. They further suggest that deformation of the austenite by the martensite reaction may be responsible for hastening subsequent bainite transformation. I would like to ask them if any work has been done, to their knowledge, to show the effect of plastic deformation of austenite prior to isothermal transformation, or if they have done any work of this nature which might substantiate the "deformation" theory?

C. T. PATTERSON†—The well known Hadfield manganese steel used for crusher jaws is quenched to austenite which is supposed to transform to martensite only when distorted. This phenomenon is well known and does it not have a considerable bearing on the question previously raised?

L. D. JAFFE‡—In an earlier paper,⁹ the authors established the reliability of the Hurlbut lineal counter method for determining the percentages of microconstituents about 15 times as coarse as some of those studied in the present work. A question still remains as to the reliability of the method for structures as fine as those of Fig 16, for example. The data of the previous paper indicate that a field at 1500 \times moved across the microscope cross-hairs at 0.16 in. per sec. Since much of the transforma-

* American Foundry and Machine Co., Salt Lake City, Utah.

† Solvay Process Co., Syracuse, N. Y.

‡ Watertown Arsenal, Watertown, Mass.

* Standard Oil Company (Indiana).

† Bethlehem Steel Co., Bethlehem, Pa.

tion product in Fig 16 appears thinner than 0.16 in. the counter keys must have been depressed, held for the proper time, and then released, all within a fraction of a second. Was any check made of the reliability of the method under such conditions?

If no such check was made, it seems possible that anomaly observed for the 5 pct transformation in the 1.35 pct carbon steel might arise from the difficulty of accurately determining the percentage of very fine microconstituents. If the operator could not depress and release the keys rapidly enough, he would necessarily obtain a high reading on very fine constituents.

R. T. HOWARD, JR. and M. COHEN (authors' reply)—As Mr. Grange points out, there is some question as to the exact shape of the martensite formation curve just below M_s . His explanation of the influence of segregation is entirely reasonable. If M_s is taken as the temperature at which the first few martensite plates are observed, there is no assurance that the areas exhibiting these plates are truly representative of the whole steel. This is why we have placed more weight on the extrapolation to zero of the martensite curve which is based on many points quantitatively determined at the lower temperatures. Presumably both methods of M_s measurement will tend toward the same result if the steel is sufficiently homogeneous. However, even in the present study, it was generally possible to detect minute traces of martensite about 5°C above the extrapolated M_s temperature.

Although the progress of the austenite-martensite reaction below M_s is affected by the rate of cooling, this variable is only a secondary factor. The blending of the martensite and bainite ranges is properly depictable on an isothermal diagram with just as much rigor as the pearlite *C*-curves because the latter are also influenced by the rate of cooling, at least to a minor degree. In both cases, we represent the course of isothermal austenite decomposition after quenching as rapidly as possible to the temperature in question. And in neither case can the data be quantitatively applied to considerably larger pieces of steel.

Our use of brine quenching has been recently extended to 80°C (175°F) and the course of the martensite reaction from this temperature down to 20°C (68°F) plots on the

same smooth curve determined by quenching into lead-alloy baths between M_s and 90°C. As far as this transformation is concerned, brine and lead-alloy baths seem to match quite well.

According to our findings, the martensite range is not widened by increasing carbon, unlike the published data of Grange and Stewart.⁷ The real point at issue lies in the determination of M_f , which is most uncertain by metallographic methods because of the difficulty in ascertaining when all the austenite (or 99 pct) is converted. In fact, the higher carbon austenites do not transform completely even on sub-zero cooling. Over the limited range of carbon contents investigated here, dilatometric runs show that the austenite-martensite reaction stops at about -155°C (-250°F). Since the M_s definitely drops with increasing carbon, it appears that the martensite range becomes narrower rather than wider as the carbon content is raised.

The possibility of "isothermal martensite formation" was mentioned by the authors because precision length determinations in a companion program have given just such evidence. The distinction between isothermal martensite and bainite was established by the kinetics of the reaction, not by the microscopic appearance. The details are presented in a recent paper.*

In reply to Dr. Koh, we regret to advise that no microhardness measurements have been made on the transformation products. Undoubtedly, these products do change in hardness as a function of reaction time and temperature, but the magnitude is not known. It is not believed, however, that isothermal transformation below M_s is a practical way of hardening these steels. The holding time for anything like complete transformation is excessively long, and the attendant tempering of the product causes undue softening. Perhaps the optimum combination of high hardness and minimum internal stress can be attained by martempering, rather than by isothermal transformation within the martensite range.

We cannot answer Dr. Epstein's question relative to the martensite range in a 0.2 pct carbon steel. No detailed measurements have

* B. L. Averbach and M. Cohen: Isothermal Decomposition of Martensite and Retained Austenite. Submitted to the American Society for Metals.

been made. However, inasmuch as retained austenite has been detected in 0.45 pct carbon steel, it is evident that at least down to this carbon level, the hardening transformation continues to room temperature. Nevertheless this does not mean that the steel undergoes expansion on approaching room temperature. The expansion due to the austenite-martensite reaction at this stage is probably not sufficient to offset the normal contraction due to cooling.

Mr. Rosenblatt has inquired about the bainite in Fig 7 that has not been nucleated by the martensite. The authors have suggested that deformation of the austenite by the martensite may accelerate this isothermal bainitic transformation. This effect has been studied by Elmendor⁶ who followed the rate of bainite formation in the presence of various amounts of martensite. Also, the isothermal transformation of austenite into bainite (and pearlite) is definitely accelerated by plastic deformation. Furthermore the Hadfield manganese steel, mentioned by Mr. Patterson, is commonly believed to undergo some sort of austenite decomposition when cold worked, but the product has not been clearly ascertained.

The lineal analysis method, questioned by Mr. Jaffe, has received a great deal of use at M.I.T. by several independent observers since

our first description of the technique,⁹ and has been found reliable and easily applicable to the fine structures at hand. In fact, even when dealing with amounts of retained austenite down to a few percent, reasonably good agreement has been obtained between lineal analysis and X ray diffraction.* The measurement of a few percent of a fine product by lineal analysis (dark structure against a light background) is a relatively simple problem, and can be carried out with considerable certainty. Although, as Mr. Jaffe indicates, the experimental error tends to become larger as the structure becomes finer, this cannot explain the anomaly in the 1.35 pct carbon transformation diagram. It may be pointed out that not only the 5 pct curve, but also the 15 and 25 pct curves in Fig 8, show faster transformation at 120°C (250°F) than would be anticipated from the normal trend at the higher temperatures. Since the lineal analysis cannot be in error by the 10-20 pct necessary to explain away this anomaly, the authors must conclude that the acceleration of the reaction at 120°C is real.

* B. L. Averbach and M. Cohen: X ray Determination of Retained Austenite by Integrated Intensities, TP 2342, *Metals Tech.*, Feb. 1948. This volume, p. 401

X Ray Determination of Retained Austenite by Integrated Intensities*

By B. L. AVERBACH,[†] JUNIOR MEMBER, AND M. COHEN,[†] MEMBER AIME

(New York Meeting, February 1948)

THE PROBLEM

MANY hardened steels contain significant quantities of retained austenite even in cases where the carbon and alloy contents are low. In fact austenite has been detected in plain carbon steels containing as little as 0.50 pct carbon.¹ Although the austenite may not be visible metallographically it causes definite dilatometric and magnetic effects during subsequent tempering or sub-atmospheric cooling.^{1,2,3} Therefore if the reactions which hardened steels undergo during later treatment are to be understood in quantitative fashion it is most essential to have some kind of absolute analysis for the austenite content in hardened steels. Once this analysis has been made, the austenite transformations can be followed precisely by observing such sensitive phenomena as changes in length or in magnetization but the latter techniques can only determine differences in the amount of retained austenite and usually an independent method must be found to put these differences on an absolute basis.

In certain instances the microscope can be used advantageously to determine the percentage of retained austenite. The quenched sample is tempered to "darken"

the martensite with minimum decomposition of the coexisting austenite, and then is polished and etched in the usual fashion. If the austenite is clearly distinguishable from the tempered martensite and other possible constituents its volume percentage can be measured quantitatively by point counting or lineal analysis.⁴ Such microscopic methods, however, depend on the etch being sufficiently discriminatory. In fairly coarse structures, if the austenite content is greater than 10-15 pct, there is probably little smearing of the etch, and point counting or lineal analysis seems to be quite accurate. On the other hand if the structure is difficult to resolve, as in commercially treated fine-grained steels which contain less than 10-15 pct retained austenite, the latter may be completely obliterated by the dark etching martensite or it may appear disproportionately low as the interfaces between the two constituents become difficult to distinguish. Another disadvantage of the metallographic method is the need for "darkening" the martensite and hence the determination cannot be applied to as-hardened steels. The required tempering may spoil the structure for other tests or may even remove a small part of the austenite which is being sought.

X ray methods hold more promise for covering the range under 15 pct retained austenite. Although austenite and martensite in the hardened steel may be chemically identical, their crystal structures and lattice parameters differ, and the intensity of an austenite diffraction line is some continuous function of the percentage of re-

Manuscript received at the office of the Institute November 12, 1947. Issued as TP 2342 in METALS TECHNOLOGY, February 1948.

* This paper is based on a portion of the thesis submitted by B. L. Averbach in fulfillment of the requirements for the degree of Doctor of Science in Metallurgy at the Massachusetts Institute of Technology, September, 1947.

[†] Assistant Professor and Professor of Physical Metallurgy, respectively, Massachusetts Institute of Technology.

¹ References are at the end of the paper.

tained austenite in the sample. Because of the theoretical advantages of the X ray approach it was felt desirable to reexamine critically the potentialities of the method despite previous work on the subject by one of the authors^{2,6} and others.⁵

PREVIOUS X RAY METHODS

Tamaru and Sekito⁵ employed a Debye-Scherrer camera in which a rotating steel specimen was exposed alternately with a strip of gold, the latter providing reference lines for standardizing the exposure and developing conditions. This method was calibrated with a completely austenitic structure of high-manganese steel and was therefore open to question when applied to plain carbon steels. Moreover the investigators used only the peaks of the microphotometer traces rather than the actual peak intensities of the diffraction lines.

In the method of Gardner, Antia and Cohen,⁶ the same X ray principle was applied by exposing the sample simultaneously with a standard aluminum foil in a Phragmen camera. The ratio of the peak intensity (or maximum blackening on the photographic film) of the (200) austenite line to that of the (200) aluminum line, as determined from a microphotometer trace, was taken as a measure of the austenite content. This method was calibrated with a series of steels whose austenite contents were previously known from point-counting measurements. At high austenite contents the calibration was probably quite accurate and resulted in a straight line which apparently passed through the origin. However, close to the origin the accuracy was rather low and the calibration became uncertain in the region under 10 pct austenite. Fletcher's modification² consisted of tempering the sample at 150°C (300°F) to collapse the martensite (110-101) doublet thus exposing the (111) austenite line which is considerably more intense than the (200) line.

In addition to the uncertainty in the

microscopic calibration there is an inherent error in extending the calibration plot as a straight line through the origin. The peak intensity of a diffraction line is not only a function of the amount of a given phase but is also influenced greatly by the physical condition of the diffracting crystals. As the hardening reaction proceeds, the particle size of the retained austenite becomes smaller and soon after it reaches the point where it can no longer be resolved under the microscope, line broadening begins to occur with a corresponding decrease in the peak intensity.

Retained austenite crystallites are also apt to be considerably distorted because the transformation product has a greater specific volume than the austenite from which it forms and such distortion further reduces the peak intensities appreciably. These factors cannot be circumvented by an independent calibration with point counting or lineal analysis because of the metallographic difficulties with low percentages of austenite, and thus the X ray determination tends to err on the low side. However, the total diffracted energy in each line is essentially independent of particle size and lattice distortion and hence the integrated intensity (which is directly proportional to the diffracted energy) should be a more reliable measure of austenite content than the peak intensity.

The present paper describes an X ray procedure for the quantitative determination of retained austenite based on integrated intensities rather than peak intensities. Not only does the method work satisfactorily on as-hardened steels containing metallographically invisible quantities of austenite but it requires no prior tempering or independent calibration. Furthermore a reference foil for standardizing the exposures and developing conditions becomes unnecessary because, in effect, the coexisting martensite is used as an internal standard. Good agreement is found with lineal analysis in those cases where the

latter may be properly applied. Finally, several examples are given of the results obtained with the new X ray method.

QUANTITATIVE ANALYSIS BY THE INTEGRATED-INTENSITY METHOD

If a mixture of martensite and austenite (with or without other phases) is irradiated with X rays, each crystal will diffract in accordance with the Bragg law. The diffracted energy at each Bragg angle from a polycrystalline sample may be written for given camera and exposure conditions as:

$$P_{\alpha} = \text{const.} \cdot \frac{1}{v_{\alpha}^2} F^2 m (L.P.) e^{-2M} V_{\alpha} A(\theta) \quad \text{Eq 1}$$

$$P_{\alpha} = \text{const.} \cdot R V_{\alpha} A(\theta) \quad \text{Eq 2}$$

where:

- P_{α} = power per unit length of diffraction line for a particular diffraction line of substance α , in arbitrary units
- v_{α} = volume of unit cell of substance α , in $(kX)^3$ units
- F = structure factor per unit cell
- m = multiplicity of diffracting plane
- $(L.P.)$ = Lorenz and polarization factor
- e^{-2M} = Debye-Waller temperature factor
- V_{α} = volume of substance α irradiated, in cm^3
- $A(\theta)$ = sample absorption factor
- θ = Bragg angle

The constant is independent of the kind and quantity of the diffracting substance.

If martensite is taken as the substance α than a similar equation may be written for each diffraction line of austenite (γ), in which V_{γ} and v_{γ} appear instead of V_{α} and v_{α} . For each line the factors v , F , m , $(L.P.)$ and e^{-2M} may readily be calculated from tabulated or measured data and may be lumped into the coefficient R in Eq 2. However the volume irradiated (V) remains as an unknown and the absorption factor ($A(\theta)$) depends on the geometry of the sample (Appendix A). With a flat sample

set at a grazing angle (ϕ) the absorption factor has been shown to be⁷:

$$A(\theta) = \frac{a}{\bar{\mu}} \cdot \frac{\sin(2\theta - \phi) \sin \phi}{\sin(2\theta - \phi) + \sin \phi} = \frac{a}{\bar{\mu}} \cdot A'(\theta) \quad \text{Eq 3}$$

where:

a = cross-sectional area of collimated X ray beam

$\bar{\mu}$ = average linear absorption coefficient for the overall specimen

Since ϕ is a constant for a given exposure, the factor $A'(\theta)$ varies only with θ in a smooth curve such as the one plotted in Fig 1 for the case when $\phi = 60^\circ$. However, a and $\bar{\mu}$ are also constants for a given exposure and specimen and therefore Fig 1 has the shape of the $A(\theta)$ vs. θ curve.

To determine the volume ratio $\frac{V_{\alpha}}{V_{\gamma}}$ the diffraction lines of the steel specimen are microphotometered and the integrated intensity (P) for each line is determined in arbitrary units. Division of these observed intensities by the appropriate values of R (Appendix A) will leave the product $V_{\alpha} \cdot A(\theta)$ for the martensite lines and $V_{\gamma} \cdot A(\theta)$ for the austenite lines. Since V_{α} is a constant for all the diffraction lines from the martensite, a plot of $V_{\alpha} \cdot A(\theta)$ vs. θ should have the same general shape as the curve in Fig 1. Similarly, V_{γ} is a constant for all the austenite lines and a plot of $V_{\gamma} \cdot A(\theta)$ vs. θ should also have the same shape as in Fig 1. Inasmuch as $A(\theta)$ varies only with θ for a given exposure and sample, the relative displacement of the γ -curve from the α -curve is due only to the fact that V_{α} is different from V_{γ} . The constant factor by which the ordinates of the γ -curve must be multiplied to place them on the α -curve is thus equal to the volume ratio $\frac{V_{\alpha}}{V_{\gamma}}$ or the volume percentage ratio $\frac{\alpha}{\gamma}$.

If no other diffracting medium is present in the sample, the volume percentage of each constituent may then be calculated from the additional fact that $\alpha + \gamma = 100$.

On the other hand if a third phase such as undissolved carbide is also present, the latter may be determined by lineal analysis, and $\alpha + \gamma = 100 - \text{vol pct of carbide}$. Eq 4

error, or as in the present work they may be measured by lineal analysis and taken into account. It should be noted that such metallographic data are used here only for

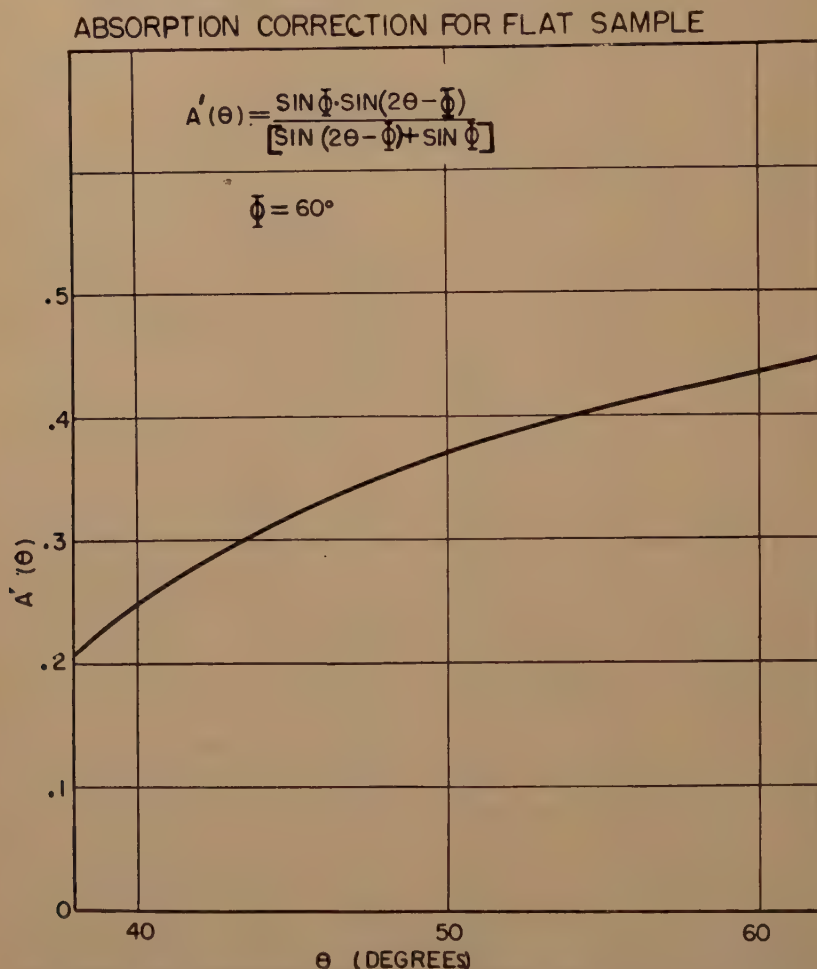


FIG 1—VARIATION OF ABSORPTION FACTOR $A'(\theta)$ WITH DIFFRACTION ANGLE FOR A FLAT SAMPLE.

For example if $\frac{\alpha}{\gamma}$ were found equal to 9.0 by the above X ray method and lineal analysis showed the carbide volume to be 2.0 pct, then γ would be 9.8 pct; whereas if the carbide were neglected, γ would be 10.0 pct. Thus because of the nature of the problem, appreciable quantities of a third phase may be neglected without significant

secondary correction purposes and not for calibration of the X ray method.

EXPERIMENTAL PROCEDURE

The procedure may be illustrated by describing the determination of retained austenite in a plain carbon tool steel whose composition is listed in Table 1. The sample was a cylinder $\frac{3}{8}$ -in. diam by $\frac{5}{8}$ -in. long austenitized for 30 min. at $790 \pm 3^\circ\text{C}$

($1450 \pm 5^\circ\text{F}$) in a lead pot and quenched into agitated water at 20°C (68°F). After heat treatment about $\frac{1}{8}$ in. was slowly removed from the flat surface on a wet grinder with precautions taken not to temper the specimen. After a standard metallographic polish and etch with 1 pct nital, the sample was examined for evidence of tempering and flow. Pitting of the undissolved carbides was avoided since the diluting effect of these carbides was considered in subsequent calculations.

The specimen was then mounted in a Debye camera (radius 4.72 cm) so arranged that the grazing angle (ϕ) with the flat polished section was 60° . This angle was experimentally determined as being small enough to allow the (200) martensite line to diffract and large enough to prevent excessive line broadening on account of the obliqueness of the irradiated surface. A flat sample was used because of the ease of duplicating the surface preparation and because it was possible to remove sufficient metal from the surface to avoid edge effects. A plane surface is also an efficient diffracting shape and exposure times were considerably less than for a wedge or a thin rod. Monochromatic $\text{Co K}\alpha$ X rays were obtained by the diffraction of cobalt radiation from the (200) face of a rock salt crystal mounted directly on the camera in front of the collimating system which defined a beam of approx. 1 mm diam. Although the half and third wavelengths

radiation was necessary to minimize the background intensity so that the very weak lines for low percentages of austenite would be visible, and the camera was evacuated also to reduce air scattering. Segregated areas in the specimen were avoided and in view of the fine grain size (ASTM No. 9) obtained from this particular heat treatment no sample oscillation was necessary to obtain uniform diffraction lines. Exposure times were about 24 hr and the central reproduction in Fig 2 shows the diffraction pattern obtained by this method for the plain carbon steel quenched from 790°C (1450°F).

The X ray patterns were recorded on Eastman No-Screen film, and all films were processed so as to produce a linear blackening vs. intensity curve up to a blackening of 1.5. In practice, however, the maximum blackening used was approximately 1.2. These films were then microphotometered in a Kipp and Zonen recording microphotometer with the light intensity adjusted to provide the greatest possible sensitivity. The central trace of Fig 3 shows the microphotometer record of the corresponding film of Fig 2. This densitometer trace was then converted to a blackening curve and the area under each peak was measured. This area is proportional to the integrated intensity which, in turn, is proportional to P in arbitrary units in Eq 1 and 2.

Most of the factors for the quantity R in Eq 2 have been tabulated and their calculation is discussed in Appendix A. The quantitative analysis of multiphase alloys by X ray diffraction may, however, be subject to serious error if extinction and microabsorption effects are present. A discussion of these factors is included in Appendix B to demonstrate that they introduce little or no error in retained austenite determinations but that they may be far from negligible in other multiphase systems. Another possible source of error occurs in the tempering of the steel because tetragonal martensite

TABLE 1—Analyses of Steels

Type	Code	Weight, Per Cent						
		C	Si	Mn	S	P	Cr	V
Plain Carbon.....	K	1.07	0.23	0.25	0.014	0.011		
Ball-bearing.....	T	1.00	0.35	0.37			1.56	0.21

were also present, they did not interfere with the determination since only the relatively weak lines of the austenite and martensite were used. Monochromatic

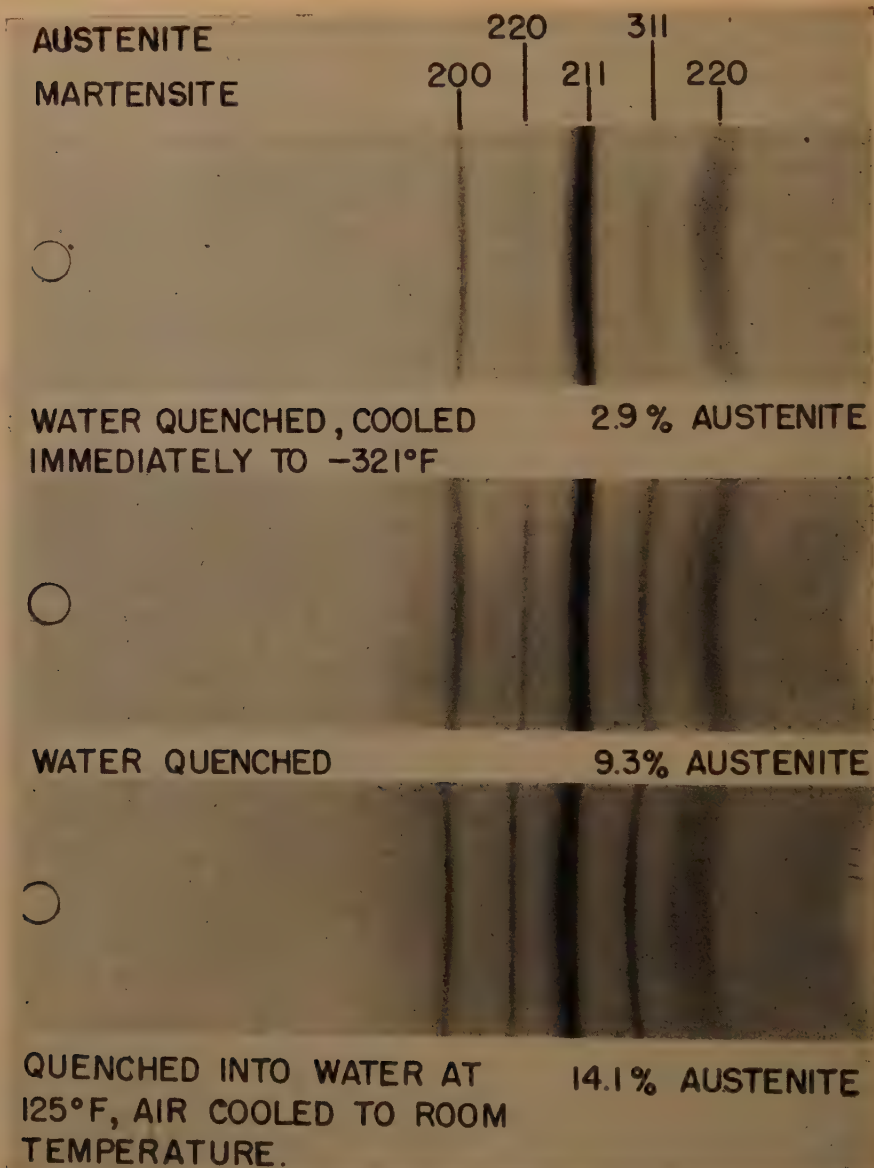


FIG 2—X RAY DIFFRACTION PATTERNS (FULL SIZE) WITH $\text{CoK}\alpha$ MONOCHROMATIC RADIATION, SHOWING AUSTENITE AND MARTENSITE LINES IN A PLAIN CARBON (1.07 C) STEEL.

undergoes partial decomposition even on aging at room temperature.⁹ The attendant precipitation removes iron atoms from the martensite and detracts from the diffracted energy of the martensite lines. However, even with the generous assumption that the

initial precipitate is Fe_3C instead of Fe_2C the extent of precipitation below 120°C (250°F) is not sufficient to cause a detectable change in the integrated intensity of the martensite lines although of course their shape and peak intensities are altered

appreciably. On this same basis tempering for 1 hr at 150°C (300°F) results in less than a 10 pct decrease in the integrated intensity. Accordingly the X ray method may be

units for the lines of plain carbon steel (1.07 C) exposed 30 hr after hardening are listed in Table 2. On plotting the values of $V_{\alpha} \cdot A(\theta)$ for the martensite lines in Fig 4

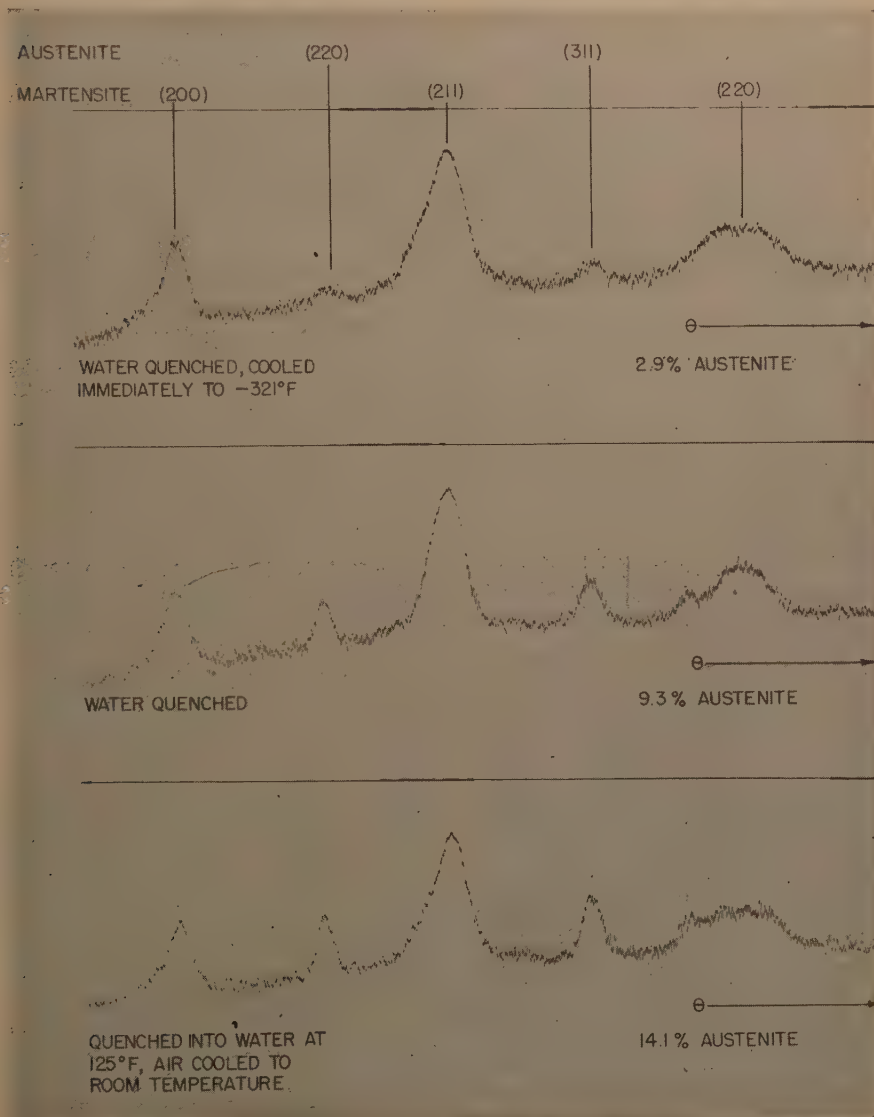


FIG 3—MICROPHOTOMETER TRACES OF DIFFRACTION PATTERNS SHOWN IN FIG 2.

safely applied to hardened steels despite long aging at room temperature or slightly above.

The integrated intensities in arbitrary

it is seen that the shape of the absorption curve is the same as that predicted by the calculated curve in Fig 1. Similarly the values of $V_{\gamma} \cdot A(\theta)$ for the austenite points

lie on a curve considerably lower than that for martensite. From Fig 4 it is evident that the γ (200) must be multiplied by 9.7 and the γ (311) by 9.2 to bring them up to the martensite curve. On averaging, the ratio $\frac{\alpha}{\gamma} = 9.5$.

TABLE 2—Integrated Intensities for Austenite Determination

K Steel (1.07 C), austenitized at 790°C, quenched into water at 20°C. 2.6 pct carbides

Phase	Line	Integrated Intensity, P	R	$P/R = V \cdot A(\theta)$	$\frac{\alpha}{\gamma}$	γ Volume, Per Cent
Martensite.....	(200)	4.849	6.01	0.702	9.7 9.2 Av. 9.5	9.3
	(211)	19.431	15.05	1.295		
	(220)	9.591	6.54	1.470		
Austenite.....	(220)	1.095	9.80	0.112	Av. 9.5	9.3
	(311)	2.318	14.75	0.163		

$\frac{\alpha}{\gamma} = 9.5$
 $\alpha + \gamma = 100 - 2.6 = 97.4$
 $\gamma = 9.3$ volume per cent

TABLE 3—Effect of Room Temperature Aging on Retained Austenite Contents

K Steel (1.07 C), austenitized at 790°C, quenched into water at 20°C

Sample	Time after Quench (Hr)	Volume Percentage		
		Carbides	Retained Austenite	Martensite
1	30	2.6	9.3	89.1
1	54	2.6	9.5	88.9
2	72	2.6	9.4	89.0
3	240	2.6	9.0	89.4
4	480	2.6	9.1	89.3
5	6000	2.6	8.8	89.6

If the whole sample were composed entirely of austenite and martensite, the percentage of austenite would be 9.5 pct. Undissolved carbides were, however, plainly visible under the microscope and were measured by lineal analysis as 2.6 pct by volume. Hence, with the aid of Eq 4 the austenite content turned out to be 9.3 pct.

The carbide volume can also be checked from the M_s point determination. If we assume for the plain carbon steel (1.07 C) that the undissolved carbides are present as Fe_3C , on subtraction of the carbon in the

2.6 pct of carbides from the total carbon, it would seem that about 0.9 pct carbon is in solution. The M_s point for such a steel has been given as about 205°C (400°F) by Greninger and Troiano¹⁰ and this corresponds exactly with the M_s point measured under the conditions at hand.

To check on the reproducibility of the austenite determination another exposure was made on the same sample immediately afterwards. This result and the results on several other samples hardened identically are shown in Table 3 from which it is evident that aging at room temperature produces a progressive decrease in the austenite content. The error in the determination was estimated to be ± 5 pct of the amount of retained austenite or ± 0.3 pct austenite, whichever is the greater. The sensitivity of the method is quite high since the exposure time can be increased to bring out very weak austenite lines without a corresponding increase in the background. Fig 2 and 3 illustrate the X ray patterns and microphotometer traces for cases where the austenite contents are as low as 2.9 pct and as high as 14.3 pct. It is possible to detect as little as $\frac{1}{2}$ pct austenite with the exposure conditions used here.

It is also interesting to note in Fig 3 that the austenite lines become relatively broader as the austenite percentage decreases. This effect is caused either by fine particle size or lattice distortion and con-

tributes to the error caused when peak intensities rather than integrated intensities are used as a criterion of austenite content.

COMPARISON OF THE X RAY METHOD WITH LINEAL ANALYSIS

A check of the X ray method against lineal analysis is summarized in Table 4. Samples of the ball-bearing steel were quenched into oil from a series of austenitizing temperatures from 790 to 955°C (1450 to 1750°F). Austenite contents were determined by X ray after which the martensite was "darkened" for 10 sec at 320°C (610°F) and the austenite redetermined by lineal analysis.

TABLE 4—Comparison of X ray Determinations with Lineal Analysis

Treatment				Per Cent Carbides	Per Cent Retained Austenite	
					Lineal Analysis	X ray
T Steel (1.0 C, 1.5 Cr, 0.2 V)						
	Deg C	Deg F	Min.			
Austenitized	790	(1450)	30 oil quenched.....	10.0	2.0 ± 1.0	3.1 ± 0.3
Austenitized	845	(1550)	30 oil quenched.....	4.0	6.0 ± 1.0	7.0 ± 0.4
Austenitized	900	(1650)	30 oil quenched.....	2.6	13.8 ± 1.0	14.0 ± 0.8
Austenitized	955	(1750)	30 oil quenched.....	0.2	20.1 ± 1.0	20.0 ± 1.0
K Steel (1.07 C)						
Austenitized	790	(1450)	30 water quenched.....	2.6	9.7 ± 2.0	9.0 ± 0.5

It should be emphasized that extraordinary care was necessary with the chromium steel in the metallographic technique preceding the lineal analysis to obtain the data shown in Table 4. The usual nital and picral etches were susceptible to large errors because of obscurement of the austenite when present in quantities under 10 pct, until it was found* that 1 pct of zephiran chloride¹¹ in 4 pct nital provided a marked improvement in structural detail. The lower quantities of austenite could then be resolved with some clarity.

Table 4 shows that the two methods checked quite well; but as the austenite particles became finer with decreasing tem-

perature, the lineal analysis tended to show austenite contents somewhat lower than those indicated by the X ray method. These results lent considerable weight to the newer method and the X ray determinations could be regarded with confidence.

RESULTS OF SOME AUSTENITE DETERMINATIONS

Table 5 lists the austenite contents for the K steel (1.07 C) as a function of quenching conditions and each value is the average of at least two determinations. These results are somewhat higher than the corresponding values shown in earlier work.² In fact a surprisingly large amount of aus-

tenite is present even after immediate refrigeration in liquid nitrogen. Although previous X ray data had indicated that this subcooling treatment leaves only a negligible trace of residual austenite, recent observations of dimensional changes during the tempering of such specimens have indicated that over 2 pct austenite must be present.* This is confirmed by the newer X ray measurements.

Of interest also is the significant increase in retained austenite as the quenching bath is raised to only 50°C (125°F). During some commercial quenching the work is removed from the quench before cooling to room temperature and it is seen that such practice may result in appreciably higher retained austenite.

* Private communication from W. J. Harris, National Research Fellow, Mass. Institute of Technology.

* To be published elsewhere.

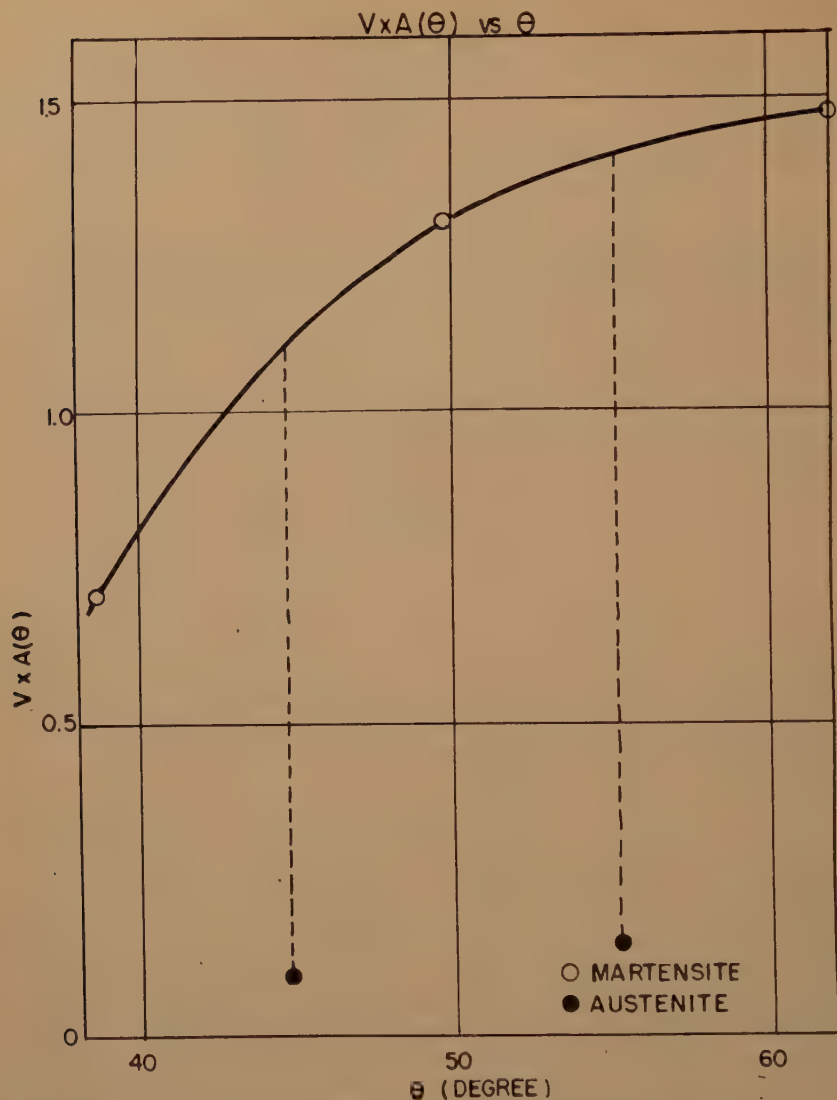


FIG 4—THE VARIATION OF $V A(\theta)$ WITH DIFFRACTION ANGLE OBTAINED FOR A PLAIN CARBON STEEL (1.07 C) AUSTENITIZED AT 790°C (1450°F) AND QUENCHED INTO WATER.

The constant factor needed to bring the austenite points on to the martensite curve is equal to the volume ratio of martensite to austenite.

Similarly, Table 6 shows the retained austenite contents in the ball-bearing steel (T steel, 1.0 C, 1.5 Cr, 0.2 V) for various quenching conditions. Here again the austenite content rises somewhat with the temperature of the quenching bath and on quenching above the M_s point (215°C for

this steel when austenitized at 845°C) as in martempering, over 10 pct of austenite is retained. The rate of cooling through the martensite region also has a measurable effect on the amount of retained austenite. Table 7 indicates that as the rate of cooling is increased the percentage of retained aus-

tenite decreases. A specimen quenched from 845°C (1550°F) into oil contains 7.0 pct austenite compared to 5.8 pct for a water quenched specimen. The effect of cooling

TABLE 5—*Retained Austenite Content as a Function of Quenching Conditions*

K Steel (1.07 C), austenitized at 790°C, quenched as shown. 2.6 pct carbides

Treatment	Hardness, Rockwell C	Per Cent Retained Austenite*
Water quenched to 50°C (125°F), air cooled to room temperature	65.9	14.1
Water quenched to 20°C (68°F) ..	67.0	9.0
Quenched into iced brine at -5°C (23°F)	67.2	8.5
Water quenched to 20°C (68°F), refrigerated immediately to 195°C (-320°F)	68.0	2.9

* 10 days after treatment.

TABLE 6—*Retained Austenite Content as a Function of Quenching Conditions*

T Steel (1.0 C, 1.5 Cr, 0.2 V)

Treatment	Hardness, Rockwell C	Per Cent Retained Austenite*
Austenitized at 845°C (4.0 pct carbides)		
Oil quenched to 20°C	66.5	7.0
Oil quenched to 50°C, air cooled to room temperature ..	64.9	9.0
Oil quenched to 120°C, air cooled to room temperature ..	64.4	9.5
Quenched into molten salt at 230°C, air cooled to room temperature	64.0	10.6
Oil quenched to 20°F, refrigerated immediately to -195°C	67.0	2.0
Quenched into iced brine at -5°C (23°F)		4.9
Quenched into iced brine at -5°C, refrigerated immediately to -195°C (-320°F) ..		0.7
Austenitized at 790°C (10.0 pct carbides)		
Quenched into water at 20°C ..	65.5	3.1
Quenched into water at 20°C, refrigerated immediately to -195°C	65.6	0.5

* 10 days after treatment.

rate was shown in another way by quenching specimens into molten salt at 230°C (450°F), which is above the M_s temperature, and then air cooling, oil quenching, and water quenching to 20°C (68°F). The data for this series in Table 7 indicate that an increase in cooling rate below the M_s

point reduces the austenite content. This influence of cooling rate is probably caused by the very rapid stabilization of austenite towards transformation on cooling such as occurs during aging at and slightly above room temperature. It is well known that aging of retained austenite at room temperature or tempering at elevated temperatures progressively stabilizes it against further transformation on subcooling.^{2,9,12}

TABLE 7—*Effect of Cooling Rate on Retained Austenite Content*

T Steel (1.0 C, 1.5 Cr, 0.2 V), austenitized at 845°C, 4.0 pct carbides

TREATMENT	PER CENT RETAINED AUSTENITE*
Quenched into oil at 20°C (68°F)	7.0
Quenched into water at 20°C (68°F) ..	5.8
Quenched into molten salt at 230°C (450°F), air cooled to room temperature	10.6
Quenched into molten salt at 230°C (450°F), oil quenched to room temperature	6.2
Quenched into molten salt at 230°C (450°F), water quenched to room temperature	6.1
Quenched into molten salt at 230°C (450°F), quenched into liquid nitrogen at -195°C	0.9

* 10 days after treatment.

It also appears that even a quench into liquid nitrogen from above the M_s temperature is unable to transform all of the austenite into martensite. About 0.9 pct remains after this treatment even though the cooling is continuous from the M_s temperature down to -195°C (320°F) without any interruption at room temperature. Perhaps it is impossible to transform completely all of the retained austenite in a specimen of this size ($\frac{3}{8}$ -in. diam, $\frac{5}{8}$ -in. long) by merely cooling through the martensite range. Direct quenching in liquid nitrogen from the austenitizing temperature is ineffective because it leads to some pearlite formation.

SUMMARY

An X ray method based on integrated intensities has been developed for the determination of retained austenite in hardened steels. No external calibration or standard

reference foil is necessary and the procedure can be applied to steels in the as-hardened condition prior to any tempering treatment.

Some typical results which have been obtained by this method are:

1. Normally hardened 1 pct carbon, plain and chromium bearing tool steels retain 7-10 pct austenite after quenching and remaining at room temperature for several days.

2. Retained austenite undergoes slow isothermal decomposition on aging at room temperature.

3. Cooling below room temperature does not transform austenite completely in $\frac{3}{8}$ -in. diam by $\frac{5}{8}$ -in. long specimens and even continuous cooling from above the M_s point into liquid nitrogen leaves about 1 pct of retained austenite.

4. A retarded rate of cooling through the martensite region increases the quantity of retained austenite; and if the cooling is arrested by an interrupted quench followed by air cooling the amount of retained austenite is also increased.

ACKNOWLEDGMENT

The authors are pleased to acknowledge the valuable aid of Professor B. E. Warren in the development of the X ray method and the cooperation of W. J. Harris in performing the lineal analyses. They are also indebted to the Sheffield Foundation of Dayton, O., for a grant-in-aid under which this work was conducted.

APPENDIX A

Calculation of R Factor in Eq 2

Most of the factors for the value of R in Eq 2 have been tabulated by Taylor.¹³

The volume of the unit cell is computed in each case from the known parameters of austenite and martensite for the appropriate carbon content.¹

In the calculation of the structure factor, a correction for dispersion must be made in the listed atomic scattering factors since

the wavelength of the $\text{CoK}\alpha$ X radiation (1.7872 k X units) is very close to that of the absorption edge of iron (1.7394 k X units). This correction has been tabulated by Hönl¹³ and takes the form:

$$f = f_0 - \Delta f \quad \text{Eq 5}$$

where:

f = effective atomic scattering factor.

f_0 = usual atomic scattering factor for the case where the irradiating wavelength is not close to an absorption edge of the sample.

Δf = decrement of the atomic scattering factor due to interaction with the K electrons.

For the case of $\text{CoK}\alpha$ radiation on iron the dispersion correction is quite large and $\Delta f = 4.0$ units.

Inasmuch as the camera was too small and the lines too diffuse to permit good resolution of the body-centered tetragonal doublets of the martensite both the structure factor and multiplicity are calculated on the basis of a body-centered cubic structure. This introduces no error since in each case the total diffracted power for each set of doublets is combined in the measurement of integrated intensity. The austenite calculations are straightforward.

The Debye-Waller temperature factor is computed by taking 420°K as the Debye temperature for iron and then using the tabulated values given by Taylor.¹³

In the Lorenz and polarization factor, account is taken of the fact that a beam of X rays monochromated by a rock salt crystal is not completely unpolarized and the ($L.P.$) factor is calculated from*

$$(L.P.) = \frac{1 + \cos^2 2\theta_c \cos^2 \theta}{\sin \theta \cdot \sin 2\theta} \quad \text{Eq 6}$$

where:

θ = Bragg angle for the sample

θ_c = Bragg angle for the monochromating crystal.

* Private communication from Professor B. E. Warren, Physics Dept., Mass. Inst. of Tech.

The values for each of these factors are listed for the austenite martensite lines in Table 8.

TABLE 8—*X ray Constants for Martensite and Austenite Lines*

CoK α radiation (1.7872 kX units) crystal monochromated

Martensite: Body-centered tetragonal
 $a = 2.852$ kX $v_{\alpha} = 24.2$ (kX)³
 $c = 2.975$ kX

Line	θ°	f	F	m	L.P.	e^{-2M}	R
(200)	38.60	10.4	20.8	6	1.70	0.920	6.91
(002)							
(211)	49.90	8.8	17.6	24	1.35	0.875	15.05
(112)							
(220)	61.90	7.6	15.2	12	1.65	0.835	6.54
(022)							

Austenite: Face-centered cubic
 $a_0 = 3.597$ $v_{\gamma} = 46.4$ (kX)³

(220)	44.68	9.4	37.6	12	1.40	0.890	9.80
(311)	55.18	8.2	32.8	24	1.42	0.860	14.75

APPENDIX B

Extinction and Microabsorption Effects

Before this X ray method could be accepted with confidence several additional factors had to be considered. Eq 1 is applicable only in the absence of extinction. Primary extinction is caused by the cancellation of energy caused by a 180° phase shift as the primary beam proceeds through a given set of planes in a crystal. As the crystal becomes smaller the extinction decreases but the particle size in steel is not necessarily small enough to justify the assumption that extinction is absent. There is, however, considerable distortion in both the austenite and martensite crystals and it has been shown that plastic deformation practically eliminates extinction especially for the weaker reflections. In addition, extinction has its greatest influence on the very strong reflections, (111) γ and (110) α , which are not used in this determination. It seems reasonable to assume therefore that the extinction effects are negligible here.

Eq 1 is also limited to the case where the particle size is so small that the absorption in the individual particle produces a neg-

ligible reduction of intensity of the transmitted beam. Unfortunately, although this effect is quite troublesome, it has generally been overlooked. This phenomenon is termed microabsorption and has recently been treated theoretically by Brindley,¹⁴ Taylor¹⁵ and Brentano.¹⁶ Following the reasoning of Brindley, a given crystal A in a mixture of A and B crystals is considered as it is irradiated by X rays. The path of the incident beam to the crystal and of the diffracted beam from the crystal may be considered as a statistical average of A and B according to the average composition of the sample. For this part of the path, the average absorption coefficient $\bar{\mu}$ may be used as calculated from the composition in the usual fashion and it is this absorption coefficient which appears in the absorption factor given by Eq 3. In this case, the absorption coefficients of A and B appear only as part of an average for the absorption of the entire sample. For a diffraction line of A however, part of the path must lie completely within A . Similarly for the diffraction lines of B part of the path must lie completely within B . If the absorption coefficient for A is greater than that for B or if the average particle size of A is larger than that of B a larger fraction of the energy will be lost by absorption in A , and the A phase will be disproportionately suppressed on the pattern. Such an effect may seem trivial but a large number of particles must diffract to produce an observable diffraction line, and this factor can become the most important single cause of error in a quantitative determination of phases by X rays. Fitzwilliam⁸ has shown for example that with powdered mixtures of iron and nickel and of copper and aluminum, errors of several hundred percent may be observed in the ratio of the two phases if microabsorption effects are neglected.

Corrections for microabsorption have been proposed by Brentano¹⁶ and by Brindley¹⁴ and Fitzwilliam's data support the Brentano theory reasonably well. However

either theory can be used to demonstrate that in the case at hand microabsorption may be safely disregarded. This fortunate circumstance is caused by the fact austenite and martensite in a hardened steel have the same composition and only a 4 pct difference in density. Hence their absorption coefficients differ only by 4 pct and despite generous assumptions with regard to differences in average particle size, the resulting microabsorption correction turns out to be negligible.

REFERENCES

1. S. G. Fletcher and M. Cohen: The Effect of Carbon on the Tempering of Steel. (1944) *Trans. A.S.M.*, **32**, 333.
2. S. G. Fletcher and M. Cohen: The Dimensional Stability of Steel. Part I—Subatmospheric Transformation of Retained Austenite, (1945) *Trans. A.S.M.*, **34**, 216.
3. M. A. Grossmann: Toughness and Fracture of Hardened Steels, (1946) *Trans. AIME*, **167**, 39. *Metals Tech.*, Apr. 1946.
4. T. R. Howard and M. Cohen: Quantitative Metallography by Point Counting and Lineal Analysis. *Met. Tech.* (August 1947). *Trans. AIME*, **172**, 413.
5. K. Tamaru and S. Sakito: On the Quantitative Determination of Retained Austenite in Quenched Steels. (1931) *Sci. Repts.*, Tohoku Imp. Univ., **20**, 1.
6. F. S. Gardner, M. Cohen and D. P. Antia: Quantitative Determination of Retained Austenite by X rays. (1943) *Trans. AIME*, **154**, 306.
7. Z. W. Wilchinsky: X ray Measurement of Order in the Alloy Cu₃Au. (1944) *Jnl. Appl. Phys.*, **15**, No. 12, 806.
8. J. W. Fitzwilliam: X ray Study of Order in Binary Systems (June 1947). Ph.D. Thesis, Phys. Dept., M.I.T.
9. S. G. Fletcher, B. L. Averbach, and M. Cohen: The Dimensional Stability of Steel. Part II—Further Experiments on Subatmospheric Transformations. (1948) A.S.M. preprint No. 7, 40.
10. A. B. Greninger and A. R. Troiano: Kinetics of the Austenite-Martensite Transformation in Steel. (1940) A.S.M. **28**, 537.
11. J. B. Cohen, A. Hurlich and M. Jacobson: A Metallographic Etchant to Reveal Temper Brittleness in Steel. (1947) *Trans. A.S.M.*, **39**, 109.
12. J. H. Hollomon, L. D. Jaffe and D. C. Buffum: Stabilization, Tempering, and Relaxation in the Austenite-Martensite Transformation. (August 1947) *Jnl. Appl. Phys.*, **18**, 784.
13. A. Taylor: An Introduction to X ray Metallography. (1945) John Wiley and Sons.
14. G. W. Brindley: The Effect of Grain or Particle Size on X ray Reflections from Mixed Powders and Alloys Considered in Relation to the Quantitative Determination of Crystalline Substances by X ray Methods. (1945) *Phil. Mag.*, Series 7, **36**, 347.
15. A. Taylor: On the Application of the Micro-Absorption Factor to Problems of Lattice Distortion and the Nature of Anti-Phase Domains. (1944) *Phil. Mag.*, Series 7, **35**, 404.
16. J. C. M. Brentano: The Quantitative Measurement of the Intensity of X ray Reflections from Crystalline Powders. (1935) *Proc. Phys. Soc. (London)* **47**, 932.

DISCUSSION

(B. R. Queneau presiding)

B. R. QUENEAU—One of the difficulties in metallurgy has always been a lack of precision in measurement, and I think the authors are to be congratulated on developing a method which will give us an accurate and dependable quantitative estimate of the amount of retained austenite.

O. ZMESKAL*—As Chairman Queneau said, this is indeed an ingenious and needed determination.

We have seen figures presented of $\frac{1}{2}$ pct retained austenite determined, and I would like to ask the authors the lower limits of this method. How far down do they feel they can go in improving the technique still more?

The other question is concerned with the effect of retained austenite on the properties of tool steel. As Dr. Averbach shows, we cannot get rid of retained austenite in a quench, but can get rid of it fairly well in tempering. How significant is it whether you have $\frac{1}{2}$ pct going into the temper or whether you have 9 pct, assuming you double-temper or multiple-temper? Just what relation is there between the amounts of retained austenite in the as-quenched tool and the properties we should expect in this tool after multiple tempering?

J. A. FELLOWS†—I would like to ask the authors if they have any comment to make about the range of grain size which will permit this precision, especially at the lower limits of retained austenite.

* Illinois Institute of Technology.

† American Brake Shoe Co.

E. S. ROWLAND*—Do you have any data on the effect of the vanadium in this so-called ball bearing steel? We have been asked from time to time, in regard to your work, about this particular analysis. About 95 pct of the ball-bearing steel made in this country does not contain more than 0.02 or 0.03 pct vanadium as a maximum. The majority of our questioners are very vitally interested in the austenite contents under normal heat treating conditions. I think if you have any data on the relative effects with and without this vanadium addition, they would be very much worth while.

A. H. GEISLER†—I would like to inquire about the possible variation in amount of retained austenite across the cross-section of the tool steels which have been investigated. With such a precise method as the one described this should not be a limitation but should present an additional potentiality of the method. We have recently been studying the structure of some heat treated iron-cobalt alloys. Specimens in the form of 0.020-in. wire were used. In some extreme cases we have noticed that patterns for lightly etched specimens reveal 100 pct ferrite but when the specimens were etched to about one half of the original diameter the patterns reveal 100 pct austenite. The original specimens were magnetic but after heavy etching they were non-magnetic. Thus, at least in this material and probably in many high alloy steels the location of the area analyzed is quite important. Have the authors made a survey of the amount of retained austenite across the section of any of their tool steels?

B. L. AVERBACH (authors' reply)—Under the exposure conditions which have been described in the paper, we were able to measure amounts of retained austenite down to approximately $\frac{1}{2}$ pct. Smaller austenite contents were detectable, but because of difficulties in the microphotometry of very diffuse lines, the accuracy became questionable at these lower

levels. However, in principle, this is not the lowest limit of the X ray method. It is possible to mask off the high-intensity martensite lines with aluminum foil in the camera and to make longer exposures so that even smaller quantities of austenite will give measurable diffraction lines. Line broadening also becomes troublesome at these very low austenite contents, and attempts are being made to overcome this difficulty.

The second portion of Dr. Zmeskal's question is one which offers many possibilities for future research. Very little data are available on the relationship between austenite content and the physical properties of steels. We expect to be in a position to supply such information sometime in the future.

The effect of grain size on the austenite determination is evidenced by a spottiness in the reflections and this limitation appears as soon as the grain size becomes larger than A.S.T.M. No. 6. In the investigation at hand, the grain size was so fine that it was necessary to rotate the specimen to obtain smooth diffraction lines. For coarser grained materials, the specimen must be moved during the exposure, and arrangements are being made to oscillate the sample in our present camera. Under these conditions, determinations on coarse grained materials should have an accuracy equivalent to that which we have shown here.

Dr. Rowland has inquired about the effect of 0.20 pct vanadium on the quantity of retained austenite. We cannot answer this question at the moment, but are taking steps to obtain the necessary data.

Dr. Geisler has emphasized a point upon which we did not elaborate in our paper. There were rather large edge effects in our samples, and this method could have been used to study the variation in austenite content across the diameter. For this present investigation, however, we were careful to stay away from the edges as well as from the center of the sample where segregation might exist. In other applications, such as in carburizing, it would be very appropriate to determine the austenite content as a function of distance from the surface.

* Timken Roller Bearing Co.

† General Electric Research Laboratory.

An Evaluation of Quenching Oils by Means of the End Quench Test

By C. A. SIEBERT* MEMBER AIME AND G. SANDOZ†

(New York Meeting, February 1948)

OIL quenching of steel, in good commercial practice, is carried out using a great deal of agitation in the quenching bath. Many of the tests reported in the literature represent the results obtained on steels quenched into still oil.

Scott¹ describes three stages of cooling in liquid quenching baths, namely:

"State 'A'—*Vapor Blanket Cooling*—In this, the first stage, a thin stable vapor film surrounds the hot metal. Cooling is by conduction and radiation through the gaseous film and is therefore relatively slow.

"Stage 'B'—*Vapor Transport Cooling*—Termination of the 'A' stage is marked by wetting of the metal surface. Vapor forms copiously in bubbles and is carried away by gravity and convection currents to condense in cooler surrounding liquid. This is the fastest stage of cooling.

"Stage 'C'—*Liquid Cooling*—The 'B' stage ends as the surface temperature of the metal approaches the boiling point of the quenching liquid. Vapor no longer forms, so cooling is by conduction and convection and the temperature difference is greatly decreased. This mode of cooling is slower than that of the 'B' stage."

Mechanical agitation of the quenching

medium will accelerate all three stages of cooling. The greatest effect, however, will be noted on stage 'B' because the removal of the bubbles from the surface of the steel will not be entirely dependent upon gravity and natural convection currents.

The method employed in this investigation for evaluating the oils was the end quench test. The various oils were substituted for water as the quenching liquid and hardness determinations were made at various distances from the quenched end. Most of the tests were run using a $\frac{3}{8}$ -in. orifice with a $2\frac{1}{2}$ -in. stream height. However, to check the effect of other velocities two additional conditions were used, namely: (1) A $\frac{3}{8}$ -in. orifice and 1-in. stream height, and (2) a $\frac{1}{2}$ -in. orifice and a $3\frac{1}{2}$ -in. stream height. In all cases the samples were suspended so that the quenched end was $\frac{1}{2}$ -in. above the orifice.

The steel used was an NE 9450 having the following analysis:

C	Mn	P	S	Si	Cr	Ni	Mo	Cu
0.52	0.81	0.013	0.019	0.26	0.30	0.38	0.10	0.06

Some tests were run on an NE 8740, 3312, and a 4340 steel. The results obtained on these steels confirmed those obtained on the NE 9450 and have therefore been omitted from this paper. The test bars were machined from $1\frac{1}{8}$ -in. stock to 1-in. diam by 4 in. long.

Manuscript received at the office of the Institute November 1, 1947; this amplified version received January 9, 1948. Issued as TP 2353 in METALS TECHNOLOGY, April 1948.

* Associate Professor of Metallurgical Engineering at the University of Michigan and Consulting Metallurgical Engineer.

† Graduate Student at the University of Michigan.

¹ References are at the end of the paper.

Five commercial quenching oils were investigated representing three different sources. Oils No. 1 and 2 were the conventional "ten cents a gallon" type, while oils

The properties of the oils are shown in Table 1. Oils No. 1, 2, 4 and 5 are quite similar at all of the temperatures investigated, while oil No. 3 shows a

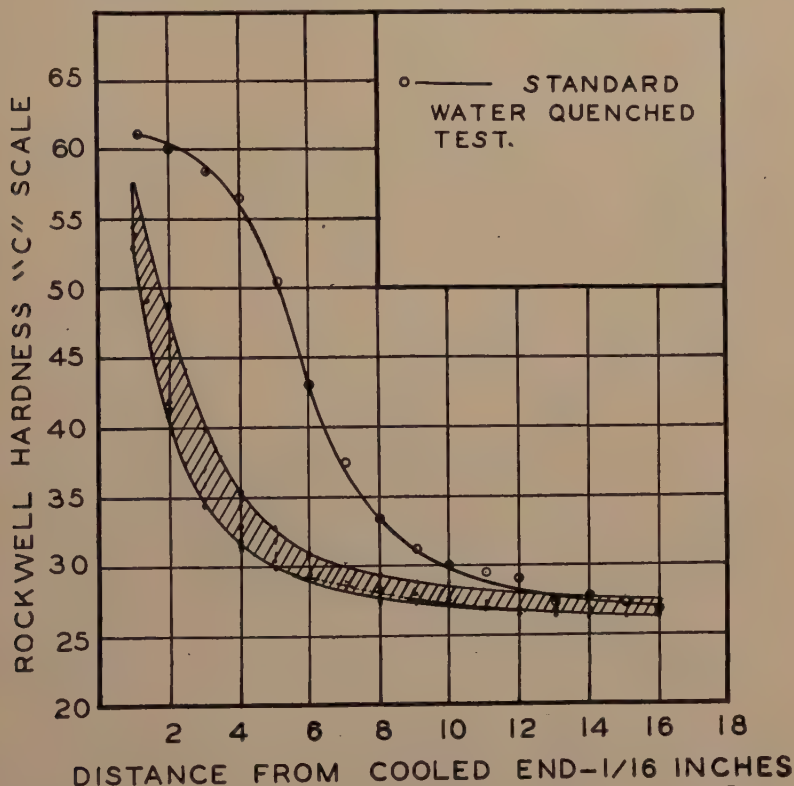


FIG 1—HARDNESS BAND OBTAINED USING FIVE DIFFERENT OILS AT 80°F.

TABLE 1—*Properties of Oils*

Oil No.	Source	Con- dition	API Gravity	Flash Point °F	Fire Point °F	Saybolt Viscosity—Seconds			DuNouy Surface Tension Dynes per Centimeter at 90°F
						77°F	100°F	140°F	
1	A	Used	26.8	360	405	217	122	66	32.3
2	A	New	26.8	370	420	195	112	61	32.3
3	B	New	31.8	360	395	133	87	55	31.8
4	C	Used	29.7	370	420	205	116	64	32.3
5	C	New	29.5	375	425	205	118	66	32.3

No. 3, 4 and 5 were of the proprietary compounded variety. Oils No. 1 and 4 were used oils from commercial quenching systems through which several hundred tons of steel had been processed.

marked difference in viscosity, especially at 77 and 100°F.

RESULTS

Hardness results obtained by quenching with the various oils are given in Table 2.

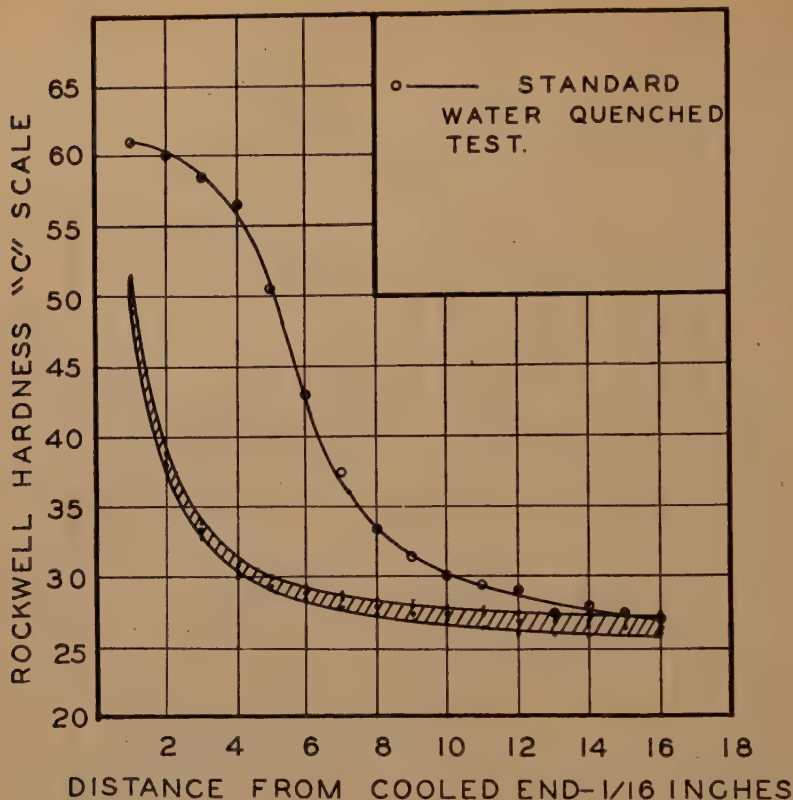


FIG 2—HARDNESS BAND OBTAINED USING FIVE DIFFERENT OILS AT 140°F.

TABLE 2—Hardness Results Obtained

Oil no.....	1	2	3	4	5	1	2	3	4	5	3	3	3	Standard Water Quench
Oil Temp., °F....	80	80	80	80	80	140	140	140	140	140	80	80	185	
Orifice.....	$\frac{3}{8}$	$\frac{3}{8}$	$\frac{3}{8}$	$\frac{3}{8}$	$\frac{3}{8}$	$\frac{3}{8}$	$\frac{3}{8}$	$\frac{3}{8}$	$\frac{3}{8}$	$\frac{3}{8}$	$\frac{3}{8}$	$\frac{1}{2}$	$\frac{3}{8}$	
Height in Inches..	2.5	2.5	2.5	2.5	2.5	2.5	2.5	2.5	2.5	2.5	1	3.5	2.5	
Distance from Quenched End, $\frac{1}{16}$ In.	Rockwell "C" Hardness													
1.....	54	53	53	54.5	57.5	51.5	49.5	50	51	49.5	44	56	45.5	61
2.....	42	41.5	42	46	49	38	38	39	39	39	38	47	35	60
3.....	36	34.2	34.5	37	40	33	33	33.5	33	34	32	37.5	32	58.5
4.....	33	32	31.5	34.5	35.5	30	30.5	31	31	31	29	34	30	56.5
5.....	31	30.5	30	32	33	29.5	29.5	30	29.5	30	29	32	29.5	50.5
6.....	29.5	29.5	29.5	31	31	29	28.5	29.5	29	29.5	28	31	29	43
7.....	29	28.5	28.5	28.5	30.5	28.5	28	29	28	29	28	30	29	37.5
8.....	28.5	28	28.5	27.5	29.5	28	27.5	28	27.5	28.5	28	29	28.5	33.5
9.....	28	28	28	27.5	29	28	27.5	27.5	27	28.5	27	28	27	31.5
10.....	28	27.5	27.5	27.5	29	27.5	27.5	28	27	28.5	27	28	27.5	30
11.....	27	27	27.5	27	29	27.5	27.5	27.5	26.5	28	27	28	27.5	29.5
12.....	27	26.5	27	27	28.5	27.5	27	27.5	26	28	27	28	27.5	29
13.....	27	27	27	26.5	28	27	27	27	26	27.5	27	28	27	27.5
14.....	27	27	27	26.5	28	26.5	27	27	26	27.5	27	28	27	28
15.....	27	27	27	26.5	28	26.5	27	27	26	27.5	27	27.5	27	27.5
16.....	27	27	27	26.5	27.5	26.5	27	27	26	27.5	27	27.5	26.5	27

The hardness values are the average of several tests. The reproducibility of results was usually within $\frac{1}{32}$ of an in. on the end quench bar. The data for the 80°F. oil are

is less than $\frac{1}{16}$ in. on the end quenched test. The difference in the hardening power of these oils at 140°F is approximately $\frac{1}{32}$ of an in., which is within the scope of

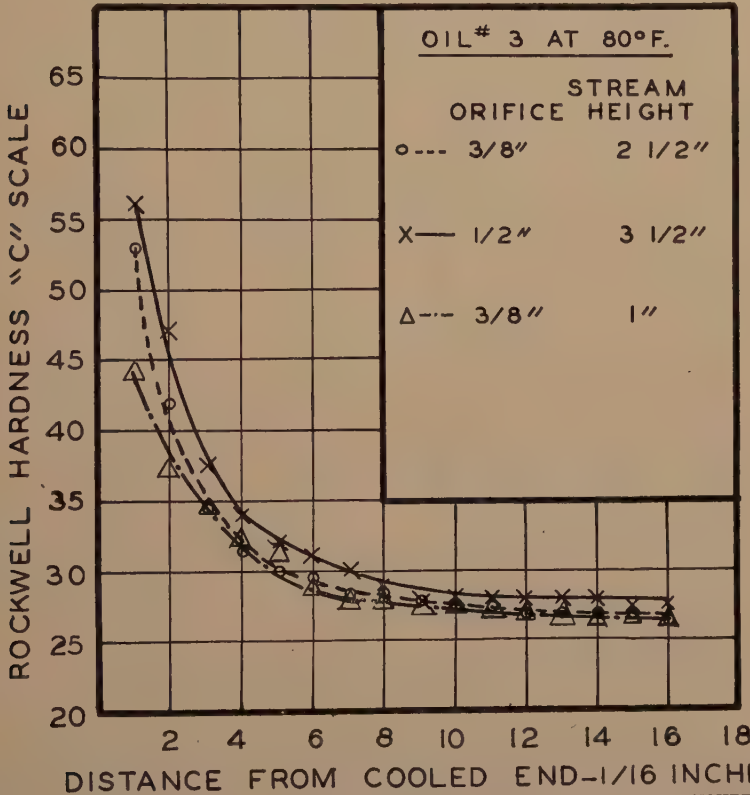


FIG 3—THE EFFECT OF OIL VELOCITY ON THE HARDNESS OF THE END QUENCHED BARS.

plotted in Fig 1 along with the results from the standard end quench test. The curve is shown as a band to portray the extent of the difference in quenching power of the oils. The new proprietary compounded oil No. 5 produced results which follow the upper curve of the band, while the new proprietary compounded oil No. 3 follows the lower curve of the band. The other oils produced results that fall within the band.

The hardness data for the 140°F oil are plotted in Fig 2.

Fig 1 shows that the difference in hardening power of the various oils tested at 80°F

reproducibility of the end quench test. The colder oil appears to show a greater difference in hardening power than the oil at 140°F. In all cases the effect of the flow of the oil past the surface being cooled was to minimize any differences in the quenching power of the oils which may be present when quenching is carried out in still oil, especially at the higher oil temperature.

In order to determine the effect of oil velocity on the quenching power of the oil three different conditions of orifice diameters and stream heights were investigated and all showed similar results to those

plotted in Fig 3. Increasing the orifice size and stream height increased the hardening power, although the difference between the $\frac{3}{8}$ -in. orifice with a $2\frac{1}{2}$ -in. stream height

data were obtained by quenching in still oil which may account for the difference noted.

When the agitation of the oil is small the removal of the vapor bubbles depends to a

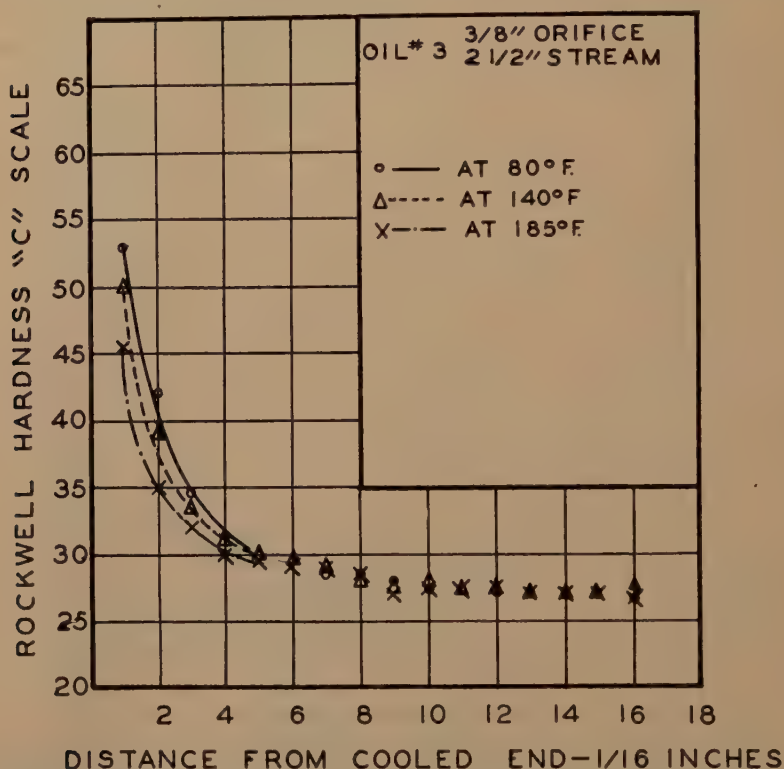


FIG 4—THE EFFECT OF OIL TEMPERATURES ON THE HARDNESS OF THE END QUENCHED BARS.

and the $\frac{1}{2}$ -in. orifice with a $3\frac{1}{2}$ -in. stream height is small. This would indicate that the highest flow condition used in these tests is approaching the optimum flow condition. The oil bubbles forming at the oil-steel interface must be removed at a very rapid rate by a mechanical action caused by the flow of the oil.

Fig 4 shows the effect of varying the oil temperature on the hardening power of No. 3 oil. It can be seen that increasing the oil temperature resulted in a decrease in the hardening power of the oil. This finding is contrary to the data reported by Spring, Lansdale, and Alexander.² However, their

great extent upon natural convection. An increase in the oil temperature results in a decrease in the viscosity of the oil which permits the vapor bubbles to escape from the surface of the steel more readily than is the case when the oil temperature is low. However, it would appear that the degree of agitation obtained in the end quench test minimizes the effect of viscosity and the like on bubble removal, and the extraction of heat from the steel becomes more dependent upon the temperature difference between the surface of the steel and the oil, than on the properties of the oil.

SUMMARY AND CONCLUSIONS

1. Data are presented on the hardening power of five different oils representing three sources of supply. 2. The end quench test was used as a means of evaluating the quenching power of the oils. 3. The difference in quenching power of two different proprietary compounded oils was found to be greater than the difference between the compounded oil and a straight mineral oil. 4. Increasing the flow of the oil caused an increase in the hardening power observed. 5. Increasing the temperature of the oil resulted in a decrease in the hardening power of the oil. 6. With high rates of agitation, such as those encountered in these tests, there is little, if any, advantage to be gained by using a proprietary compounded oil in place of a straight mineral oil.

REFERENCES

1. Scott, H.: Metals Handbook, (1939) 328 A.S.M.
2. Spring, Lansdale, and Alexander: (1944) *Trans.*, A.S.M. 33, 42.

DISCUSSION

(H. B. Knowlton presiding)

H. L. WALKER*—All I want to record is that about four years ago our laboratory, under the direction of Prof. E. J. Eckel, started a program of attempting to evaluate quenchants. We came to the conclusion that the conditions of the Jominy test would best fulfill the requirements.

I might say one of the good ideas we had for a while was to measure the amount of current necessary to maintain a given temperature in the resistor wire, which was immersed in various quenchants. The method failed at the higher temperatures because a vapor blanket formed at the boiling point of the quenchant and the heavy current passing through the resistor would suddenly increase the temperature above its melting point.

We have standardized on two steels and have been working on them continuously. We

find we are able to duplicate our results for any given set of conditions to ± 1 Rc.

We have been interested in velocity, composition of quenchant and temperature mostly, but we have also evaluated air, water, brines, ethylene glycol-water mixtures, oils of the straight mineral and compounded type. As far as the oil data are concerned, we concur in Dr. Siebert's conclusions, that both types of oil have equal hardening power when agitated.

We have also devised a method of determining Jominy hardenability under still-quench conditions. The still-quench data are being correlated with the data for agitated conditions.

You can get a tremendous amount of information from these methods because you can calculate velocities as the quenchant is moving over the surface of the specimen. That is not difficult to do because you can measure the umbrella. For the agitated condition we have used stream heights from $\frac{1}{2}$ in. to 5 ft of quenchant. We arrive at a certain velocity of quenchant in which the heat is being conducted away from the specimen faster than the specimen conducts heat to the surface.

We also have hardenability data in terms of temperature of quenchant. We have run into a very queer phenomenon at the higher temperatures. In some cases we found a lower hardness at the quenched end than was found from the quenched end of the Jominy bar. Soft surfaces of heat-treated bar have always been explained as due to (1) decarburization; or (2) retained austenite. This is not the true explanation, but rather the lowered hardness on the surface is due to a persistent vapor blanket stage. For a water temperature of 210°F , the vapor blanket was maintained for as much as 10 min. This means the quenchant never reached, nor wetted the surface of the specimen for this time interval.

The effect of the vapor blanket is to cool the surface quite slowly through the critical range, but farther along the bar the temperature is above the critical range. When the vapor blanket collapses and the quenchant wets the specimen, quench conditions are established away from the surface and a higher hardness results.

The literature reports the maximum effect of sodium chloride for brine concentration is about 9 pct. That is wrong because we find no decrease in hardness for solutions containing 25

* University of Illinois.

pct salt. We did not test higher concentrations because 25 pct is almost at the saturation point.

For water depending upon agitation, we find about 150 to 160°F to be the critical temperature as far as temperature of water is concerned where the vapor blanket forms. The reason brine is a better quenchant is because the vapor blanket stage is of much shorter duration. In other words, when you turn on the brine quenchant it wets the specimen, and you have practically no vapor blanket stage. With water it may run to 10 min. before you get the water wetting the specimen.

We are trying to work out what brine does. It does not appreciably raise the boiling temperature, but we believe a modification in the surface tension of the solution may be responsible. It is not that brine quenches any faster than water does. It merely does not have a prolonged vapor blanket stage.

M. COHEN*—What is the name of the steel you standardized?

H. L. WALKER—It is one of the nickel steels. It is SAE 2340.

D. V. DOANE†—I just wanted to inquire as to the height of the water stream in the test in which you obtained this phenomenon of the vapor phase adjacent to the specimen.

H. L. WALKER—The vapor blanket will form with a free height of $3\frac{1}{2}$ in., which was the highest tested. The quenchant must, of course, be hot. We do not know what the maximum free height is. Two and a half inch free height is standard conditions.

D. V. DOANE—That should occur then for any full hardening steel such as 4340, and I wanted to ask Dr. Siebert, then, if he encountered the same phenomenon on 4340 in his investigation.

H. L. WALKER—Dr. Siebert is working with oil, and I am talking about water. The vapor blanket is not nearly so prominent with oil. The data will be published as a bulletin of the University of Illinois Engineering Experiment Station in the future. We shall be glad to send anyone interested a copy.

R. S. KOMARNITSKY*—Professor Walker, in your experimental work did you try to correlate ability to carry away the vapor blanket with the conditions of boundary layer of the quenching liquid flow—whether it was laminar or turbulent, also depth and type of turbulence? Was any attempt made to correlate flow characteristics with Reynolds number? However, in your experiments using amount of electric current passing through the wire as measure of intensity of quench, it would perhaps be easier to do that, than in Jominy test, if direction of the flow was parallel instead of across the wire.

H. L. WALKER—I do not believe this to be true because the resistors failed at too low a temperature to give reliable data. We have not tested quenchant containing wetting agents.

H. B. KNOWLTON†—We have all heard a lot of claims concerning oils which produce fast speeds of cooling, and at the same time are not as prone to produce cracking as ordinary quenching oils. We could probably spend the rest of the morning discussing what causes cracking. We would appreciate the opinion of the authors with regard to the relation between the end quench test and quenching by complete immersion. Presumably cracking is associated with the formation of martensite between the M_s and M_f points.

Is there any possibility that any of these oils would change the speed of cooling, while a steel is passing from the M_s to the M_f point during quenching by complete immersion? Would there be any difference between this condition and that produced by the rapid flow of oil over the end of the Jominy specimen?

C. A. SIEBERT (authors' reply)—We are happy to learn that Professor Walker's investigations confirm our findings on quenching oils and that they have standardized on the end quench method as best fulfilling the requirements for evaluating quenchant.

We did not measure the hardness of the quenched end of the bars; therefore we have no data to determine whether or not a soft surface developed on any of the bars as reported by Professor Walker.

* Massachusetts Institute of Technology.

† M. W. Kellogg Co.

* Standard Steel Spring Co., Coraopolis, Pa.

† International Harvester Co., Chicago, Ill.

The end quench method, as used in this investigation, cannot be used to evaluate the cooling power of various oils in the temperature range between the M_s and M_f temperatures. The work of Spring, Lansdale, and Alexander² shows that oils do differ in their cooling power when the steel temperature is within the martensite formation range, and that the cooling rate is a function of the oil temperature. However, the difference in rate of cooling for any given temperature is rather small for the

oils they tested, and would probably be much smaller if the oil were highly agitated.

It is our opinion that good quenching practice requires high rates of agitation to insure uniform cooling, and to minimize distortion. In production quenching it is possible to have the conveyors moving fast enough so that the parts will come out of the oil at a temperature just low enough to prevent flashing of the oil. The parts will then cool slowly in air.

Notch-tensile Characteristics of a Partially Austempered, Low Alloy Steel*

By G. SACHS,† MEMBER AIME, L. J. EBERT,‡ AND W. F. BROWN, JR.§

(New York Meeting, February 1948)

INTRODUCTION

ISOTHERMAL transformation, or "austempering," of a carbon-containing austenite at elevated temperatures yields so-called "intermediate products." Their structure and properties are, for a given hardness, rather different from those of "tempered martensite" obtained on conventional quenching and tempering.¹

Several investigators^{2,3} have found that for high carbon and slightly alloyed steels the intermediate products formed at temperatures close to that of the martensite reaction possess strength properties superior to those of tempered martensite. The structure of these low temperature, intermediate products is generally acicular (bainite) but clearly different from that of martensite.

However, at higher austempering temperatures, between 1000 and 1300°F (540 and 700°C) carbon steels were found to exhibit a rather low ductility.^{4,5} Thus notch bar tensile tests showed the ratio between notch strength and regular tensile strength to decrease with increasing austempering temperature. For ductilities below a few

percent this notch strength ratio is a measure of ductility, according to investigations on low alloy steels.^{6,7} Furthermore the presence of intermediate products formed unintentionally on quenching was considered as responsible for the low ductility and impact energy of some heat treated steels.⁸ These intermediate products could result from partial transformation at the so-called "nose-temperature" where the rate of the transformation is a maximum. Tempering improved such mixtures of martensite and intermediate products, their properties approaching those of tempered martensite of equal hardness.

The following investigation constitutes an attempt to determine certain strength properties of a partially austempered and subsequently quenched low alloy steel, namely, a chromium steel (SAE 5140). The structures formed by such a treatment should consist of a mixture of intermediate products formed on austempering and a martensite formed on oil quenching from the austempering temperature. It was intended, by varying the austempering time, to vary the quantity of the intermediate products between zero and 100 pct.

The austempering temperature of 860°F was selected after extensive preliminary tests close to the nose-temperature. Austempering at this temperature yielded an acicular intermediate product. Additional tests under less exacting conditions were made for an austempering temperature of 950°F where the intermediate product appeared to be very fine pearlite.

To determine the effects of tempering on structures containing various amounts of

Manuscript received at the office of the Institute October 30, 1947. Issued as TP 2321 in METALS TECHNOLOGY, February 1948.

* This paper is one of a series of reports on the research program conducted at Case Institute of Technology (formerly Case School of Applied Science) under the sponsorship of the International Nickel Co.

† Director, Research Laboratory for Mechanical Metallurgy, and Professor of Physical Metallurgy, Case Institute of Technology, Cleveland, O.

‡ Research Laboratory for Mechanical Metallurgy, Case Institute of Technology, Cleveland, O.

§ Research Metallurgist, Flight Propulsion Laboratory, NACA, Cleveland, O.

¹ References are at the end of the paper.

intermediate products, a few additional tests were made on partially and fully austempered specimens subjected to an additional tempering for one hour at the austempering temperature (950°F). The structure of such specimens consisted of mixtures of tempered intermediate products and tempered martensite.

The properties of such specimens, as investigated here, must be considered as dependent upon at least two major variables, their structure (composed of mixtures of tempered martensite and a particular intermediate product in various proportions) and the hardness of this mixture. A large amount of experimentation would be required to separate these variables, that is to obtain relations for either constant structures or constant hardness. Therefore on the basis of only a few series of tests in which large hardness changes occur it is impossible to explain fully the significance of the test results.

On the other hand it is possible to compare the properties of partially austempered specimens with those of conventionally quenched and tempered specimens of equal hardness. Because of the very large differences revealed in this investigation, it appears that certain of the observed effects of intermediate products are of general significance.

Attempts to determine the regular tensile properties of the austempered specimens were in general unsuccessful. Even with special precautions such as a very small test section and high concentricity of loading⁶ most of the harder specimens containing a small amount of intermediate products failed outside the gauge length.

Therefore this paper describes only the results obtained on static testing (concentrically and eccentrically) notched specimens in tension. Previous investigations have shown that such tests indicate differences in heat treated steels which more conventional static test methods have failed to reveal.⁷

MATERIAL AND PROCEDURE

The SAE 5140 steel investigated was a ladle killed, open hearth steel of the following chemical composition:

C	Ni	Cr	Mn	P	S	Si
0.40	—	1.00	0.69	0.014	0.023	0.16

Hot rolled $\frac{3}{4}$ -in. bar stock was used.

The notched test bars had a cylindrical section of 0.500 ± 0.02 in. diam and were provided with a 50 pct (reduction in cross-section), 60° circumferential V-notch. The radius at the root of the notch was in all cases less than 0.001 in.

Specimens for the concentric tests were provided with buttonhead ends and tested in fixtures designed to yield high concentricity. Threaded ends were used on eccentric specimens tested with the axis of load application initially $\frac{1}{4}$ in. apart from the longitudinal specimen axis.

The heat treatment consisted of austenitizing for one hour at 1550°F, quenching into a lead bath* at the austempering temperature (860°F), holding for various times and then quenching into oil. Following austempering specimens were tempered at 300°F to reduce quenching stresses.† In addition, a few bars austempered at 950°F were tempered at the austempering temperature for one hour. Specimens were finish machined following the heat treatment. Details of specimen preparation and experimental technique have been previously reported.^{6,7}

The notch strength (ratio of maximum load to initial area of the notched section)

* Specimens austempered at 950°F were quenched into a salt bath. This yielded a non-uniform distribution of hardness on the notched cross-section presumably because of the slower cooling rate yielded by molten salt.

† This low temperature should not cause significant changes in either the structure of the intermediate products or the martensite. However according to general experience, it should improve the reliability of the tests, possibly because of the reduction of residual quenching stresses.

was determined for both types of specimens. Also, for the concentric specimens the notch ductility was measured, that is, the contraction in area at the root of the notch, by a radial strain gauge of the type previously described.⁷

The hardness of a structure corresponding to a particular austempering time was determined on eccentric notch specimens after testing. The fractured surface of these specimens was ground flat (with flood lubrication) and then a layer of metal 0.015-in. thick removed. The Rockwell "C" hardness distribution was determined across a diameter and the average of five hardness readings taken in this manner is reported for a particular specimen.*

The quantity of intermediate products was estimated visually under the microscope. Four areas were selected for these measurements located midway between the center and the periphery of the notched cross section. Results of two observers were averaged. It appears possible that this method yielded results which are somewhat in error, since it might be expected that less decomposition would occur at the center than near the surface of the specimens. However for the purpose of this paper such an estimate of the extent of decomposition was considered satisfactory.

RESULTS

The fundamental effects on the metal properties caused by the addition of intermediate products to tempered martensite could be shown by an analysis of the data for either of the two austempering temperatures investigated. However, since the data for austempering at 860°F were obtained under more closely con-

trolled conditions, these are presented and discussed below. For the purposes of comparison, trend curves for the properties obtained on austempering at 950°F have been added to some of the graphical representations.

MICROSTRUCTURES

Fig 1 shows the microstructures* for SAE 5140 austempered at 860°F for various times. The intermediate products (other than ferrite) were found to be of the acicular type (bainite). After austempering for 4 sec the structure exhibits a small quantity of ferrite.† With increasing time the amount of intermediate products increases. A completely transformed structure is represented by the specimens austempered for 120 sec. The quantity of intermediate products (including ferrite) as estimated from the microstructures is shown in Fig 2 as a function of the austempering time. At 860°F the structure is composed of 50 pct austempered product after only approximately 15 sec transformation and the reaction is complete after 60 sec.

Notch Properties of the Austempered Structures

In Fig 3 the notch properties are represented as a function of the austempering time. The structure and properties for zero austempering time are not known and cannot be definitely determined. However, the properties assembled in Fig 3 are in agreement with the assumption that the structure after austempering for zero time and subsequent quenching consists of martensite. The properties of such martensite (tempered at 300°F) have been previously determined⁷ and these values are added to

* In general the hardness of the specimens austempered for the shorter times, 15 sec or less, was uniform across the cross-section. Specimens austempered for longer than 15 sec were approximately 10 pct harder at the surface than at the center. These variations indicate that the transformation was not uniform; however this should not affect the validity of the results, as will be discussed later.

* The micrographs were taken on the notched cross-section at a point midway between the center and the surface of the specimens.

† Previous investigations⁷ show that oil-quenched 0.500-in. cylindrical-diam notch specimens of SAE 5140 contain a very small quantity of ferrite. Apparently this section size can not be obtained entirely free of ferrite on oil quenching.

Fig 3. Then with increasing austempering time, all notch properties decrease until a pronounced minimum is reached at a very

function of the quantity of intermediate products* in Fig 4. This graph again illustrates the reduction in strength and

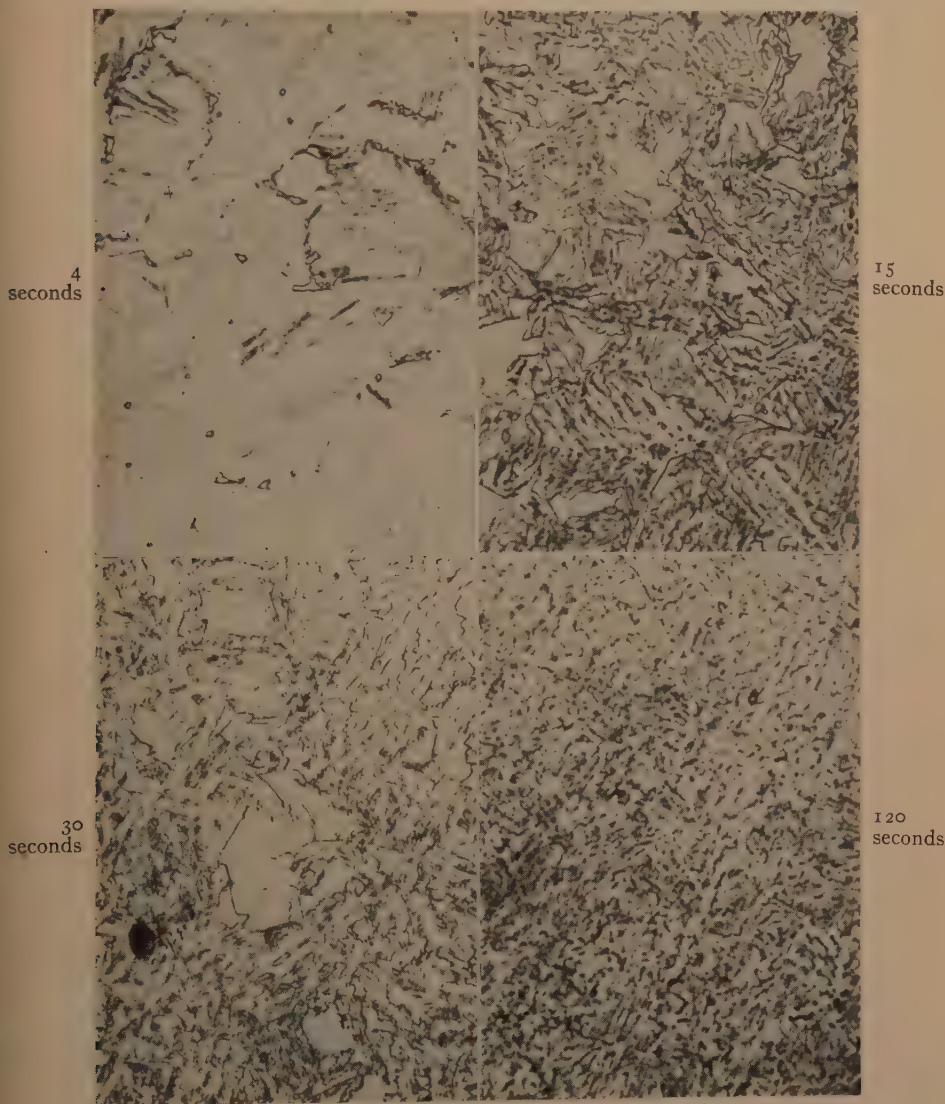


FIG 1—STRUCTURES OF SAE 5140 AUSTEMPERED FOR VARIOUS TIMES AT 860°F AND TEMPERED AT 300°F FOR ONE HOUR (1000 X).

short time, approximately 7 sec. With further increasing austempering time the notch properties rise rapidly to an almost constant value.

The notch properties are replotted as a

ductility if a small portion of martensite

* In determining the quantity of intermediate products, the values for a given austempering time have been derived from the trend curves, Fig 2, rather than from the individual data points.

is replaced by intermediate products. Thus the tempered martensite (zero quantity of intermediate products) loses approximately 40 pct in concentric notch strength and

Relation between Notch Properties and Hardness

The hardness, (Fig 3) continuously decreases with increasing austempering time

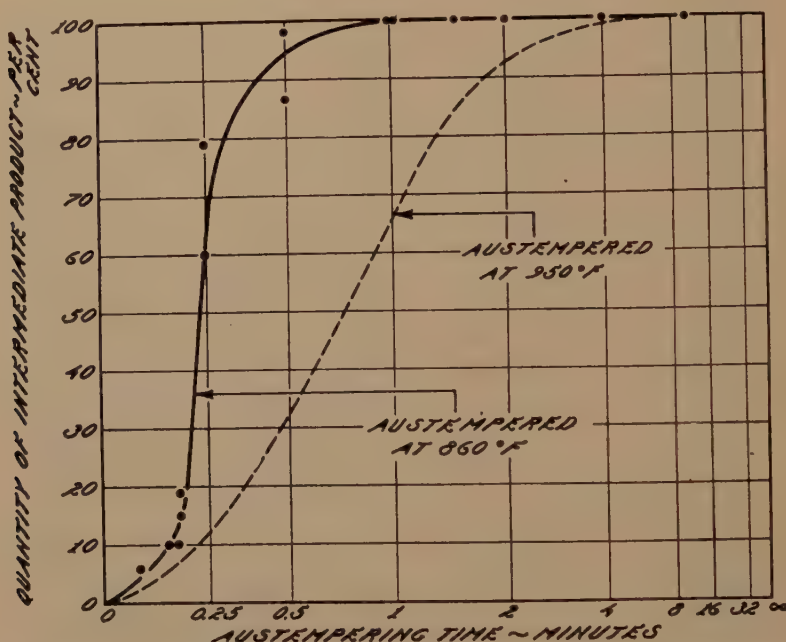


FIG 2—QUANTITY OF INTERMEDIATE PRODUCT (INCLUDING FERRITE) AS A FUNCTION OF THE AUSTEMPERING TIME FOR SAE 5140.

approximately 30 pct in eccentric notch strength with the addition of intermediate products to compose 15 pct of the structure. The corresponding decrease in notch ductility is from 0.2 or 0.1 pct to less than 0.05 pct. More than one half of these reductions in notch properties occur after austempering times which yield only 2 pct of the intermediate products.

With increasing quantity of these products, up to approximately 60 pct, only small further changes result in the notch properties. These notch properties of structures containing more than 60 pct intermediate products rise with increasing quantity to a maximum value for the fully austempered specimens.

from a maximum of 52 R_C to a value of approximately 23 R_C for the fully austempered structure. The relation between the hardness and the quantity of intermediate products, Fig 4, is practically a straight line as would be predicted from the law of mixtures. However, a deviation to lower values was observed at approximately 25 pct transformation.*

In Fig 5, the notch properties of the austempered structures are shown as a function of the hardness. In general, the properties decrease with increasing hard-

* This observation cannot be explained at present. However, it should be noted that this decrease in hardness is associated with the minimum notch properties.

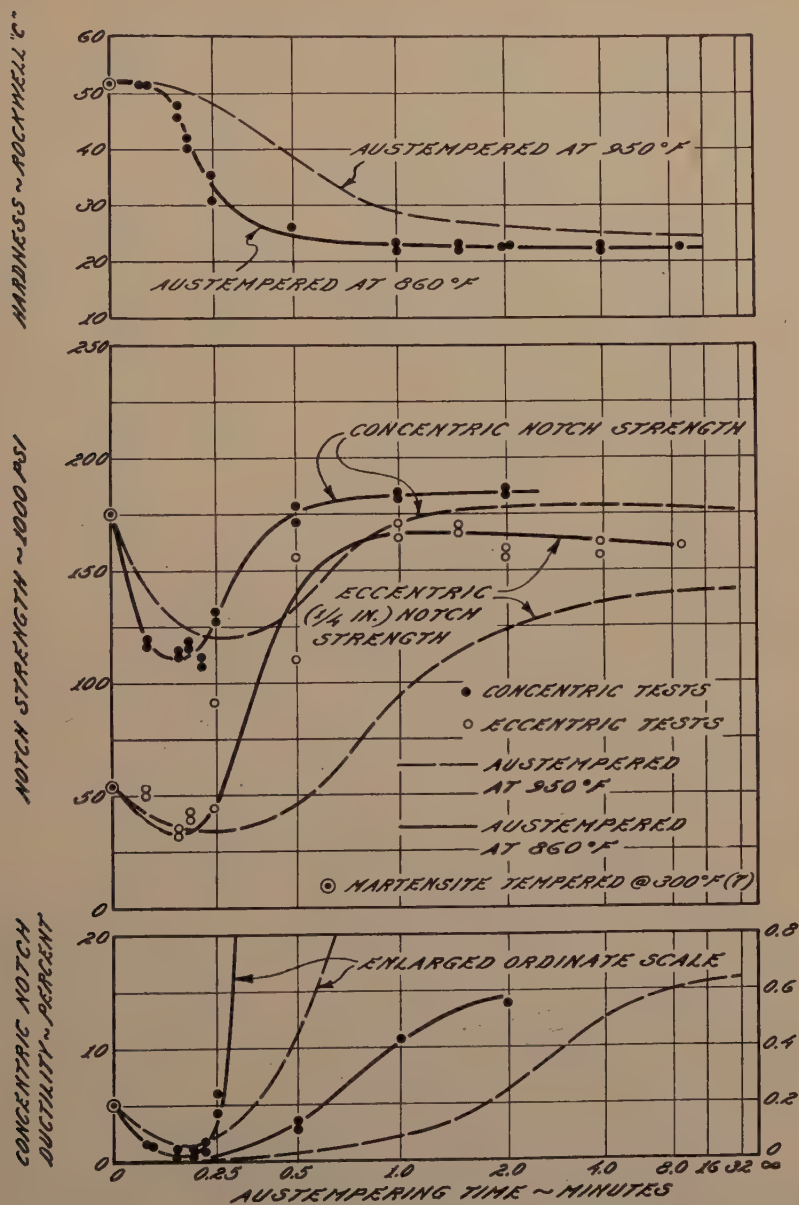


FIG 3—EFFECT OF AUSTEMPERING TIME ON THE NOTCH PROPERTIES AND HARDNESS OF SAE 5140.

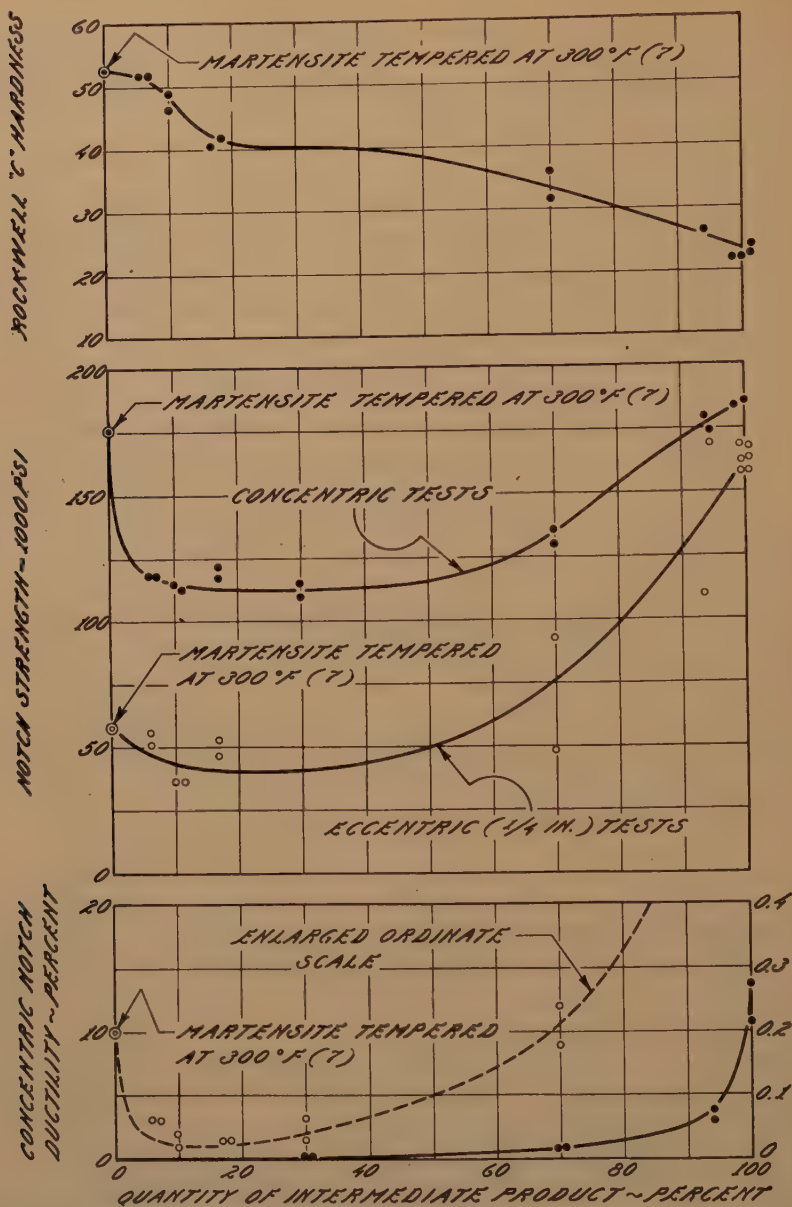


FIG 4—NOTCH PROPERTIES AND HARDNESS OF SAE 5140 AS A FUNCTION OF THE QUANTITY OF INTERMEDIATE PRODUCT FORMED BY AUSTEMPERING AT 860°F.

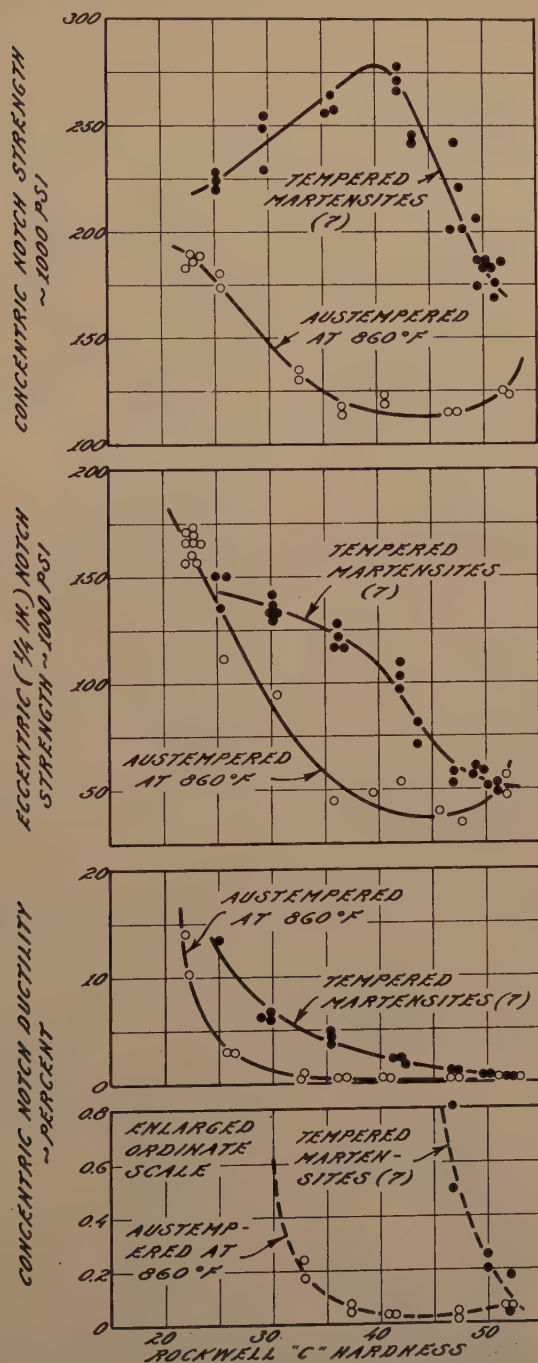


FIG 5—NOTCH PROPERTIES AS A FUNCTION OF SPECIMEN HARDNESS FOR SAE 5140 AUSTEMPERED FOR VARIOUS LENGTHS OF TIME AT 860°F AND FOR SAE 5140 TEMPERED MARTENSITES.

ness from a maximum value at minimum hardness to a minimum value at a hardness of approximately 40 R_C . Between 40 and 50 R_C the notch strengths and ductilities remain practically constant. Approaching the conditions of maximum hardness, small increases in hardness are associated with comparatively large increases in the notch properties.

DISCUSSION OF RESULTS

The properties of the partially austempered steels may be compared with those of tempered martensite on the basis of equivalent hardness. Also considering the results for both austempering at 860 and 950°F some general conclusions may be drawn regarding the effects of intermediate products on the properties of a tempered martensite.

Notch Properties of Tempered Martensites

The notch properties of tempered martensites have previously been determined over a wide range of hardnesses (strength levels) by Sachs, Ebert, and Brown.⁷ These data have been added to Fig 5 and reveal that any alloy steel becomes extremely notch brittle if the hardness exceeds approximately 40 R_C (or if the regular tensile strength exceeds 200,000 psi). Below this hardness the concentric notch strength is generally about 50 pct higher than the tensile strength. With further increasing hardness the concentric notch strength passes through a maximum and then, for 5140 steel, decreases rapidly to low values.

The notch ductility decreases continuously with increasing hardness from a maximum of about 12 pct to a very low value for the high hardnesses.

The results of eccentric notch tests also illustrate this gradual embrittlement of the steel even at low hardnesses. The eccentric notch strength is considerably lower than the concentric notch strength over the entire range of hardnesses so far investigated.

Comparison of the Notch Properties of the Partially Austempered Structures with Those of Tempered Martensites

A comparison, Fig 5, of the notch properties of the austempered structures and those of the tempered martensites reveals large differences in strength and ductility between these two structures. The magnitude of these differences varies with the hardness. These differences are directly represented in Fig 6 as a function of the hardness, in other words the properties of the austempered structure are subtracted from those of the tempered martensite at a given hardness.

For the lowest hardnesses* the notch properties of the austempered structures and the tempered martensites approach each other closely. In fact at hardnesses below 25 R_C the eccentric notch strength† of the austempered structures appears to be slightly higher than that of tempered martensite (indicated by negative values in Fig 6). In this region of low hardness the austempering was practically complete. Thus a fully austempered (at 860°F) structure has properties approximately equal to those of a tempered martensite of equivalent hardness.

With increasing hardness (above 25 R_C) the notch properties of the tempered martensite become increasingly superior to those of the partially austempered structures. The largest difference between the two conditions in terms of the concentric notch strength occurs at a hardness of approximately 40 R_C . The maximum difference in eccentric notch strength occurs at a

* The properties of the tempered martensites at hardnesses less than 25 R_C have not been determined experimentally. However the curves for tempered martensites in Fig 5 can be extrapolated to the hardness of the fully austempered specimens with sufficient accuracy.

† The notch ductility of these structures is relatively high (above 15 pct). Under such conditions it might be expected that the strength values derived from the eccentric test would be more sensitive to differences between the structures than those derived from the concentric tests.⁷

lower hardness, approximately 35 R_C. The largest difference in ductility occurs at a hardness of approximately 27 R_C.

As the hardness increases beyond the value corresponding to the maximum dif-

ferences in properties these differences become again smaller. It might be expected, as was mentioned previously, that with decreasing amounts of intermediate products approaching a structure of pure mar-

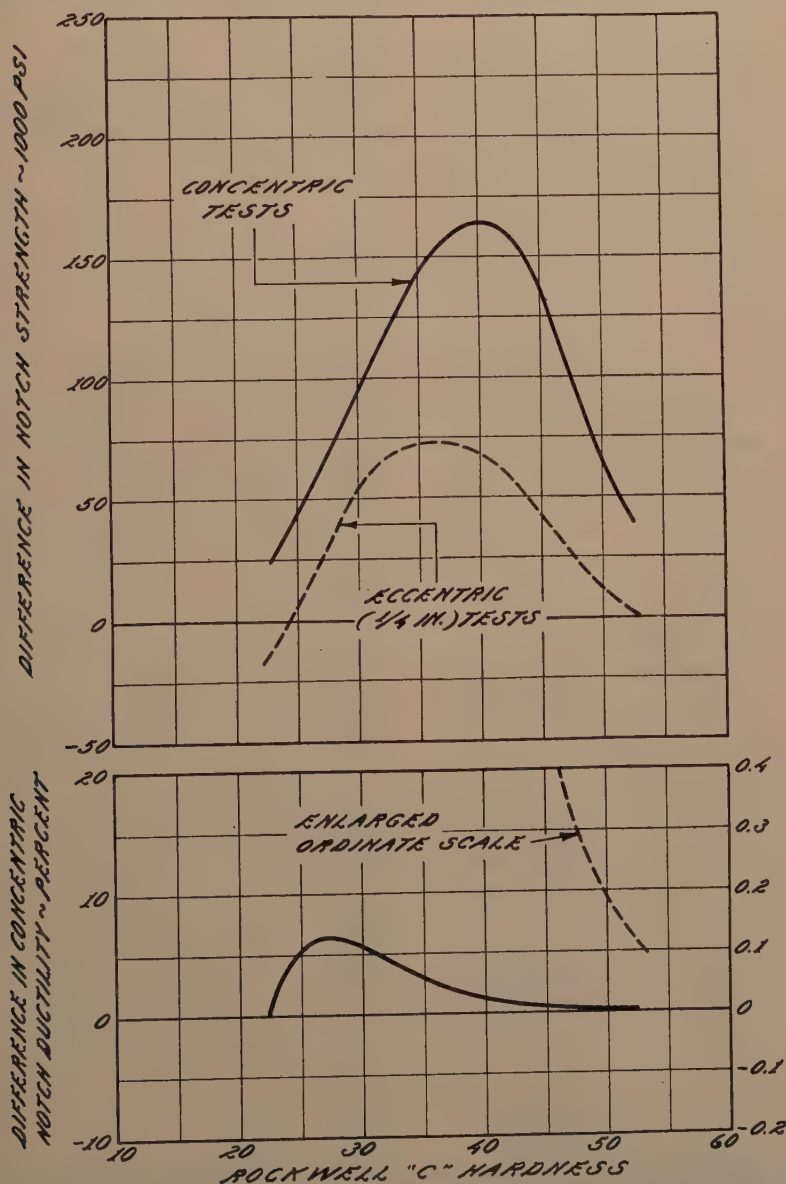


FIG 6—DIFFERENCE BETWEEN THE NOTCH PROPERTIES OF SAE 5140 STEEL TEMPERED MARTENSITES AND THOSE OF SAE 5140 STEEL PARTIALLY AUTEMPERED AT 860°F FOR CORRESPONDING HARDNESSES.

tensite (maximum hardness) the differences in the properties between the two structures would approach zero.

Comparison between the Notch Properties for Austempering at 860 and 950°F

Referring to Fig 3, a comparison may be made between the hardness and notch properties of SAE 5140 structures austempered for various times at 860 and 950°F.

The hardnesses of the fully transformed structures for both temperatures of austempering were found to be practically identical; however the hardness decreased less rapidly with increasing austempering time at 950°F.

The minimum in the curves relating notch properties to austempering time is somewhat less pronounced and displaced to longer times, and it appears that the concentric notch strength of the structures yielding minimum properties was slightly higher at 950°F than at 860°F. The concentric notch strengths of the fully austempered structures at both temperatures are practically identical. This might be expected since these specimens possess identical hardnesses and high ductilities. However eccentric notch strength of the fully transformed structure at 950°F was lower than that formed at 860°F.*

The differences in notch properties between the structures formed at 860 and 950°F are explained by (1) the difference in reaction rates and (2) the difference in the structure and hardness of the intermediate products. Thus the reaction rate is considerably slower at the higher austempering temperature (Fig 2) and therefore a longer austempering time would be required to produce a given quantity of the intermediate products. This would explain the less rapid decrease in hardness with time for

austempering at 950°F than at 860°F. It would also explain the shift in the minimum notch properties to longer times and the broadening of the belly in the curves of Fig 3, when the austempering was carried out at the higher temperature.

PRACTICAL SIGNIFICANCE OF THE RESULTS

The data clearly show that very small quantities of intermediate products constitute potent embrittling factors when present in a matrix of hard martensite. It may be very difficult to avoid the formation of such transformation products during conventional quenching of some low alloy steels. In SAE 5140 steel austenite begins to transform after less than 2 sec at temperatures between 850 and 1100°F and this reaction proceeds very rapidly, particularly at the lower limit of this temperature range. Thus a slight delay in quenching or too large a section size may result in a portion of the section containing small amounts of ferrite and/or intermediate products. Such mixed structures could be expected to behave in a very brittle manner if tempered to high hardnesses. It is impossible to state at this time the effect of tempering temperature on the properties of a structure containing a small amount of intermediate products (including ferrite). However a few tests on specimens austempered at 950°F for various lengths of time and then tempered for one hour at 950°F indicate that a mixed structure tempered at a sufficiently high temperature possesses approximately the same notch properties as a pure tempered martensite of the same hardness. Probably this is explained by the fact that the hardness of the tempered martensite and intermediate products approach each other as the tempering temperature is increased.

CONCLUSIONS

1. The concentric and eccentric (static) notch bar tensile test may be used to evaluate the embrittlement occurring on par-

* The data are not available which would permit a comparison of the notch ductilities for fully transformed specimens. However the higher eccentric notch strength at 860°F would indicate a higher concentric notch ductility for this temperature of austempering.

tially austempering a low alloy steel. On the contrary accurate data cannot be obtained from regular tensile tests since such partially austempered specimens may be excessively brittle and therefore cannot be made to fail in the cylindrical test section.

2. The notch properties of a partially austempered SAE 5140 steel appear to be determined primarily by two factors: (a) the quantity of the intermediate products and (b) the strength properties, particularly the hardness, of the intermediate products.

3. The strength properties of partially austempered SAE 5140 steel may be considerably inferior to those of tempered martensite of equal hardness. The maximum difference occurs when 30 to 50 pct of the structure consists of intermediate products.

4. Austempering for a sufficient length of time to produce complete transformation results in a structure which possesses properties approximately equal to tempered martensite of the same hardness.

5. Austempering for extremely short times, resulting in a structure containing very small amounts of intermediate products, causes a large detrimental effect on the notch properties of martensite as quenched or tempered at low temperatures.

6. Because of the relatively large specimen size used in this investigation, it is impossible to state that the transformation of the entire cross-section occurred isothermally. Therefore it is not possible to evaluate the results in terms of the notch properties of those austempered structures which would be predicted from published, isothermal transformation diagrams. Such data are generally derived from tests on much smaller sections than were used in this investigation.

However some additional tests, in which not only the transformation conditions such as temperature and cooling rate, but also the chemical composition of the steel was varied, yielded throughout results in

agreement with the above conclusions. This, consequently, indicates that very small quantities of intermediate products which may be formed during conventional quenching may cause any low alloy steel in hard tempers to become extremely brittle.

ACKNOWLEDGMENTS

This investigation was suggested by Mr. H. J. French, Vice President, International Nickel Co., New York. The authors wish to acknowledge his constructive criticism and assistance in evaluation of the results. They also wish to express particular appreciation to Mr. G. R. Brophy who carried out the austempering heat treatments and the subsequent metallographic examinations.

In addition the authors are indebted to Mr. M. H. Jones of the Research Laboratory for Mechanical Metallurgy, Case Institute of Technology, for his aid in testing the specimens.

REFERENCES

1. E. S. Davenport and E. C. Bain: Transformation of Austenite at Constant Subcritical Temperatures. *Trans. AIME* (1930) **30**, 117-154.
2. E. S. Davenport, E. L. Roff and E. C. Bain: Microscopic Cracks in Hardened Steel, Their Effects and Elimination. *Trans. Amer. Soc. Metals* (1934) **22**, 289-310.
3. E. E. Legge: Industrial Application of Austempering. *Metals and Alloys* (1939) **10**, 228-242.
4. M. Gensamer, E. B. Pearsall and G. V. Smith: The Mechanical Properties of the Isothermal Decomposition Products of Austenite. *Trans. Amer. Soc. Metals* (1940) **28**, 380-398.
5. M. Gensamer, E. B. Pearsall, W. S. Pellini and J. R. Low: The Tensile Properties of Pearlite, Bainite, and Spheroidite. *Trans. Amer. Soc. Metals* (1942) **30**, 983-1020.
6. G. Sachs, J. D. Lubahn and L. J. Ebert: Notched Bar Tensile Test Characteristics of Heat Treated Low Alloy Steels. *Trans. Amer. Soc. Metals* (1944) **33**, 340-395.
7. G. Sachs, L. J. Ebert and W. F. Brown, Jr.: Comparison of Various Structural Alloy Steels by Means of the Static Notch Bar Tensile Test. *Metals Tech.*, Dec., TP 2110. *Trans. AIME* (1947) **172**.
8. W. T. Griffiths, L. B. Pfeil and N. P. Allen: The Intermediate Transformation in Alloy Steels. Iron Steel Inst. (London) Second Rep., Alloy Steels Res. Com., Spec. Rep. No. 24 (1939), 343-367.

Influence of Strain Aging on the Fracture Stress of Low-carbon Steel

By D. J. McADAM, JR., MEMBER AIME,* G. W. GEIL,† D. H. WOODARD,† AND W. D. JENKINS†

(New York Meeting, February, 1948)

INTRODUCTION

IN a series of papers, the authors and their associates have shown the influence of four important factors on the technical cohesion limit.³⁻¹⁶ By "technical cohesion limit" is meant the technically determinable resistance to fracture. The four important factors are the stress system, plastic deformation, temperature, and the strain rate. The influence of any one of these factors may be represented by a curve of cohesion limits, although only one point on the curve may represent actual fracture. As the term "fracture stress" has come into general use with the same significance as technical cohesion limit, the authors are here using the shorter term with the understanding that it does not always refer to actual fracture.

The previously mentioned series of papers contains ample evidence that plastic extension increases the fracture stress of any polycrystalline metal. In a recent paper of the series,¹⁶ moreover, it has been shown that the effect of plastic deformation on the fracture stress cannot be attributed to reorientation of internal flaws but is a work-strengthening effect, similar to the effect on the flow stress.‡

Manuscript received at the office of the Institute October 10, 1947. Issued as TP 2318 in METALS TECHNOLOGY, January 1948.

* Chief, Section on Thermal Metallurgy, National Bureau of Standards, Washington, D. C.

† Metallurgists, National Bureau of Standards, Washington, D. C.

‡ "Flow stress" is here used in its generally accepted significance, to designate the greatest principal stress during flow.

³⁻¹⁶ References are at the end of the paper.

Plastic deformation of steels, however, may not only cause work hardening, but may result in additional hardness because of strain aging. Some evidence that strain aging affects not only the flow stress but also the fracture stress, has been presented in a recent paper.¹⁴ In that paper, a study is made of the influence of plastic deformation at room temperature on the fracture stress of ferritic steels at -188°C . The study is based on the results of two-stage tests. In the first stage each specimen was extended a predetermined amount at room temperature; in the second stage the specimen was tested to fracture in liquid air. In most of these tests the specimen remained in the testing machine during the interval of about one hour between the first and second stages, it was kept under a tensile load of about 500 lb and maintained at liquid air temperature. The effects of various amounts of plastic deformation on the fracture stress were thus determined and curves were obtained to represent the influence of plastic deformation at room temperature on the stress at brittle fracture in liquid air.¹⁴ Two specimens of ingot iron, however, were removed from the testing machine at the end of the first stage and several days elapsed before the specimens were tested to fracture in liquid air. As shown in Fig 8 of that paper,¹⁴ the points representing fracture of these specimens are far above the curve representing the results of two-stage tests without a rest interval between the stages. The evidence thus indicated that the fracture stresses of these two specimens were increased not

only by the work-strengthening, but also by strain aging. The present paper presents results of further investigation of the influence of strain aging on the fracture stress.

There are two kinds of aging of steel. Both kinds probably are caused by precipitation of particles from supersaturated solution in the ferrite.¹ One kind, known as "quench aging" or "carbon aging," occurs after quenching from elevated temperatures and is caused probably by precipitation of carbides. The other kind, known as "strain aging," is induced by plastic deformation, and may continue, probably at a decreasing rate, for some time after plastic deformation has ceased. Whereas the hardness induced by quench aging varies considerably with the temperature, the hardness induced by strain aging varies little over a wide range of temperature and softening does not occur even after 500 to 1000 hr. Evidently the precipitated compound forms at low temperatures and the diffusion rate is so slow that the particles do not increase greatly in size. It has been suggested that aging is caused by precipitation of iron oxide from supersaturated solution in the ferrite.¹

In addition to the hardening effect of strain aging, there is a change in the form of the stress-strain curve. The curve obtained in a tension test of steel that has been plastically deformed but not allowed to age, shows no drop in stress or discontinuity at the yield point; it rises continuously from the origin. With aging, however, the curve reverts to the form obtained with annealed steel and eventually shows a drop in stress at the yield point. J. Muir¹⁸ investigated the effects of time and temperature on the slow return from the "semi-plastic state" to the "elastic state." Since then, the two effects of strain aging have been the subject of much investigation.^{2,17,20} Little attention, however, has been given to the influence of strain aging on the fracture stress.

METHOD OF INVESTIGATION, MATERIALS, AND SPECIMENS

In this investigation, specimens of annealed steels were plastically deformed various amounts at room temperature. Some of the specimens were then cooled immediately in liquid air and tested to fracture; others were aged before testing in liquid air and still others were aged, plastically deformed again and finally tested to fracture in liquid air. With each metal, therefore, three curves were obtained to represent the influence of plastic deformation and strain aging on the fracture stress at -188°C . One of the curves represents the influence of plastic deformation alone, one represents the influence of plastic deformation plus strain aging, and the other represents the influence of plastic deformation of strain aged metal.

No attempt has been made to investigate the variation of strain aging with time and the effect of this variation on the fracture stress. Attention has been confined to the effects of practically complete strain aging. Since the strain aging of low-carbon steels is practically complete after about three weeks at room temperature, most of the specimens to be aged were kept at room temperature for 25 to 30 days. To hasten the aging of a few of the specimens, however, they were heated for about 30 min. in boiling water. As shown by Muir,¹⁸ Mehringer and MacGregor¹⁷ and others, aging is practically complete in that length of time at 100°C .

For a description of the apparatus and methods used in the tension tests, reference may be made to a previous paper.⁵ For a description of the methods of testing at low temperatures, reference may be made to another paper.⁶ In the tension tests, especially in the tests at -188°C , the load was increased or decreased more slowly than is usual. In the approach to fracture, the stress generally did not change more than 1000 psi in 30 to 60 sec. During the tension tests at room temperature the

change in diameter was measured by means of a dial micrometer to an accuracy of about 0.0002 in. In obtaining a complete flow stress curve, the measurements were continued to the beginning of fracture.^{14,15,16}

The metals used in the investigation were annealed ingot iron and annealed 0.12 pct carbon steel. The chemical compositions are given in Table 1 and details of the annealing treatment are given in Table 2. As indicated by the analysis, which was reported after the experiments were started, the 0.12 pct carbon steel is evidently Bessemer steel.

TABLE 1—Description of Metals

Material	Designation	Rod Diam., In.	Chemical Composition Per Cent				
			Carbon	Manganese	Phosphorus	Sulphur	Silicon
Ingot iron. 0.12 pct Carbon Steel...	DK	1.000	0.01	0.028	0.003	0.017	0.002
	AD	0.875	0.12	0.74	0.109	0.213	0.02

TABLE 2—Heat Treatment

Material	Designation	Rod Diam In.	Temp Deg F	Time Held Hr	Cooled in
Ingot iron. 0.12 pct Carbon Steel...	DK-17.5	1.000	1750	1	Furnace
	AD-17	0.875	1700	1	Furnace

The specimens were circular in cross-section and were unnotched. The threaded ends were 0.75 in. in diam and the gauge length was 2 in. For the tests at room temperature, the gauge diam was 0.505 in.; for the tests in liquid air the diameter was smaller—about 0.4 in., to avoid fracture in the threaded ends.

INFLUENCE OF PLASTIC DEFORMATION AT ROOM TEMPERATURE ON THE FRACTURE STRESS AT -188°C

Fig 1 and 2 show the influence of plastic deformation and strain aging on the flow

stress at room temperature and on the fracture stress at -188°C . Plastic deformation is expressed in terms of A_0/A , in which A_0 and A represent the initial and current areas of cross-section. Since values of A_0/A are represented on a logarithmic scale, abscissas represent true strains. Curves F and F_A in each figure represent results of tests at room temperature, and curves T , T_A and T_B represent results of tests to fracture at -188°C . Attention will be given first to the influence of plastic deformation at room temperature without strain aging on the fracture stress at -188°C .

Curve F in each figure shows the variation of the flow stress of unaged metal during a test to fracture at room temperature, and the small open circles indicate results of measurements made during the test. The symbol at the end of curve F represents the beginning of fracture. Points representing the completion of fracture are not shown. Such points are determined in the usual way by dividing the "breaking load" by the area of cross-section measured after fracture. The area so determined generally is less than the area at the beginning of fracture, because the metal at the rim of the cross-section continues to extend after fracture begins at the axis. Breaking stresses based on this smaller area, therefore, are too high. The symbol at the end of curve F represents the true fracture stress.^{14,15,16}

Each of the other symbols along curve F indicates the end of the first stage in either a two-stage or a three-stage test. The dot-and-dash lines rising from some of these symbols represent the increases of stress between the ends of first stages and the beginnings of the second stages. Each small black circle along curves F indicates the end of a first stage which was followed immediately by cooling to -188°C and test to fracture. Directly above each of these circles is a symbol indicating either fracture or yield in the test at -188°C . When the plastic deformation in the first

stage was less than a certain amount, the specimen showed no appreciable ductility in liquid air. When this amount of plastic deformation was exceeded in the first stage, however, the steel was ductile in the second stage. The ductility of the 0.12 pct carbon steel at -188°C began at less prior plastic deformation and was much greater than that of the ingot iron. As shown in a previous paper,¹⁴ the ductility of a 0.12 pct carbon steel first increased with increase in the prior plastic deformation then decreased rapidly and disappeared. The reason for the increase in ductility is not known. It can hardly be attributed to reorientation of cementite particles since the carbon content of the ingot iron was only 0.01 pct. As shown in previous papers⁸⁻¹⁶ any variable that has even a slight differential effect on the flow stress and fracture stress may have a great effect on the ductility.

Since curves *T* in Fig 1 and 2 are intended to represent the influence of plastic deformation at room temperature alone on the fracture stress at -188°C , the curves have been drawn so as to make allowance for the influence of any plastic deformation at -188°C on the fracture stress. The fracture stress of any specimen that is ductile at -188°C is increased by the plastic deformation at that temperature. A point representing the *initial* fracture stress of such a specimen in liquid air, therefore, must be between the points representing yield and fracture. Since the resistance of a severely cold-worked metal to fracture is only slightly greater than its resistance to flow,³⁻¹⁶ curves *T* have been drawn so as to pass only a little above the points representing yield of the ductile specimens.

As shown in two previous papers,^{14,15} the curve of fracture stresses in liquid air is generally similar in form to the curve of flow stresses at room temperature. When the yield stress drops abruptly to a minimum at room temperature, the curve of fracture stresses at -188°C shows a similar

steep descent to a minimum. Such a relationship was obtained with the 0.12 pct carbon steel (Fig 1). The specimen tested entirely at -188°C fractured immediately after an abrupt drop in stress at yield. Curve *T* in Fig 1 drops far below the upper yield point of this specimen and even below the point representing fracture. In Fig 2, however, the correspondence between curves *T* and *F* near the origin is not clearly revealed. Although there was a slight drop in stress at yield of the specimen tested at room temperature, there was a continuous rise of stress between yield and fracture of the specimen tested entirely at -188°C . However, downward extension of curve *T* might carry it to a minimum lower than the yield point of the specimen tested entirely at -188°C .

The course of curve *F* beyond the point representing the maximum load is affected by the increase in the radial stress ratio (ratio of transverse radial to longitudinal stress) because of the notch effect of the local contraction of the specimen. If the radial stress ratio did not increase, the course of curve *F* would depend only on the work-hardening effect of the plastic deformation, and the curvature would be much greater than it is between the points representing maximum load and fracture. The similarity in form between curves *T* and *F* indicates that the fracture stress is affected not only by the plastic deformation, but also by the increase in the radial stress ratio during the local contraction of the specimen.¹⁴

INFLUENCE OF PLASTIC DEFORMATION AT ROOM TEMPERATURE FOLLOWED BY AGING ON THE FRACTURE STRESS AT -188°C AND ON THE FLOW STRESS AT ROOM TEMPERATURE

Curves *T_A* in Fig 1 and 2 are based on the results of two-stage tests in which specimens were plastically deformed various amounts at room temperature, aged for 25 to 30 days at room temperature or

for 30 min. in boiling water and tested to fracture in liquid air. The small open squares along curves F mark the ends of the first stages. Directly above each of these squares is a symbol indicating the stress at yield or at fracture of the aged specimen at -188°C . The aged specimens of the 0.12 pct carbon steel showed some ductility in liquid air when the prior plastic deformation at room temperature exceeded a certain amount but the ductility was much less than that of the unaged metal. The results obtained with this steel have made it possible to extend curve T_A in Fig 1 to about the same length as that of curve T . In Fig 2, however, curve T_A could not be extended far because of the lack of material for further tests. The small black square near the upper right corner of the figure possibly is too low because of incipient fracture in the first stage; the prior plastic deformation was nearly enough to cause fracture. Illustrations of such an effect are shown in Fig 6 and 8 of a previous paper.¹⁴

Comparison of curve T_A with curve T in each figure reveals the influence of the aging after various amounts of plastic deformation at room temperature. Comparison of corresponding ordinates of the two curves shows that the percent-increase in the fracture stress because of the aging varied only slightly with the prior plastic deformation. The evidence indicates that the difference between corresponding fracture stresses for the 0.12 pct carbon steel was about 10 pct whether the prior plastic strain was large or small. For the ingot iron, the percent difference between corresponding fracture stresses possibly decreases slightly with increase in the prior plastic strain. With decrease of the prior plastic strain below about 2 pct, curve T_A for the 0.12 pct carbon steel evidently would descend below the upper yield point of the specimen that was tested entirely at -188°C . Before the yield of this specimen, therefore, the fracture stress evidently was

higher than the fracture stress of steel that had been aged after slight plastic strain. This relationship illustrates the fact that unstrained annealed low-carbon steel is similar in some respects to strain aged steel. If curve T_A were extended to zero strain it would traverse a minimum and rise to a point not far above the upper yield point of the annealed steel. Curve T_A thus would be similar in form to curve T . The evidence in Fig 2 is not sufficient to show whether curves T and T_A traverse a minimum and are thus similar in form to curve T .

Curves F_A in Fig 1 and 2 show the influence of plastic deformation at room temperature followed by aging on the flow stress at room temperature. These curves are derived from results of three-stage tests in which the specimens were plastically deformed various amounts at room temperature, aged as usual, again plastically deformed to predetermined amounts at room temperature, and finally tested to fracture in liquid air. The first two stages of these tests have been used in deriving curves F_A . The plus marks along curves F indicate the ends of the first stages. Directly above each of these marks is a symbol indicating yield of the aged metal at room temperature and a flow-stress curve extends from this symbol to an open triangle indicating the end of the second stage. Curves F_A are based primarily on the lower yield points obtained in the second stages.

Comparison of curve F_A with curve F in each figure reveals the influence of aging after various amounts of plastic deformation on the flow stress at room temperature. Comparison of corresponding ordinates of the two curves shows that the percent increases in the flow stress caused by the aging varied only slightly with the prior plastic deformation. The evidence in Fig 1 indicates that the difference between corresponding flow stresses for the 0.12 pct carbon steel was about 10 pct whether

the prior plastic strain was large or small, Fig 1. Evidence in Fig 2 seems to indicate that the percent difference between the flow stresses of aged and unaged ingot iron decreased very slightly with increase in the prior plastic strain.* For both metals the percent increase in the flow stress because of the aging was practically the same as the percent increase in the fracture stress at -188°C .

With decrease in the prior strain below about 2 pct curve F_A in Fig 1 falls below the initial upper yield point of the 0.12 pct carbon steel. If curve F_A were extended to zero strain, it would traverse a minimum and rise to the point representing the initial upper yield stress. The evidence in Fig 2 is not sufficient to show whether curve F_A would traverse a minimum if extended to zero strain.

INFLUENCE OF PLASTIC DEFORMATION OF PREVIOUSLY STRAIN-AGED STEEL ON THE FRACTURE STRESS AT -188°C

As illustrated by curves F_A in Fig 1 and 2 and by the short flow-stress curves along curves F_A , plastic deformation after aging had no adverse effect on the flow stress at room temperature. When the strain before aging exceeded a certain amount the stress at yield in the subsequent test at room temperature dropped abruptly. After this drop, however, the flow-stress curve follows curve F . This gives no evidence of damage during the flow of the previously strain-aged metal.

Consideration will now be given to the influence of plastic deformation of previously strain-aged metal on the fracture at -188°C . After the strain-aged specimens had been extended the amounts indicated by the small open triangles along curves F_A , each specimen was tested to fracture in liquid air. Directly above each open triangle is a symbol indicating either

yield or fracture at -188°C . Curve T_B , based on the results of these tests to fracture, shows the influence of plastic deformation of the aged metal at room temperature on the fracture stress in liquid air. If plastic deformation of strain-aged metal at room temperature had no adverse effect on the fracture stress at -188°C , curve T_B would coincide with curve T_A which represents the effect of strain aging with no subsequent plastic deformation. Curve T_B , however, ranges between the curve for unaged metal (T) and curve T_A . When the plastic deformation before and after aging was slight, the fracture stress in liquid air was no higher than that of unaged metal. With increase in the total plastic deformation of the 0.12 pct carbon steel, the curve of fracture stresses (T_B) rises rapidly until it practically coincides with curve T_A . Curve T_B for ingot iron, however, rises much more slowly, and remains below curve T_A .

Comparison of curves C and C' (Fig 1 and 2) reveals qualitatively the variation of the fracture stress at -188°C with plastic deformation of specimens of aged steels. When the prior plastic strain of a specimen of 0.12 pct carbon steel before aging was only about 3 pct, plastic strain after aging evidently lowered the fracture stress at -188°C . (Fig 1.) When the prior plastic deformation before aging was about 10 pct, however, plastic strain of the aged metal increased both the flow stress and the fracture stress. Over a wide range of prior plastic deformation of ingot iron (Fig 2) plastic strain of the aged metal at room temperature evidently decreased the fracture stress at -188°C (Fig 2).

INFLUENCE OF PLASTIC DEFORMATION AND STRAIN AGING ON THE FRACTURE STRESS AT ROOM TEMPERATURE

The previously discussed variations of the fracture stress at -188°C with plastic

* The evidence in these two figures is not in accordance with the view of Davenport and Bain¹ that maximum strain aging occurs after about 15 pct prior strain.

deformation and with strain aging must be attributed to qualitatively similar variations of the technical cohesive strength at room temperature. In previous papers³⁻¹⁶ the influence of plastic deformation on the fracture stress of a metal at room temperature has been represented by a curve a little above the corresponding flow-stress curve; both curves rise and intersect at a small angle at the point representing actual fracture. Because only one point on such a cohesion curve represents actual fracture, the curve can be established only by indirect methods. However, by a comparison of fracture-stress curves obtained at -188°C with the corresponding flow-stress curves obtained at room temperature, it is possible to establish definitely the relation between the flow stress and fracture stress during the plastic deformation of ferritic steels at room temperature.^{14,15} In making such a comparison, however, the curves obtained at -188°C must be converted into equivalent curves representing the variation of the fracture stress with plastic deformation at room temperature. Such a conversion can be made by proportionate reduction of the ordinates of the curves obtained at -188°C .^{14,15}

In Fig 3 converted fracture-stress curves for the 0.12 pct carbon steel thus obtained are shown together with the corresponding flow-stress curves. The conversion factor (0.67) was chosen so that each converted fracture-stress curve touches the corresponding flow-stress curve at the point representing actual fracture at room temperature. Curves T' , T_A' and T_B' thus have been derived by multiplying ordinates of curves T , T_A and T_B by the constant conversion factor 0.67.

Comparison of curves F and T shows the relation between the flow stress and the fracture stress during the plastic deformation of unaged steel at room temperature. Comparison of curves F_A and T_A shows the influence of plastic deformation at room temperature followed by aging on the

relation between the flow stress and the fracture stress. If plastic deformation of aged steel affects the fracture stress at room temperature in the same way that it affects the fracture stress at -188°C , curve T_B' represents the influence of plastic deformation before and after aging on the fracture stress at room temperature, and curve F_A represents the corresponding variation of the flow stress. Since the ductility of a metal depends on the initial difference between the curves of fracture stress and flow stress, the relation between curves T_B' and T_A' seems to indicate that slight plastic deformation followed by aging would decrease the ductility of 0.12 pct carbon steel but that plastic extension of 20 pct or more followed by aging would not decrease the ductility. Since curve T_B in Fig 2 rises only slowly above curve T and remains below curve T_A , this relationship indicates that strain aging would decrease the ductility of ingot iron more than that of the 0.12 pct carbon steel. This supposition is confirmed by evidence in the literature. For example, in Fig 9 of a previous paper⁶ the ductility of ingot iron is shown to be much less at 100°C than at room temperature. The lower ductility at 100°C was caused by the strain aging.

CONCLUSIONS

The results of the experiments confirm the conclusion expressed in previous papers³⁻¹⁶ that plastic deformation increases the fracture stress of metals.

Aging after plastic deformation at room temperature increases the fracture stress at -188°C nearly in proportion to the increase in the flow stress at room temperature.

The percent increase in the flow stress and fracture stress caused by aging varies little but may decrease slightly with increase in the plastic deformation before aging.

When the deformation of either 0.12 pct carbon steel or ingot iron before aging is slight, subsequent moderate plastic de-

formation lowers the fracture stress at -188°C and probably also lowers the fracture stress at room temperature. This adverse effect of plastic deformation of aged steel decreases with increase in the plastic deformation before aging. The decrease of the adverse effect with prior plastic deformation is rapid for the 0.12 pct carbon steel but is very slow for the ingot iron.

Since strain aging increases the flow stress the ductility is decreased when conditions are such that the strain aging decreases the fracture stress.

The results of the experiments confirm the conclusion expressed in previous papers that the variation of the fracture stress with plastic extension may be represented by a curve above the flow-stress curve; both curves rise at a decreasing rate and intersect at a small angle at the point representing actual fracture.

ACKNOWLEDGMENTS

Acknowledgment is due to Miss Frances J. Cromwell for general assistance and for preparing the illustrations, to Mrs. Fannie Wilkinson and Miss Lavaria Weinrich for general assistance.

REFERENCES

1. E. S. Davenport and E. C. Bain: The Aging of Steels. *Trans. Amer. Soc. Metals* (1935) **23**, 1047-1096.
2. R. L. Kenyon and R. S. Burns: Amer. Soc. Metals, Symposium on Age Hardening of Metals (1940), 262-313.
3. D. J. McAdam, Jr.: The Technical Cohesive Strength of Metals. *Trans. Amer. Soc. Mech. Eng.* **63**, *Jnl. Appl. Mech.* (1941) **8**, A 155-165.
4. D. J. McAdam, Jr.: The Technical Cohesive Strength and Yield Strength of Metals. *Trans. AIME* (1942) **150**, 311-357.
5. D. J. McAdam, Jr., and R. W. Mebs: An Investigation of the Technical Cohesive Strength of Metals. *Trans. AIME* (1945) **162**, 474-536.
6. D. J. McAdam, Jr. and R. W. Mebs: The Technical Cohesive Strength and Other Mechanical Properties of Metals at Low Temperatures. *Proc. Amer. Soc. Test. Materials* (1943) **43**, 661-703.
7. D. J. McAdam, Jr., R. W. Mebs and G. W. Geil: The Technical Cohesive Strength of Some Steels and Light Alloys at Low Temperatures. *Proc. Amer. Soc. Test. Materials* (1944) **44**, 593-623.
8. D. J. McAdam, Jr.: The Technical Cohesive Strength of Metals in Terms of the Principal Stresses. *Trans. AIME* (1945) **162**, 542-568.
9. D. J. McAdam, Jr., G. W. Geil, and R. W. Mebs: The Effect of Combined Stresses on the Mechanical Properties of Steels between Room Temperature and -188°C . *Proc. Amer. Soc. Test. Materials* (1945) **45**, 448-485.
10. D. J. McAdam, Jr., G. W. Geil, and R. W. Mebs: Effects of Combined Stresses and Low Temperatures on the Mechanical Properties of Some Non-ferrous Metals. *Trans. Amer. Soc. Metals* (1946) **37**, 497-537.
11. D. J. McAdam, Jr.: Fracture of Metals under Combined Stresses. *Trans. Amer. Soc. Metals* (1946) **37**, 538-566.
12. D. J. McAdam, Jr., G. W. Geil, and D. H. Woodard: Influence of Strain Rate and Temperature on the Mechanical Properties of Monel Metal and Copper. *Proc. Amer. Soc. Test. Materials* (1946) **46**, 902-950.
13. D. J. McAdam, Jr., G. W. Geil, and D. H. Woodard: Influence of the Strain Rate and the Stress System on the Mechanical Properties of Copper. *Trans. Amer. Soc. Metals* (1947) **38**, 551-576.
14. D. J. McAdam, Jr., G. W. Geil, and R. W. Mebs: Influence of Plastic Deformation, Combined Stresses, and Low Temperatures on the Breaking Stress of Ferritic Steels. *Metals Tech.*, August 1947, TP 2220. *Trans. AIME* (1947) **172**.
15. D. J. McAdam, Jr., G. W. Geil, and W. D. Jenkins: Influence of Plastic Extension and Compression on the Fracture Stress of Metals. *Amer. Soc. Test. Materials*, Preprint No. 30, 1947.
16. D. J. McAdam, Jr., G. W. Geil, and Miss Frances J. Cromwell: Flow, Fracture, and Ductility of Metals. *Metals Tech.*, Jan. 1948, TP 2296. *Trans. AIME* (1948) **175**, 306.
17. F. J. Mehringer and C. W. MacGregor: Effects of Cold-Rolling on the True Stress-strain Properties of Low-Carbon Steel. *Trans. AIME* (1945) **162**, 291-309.
18. J. Muir: On the Recovery of Iron from Overstrain. *Phil. Trans. Roy. Soc.* (1900) **193-A** 1-46.
19. L. B. Pfeil: The Change in Tensile Strength due to Aging of Cold Drawn Iron and Steel. *Jnl. Iron and Steel Inst.* (1928) **118**, Part 2, 167-194.
20. J. W. Winlock and R. W. E. Leiter: Some Factors Affecting the Plastic Deformation of Sheet and Strip Steels, and their Relation to Deep Drawing Qualities. *Trans. Amer. Soc. Metals*, (1937) **25**, 163-185.

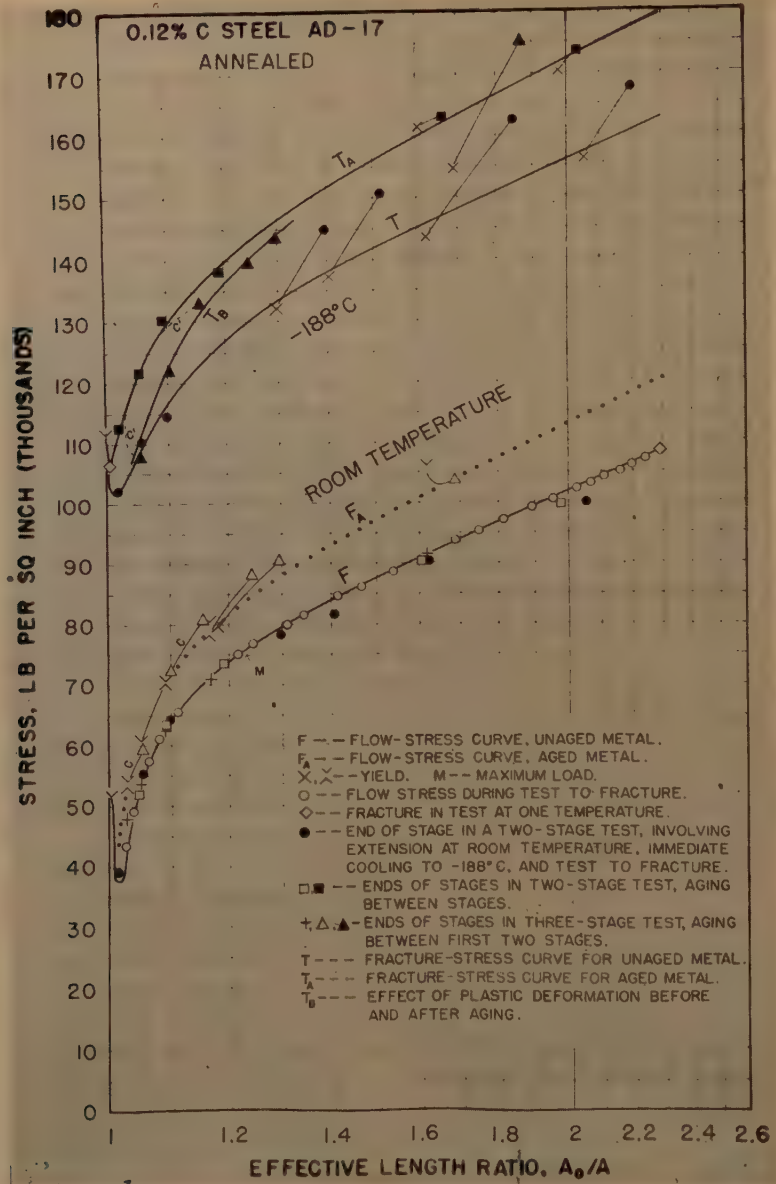


FIG 1—INFLUENCE OF PLASTIC DEFORMATION AND STRAIN AGING ON THE FLOW STRESS OF 0.12 PCT CARBON STEEL AT ROOM TEMPERATURE AND ON THE FRACTURE STRESS AT -188°C.

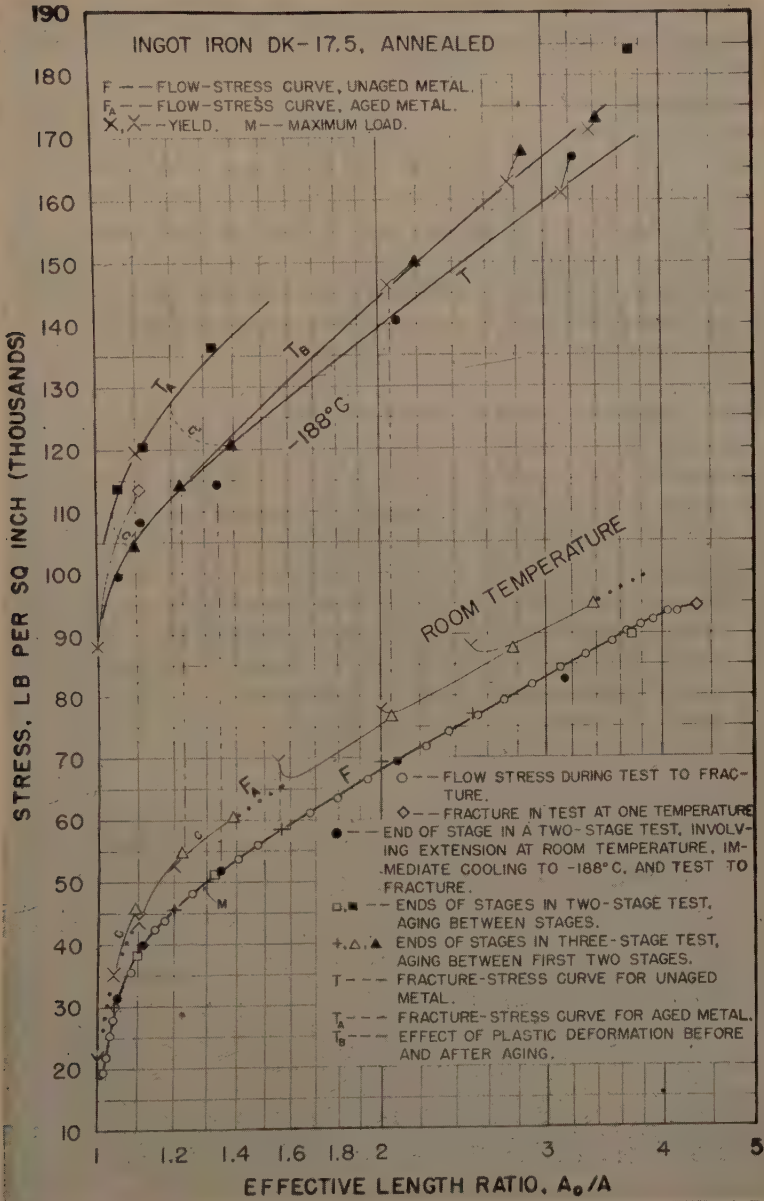


FIG 2—INFLUENCE OF PLASTIC DEFORMATION AND STRAIN AGING ON THE FLOW STRESS OF INGOT IRON AT ROOM TEMPERATURE AND ON THE FRACTURE STRESS AT -188°C.

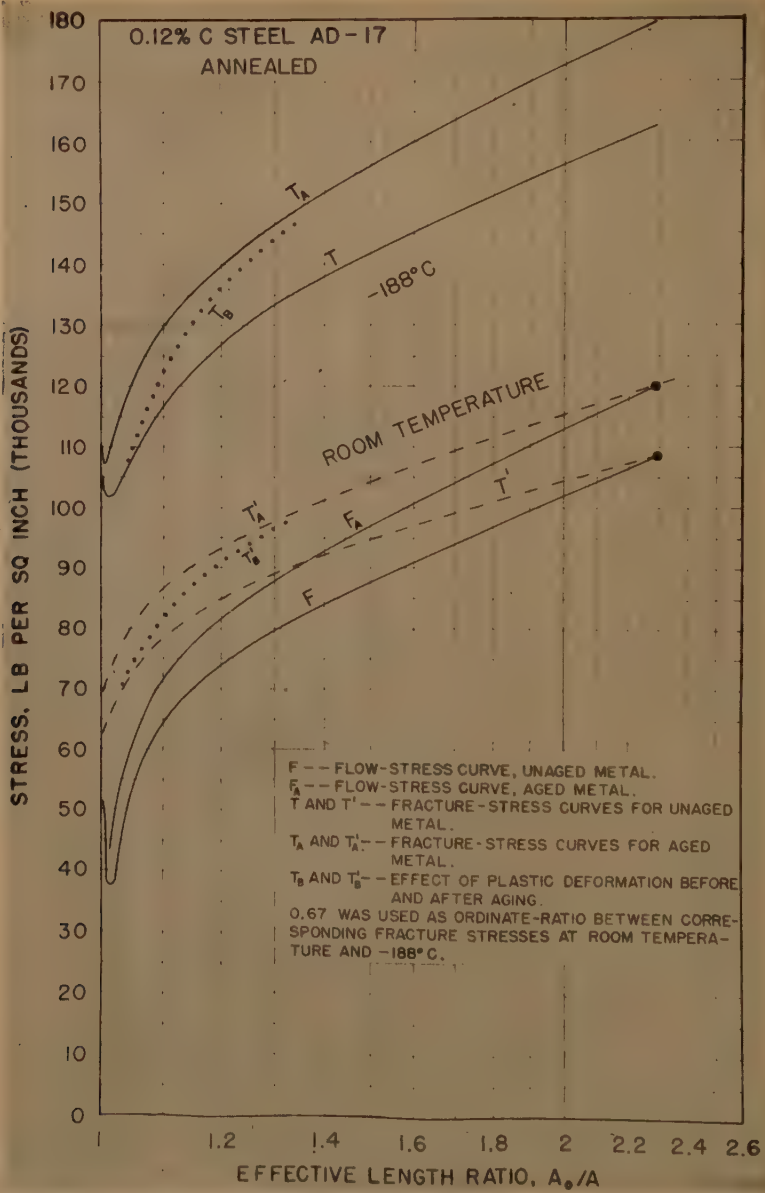


FIG 3--INFLUENCE OF PLASTIC DEFORMATION AND STRAIN AGING ON THE FRACTURE STRESS AT ROOM TEMPERATURE.

DISCUSSION

JOHN R. LOW, JR.*—From the analysis shown for steel No. 12 one might suspect that it was a Bessemer steel whereas the others are presumably open-hearth steels. If this is true, it should be clearly indicated in the paper since Bessemer steels normally can be expected to exhibit strain aging effects to a more marked degree than other grades.

D. J. McADAM, JR. (authors' reply)—As stated in the paper, this was a Bessemer steel. We did not know that until after the tests were started.

JOHN R. LOW—The fracture stress curve in

Fig 1 appears to be drawn through the yield point values at -188°C rather than through the fracture stress points. We would appreciate an explanation by the authors of why this was done.

D. J. McADAM, JR.—The fracture stress curve is supposed to represent the influence of plastic deformation at room temperature on the fracture stress in liquid air. Since the steel had some ductility in liquid air, and since the breaking stress of any specimen in liquid air depends on the total plastic deformation, a curve to represent the influence of plastic deformation at room temperature on the fracture stress in liquid air must be below the points representing actual fracture in liquid air but above the points representing yield.

* Pennsylvania State College.

Anelastic Properties of Iron*

By T'ING-SUI KÊ† MEMBER AIME

(New York Meeting, February 1948)

INTRODUCTION

ACCORDING to the classical theory of elasticity, the elastic portion of the stress-strain curve is represented by a straight line. Such a representation implies that there is a linear relationship between strain and stress and also that strain is a single-valued function of stress and vice versa. Actually, such a one-to-one correspondence between strain and stress does not exist in real metals. A well-known example is the elastic after-effect on unloading. Another familiar example is damping or internal friction, that is, the dissipation of energy attending vibration. In an extensive review of such phenomena, Zener^{1,2} has proposed the term "anelasticity" to denote that property of a solid in virtue of which strain is not a unique function of stress in the non-plastic region. The phenomena arising from anelasticity are called anelastic effects.

The measurements on anelastic effects are important in many fields of metals technology. Thus, in precise instruments such as watch springs, difficulties often arise from the slight dimensional changes after fabrication. The internal friction or damping capacity of metals is often an important factor in deciding whether they are appropriate for instruments in which there are accompanying vibrations.³ However, for metal scientists, the study of anelastic

effects furnishes a powerful tool for understanding many properties of metals in terms of their microstructures or atomic interactions. In order to utilize the anelastic measurements to their fullest extent for acquiring such information, the experimental studies of anelasticity must be interpreted by appropriate mathematical analysis. For a great many problems, however, the necessary information often can be obtained by general qualitative arguments.

From the definition of anelasticity, any physical changes occurring in a specimen as a result of the applied stress will cause anelastic effects if such physical changes are accompanied by a delayed change of elastic strain. Under these circumstances, we have the condition that strain lags behind the stress. We may mention the stress-induced transportation phenomena as examples. These include the stress-induced thermal diffusion,⁴⁻⁷ the stress-induced diffusion of particles,⁸⁻¹² and the stress-induced viscous slip along the microelements in metals.¹²⁻¹⁵ The differential equations describing the microscopic mechanism in these phenomena lead to relations in which stress is linear with respect to strain (and/or their derivatives). Thus if we can demonstrate that the superposition principle is valid under the circumstances in which the anelastic effects are observed, we would expect in the macroscopic relation a linear relationship between stress and strain and their derivatives.

This report is to describe a number of anelastic effects observed in alpha-iron, and an attempt is made to derive valuable information from a critical study of these

* This research has been supported by ONR (Contract No. N-6ori-20-IV). Manuscript received at the office of the Institute December 2, 1947; revision received February 16, 1948. Issued as TP 2370 in METALS TECHNOLOGY, June 1948.

† Research Associate with the rank of Assistant Professor, Institute for the Study of Metals, University of Chicago.

¹ References are at the end of the paper.

effects. Before proceeding to a description of the experiments, it may be helpful to make a correlation of various kinds of anelastic effects so that we can compare the results obtained by various anelastic measurements on alpha-iron by earlier workers^{9,16} and by this writer.

INTERRELATION BETWEEN VARIOUS ANELASTIC EFFECTS

There are many manifestations of the anelasticity of metals in virtue of which stress and strain are not unique functions of one another in the pre-plastic range. To mention a few: (1) the recoverable creep under constant stress; (2) the elastic after-effect on unloading; (3) the stress relaxation at a constant deformation; (4) the variation of dynamic elastic modulus with the frequency of vibration; and (5) the internal friction. These effects are interrelated and are observed under different experimental conditions. Let us illustrate how these effects should be observed in a polycrystalline metal if the applied stress induces a viscous slip along the grain boundaries.^{13,14}

1. When a stress is applied to a metal, an elastic deformation is instantaneously produced. If the grain boundaries behave in a viscous manner, they cannot sustain a shearing stress permanently however small the stress may be. There will therefore be a viscous flow along the grain boundaries, and the shearing stress across these boundaries will at once start to relax. This stress relaxation will cause an over-all slow yielding of the metal after the instantaneous deformation. Thus, if the applied stress is kept constant, there will be a creep under constant stress. The locking effect of the grain edges and corners will insure that the over-all creep will be of limited extent for a fixed over-all stress.

2. When the applied stress is removed, there will be an instantaneous partial recovery of the specimen. However, the strain lags behind in the grain boundaries. This will cause residual stress in the neighboring

grains and this residual stress will, in turn, cause shear stress across the grain boundaries. The gradual relaxation of this shear stress will result in a delayed complete recovery of the specimen which manifests itself as the elastic after-effect.

3. The stress relaxation under constant deformation is but another way of describing the recoverable creep under constant stress. It is evident that the applied stress should be gradually reduced if the over-all deformation of the specimen is to be kept constant. Likewise, as in the case of creep under constant stress, the over-all reduction of stress or stress relaxation will also be of limited extent for a fixed over-all strain.

4. When the specimen is set into vibration, a periodic stress gives rise to a periodic displacement. The dynamic modulus is the ratio of the stress to that component of the strain which is in phase with the stress. It is this modulus which is measured by dynamic methods. Since the amount of creep and stress relaxation varies with the time of observation, the amount that the strain lags behind the stress will also vary with the frequency of vibration. Accordingly the dynamic modulus will vary with the frequency of vibration.

5. The internal friction is measured by the dissipation of energy attending vibration. In a periodic vibration where the stress and strain are not uniquely related, the corresponding stress-strain diagram for the conventional elastic region is an ellipse instead of a straight line for the case where the stress and strain are in phase. The area enclosed by this ellipse is a measure of the energy dissipated in a cycle of vibration. For an unambiguous and convenient measure of this energy dissipation, we can define $\tan \alpha$, where α is the angle that strain lags behind the applied stress, as the internal friction. This expression is often referred to as Q^{-1} by analogy with electrical oscillation. Using this definition, the internal friction is zero when stress and strain are in

phase and is infinity when they are completely out of phase, having a phase difference of 90° . The anelastic effect manifested in this type of measurement is thus the internal friction and its variation with the frequency of vibration. This definition of internal friction has sense even when the energy dissipation is extremely large so that the free vibration becomes aperiodic. When the energy dissipation is not too large, it turns out that $\tan \alpha$ is identical with the logarithmic decrement measured in free decay experiments divided by π . A discussion of very large energy dissipation for a particular case has been given recently by Zener.¹⁷

In the above discussions, the pertinent anelastic effects in the dynamic case are the variations of elastic modulus and of internal friction with the frequency of vibration. A variation of the frequency of vibration through a wide range involves much experimental difficulty. However, in most of the anelastic effects, in which we are interested (except those associated with thermal diffusion and magnetic flux diffusion), the temperature and the rate of delayed deformation, or relaxation, are interrelated through a heat of activation. In such cases, the variation of a dynamic modulus with frequency of vibration will be associated with a variation of this modulus with the temperature of measurement. Similarly the internal friction, which is a function of the frequency of vibration, will also be a function of temperature. In these cases we can measure the dynamic modulus and internal friction as a function of temperature instead of as a function of frequency.

A set of relations correlating these anelastic effects mentioned above has been derived by Zener,² which is valid independent of the magnitude of the effects concerned. An experimental demonstration of the validity of these relations has been presented by the writer in his study on the viscous behavior of grain boundaries in aluminum.¹³

EXPERIMENTAL METHODS OF MEASURING ANELASTIC EFFECTS

In the measurement of anelastic effects, the applied stress should be so small that the following conditions are fulfilled: (1) there should be no permanent set after the stress is removed; (2) the observed anelastic effects should be linear with the applied stress or prior strain in the static case and independent of the stress levels in the dynamic case. Thus the internal friction and the dynamic rigidity should be independent of the amplitude of vibration; the creep per unit elastic strain (or instantaneous strain) independent of the magnitude of the elastic strain; and the stress relaxation per unit initial stress independent of the magnitude of the initial stress.

Anelastic effects in metals can be observed in all or one of the following types of deformation: tension, bending and torsion. The torsional method was chosen in the present investigation because it is much simpler experimentally than the other methods when the strain to be measured or the stress applied is very small. One objection to the torsional method is that the strain in the specimen is inhomogeneous. But this will have no consequence if the effects concerned are observed under such conditions that they are linear with strain and stress.

As the various kinds of anelastic effects can be interrelated, only one type of anelastic measurement, that is internal friction, was taken in the following investigation. The shear modulus was also determined occasionally. The frequency of vibration was adjusted to be about one cycle per second by attaching a small inertial bar to the specimen. Visual observations could therefore be made easily. The measure of internal friction herein adopted is the logarithmic decrement divided by π . When the logarithmic decrement is small, the shear modulus G of the wire is proportional to the square of the frequency of vibration

provided the length and radius of the wire are kept constant.

The apparatus used was essentially an elaborated torsional pendulum with the

ANELASTIC RELAXATIONS IN ALPHA-IRON

The material used in this investigation was Westinghouse "Puron," a high purity iron, containing as its chief impurities

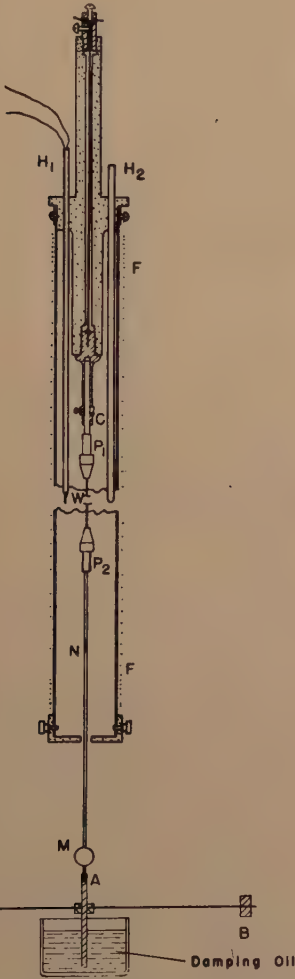


FIG 1—TORSIONAL APPARATUS FOR MEASURING INTERNAL FRICTION AND DYNAMIC SHEAR MODULUS OF WIRE SPECIMEN UNDER VERY SMALL STRESS.

wire specimen as the suspension fiber. The temperature of the specimen can be either raised or lowered. A diagrammatical description of the apparatus is shown in Fig 1 and the actual form in Fig 2. A detailed description of it has been given elsewhere.¹³

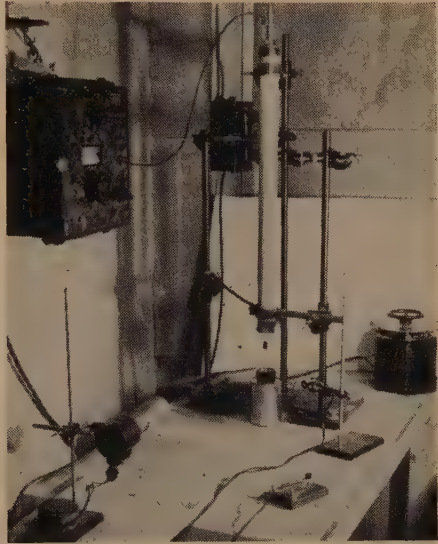


FIG 2—ARRANGEMENT USED IN THE TORSIONAL EXPERIMENT.

approximately 0.040 pct oxygen, 0.005 pct carbon and 0.004 pct nitrogen. It was supplied in $\frac{3}{8}$ in. rod and was swaged to 0.178 in., then it was recrystallized by annealing at 550°C for 30 min. in a salt bath. This material was swaged and then drawn to 0.026 in. with several intermediate 30-min. anneals at 650°C in vacuum. The amount of final cold-working was about 58 pct RA. A test wire 12-in. long was mounted between the two pin vises, P_1 , P_2 , shown in Fig 1 so that it was situated in the uniform temperature region of a non-inductively wound electric furnace FF . The temperature of the wire specimen was controlled and measured with a relative accuracy of 1°C with a chromel p-alumel thermocouple inserted into the furnace through the hole H_1 and a Tag Celestray indicating temperature controller (Fig 2). The measurements were taken in an atmosphere of 99.8 pct argon by keeping a con-

stant flow of argon through the furnace through the Pyrex glass tube H_2 . For measurements at temperatures below room temperature, the argon flow was substi-

vibration were plotted on semi-logarithmic paper against ordinal number of vibrations, a straight line has always been obtained. This indicates that under the experimental

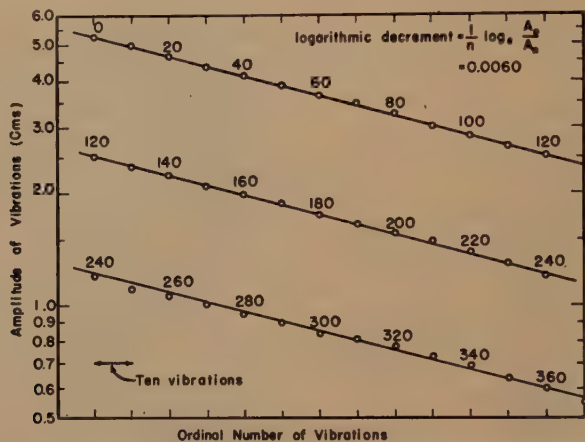


FIG 3—CURVES ILLUSTRATING THAT THE LOGARITHMIC DECREMENT DETERMINED IN THE TORSIONAL EXPERIMENT IS INDEPENDENT OF THE STRESS AS THE STRESS AMPLITUDE VARIED TENFOLD.

The internal friction is equal to the logarithmic decrement divided by π . These logarithmic decrement curves were obtained for cold-worked Puron specimen (58 pct RA) at 139°C after it was annealed at 300°C for one hour (See Fig 5).

tuted by a stream of nitrogen cooled by passing through liquid nitrogen.

The total longitudinal load on the test wire, including the lower pin vise P_2 , the Kanthal A-1 rod N , the concave mirror M , the torsional arm BB and the damping pin A , is about 37 g (except in the experiments designed to test the effect of this longitudinal load, to be described later). This corresponds to a longitudinal stress of about 150 psi, a value much lower than the yield point of iron which is about 10^4 psi at room temperature. The maximum amplitude of vibration observed on a scale situated 3 m away from the mirror was made to be less than 3 cm in most of the measurements, and was less than 2 cm for measurements at high temperatures. With a test wire of 0.026-in. diameter and 12 in. long, this amplitude of vibration corresponds to a maximum shearing strain on the surface of the test wire of 4×10^{-6} . When the consecutive amplitudes of

conditions: (1) the twist on the wire was sufficiently small so that the logarithmic decrement, and thus the internal friction, is independent of the stress amplitude; (2) the twist applied to the wire and the longitudinal load on the wire have caused no change in the wire specimen during the measurement. Typical examples illustrating the stress independence of logarithmic decrement in the iron specimen at 139°C and 475°C are shown respectively in Fig 3, 4 and 5 where the amplitude of vibration varies tenfold.

In Snoek's experiments on the internal friction of iron, a longitudinal magnetic field of 40 oersted was applied during the measurements to suppress the damping caused by magneto-mechanical hysteresis effects.⁹ However, it is well-known that such hysteresis loss decreases when the stress amplitude is reduced. Using the stress amplitude described above, the lowest internal friction observed with the present

apparatus without a "saturation magnetic field" was about 0.0007. This value includes the air damping and apparatus losses. The ferromagnetic hysteresis loss is appar-

glass tube H_2 for microscopic examination. These test pieces had the same past history as the wire specimen and had received the same annealing treatment except no

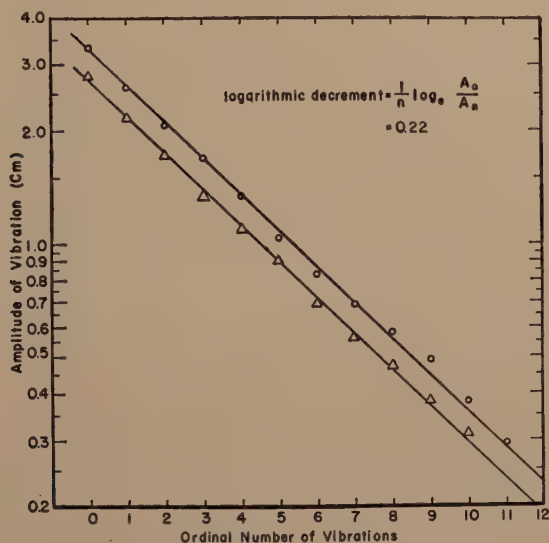


FIG 4—SIMILAR AS IN FIG 3 EXCEPT THAT THESE CURVES WERE DETERMINED AT 475°C AFTER THE COLD-WORKED SPECIMEN WAS ANNEALED AT 600°C FOR ONE HOUR (SEE FIG 5).

It is to be noticed that the logarithmic decrement given by these curves are about 37 times larger than that given in Fig 3.

ently negligibly small under the stress level used. Consequently no saturation field was used in the present experiment.

The internal friction of the 58 pct RA Puron wire was measured at room temperature. It was then annealed at 200°C for one hour "in situ" and the internal friction measured at 200°C and lower temperatures. The same wire was successively annealed at higher temperatures (with 50°C steps) for one hour and measurements were taken at the annealing temperatures and lower temperatures as before. During the annealing at high temperatures, the longitudinal load on the wire was supported so that no stretching could be made on the wire during annealing. This series of measurements was made up to 600°C. After each annealing, a short test piece of Puron wire was taken out from the Pyrex

longitudinal load was applied during annealing. Preliminary experiments have demonstrated that the longitudinal load applied has no effect on the microstructure of the specimen. The wire was found by metallographic examination to be completely recrystallized after the one hour anneal at 500°C. The etchant used was 2 pct nital.

The variation of internal friction with temperature after successive annealings is shown in Fig 5. The frequency of vibration used was about half a cycle per second at room temperature. There are three internal friction peaks, A, C, and E. They occur at temperatures around 20, 225 and 490°C. In addition to these peaks, there are three regions, B, D and F, over which the internal friction varies with temperature. It is to be noted that these three internal friction

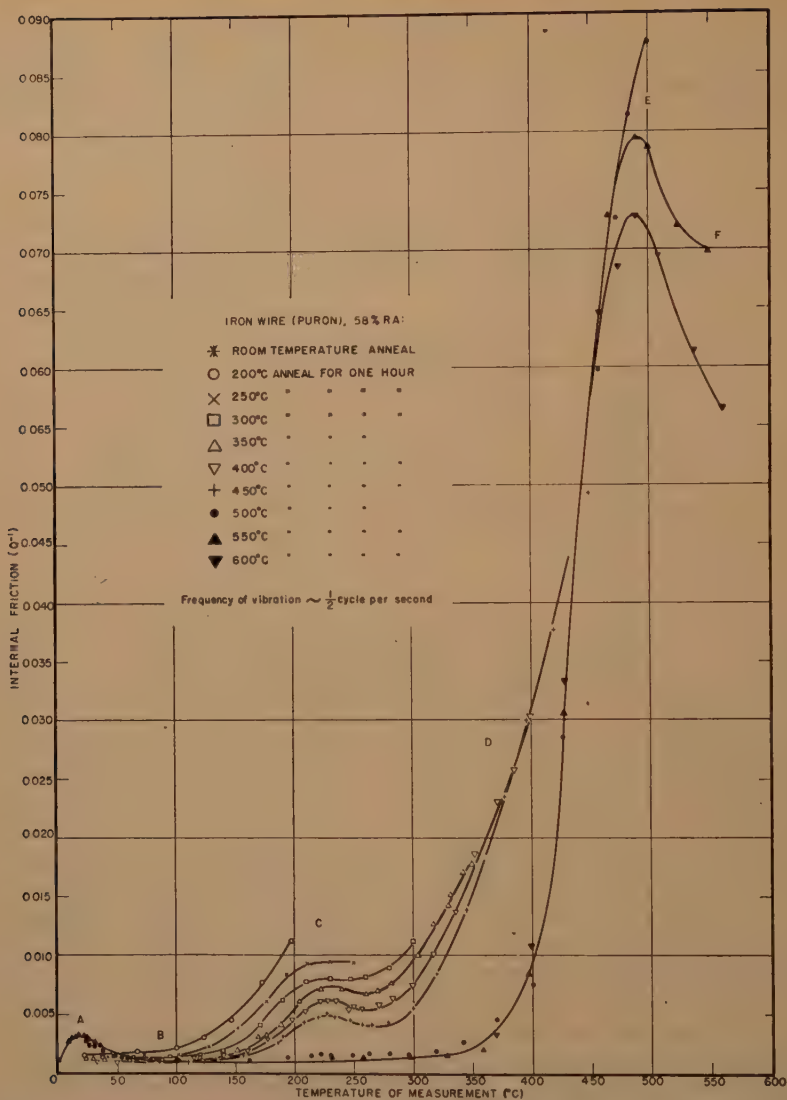


FIG 5—VARIATION OF INTERNAL FRICTION WITH TEMPERATURE OF COLD-WORKED WESTINGHOUSE PURON SPECIMEN (58 PCT RA) AFTER IT WAS SUCCESSIVELY ANNEALED AT VARIOUS TEMPERATURES AS INDICATED IN AT ATMOSPHERE OF ARGON FOR ONE HOUR.

The frequency of vibration was about $\frac{1}{2}$ cycle per second at room temperature. The capital letters A, B, C, D, E, F, are used to mark out the six different relaxations which occurred in the temperature range studied. These relaxations will be discussed separately in the following sections.

peaks occur under different treatments. Thus there is no 20°C peak for the cold-worked specimen and the 225°C peak disappears when the specimen was recrystallized. Fig 5 indicates that the 20°C and the 225°C peaks are somewhat complementary:

one rises while the other sinks. Before we proceed to discuss these relaxations separately, let us examine what general conclusion can be drawn from the fact that there is an optimum temperature for maximum internal friction.

When a stress is applied to a specimen, an anelastic effect is expected if the applied stress causes a delayed change of strain. This delayed deformation of the specimen can be called a relaxation which may be limited or unlimited. Amorphous substances such as pitch are good examples of solids manifesting unlimited relaxation. In such cases the creep under constant stress will not be recoverable when the applied stress is removed and the internal friction will continue to increase indefinitely as the frequency of vibration is lowered or when the temperature of measurement is raised. In a strict sense, therefore, the anelastic effects which are nonplastic and recoverable should include only the relaxation phenomena of the limited type. In solids with limited relaxation, the creep under constant stress will also be limited, or only a certain fraction of a macroscopic stress associated with a given strain can be relaxed. The internal friction will have a maximum value when the frequency of vibration is varied, or, in the case where there is a time-temperature relationship, there will be an optimum temperature for maximum internal friction. The relaxation phenomena of the limited type signify that the diffusion distance must be finite in cases where anelastic effects were caused by stress-induced diffusion. In the case of viscous phenomena, the viscous regions must be confined by non-viscous matrices so that there can be only a limited amount of viscous slip. The existence of an internal friction peak (either versus frequency of vibration or versus temperature of measurement) is thus a necessary and sufficient condition for establishing an anelastic effect in the strict sense; and valuable information can be derived from internal friction measurements only when an internal friction peak is observed.

Analysis of the 20°C Peak (Peak A)

The physical origin of the 20°C peak observed in annealed Puron with a fre-

quency of vibration of half a cycle per second is believed to have the same origin as that observed by Snoek⁹ in annealed iron containing a small amount of carbon or nitrogen. According to Snoek and later verified by Dijkstra,¹³ this internal friction peak is caused by the anelasticity associated with the stress-induced preferential distribution of carbon and nitrogen atoms among various interstitial positions in primary solid solution of alpha-iron. In body-centered cubic iron the carbon or nitrogen can go into the interstitial positions, that is, the center of the faces or the middle of the edges of an elementary cell. These interstitial positions have tetragonal symmetry with the tetragonal axis parallel to one of the principal axes. This implies that the lattice distortion produced by carbon or nitrogen atoms in these positions will also have tetragonal symmetry. Along the tetragonal axis the interstitial atom lies closer to the neighboring iron atoms and thus the elastic distortion is greater. In a stress-free specimen containing interstitial solute atoms, these atoms will be distributed equally among interstitial positions having tetragonal axes parallel to any one of the three principal axes. When a tensile stress is applied along one of the principal axes, as *X*-axis, there will be a greater probability that a solute atom will be in an interstitial position whose tetragonal axis is along the *X*-axis. Some time is required for the establishment of this preferential distribution of solute atoms and consequently strain lags behind the stress. This will cause internal friction and other anelastic effects.

In the picture presented above, it is evident that the diffusion of the solute atoms is from one interstitial position to another and the distance over which diffusion takes place for relaxation is of the order of one atomic distance. For atomic diffusion processes, the relaxation time τ varies with the temperature of measurement T (in °K) according to the relation:

$$\tau = \tau_0 e^{H/RT} \quad [1]$$

where τ_0 is a constant, R the gas constant and H the heat of activation. At low temperatures, the relaxation time associated with the diffusion induced by the applied stress is so large that practically nothing has been relaxed during a half cycle of the applied stress. The strain is thus essentially in phase with the applied stress all the time during the half-cycle and therefore the internal friction should be small. At very high temperatures, the relaxation time is so short that the relaxation will be completed in but a very small fraction of a half-cycle of the stress. So again the strain is essentially in phase with the applied stress and thus the internal friction is again small. Only in intermediate temperature ranges where the relaxation time is comparable with the period of vibration do we have a partial relaxation, and the internal friction will be large. The internal friction will reach its maximum value when

$$\tau\omega \cong 1 \quad [2]$$

where ω is the angular frequency of the applied stress. We have thus

$$\tau \cong \frac{1}{(2\pi f)} \quad [3]$$

where f is the frequency of vibration. This furnishes us a method for estimating the time of relaxation.

Confirming Snoek's observation, it was found that the 20°C peak disappears after the Puron wire was "purified" from carbon and nitrogen by the conventional wet hydrogen treatment. This is shown in the left end of Fig 8 to be compared with Fig 5. In order to find out whether the observed peak in Puron is due to carbon or nitrogen, a "purified" Puron specimen was loaded with nitrogen by annealing the specimen in an atmosphere of hydrogen-ammonia mixture (4 pct ammonia by volume) at 550°C for one hour. The specimen enriched with

nitrogen gives a much higher peak at the same temperature with the same frequency of vibration. Accordingly the 20°C peak observed in the original Puron wire corresponds to the nitrogen peak observed by Snoek. This wire contains only about 0.004 pct of nitrogen.

It can be seen from Snoek's picture that the heat of activation associated with the stress-induced preferential distribution of nitrogen atoms among various interstitial positions in alpha-iron corresponds to the activation energy for the diffusion of nitrogen in alpha-iron. In the present experiment where the applied stress is extremely small, the effect of the applied stress on the activation energy should be negligibly small. Consequently the heat of activation determined by anelastic measurements is actually equal to the heat of activation for diffusion in absence of applied stress. As one purpose of the present paper is to elucidate what anelastic measurements can achieve when used as a tool for research, it seems to be proper to describe here the procedure for determining the heat of activation from internal friction measurements.

For any relaxation process having a heat of activation, we have the relation Eq 1:

$$\tau = \tau_0 e^{H/RT}$$

The internal friction is a function of the phase difference between stress and strain, and this is, in turn, a function of the total amount of relaxation during half a cycle of the applied stress. The amount of relaxation during a half-cycle depends on the relaxation time and the frequency of vibration. Consequently, the internal friction must be a function of the relaxation time and the frequency of vibration f .

By dimensional analysis, the internal friction, being dimensionless, must be a function of the parameter τf , or

$$Q^{-1} = A \text{fcn}(f\tau) \quad [4]$$

where the factor A is independent of f but

may be a function of T . However, if there is a heat of activation associated with the relaxation process concerned, the factor A can only be a slowly varying function of T . This means that the necessary condition for the existence of a unique heat of activation is that the internal friction is determined primarily by the parameter $fe^{H/RT}$. Under this condition, an increase of the frequency of vibration would shift the internal friction curve to higher temperatures without changing the shape of the curve when plotted with Q^{-1} against $1/T$. The internal friction is now measured with two or more frequencies of vibration and the temperatures selected at which the value of the internal friction is the same in both (or all) measurements. In this procedure, then, we can consider that the internal friction is independent of the temperature of measurement. By differentiating both sides of Eq 4 with respect to $1/T$ where T is the temperature in absolute scale, we get on neglecting the term containing $dA/d(1/T)$,

$$\frac{dQ^{-1}}{d(1/T)} = 0 = A f c n' (f e^{H/RT}) e^{H/RT} \left(\frac{df}{d(1/T)} + \frac{fH}{R} \right) \quad [5]$$

in which the prime sign indicates the first derivative of the function with respect to its argument. From Eq 5 we get

$$\frac{df}{d(1/T)} = -f \frac{H}{R}$$

or

$$\frac{df}{f} = - \left(\frac{H}{R} \right) d \left(\frac{1}{T} \right)$$

$$d \ln f = - \left(\frac{H}{R} \right) d \left(\frac{1}{T} \right)$$

and

$$\frac{d \ln f}{d(1/T)} = - \frac{H}{R} \quad [6]$$

Hence

$$H = -2.3R \frac{d \log_{10} f}{d(1/T)} \quad [7]$$

When two frequencies of vibration f_1 and f_2 are used, we have

$$H = 2.3R \frac{\log_{10} (f_2/f_1)}{1/T_1 - 1/T_2} \quad [8]$$

It is obvious then that the procedure for determining the heat of activation is to measure the internal friction curve (versus temperature) with two (or more) frequencies of vibration and plot each curve against $1/T$ as abscissa. Then one curve is to be shifted horizontally until it superposes on the other. The heat of activation can thus be determined according to Eq 8 from the amount of horizontal shift. It is evident that there is a unique value of activation energy for the whole relaxation process when and only when the whole internal friction curves can be made to superpose on one another through one single horizontal shift.

In Snoek's original work, the heat of activation associated with the nitrogen peak was assumed to have the same value as in the magnetic after-effect experiments ($H = 16,400$ cal per mole). However, the observed curve was found to be narrower than the calculated curve assuming this heat of activation. It is apparent that the value from magnetic data is too low. As this value is important in diffusion studies, a direct determination from internal friction measurements is desirable.

There are intrinsic difficulties in the determination of the heat of activation associated with the nitrogen peak. In order to avoid the uncertainty introduced by the background it is necessary to have a large internal friction peak. However, when this peak is raised by loading more nitrogen into the specimen, "segregation" usually comes in. It has been found that specimens annealed at temperatures over 850°C for several hours can hold the nitrogen in solid solution for a period of a few days without appreciable segregation.¹⁹ In the following determinations the specimen used was annealed at 850°C for about 10 hr

after being stretched 3 pct. After such treatment, it has very large grains, being several times larger than the diameter of the wire. This wire was then loaded with nitrogen (6 pct NH_3 in H_2) at 550°C for 3 hr

0.1575. As the two frequencies of vibration used have a constant ratio of 4.74 over the temperature range concerned, we have from Eq 8, $H = 20,000$ cal per mole, which should be accurate to within 10 pct.

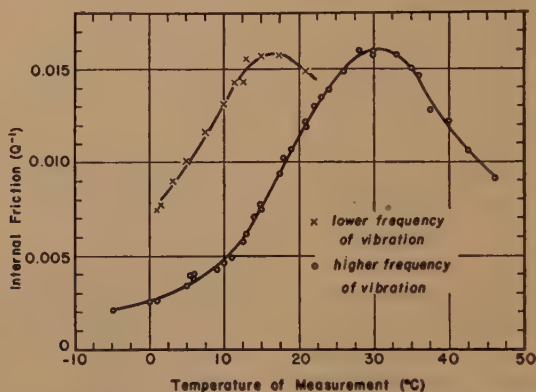


FIG 6—RELAXATION PEAK *A* IN PURON SPECIMEN WHICH WAS FIRST TREATED WITH WET HYDROGEN TO REMOVE CARBON AND NITROGEN AND THEN "LOADED" WITH NITROGEN BY ANNEALING IN AN ATMOSPHERE OF 6 PCT NH_3 IN H_2 AT 550°C FOR 3 HOURS AND QUENCHED IN COLD WATER.

The frequencies of vibration used in determining the two internal friction curves shown in the figure were respectively about 1.8 and 0.38 cycles per second.

and quenched in cold water. Preliminary measurements showed that this specimen, after being tempered at 50°C for one hour, has no appreciable segregation in a period of about four days. The internal friction of this specimen was measured from -5°C to 46°C with a frequency of about 1.8 cycles per sec (Fig 6). The frequency of vibration was then lowered about five times by attaching a heavier and longer torsional arm to the specimen and the internal friction measured again from 0°C up. The measurements for this frequency were made only to 21°C in one trial. The curve could not be completed because it was found next morning that the internal friction had decreased about 5 pct at the same temperature. However, as the curve has passed over the maximum value, we can determine the heat of activation with a fair degree of accuracy.

In Fig 7 these two internal friction curves were superposed on each other by a horizontal shift of the $1000/T$ scale through

We should like to mention in passing that such an internal friction peak has been recently observed also in the interstitial solid solutions of C, N and O in tantalum which has a body-centered cubic structure.¹¹ This indicates that such anelastic phenomenon is characteristic of all interstitial solid solutions of body-centered cubic metals.

Analysis of the 225°C Peak (Peak C)

Working with 99.8 pct Baker's iron wire in cold-drawn form, West has observed elastic after-effects in the temperature range of 100 – 200°C .¹⁶ He found that low-temperature anneals diminish the ability of cold-worked material to show such after-effect, the after-effect observed at low temperatures being eliminated first. These after-effects were analyzed in terms of relaxation spectrum ψ , and the value of ψ (roughly equal to internal friction) for 6-sec relaxations at each temperature being calculated from the slope of the elastic

after-effect curves. When the ψ -values were plotted against the temperature of measurement, an "apparent" peak was found around 165°C which he considered

It is seen in Fig 5 that the height of the 225°C peak decreases with an increase of annealing temperature. It was eliminated when the specimen was completely re-

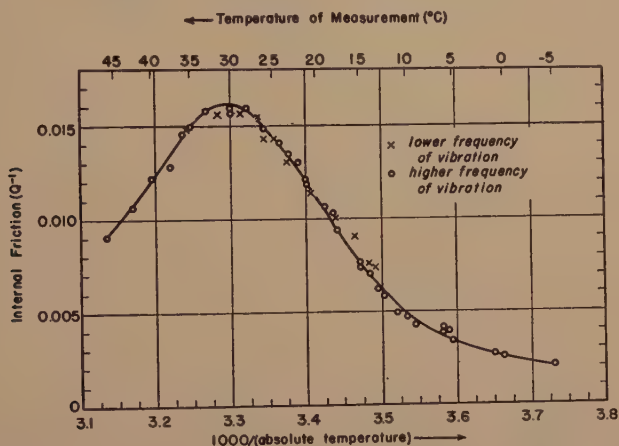


FIG 7—DETERMINATION OF HEAT OF ACTIVATION ASSOCIATED WITH PEAK A BY A RELATIVE SHIFT OF THE TWO INTERNAL FRICTION CURVES SHOWN IN FIG 6 (AFTER THEY WERE REPLOTED WITH THE INTERNAL FRICTION AGAINST $1000/T$).

These two curves were superposed on each other by a horizontal shift of the $1000/T$ scale through 0.1575.

was caused by the viscosity of slip bands. However, Snoek⁹ has observed earlier in cold-worked iron containing carbon or nitrogen a conspicuous maximum in internal friction at about 200°C with a frequency of vibration of about 0.2 cycles per sec, and he thinks the most plausible inference is that the observed damping has something to do with a pure Gorsky damping,⁸ that is, carbon or nitrogen particles migrate from regions of positive stress to regions of negative stress in the way proposed for the first time by Gorsky. Comparing the results obtained by these two workers, one finds that the relaxation phenomena they observed are the same. The shift of the relaxation peak to a lower temperature in West's work is because his data on 6-sec relaxation corresponds to a lower frequency of vibration (about 0.02 cycles per sec). As they have different opinions concerning the physical origin of this peak, it seems desirable to make a further study.

crystallized by annealing at 500°C for one hour. Consequently it must be connected in some way with the state of cold-working in the specimen.

The curves shown in Fig 8 were obtained under identical conditions as those in Fig 5, except that the Puron specimen was treated with wet hydrogen before it was cold-drawn to 56 pct RA. There is practically no 225°C peak for this specimen. After this specimen was completely recrystallized (500°C anneal for one hour), the 20°C peak rises barely over its background. This indicates that the wet hydrogen treatment did not remove every trace of nitrogen or carbon originally contained in the Puron specimen. A comparison of Fig 8 with Fig 5 is, however, sufficiently convincing to infer that the observed 225°C relaxation peak must have something to do with nitrogen or carbon. In order to find out whether the observed peak in Puron is due to carbon or nitrogen, a Puron specimen was first "purified" from nitrogen and car-

bon by wet hydrogen treatment. This specimen was loaded with nitrogen by the ammonia treatment described above. It was then drawn to about 60 pct RA and

ing is necessary for the observed relaxation peak.

The iron specimen used by West in his study was Baker's iron wire. Although an

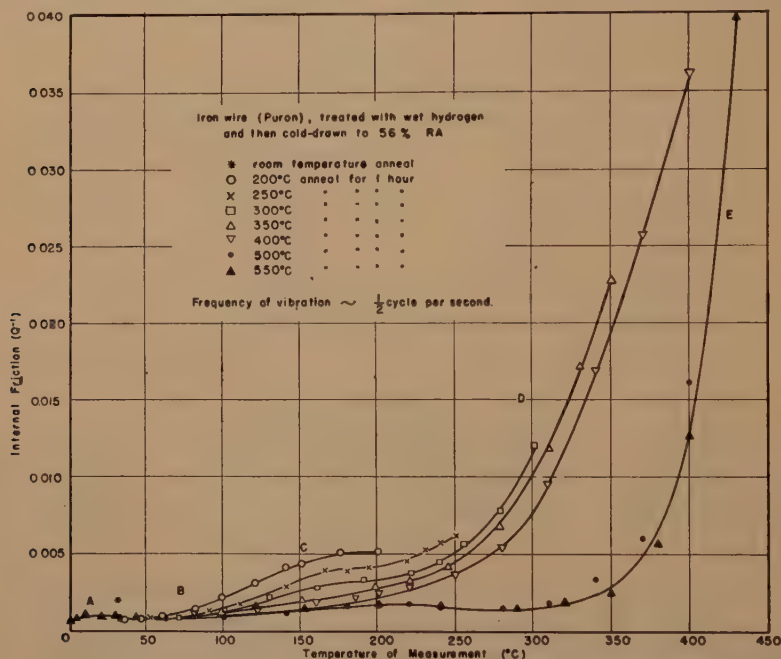


FIG 8—A SET OF CURVES OBTAINED UNDER IDENTICAL CONDITIONS AS THOSE SHOWN IN FIG 5 EXCEPT THAT THE PURON SPECIMEN WAS TREATED WITH WET HYDROGEN BEFORE IT WAS COLD-DRAWN TO 56 PCT RA.

was tempered at 350°C for one hour. The internal friction measurements were taken from room temperature up to 320°C and the results are shown in Fig 9. The frequency of vibration used was about 0.13 cycles per sec. Here the maximum internal friction occurs at the same temperature as in the case of the Puron specimen when account was taken of the difference of frequencies of vibration used in these measurements. This indicates that the peak observed in the Puron specimen used is due to nitrogen.

Experiments on annealed specimen loaded with nitrogen but without being subjected to cold-work show no relaxation peak up to 300°C. Accordingly, cold-work-

analysis of the carbon and nitrogen content in the specimen was not given, it must contain an appreciable amount either of carbon or nitrogen as the wire showed a marked lower yield after it was annealed at 850°C. Consequently the relaxation peak he observed is associated with the presence of either carbon or nitrogen in cold-worked iron and is not likely to be caused by the viscosity of slip bands.

Attempts were made to determine the heat of activation associated with the relaxation peak with the nitrogen-loaded specimen (Fig 9). It was found that this peak decreases with annealing and is not stable enough to give an accurate determination.

The heat of activation was finally deter-

mined with an original Puron specimen. The specimen was cold-drawn to 58 pct RA and then annealed at 450°C for one hour. Internal friction measurements were made with two frequencies of vibration having a

curve were brought to superpose on one another by a horizontal shift of the $1000/T$ scale through 0.15. According to Eq 8 this gives a heat of activation of

$$H = 32,000 \text{ cal per mol}$$

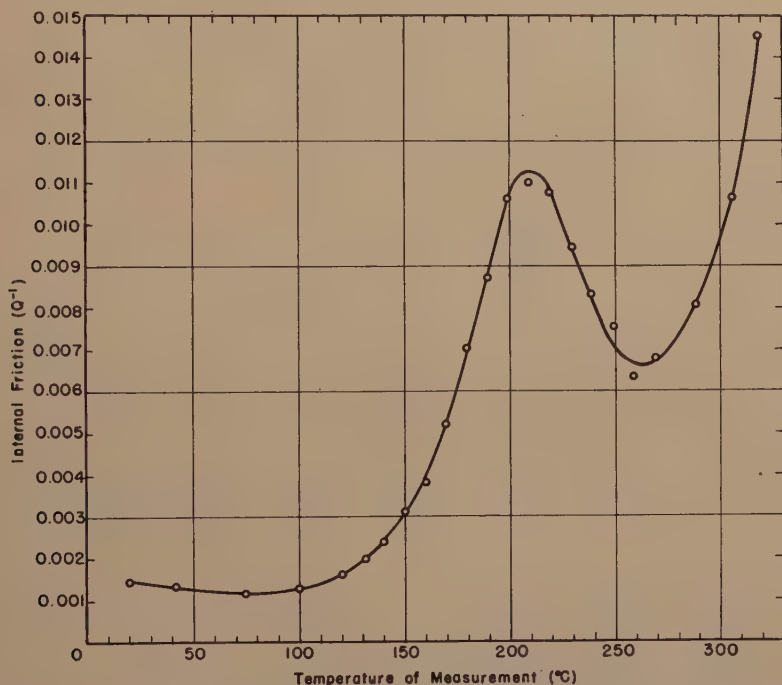


FIG 9—RELAXATION PEAK C IN PURON SPECIMEN WHICH WAS FIRST TREATED WITH WET HYDROGEN AND THEN LOADED WITH NITROGEN.

Before the internal friction measurements, the nitrogen loaded specimen was cold-drawn to 60 pct RA and then tempered at 350°C for one hour. Frequency of vibration used was about 0.13 cycles per second. Peak is C. Upper right hand branch is "relaxation D."

ratio of 11.2 (the frequencies are about 0.156 and 1.75 cycles per sec). Both internal friction curves, which are quite stable and reproducible, are shown in Fig 10 with the internal friction plotted against $1000/T$, where T is the temperature of measurement in absolute scale. At the higher-temperature side of both curves, the "relaxation peak C" is overlapping with "relaxation D" to be discussed later. Consequently only the low-temperature side of the curves can be relied upon in the determination of the heat of activation. In Fig 11, the low-temperature parts of each

This value is much larger than the value 21,000 cal per mole found by West, but lies within the limit of Snoek's value of from 24,000 to 40,000 cal per mole.

In Fig 10 a smaller shift brings "relaxation D" of two corresponding curves to superpose. This indicates that the heat of activation associated with "relaxation D" is larger. A crude estimation gives a value of about 50,000 cal per mole.

A glance at Fig 10 shows that the two relaxations have resolved better in the lower frequency curve than in the higher frequency curve. This illustrates a general

principle of resolving two over-lapping relaxations having different heats of activation by changing the frequency of vibration.

peak in a stress-induced diffusion process implies that the diffusion distance involved is finite. Although the exact diffusion mechanism is not known, we can estimate

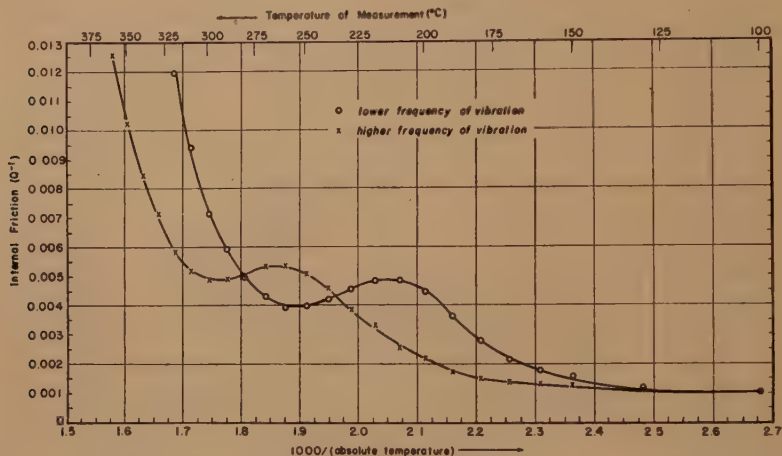


FIG 10—RELAXATION PEAK C IN ORIGINAL PURON SPECIMEN AFTER IT WAS COLD-DRAWN TO 58 PCT RA AND THEN ANNEALED AT 450°C FOR ONE HOUR.

The two frequencies of vibration used in determining the two internal friction curves shown in the figure were respectively about 0.156 and 1.75 cycles per second. Notice that high-temperature side of each curve was mixed up with "relaxation D." Peak is C. Upper left hand branch is "relaxation D."

Summarizing the information obtained so far concerning the 225°C peak, we can conclude that the sufficient conditions for the occurrence of this relaxation peak are that an iron specimen contains a small amount of nitrogen and has been subjected to cold-work. Since there is a heat of activation associated with this relaxation, these observations suggest that we are concerned with the stress-induced diffusion of nitrogen within some peculiar type of stress regions produced by cold-working. The diffusion process involved must be quite different from the interstitial diffusion of nitrogen in solid solution of iron because the relaxation peak now concerned is mutually exclusive with the 20°C peak which is caused by the stress-induced interstitial diffusion of nitrogen atoms in annealed iron. This also indicates that the simple picture of Gorsky's type of damping mentioned by Snoek cannot be adequate.

The existence of an internal friction

the over-all distance over which the nitrogen is diffusing under the influence of the applied stress.

For a diffusion process, we have the general relation

$$x^2 \sim Dt$$

where x is the average distance covered by the diffusing particle, D the diffusion coefficient and t the time of diffusion which can be taken in the present case as the relaxation time τ . At a temperature T we have

$$x^2 \sim D_0 e^{-H/RT} \cdot \tau_T \quad [9]$$

where D_0 is the diffusion constant and H the heat of activation for diffusion which can be taken as the heat of activation associated with the relaxation (32,000 cal per mole). At 210°C (438°K), the temperature at which the internal friction is a maximum (see Fig 10), the frequency of vibration is 0.124 cycle per sec. The time of

relaxation at this temperature is thus, according to Eq 3, 1.28 sec. To estimate the diffusion distance which is independent of temperature, we have all the

a maximum value of about 0.08. Converting this to the engineering term specific damping capacity defined as the ratio of the energy ΔE dissipated per cycle to the

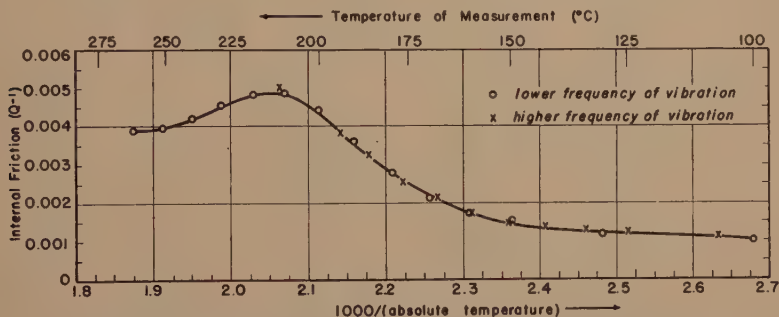


FIG 11—DETERMINATION OF THE HEAT OF ACTIVATION ASSOCIATED WITH PEAK C BY A RELATIVE SHIFT OF THE TWO INTERNAL FRICTION CURVES SHOWN IN FIG 10.

These two curves were superposed on each other by a horizontal shift of the $1000/T$ scale through 0.15.

necessary data except D_0 which can not be evaluated unless the mechanism of diffusion was understood. Fortunately, this constant does not change appreciably for different diffusion processes and its contribution to x^2 in Eq 9 is much less important in comparison with that of the exponential term. If we can apply Dushman-Langmuir diffusion formula²⁰ to the present case, we have

$$D_0 = HJd^2/N_0h$$

where h is Planck's constant, N_0 the Avogadro's number, J the mechanical equivalent of heat, H the heat of activation in cal per mol and d the distance involved in an elementary jump which can be taken as approximately equal to the lattice constant (2.86 Å for iron). This gives $D_0 = 0.28$ cm²/sec. Substituting this and $T = 483^\circ\text{K}$, $\tau\tau = 1.28$ sec and $H = 32,000$ cal per mol in Eq 9 we get $x \sim 4\text{Å}$, indicating that the average diffusion distance of nitrogen atoms is of the order of a few atomic diameters.

Analysis of the 490°C Peak (Peak E)

The 490°C peak shown in Fig 5 is unique in its magnitude. The internal friction has

average energy E of vibration per cycle, we have

$$\Delta E/E = 2\pi Q^{-1} = 50 \text{ pct}$$

Although this conversion formula is strictly true only when the quantities involved are small, nevertheless it gives a fairly good idea as to the damping magnitude. Such a high damping capacity deserves special attention because it seems to occur in all polycrystalline metals under appropriate conditions but not in single crystals.^{12,13,14} By an extensive quantitative study with various kinds of anelastic measurements, it has been demonstrated in the case of 99.991 pct aluminum that this damping peak has its physical origin in the viscous behavior of the grain boundaries in metals.^{13,14} In the present study of this grain boundary peak in iron, more evidence was obtained which should be able to clarify some skepticism on the viscous behavior of grain boundaries. Furthermore, an attempt is made to understand the mechanism of grain boundary slip which may contribute to the study of creep of metals.

There is no method known at present of determining the actual structure of grain

boundaries in metals. However, when two crystals of different orientations meet, the transition zone between the two crystals must possess a disturbed crystallinity. Consequently, whatever the nature of the grain boundary may be, an intercrystalline amorphous cement or a transitional atomic layer, it can equally well behave in a viscous manner when the boundary region is considered as an entity. Such a phenomenological consideration is fruitful for the purpose of understanding the mechanism of plastic deformation and fracture in polycrystalline metals. By viscous behavior we mean that the grain boundary can not sustain a shear stress permanently and it has a coefficient of viscosity decreasing with an increase of temperature. In the introductory chapter of this paper, we have described in some detail how the viscous behavior of grain boundaries can cause anelastic effects under appropriate conditions. In the case of internal friction measurements, one can predict that as the temperature of the polycrystalline specimen is raised, the internal friction associated with the viscous slip along the grain boundaries will have a maximum value. The reason for this is similar to the case of stress-induced atomic diffusion described above. At low temperatures, the rate of slip at the boundary is low because the viscosity is high. The distance slipped in a half-cycle of the applied stress will thus be negligibly small in comparison with the total amount of possible slip which is a function of the grain size of the specimen. The deformation is thus essentially in phase with the stress and consequently the internal friction is small. At very high temperatures, the rate of slip is very high because of the low viscosity at the boundary. The total permissible slip will be completed in but a small fraction of the time in a half-cycle and again the deformation is essentially in phase with the stress most of the time. Consequently the internal friction will again be small. Only

in an intermediate temperature range when the time for the completion of the slip (or roughly speaking, the relaxation time) is comparable with the period of the applied cyclic stress will the internal friction be appreciable. Such a maximum has been observed in the case of aluminum,¹³ magnesium¹³ and alpha-brass.¹² Using elastic after-effect on unloading, West¹⁶ has observed in 99.8 pct iron some high-temperature after-effect for which the relaxation spectrum (roughly equal to internal friction) increases rapidly up to 550°C, the highest temperature of measurement. He suggested that this after-effect is due to shear-stress relaxation along grain boundaries. With reference to the previous results obtained in other metals, it is natural to believe that the 490°C peak (Peak *E*) obtained in recrystallized Puron as shown in Fig 5 has its origin in the grain boundaries. In order to demonstrate the effect of grain size of the specimen upon the observed internal friction peak, the recrystallized Puron specimen was annealed at still higher temperatures, namely at 750°C and at 850°C for one hour in vacuum. However, no appreciable change in the internal friction peak was observed after such treatment except that there was a slight decrease in the high-temperature branch of the curve, probably due to the decrease of the "relaxation *F*" by annealing (Fig 5). Metallographic examination of the specimens showed that no detectable grain growth had occurred. In the case of 99.991 pct aluminum where grain growth was obtained by annealing at successively higher temperatures, an increase of grain size of the specimen had shifted the internal friction curve (versus temperature) to higher temperatures.¹⁴ An attempt had been made to achieve grain growth by annealing the specimen in an atmosphere of wet hydrogen before the final annealing but the procedure met with little success. It was thus decided to prepare large grains following the general procedure used by

Edward and Pfeil.²¹ The original Puron specimen was first treated with wet hydrogen at 750°C, stretched about 3 pct, annealed at 850°C for about 10 hr in vacuum

ration of the specimen having very large grains. This specimen was annealed also at 850°C for about 10 hr; the only difference was that the 3 pct intermediate stretching

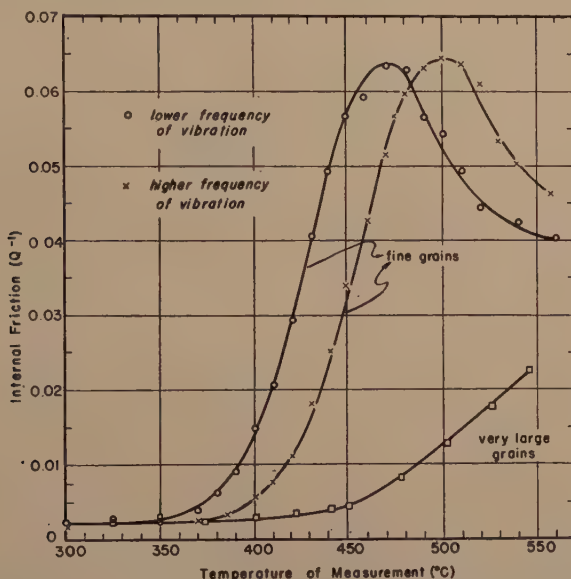


FIG 12—VARIATION OF INTERNAL FRICTION WITH TEMPERATURE OF VERY FINE-GRAINED AND VERY LARGE-GRAINED PURON SPECIMENS PREPARED BY IDENTICAL HEAT TREATMENT (850°C ANNEAL IN VACUUM) EXCEPT THAT THE 3 PCT INTERMEDIATE STRETCHING WAS OMITTED IN THE PREPARATION OF THE FINE-GRAINED SPECIMEN.

The two internal friction curves for the fine-grained specimen were determined with frequencies of vibration of respectively about 1.76 and 0.26 cycles per second at room temperature. The longitudinal load on the wire in the measurements with the lower-frequency of vibration was about seven times greater.

and then furnace-cooled. Very large grains were obtained after such treatment. They were several millimeters long, which was much larger than the diameter of the wire specimen. The variation of internal friction with temperature for this specimen was determined and shown in Fig 12. The internal friction is comparatively small up to a temperature of 550°C with no peak around 490°C as in the case of fine-grained specimen.

In order to demonstrate that the peak E shown in Fig 5 can not be due to the effect of cold-working which might persist even after the specimen was recrystallized, a fine-grained specimen was prepared following the same procedure as for the prepa-

ration of the specimen having very large grains. This specimen was annealed also at 850°C for about 10 hr; the only difference was that the 3 pct intermediate stretching was omitted. In this case a rather fine-grained specimen was obtained, having an average grain size of about 0.003 cm. The 850°C annealings were all done in a vacuum furnace with the specimen lying straight and free. After this treatment, the specimen was mounted for measurement in the torsional apparatus. Extra care was taken to reduce the disturbance to the wire to a minimum. A very light torsional arm was used for the measurements. The total load on the wire was about 23 g. Since the diameter of the wire was about 0.033 in., this longitudinal load amounted to about 60 psi. The internal friction curve for this specimen is shown in Fig 12 (the curve with crosses). It is seen that the in-

ternal friction peak occurs around 500°C; and at this temperature, the frequency of vibration is 1.62 cycles per sec (see the lower curve in Fig 13). As the fine-grained

quite stable with respect to the time and temperature of annealing provided that the annealing temperature did not exceed the highest temperature at which the specimen was previously annealed.

To make a decisive test on this point, a torsional arm about seven times heavier than the first arm was attached to the same specimen. The frequency of vibration was then much lower. With this torsional arm, the longitudinal load on the wire was about 400 psi. The internal friction curve determined under this condition is shown in Fig 12 (the curve with circles). The shape and the height of the curve are similar to the higher frequency curve except it was shifted to lower temperatures as is expected in a relaxation process.

From the relative shift of these two curves, the heat of activation associated with the grain boundary relaxation can be determined according to Eq 8. As the relaxation effect concerned is very large, the natural frequency of vibration is no longer constant over the whole range of the temperature of measurement. The variation of the frequency with temperature is shown in Fig 13 for both frequencies. It was found, however, that the ratio of the two frequencies is almost constant over the whole temperature range. The average ratio was found from Fig 13 to be 7.73. In Fig 14 it is shown that the two curves (plotted against $1000/T$) can be brought to superpose on each other by a horizontal shift of the $1000/T$ scale through 0.048. This gives a heat of activation of

$$H = 85,000 \text{ cal per mol}$$

which should be accurate to within 10 pct.

The higher temperature branch of the internal friction peak did not descend as it should if the entire peak were due to the grain boundary relaxation. This has also been observed in the case of other metals (aluminum, magnesium and alpha-brass). It was thought that a new type of relaxation came in and it was labeled F in

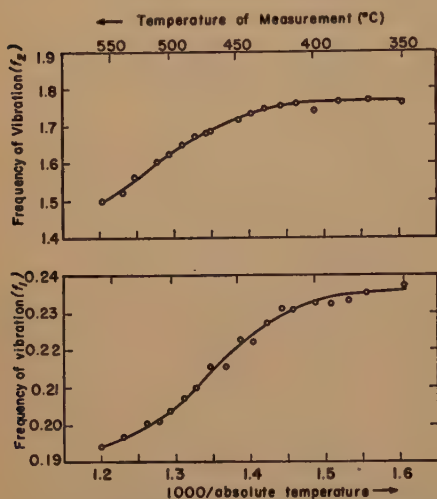


FIG 13—VARIATION OF NATURAL FREQUENCY OF VIBRATION WITH TEMPERATURE OF THE FINE-GRAINED PURON SPECIMEN.

The upper curve is for the higher and the lower curve is for the lower frequency of vibration. The ratio of the two frequencies was found to have a constant value of 7.73, over the temperature range concerned.

specimen and the very large grained specimen were prepared using similar procedures, we have reason to believe that the existence of a peak in the case of the fine-grained specimen can be attributed only to the grain boundaries.

In the above measurements, the longitudinal load on the wire was about 60 psi. The question may arise as to whether this longitudinal load might have stretched the wire during the measurement especially at higher temperatures and this might cause the observed internal friction peak. It seems improbable that such a small load should cause any appreciable change in the specimen. The logarithmic decrement curves shown in Fig 4 seem to indicate that no change could have been made during the measurement. Furthermore, the internal friction peak was found to be

Fig 5 to be discussed later. As can be seen from Fig 12, however, when the frequency of vibration is changed, the higher temperature branch of the internal friction curve, which is presumably a combination of the grain boundary relaxation and "relaxation

can be estimated according to Eq 3. We have thus

$$\tau = \frac{1}{2}\pi f$$

or

$$\tau_{470^{\circ}\text{C}} = 0.748 \text{ sec}$$

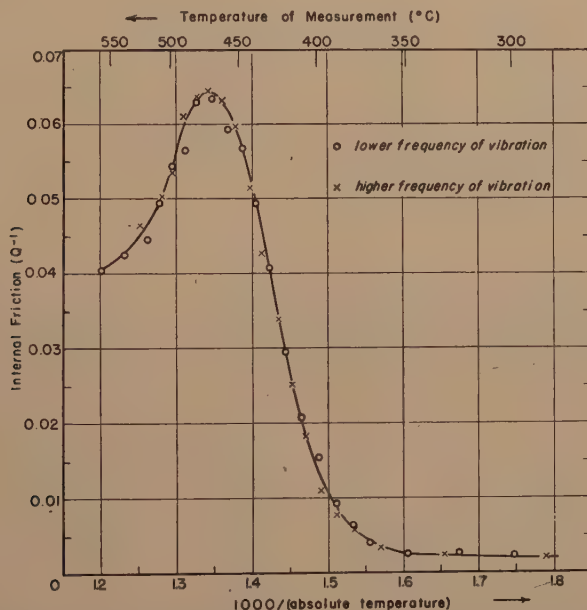


FIG 14—DETERMINATION OF THE HEAT OF ACTIVATION ASSOCIATED WITH RELAXATION PEAK *E* BY A RELATIVE SHIFT OF THE TWO INTERNAL FRICTION CURVES SHOWN IN FIG 13, AFTER THEY WERE REPLOTTED WITH INTERNAL FRICTION AGAINST $1000/T$.

These two curves were superposed on each other by a horizontal shift of the $1000/T$ scale through 0.048.

F," shifted the same amount as the lower-temperature branch of the curve which is presumably entirely due to grain boundary relaxation. This may indicate that the heat of activation associated with "relaxation *F*" is nearly equal to that associated with grain boundary relaxation.

From the lower-frequency curve shown in Fig 12, we can see that the optimum internal friction occurs at a temperature of 470°C . The natural frequency of vibration at this temperature is, from the lower curve of Fig 13, 0.213 cycles per sec. With these data, the "mean" relaxation time associated with the grain boundary relaxation

Now from Eq 1, we have

$$\tau = \tau_0 e^{H/RT}$$

and τ_0 can be determined from the condition that $\tau = 0.748 \text{ sec}$ at 470°C , whence we get

$$\tau = 1.09 \times 10^{-25} e^{42,500/T} \quad [9]$$

We have emphasized repeatedly that our study on grain boundary is only phenomenological and that the viscous behavior of the grain boundaries is contemplated in the sense that the grain boundary can not sustain a shear stress permanently and it has a coefficient of viscosity decreasing

with an increase of temperature. Following is an estimation of the viscosity of the grain boundary as manifested by its behavior of relaxing shear stress.

Consider a grain boundary with an "effective thickness" d . Then the coefficient

and thus $v \cong s(G.S.)/G_U\tau$, whence we may estimate η from the following formula

$$\eta = G_U\tau d/(G.S.) \quad [11]$$

It is seen from Eq 11 that the temperature dependence of η is primarily

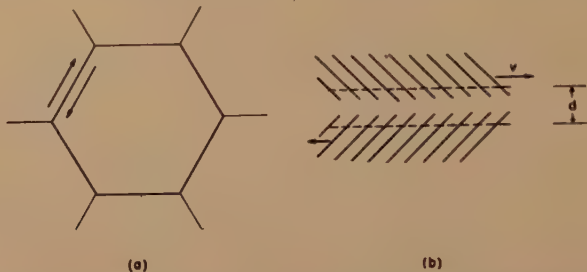


FIG 15—(a) EXAMPLE OF EQUIAXED GRAINS. (b) ILLUSTRATION OF THE POSSIBLE CONDITION AT THE GRAIN BOUNDARY.

The parallel lines indicate the regular lattice planes. The effective thickness of the grain boundary was indicated by d which includes the region in which the atoms belonging to the lattice of one grain are influenced by those in the adjacent grain.

cient of viscosity may be defined in a conventional way by

$$\eta = s/(v/d) \quad [10]$$

where s is the shearing stress and v is the rate of relative displacement of the two sides of the boundary. The thickness of the grain boundary is not known from experimental work. However, if the grain boundary is assumed to include the region in which the atoms belonging to the lattice of one grain are influenced by those in the adjacent grain (Fig 15b), then the effective thickness of the grain boundary may be considered of the order of a few atomic distances. Take the case of equiaxed grains as shown in Fig 15a. Let Δx be the distance slipped along the grain boundary during the time τ where τ is the time of relaxation, then $v \cong \Delta x/\tau$. The elastic shear strain in the immediate vicinity of the boundary accompanying this slip is given approximately by $e \cong \Delta x/(G.S.)$, where $(G.S.)$ is the average grain diameter of the specimen. As this elastic strain is defined by $e = s/G_U$, where G_U is the unrelaxed shear modulus or the shear modulus when no relaxation has taken place, we have $\Delta x/(G.S.) \cong s/G_U$,

through the time of relaxation τ because d and $(G.S.)$ are independent of and G_U varies only slightly with the temperature of measurement.

The unrelaxed shear modulus of iron is of the order of magnitude of 10^{12} dynes per cm^2 and we can take d as of the order of magnitude of 10 \AA . Since the average grain diameter for the alpha-iron specimen is about 0.003 cm , we have, by combining Eq 11 and Eq 9

$$\eta\tau = 4 \times 10^{-18} e^{42,000/T} \quad [12]$$

by which we can estimate the grain boundary viscosity in the alpha-iron specimen at various temperatures.

It is evident that the grain boundary viscosity as manifested by its behavior of relaxing shear stress will depend upon many metallurgical factors in addition to grain size. In the case of 99.991 pct aluminum, internal friction measurements have demonstrated that the grain boundary viscosity is lower in a specimen subjected to a heavier plastic deformation prior to recrystallization.²² A study of the effect of impurities upon grain boundary viscosity has also been made and will be reported

in a later paper. In spite of all these, the estimated values of grain boundary viscosity at some particular temperatures shown in Table 1 are quite illustrative.

TABLE 1—*Estimated Values of the "Grain Boundary Viscosity" in Alpha-Iron at Several Temperatures.*

T		η (poise)
(°C)	(°K)	
20	293	10^{45}
400	673	10^{10}
500	773	10^6
600	873	10^4
910	1183	10^{-2}

The viscosity at room temperature is extremely high and therefore no grain boundary relaxation can occur. The internal friction peak observed in alpha-iron covers approximately the temperature range of 400–600°C, where the coefficient of viscosity decreases from 10^{10} to 10^3 poise. If we should take phenomenological analogy literally, we might compare these figures with those of Pyrex glass which is known to behave in a viscous manner. The working range for glass blowing is when the viscosity of the glass lies between 10^{10} to 10^4 poise.²³ It is to be noted that the grain boundary viscosity at 910°C, the transition temperature of alpha-iron to gamma-iron, is 10^{-2} poise, which is of the same order of magnitude as the coefficient of viscosity of molten iron.

As described above, the heat of activation associated with grain boundary relaxation in alpha-iron as determined by internal friction measurements is 85,000 cal per mole within an accuracy of 10 pct. Using radioactive iron from the atomic pile and Westinghouse Puron iron, the self-diffusion coefficients in alpha and gamma iron have been recently determined by Birchenall and Mehl.²⁴ The preliminary results they reported gave a value of 77,200 cal per mol for the activation energy of alpha-iron. These two values agree within

experimental error. Such an agreement has also been found in the case of alpha-brass (29 pct Zn),¹² where the activation energy associated with the grain boundary relaxation was found to be 41,000 cal per mol which is close to the value of 41,700 cal per mol for the diffusion of zinc (29.08 pct) in alpha-brass. In the case of aluminum, the heat of activation associated with the grain boundary relaxation has been found to be 34,500 cal per mol.¹³ Unfortunately the activation energy for self-diffusion in aluminum has not been determined by direct experiment because there are no known radio-active isotopes of satisfactory half-life. However, this activation energy may be estimated roughly on the basis of melting point and of binding energy of aluminum.²⁵ It was observed by Johnson²⁶ that the ratio of the activation energy to the melting temperature for certain face-centered cubic metals ranges from about 37 to 45, and the ratio of the activation energy to the binding energy for the same metals ranges from about 0.6 to 0.75. From these limits, the activation energy for the self-diffusion of aluminum, which is a face-centered cubic metal, was estimated to be $37,500 \pm 4,000$ cal per mol. The grain boundary activation energy for aluminum lies within these limits.

If such an agreement in activation energies for grain boundary slip and for volume diffusion were found to be a general phenomenon for all metals, this would indicate that the grain boundary slip involves the same mechanism as does volume diffusion. In our study of the mechanical behavior of the grain boundaries in metals, the grain boundary is considered as an entity whatever its nature may be, an intercrystalline amorphous cement or an atomic transitional layer. If the grain boundary slip involves the same mechanism as does the volume diffusion in the interior of the grains, that would imply, as far as the local order is concerned, the structure of the grain boundary region can not be markedly different

from that of the interior of the grains. The grain boundary slip can thus be considered as creep on a microscopic scale, and this creep occurs at a lower temperature than creep in single crystals because

boundaries has been complete, G_U the shear modulus when no slip occurs across the grain boundaries, and s is the Poisson's ratio. As the value of s covers the range from $\frac{1}{2}$ to $\frac{1}{4}$ for most metals, the theoretic-

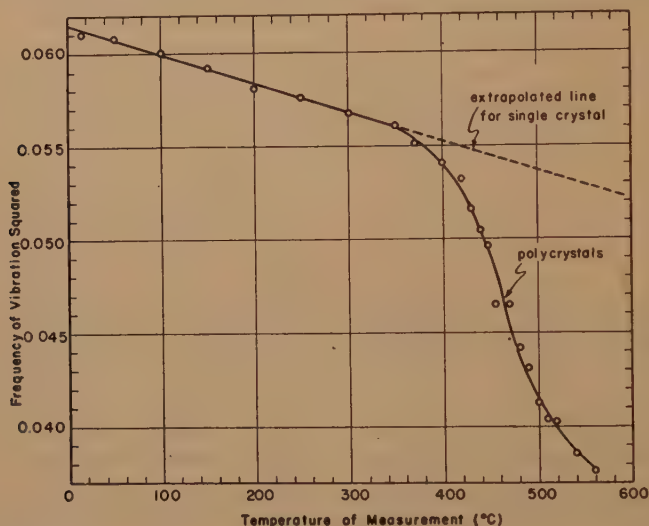


FIG 16—VARIATION OF "SHEAR MODULUS" WITH TEMPERATURE OF FINE-GRAINED PURON SPECIMEN

of the disturbed crystallinity at the grain boundary. This viewpoint is strengthened by the observation that the activation energies for the creep in these metals mentioned above are comparable with that of grain boundary slip.²⁷

The viscous behavior of grain boundaries in metals implies also that when an over-all stress, however small, is applied to a polycrystalline specimen, the shear stress across all grain boundaries will gradually relax. The locking effect of the grain edges and corners will insure that the over-all stress relaxation will be of limited extent for a fixed over-all strain. The theoretical maximum shear relaxation is²⁸

$$1 - G_R/G_U = 1 - 2(7 + 5s)/5(7 - 4s) \quad [13]$$

where G_R is the shear modulus of a polycrystalline specimen in the case where the grain boundaries are viscous and the relaxation of shear stress across the grain

cal value of the maximum shear stress relaxation is, according to Eq 13, from 24 to 45 pct.

The temperature variation of the shear modulus (which is proportional to the square of the natural frequency of vibration) in a fine-grained Puron specimen is shown in Fig 16. The curve is essentially a straight line at low temperatures and there is a rapid change in curvature around 320°C. This rapid change occurs at a higher temperature for specimens having very large grains. Reference to the previous works on other metals^{12,13} justifies the statement that the curve for single crystals will run along the extended line indicated in Fig 16.

Since there is no grain boundary in a single crystal, the extended line can be considered as the curve for the unrelaxed modulus G_U . Let $G(T)$ be the dynamic shear modulus in polycrystalline iron at

the temperature T , then we have

$$G(T)/G_U = (f_p/f_s)^2 \quad [14]$$

where f_p and f_s are respectively the frequency of vibration in polycrystalline and

relative to the viscous slip along the grain boundaries. When we consider the grain boundary as a transitional region, this boundary region and the neighboring grains are not sharply divided. If the grain

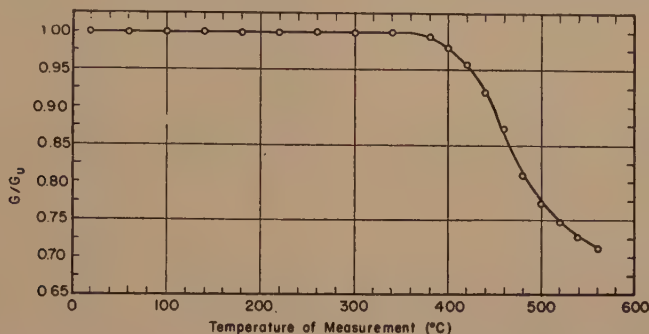


FIG 17—RELAXATION OF SHEAR MODULUS IN FINE-GRAINED PURON SPECIMEN.

single crystal iron at the temperature T . The ratio $G(T)/G_U$, calculated from Fig 16, is plotted as a function of the temperature of measurement in Fig 17. It can be seen that the grain boundary relaxation has not been completed at the highest temperature of measurement but we can infer that G_R/G_U is smaller than, but is close to, 0.70. The over-all stress relaxation across the grain boundaries in the Puron iron specimen is thus greater than, but is close to, 30 pct. This lies within the theoretical value of from 24 to 45 pct given above.

The percentage over-all shear stress relaxation across the grain boundaries is of limited extent as demonstrated above. This implies that the viscous slip along the grain boundaries is also of limited extent. Such a limited creep has been observed in the case of aluminum in measurements of creep under constant stress.¹³ This creep is limited because of the blocking effect of the grain edges and corners. When stress is applied to a polycrystalline specimen, undoubtedly there will be some sort of readjustment at the grain edges and corners. However, when the applied stress is very small as in the present experiments, the edges and corners will move very little so they can be considered as essentially fixed

boundary is blocked at grain corners, the question may arise as to what will happen to the regions of the grains next to the grain boundary when viscous slip is occurring at the boundary. This situation may be illustrated in Fig 18, in which the grain boundary region is indicated by the region between the two dotted lines and its neighboring regions in the grains by two elastic springs. These springs are fastened on two supports representing the grain corners shown in Fig 15a. As illustrated, the springs can be elastically deformed even when they are fixed at both ends. If the viscous slip along the boundary is Δx , then the elastic displacement at the immediate vicinity of the boundary must also be Δx . Such a relationship has been utilized before in deriving a formula for the estimation of grain boundary viscosity.

If shear stress is relaxed along the grain boundaries, then stress must be concentrated at the grain edges or corners. Under proper conditions, the local stress concentration may be large enough to initiate cracks or slip at the grain edges or corners.

Relaxations B, D and F

On comparing Fig 5 with Fig 8, it can be seen that if we could remove the carbon

and nitrogen completely from the Puron specimen with the complete elimination of the relaxation peak *C*, then relaxations *B* and *D* would merge into a single region in

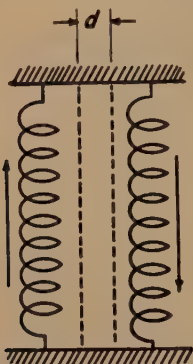


FIG 18—FIGURATIVE ILLUSTRATION OF THE SITUATION AT THE GRAIN BOUNDARY.

which the internal friction increases continuously with an increase of temperature. As the existence of an internal friction peak (either versus frequency of vibration or versus temperature of measurement) is a necessary and sufficient condition for establishing an anelastic effect in the strict sense, no conclusive information can be derived from relaxations *B* and *D* because no peak has been observed. However, a plausible argument can be made based on experimental results on these relaxations. These results are consistent with the viewpoint that the slip bands or the highly disorganized regions formed in cold-worked material behave in a viscous manner similar to grain boundaries. As shown in Fig 8 the internal friction associated with relaxations *B* and *D* at any given temperature is lower the higher the temperature of prior anneal. This is consistent with the concept that the highly disorganized material in the slip bands acquires gradually the order of the surrounding undeformed material as the specimen is annealed. For any given temperature of prior anneal, the internal friction is higher the higher the temperature of measurement. This is consistent with the

viewpoint that the rate of shearing strain within the slip band material increases rapidly with an increase of temperature. In other words, the viscosity associated with the slip band material decreases rapidly with an increase of temperature. Extensive results have been obtained in the case of cold-worked polycrystalline and single crystal aluminum,²⁹ indicating that this phenomenon is common to all metals.

Experiments show that relaxation *D* does not depend on the original grain size of the specimen before it was subjected to cold-work. This indicates that relaxation *D* is not caused by the stress relaxation across the old grain boundaries in the deformed metal.

The viscous behavior of slip band material is only one of the plausible concepts which can give a consistent explanation to the variation of internal friction with the temperature of measurement and of annealing. There was no conclusive experimental evidence, so far, to show that the internal friction in regions *B* and *D* is necessarily due to the slip bands in cold-worked material. However, it has been recently observed by Burke and Barrett³⁰ that the slip lines in deformed alpha-brass specimens are eliminated only after the specimens were completely recrystallized. If this is also true in the case of deformed alpha-iron, that would indicate the relaxation *D* is connected with these slip lines. In both Fig 5 and 8 there is an abrupt drop in internal friction in region *D* after the specimen was completely recrystallized (500°C anneal for one hour).

Very little can be said about the relaxation *F* which occurs at the highest temperature of measurement. As has been described above, the internal friction associated with this relaxation decreases when the specimen is annealed at successively higher temperatures after the specimen has recrystallized (Fig 5). This suggests that this relaxation might be caused by the imperfections in the specimen created by cold-working which could not be removed even after the speci-

men was recrystallized. This viewpoint is supported by previous observations in the case of aluminum¹³ which showed that this relaxation is quite sensitive to the amount of cold-working on the specimen prior to recrystallization. As the heat of activation associated with this relaxation is comparable to that associated with creep in metals, this relaxation might be a manifestation of creep in metal crystals.

SUMMARY

Internal friction measurements in torsion were made on Westinghouse Puron specimens containing as chief impurities approximately 0.040 pct oxygen, 0.005 pct carbon and 0.004 pct nitrogen. Starting with a cold-worked Puron wire, the internal friction was determined by free decay method after the specimen had been annealed at successively higher temperatures from 50°C to 600°C. Measurements were made after each anneal from room temperature up to the annealing temperature and the frequency of vibration used in each case was of the order of one cycle per second. When the internal friction was plotted as a function of temperature of measurement, three internal friction peaks were found around the temperatures 20, 225 and 490°C, and in addition, three regions were found over which the internal friction varies with temperature.

Experiments were then designed to analyze these relaxation phenomena separately with special emphasis placed on the three internal friction peaks.

(1) It has been found that the 20°C peak is caused by the anelasticity associated with the stress-induced preferential distribution of nitrogen atoms among the various interstitial positions in the solid solution of iron, an extensive study of which had been previously made by Snoek. The heat of activation associated with this relaxation for the case of nitrogen was determined by internal friction measure-

ments to be 20,000 cal per mol with an accuracy of within 10 pct.

(2) The 225°C peak which had been observed previously by Snoek and by West was found to be caused by the stress-induced diffusion of nitrogen atoms within some peculiar type of stress regions created in the specimen after it was subjected to cold-work. Although the mechanism of this diffusion is not understood, relaxation experiments indicated that the heat of activation for this diffusion is 32,000 cal per mol and the diffusion distance is of the order of a few atomic diameters.

(3) The 490°C peak was found to be caused by the grain boundary relaxation in alpha-iron, and is similar to the grain boundary relaxation previously observed in the case of aluminum, magnesium and alpha-brass. The heat of activation associated with this relaxation was found to be 85,000 cal per mol, which agrees, within experimental error, with the activation energy for self-diffusion in alpha-iron. Such an agreement in activation energies for grain boundary relaxation and for volume diffusion had been previously found in the case of alpha-brass and probably also in aluminum. This may indicate that the viscous slip along grain boundaries involves a process of volume diffusion or accelerated creep.

(4) By plausible arguments the additional relaxations observed in the temperature range from room temperature to the recrystallization temperature of the specimen were shown to be caused by the viscous behavior of the slip band material, and the relaxation at very high temperatures might probably be due to the imperfections in the specimen created by cold-working which could not be removed even after the specimen was recrystallized.

ACKNOWLEDGMENT

The author is indebted to Professor Clarence M. Zener for his active interest in the research program. Thanks are due to

him, Professor Cyril S. Smith and Professor Charles S. Barrett for their reading of the manuscript with valuable criticisms. It is a pleasure to acknowledge the help of many members of this Institute, especially that of Mr. Edward C. Garst and Mr. Morton Schneider in taking the measurements.

REFERENCES

1. C. Zener: Anelasticity of Metals. TP 1992, *Mel. Tech.* (Aug. 1946); *Trans. AIME* (1946), **167**, 155.
2. C. Zener: Elasticity and Anelasticity of Metals. Univ. of Chic. Press, (1948).
3. Andrew Gemant: The Problem of Reduction of Vibrations by Use of Materials of High Damping Capacity. *Jnl. Appl. Phys.* (1944), **15**, 33.
4. C. Zener: Theory of Internal Friction in Reeds. *Phys. Rev.* (1937), **52**, 230; General Theory of Thermoelastic Internal Friction. *Phys. Rev.* (1937) **53**, 90.
5. C. Zener, W. Otis and R. Nuckolls: Experimental Demonstration of Thermoelastic Internal Friction. *Phys. Rev.* (1937), **53**, 100.
6. R. H. Randall, F. C. Rose and C. Zener: Intercrystalline thermal currents as a source of internal friction. *Phys. Rev.* (1939), **56**, 343.
7. C. Zener and R. H. Randall: Variation of Internal Friction with Grain Size. *Trans. AIME* (1940), **137**, 41.
8. W. S. Gorsky: On the Transitions in the CuAu Alloy, III, On the Influence of Strain on the Equilibrium in the Ordered Lattice of CuAu. *Phys. Ztsch. Sow.* (1934), **6**, 77.
9. J. L. Snoek: Effect of Small Quantities of Carbon and Nitrogen on the Elastic and Plastic Properties of Iron. *Physica* (1941), **8**, 711.
10. C. Zener: Stress Induced Preferential Orientation of Pairs of Solute Atoms in Metallic Solid Solution. *Phys. Rev.* (1947), **71**, 34.
11. T. S. Kê: Internal Friction in the Interstitial Solid Solutions of C and O in Tantalum. *Phys. Rev.* (1948), **74**, 9.
Stress Relaxation by Interstitial Atomic Diffusion in Tantalum. *Phys. Rev.* (1948), **74**, 16.
Internal Friction and Precipitation from the Solid Solution of N in Tantalum. *Phys. Rev.* (1948), **74**, Oct. 15 issue.
12. T. S. Kê: Viscous Slip Along Grain Boundaries and Diffusion of Zinc in Alpha-brass. *Jnl. Appl. Phys.* (1948), **19**, 285.
13. T. S. Kê: Experimental Evidence on the Viscous Behavior of Grain Boundaries in Metals. *Phys. Rev.* (1947), **71**, 533.
14. T. S. Kê: Stress Relaxation Across Grain Boundaries in Metals. *Phys. Rev.* (1947), **72**, 41.
15. T. S. Kê: On the Viscous Behavior of Slip Bands. Unpublished technical reports.
16. W. A. West: Elastic After-effects in Iron Wires from 20°C to 550°C. TP 1993, *Mel. Tech.* (Aug. 1946); *Trans. AIME* (1946), **167**, 192.
17. C. Zener: Mechanical Behavior of High Damping Metals. *Jnl. Appl. Phys.* (1947), **18**, 1022.
18. L. J. Dijkstra: Elastic Relaxation and Some Other Properties of the Solid Solution of Carbon and Nitrogen in Iron. Philips Res. Reports (1947), **2**, 357.
19. L. J. Dijkstra: private communication.
20. S. Dushman and I. Langmuir: The Diffusion Coefficient in Solids and its Temperature Coefficient. *Phys. Rev.* (1922), **20**, 113.
21. C. A. Edwards and L. B. Pfeil: The Production of Large Crystals by Annealing Strained Iron. *Jnl. Iron and Steel Inst.* (1924), **109**, 129.
22. T. S. Kê: Atomic Vacancy and the Viscosity of Grain Boundaries in Metals. *Phys. Rev.* (1947), **72**, 534A.
23. J. Strong: Procedures in Experimental Physics. Prentice-Hall, N. Y., (1943), p. 6.
24. C. E. Birchenall and R. F. Mehl: Self-Diffusion in Iron. *Jnl. Appl. Phys.* (1948), **19**, 217.
25. Thanks are due to Dr. W. A. Johnson for correspondence concerning the activation energy for self-diffusion in aluminum.
26. W. A. Johnson: Self Diffusion of Silver. *Trans. AIME* (1941), **143**, 107.
27. T. S. Kê: On the Structure of Grain Boundaries in Metals. *Phys. Rev.* (1948), **73**, 267.
28. C. Zener: Theory of the Elasticity of Polycrystals with Viscous Grain Boundaries. *Phys. Rev.* (1941), **61**, 906; see also ref. 13.
29. T. S. Kê: Internal Friction of Cold-worked Polycrystalline and Single Crystal Aluminum. (To be published.)
30. J. E. Burke and C. S. Barrett: The Nature of Strain Markings in Alpha Brass. *Mel. Tech.* (Feb., 1948). *Trans. AIME*, **175**, 106.

DISCUSSION

(G. Sacks and W. M. Baldwin, Jr. presiding)

L. D. JAFFE*—I want to compliment Dr. Kê on this valuable addition to our scant knowledge of anelastic phenomena and ask only two very minor questions. One is, if the two lower peaks are both associated with diffusion of nitrogen, why is it that the activation energies are different? If I recall correctly, you mentioned for the first peak the energy was 20,000 cal per g mol, and for the second about 32,000.

I also want to ask whether you had actually tried carburizing the pure iron to make sure that the peak attributable to carbon did not also coincide with the measured peaks that you observed, because, after all, we know

* Watertown Arsenal, Watertown, Massachusetts.

that the carbon and nitrogen peaks are not very far apart.

T'ING-SUI KÊ (author's reply)—The heats of activation are different in peaks *A* and *C* because the mechanisms of diffusion involved in these two peaks are different.

I did not work with carbon. However, for peak *A*, the carbon peak is, according to Dr. Snoek, 20°C higher than the corresponding nitrogen peak and should thus be easily differentiable. For peak *C*, Dr. Dijkstra of our laboratory has carburized a specimen previously purified from C and N and has found that the carbon peak is very unstable and is very much smaller than the corresponding nitrogen peak.

J. L. SNOEK*—Stress-induced preferential diffusion in cubic body centered metals in the annealed state provides us with a powerful tool for determining the mobility of interstitially solved atoms as well as their location in the lattice and the exact nature of the distortion brought about in the lattice by their presence.

Calculations given by D. Polder³¹ show that the distortion of the lattice, besides being proportional to the applied stress *P*, is also proportional to

$$\frac{VC_0}{RT + \alpha VC_0}$$

where *T*, *V* and *C*₀ are the temperature, molar volume of the solvent and molar concentration of the solute respectively and α is a constant describing the mutual interaction energy of the dissolved particles. This calculation obviously is no longer valid if α is negative and the absolute value of αVC_0 surpasses that of *RT*. The lattice may then be expected to become tetragonal spontaneously. Such a spontaneous tetragonality seems to have been observed by W. Klemm and L. Grimm for the case of oxygen solved in vanadium.³²

Measurements of the internal friction in cold worked iron containing carbon or nitrogen should provide us with information on the mobility as well as the preferential location of

these particles in the iron lattice in the cold worked state: The work by T'ing-Sui Kê is a valuable contribution to this problem. The data obtained by T'ing Sui Kê and myself on cold worked samples of iron seem to indicate that carbon and nitrogen in these samples are found either in the normal ($\frac{1}{2}$, 0, 0) interstices or in a new preferential position created by the cold working.

The latter positions in my opinion can hardly be anything else but the edges of the dislocations. The observed larger distances of diffusion might be explained by assuming that the carbon atoms when freed from a certain dislocation by thermal agitation must diffuse over several atom distances before being caught in another dislocation. The theory however needs working out and no doubt will be much more complicated than the one valid for the annealed state.

T'ING-SUI KÊ (author's reply)—It is highly encouraging to read the written discussion given by Dr. Snoek who initiated the theory of stress-induced preferential diffusion in cubic body centered metals in the annealed state. Since the presentation of this paper, the author has done more experimental work on this subject which seems to be able to settle several of the points raised by Dr. Snoek.

It has been found that such stress-induced preferential diffusion occurs also in the solid solutions of carbon,¹¹ oxygen,¹¹ and nitrogen³³ in tantalum which has a body centered cubic structure. Analysis of the shape of the observed internal friction peaks indicates that the interstitial atoms responsible for the observed peaks in tantalum are situated at the octahedral positions in the case of carbon and at both octahedral and tetrahedral positions in the case of oxygen and nitrogen.

The spontaneous tetragonity mentioned by Dr. Snoek has also been sought in the case of oxygen dissolved in tantalum. The result showed that the temperature at which such a spontaneous tetragonity might occur is close to absolute zero. Dr. Zener³⁴ has recently pointed out that the observation for the case of oxygen in tantalum may not be generalized to other similar solid solutions. This is apparently so if such a spontaneous tetragonity has been observed for the case of oxygen dissolved in vanadium. The answer to spontaneous tetra-

* Philips' Research Laboratories, N. V. Philips' Gloeilampenfabrieken, Eindhoven, Netherlands.

³¹ References are at the end of the discussion.

gonity should be in the affirmative if Dr. Zener's theory³⁵ of tetragonal martensite is to be upheld. More experiments are needed to settle this point.

REFERENCES

31. D. Polder: Philips' Res. Rep. (1945) **1**, 1.
32. W. Klemm and L. Grimm: *Ztsch. an. all. Chem.* (1942-43) **250**, 47.
33. T. S. Kê: Internal Friction and Precipitation from the Solid Solution of N in Tantalum. *Phys. Rev.* (1948), **74**, Oct. 15.
34. C. Zener: Theory of Strain Interaction of Solute Atoms. *Phys. Rev.* (1948), **74**, Sept. 15.
35. C. Zener: Kinetics of the Decomposition of Austenite. TP 1925, *Metals Tech.*, Jan. 1946; *Trans. AIME* (1946), **167**, 550.

Testing Gun Steel and Other Alloys and Metals for Resistance to Surface Cracking

By EARL INGERSON*

(Chicago Meeting, October 1947)

BORE surfaces of used guns commonly show a pattern of cracks in various degrees of development. It has been suggested that these cracks may aid erosion by providing channelways for the gases, eventually leading to the tearing out of blocks of metal. Under the general studies of gun erosion conducted at the Geophysical Laboratory it appeared desirable to consider this factor, and to determine the resistance to surface cracking offered by gun steel and by various other materials that might be used in the bores of guns.

METHOD AND APPARATUS

In order to make such a determination it is necessary to have (1) an arrangement in which the surface to be studied can be subjected to conditions similar to those in a gun with respect to temperature, pressure (developed by explosion gases), composition of the gases and length of time the surface is exposed to the gases; and (2) a specimen that can be examined readily after any number of shots, and then fired again, if necessary.

The first of these conditions can be met by using an explosion vessel designed by H. S. Roberts of the Geophysical Laboratory. Fig 1 shows a cross-section of the apparatus. The "gun" *G* from which

the charge is fired is made from the receiver of a caliber 0.30 army rifle, M1903, and the charges are prepared in caliber 0.30 cartridge cases. The test specimen *S* is held in place by a cone-shaped plug *P* and by a steel bridge *B* which is bolted to the outside of the explosion vessel on either side of the section shown. The plug, in turn, is held in place by a screw collar *C*. Maximum pressure is controlled by a brass rupture disk *R*. Part of the explosion gases flow past the two flat areas on *S*.

Temperature and composition of gases, and the time before the rupture disk breaks, can be controlled by amount and kind of powder used, and pressure can be controlled by using rupture disks of different thickness. While the explosion vessel used was not designed so that temperature and pressure could be measured, in other vessels of closely similar size and shape containing proportionate charges of the same kind of powder as that used for standard testing procedure, values of 2700°K and 50,000 psi were obtained. Since the orifices past the flat areas on the plug are small compared to the rupture disk hole (1:16), most of the gas goes out through the rupture disk when it breaks. The amount that goes by the plug depends on (1) the pressure attained before the rupture disk breaks and (2) the time it takes for this pressure to be built up.

The second condition (examination at will after any firing) is met by using for specimens short rods that have flat areas ground on opposite sides. These flat

Manuscript received at the office of the Institute Jan. 25, 1947; revision received Mar. 3, 1947. Issued as TP 2223 in METALS TECHNOLOGY, August 1947.

The information described in this article was obtained under contract OEMsr-51 with the Office of Scientific Research and Development, under the supervision of the National Defense Research Committee.

* Geophysical Laboratory, Carnegie Institution of Washington.

areas are readily examined and photographed under a metallographic microscope. The rods used in most of the tests herein described were $1\frac{1}{4}$ -in. long, $\frac{3}{16}$ -in. diam

begins in a few rounds so that a given material can be tested in a short time.

Various quantities of different kinds of powders were tried with rupture disks

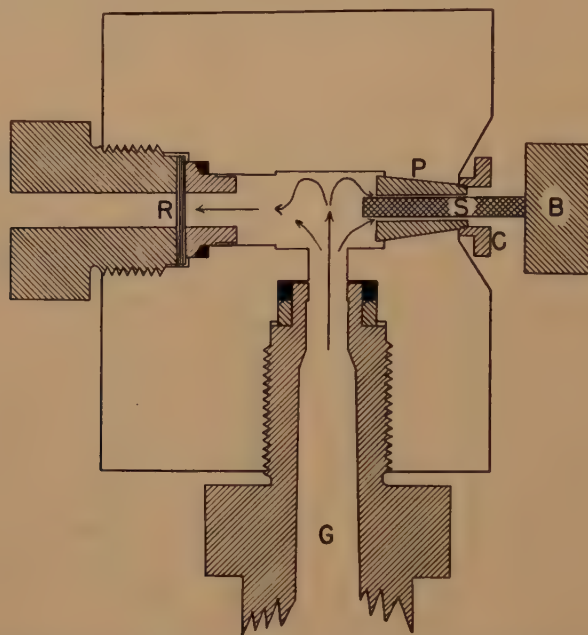


FIG. 1.—CROSS-SECTION OF THE EXPLOSION VESSEL USED. G, "GUN"; S, TEST SPECIMEN; P, CONE-SHAPED PLUG TO HOLD THE SPECIMEN; B, BRIDGE TO KEEP SPECIMEN IN PLUG DURING EXPLOSION; C, SCREW COLLAR TO HOLD PLUG IN WALL OF VESSEL; R, RUPTURE DISK.

and had flat areas of such size that the total orifice area was equal to the cross-sectional area of a hole $\frac{1}{16}$ -in. diam, with the area of one of the two orifices twice that of the other. When the rod is placed in the testing apparatus, the larger of the two areas is on the lower side of the rod. The hole in the plug that holds the rupture disk is $\frac{1}{4}$ -in. diam.

Charge

For a study of surface cracking the charge used should be such as to produce the following two conditions. (1) The temperature-time relation should be such that little or no melting of gun steel or similar materials occurs. (2) Conditions should be severe enough that cracking

of different thicknesses. A "standard shot" of 2.5 g of pistol powder with $\frac{1}{16}$ -in. rupture disk was adopted for the tests. Pistol powder gives a comparatively low flame temperature (2850°K) and burns very rapidly, only 0.2 millisecc being required for the pressure to build from 20 pct to 80 pct of the maximum. With this charge melting of the surface does not occur, but materials similar to gun steel begin to crack after a few rounds.

With the manner of firing determined, it is still necessary to set up a standard procedure for comparing the resistance of various materials to cracking. There are two obvious methods: (1) To continue firing until some predetermined state of cracking is attained and let the number of

rounds required to develop the cracking be a measure of the resistance of the material. (2) To fire a standard number of rounds and compare the amounts of cracking developed on various materials and rate them accordingly.

There are advantages and disadvantages to either method. The first one would give a better quantitative result, or at least a more definite method of expressing it. However, it is much more time consuming, because a specimen has to be cleaned and examined after each shot, or at any rate after a given number of shots, if an advanced degree of cracking is selected as a standard. Moreover, this cleaning after each round affects the cracking markedly. For example, after four shots, without cleaning the rod, cold-rolled steel shows a fairly well integrated crack pattern. However, if a rod of the same material is cleaned after each of four shots, it is difficult to find any cracks at all.

Under "standard conditions" of 2.5 g of pistol powder and $\frac{1}{16}$ -in. rupture disk, gun steel (SAE 4140) is noticeably cracked after 4 rounds, Fig 2.* Different specimens of the same material are cracked essentially the same amount by the same number of rounds. Four rounds can be fired in 4 min., thus providing a rapid test for materials which, in their resistance to cracking, are similar to gun steel. A "standard procedure" of firing four rounds with 2.5 g of pistol powder and $\frac{1}{16}$ -in. rupture disks, and then polishing and examining the specimen was adopted.

By using this procedure, materials can readily be divided into three groups,

(1) those that are badly cracked over a large part of the surfaces in the plug after four rounds, (2) those that behave roughly the same as gun steel, and (3) those that

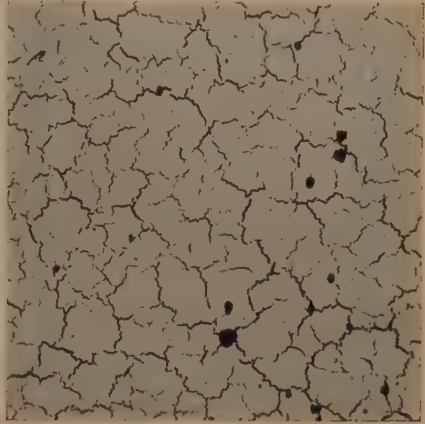


FIG 2—GUN STEEL AFTER 4 STANDARD SHOTS.
X 250.

show little or no cracking after four rounds and are therefore better than gun steel with respect to this particular property.

To classify materials with high resistance more accurately, or for special studies—such as observing the mechanism of erosion under these conditions—it may be necessary to fire many times the standard 4-round series.

After a series of rounds has been fired, the rod is put on a polishing lap with levigated alumina for 5 to 10 sec. A "series" begins as a four shot series, but for very resistant materials the number of shots in a series may be increased as desired to save unnecessary examinations of surfaces that erode slowly. This polishing removes the fouling, as well as thin gray coating, which has not been definitely identified but appears to be oxide, without taking off a significant amount of the metal.

RESULTS OF TESTS

No systematic or comprehensive series of tests has been undertaken, but several

* All micrographs were taken after the coatings had been removed and the surfaces had been polished. Where the surface was etched after polishing, that fact is stated in the individual legends.

In all the micrographs, except the cross-section of Fig 27, gas motion was toward the top of the page; that is, away from the reader.

Where powder and rupture disk are not specified, the "standard shot" of 2.5 gram of pistol powder and a $\frac{1}{16}$ -in. rupture disk were used.

TABLE 1—Tests of Resistance of Metals to Surface Cracking

Material	Shots	Results and Remarks	Figures
28 pct Cr steel.....	4	Very many intracrystalline cracks even after one shot. More after 2, then not much more change.	
4.85 pct Si transformer steel..	2	Intercrystalline cracks well developed.	
	6	Many inter- and intracrystalline cracks.	14, 15
4024 austenitic steel.....	4	Intercrystalline cracks.	9, 10
Nickel.....	4	Intercrystalline cracks.	
	8	Intercrystalline cracks.	11, 12
Gun steel.....	2	Cracks just beginning.	
	4	Well-integrated heat-check pattern.	2
	20	Edges of cracks being torn away.	19
	85	Original surface largely destroyed near notch.	20
Drill rod.....	4	Moderately-integrated heat-check pattern.	
	8	Well-integrated heat-check pattern.	
	24	Edges of many cracks torn away.	
	54	Most of the cracks widening.	
Cold-rolled steel.....	2	Heat checks just beginning.	
	6	Well-integrated heat-check pattern.	
	24	Edges of many cracks torn away.	18
	54	Individual cracks followed through previous series of shots now largely obliterated.	
Armco Iron.....	4	Moderate amount of heat checking.	
Copper.....	14	No cracks; surface "ripple marked."	
Chromium.....	4	No heat checking, but rod was so brittle that it shattered and no further shots were possible.	
Molybdenum.....	60	No heat checking. Slight pitting, but no important erosion, because shallow original tool marks still remain.	
Tantalum.....	6	No heat checks, but a few small cracks developed parallel to the axis of the rod.	
50 pct Molybdenum.....	4	No heat checks; broke up much as chromium did.	
50 pct Tungsten			

TABLE 2—Compositions of Alloys

Alloy	C	P	S	Si	Cr	Ni	Co	Ti	Al	Mn	N
28 pct Cr Steel ¹	0.13			0.30	27.71					0.57	0.17
Transformer steel ¹	0.05	0.006	0.01	4.85						0.24	
4024 ²				1.59	19.0	13	17	1.4	0.24	1.50	
5 in. per 38 cal gun steel.....					SAE 4140						
Drill rod ³					SAE 1060						
Cold rolled steel ³					No analysis available						

¹ Furnished by U.S. Steel Research Laboratory.² Furnished by Westinghouse.³ Furnished by Geophysical Laboratory.

TABLE 3—Microstructures of Metals and Alloys Used

Material	Treatment	Original Microstructure
28 pct Cr steel.....		Ferrite with small amounts of austenite
High silicon transformer steel...	Heat-treated	Coarse ferrite with a precipitated phase at grain boundaries
4024.....	Probably annealed	Austenitic; small amounts of angular constituent
Nickel.....	Cold-worked	Distorted grains
Gun steel.....	Heat-treated	Sorbitic
Drill rod.....	Spheroidized	Spheroidized carbides in ferrite matrix
Cold-rolled steel.....	Cold-rolled	Ferrite and pearlite in stringers
Armco iron.....	Annealed	Ferrite
Copper.....	Cold-rolled	Distorted grains
Chromium.....	Heat-treated at 1000°C in H ₂	Annealed grain boundaries; spheroidized inclusions
Molybdenum.....	Hot-rolled	Elongate grains
Tantalum.....	Cold drawn and hardened	Elongate grains

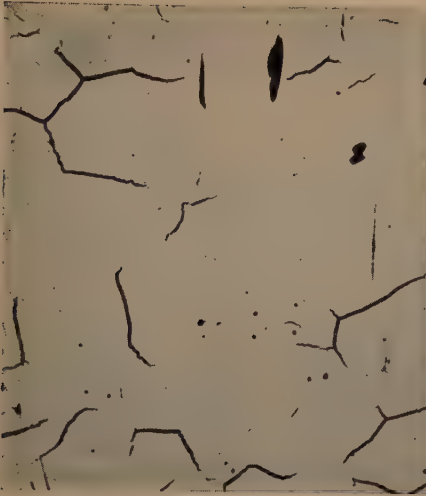


FIG 3.

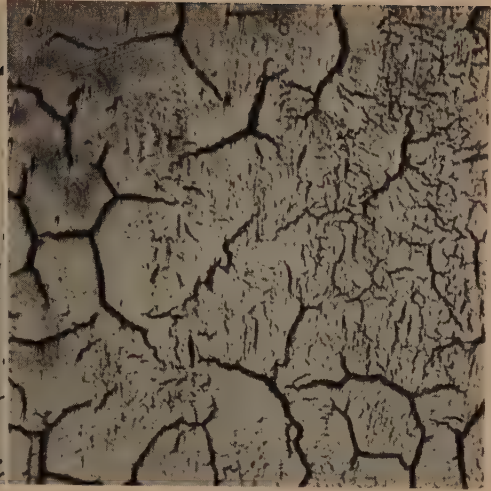


FIG 4.

FIG 3—COARSE CRACKS ON THE SURFACE OF A ROD OF GUN STEEL AFTER 20 ROUNDS. THESE CRACKS FORMED *outside* OF THE PLUG, WHICH MEANS THAT THIS PART OF THE ROD WAS ENTIRELY OUT OF THE EXPLOSION CHAMBER. $\times 250$.

FIG 4—SAME ROD AS THAT OF FIG 3, BUT AFTER 85 SHOTS, SHOWING BOTH TYPES OF CRACKING. $\times 250$.



FIG 5.



FIG 6.

FIG 5—COARSE CRACKING OF MELTED SURFACE ON A ROD OF COLD-ROLLED STEEL AFTER A SHOT WITH 2.0 GRAM OF A SINGLE BASE POWDER WHEN THE RUPTURE DISK FAILED TO GO. $\times 100$.

FIG 6—EDGE OF CRACKED AREA ON A ROD OF GUN STEEL AFTER 4 ROUNDS. ETCHED 2 SEC WITH HCl + PICRIC ACID TO BRING OUT ORIGINAL AUSTENITE GRAIN BOUNDARIES (LEFT). NOTE DIFFERENT SIZE AND SHAPE OF GRAINS AND POLYGONS ENCLOSED BY CRACKS. $\times 250$.

kinds of materials have been tried, as summarized in Table 1 where reference is also made to the photographs that illustrate the results. Compositions of the alloys are given in Table 2 and a summary of previous treatment and microstructures in Table 3. The samples were obtained under the contract for testing and no details of previous history are known except those recorded in the table.

KINDS OF CRACKING

In studying the rods of various materials at least three general types of cracks were observed: heat checking, coarse cracking, and post-fusion cracks.

Heat Checking

When gun steel and other steels closely related in composition are treated as outlined above, the first cracks to appear are very similar to the "heat checking" so prevalent in eroded guns. These cracks appear first where the hot gases enter the plug. This point is referred to as the "notch" because the hot gases almost invariably cut little notches in the edges of the flat areas of the rods where they enter the plug. As firing is continued the cracks work their way progressively downstream on the flat surfaces of the rod. Fig 2 shows typical heat checking on gun steel. The distance between these cracks averages about 0.03 mm. In cross section the cracks that show up are at an average spacing of about 0.045 mm. These values are of the same order of magnitude as those reported by Kosting¹ (0.076 mm) for a worn out 37-mm Browning automatic gun M1, and by Kosting and Peterson² (0.066 mm) for a worn out 37-mm gun M1A2. Fig 7 shows such cracks on drill rod. The random pattern of these cracks

indicates that they are probably independent of grain boundaries. This is borne out by a study of etched specimens, Fig 8.

Coarse Cracking

Another type of cracking has been observed which develops very readily in brittle materials and appears eventually even in materials like gun steel. This type of cracking is not confined to the area near the notch where the heat checks begin. In fact, on some materials (for example, gun steel) these cracks start near the exit and do not overlap the area of heat checks until many rounds have been fired. On gun steel they are not observed until some 20 rounds have been fired, whereas on brittle materials they may be quite prominent after one round. These cracks are of a larger order of magnitude than the typical heat checks. From their size and arrangement they were at first called "intercrystalline cracks," but study of etched surfaces of various materials showed that they are by no means always intercrystalline.

Fig 3 is from a gun-steel rod after the firing of 20 rounds. It is from near the downstream end of the plug and shows these cracks in the area where they first appear in gun steel, away from the heat checks. Near the center of the rod these larger cracks and the heat checking occur in the same area. Fig 4 shows this overlap of the two types on the same rod from which Fig 3 was taken, after 85 rounds.

Other materials, for instance, nickel, chromium, austenitic steels and high silicon steels, show as much of this coarser cracking after 1 to 8 rounds as gun steel shows after 20 to 30 rounds. Fig 11 shows this type of cracking in nickel after 8 rounds. Fig 14 shows it in high-silicon (4.85 pct) transformer steel after 6 rounds. Fig 9 is an austenitic steel (4024) after 4 rounds. High chromium stainless steel shows a similar cracking, but with a different pattern (Fig 13).

¹ P. R. Kosting: 37-mm Browning automatic gun M1, No. 1 barrel. Watertown Arsenal Report No. 731/45 (Oct. 17, 1940).

² P. R. Kosting and R. E. Peterson: 37-mm gun M1A2, No. 109, Watertown Arsenal Report No. 731/59 (May 29, 1942).

The physical separation and the quite different appearance of the two sets of cracks lead naturally to the supposition

where it heat-checks, but shows no change other than the cracking in the area where the coarser cracks are developed.

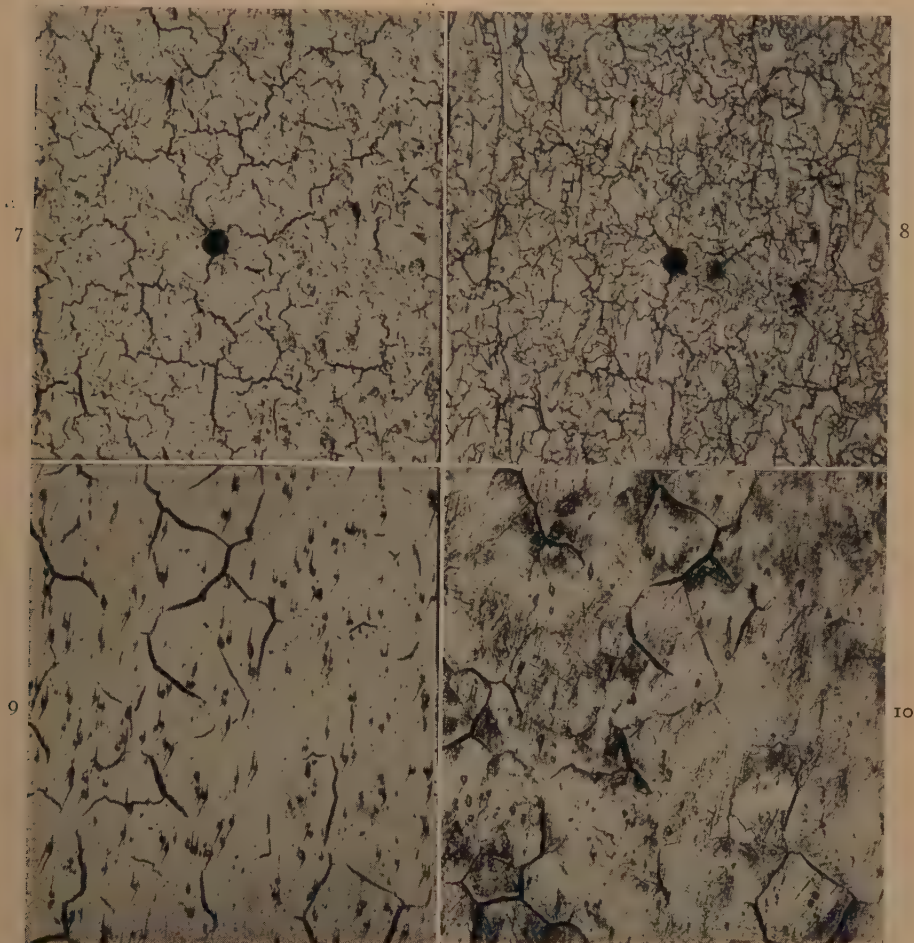


FIG 7—DRILL ROD AFTER 4 CONSECUTIVE SHOTS. POLISHED, BUT NOT ETCHED. $\times 250$

FIG 8—SAME FIELD AS FIG 7, AFTER 10-SEC ETCH IN $\text{FeCl}_3 + \text{HCl}$. $\times 250$.

FIG 9—COARSE CRACKING ON AUSTENITIC STEEL (4024) AFTER 4 SHOTS. POLISHED, BUT NOT ETCHED. $\times 250$.

FIG 10—SAME FIELD AS FIG 9 AFTER 10-SEC ETCH WITH $\text{HCl} + \text{PICRIC ACID}$. SHOWS CRACKING TO BE ENTIRELY INTERCRYSTALLINE. $\times 250$.

that they have separate causes. It is possible that the heat checking is due to rapid heating and cooling of the surface layers, while the other type of cracking is brought about by mechanical shock. This suggestion is upheld by the observation that the surface is considerably altered

Post-fusion Cracks

A third type of cracking develops when heating of the surface is more intense, as when a double-base powder is used, or when a rupture disk fails to break and part of the surface of the rod actually melts. As it cools rapidly and contracts,

a crack pattern develops which resembles the pattern that is formed when mud cracks upon drying. Fig 5 shows this type of cracking at the end of the tongue formed on cold-rolled steel with 2.0 g of a single-base powder when a rupture disk failed to function. These cracks resemble heat checks, but the pattern is much coarser, the individual polygons being two or three times the diameter of those of typical heat checking. They are found only on the tongues where the surface has been melted. Post-fusion cracking is encountered in erosion plugs where melting occurs during each round fired, but it is not important in the experiments under discussion.

RELATION OF CRACKS TO GRAIN BOUNDARIES

Different kinds of cracks in various kinds of materials show quite different relations to the grain boundaries. On some of the materials tested it is difficult to observe the relation between cracks and grain boundaries, because in the cracked areas some change has occurred in the surface layer so that etching fails to bring out the grain boundaries clearly. Gun steel and soft iron both fall in this category.

Fig 6 is from a rod of gun steel etched to bring out the boundaries of the original austenite grains. Some of the boundaries are visible in the left part of the picture, but they are missing completely in the cracked area to the right. Although cracks and grain boundaries are not visible in the same area, it is evident from the size and shape of the grains that the cracks are not controlled by the austenite boundaries. Cracked gun steel was etched to bring out the needles of martensite and it was studied carefully under higher magnifications, but no more consistent relationship between martensite needles and cracks could be determined

than between cracks and austenite grain boundaries.

Soft Armco iron showed a pattern not unlike that of gun steel. Study of etched specimens failed to show any correlation between cracks and the boundaries of the ferrite grains.

Fig 17 shows cracking on a rod of cold-rolled steel at four rounds after etching. The elongate clear grains were pearlite before firing took place. During firing the carbide is dissolved and martensite forms because very rapid cooling takes place immediately. Here, again, the cracks are not for the most part along grain boundaries. They are related to the kind of grains, however, and are mostly in the ferrite "groundmass," comparatively few cracks occurring in, or crossing, the pearlite grains.

Drill rod shows very much the same relations as cold-rolled steel. Fig 7 is from drill rod after four rounds, and Fig 8 is of the same area after etching. The clear, elongate areas were pearlite before firing. Again, most of the cracks are in the ferrite groundmass.

The coarse cracks are more definitely related to grains and grain boundaries than the heat checks in any material thus far studied. In an austenitic steel (4024) these cracks are entirely intercrystalline. Fig 9 is from a rod of this material after 4 rounds, and Fig 10 pictures the same area after etching. Nickel shows these intercrystalline cracks even better. Fig 11 is from a nickel rod after eight rounds, and Fig 12 is the same area after etching to bring out the grain boundaries.

In a high-chromium, stainless steel (28 pct Cr) the cracks are almost entirely *intracrystalline*. Fig 13 is from a rod of this material after four rounds, and then polished and etched to bring out the grain boundaries. Few, if any, of the cracks cross grain boundaries.

A high-silicon (4.85 pct Si) transformer steel shows a behavior intermediate be-

tween that of nickel and of the 28 pct chromium steel. In other words, roughly half of the cracks are intercrystalline and

others "dead end" within grains. Some follow grain boundaries for part of the width of a grain and leave at a low angle.

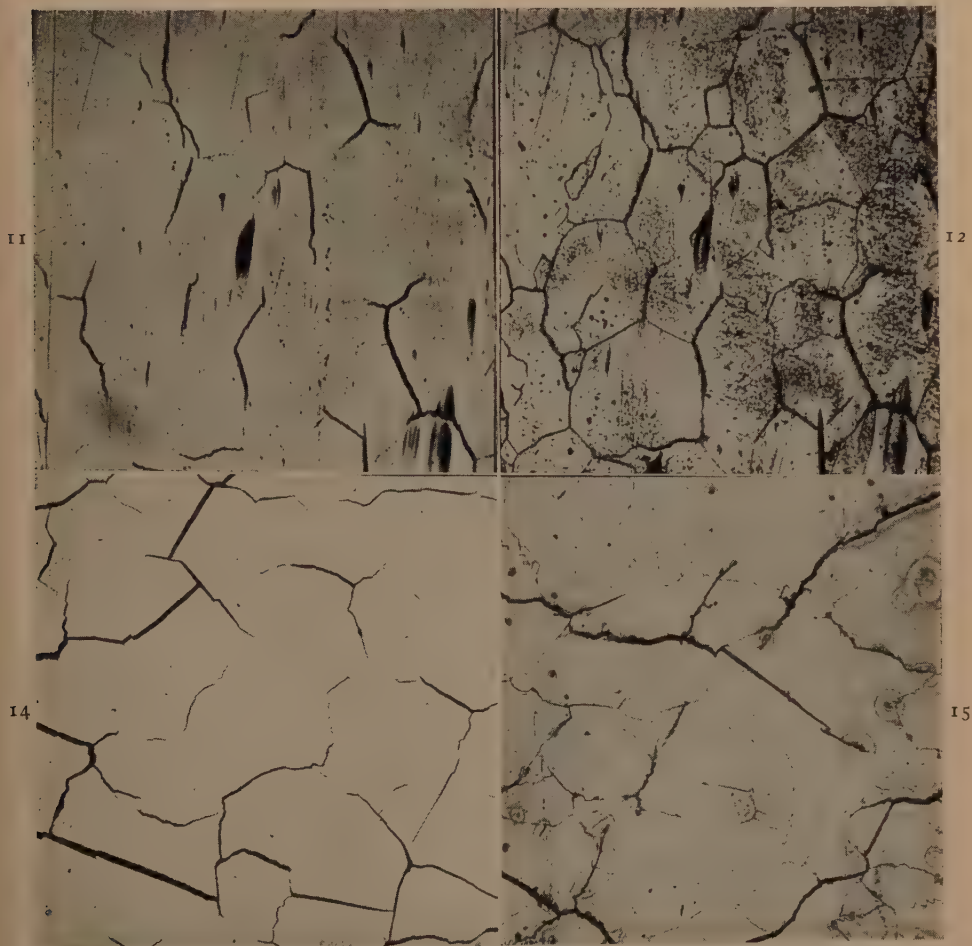


FIG 11—NICKEL AFTER 8 SHOTS. POLISHED, BUT NOT ETCHED. $\times 250$.

FIG 12—SAME FIELD AS FIG 11 AFTER 10-SEC ETCH WITH MIXTURE OF 50 PCT CONCENTRATED HNO_3 AND 50 PCT GLACIAL ACETIC ACID. ALL CRACKS FOLLOW GRAIN BOUNDARIES. $\times 250$.

FIG 14—HIGH-SILICON STEEL (4.85 PCT) AFTER 6 SHOTS. POLISHED, BUT NOT ETCHED. $\times 100$.

FIG 15—ANOTHER FIELD FROM NEAR THE ONE SHOWN IN FIG 14, AFTER ETCH WITH NITAL TO BRING OUT THE GRAIN BOUNDARIES. PART OF THE CRACKS FOLLOW GRAIN BOUNDARIES, PART CUT GRAINS. $\times 100$.

half intracrystalline. Fig 14 is from a rod of this material after six shots. Fig 15 shows a near-by area after etching to bring out the grain boundaries. Many of the cracks are intercrystalline. Others cut all the way through grains and still

A piece of a very similar alloy made by the United States Steel Corporation with 4.7 pct Si and measuring 1 in. in diameter by about 7 in. long was sent by Dr. Posnjak of the Geophysical Laboratory to the Franklin Institute where it

was made into a short liner and subjected to the accelerated erosion testing. The liner was badly shattered in the first few rounds. This behavior was to be



FIG 13—HIGH CHROMIUM STAINLESS STEEL AFTER 4 SHOTS. POLISHED AND ETCHED 25 SEC WITH $\text{HCl} + \text{HNO}_3 + \text{GLYCERINE}$. $\times 250$.

expected from the extreme cracking of the test rod after only two rounds.

The post-fusion cracks are like the heat checks in that they are independent of grain boundaries. These cracks are unimportant in the present investigation and no photographs of etched surfaces were taken.

EXPLANATION OF THE HEAT CHECKING

It has been suggested above that the intercrystalline and intracrystalline cracks may result from mechanical shock, whereas the heat checks are caused by rapid heating and cooling of the surface. This is not the complete explanation, however. The surface is changed during firing. The first evidence of change is a peculiar "mottling" of the polished surface that on gun steel always precedes the development of heat checks.

By the time an area has become well checked the mottling has disappeared and the relation of cracks to mottle

pattern cannot be observed. Immediately downstream from a well-checked area, however, a few small cracks sometimes appear in an area that still shows mottling.



FIG 16—CROSS-SECTION OF ROD OF GUN STEEL NEAR THE NOTCH AFTER 85 ROUNDS. ETCHED TO SHOW ALTERED LAYER. $\times 250$.

There is no apparent relation between the two patterns. The mottling may be a mechanical etching that makes the martensite needles stand out. This is suggested by a careful study of the mottled area on a rod of gun steel, after etching so as to bring out the martensite pattern. The lines of mottling appear to be simply the more prominent martensite needles, or possibly plates of cementite.

Continued firing causes the mottling to disappear as heat checking develops. In gun steel the martensite needles disappear and the surface becomes uniform between cracks (Fig 6). At first this was interpreted as decarburization. This interpretation was favored by a study of cross-sections of gun-steel rods, which showed a progressive decrease in carbide particles until at the very surface the material appeared homogeneous and developed no pattern on etching. Fig 16 shows the altered layer at the surface of gun steel after 85 rounds. Note that the cracks go through the altered layer into the unaltered steel.

Study of other types of steel shows that this disappearance of carbide particles

results from reabsorption rather than from decarburization. In drill rod and cold-rolled steel, for example, where the carbide is in plates in pearlite grains, the behavior is quite different. Fig 17 is from cold-rolled steel after four shots, etched with a reagent to bring out the structure. Pearlite shows up unaltered outside of the heat-affected "tongue" (the right side of each picture), but on the tongue (left side) the carbide has been reabsorbed. If it were decarburization, then all of the grains would be ferrite and the surface would be more or less uniform. The grains that were pearlite retain their carbon because they maintain their identity, have a decidedly different luster, stand above the ferrite grains on polishing, and when cracks appear they develop differently in the two kinds of grains. Also, just at the edge of the tongue the carbide of the pearlite grains is spheroidized.

From these considerations it is evident that the change in the surface of gun steel is also reabsorption. The difference in appearance results from the fact that the carbide particles in the gun steel are so much more uniformly distributed that when they are reabsorbed the resulting surface appears homogeneous, even if it is not entirely so.

Whether there is a direct relation between the alteration of the surface and heat checking has not been definitely established. It is quite possible that both phenomena are functions of the heating of the surface, but that there is no causal relation between them. There is meager indirect evidence that such is the case. It has been previously pointed out that the cracking is not confined to the altered layer. Then, in pure iron in which reabsorption cannot play a part, the same kind of cracks develop. Theories that heat checking is caused by a change of phase, or an alteration of the surface, must at least for the present remain theories.

The crack pattern sometimes shows a

definite relation to the long axis of the rods. In tantalum, for example, the *only* cracks formed near the edge of the rod and parallel to its long axis. In soft iron



FIG 17—EDGE OF ALTERED AREA ON ROD OF COLD-ROLLED STEEL AFTER 4 SHOTS. ETCHED 20 SEC WITH NITAL TO SHOW REABSORPTION OF CARBIDE IN PEARLITE GRAINS. $\times 250$.

the most prominent cracks showed the same relation. One specimen of drill rod showed a prominent system of cracks normal to the axis of the rod. One rod of gun steel, the axis of which was parallel to the axis of the gun, developed a prominent crack system forming an angle of 45° with the rod axis.

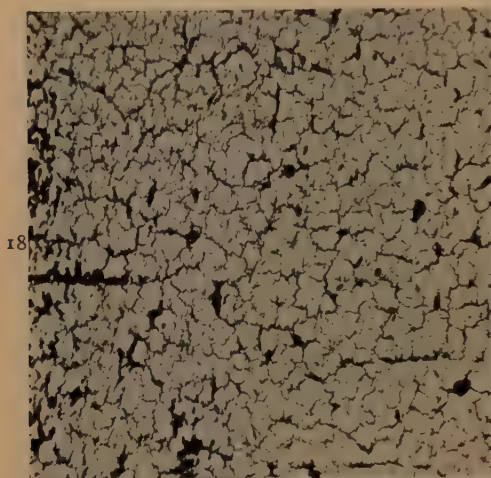
Sometimes the cracks appear to be initiated by pits on the surface that are formed by solid material in the powder gases striking the surface. In soft iron, for example, almost all of the cracks radiate from such pits.

MECHANISM OF EROSION IN THESE TEST SPECIMENS

There is good evidence that the surface of a test rod does not melt with the "standard" charge of pistol powder. In the first place, when double-base powder is used, or the rupture disk fails

to break, the whole surface within the plug, or at least a considerable part of it is "wiped off" and moves downstream, and a little ridge of metal is piled up at the

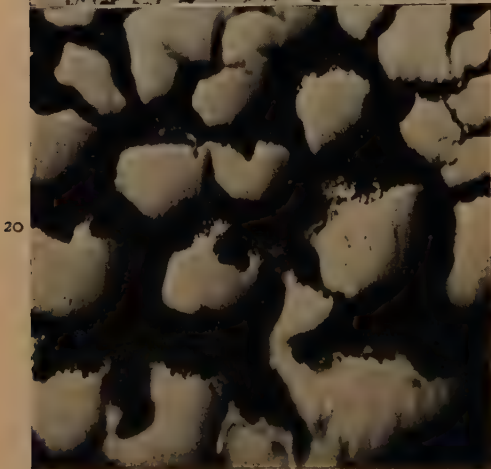
scale in the restricted area where the heat checks occur is indicated by the fact that during a long series of shots the individual cracks can be studied after



18



19



20

FIG 18—COLD-ROLLED STEEL AFTER 24 SHOTS. MANY EDGES BEGIN TO GO, ESPECIALLY IN LOWER LEFT PART OF PICTURE. THIS AREA IS IMMEDIATELY DOWNSTREAM FROM THE LEFT-HAND NOTCH. $\times 100$.

FIG 19—GUN STEEL AFTER 20 SHOTS. EDGES OF CRACKS BEING TORN AWAY. $\times 250$.

FIG 20—GUN STEEL AFTER 85 SHOTS. ORIGINAL SURFACE LARGELY DESTROYED NEAR NOTCH. $\times 250$.

end of the "tongue" thus formed (Fig 5). Original grain boundaries are obscured and irregularities in the surface are covered over. Each shot destroys the crack pattern produced by the preceding shot and a new pattern is formed on the freshly melted surface.

With the "standard" shots, however, no such melted tongue is formed. The absence of melting even on a smaller

each shot, or series of shots, and no indication can be found that even the smallest ones are covered over by a layer of melted material, or that there is any melting of the edges of the cracks. After long-continued firing the edges become rounded, of course, but this appears to be the result of gas abrasion (probably with the aid of solid particles in the gas) and breaking of the sharp edges, rather than

of melting (Figs 18 to 20). Each crack develops progressively and can be followed through a long series of shots.

Figs 19 and 20 show advanced erosion in gun steel. Fig 19 shows how the edges of the cracks begin to tear away after 20 rounds; Fig 20 shows the surface well eroded after 85 rounds.

It is possible that this kind of erosion is more nearly like that which takes place in most guns than that found in those erosion plug experiments which involve melting of a surface layer. The test method described herein has the drawback of requiring many more rounds than are necessary with an erosion plug, but for some types of tests it is probably worth the extra time involved. Erosion per round increases with increasing number of rounds.

DISCUSSION

E. A. LORIA*—The method of testing gun steel for resistance to surface cracking described in this paper was restricted to the examination of small, rod-shaped specimens. The writer would like to point out the importance of other factors in producing defects in forged and bored gun tubes which would not be apparent in this investigation because of the nature of the test. Actual section size would accentuate the possibility of internal wall (bore) defects arising from unequal expansion between the internal and external wall surfaces on firing, resulting in internal tearing. Checks and tears on the inside walls arise from internal tensions and nonuniformity on cooling, but the internal tearing can be reduced by using alloys of low expansion and of good thermal conductivity so as to reduce the difference between the outer and inner wall surfaces. Also, the possibility of the location of inclusion segregates within a machined gun tube becomes more likely than in a small test specimen. The effect of these nonmetallics on gun life and performance is evident when one realizes that the inclusions are soft yet brittle. They reduce the amount of plastic deformation which can take place before cohesive failure occurs. Once

localized fracture has occurred at the position of a chain of these inclusions, a sharp notch (crack) is formed which produces stress conditions more favorable to cohesive failure than to plastic deformation. These cracks aid erosion by providing channelways for the explosive gases, eventually leading to the tearing out or spalling of blocks of metal.

Oxidation of the surface may be partly responsible for the change in the surface of gun steel during firing observed by the author. The appearance of burn on the surface is an indication that high temperatures were reached on firing, resulting in a slight oxidation of the surface. Since the color of the oxidized film depends on both temperature and time, a higher temperature is required for a given color to form when it is caused by explosive heat, which acts for only an extremely short time at a given spot, than when it is caused by ordinary tempering. The cross-section of the gun steel specimen, Fig 16, illustrates that the repeated firing temperatures were high enough to cause some softening of the surface region, resulting in the well-known phenomenon of soft skin. This softening is one form of what may be conveniently termed metallurgical burn, to distinguish it from visible burn arising from surface oxidation.

Fig 3 and 4 show an interesting sequence in crack propagation. After continued firing, the increased severity of cracking leads to a branching of some of the cracks such as can be seen in Fig 4. When the branching is frequent enough, the cracks begin to form an irregular network in which the most pronounced (primary) cracks remain more or less in the grain boundaries. After a further series of rounds have been fired, the network is likely to become a regular one having the cracks both perpendicular and parallel to the grains. This can be considered to be a second type of crack pattern but no sharp dividing line can be drawn between it and the first type of crack pattern since one type gradually merges into the other.

EARL INGERSON (author's reply)—It was realized that tests on the small rods did not simulate conditions in guns closely enough for this method to serve as a final test. It was used in a preliminary rating and the materials that showed up well in this test were made into gun barrels and/or liners for final testing.

* Mellon Institute of Industrial Research.

Wear Tests on Grinding Balls

By T. E. NORMAN,* JUNIOR MEMBER, AND C. M. LOEB, JR., MEMBER AIME

(New York Meeting February 1948)

THE use of ball, rod and tube mills for grinding ore, cement and other materials has grown so rapidly during the past forty years that the world's annual consumption of ferrous grinding media for these mills is now estimated to be between one half million and one million tons per year. Ferrous grinding balls constitute the major portion of this tonnage. Obviously they represent sufficient value to justify thorough studies of the factors governing their performance.

The selection of grinding balls is governed principally by: 1. Quality (wear resistance, impact resistance, soundness, and the like). 2. Sources of supply and delivered cost. 3. Grinding characteristics or efficiency in the ball mill. This paper deals principally with the quality of ferrous grinding balls. In the study of these factors certain data relative to the fundamental nature of ball wear in ball mills have been obtained. These data are also presented and discussed briefly.

THE DEVELOPMENT OF A SUITABLE WEAR TEST

A study of the fundamental factors governing the quality of grinding balls has been hampered seriously by the fact that a competent test has, in the past, involved the purchase of several hundred tons of balls of a specific type which were then run

in one or more ball mills for a period ranging from several months' to several years' duration. Often, during the period of test, it became necessary to change operating conditions or the character of the ore fed to the test mill with the result that the rate of ball consumption changed and the test figures became of little value. Under such circumstances, progress in the development of better grinding balls, has been necessarily slow.

Economic factors and variations in the quality of balls produced by different sources of supply generally make it necessary for each mill operator to determine for himself the most suitable type of balls for his mills. In our own ball mill grinding operations at Climax, Colo., we were faced with this problem. After we had run a few large scale wear tests at considerable expense we decided to investigate the possibilities of a small scale wear test which would be capable of testing numerous types of balls within a relatively short time.

The most important requirement of any test is, of course, that it give results which can be used to predict accurately the wear in full scale operations. It was known that Ellis and his associates^{1,2} had developed a method of testing grinding balls by small scale tests run at the Ontario Research Foundation. Ellis' method of testing was used as a starting point in our investigations. In the course of our tests a number of modifications of the original method were found to be desirable so that, by an evolutionary procedure, a method of small scale

Manuscript received at the office of the Institute September 12, 1947. Issued as TP 2319 in METALS TECHNOLOGY, April 1948, and MINING TECHNOLOGY, May 1948.

* Metallurgical Engineer and Vice President, respectively, Climax Molybdenum Co., Denver, Colo. and New York City, N. Y.

¹ References are at the end of the paper.

testing has been developed which we believe makes possible an accurate estimation of the wear in full scale operations.

Our first small scale tests were run at the

The balls tested were, in most cases, nominally 3 in. in diam.

Our preliminary tests differed from Ellis' method principally in the matter of dimen-

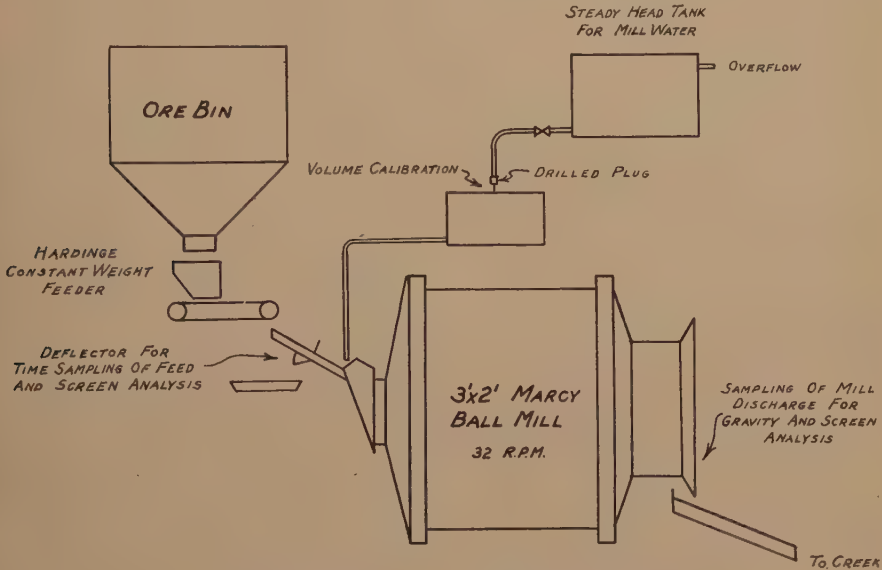


FIG 1—FLOWSHEET OF WEAR TESTS AT GOLDEN.

Colorado School of Mines State Experimental Plant in Golden, Colo. These were run in a Marcy ball mill approximately 3 ft id by 2 ft long, lined with ship-lap steel liners and equipped with a discharge grate which could be adjusted by means of diaphragm rings to discharge the ground pulp at various levels. The discharge could also be sealed for batch grinding tests. Fig 1 illustrates the arrangement used for the test when operating on open circuit grinding with a continuous feed and discharge. This arrangement was used for most of our preliminary tests though in a few cases it was found desirable to run a series of batch tests for the study of certain variables. Abrasives used in the tests were crushed Climax ore, a river sand very similar in abrasive characteristics to Climax ore, commercially pure crushed feldspar and a relatively pure type of crushed calcite.

We used balls 3 in. in diam in a mill 3 ft in diam where Ellis, in most of his tests, used balls 1 in. in diam in a mill 1 ft in diam or smaller.

Our tests in the 3-ft mill were found to be useful for preliminary testing or for the study of certain fundamental factors affecting ball wear. Usually the order of merit of a series of balls could be quite well established in such tests. The test was found, however, to have certain limitations. For instance, the impact conditions in the 3 ft mill did not duplicate those in our large 9 ft diam mills at Climax. Also, the spread in relative wear resistance between a good and a poor type of ball was generally different from that obtained in our larger mills at Climax, or in the mills at other mining operations:

Ellis¹ has demonstrated that the character of the abrasive has a marked influence

on the relative wear resistance of various types of balls. This was confirmed in our preliminary tests. Ordinarily the hard abrasives such as quartz give a relatively small spread while the softer abrasives, such as feldspar and calcite, tend to produce a relatively large spread between the wear resistance of a good and a poor type of ball.

Because of the foregoing limitations of the tests in the 3 ft mill, a new testing technique was developed whereby many types of balls could be tested on a small scale in a commercial mill without seriously interfering with its regular operation. Results of such tests, when comparisons have been available, show excellent agreement with large scale tests made in the same mills where only one composition was used for the entire ball charge.

DETAILED PROCEDURE FOR RUNNING WEAR TESTS IN COMMERCIAL MILLS

The technique used in running our wear tests, in its final stage of evolution, was as follows:

1. A series of groups of balls was selected with the balls in each group representing steel or iron of a specific type and treatment. A "group" usually consisted of from 5 to 15 balls. Our tests have indicated that if all the balls in any group are similar each ball will show, within the limits of experimental error, exactly the same weight loss per unit of area. There was very little advantage to be gained therefore from the use of large groups. One group of balls in each series was of the type used as a standard for comparison.

2. The balls in each group were marked with a distinctive mark, such as one or two notches or drilled holes or a combination of a notch and a drilled hole. Where two notches or drilled holes and notches were used on a ball, they were placed at definite angular distances from each other on the ball surface. Generally the marks were about $\frac{1}{4}$ in. deep with the holes $\frac{1}{4}$ in. diam and the notches $\frac{1}{16}$ or $\frac{1}{8}$ in. wide by 1 in.

long. The notches were cut with a small abrasive cut-off wheel.

Comparative tests have indicated that the one or two notches or holes placed in these test balls produced no measurable difference in rate of wear except in cases where spalling occurred at the edge of the notches. Where spalling did occur, it was generally of such a nature that the weight loss due to this spalling could be estimated and the necessary corrections made to determine the weight loss caused by wear alone.

3. After marking, the surface defects such as scaling and decarburization were removed from the test balls by a "wear-in" in a small ball mill for a sufficient time to remove metal to a depth of at least 0.040 in. below the original surface of the ball.

4. Where the groups of test balls were to be run in a large mill along with the regular charge from which it would be difficult to recover all the test balls, it was found necessary to adjust the weight (after the wear-in) of each ball in a group to an identical value. This was done by grinding on an abrasive grinding wheel. By having all balls in a group of equal weight at the beginning of the wear test it was unnecessary to recover all the balls in the group from the mill when the test was complete.

5. All the balls were weighed carefully both in air and while suspended in water containing a wetting agent. From these data the density, volume and surface area of each ball were calculated by assuming that the ratio of volume to surface area was equal to that of a perfect sphere.

6. The mill in which the wear test was to be run was selected and the entire series of test balls charged at once. They were allowed to run in this mill, along with the regular charge of balls under normal operating conditions, for a sufficient period of time to establish a reliable wear factor. In commercial mills the test balls were generally run for a sufficient length of time to wear off a layer of metal about $\frac{1}{8}$ in. thick

from their surface. The mill was then stopped and the marked test balls were sorted out from the rest of the charge. Sorting was accomplished by dumping the entire charge of balls on the floor, or preferably in large mills, by having two or three men pick the marked balls from the surface of the ball charge inside the mill while it was slowly rotated 180° with a crane and rope.

The time for shutdown and recovery of balls from a test mill was generally chosen so that it would coincide with the time the mill was to be shut down for relining or other repairs. By doing this the wear test did not interfere with normal operations of the ball mill. We did not attempt to find 100 pct of the test balls. Generally, however, from 60 to 80 pct of them were found without difficulty within about 2 hr. During the search period a close watch was kept for test balls which had broken or spalled during the test.

7. The test balls were sorted, cleaned and weighed and their weight loss per unit of surface area was calculated. This figure was compared to the loss per unit of area on the standard balls included in the test. From this comparison an "abrasion factor" or relative rate of wear was calculated. For instance on a typical test the standard balls lost 116.0 g per 100 sq cm of original surface area. The balls in "group 1" showed an average loss of 128.7 g per 100 sq cm. The standard ball was always nominally assigned an abrasion factor of 100. The abrasion factor (relative rate of wear) of the balls in group 1 was, therefore, $\frac{128.7}{116.0} \times 100 = 111.0$. In this paper all abrasion factors are given to the nearest whole number.

All abrasion factors listed in this paper have been obtained by the foregoing procedure. In all cases our standard for comparison was a group of martensitic forged steel balls containing 0.75 to 0.88 pct carbon and 0.20 to 0.30 pct molybdenum.

These standard balls had been made in regular commercial practice under carefully controlled conditions and were found to be very uniform in quality.

In studying the abrasion factors given in this review it should be clearly realized that they represent relative rates of wear. Balls with an abrasion factor higher than 100 wear away faster and are, therefore, poorer than the standard, while balls with an abrasion factor of less than 100 wear more slowly and are, therefore, superior to the standard.

The abrasion factor represents the relative rate of wear of that portion of the ball which was worn away during the test. If the ball is homogeneous from surface to center the abrasion factor should be representative of relative wear resistance of the entire ball. In some cases, however, the ball may be less wear resistant at its center than at its surface. When this condition exists, allowances must be made in evaluating the relative wear resistance of the entire ball. Generally, however, the correction necessary is very slight. For instance, if a steel ball 3 in. in diam is fully hardened to a depth of 1 in. below its surface, then the weight of hardened steel in the ball is 96.3 pct of the total weight with the unhardened core representing only 3.7 pct of the total weight. Under such circumstances the correction necessary for the more rapid wear rate of this core will probably be less than 1 pct when applied to the average wear rate of the entire ball.

Surface decarburization to a depth of 0.030 in. may increase the rate of wear of a ball 3 in. in diam by a greater amount than a soft core 1 in. in diam. Such a layer represents approximately 6 pct of the total weight of the ball. We estimate that such a zone of decarburization will generally shorten the life of a 3 in. ball by 1 to 2 pct. On smaller balls the influence of decarburization would be still greater.

The data and conclusions presented in this paper are supported by wear tests run

over a 7 yr period on over 200 metallurgical classifications of steel and iron balls. A total of 94 wear tests was run to study numerous variables under a wide variety of operating conditions. The entire mass of data collected, if presented in this paper, would increase its length excessively and tend to obscure many of the more important findings which we feel the investigation has brought forth. The data presented in this paper will, therefore, be confined principally to illustrative examples rather than to a complete compilation of all results.

RATES OF WEAR AND LIMITS OF ACCURACY

Once the surface of a test ball has been suitably prepared, the determination of an accurate abrasion factor is merely a matter of running the test ball along with a standard for a sufficient length of time to wear off an accurately measurable amount of metal. In our tests we attempted to wear off a sufficient weight of metal on each test so that our limit of experimental error in weighing was less than 1 pct. In the 3 ft diam test mill at Golden, Colo., we found that a 24 hr test, using a continuous feed of crushed Climax ore, washed river sand or washed river pea gravel would wear 15 to 30 g from a ball 3 in. in diam. For a group of 5 to 15 balls, this was sufficient to obtain the desired degree of accuracy.

When running tests in which it was necessary to add the abrasive and water in batches instead of continuously we usually ran each test for a period of 6 hr with the abrasive being changed every 2 hr. Two or more of these 6-hr tests were generally run in order to obtain a check on our results.

In the tests in commercial mills the average period of the wear test was from one to two weeks which in most cases wore off 75 to 400 g per ball. This was ample to establish wear factors with a high degree of accuracy. In one case, however, in which we ran a test in a mill grinding cement clinker the rate of wear was so low that only 4.5 g were worn off each 3 in. standard ball

after a 222 hr run. While the limit of experimental error on this test was relatively high, a compensating factor was found in the fact that the spread in wear resistance between the good and poor types of balls was so great that there was no doubt about the relative merits of the various types tested.

Table 1 gives the actual rates of wear obtained on our standard balls when run in ten tests representing a rather wide variety of operating conditions. From these values of wear rates per unit of area, the rate at which the balls decrease in diameter and their useful life period have been calculated for each condition. This calculation assumes that mill operating conditions remain constant and that the wear on each ball continues to be in direct proportion to its surface area for its entire life. The life of individual balls in a mill is of particular interest when large scale wear tests are planned on one or more types of balls. General practice on such tests is to start adding the test balls to the mills daily in the quantity needed to maintain the ball charge at a desired level. When the operator is satisfied that the balls formerly used in the mill are substantially all worn out, and the test balls have worn in sufficiently to form an equilibrium ball charge, he then starts to keep an accurate record of the weight of test balls added to the mill. It may be seen from Table 1 that this method of testing can develop into a long, tedious process because of the fact that it requires months and in some cases years to replace the former charge of balls with the test balls.

The rate at which individual balls wear will tend to be faster in mills of large diameter than in mills of small diameter. Theoretically the wear rate of an individual ball in a charge will increase as the 0.6 power of the mill diameter. This general trend for the balls to wear faster in the larger diameter mills is observable from the data in Table 1. An accurate experimental

TABLE 1—Wear Rates on Standard Martensitic Forged Steel Balls in Various Mills

Company	Location	Abrasive	Mill Diameter (Feet)	Ball Makeup Diameter (Inches)	Wear per 100 Sq. Cnt. per 24 Hrs (Grams)	Loss in Diameter per 24 Hr. (Inches)	Approximate* Life (Days)
Climax Molybdenum Co.	Climax, Colo.	Mo ore	9	100 pct—3 in.	22.7	0.0228	99
Climax Molybdenum Co.	Climax, Colo.	Mo ore	9	50 pct—3 in.	17.1	0.0172	131 on 3 in. 73 on 2 in.
Climax Molybdenum Co.	Climax, Colo.	Mo ore	6	100 pct—2 in.	13.3	0.0134	108
Homesake Mining Co.	Lead, S. Dak.	Gold ore	5	100 pct—3 in.	9.0	0.0090	139
Belts-Podge Corp.	Ajo, Ariz.	Copper ore	6½	100 pct—2 in.	8.6	0.0086	202
Miami Copper Co.	Miami, Ariz.	Copper ore	8	100 pct—3 in.	10.4	0.0105	214
Colo. Portland Cement Co.	Portland, Colo.	Dry cement clinker	8	4 in. and smaller	0.24	0.00024	13,500 on 4 in.
Colo. School of Mines.	Golden, Colo.	River sand	3	3 in.	8.3	0.0083	271†
Colo. School of Mines.	Golden, Colo.	Feldspar	3	3 in.	3.7	0.0037	608†
Colo. School of Mines.	Golden, Colo.	Calcite	3	3 in.	0.31	0.00031	7200†

* The "life" of a ball is calculated here as the time required to wear it from its original diameter down to 0.75 in. diameter.

† This life is on a charge consisting entirely of 3 in. balls. If the charge had been an equilibrium charge containing balls graduated from 3 in. diam down to 0.75 in. then the wear rate would have been less and the life longer due to the greater total surface area of such a charge.

determination of this 0.6 power rule is however, rather difficult because of the numerous other variables which generally enter the picture when we change from a mill of one diameter to that of another diameter.

FUNDAMENTAL FACTORS GOVERNING BALL WEAR IN A MILL

In the development of a suitable testing technique, one of the first things we had to determine was the basis on which we could compare the wear of balls which varied in diameter or weight. Davis³ had stated that balls wore in direct proportion to their weight (or cube of their diameter). Ellis¹ in most of his tests based his wear rates on weight loss per unit of surface area, that is, he assumed that balls wore in direct proportion to the square of their diameter. Bond⁴ states that the balls in his tests wore as the 2.29 power of their diameter. Since both Davis' and Bond's methods of determining the proportionality of ball wear were of an indirect nature, we felt that further evidence on this subject should be obtained by more direct methods of observation. Groups of balls were, therefore, prepared which were metallurgically and chemically similar, the only variable being their diameter. These groups were run on various tests in a number of mills. It was found that the balls in these groups wore in direct proportion to their surface area, that is, in proportion to the square of their diameter. An exception to this surface area rule was found in the case where a few balls 4 to 5 in. in diam were run in a charge which consisted principally of balls 3 in. in diam and smaller. It was found that under such conditions the abnormally large balls tended to segregate to the outside of the mill charge where they would naturally absorb a greater than average amount of energy and, therefore, wore somewhat faster than was called for by the surface area law.

The mills in which these tests were run have varied from 3 to 9 ft in diam. Mill speeds ranged from 65 to 78 pct of critical while pulp densities and pulp levels varied sufficiently to produce a wide variation in the degree of impact to which the balls were subjected. In spite of these wide variations in operating conditions, we have been unable to find any deviation from this surface area law for ball wear except for the case mentioned where the large balls segregated to the outside of the mill.

Since, in the absence of size segregation, grinding balls in a mill will tend to wear in direct proportion to their surface area, the wear per unit of area will be the same on metallurgically and chemically similar balls even though these balls vary in size. Data from a number of our tests which confirm this observation are given in Table 2. It will be noted that within the limits of experimental error, for any given test, the wear per unit of area on balls of various diameters is practically identical.

Since grinding balls tend to wear in direct proportion to their surface area, it also follows that they will tend to lose diameter at a constant rate. This has been very nicely confirmed by Prentice's⁵ investigations. Garms and Stevens⁶ show a further confirmation of this in Fig 2 of their paper.

Davis³ based his conclusion that balls wear in proportion to their weight on the screen analysis of a number of ball charges. Prentice⁵ has compiled more recent data on the screen analysis of a number of ball charges. His compilation, and unpublished data from the screen analysis of ball charges in our Climax mills, tend to confirm the surface area theory of ball wear.

The nature of ball wear in a ball mill has been the object of much discussion ever since Davis³ published his original paper on this subject. It is suggested that our technique of wear testing can be used to yield further experimental data on this problem. Our tests indicate that the wear in a ball

TABLE 2—*Wear Rates of Balls of Various Diameters in Several Tests**

a. Annealed, Forged Steel, Plain Carbon Balls in 3-ft Diam Mill at Golden. Results from one 24-hr Test in River Sand and one 24-hr Test in Climax Ore

Nominal Diameter (Inches)	Actual Area (Sq Cm)	Grams Lost per 100 Sq Cm	
		Sand	Climax Ore
3	178.1	11.0	10.1
2	78.6	10.6	9.8

b. Martensitic Forged Steel (Standard) Balls in a 5-ft Diam Mill at Homestake Mining Co. Results from 239-hr Test in Partially Ground Homestake Ore

Nominal Diameter (Inches)	Actual Area (Sq Cm)	Grams Lost per 100 Sq Cm
3	170.0	89.8
3	176.6	89.1
2½	124.8	90.3

c. Soft Pearlitic Forged Steel Balls (277 Brinell) in a 5-ft Diam Mill at Homestake Mining Co. Results from a 239-hr Test in Partially Ground Homestake Ore

Nominal Diameter (Inches)	Actual Area (Sq Cm)	Grams Lost per 100 Sq Cm
3	164.9	110.1
3½	224.5	109.7

d. Soft Pearlitic Forged Steel Balls (277 Brinell) in a 6¼-ft Diam Mill at Phelps Dodge Corp., Ajo, Ariz. Results from a 168-hr Test in Ajo Ore

Nominal Diameter (Inches)	Actual Area (Sq Cm)	Grams Lost per 100 Sq Cm
2¾	151.4	94.8
3¼	209.0	95.3

e. Martensitic Forged Steel (Standard) Balls in a 3-ft Diam Mill at Golden. Results from one 24-hr Test in River Sand and one 24-hr Test in Climax Ore

Nominal Diameter (Inches)	Actual Area (Sq Cm)	Grams Lost per 100 Sq Cm	
		Sand	Climax Ore
3	163.0	8.28	8.43
2½	113.9	8.31	8.30

f. Martensitic Forged Steel (Standard) Balls in a 9-ft Diam Mill at Climax, Colo. Results from one 162-hr Test in Climax Ore

Nominal Diameter (Inches)	Actual Area (Sq Cm)	Grams Lost per 100 Sq Cm
3	175.5	116.3
3	170.0	115.8

* The results given represent averages. A total of five to twenty balls of each type was run in each test.

charge tends to be uniformly distributed over the surface so that the wear on any one ball is proportional to its surface area. It would seem to follow that the energy induced by rotation of the mill and the grinding effect are similarly distributed.

THE MECHANISM OF WEAR

Our wear tests lead us to believe that wear may be classified in all cases as occurring by two mechanisms. One is by the removal of oxide films or other chemical coatings which form on the freshly exposed metallic surface of the wearing part. When wear occurs by this mechanism, the chemical composition of the metal is the dominating factor. A reduction of wear under these conditions can be most readily accomplished by selecting a metal or alloy which forms a hard and adherent oxide film such as that obtained on high chromium alloys.

The other classification of wear involves the removal of the surface of the part as metallic particles. When wear occurs by this mechanism, we believe the controlling factors governing rate of wear are determined by the distribution and characteristics of the micro-constituents in the metal or alloy. In the case of grinding balls, operating in mills of commercial size, our tests indicate that most of the wear occurs by the removal of metallic particles since the microstructure of all balls tested has been the dominant factor in the determination of their wear resistance. For instance, we have found that balls of the same analysis but of different microstructure will generally show a corresponding difference in wear resistance. On the other hand, balls of widely different alloy content but with practically the same microstructure will show relatively small differences in wear resistance.

Ellis² has found, under the conditions existing in his laboratory testing of grinding balls, that wear caused by the removal of oxide films was a dominating factor.

His tests were run in small jar mills on balls 1 in. in diam. Under these conditions the addition of chromium to his steel or iron composition was found to be very effective in reducing ball wear. We suspect that when wear in grinding balls occurs primarily by the removal of oxide films, the forces causing abrasion are unusually mild. Where larger balls are used in the larger test mills, or in mills of commercial size, the metallic particles worn from balls during a wet grinding operation can generally be removed from the ground pulp by gravity or magnetic concentration, though a complete separation is difficult. Probably the finer particles are rapidly oxidized, so quantitative determinations of metallic iron in the ground pulp may be misleading. These ground pulps, when allowed to stand, will often generate surprisingly large volumes of hydrogen, indicating the reduction of hydrogen ions by the metallic iron. This hydrogen evolution is the basis of one quantitative method of determining the amount of metallic iron in these pulps.

We believe that the oxide films play only a minor part in determining the wear of grinding balls in most ball mills. In acid or corrosive pulps, or where small balls are used in mills of small diameter, the influence of oxide films on the balls may become an important consideration. The microstructure of the steel or iron balls may also have a definite influence on the formation of the oxide films. Metallographists are all familiar with the fact that pearlite etches more rapidly than martensite when exposed to oxidizing acids. We have indications that a similar condition exists during the formation of oxide films on the freshly abraded surfaces of grinding balls. For instance, on a series of batch tests in the 3 ft diam mill at Golden, using crushed Climax ore as the abrasive, when the mill atmosphere was changed from air to a pure oxygen atmosphere, a group of pearlitic steel balls showed a 39 pct increase in rate of wear while the standard martensitic

balls showed only a 19 pct increase in rate of wear. On the other hand, when we attempted to reduce the rate of oxidation of the balls by operating in an air atmosphere with an alkaline pulp, the pearlitic balls showed a 10.7 pct decrease in rate of wear while the martensitic balls showed only a 7.4 pct decrease. The martensitic steel was, therefore, less affected by changes in oxidizing conditions than the pearlitic steel. Since the oxygen in an air atmosphere apparently did have some influence on rate of wear, it is reasonable to expect that at least some reduction in rate of wear by oxidation may be achieved by making the steel martensitic.

The changes in rate of wear which we obtained by the use of an oxygen atmosphere or by making the pulp alkaline are not nearly so great as those obtained by Ellis² in his small jar mills. We believe the reason for this is that in our tests the wear by removal of oxide films did not represent nearly as great a proportion of the total as it did in Ellis' small laboratory mills.

DEFINITION OF MICROSTRUCTURAL CLASSIFICATIONS

Since the balls in our wear tests were studied with particular reference to their microstructure, a brief definition of the terms used to describe these microstructures is in order.

During the solidification of a medium or high carbon steel or of hypoeutectic compositions within the white iron range, the first constituent to solidify is austenite. Upon cooling, this austenite may transform to pearlite, bainite, or martensite with the product of transformation depending on the temperature at which the austenite transforms. The austenite and its transformation products are often referred to as the "matrix" of the steel or iron, and are, at times, so designated in this paper. During the cooling of the solidified austenite, pro-eutectoid carbides or ferrite may be rejected. Since these constituents are

rejected around the austenite grains, they are referred to as grain boundary carbides or ferrite.

Spheroidized carbides, which occurred in several groups of balls which we studied, were produced by reheating operations after casting or forging. They existed in all cases as very small globular particles finely disseminated throughout the matrix of the steel.

Sulphides were observable and easily identified in several cast steels of high sulphur content. Where they occurred as envelopes or partial envelopes around the original austenite grains, they are classed as grain boundary sulphides. Where they occurred as globules within the original austenite grain boundaries they are classed as globular sulphides.

When ferrous alloys within the cast iron range of compositions solidify, there will form around or adjacent to the original austenite grains: carbides, which we shall designate as primary or massive carbides; graphite, which will be so designated; and steadite, an iron phosphorus eutectic. In one case, ledeburite, which is a eutectic of austenite or its transformation products and primary iron carbide, is mentioned.

Pearlite is the lamellar product resulting from transformation of austenite at temperatures from the A_{e1} temperatures (approximately 1350°F (730°C) for most of the compositions studied) and about 1000°F (540°C). It will be further classified into coarse, medium and fine pearlite depending on the size and spacing of the lamellae. Bainite is the acicular product resulting from transformation of austenite at temperatures which are generally below 900°F (480°C) and above 450°F (230°C). For most of our compositions, the bainite was formed between 800 and 500°F (430-260°C). Substantial amounts of retained austenite generally were found along with the bainite. Martensite refers to the hard acicular product formed below the $A_{r''}$ temperature of the steel. This $A_{r''}$

temperature was within a range of 550 to 350°F (290–180°C) for most of the compositions which we studied. There were, however, a few compositions which contained a total alloy content sufficient to depress the A_1'' temperature to values near or below room temperature so that refrigeration was necessary to obtain appreciable transformation from austenite to martensite.

The similarity in appearance between martensite and low temperature bainite is such that we may, in a number of cases, have confused one with the other. On our more recent investigations we have attempted to distinguish between bainite and martensite by determining the temperatures at which the balls transformed with "Tempilstiks" and a magnet.

Spheroidite as described by Payson⁷ has also been studied in a few of these wear tests. This structure was obtained in a few of the normalized high carbon, low alloy steels.

WEAR RESISTANCE OF STEEL OF VARIOUS MICROSTRUCTURES

Microstructure seems to be the dominating factor insofar as the wear resistance of steel grinding balls is concerned. Structure of the matrix appears to be most important. Grain boundary carbides and undissolved spheroidized carbides have a minor, though by no means negligible, effect on wear resistance. The effect of massive carbides is variable and appears to depend to some extent on the character of the matrix. Grain boundary and massive carbides have a pronounced influence on the resistance shown by the balls to spalling and breakage under severe impact. Grain boundary ferrite is harmful to wear resistance.

Carbon content plays such a dominant part in determining the microstructure of a steel or iron that its influence will be discussed in this section on microstructure rather than in a later section on the influence of chemical composition on wear resistance.

The relative wear resistance (abrasion factors) of eleven of the more important types of steel and iron representing certain typical microstructures is listed in Table 3. The abrasion factors obtained under seven different operating conditions are given. The eleven analyses are listed in their approximate order of merit.

Generally, in the conduct of our wear tests, a wide variety of types was included in each test. The complete data from two of our more comprehensive tests are listed in Tables 4 and 5 for illustrative purposes. It is from such data as these that we have taken the selected data for Table 3.

In studying the influence of microstructure on wear resistance, our discussion can be conveniently divided into three parts, one dealing with a matrix structure made up of austenite, martensite, or bainite or a combination of these, and the second with a matrix structure of fine, medium or coarse pearlite. The third part deals with structures containing a matrix of spheroidal carbides in ferrite.

1. *Balls with a Matrix of Austenite, Martensite or Bainite*

A well known form of steel containing austenite is found in the 12 to 14 pct manganese, 1.0 to 1.3 pct carbon Hadfield manganese steel which has been reheated after casting to about 1900°F (1040°C) and water quenched. This steel represents a rather stable form of austenite which can be work hardened from its as-quenched hardness value of about 10 R_C to a maximum of 58 R_C . In our work on grinding balls the highest hardness observed on the work hardened surface of Hadfield manganese steel was 54 R_C . We have never been able to detect the transformation of this austenite to ferro-magnetic products (such as martensite) by work hardening of the surface. This applies to both balls and crusher parts. This finding is supported by the work of Goss⁸ who concluded that no such products are formed from the work

TABLE 3—Abrasion Factors of Typical Microstructures When Tested as 3-in. Grinding Balls in Various Mills

				Conditions of Test						
Mill Location.....				Lead, S. D.	Golden, Colo.	Climax, Colo.	Climax, Colo.	Ajo, Ariz.	Golden, Colo.	Portland, Colo.
Mill Diameter (Feet).....				5	3	6	9	6½	3	8
Mill Speed (rpm).....				27	32	25	20	23.1	32	17.5
Pulp Density (pct Solids).....				75	3	77	75	70	70	Dry
Discharge Level of Pulp.....				High	High	High	Low	High	High	Low
Duration of Test (Hours).....				239	48	145	162	168	36	222
Type of Ore.....				Gold	River Sand	Molybdenum	Molybdenum	Copper	Feldspar	Cement Clinker
Principal Abrasives.....				Iron-Magne- sium-Sili- cate	Quartz and Feldspar	Quartz and Feldspar	Quartz and Feldspar	Feldspar and Quartz	Albite and Orthoclase	Ca. Aluminate Ca. Silicate
				Abrasion Factors						
Item No.	Microstructure	Hard- ness Bhn	Carbon Per Cent	Lead, S. D.	Golden, Colo.	Climax, Colo.	Climax, Colo.	Ajo, Ariz.	Golden, Colo.	Portland, Colo.
1	Mart., Aust., primary Carb. (sand cast).....	601	3.23	95	101	95	95	84	72	
2	Bainite or Martensite plus Aus- tenite.....	512-627	0.90-1.01	96			96	90	77	
3	Martensite, some retained Aust. (Std.).....	652-683	0.80-0.86	100	100	100	100	100	100	100
4	Mart., Aust., primary Carb. (chill cast).....	637	3.27		106	104	Spalled			Broke
5	Fine high carbon Pearlite.....	364	1.01	104	107	110	110	128	244	
6	Fine eutectoid Pearlite.....	375	0.71	110	110	115	115	132	264	366
7	Austenite (Hadfield Mn Steel).....	207	1.14	120	133	130	124	154	364	
8	Coarse Pearlite.....	269	0.70	123		134	127	158		
9	Fine Pearl., primary Carb. (chill cast).....	475	3.20	128		138	Spalled	163		
10	Coarse Pearl., primary Carb. (chill cast).....	444-460	2.70-3.20	139	160	154	Broke	175	247	
11	Coarse Pearl., primary Carb. (sand cast).....	475	3.20		178	176				

Abbreviations: Mart. = Martensite.
 Carb. = Carbide.
 Aust. = Austenite.
 Pearl = Pearlite.

hardening of Hadfield manganese steel. This steel has shown relatively poor wear resistance in all our wear tests in which it has been included. This is observable from the abrasion factors for item 7 of Table 3, from item 42 of Table 4, and items 31 or 32 of Table 5. The influence of the carbon content on this type of austenitic steel has not been investigated by us.

One should not conclude from the results for Hadfield manganese steel that all types of austenite will have poor wear resistance when tested as grinding balls. Other types of austenite, which tend to transform quite readily to martensite when work hardened, exist at room temperature. Many of the groups of balls which we have tested contained austenite of this latter type. These groups have in all cases stood at the top of the list insofar as wear resistance is concerned, which leads us to believe that those types of austenite which will transform readily to martensite when cold worked are not harmful to wear resistance of grinding balls. This is demonstrated in Table 6 which lists the results obtained from nine steel compositions containing retained austenite.

The groups of balls listed in Table 6 were selected from Table 5. Tables 3 and 4 list a number of additional results on groups which contained retained austenite. It will be noted that these groups all show excellent wear resistance.

Some of the most wear resistant groups of balls in our tests had relatively low initial hardness because of their large amount of retained austenite. These balls have shown a substantial amount of work hardening on their surface as determined by Rockwell C impressions. For instance the balls in item 8 of Table 5 had a hardness of 40-41 R_C before testing. After a series of wear tests, which concluded with the test at Ajo, the balls in this group had surface hardnesses in the range of 50-56 R_C . Similarly, the surface hardness of the balls in item 10 of Table 5 increased from 53-55

R_C to 61-64 R_C . These surface hardness readings are possibly low since the Rockwell C impressions have probably penetrated into the softer metal below the surface. Balls which did not contain retained austenite showed no appreciable work hardening at the surface, as measured by the Rockwell C test.

To study more fully the influence of retained austenite in the matrix of grinding balls, tests were run on five steel compositions of varying austenite stability. The composition, heat treatment and hardness of these steels, together with the abrasion factors obtained from them on a wear test in the test mill at Golden, are given in Table 7. The groups are listed in order of decreasing austenite stability. Group 1-WQ represents austenitic manganese steel water quenched directly from the mold. It was completely austenitic except for a small amount of primary carbide around the dendritic grain boundaries. The relatively high rate of wear which we obtained from this type of austenite is similar to that obtained from items 31 or 32 of Table 5.

Microscopic observation and magnetic permeability tests indicated that groups 2-WQ and 2-AQ were similar and were completely austenitic except for some primary carbides around the dendritic grain boundaries. Magnetic permeability tests indicated that a slight amount of transformation to martensite occurred in group 2-WQR when it was refrigerated to -70°F (-57°C). Small specimens of steels 2-WQ and 2-AQ could be work hardened to a maximum of 44 R_C by hammering. This work hardening brought about some transformation to ferromagnetic products, indicating the formation of martensite.

Tests similar to those run on the three groups of composition 2 were also run on the three groups of composition 3. Groups 3-WQ and 3-AQ appeared to be completely austenitic except for the primary carbides around the grain boundaries. Group 3-WQR showed appreciable transformation

TABLE 4—Relative Rates of Wear of 3-in. Diameter Grinding Balls in a 6 X 6-ft. Mill at Climax, Colo. (May 1941)

Item No.	No. of Balls	Heat Treatment	Microstructure	Hardness† Bhn	Analysis, Per Cent							Abrasion Factor G. per cc		
					C	Mn	Cr	Mo	Ni	Cu	Si		S	P
(a) Forged Steel														
1	5	Oil Quench from forge, T. 375°F.	Mart., Bain. (?), Aust.	627	1.01	0.44	1.06	0.21				0.34		7.77
2	6	Oil Quench from forge, T. 375°F.	Mart., Bain. (?), Aust.	578	1.03	1.32	1.06	0.22				0.40		7.80
3	12	Forged, reheated 1525°F., W.Q., T. 375°	Mart., Spheroidized Carbide	683	1.01	0.44	1.06	0.21				0.34		7.81
4	7	Oil Quench from forge, T. 375°F.	Mart., Bain. (?), Aust.	683	0.75	0.45	0.42	0.26				0.65		7.75
5	15	Forged, reheated, W.Q. T. 300°F.	Martensite, austenite	652	0.86	0.32	0.20	0.29				0.26	0.029	0.011
6	12	Forged, reheated, O.Q. T. 375°F.	Mart., Bain., Aust.	652	0.75	0.45	0.42	0.26				0.65		7.78
7	10	Water quench from forge.....	Martensite	745	0.70	0.66						0.15	0.033	0.013
8	14	Forged, reheated, W.Q.....	Martensite	668	0.71	0.63						0.22	0.033	0.013
9	15	Forged, reheated, O.Q.....	Not observed	534	0.86	0.59		0.29				0.26	0.029	0.011
10	3	Delayed O.Q. from forge, T. 450°F.	Mart., Aust., G.B. Carbide	600	1.03	1.32	1.06	0.22				0.40		7.79
11	15	Forged, air cooled.....	Fine pearlite, G.B. Carbide	387	1.03	1.32	1.06	0.22				0.40		7.81
12	15	Forged, air cooled.....	Fine pearlite, G.B. Carbide	304	1.01	0.44	1.06	0.21				0.34		7.80
13	10	Oil quench from forge.....	Fine pearlite	370	0.75	0.60*						0.20*		7.85
14	7	Forged, oil quenched, T. 1050°F.	Tempered martensite	387	1.01	0.44	1.06	0.21				0.34		7.80
15	6	Forged, oil quenched, T. 1050°F.	Tempered martensite	402	1.03	1.32	1.06	0.22				0.40		7.78
16	15	Forged, air cooled.....	Fine pearlite	387	0.75	0.45	0.42	0.26				0.65		7.79
17	15	Oil quench from forge.....	Fine pearlite	375	0.71	0.63						0.22	0.033	0.013
18	14	Oil quench from forge.....	Fine pearlite, a little ferrite	375	0.70	0.66						0.15		7.82
19	8	Forged, oil quenched, T. 1050°F.	Bainite, Martensite	387	0.75	0.45	0.42	0.26				0.65		7.80
20	14	Oil quench from forge.....	Not observed	408	0.46	1.74						0.19	0.042	0.026
21	10	Forged, air cooled.....	Pearlite	340	0.52	1.45	0.85					0.29	0.020	0.011
22	15	Forged, air cooled.....	Coarse Pearlite	302	0.86	0.59						0.27	0.033	0.013
23	20	Forged, air cooled.....	Coarse Pearlite	286	0.70	0.88						0.22		7.83
24	15	Forged, air cooled.....	Coarse Pearlite	258	0.71	0.63						0.22		7.83
(b) Cast Steel														
25	8	Sand Cast, norm. 1800°F., T. 600°F.	Spheroid. Carb., T. Mart.	555	1.10	0.47	5.45	0.51				0.73	0.02*	0.04*
26	4	Sand Cast, norm. 1800°F., T. 600°F.	Spheroid. Carb., T. Mart.	600	0.85	0.48	5.88	0.47				0.70	0.02*	0.04*
27	6	Chill Cast, air cooled.....	Martensite, Austenite	512	0.84	1.14	2.61	0.43	1.51			0.47	0.02*	0.04*
28	4	Sand Cast, norm. 1800°F., T. 1000°F.	Spheroid. Carb., T. Mart.	555	0.85	0.48	5.88	0.47				0.70	0.02*	0.04*
29	8	Sand Cast, cooled in sand.....	Aust., Pearl., G.B. Carb.	375	1.10	0.47	5.45	0.51				0.73	0.02*	0.04*
30	9	Chill Cast, air cooled, T. 600°F.	Tempered Martensite	555	0.73	0.95	1.84	0.42	0.99			0.47	0.02*	0.04*

31	5	Sand Cast, norm. 1650°F., T. 600°F.,.....	601	0.78	0.93	1.63	0.48	0.87	0.44	0.02*	0.04*	7.69	104
32	14	Chill Cast, air cooled,.....	408	1.36	0.93	1.68	0.39	0.98	0.55	0.02*	0.04*	7.71	104
33	13	Sand Cast, cooled in sand,.....	352	1.06	1.51	2.63	0.53		0.44	0.02	0.04	7.78	106
34	14	Sand Cast, cooled in sand,.....	341	1.06	2.02	3.05	0.26		0.42	0.05	0.01	7.83	107
35	4	Sand Cast, cooled in sand,.....	351	0.85	0.48	5.88	0.47		0.72	0.02*	0.04*	7.63	108
36	4	Sand Cast, cooled in sand, T. 1000°F.,.....	341	0.85	0.48	5.88	0.47		0.70	0.02*	0.04*	7.62	108
37	14	Sand Cast, cooled in sand,.....	388	1.29	1.03	1.60	0.42	0.99	0.41	0.03	0.06	7.77	109
38	7	Sand Cast, cooled in sand,.....	375	0.91	1.04	1.66	0.43	0.78	0.61	0.02	0.04	7.62	110
39	7	Sand Cast, cooled in sand,.....	364	0.86	1.04	1.66	0.43	0.78	0.61	0.02	0.04	7.67	110
40	7	Sand Cast, cooled in sand,.....	369	0.78	0.93	1.63	0.48	0.87	0.44	0.02*	0.04*	7.74	111
41	6	Sand Cast, ann. 1800°F., norm. 1050°F.,.....	351	0.86	1.04	1.66	0.43	0.78	0.61	0.02*	0.04*	7.64	113
42	8	Sand Cast, reheated 1900°F., W.Q.,.....	200	1.14	12.38				0.54	0.02*	0.04*	7.72	130

(c) Chill Cast Iron

43	4	Cooled in air,.....	637	3.27	0.50*	1.50*	4.50*		0.50*			7.74	104
44	15	Cooled in air,.....	475	3.20*	0.40*	0.90*	0.25*		1.70*			7.51	138
45	10	Cooled in air,.....	460	2.75	0.75*				0.30*	0.15*	0.15*	7.57	153
46	13	Cooled in sand,.....	477	3.66*	0.50*				0.55	0.10*	0.30*	7.58	154
47	7	Cooled in air,.....	444	2.70	0.21	0.02	0.02		0.22	0.10	0.12	7.59	163

(d) Sand Cast White Iron and High Metalloid Steels

48	7	Cooled in sand,.....	600	3.23	0.64	1.89		4.26	0.62	0.11	0.10	7.71	95
49	8	Cooled in sand, T. 400°F.,.....	600	3.23	0.64	1.89		4.26	0.62	0.11	0.10	7.72	96
50	15	Cooled in sand,.....	364	0.99	0.55	2.69	0.35		0.50	0.19	0.33	7.72	119
51	14	Cooled in sand,.....	387	1.24	1.03	2.63	0.28		0.36	0.12	0.31	7.72	122
52	15	Cooled in sand,.....	401	1.53	1.68	2.56	0.54		0.36	0.16	0.32	7.71	127
53	15	Cooled in sand,.....	415	1.33	1.66	2.61	0.26		0.49	0.17	0.33	7.73	130
54	15	Cooled in sand,.....	331	1.02	0.50	0.19	0.57	1.04	0.42	0.17	0.30	7.75	130
55	14	Cooled in sand,.....	285	1.02	1.07				0.46	0.19	0.33	7.72	141
56	5	Cooled in sand,.....	460	1.54	2.52	1.10			0.51	0.15	0.26	7.72	141
57	14	Cooled in sand,.....	532	3.00	1.51	1.94		2.75	0.64	0.13	0.29	7.70	151
58	15	Cooled in sand,.....	477	3.00*	0.65*	0.80*	0.25*		0.90*	0.17*	0.40*	7.62	176
59	14	Cooled in sand,.....	578	3.20*	0.70*	2.55*			2.50*	0.80*		7.69	182

* Approximate analysis.

† Hardness refers to the hardness of the metal actually removed by wear.
 Abbreviations: T. = Tempered
 Norm. = Normalized
 Bain. = Bainite
 Carb. = Carbide
 Spheroid. = Spheroidized
 O.Q. = Oil Quenched
 G.B. = Grain Boundary
 Mart. = Martensite
 Aust. = Austenite
 Sulph. = Sulphide
 Mass. = Massive
 Glob. = Globular

TABLE 5—Relative Rates of Wear of 3-in. Diameter Grinding Balls in $6\frac{1}{2} \times 15$ -ft. Mill at Phelps Dodge Corp., Ajo, Ariz. (November 1941)

Item No.	No. of Balls	Heat Treatment	Microstructure	Hardness† (Bhn)	Analysis, Per Cent								Abrasion Factor	Density, G per cc
					C	Mn	Cr	Mo	Ni	Cu	Si	S		

(a) Forged Steel																
1	5	Oil quench from forge. T. 375°F.	Mart., Bain., Aust.	627	1.01	0.44	1.06	0.21				0.34			7.77	90
2	6	Oil quench from forge. T. 375°F.	Mart., Bain., Aust.	578	1.03	1.32	1.06	0.22				0.40			7.80	92
3	15	Forged, reheated, W.Q., T. 300°F.	Mart., Aust.	652	0.80	0.60		0.29				0.26			7.81	100 Std.
4	10	Oil quench from forge.	Fine pearlite	370	0.75	0.60*						0.20*			7.85	131.
5	14	Oil quench from forge.	Fine pearlite, a little ferrite	375	0.70	0.66						0.15			7.82	133
6	15	Forged, air cooled (2¾ in.)	Coarse pearlite	286	0.70	0.88						0.27			7.80	157
7	15	Forged, air cooled (3¼ in.)	Coarse pearlite	269	0.70	0.88						0.27			7.82	158

(b) Cast Steel																	
8	10	Chill cast, air cooled.	Aust., Bain., trace of pearl.	364	0.90	1.68	2.85	0.41				0.58	0.02*	0.04*	7.75	94	
9	5	Chill cast, air cooled.	Aust., Bain., Pear.	452	0.96	1.68	3.43	0.32				0.65	0.03*	0.04*	7.77	94	
10	5	Chill cast, air cooled.	Bain., Aust.	512	0.88	0.97	1.56	0.33	0.59			0.92	0.03*	0.04*	7.72	96	
11	1	Chill cast, W.Q. ½ min. air cooled.	Bain., Aust., globular Sulph.	555	1.00	1.21		0.30*				0.35*	0.06*	0.17*	7.76	97	
12	1	Chill cast, W.Q. ½ min. air cooled.	Bain., Aust., globular Sulph.	555	1.01	1.19		0.30*				0.35*	0.06*	0.17*	7.76	98	
13	3	Chill cast, water quenched.	Mart., Aust., G.B. Sulph.	627	0.95	0.90				0.30*		0.30*	0.35*	0.06*	0.17*	7.69	98
14	3	Chill cast, water quenched.	Mart., Aust., G.B. Sulph.	682	0.90	0.85				0.30*		0.30*	0.35*	0.06*	0.17*	7.72	99
15	1	Chill cast, water quenched.	Mart., Aust., G.B. Sulph.	601	1.00	1.21		0.30*				0.35*	0.06*	0.17*	7.72	100	
16	2	Chill cast, water quenched.	Mart., Aust., G.B. Sulph.	640	0.94	1.36		0.30*				0.35*	0.06*	0.17*	7.71	100	
17	4	Chill cast, water quenched.	Mart., Aust., G.B. Sulph.	682	0.78	0.75		0.30*				0.30*	0.35*	0.06*	0.17*	7.68	100
18	20	Chill cast, air cooled.	Bain., Aust., Pear.	582	0.79	0.92	1.32	0.27				0.47	0.05	0.13	7.62	104	
19	8	Sand cast, norm. 1800°F., T. 600°F.	Spheroid. Carb., T. Mart.	555	1.10	0.47	5.45	0.51				0.73	0.02*	0.04*	7.69	107	
20	5	Chill cast, air cooled.	Pearl., Mart., Aust.	534	1.03	1.36	2.00	0.30*				1.00*	0.35*	0.06*	0.17*	7.75	112
21	5	Chill cast, air cooled.	Pearl., Mart., Aust.	535	1.03	1.35	2.00	0.30*				2.00*	0.35*	0.06*	0.17*	7.76	112
22	13	Chill cast, air cooled.	Fine Pearl., G.B. Carbide	408	1.36	0.93	1.68	0.39	0.98			0.55	0.02*	0.04*	7.71	121	
23	1	Chill cast, W.Q. ½ min. air cooled.	Bain., Mart., Aust., G.B. Sulphide	444	0.94	1.36		0.30*				0.35*	0.06*	0.17*	7.77	125	
24	8	Sand cast, cooled in sand.	Aust., Pear., G.B. Carbide	375	1.10	0.47	5.45	0.51				0.73	0.02*	0.04*	7.68	126	
25	13	Sand cast, cooled in sand.	Fine Pearlite	352	1.06	1.51	2.63	0.53				0.44	0.02	0.04	7.78	128	

TABLE 5—(Continued)

Item No.	No. of Balls	Heat Treatment	Microstructure	Hardness (Bhn)	Analysis, Per Cent										Density, G per cc	Abrasion Factor
					C	Mn	Cr	Mo	Ni	Cu	Si	S	P			
26	7	Sand cast, cooled in sand.....	Fine Pearlite	364	0.86	1.04	1.66	0.43	0.78			0.61	0.02*	0.04*	7.67	132
27	6	Sand cast, ann. 1800°F., norm. 1650°F.....	Spheroidite	351	0.86	1.04	1.66	0.43	0.78			0.61	0.02*	0.04*	7.64	135
28	1	Chill cast, W.Q. ½ min., air cooled.....	Pearl., Bain., G.B. Sulphide	363	0.92	0.92						0.35*	0.06*	0.17*	7.77	137
29	5	Chill cast, air cooled.....	Pearl., Mart., G.B. Carb., and Sulph.	401	1.02	1.16		0.30*		1.00*	0.35*	0.06*	0.17*	7.75	143	
30	1	Chill cast, W.Q. ½ min., air cooled.....	Pearl., G.B. Sulphide	363	0.92	0.90				0.30*	0.35*	0.06*	0.17*	7.78	153	
31	5	Chill cast, reheated 1900°F., W.Q.....	Austenite	207	1.15	12.50						0.60*	0.02*	0.04*	7.75	154
32	5	Chill cast, air cooled.....	Aust., G.B. Carbides	207	1.15	12.50						0.60*	0.02*	0.04*	7.74	155
(c) Sand and Chill Cast Iron																
33	7	Sand cast, cooled in sand.....	Mart., Aust., Massive Carb.	601	3.23	0.64	1.89		4.26			0.62	0.11	0.10	7.71	84
34	8	Sand cast, cooled in sand, T. 400°F.....	Mart., Aust., Massive Carb. Pearl., Massive Carbide	601	3.23	0.64	1.89		4.26			0.62	0.11	0.10	7.72	87
35	15	Chill cast, air cooled.....	Pearl., Massive Carbide	512	3.20*	0.40*	0.90*	0.25*				1.70*			7.51	103
36	10	Chill cast, air cooled.....	Pearlite, massive Carbide	460	2.75	0.75						0.30*	0.16*	0.15*	7.57	168
37	10	Chill cast, air cooled.....	Pearlite, massive Carbide	444	3.00*	0.50*						0.60*	0.15*	0.25*	7.60	170
38	27	Chill cast, air cooled.....	Pearlite, massive Carbide	409	2.75*	0.75*						0.30*	0.16*	0.15*	7.57	173
39	15	Chill cast, air cooled.....	Pearlite, massive Carbide	486	2.75*	0.75*						0.30*	0.16*	0.15*	7.55	181
40	7	Chill cast, air cooled.....	Pearlite, massive Carbide	444	2.70	0.21	0.02	0.02				0.22	0.16	0.12	7.59	185

* Approximate analysis.

† Hardness refers to the hardness of the metal actually removed by wear.

Abbreviations: W.Q. = Water Quenched

G.B. = Grain Boundary

Bain. = Bainite

Pearl. = Pearlite

Carb. = Carbide

T. = Tempered

Mart. = Martensite

Aust. = Austenite

Sulph. = Sulphide

Spheroid. = Spheroidized

TABLE 6—*Relative Rates of Wear of Nine Steel Compositions Containing Retained Austenite*
(168 Hr Wear Test in $6\frac{1}{2} \times 15$ -ft Mill at Phelps Dodge Corp., Ajo, Ariz.)

Group No.	Heat Treatment	Microstructure	Hardness (Bhn)	Analysis, Per Cent								Abrasion Factor
				C	Mn	Cr	Mo	Ni	Si	S	P	

(a) Forged Steel												
1	Oil Quenched from forge, T. 375°F.	Martensite, bainite, austenite	627	1.01	0.44	1.06	0.21		0.34			90
2	Oil Quenched from forge, T. 375°F.	Martensite, bainite, austenite	578	1.03	1.32	1.06	0.22		0.40			92
3	Forged, reheated, W.Q., T. 300°F.	Martensite, austenite	652	0.80	0.60		0.29		0.26			100 Std.

(b) Cast Steel												
4	Chill cast, air cooled.	Austenite, bainite, trace pearlite	364	0.90	1.68	2.85	0.41		0.58	0.02*	0.04*	94
5	Chill cast, air cooled.	Austenite, bainite, trace pearlite	452	0.06	1.68	3.43	0.32		0.95	0.03*	0.04*	94
6	Chill cast, air cooled.	Bainite, austenite	512	0.88	0.97	1.56	0.33	0.59	0.92	0.03*	0.04*	96
7	Chill cast, W.Q. $\frac{1}{2}$ min. air cooled.	Bainite, austenite, globular sulph.	555	1.00	1.21		0.30*		0.35*	0.06*	0.17*	97
8	Chill cast, water quenched.	Martensite, austenite, G.B. sulph.	637	0.95	0.90				0.35*	0.06*	0.17*	98
9	Chill cast, water quenched.	Martensite, austenite, G.B. sulph.	682	0.90	0.85				0.35*	0.06*	0.17*	99

* Approximate analysis.

TABLE 7—Relative Rates of Wear on Five Steel Compositions of Varying Austenite Stability
(24-hour Wear Test in 3 × 2 ft Mill at Golden Washed Pea Gravel Abrasive, 72.5 Pct Solids)

Group No.	Heat Treatment	Microstructure	Hardness* (RC)	Analysis, Per Cent						Abrasion Factor
				C	Mn	Cr	Mo	Ni	Si	
1-WQ	Chill cast, water quenched.....	Austenite, grain boundary carbide	12	1.15	13.00				0.60	154
2-WQ	Chill cast, water quenched.....	Austenite, grain boundary carbide	20	1.04	1.10	10.76	1.11	3.94	1.10	120
2-WQR	Chill cast, water quenched, refig. -70°F.....	Austenite, grain boundary carbide	23	1.04	1.10	10.76	1.11	3.94	1.10	120
2-AQ	Chill cast, air cooled.....	Austenite, grain boundary carbide	22	1.04	1.10	10.76	1.11	3.94	1.10	121
3-WQ	Chill cast, water quenched.....	Austenite, grain boundary carbide	23	0.96	1.35	9.48	1.08	1.53	0.90	105
3-WQR	Chill cast, water quenched, refig. -70°F.....	Austenite, martensite, G.B. carbide	37	0.96	1.35	9.48	1.08	1.53	0.90	105
3-AQ	Chill cast, air cooled.....	Austenite, grain boundary carbide	23	0.96	1.35	9.48	1.08	1.53	0.90	104
4-AQ	Chill cast, air cooled.....	Martensite, bainite (?), austenite	51	0.72	0.70	2.60	0.36	0.32	0.74	96
5-WQ	Forged, reheated, water quenched, T. 300°F.....	Martensite, austenite	62	0.80	0.60		0.29		0.26	100 Std.

* This represents the hardness of the metal before it was cold worked by the wear test.

to martensite on cooling to -25°F (-32°C) and additional transformation when cooled to -70°F (-57°C). This is also indicated by the higher hardness of group 3-WQR. Groups 3-WQ and 3-AQ could be work hardened to 53 R_C by hammering, and also showed substantial transformation to ferro-magnetic products. It is clear from these tests that the austenite in the groups of composition 3 was less stable than that of composition 2. This was apparently caused by the higher nickel content of composition 2, since there was very little difference in the content of the other austenite stabilizing elements (carbon, manganese, and chromium) in the two compositions.

Group 4-AQ contained fairly substantial amounts of austenite of relatively low alloy content. It is reasonable to expect that this austenite would be rather unstable and, therefore, easily subject to transformation to martensite when work hardened.

Group 5-WQ was our standard martensitic forged steel with which all test groups are compared. It represents mainly martensite in a mildly tempered condition. This mild temper consisted of a brief reheat at approximately 300°F (150°C) which each ball received as a result of its removal from the water quench before its center was completely cooled.

The wearing characteristics of the groups listed in Table 7 improve with decreasing stability of the retained austenite and reach an optimum in group 4-AQ which represents a relatively low alloy steel containing appreciable amounts of retained austenite. The type of martensite found in group 5-WQ causes a slight falling off in wear resistance.

Refrigeration had no effect on the wear resistance of group 3-WQR even though it raised the initial hardness from 23 R_C to 37 R_C . However this steel was subjected to cold work by the forces of impact involved in the wear test which may have raised its hardness at the wearing surface to a value above 50 R_C . A substantial amount of work

hardening occurred on the surface of all the austenitic balls though to such a shallow depth that we were unable to measure the surface hardness with any reasonable degree of accuracy.

It has been brought out that retained austenite at the wearing surface of low alloy, high carbon steel grinding balls will transform to martensite by the cold working effect which normally exists in a ball mill grinding operation. This retained austenite can also be transformed to martensite by refrigeration though the one result of such treatment, obtained from group 3-WQR in Table 7, does not indicate that transformation in this manner will appreciably improve the wear resistance of grinding balls.

Another method used for transforming retained austenite was to temper it for a short time at 600°F (315°C). The influence of tempering treatments up to 600°F (315°C) on the wear rates and hardnesses of three martensitic or bainitic steel compositions containing retained austenite is shown in Table 8. Tempering these compositions at 375°F (190°C) brought about a slight increase in hardness but very little, if any, change in wear resistance. By tempering the compositions at 600°F (315°C), however, the austenite in the steel was transformed to tempered martensite or bainite. Little overall change in hardness occurred as a result of this treatment. A marked drop in wear resistance did occur, however, with the average rate of wear for the three compositions almost doubling as a result of the 600°F (315°C) temper.

It should be noted that the wear tests listed in Table 8 were batch runs in a crushed feldspar abrasive. This abrasive was selected because abrasion tests run in feldspar tend to show a wide spread between balls of different wearing quality. This allows the detection of relatively minor differences in the wearing quality of balls. In this series of 6-hr tests the amount worn off the balls was quite small so that the limit of experimental error was

about ± 5 pct. For this reason we have listed wear rates in Table 8 instead of abrasion factors which require a higher degree of accuracy.

The abrasives and operating conditions in many commercial ball mills are such that the loss in wear resistance caused by the tempering of hardened balls at 600°F (315°C) will be much less than that shown for Table 8. For instance in Table 4, items 25, 26, 30, and 31 represent groups of balls which contained martensite or bainite plus retained austenite before they were tempered. Item 25 in Table 4 is also represented as item 19 in Table 5. These groups do not have as good wear resistance as we would expect from them if they had not been tempered. However, their loss in wear resistance was obviously not very great since they still show relatively good abrasion factors.

Further tests, of a more comprehensive nature, on the influence of tempering hardened steel balls should have practical value. Antia, Fletcher and Cohen⁹ have demonstrated that three separate tempering reactions occur between 180°F (80°C) and 675°F (355°C). A study of the wear resistance of the hardened steel before and after each of the tempering reactions should be of value.

The influence of carbon content on steels and irons having a matrix of martensite, bainite or austenite is of interest. This variable has not been fully investigated over the entire range of compositions by our tests. Quite a few martensitic steels within the range of 0.70 to 0.90 pct carbon have, however, been tested and found to be remarkably similar in wearing characteristics. It was for this reason that we chose a martensitic steel within this range of carbon content as our test standard.

When the carbon content of a martensitic steel was dropped to 0.60 pct or lower a definite falling off in wear resistance was noted. Martensitic 0.50 to 0.60 pct carbon low alloy steels when tested by grinding

TABLE 8—Influence of Tempering on the Wear Rates of 4 Groups of Hardened Steel Balls
(Averages from Two 6-hr Wear Tests in 3×2 -ft Mill at Golden. Feldspar Abrasive. 70 pct Solids)

Group No.	Heat Treatment	Microstructure	Hardness (Bhn)	Analysis, Per Cent					Wear Rate Grams per 100 Sq Cm per Test
				C	Mn	Cr	Mo	Ni	Si
1-a	O.Q. from forge.....	Martensite, bainite (?), austenite	606	1.01	0.44	1.06	0.21		0.34
1-b	O.Q. from forge temper 375°F, 1 hr.....	Martensite, bainite (?), austenite	627	1.01	0.44	1.06	0.21		0.34
1-c	O.Q. from forge temper 600°F, 1 hr.....	Bainite (?), Tempered martensite	600	1.01	0.44	1.06	0.21		0.34
2-a	O.Q. from forge.....	Martensite, bainite (?), austenite	482	1.03	1.32	1.06	0.22		0.40
2-b	O.Q. from forge temper 375°F, 1 hr.....	Martensite, bainite (?), austenite	578	1.03	1.32	1.06	0.22		0.40
2-c	O.Q. from forge temper 600°F, 1 hr.....	Bainite (?), Tempered martensite	578	1.03	1.32	1.06	0.22		0.40
3-a	Chill cast, air cooled.....	Bainite, austenite	642	0.73	0.95	1.84	0.42	0.99	0.47
3-b	Chill cast, air cooled, tempered 375°F.....	Bainite, austenite	555	0.73	0.95	1.84	0.42	0.99	0.47
3-c	Chill cast, air cooled, tempered 600°F, 1 hr.....	Bainite, tempered martensite	555	0.73	0.95	1.84	0.42	0.99	0.47
4-a	Forged, re-heated, water quenched, T. 300°F.....	Martensite, austenite	652	0.88	0.50		0.20		0.8 Std.

river sand in the test mill at Golden or by grinding molybdenum ore at Climax have been found to wear from 5 to 15 pct faster than our standard 0.80 pct carbon, low alloy martensitic steel.

When the carbon content of a martensitic steel was raised to about 1.0 pct the wear resistance of the steel was somewhat better than that of our standard. Such steels generally have a very substantial amount of retained austenite in their structure.

High carbon steels containing over 0.90 pct carbon suffer from the disadvantage of brittleness and susceptibility to quench cracking. Recent tests have indicated that reduced cracking of the high carbon steel would be obtained by quenching the balls from a temperature just above the *Acl* to produce a structure of spheroidized carbides in martensite. A limited amount of data which we have on this structure indicates that it has somewhat better wear resistance than martensitic steels of eutectoid composition. This is in line with experience in the ball bearing field and with experience on the wearing properties of rock drill bits for percussion drilling.

It has been found that relatively high alloy contents are necessary for the production of a matrix of martensite, bainite, or austenite in high carbon irons. Chromium and molybdenum, at least up to a certain amount, are contained principally within the massive primary carbides, having little effect on the matrix structure. Nickel is effective on the matrix structure and is, therefore, used to produce "Ni-Hard" white irons with a matrix of martensite plus austenite. Chromium is used in these Ni-Hard irons to suppress the formation of graphite in the structure. Two typical Ni-Hard irons are listed as items 1 and 4 in Table 3 and items 48 and 43, respectively, in Table 4.

2. Balls with a Pearlitic Matrix

Generally speaking, balls with a pearlitic matrix will be inferior in wear resistance to

those with a matrix of martensite or bainite, plus retained austenite. A very large proportion of the grinding balls used commercially is, however, still of the pearlitic type so the characteristics of such balls have been rather fully investigated. The inferior wearing characteristics of the pearlitic steels and irons are quite evident from a study of the data in Tables 3, 4, and 5. It is also evident, however, that there is a rather wide range in wearing characteristics of various pearlitic steels and irons. Some of the harder, high carbon pearlitic steels are capable of giving a fairly good account of themselves in the harder types of ore. In grinding the softer types of abrasives, such as feldspar or calcite, none of the pearlitic steels or irons showed up well in comparison with the standard martensitic steel balls.

Pearlitic steels of eutectoid carbon content tend to wear better with increasing fineness of the lamellar structure which is paralleled by an increase in the hardness of the steel. This is indicated by a comparison of items 6 and 8 in Table 3.

The influence of carbon content on the wear resistance of six pearlitic forged steels of similar hardness is demonstrated by Table 9. The trend towards improved wear resistance as the carbon content is raised from 0.52 to 1.03 pct is very consistent. Further data on the influence of carbon content on the wear resistance of a series of alloyed pearlitic steels of relatively high hardness are given in Table 10. Again the trend towards improved wear resistance as the carbon content increases, in this case up to 1.19 pct, is observable.

The results in Table 11 are shown to illustrate the influence of carbon content up to the cast iron range on balls having a pearlitic matrix. Further data on the performance of pearlitic white iron balls are also given in Tables 3, 4, and 5. It will be noted from these data that the introduction of sufficient carbon into a composition to cause the formation of primary massive

carbides in its structure generally causes a definite loss in wear resistance.

Data on the influence of carbon content on the wear resistance of pearlitic balls are presented by Prentice.⁵ While Prentice does not report the microstructure of the balls he tested, there are certain groups in his list which, because of their analysis, heat treatment and hardness obviously have a pearlitic matrix. Six of these groups are re-listed in Table 12. The superiority of the steel of eutectoid or slightly hyper-eutectoid carbon content is evident.

The most wear resistant balls of the pearlitic type are made of steel compositions of high hardness and hyper-eutectoid carbon content. A maximum hardness of about 477 Bhn was obtained in a purely pearlitic steel when its carbon content was in a range of 1.0 to 1.40 pct. All of our pearlitic steels within this carbon range contained an envelope or partial envelope of pro-eutectoid carbides around the grain boundaries. Such carbides are very effective in causing rapid nucleation of the austenite, so in this respect they promote the development of a pearlitic matrix. If large amounts of the pro-eutectoid carbides precipitate at the grain boundaries they will lower the wear resistance of the steel. It is apparently desirable to retain most of this pro-eutectoid carbon within the pearlitic matrix. The judicious use of alloying elements coupled with rapid cooling through the critical range has been found quite effective in accomplishing this.

The data in Table 10 indicate that a high carbon, low alloy pearlitic steel is capable of showing fairly good wear resistance when tested in Climax ore. This is confirmed by the result for item 32 in Table 4 as well as by numerous unlisted results. It should be mentioned, however, that when the softer types of ore are ground (such as some of the porphyry copper ores) none of the pearlitic steels will compare very favorably with the

TABLE 9—Influence of Carbon Content on the Wear Rates of Six Pearlitic Forged Steel Compositions
(145-hr Wear Test in a 6 × 6-ft Mill at Climax, May 1941)

Group No.	Heat Treatment	Microstructure	Hardness (Bhn)	Analysis, Per Cent						Abrasion Factor
				C	Mn	Cr	Mo	Ni	Si	
1	Air cooled from forge.....	Fine pearlite, grain boundary ferrite	340	0.52	1.45	0.85			0.19	126
2	Oil quenched from forge.....	Fine pearlite, a little ferrite	375	0.70	0.66				0.15	116
3	Oil quenched from forge.....	Fine pearlite	375	0.71	0.63				0.22	115
4	Air cooled from forge.....	Fine pearlite	387	0.75	0.45	0.42	0.26		0.65	114
5	Air cooled from forge.....	Fine pearlite, G.B. carbide	364	1.01	0.44	1.06	0.21		0.34	110
6	Air cooled from forge.....	Fine pearlite, G.B. carbide	387	1.03	1.32	1.06	0.22		0.40	109

TABLE 10—Influence of Carbon Content on the Wear Rates of Five Pearlitic Cast Steel Compositions (Low Metalloid)
(150-hr Wear Test in a 9 × 8-ft Marcy Low Discharge Mill at Climax, August 1945)

Group No.	Heat Treatment	Microstructure	Hardness (Bhn)	Analysis, Per Cent						Abrasion Factor
				C	Mn	Cr	Mo	Ni	Si	
1	Chill cast, air cooled.....	Fine pearlite	430	0.74	0.57	1.24	0.20		0.67	117
2	Chill cast, air cooled.....	Fine pearlite	418	0.91	0.61	1.37	0.21		0.47	111
3	Chill cast, air cooled.....	Fine pearlite, G.B. carbide	422	1.02	0.76	1.37	0.20		1.46	111
4	Chill cast, air cooled.....	Fine pearlite, G.B. carbide	426	1.07	0.62	1.20	0.21		0.31	111
5	Chill cast, air cooled.....	Fine pearlite, G.B. carbide	424	1.19	0.71	1.32	0.22		0.96	106

TABLE 11—*Influence of Carbon Content on the Wear Rates of Seven High Metalloid Cast Steels and Irons*
(145-hr Wear Test on a 6 × 6-ft Mill at Climax, May 1941)

Group No.	Heat Treatment	Microstructure	Hardness (Bhn)	Analysis, Per Cent							Abrasion Factor
				C	Mn	Cr	Mo	Ni	Si	P	
1	Sand cast, cooled in sand.	Pearlite, Grain boundary sulphide	364	0.99	0.55	2.69	0.35	—	—	—	119
2	Sand cast, cooled in sand.	Pearlite, G.B. sulphide and carbide	387	1.24	0.82	2.63	0.28	—	0.50	0.19	122
3	Sand cast, cooled in sand.	Pearlite, mass. carbide, globular sulphide	401	1.53	1.68	2.56	0.54	—	0.36	0.12	127
4	Sand cast, cooled in sand.	Pearlite, mass. carbide, globular sulphide	415	1.53	1.66	2.61	0.26	—	0.49	0.17	130
5	Sand cast, cooled in sand.	Pearlite, G.B. sulphide and carbide	460	1.54	2.02	1.10	—	—	0.51	0.15	141
6	Sand cast, cooled in sand.	Fine pearlite, massive carbide	532	3.00	1.51	1.94	—	2.75	0.54	0.13	151
7	Sand cast, cooled in sand.	Pearlite, steadite, massive carbide	477	3.00	0.95	0.80	0.25	—	0.90	0.17	176

TABLE 12—*Influence of Carbon Content on the Wear Rates of Six Pearlitic Steels and Irons, from Prentice⁵*
(Wear Test in a 32 × 17-in. Mill at City Deep Ltd., Johannesburg)

Test No.	Heat Treatment	Probable Microstructure	Hardness I(RC)	Analysis, Per Cent							Life (Days)
				C	Mn	Cr	Si	S	P		
28	Forged, air cooled (?).	Fine pearlite	40	0.90	0.89	0.85	0.20	0.03	0.04	0.04	147
35	Roll, air cooled.	Fine pearlite	35	0.78	0.87	1.10	—	0.05	0.07	0.07	120
20	Roll, air cooled.	Fine pearlite	34	0.65	0.59	2.10	0.90	0.03	0.04	0.04	119
22	Roll, air cooled.	Pearlite	27	0.53	1.53	0.28	0.11	0.03	0.05	0.05	113
7	Roll, water quenched.	Pearlite, grain boundary ferrite	33*	0.53	0.30	—	0.24	0.05	0.05	0.05	87
29	Cast, Sand cooled (?).	Pearlite, Massive carbide	44	3.14	0.50	Tr	0.30	0.16	0.13	0.13	83

* This was the hardness near the center of these balls. They were probably harder near their surface.

compositions containing a matrix of martensite or bainite, plus retained austenite.

3. Balls Containing Spheroidal Carbides

Spheroidal carbides may be developed in steel compositions by tempering martensite or bainite or, under certain circumstances, by direct transformation from austenite

of the steel balls we have studied in order of decreasing grain size follows: 1. Sand cast steel, as cast. 2. Chill cast steel, as cast. 3. Forged steel, as forged. 4. Forged or cast steel, reheated between 1400 and 1600°F (760–870°C) and quenched in air, oil or water.

Numerous tests have been run in which

TABLE 13—*Relative Wear Rates of Lamellar and Spheroidal Structures of Approximately Equal Hardness*
(145-hr Wear Test in a 6 × 6-ft Mill at Climax, May 1941)

Analysis, Per Cent					Lamellar Structure (Air Cooled from Forge, Pearlitic)		Spheroidal Structure (Oil Quenched, Tempered 1050°F, Tempered Martensite)	
C	Mn	Cr	Mo	Si	Hardness (Bhn)	Abrasion Factor	Hardness (Bhn)	Abrasion Factor
0.75	0.45	0.42	0.26	0.65	387	114	387	124
1.01	0.44	1.06	0.21	0.34	364	110	387	113
1.03	1.32	1.06	0.22	0.40	387	109	402	113

as described by Payson, Hodapp and Leder.⁷ Indications from our tests are that these spheroidal structures are not as wear resistant as lamellar (pearlitic) structures of the same hardness. A comparison of the wear resistance of three compositions which were heat treated to develop lamellar (pearlitic) and spheroidal structures of approximately equal hardness is given in Table 13. The poorer wear resistance of the spheroidal (tempered martensite) structures is evident.

An exception to the theory that spheroidal structures tend to have inferior wear resistance may be found in the case of structures in which the spheroidal carbides exist in a matrix of martensite. (See (1) above.)

THE INFLUENCE OF GRAIN SIZE

In steel compositions the prior austenitic grain size of the structure seems to have no influence on the wear resistance of grinding balls provided the microstructure within the grains is the same. This has been demonstrated on both cast and forged balls of various types. A rough classification

all four types of steel, similar in composition and microstructure, were included. No appreciable difference in the wear resistance of the four types has been found. Under severe conditions of impact, however, the martensitic or bainitic coarse-grained types often failed by spalling or breakage. Pearlitic steels, irrespective of their grain size, have not spalled or broken on any of our tests. For the martensitic steels, however, indications are that a grain refining heat treatment is desirable on balls which must withstand severe conditions of impact or combinations of impact plus low rates of wear such as are encountered in the grinding of limestone or other very soft abrasives.

Grain size is an important factor governing the wear resistance of cast white iron balls. This is particularly true for cast white iron with a pearlitic matrix. Sand cast pearlitic white iron balls have always had poorer wear resistance than chill cast pearlitic iron in our tests. It is believed that the very coarse primary carbides which exist in sand cast white iron are responsible for this more rapid rate of wear. These

carbides may be more subject to spalling on a microscopic scale.

The wear of white iron with a matrix of martensite plus retained austenite does not appear to be so greatly influenced by grain size. It will be noted in a comparison of items 1 and 4 of Table 3 that this particular sand cast Ni-Hard white iron actually wore less than the chill cast Ni-Hard white iron.

Where severe impact occurs in a ball mill or where very large balls are used to accomplish crushing as well as grinding, breakage or spalling of all types of white iron may be expected. White iron of the Ni-Hard type seems to be somewhat more resistant to this spalling and breakage than the pearlitic types of white iron.

THE INFLUENCE OF ALLOYING ELEMENTS

Since microstructure is the dominating factor determining the wear resistance of grinding balls, we believe the primary function of alloying elements is to assist in obtaining the type of microstructure desired. A secondary function of alloying elements may be to provide corrosion resistance or to facilitate the development of an abrasion resistant oxide film on the balls.

The influence and usefulness of alloying elements will be considered for the two microstructural types of grinding balls which have, in our estimation, shown the best economic possibilities. These are: 1. Balls with a matrix of martensite plus retained austenite or bainite plus retained austenite. 2. Balls with a pearlitic matrix.

Balls of type 1 are generally superior to even the best of those of type 2 insofar as wear resistance is concerned. Impact conditions in certain ball mills may, however, be too severe for balls of type 1 particularly if they are coarse grained.

To produce the type 1 microstructures in grinding balls, they must be of a composition which possesses sufficient harden-

ability to halt transformation to pearlite during their final air or liquid quench from the austenitic state. To accomplish this without resorting to too drastic a quench it is necessary to have alloying elements present in practically all the sizes of grinding balls down to about 1 in. diam. Many combinations of alloying elements can be used. However, the selection of an alloy or alloy combination together with the type of quench should be such that it introduces a minimum of harmful effects into the balls. The development of high residual stresses or quench cracks and the presence of embrittling elements such as phosphorus, sulphur or excessively high manganese and silicon should be avoided. Overstabilization of the retained austenite in the structures should also be avoided.

Numerous compositions and methods of heat treatment used to produce the type 1 microstructures in steel or iron balls 3 in. in diam are to be found in Tables 4 to 8 inclusive. It should be noted, however, that the groups listed in these tables were tested because they contributed to the study of certain variables. In most cases these groups do not represent the best composition or heat treatment for commercial production. The commercial manufacture of some of these groups would involve an unnecessarily high alloy cost, while others, because of their composition, grain size or heat treatment, would produce balls subject to quench cracking or other forms of brittleness.

The most economical alloying element per unit of hardenability effect is manganese. We have found that this element can be used to advantage in amounts up to about 0.80 pct in grinding balls with the type 1 microstructures. Larger amounts of manganese than this are generally undesirable since they tend to cause quench cracking or spalling and breakage of the balls in service. In cast steel balls, silicon contents in excess of 0.70 pct have been found undesirable for the same reasons. The cause

of this may be that such high silicon contents were generally associated with an over-reduced condition during the finishing period in the melting furnace. For hardenabilities greater than that obtainable from 0.80 pct manganese plus 0.70 pct silicon we believe the combined use of chromium, molybdenum and nickel will give the best results. Copper, in amounts up to 0.50 pct, has also been used to advantage in cast steel balls.

To determine the most efficient chromium, molybdenum and nickel combinations for commercial production of cast or forged steel balls with the type 1 microstructures, we have found that Hostetter's method¹⁰ can be applied to good advantage. While Hostetter's method of calculation was developed to determine the most economical combinations, we have found that such combinations have also worked well from a performance standpoint insofar as wear resistance and freedom from quench cracking or breakage in service are concerned. In the interest of obtaining greater toughness in the hardened balls, certain steel ball producers prefer, however, to deviate from Hostetter's formula by replacing a part of the chromium with a further addition of molybdenum. It is thought that since molybdenum has very little effect in lowering the temperature range in which austenite begins to transform to martensite, it should be less likely to induce quench cracking or high residual stresses in balls which are quenched to below their A_{r1} temperature.

Interrupted quenching techniques, which tend to avoid the development of quench cracks or high residual stresses, can be used to advantage in the production of alloyed balls with the type 1 microstructure. They are particularly useful on coarse grained steels such as those in the as-cast or as-forged condition. A technique which we have used with good success on eutectoid carbon, low alloy, chromium molybdenum steel balls has involved a quench in

oil, water sprays, or moving air until the surface of each ball was down to between 600 and 700°F (305–370°C). The balls contained sufficient alloy content to suppress any transformation to pearlite so that they were still completely austenitic at these temperatures. The balls were then removed from the quench and allowed to cool slowly to room temperature. The transformation from austenite to bainite or martensite occurred during the slow cooling period. Usually, the balls became quite strongly ferro-magnetic while they were still at temperatures between 700 and 500°F (370–260°C), indicating that the transformation product was mostly bainite.

For steel compositions, it has been pointed out that martensite (or bainite) plus an unstable austenite is easily obtained by the addition of relatively small amounts of alloying elements. Whether the further addition of alloying elements is beneficial or not is of interest. Our tests show little improvement for any large addition of an alloying element, particularly when economic factors are considered. Chromium additions beyond that necessary for full hardening are probably beneficial when conditions are such that the removal of oxide films on the balls represents a substantial proportion of the wear. In most of our tests, however, the effect of chromium in amounts greater than that necessary for full hardening has been small.

The addition of large amounts of manganese or nickel to a full hardening steel analysis appears to be undesirable because of stabilization of the retained austenite. Molybdenum additions beyond that necessary for full hardening have shown no appreciable effect on wear resistance.

The full possibilities for the carbide-forming elements when applied in a structure of martensite plus spheroidized carbides have not been explored. Fairly highly alloyed compositions, such as those used in high-speed steel cutting tools, may

show superior wear resistance though the field of application for such costly compositions in grinding balls seems to be decidedly limited.

Alloying elements in the 1.0 to 1.4 pct carbon pearlitic balls serve to increase the fineness of the pearlitic structure and also to increase its carbon content by partially suppressing the rejection of pro-eutectoid carbides around the original austenite grain boundaries. Alloying elements such as chromium and molybdenum may have a secondary beneficial effect on pearlitic structures by the introduction of alloy carbides. Since much work remains to be done, about all that can now be said is that combinations of chromium in a range of 1.0 to 3.0 pct plus molybdenum in a range of 0.20 to 0.50 pct have given good results. Manganese has also been used in amounts up to 2.0 pct though our tests have indicated that its use above 1.0 pct has contributed little to the wear resistance of these hard pearlitic steels. The nickel which was present in many of our pearlitic compositions in amounts up to 1.0 pct apparently had little influence on wear rates.

Balls made from 1.0 to 1.4 pct carbon low alloy steels may be subjected to a fairly wide range of cooling rates from their austenitic state, while still developing a hard pearlitic structure. A fairly wide range in total alloy content is also permissible. Such balls will, therefore, lend themselves well to production under conditions where a simple fool-proof heat treatment, such as an air quench, is required.

Because of the presence in white iron of massive primary carbides which tend to rob the matrix of its carbide forming alloying elements, Hostetter's formulas do not apply. A combination of nickel in a range of 3.0 to 4.5 pct plus chromium in a range of 1.5 to 2.5 pct (the Ni-Hard irons) has been used quite successfully to produce white iron with a matrix of martensite plus retained austenite.

THE INFLUENCE OF THE METALLOIDS

As might be expected, the presence of phosphorus and sulphur above the usual limits is undesirable in steel balls. Both elements cause brittleness in steel and also injure the hot working properties of wrought steels. Table 14 gives a comparison between a number of low metalloid, and similar high metalloid, pearlitic alloy steels. The high metalloid compositions are definitely inferior in wear resistance, even though their structure, hardness, and carbon content are similar. In Table 5, a high metalloid pearlitic steel represented by item 30 compared unfavorably with items 4, 5, 25, and 26, which represent low metalloid pearlites of approximately the same hardness.

The martensitic steels appear to be less affected by metalloids than the pearlitic steels insofar as wear resistance is concerned. In Table 5, the martensitic steels of high metalloid content are represented by items 11 to 17. These groups had good wear resistance, but the balls in these high metalloid groups were very subject to quench cracking and also to breakage in our wear tests.

White iron balls generally have a relatively high sulphur and phosphorus content. Whether any improvement in their wear resistance could be obtained by lowering their metalloid content is not known.

THE INFLUENCE OF ABRASIVES ON WEAR RESISTANCE

By changing from one type of abrasive to another, very marked differences in the relative wear resistance of the various types of balls have been observed. While the order of merit of a series will generally remain the same, the spread between the performance of a good and poor type will generally be much greater when grinding soft than when grinding hard abrasives. This is readily observable from the data in Table 3. Other tests which have been run

TABLE 14—Relative Wear Rates of Pearlitic Steels of High and Low Metalloid Content
(145-hr Wear Test in a 6 × 6-ft Mill at Climax, May 1941)

Group No.	Heat Treatment	Microstructure	Hardness (Bhn)	Analysis, Per Cent								Abrasion Factor
				C	Mn	Cr	Mo	Ni	Si	S	P	
(a) Low Metalloid Steels												
1	Sand cast, cooled in sand.....	Fine pearlite	352	1.06	1.51	2.63	0.53		0.44	0.02	0.04	106
2	Sand cast, cooled in sand.....	Fine pearlite	341	1.06	2.02	3.05	0.26		0.42	0.05	0.01	107
3	Sand cast, cooled in sand.....	Fine pearlite, G.B. Carbide	388	1.29	1.03	1.60	0.42	0.99	0.41	0.03	0.06	109
4	Sand cast, cooled in sand.....	Fine pearlite	375	0.91	1.04	1.66	0.43	0.78	0.61	0.02	0.04	110
5	Sand cast, cooled in sand.....	Fine pearlite	369	0.78	0.93	1.63	0.48	0.87	0.44	0.02	0.04	111
(b) High Metalloid Steels												
6	Sand cast, cooled in sand.....	Pearlite, G.B. Sulphide	364	0.99	0.55	2.69	0.35		0.50	0.19	0.33	119
7	Sand cast, cooled in sand.....	Pearlite, G.B. Sulphide and Carbide	387	1.24	1.03	2.63	0.28		0.36	0.12	0.31	122
8	Sand cast, cooled in sand.....	Pearlite, G.B. Sulphide	331	1.02	0.50	0.19	0.57	1.04	0.42	0.17	0.30	130

in calcite, cement rock, and in commercial ores high in feldspar or talc, tend to confirm this. Ellis' data¹ confirm this observation.

A reversal in order of merit may occur among the pearlitic steels and pearlitic white irons when we change from grinding a hard abrasive to the softer abrasives. For instance, in the grinding of quartz or ores high in quartz content, the pearlitic steels are generally superior to pearlitic white iron. When grinding pure feldspar, however, this condition may be reversed. This is observable from a comparison of items 6 and 10 in Table 3.

Possibly an explanation for the way that the various abrasives influence the wear resistance of grinding balls may be obtained by a consideration of the relative indentation hardness of minerals and steel at various hardness levels. Peters and Knoop¹¹ list the following indentation hardnesses as obtained by microhardness tests with a diamond pyramid:

Calcite.....	135
Steel, Rc 25.....	276
Albite Feldspar.....	490
Steel, Rc 47.....	496
Orthoclase feldspar.....	560
Quartz.....	710-790
Steel, Rc 65-67.....	791

The foregoing table indicates that quartz has about the same hardness as the hardest steel, so it should be capable of scratching all types of steel. Feldspar minerals, which have a lower hardness than quartz, will not, according to mineralogical theory, scratch the hard martensitic steels but should scratch steels softer than about 50 Rc. This probably accounts for the fact that, in a feldspar abrasive, the martensitic steels show outstanding superiority, whereas, in grinding quartz, which is capable of scratching all steels, the superiority of the martensitic steels is not so great.

A further confirmation of this scratch theory of wear is provided by the wear rates on balls grinding calcite, which is softer than all the steel balls we have studied. Theoretically, no wear should

occur on the balls when grinding calcite. Actually some wear did occur in our tests but the wear rate was only about one tenth of that in feldspar and only about one half that of the balls when they were run in water without any abrasive. The calcite, therefore, acted more as a lubricant than as an abrasive.

Other factors which we have found to affect the spread in wear resistance obtained between a good and a poor type of ball are the coarseness of the abrasive and the pulp density in wet grinding operations. An increase in the coarseness of the abrasive has been found to increase this spread. A decrease in pulp density (more dilution by water) was found to increase this spread on a series of tests in the 3-ft diam. mill at Golden using Climax ore or washed river sand as abrasive. Whether this can be taken as a general rule for all mills or abrasives is not known. When the balls were tested in clear water the rate of wear on all balls dropped to about 10 pct of the rate of wear obtained when Climax ore was used as the abrasive.

PRACTICAL ADAPTABILITY OF THE SHORT TIME WEAR TEST

Our use of the short time wear test described in this paper has been both for the study of fundamental factors influencing the wear of balls, and for an evaluation of the merits of the types of balls which are available in commercial quantities. Resistance to wear, spalling and breakage may be studied by this test. Where possible, it is preferable to run these short time tests under normal service conditions in commercial ball mills. The test has been found very useful as a means for the selection and routine inspection of grinding balls. The method could also be applied with minor modifications to the selection and inspection of grinding rods for rod mills.

In the development of alloys for use in parts other than grinding balls which are

subject to abrasive wear, this short time wear test may have possibilities provided the wearing forces on the part in question are similar to those on a grinding ball. In this connection we have studied alloy steels for ball mill liners by testing the desired composition and structure in the form of balls 5 in. in diam. Where comparisons are available the relative wear resistance of a given composition and structure as established by this short time test on large balls has shown good agreement with actual service for the same composition and structure when tested as a liner in the same mill.

A number of correlations between the results of our small scale tests on balls and large scale tests in commercial mills are already available. The results from two commercial mills are given in Table 15.

TABLE 15—*Correlation between Relative Rates of Wear. Determined by Large and Small Scale Wear Tests in Two Commercial Mills*

Type of Ball	Relative Rates of Wear*	
	Large Scale Test	Small Scale Test
(a) Primary Grinding of Crushed Molybdenum Ore at Climax, Colorado		
Martensitic Forged Steel (Standard)	100	100
Fine Pearlritic Forged Steel.....	107-124	108-120
Sand Cast Cr-Mo White Iron.....	170-180	176
(b) Primary Grinding of Porphyry Copper Ore at Phelps Dodge Corporation, Ajo, Arizona		
Martensitic Forged Steel.....	100	100
Chill Cast White Iron.....	180-200	168-185

* Relative rates of wear on the large scale tests were calculated on the basis of the consumption of balls per ton of ore ground to a given fineness. For the small scale tests the relative rates of wear are calculated on the basis of weight lost per unit of surface area of the individual test balls in the same mill.

The agreement between the two types of testing is quite good. In the case of the test at Ajo, the correlation is better when we make allowances for the fact that the metal worn off each white iron ball during

the test was somewhat more wear resistant (because of the finer grain size near the chilled surface) than the remainder of the metal in the ball.

SUMMARY

1. By running marked balls in a ball mill along with a group of standard balls of known quality, it is possible to determine the relative merits of any type of grinding ball within a short time.

2. Barring segregation, grinding balls wear in direct proportion to their surface area and therefore decrease in diameter at a constant rate.

3. A matrix of martensite or low temperature bainite, plus retained austenite, has shown the best wear resistance of all the types studied.

4. Spheroidized carbides enhance the wear resistance of a martensitic matrix.

5. The test results indicate that retained austenite is not an undesirable component of the matrix structure providing it is unstable enough to transform to martensite when cold worked.

6. The wear resistance of steel balls improves with increasing carbon content provided it is not rejected as a grain boundary carbide.

7. The prior austenitic grain size of steel balls does not appear to influence wear resistance. Since balls which have a fine austenitic grain size are less prone to fracture or spall from impact, such grain size is advocated for steel grinding balls.

8. Alloying elements affect the wear resistance of steel grinding balls indirectly through their ability to retard the rates of austenite decomposition at subcritical temperatures. The selection of alloying elements should depend upon their ability to develop the desired matrix structure under the conditions of heat treatment selected by the manufacturer.

9. The metalloids sulphur and phosphorus are undesirable constituents in all types of steel balls because they increase

brittleness, impair the hot working properties of the steels, increase the tendency of a steel to quench crack, and decrease wear resistance.

10. The primary massive carbides which are formed during the solidification of pearlitic white cast iron are, in general, detrimental to wear resistance. They are more harmful in sand cast than in chill cast balls.

11. The spread between the performance of a structure of good wear resistance and one of poor wear resistance will vary greatly depending on the mineralogical characteristics of the ore or abrasive in the ball mill and also to some extent on such factors as abrasive size, pulp density and degree of impact. It is therefore desirable to run short time ball tests in the same mills where their use on a large scale is being contemplated.

12. Good correlation is obtained between results of short time tests and the results of large scale tests run over long periods of time.

ACKNOWLEDGMENT

We are indebted to the many firms who cooperated with us in supplying the numerous types of balls used for our wear tests. This cooperation together with that of our operating and testing staff at Climax and Golden, Colo., have made this test program possible. We are also particularly indebted to the management and operating staff of the following mining companies who have cooperated with us by running wear tests in their ball mills:

Homestake Mining Co.....	Lead, S. Dak.
Ideal Portland Cement Co.....	Portland, Colo.
Kennecott Copper Corp.....	McGill, Nev.
Miami Copper Co.....	Miami, Ariz.
Phelps Dodge Corp.....	Ajo, Ariz.

The authors wish to express their appreciation of the encouragement and assistance given them in this work by the Management and the Research Department of the Climax Molybdenum Co. and for the able assistance of Mr. Harold

Blackett who was loaned by the Research Department to assist with the wear tests.

REFERENCES

1. O. W. Ellis: Wear Tests on Ferrous Alloys, *Trans., Inst. of Brit. Foundrymen*, Thirty Fourth Annual Conference, June, 1937.
2. O. W. Ellis: Wear Tests on Ferrous Alloys, *Trans., Amer. Soc. Metals*, (1942) **30**, 249.
3. E. W. Davis: Fine Crushing in Ball Mills, *Trans. AIME* (1919), **61**, 250.
4. F. C. Bond: Wear and Size Distribution of Grinding Balls. AIME T. P. 1191, *Min. Tech.*, May 1940. *Trans.* (1943) **153**.
5. T. K. Prentice: Ball Wear in Cylindrical Mills, *Jnl. Chem., Met. and Min. Soc. of So. Africa*, Jan.-Feb., 1943.
6. W. I. Garms and J. L. Stevens: Ball Wear and Functioning of the Ball Load in a Fine-grinding Ball Mill, *AIME Trans.* **169**, 133, T. P. 1984, *Min. Tech.*, March, 1946.
7. P. Payson, W. L. Hodapp and J. Leeder: The Spheroidizing of Steel by Isothermal Transformation, *Trans., Amer. Soc. Metals*, (1940) **28**, 306.
8. N. P. Goss: The Effect of Cold Rolling on the Structure of Hadfield Manganese Steel, *Trans., Amer. Soc. Metals*, (1945) **34**, 630.
9. D. P. Antia, S. G. Fletcher, and M. Cohen: Structural Changes During the Tempering of High Carbon Steel, *Trans., Amer. Soc. Metals*, (1944) **32**, 290.
10. H. E. Hostetter: Determination of Most Efficient Alloy Combinations for Hardenability, AIME T. P. 1905, *Metals Tech.*, Sept., 1945. *Trans.* (1946) **167**.
11. C. G. Peters and F. Knoop: Metals in Thin Layers—Their Microhardness, *Metals and Alloys* (Sept. 1940), **12**, No. 3, 292

DISCUSSION

(C. Wells and M. Gensamer presiding)

R. D. HAWORTH, JR.*—The present paper by Norman and Loeb, as well as those of Ellis which the authors mentioned, have been read with interest. The contribution of the authors in obtaining much needed accurate field test data is a definite step in the right direction toward greater knowledge of the little understood subject of abrasive wear. The writer has some comments that come to mind after reading the paper.

The relatively poor life obtained with white and martensitic iron compared to the results in other types of abrasive service where impact is less of a factor has not been adequately explained. It would seem that some degree of

impact takes place in all ball mill operations and increases in severity as the size of the mill is increased with constant ball size.

In Table 3, for example, three of the nine materials tested in the 9-ft mill at Climax, Colo., either broke or spalled. No breakage or serious spalling was reported in any mills smaller than 8 ft in diam. Apparently, there is a critical impact velocity or degree of impact below which spalling is not severe enough to be mentioned but it still may be a considerable factor in the weight loss of brittle balls.

The suggestion is ventured by the writer that weight loss in ball mill service may be due to a combination of abrasion and impact. For tough alloy steels, abrasive wear may be the primary factor; for brittle materials, spalling due to impact may be a much more serious consideration.

Therefore, information on the relative resistance to spalling under repeated impact should be of value in specifying materials for use in different size mills. In addition, knowledge of the resistance of the materials to pure abrasion (that is, without impact) would also be required. For the latter purpose, an accelerated abrasion testing device has been developed at the Armour Research Foundation which has enabled predictions of field service results in several instances with considerable accuracy.

The best value shown in the authors' tables was an abrasion factor of 84 for sand cast Ni-Hard. Balls made of materials with equal or better abrasion resistance than that of Ni-Hard and with higher impact strength (a not unattainable combination) might provide greatly increased life even though such materials might be basically less shock resistant than alloy steels. The impact involved is apparently not sufficient to work-harden manganese steel which, therefore, wears rapidly.

The comment by the authors that high speed steels would seem to be of limited value appears to the writer to be valid only if the increased life, if any, is less than proportional to the increased cost. Actually, on the basis of abrasion tests in the Armour device, other high alloy, lower cost combinations offer much more promise than ordinary high speed steel compositions.

* Armour Research Foundation.

H. S. AVERY*—Mr. Norman and the Climax organization cannot be complimented too highly on this paper. So far as I know, it is the finest presentation of well-conducted field

validation of our laboratory wear tests are complicated by so many uncontrolled variables that the results are only qualitative; these which Mr. Norman has presented are quantitative.

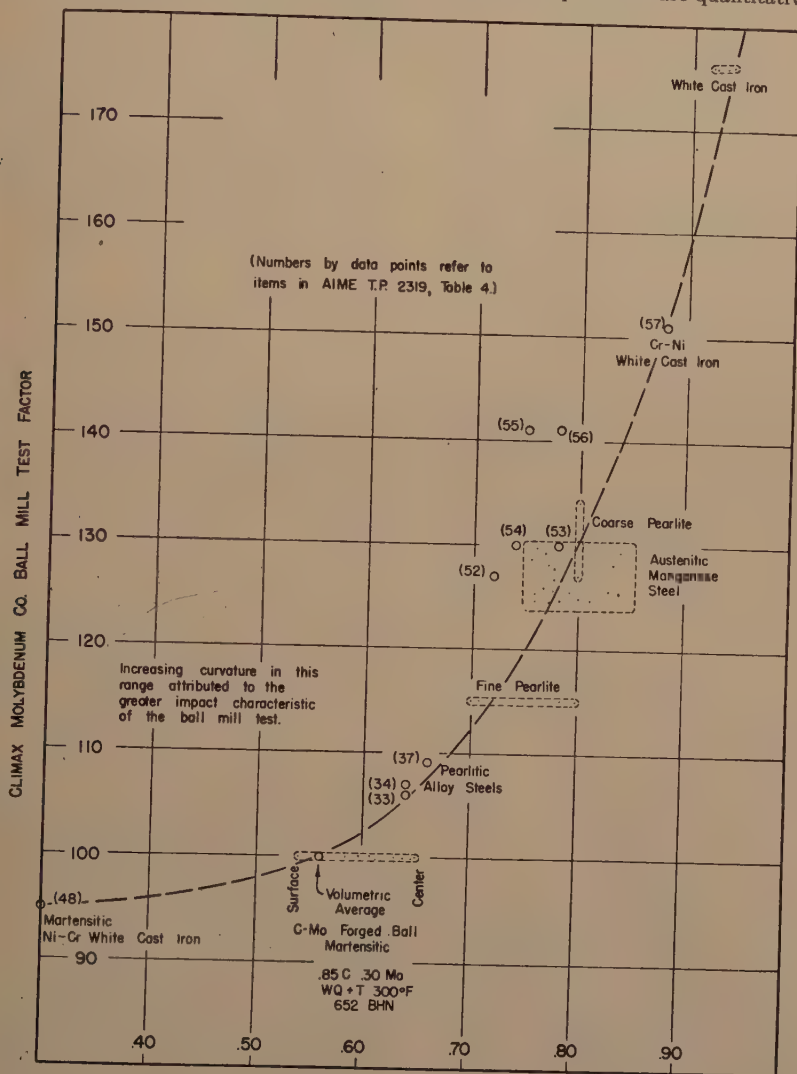


FIG 2—COMPARISON OF LABORATORY AND FIELD TESTS.

tests on abrasion that has yet appeared in mining or metallurgical literature.

It is particularly valuable because the field tests were well controlled. Most of those upon which we must depend for correlation with and

It is encouraging to note how closely the laboratory and field tests check each other when both are carefully controlled and when the same variables are studied. Some years ago the American Brake Shoe Co. provided Climax with a group of cast 3-in. diam balls for their testing program. At the same time the labora-

* American Brake Shoe Company.

tory abrasion factors were determined. Comparisons appear in Fig 2.

The laboratory test apparatus is one that the American Brake Shoe Co. has had under study for about 18 years. It consists essentially of a flat, circular copper track 2 in. wide and 4 ft in diam that acts as a lap. Against this, test specimens $1\frac{1}{2} \times 2\frac{1}{4}$ in. are held under a pressure of 38.5 psi while being moved at the rate of about 119 fpm for a total distance of 1.35 miles. Abrasion is provided by submerging the wearing surfaces in a pulp that normally consists of 40 lb of clean quartz sand (grain fineness No. 50) and 30 qt of water. The specimen is worn in against the track to conform to the surfaces; cleaned, dried and weighed; and then subjected to the standardized abrasion as above in company with a specimen of annealed SAE-1020 steel. This standard is arbitrarily assigned a factor of 1.00, just as Mr. Norman had given his martensitic forged balls a factor of 100. The data are reported in the same way, the abrasion factor being the loss in weight of the specimen under test divided by the loss in weight of the standard. However, the two standards, being of different materials represent different levels of abrasion resistance.

The reproducibility of the results has been established by considerable testing of duplicate specimens. With uniform material the probable error is 0.02; that is, 50 pct of the time the abrasion factor will be within ± 0.02 of the probable true value. The average of duplicate tests is expected to be within ± 0.02 about $\frac{2}{3}$ of the time.

In Fig 2 data for identical materials (the group of balls mentioned above, which have been designated by the item numbers in Table 4) and for similar structures have been plotted. The evidence suggests that both tests are evaluating the same quality for the tougher materials and in the range of higher factors. Speculating, it is possible to attribute the increasing curvature toward the foot of the curve to the greater influence of impact in the ball mill on the more brittle alloys. Note that impact is absent in the laboratory test.

Commenting on the performance of metallographic structures, we find that pearlitic white cast irons, coarse pearlite, austenite, fine pearlite, and martensite are ranked in the same order by the two tests. If abrasives, other than

quartz, are employed further similarities are noted. The reversal of ranking noted (p. 517 of paper) when pearlitic steel and pearlitic white cast iron are tested against quartz and against feldspar is confirmed, the latter abrasive with a hardness of 6 on Mohs' scale, giving a factor of 0.4 for the iron and 0.8-0.9 for pearlitic steels.

The rate of wear is generally lower with softer minerals. The most severe abrasive that we have employed is crushed flint (chert from the Joplin mining district), which caused a weight loss (per hour) about twice that of feldspar and about 100 times that of dolomite, for manganese steel.

In mills it is possible for balls to wear by corrosion, by abrasion, and by spalling or chipping. Mr. Norman has discounted the first (pp. 497-498) and I believe that he has also confirmed the contribution of spalling to wear rates by his observations. This would explain why Ni-Hard, which in laboratory tests and in some field situations, will considerably outwear the other alloys, appears only slightly better than the martensitic and pearlitic alloy steels.

Our experience confirms this. In some mills Ni-Hard is successful as liners. In others it fractures and is uneconomical. Where this occurs, pearlitic steels may be substituted and usually perform well because of their greater toughness, and outwear austenitic manganese steel by a modest amount because of better inherent abrasion resistance. However, when impact increases further, as represented by conditions in crushers of many kinds, all of these hardenable irons and steels are subject to breakage, leaving austenitic manganese steel as unique in its ability to provide outstanding performance in such service.

We would like to qualify the comment by Mr. Haworth that the austenitic manganese steel did not work-harden and consequently did not show its true abrasion resistance. We recognize that the unimpressive performance of this alloy where impact is absent is usually attributed to lack of work-hardening. This conclusion is repeated many times in technical literature. However, from our studies on this material over a number of years, we are inclined to question its truth. In our laboratory tests the abrasion factors tend to fall between 0.7 and 0.85, and as yet we have no good evidence

that work-hardening will move them more than a few points out of this range. There may be some minor effect, but we currently believe that the reason manganese steel stands up well under impact, and thus has gained its unique reputation, is based on its great toughness (ultimate tensile strength around 120,000 psi with about 45 pct elongation and 100 ft lb Izod), which renders it substantially immune to spalling, chipping, and other impact effects. It thus will exhibit its inherent abrasion resistance in the presence of heavy impact where other equally abrasion resistant materials wear or fail by other mechanisms.

K. A. DE LONGE*—I agree with Mr. Avery that the present authors are to be highly complimented on a well-written paper which is really a monumental work and adds a lot of knowledge to the field of abrasion resistance.

In our work on martensitic cast irons we find that we are in pretty good agreement with most of the findings in this paper. We find austenite, martensite and low temperature bainite do give the best wear resisting structures.

We also find that microstructure has the most important effect on abrasion resistance. We would like to emphasize the finding in this paper that massive carbides have a harmful effect primarily only in the pearlitic materials, because in martensitic materials there seems to be quite a bit of evidence that the presence of massive carbides is very helpful.

For instance, the best figure shown in this paper for a martensitic white iron against a martensitic steel shows a superiority of about 0.84 to 1.00. In a test now going on at Copper Cliff in our 6½-ft diam ball mills, we are comparing chill cast martensitic white iron against martensitic steel, and at the last report there was a ratio of superiority of 0.75 to 1.00 in favor of the martensitic white iron.

In grinding of paint pigments (which are softer), we find that a martensitic white iron in many cases will double the life of a martensitic steel. I think that is in agreement with the present observation of the authors that the spread of two materials is exaggerated when soft materials are being ground.

One point with which we are not in full

agreement is the relative abrasion resistance of sand cast and chill cast martensitic white irons. The paper shows the sand cast varieties are superior. We believe in this case the superiority of the sand cast product is pretty well associated with impact conditions, because in most fields of industrial service involving abrasion resistance the chill cast materials are superior. We attribute this improvement to the refinement of the carbide size.

We have another test going on at Copper Cliff at the present time, comparing sand cast and chill cast martensitic white iron balls. This test is not as yet completed but at the present time the chill cast ball is turning in a better performance than the sand cast.

I think the work-hardening data would have been more enlightening if the hardness tests of the Vickers type had been used instead of Rockwell, since I believe this would have given truer indications of the hardness at the very surface (because of shallower penetration of the indenter). The inference of Table 7 is that a material with about 4 pct nickel has an austenite which is too stable to work-harden and, hence, gives an unsatisfactory wear resistance. However, in the case of martensitic white irons with nickel contents of 2½ to 5 pct, we find that work-hardening is very pronounced. In many cases balls of this type that have come out of service have shown surface hardness from 850 to 900 Bhn. That was determined in terms of Vickers hardness.

T. E. NORMAN (authors' reply)—We wish to thank Mr. Haworth, Mr. Avery and Mr. De Longe for their discussion of this paper. We are particularly pleased to note that Mr. Avery's experimental results are in close agreement with our own.

In addition to our studies on balls, we have used our mining and concentrating operations at Climax as a field laboratory for wear tests on ball mill liners, classifier wear shoes, flotation impellers, pump runners, screen rods, mine car wheels, rock drill bits and a number of items of lesser importance. These studies, together with the experiences reported to us from other fields where abrasion resistant materials are used, have indicated to us that a rather definite dividing line can be drawn between the requirements of materials which pinch or crush mineral particles between their

* International Nickel Company.

wearing faces and the requirements of those exposed to freely suspended mineral particles, which brush or strike against the material without any pronounced crushing effect.

Materials exposed to this latter type of abrasion are definitely benefited by the presence of massive primary carbides, which apparently protect the matrix from wear. In such service, our experience has indicated that the microstructure of the matrix is not particularly important as long as it is well protected by massive carbides. Chromium and molybdenum carbides appear to be particularly beneficial. Alloys containing 3 to 30 pct chromium, 3 to 10 pct molybdenum and 1.5 to 3.5 pct carbon have shown outstanding wear resistance in parts such as sand pump runners, flotation impellers, spiral sand classifier wear shoes, sand classifier cone orifices, pug mill knives, and blades for the impellers on sand or shot blast machines. In all these classes of service, the abrasive is in free suspension and is not severely pinched or crushed. We believe this is the type of service which Mr. Haworth has in mind in his reference to the good wear resistance which has been obtained from white iron in "other types of abrasive service."

Where materials are used in abrasive service which involves pinching or crushing of hard mineral particles, the massive carbides in white iron compositions appear to offer little or no protection to the matrix. Materials which wear by pinching or crushing mineral particles include grinding balls, ball mill liners, crusher rolls, cone and jaw crusher liners, mine car wheels and the test specimens used in the laboratory wear test described by Mr. Avery. The similarity in the abrasive forces on grinding balls and those on the American Brake Shoe Laboratory's test specimen probably accounts for the relatively good agreement in the order of merit developed by these two tests on various materials.

In our wear tests on grinding balls, the degree of impact, or more possibly the localized maximum pressures, involved during the pinching or crushing of the mineral particles, is apparently responsible for the fact that the relatively hard massive carbides in pearlitic or austenitic white iron are unable to protect the matrix from wear when grinding hard minerals. They do protect the matrix to some extent

when grinding softer minerals such as the feldspars, as indicated by our tests and confirmed by Mr. Avery. It should be recognized, we believe, that in grinding hard minerals the localized unit pressures involved during the pinching or crushing of the mineral particles are very high, since they are sufficient to plastically deform (as evidenced by indenting or scratching) microconstituents having a yield strength in excess of 300,000 psi. We suspect that it may be these high unit pressures, rather than impact, which cause a crumbling of the carbides at the wearing surface, thus making it impossible for them to protect the matrix from wear. Presumably, if hard carbides could be toughened and properly supported in a martensitic matrix they should enhance the wear resistance of the material. In our tests in ball mills, however, it appears as if the unit pressures involved have been too great to make possible any noticeable benefit from the carbides in Ni-Hard, although some benefit has been indicated in the results on item 1 in Table 3, and in results reported by Mr. De Longe. Data from several sources would indicate that the wear resistance of martensitic white iron might be materially improved if the carbides could be toughened by some means. This is probably the objective which Mr. Haworth had in mind when he mentioned materials with equal or better abrasion resistance to Ni-Hard and higher impact strength.

Mr. De Longe is surprised to note that sand cast Ni-Hard was more wear resistant than chill cast Ni-Hard in our tests. We also were surprised by this result. One would naturally expect the finer-grained carbides in chill cast Ni-Hard to be less susceptible to crumbling and, therefore, be more wear resistant than the coarse grained carbides in the sand cast product. Possibly, the explanation for the poorer wear resistance of the chill cast Ni-Hard lies in differences in the amount or stability of the retained austenite in the matrix of the two irons. We are convinced that a matrix containing austenite can be over-stabilized by 4.0 pct nickel. Higher nickel contents than this in Ni-Hard appear definitely to over-stabilize the matrix. For instance, a 2.40 pct carbon, 0.8 pct manganese, 6.27 pct nickel, 3.50 pct chromium chill cast Ni-Hard (not listed in this paper) gave an abrasion factor of 122 in grinding

ing river sand at Golden and 115 in grinding ore in one of our primary mills at Climax. These factors are relatively poor for a Ni-Hard iron.

The word "spalling" as used in this paper and by the discussers requires further clarification. Where we reported spalling, we imply the removal of the metal from the ball surface as visible pieces. Such spalling left rough surfaces or indentations on the balls, and was easily observable without a microscope. Mr. Haworth has mentioned that other spalling may have occurred which was not severe enough to mention. If such spalling did occur, it was microscopic in nature and probably produced particles which had dimensions about equal to that of the individual carbide grains. We believe it might be better to refer to such spalling as crumbling of the carbide grains. Unless definite macro-spalling was reported, the balls in our tests came out of the ball mills with surfaces which could be considered as having a dull polish.

The degree of impact in ball mills and the influence of this impact on balls apparently require further clarification. No large impact is involved when individual balls collide. It is probably of the order of only a few foot-pounds of energy. Moving pictures of the action in a ball charge indicate that many of the contacts between balls involve only a rolling or pinching action with practically no impact. Our calculations on the energy input per unit of surface of a ball charge indicate that for commercial mills it is only about 0.15 ft-lb per sq in. of ball surface per sec in some of the smaller, slow speed mills and 0.4 ft-lb per sq in. per sec in the larger high speed mills such as our 9-ft mills at Climax. It would appear, therefore, that it is the countless occurrences of high unit pressure and plastic deformation on very small areas of each ball which are responsible for the work hardening of ball surfaces. There are also indications that this work hardening at the surface is responsible for the introduction of high residual stresses which eventually cause some of the more brittle types of balls to break or spall by rupturing outward from their interior.

With reference to Mr. Haworth's statement that the service in ball mills may not be sufficient to work harden manganese steel, the austenitic manganese steel balls which we tested did work harden on their surface to

values ranging from 35 to 54R_C though no transformation to martensite could be detected in this work hardened zone. We suspect it is this inability of austenitic manganese steel to transform to martensite, when work hardened, which is responsible for its relatively poor performance in grinding balls.

The diameter of ball mills as mentioned by Mr. Haworth is not the only factor influencing ball breakage. The peripheral speed of a mill, the liner contour, and the viscosity or density of the pulp in which the balls operate are some important factors influencing ball breakage. We believe the energy input per unit of ball surface area is an important factor influencing ball breakage. This factor, in turn, is controlled by the size and weight of the balls in a mill charge, by the mill diameter, and by its speed of rotation. It may be worth while to note that by running our 3-ft diam test mill at Golden with a low pulp level and low pulp viscosity we can break brittle balls as fast or faster than these same balls would break if used under normal operating conditions in our 9-ft mills at Climax.

The rate of wear also appears to influence the breakage and spalling of balls. In the primary compartment of mills grinding cement clinker, where the rate of wear on balls is low, the continual pounding without much metal removal apparently produces a highly stressed condition in the balls, since brittle balls used in this service are quite prone to spalling and breakage. For instance, the cement mill at Portland, Colo. (see Table 3), produced very severe spalling or breakage on numerous types of balls in spite of the fact that it operated at a relatively low peripheral speed.

In closing this discussion, we should like to emphasize again that the matrix structure appears to be the primary factor in determining the wear resistance of grinding balls. A matrix of martensite or low temperature bainite, plus retained austenite, has shown the best wear resistance of all types studied. The value of such a matrix has been demonstrated for both steel and white iron compositions. This general rule has been further confirmed in some tests which have been run recently on martensitic gray iron balls in which the martensitic iron has shown surprisingly good wear resistance, despite the presence of graphite, which we nor-

mally consider quite harmful in grinding balls. Further investigations on gray irons of this type are in progress.

If further improvement in the wear resistance of ferrous grinding balls is to be attained, it would appear to lie in the development of microstructures in which a high carbon matrix

of martensite or low temperature bainite, plus retained austenite, is filled with hard protective constituents. These could best be alloy carbides which are sufficiently tough to resist shattering or crumbling in normal ball mill service. As Mr. Haworth has stated, such a combination may not be unattainable.

Behavior of Metal Cavity Liners in Shaped Explosive Charges

BY GEORGE B. CLARK* AND WALTER H. BRUCKNER,† MEMBERS AIME

(New York Meeting, March 1947)

SINCE the end of World War II interest has been increasing in the use of shaped charges in the mining industry and in other industries using explosives for blasting purposes. Shaped charges employ the principle known as the "Munroe effect," which was discovered by Charles E. Munroe more than 50 years ago (in 1888). Details of their design have been explained elsewhere.^{1,2,3} Fig 1 shows the essential features of design of two types of shaped charges (with conical and hemispherical cavities) and a schematic sketch of their action upon detonation.

The following discussion deals with the behavior of the metal in the cavity liners when they are subjected to intense pressures exerted when the explosive charge is detonated. Among the conclusions reached in research on shaped explosive charges, the following have been established concerning cavity liners:^{1,2}

1. The optimum wall thickness of a conical cavity liner is dependent upon the apex angle of the cone as well as on the base diameter of the charge. Acute apex angles require thinner walls for optimum performance and more obtuse angles require thicker walls for the same base diameter.

2. Cones were more effective in forming

a penetrating jet when the walls were tapered; that is, the thickness of the wall of the cone increased from the apex down.

3. The physical and mechanical properties of metals have a marked effect upon their performance as cavity-liner material. Boiling point, ductility, malleability, tensile strength, and hardness are among the properties that influence the effectiveness of a metal used as a cavity liner. Lead, for example, makes a wide, flat crater in steel plates. Aluminum makes a deeper crater than lead, and an aluminum alloy having a high tensile strength makes a deeper hole, but slightly smaller in diameter. Cast iron makes a deep, narrow hole.

These findings, together with the following analysis under Metallographic Survey of Slug, offer solutions to many of the problems involved in solving the mechanism of the formation of Munroe jets.

It has been fairly well established that cavity liners collapse in a manner similar to that indicated in Fig 2. Conical liners are known to collapse upon themselves while hemispherical liners are believed to turn inside out in the process of jet formation. The first has been definitely proved by recovery of collapsed portions of cones, while liners from partly detonated charges show that hemispheres may turn inside out. Fig 3 shows a sketch of a recovered slug from a 6-in. shaped charge using a 45° cone made of cast iron. (This size of charge drilled holes up to 3 ft in depth in solid granodiorite.)

Manuscript received at the office of the Institute Dec. 16, 1946. Issued as TP 2158 in METALS TECHNOLOGY, Aug. 1947 and MINING TECHNOLOGY, May 1947.

* Assistant Professor of Mining Engineering, University of Illinois, Urbana, Illinois.

† Research Assistant Professor of Metallurgical Engineering, University of Illinois.

¹ References are at the end of the paper.

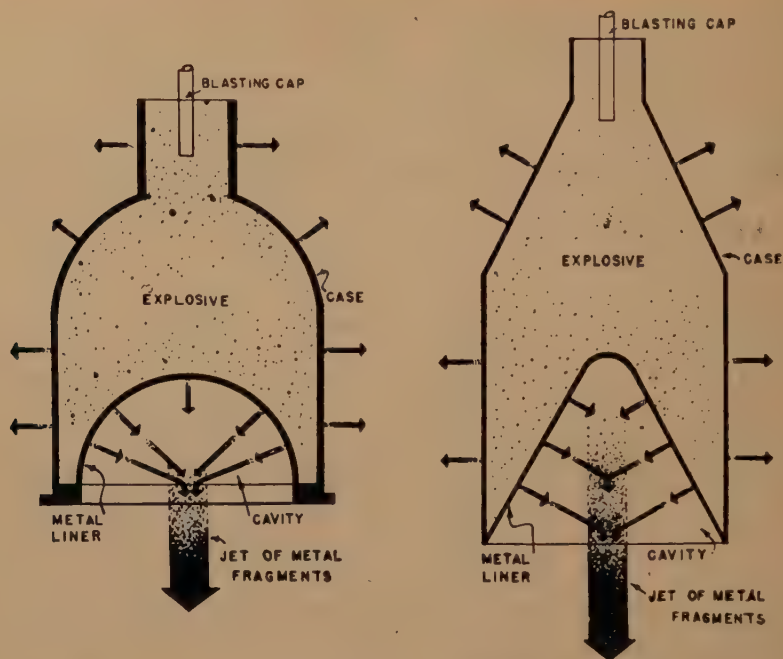


FIG 1—SKETCHES OF SHAPED CHARGES WITH (a) HEMISPHERICAL AND (b) CONICAL CAVITIES SHOWING MECHANISM OF FORMATION OF MUNROE JET.¹

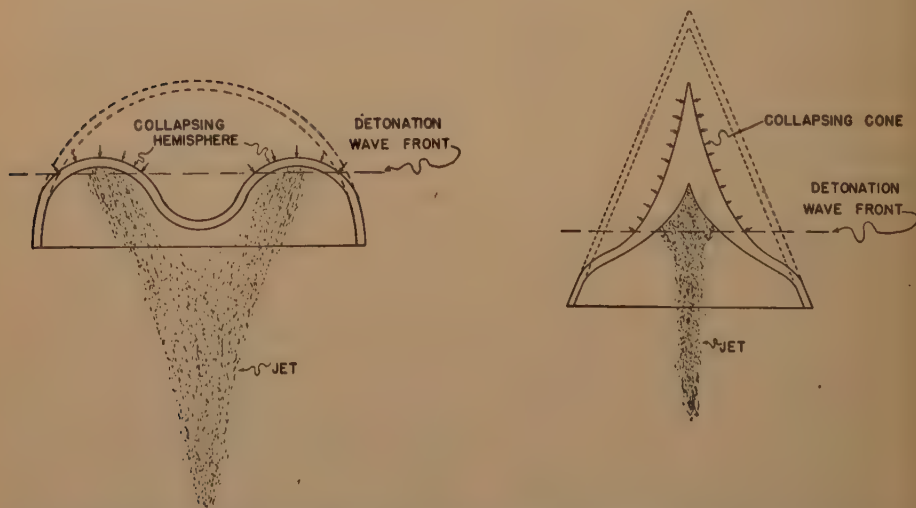


FIG 2—DIAGRAMMATIC SKETCH OF COLLAPSE OF CAVITY LINERS SHOWING APPROXIMATE POSITION OF DETONATION WAVE AND FORMATION OF JETS FROM REGIONS OF GREATEST COMPRESSION IN THE METAL.

METALLOGRAPHIC SURVEY OF CAST-IRON SLUG

The cast-iron slug was sectioned on a diametral plane through the original axis of the cone. This plane of metal received a metallographic polish and was etched with 5 pct nital to give the macrograph in Fig 4 at a magnification of approximately $2\frac{1}{2}$ diam.

A piece of the original iron casting from which the cast-iron cone had been made was also available. It was polished and etched to observe the original microstructure of the slug. A typical representation of this microstructure is shown in Fig 6. The structure shows the presence of straight-sided masses of graphite from which graphite flakes radiate (type C, ASTM). There appears to be little or no free ferrite, thus the microstructure consisted mainly of pearlite and graphite. However, it was reported that the cone had been heated after machining to a cherry red (temperature approx. 1400°F) and furnace-cooled. There was no specimen available to determine the effect on the microstructure of the heat-treatment given the iron. The structure of the recovered slug near the top outer edges and other portions representing regions of least plastic deformation are comparable with the microstructure shown in Fig 6, thus the heat-treatment was ineffective in producing any major change in microstructure.

A survey of the microstructure on the entire plane of polish of the slug illustrated in Fig 4 was made. A record was made of characteristic regions at a magnification of 100 and 500 diam. In Fig 5 a copy of Fig 4 is given with circled areas, which are lettered to correspond with the micrographs that follow in Figs 7 to 14. The micrographs are oriented the same as Fig 5 with respect to top and bottom and were taken in the circled regions shown in Fig 5.

Fig 7 shows a region at the center, top of the slug, which had suffered considerable

plastic deformation, as indicated by the "lining up" of the graphite flakes. Where the largest amount of flow or deformation took place, shown at the right side at the

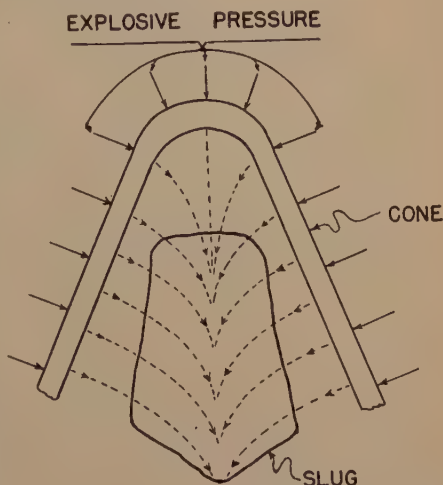


FIG 3—COLLAPSED SLUG FROM SIX-INCH CAST-IRON CONE AND PORTION OF ORIGINAL CONE FROM WHICH IT CAME.

Pressure is represented by arrows normal to the surface and curves inside the cone are probable paths of particles from the inside surface of the cone.

bottom of Fig 7, the graphite was surrounded by free ferrite and the pearlite areas were compacted. Fig 8 shows the manner in which the flow took place in this particular region. In the area in the lower right-hand side of Fig 8, the graphite, pearlite and ferrite are compacted into flow layers adjacent to a region of practically undisturbed lamellar pearlite at the top left. The structure at the right consists of free ferrite, graphite and compacted pearlite. Fig 9 shows a region in which the center field has a large amount of ferrite from which the graphite was almost completely removed. The ferrite shows a new granular structure resulting from recrystallization and the pearlite is distributed throughout as a fine dispersion. The pearlite in the surrounding areas appeared to have been partially spheroidized. The

FIG 4—CAST-IRON SLUG. $\times 2\frac{1}{2}$.

recrystallization of the ferrite and the partial spheroidization of the pearlite indicate that a temperature in the neighborhood of 1300°F was attained in the particular region.

Figs 10, 11, and 12 show a series of micrographs that form a sequence along

a horizontal line shown in Fig 5. The sequence is shown by the deformation of the ferrite in Fig 10, the partial recrystallization of the deformed ferrite in Fig 11 and the complete recrystallization of the ferrite and the partially spheroidized pearlite in Fig 12. The sequence suggests

that a temperature gradient may have been established in the slug with the temperature maximum along the center line of the slug and with the maxima increasing from top to bottom of the slug shown in Figs 4 and 5. It was also observed that in going toward the center of the slug the microstructure progressively contained less graphite, while in the central area of the slug the graphite appeared to have been squeezed out into large areas of agglomerated, practically pure graphite. In the sequence of Figs 10, 11, and 12 the direction of flow progressively changed until, as in Fig 12, it was almost parallel with the axis of the original cone.

Figs 13 and 14 show the microstructures near the bottom of the slug. Fig 13 shows a region that consists of recrystallized ferrite and recrystallized pearlite plus some graphite, while Fig 14 shows only recrystallized ferrite and spheroidized pearlite plus graphite. The areas of recrystallized pearlite in Fig 13 must have attained a temperature considerably in excess of 1300°F, below which temperature the deformed ferrite alone will recrystallize.

Near the bottom of the slug there were a number of fractures along the direction of flow. The fractures invariably went through areas of graphite that represented planes of weakness.

The extreme ductility exhibited by the interior regions of the slug is unusual for a gray cast-iron composition representative of the cone material. In tension the gray iron is notoriously a material of low strength and brittleness. Under the compressional stress of the shaped charge and the rapid application of the stress, the ductile behavior of the cast iron may have been enhanced by the heat developed internally by friction.

COLLAPSE OF CAVITY LINER

If it is assumed that approximately 25 pct of the cavity liner was ejected to

form the jet, Fig 3 shows the approximate length of the original cone that is represented by the slug. The macroscopic flow structure indicates that the paths



FIG 5—SLUG WITH AREAS LETTERED TO CORRESPOND WITH MICROGRAPHS OF FIGURES 7 TO 14. $\times 2\frac{1}{2}$.

of the grains remaining within the slug are hyperbolic in shape; that is to say, the grains appear to have been acted upon by two forces, one perpendicular to the wall of the original cone and one parallel to the axis of the cone, the velocity due to the latter increasing in magnitude as the cone collapsed and the velocity due to the force normal to the surface being changed into a velocity parallel to the axis.

The kinetic pressure against the outside of a liner is caused by the intense bombardment of molecules of the explosive gases. These molecules probably do not penetrate more than one or two atomic layers into the surface of the metal liner.

6



7



8

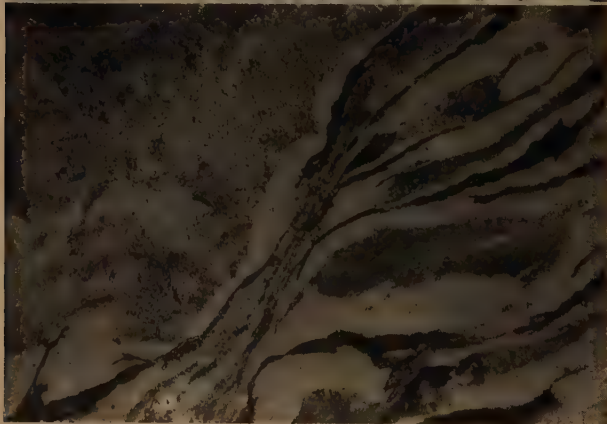


FIG 6—TYPICAL MICROSTRUCTURE OF METAL FROM WHICH SLUG WAS MADE. $\times 500$.

FIG 7—REGION AT CENTER TOP OF SLUG. $\times 100$.

Shows lining up of graphite flakes. Right bottom, graphite surrounded by free ferrite and pearlite areas.

FIG 8—MANNER OF FLOW IN REGION AT LOWER RIGHT OF FIGURE 7. $\times 500$.

Free ferrite, graphite and compacted pearlite at right.

Original magnifications given. Reduced one fourth in reproduction.

Their intense impact pressure, however, causes the wall of the liner to be forced in toward the axis of the cone. A study of the microstructure of the collapsed

properties of the metal, together with wall thickness, type of explosive, and other factors.

Microscopic examination of the col-

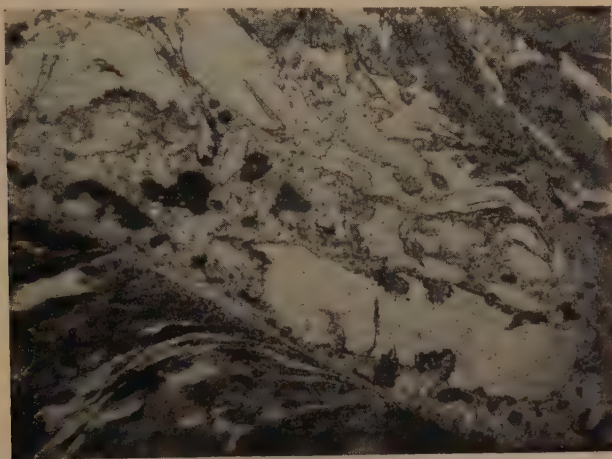


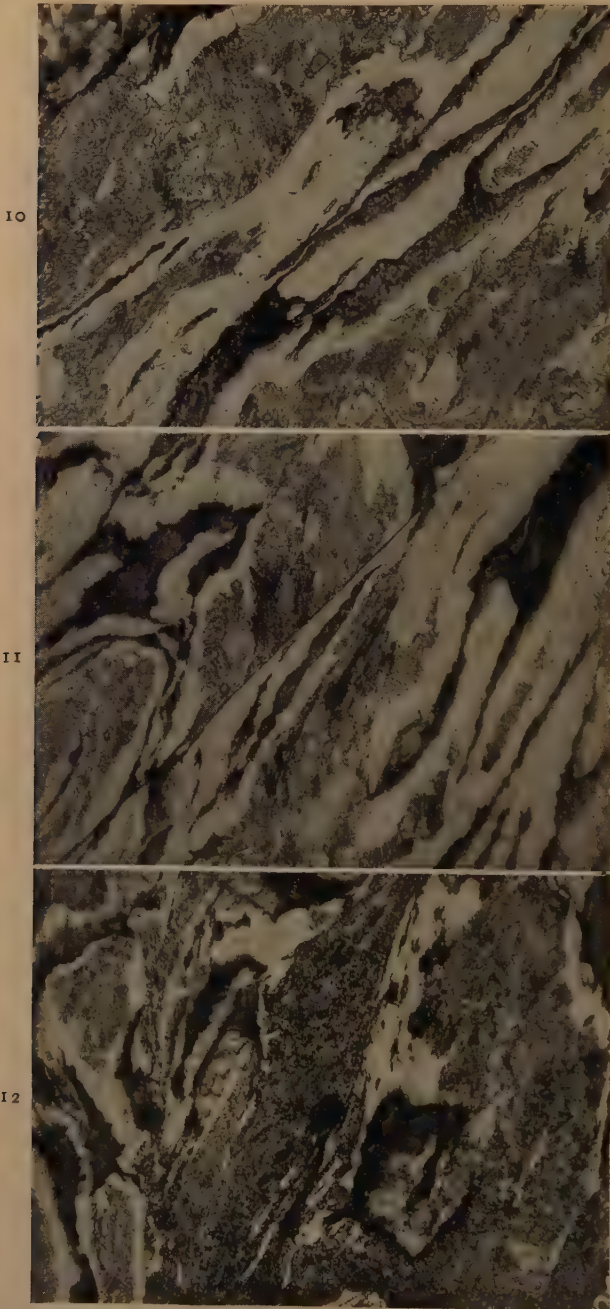
FIG 9—FERRITE FROM WHICH GRAPHITE WAS ALMOST COMPLETELY REMOVED. $\times 500$. Original magnification given. Reduced one fourth in reproduction.

slug of cast iron (Figs 4 to 14) shows that the more malleable constituents of the iron have been literally squeezed into a new structure in the direction of the axis of the slug. The total picture of the mechanism of jet formation then must include the effect of the impact of the explosive gases plus the compressive forces set up in the metal. It was concluded that in a cone the grains are in effect acted upon by two sets of compressional forces. The structure of the cast iron in Figs 4 to 13 would lead to the same conclusion; that is, that compressive forces in the collapsing liner cause the ejection of particles from the inside surface, and these particles travel in hyperbolic paths asymptotic to or coincident with the axis of the cone.

The laws that govern the division of liner material into slug and jet are not quite clear. The contact angle of impact of the collapsing walls would have a marked influence on the separation as well as the physical and mechanical

lapsed slug of cast iron shows that the metal near the center of the slug reached much higher temperatures than the metal near the outside. At the center of the slug the metal is very fine grained, grains of one and two microns in diameter being very common. As a cone collapses the metal on the inside "layers" of the cone wall, which is the metal that goes to form the jet and the center of the slug, are subject to greater heat of deformation than the outside layers of the cone. The internal heat of friction of these layers is greater than that for the outside layers, with a resulting higher temperature and greater fluidity (plasticity) in the center.

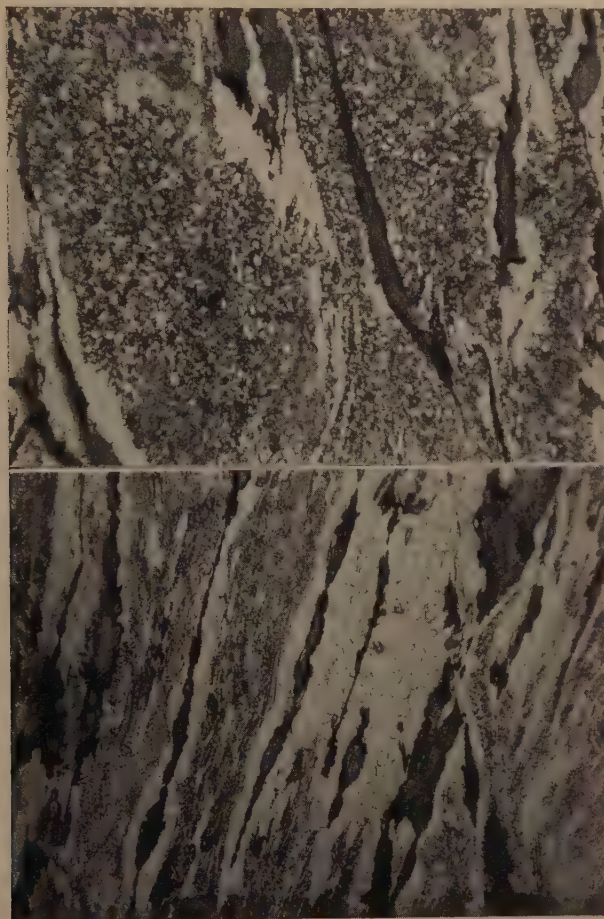
The mechanism involved probably could be described as "extrusion through a gradient orifice"; that is, the collapsing cone furnishes the extruding agent, the extruded material and the "orifice" through which the material is forced. We would have, in effect, a syringe with a self-contained moving conical metal "bulb"



FIGS 10-12—SERIES OF MICROGRAPHS ALONG HORIZONTAL LINE IN FIGURE 5. $\times 500$.
Fig 10, deformation of ferrite.
Fig 11, partial recrystallization of deformed ferrite.
Fig 12, complete recrystallization of ferrite and partially spheroidized pearlite.
Original magnification given. Reduced one fourth in reproduction.

subject to compressional forces normal to its walls. The "bulb" consists of metal of increasing fluidity from the outside to the axis, owing to the temperature

sides of the "bulb," the whole process moving progressively down the axis of the cone. The velocity of the jet with respect to a fixed point would then be



FIGS 13 AND 14—MICROSTRUCTURES NEAR BOTTOM OF SLUG. $\times 500$.
Fig 13, recrystallized ferrite and recrystallized pearlite, plus graphite.
Fig 14, recrystallized ferrite and spheroidized pearlite plus graphite.
Original magnification given. Reduced one fourth in reproduction.

gradient established by explosive pressure. The "orifice" consists of a partially constricted channel made by the flow of metal toward the axis of the cone, the metal having reached a temperature and state of fluidity just below that of the metal in the "bulb." The reservoir of fluid metal is constantly fed from the

equal to the velocity with which the metal is fed into the "bulb" plus the velocity of the point of contact of the collapsing walls.

From results of experimentation, it appears there is a relationship between the cavity-liner wall thickness and the momentum of the jet. As wall thickness

is increased from zero, the penetration effect of the jet increases also until an optimum thickness is reached, after which the penetration of the jet decreases as the walls become thicker. Then, based upon the conception of collapse described above, the property of cohesiveness of the metal also seems to be an important factor in determining the suitability of a metal for cavity liners.

When the cavity walls are too thin, apparently they do not possess the necessary mass to form both an "orifice" and a "bulb" and to furnish a quantity of plastic material to form the jet. Hence, jets from thin liners possess relatively low momentum. On the other hand, when the wall is thicker than optimum it offers too much resistance to the transmission of the energy of the explosion. As wall thickness increases above the optimum relatively less and less material goes into the jet, and if it is increased until the entire cavity is filled with metal the total mass would move forward with a velocity lower than the velocity of detonation.

The optimum thickness of a conical cavity liner probably would also vary according to the physical and mechanical properties of the metal employed.

THEORY OF JET FORMATION FOR HEMISPHERES

The mechanism of jet formation in hemispherical cavities is not as clearly defined as it is in conical cavities. Slugs from hemispherical charges have not been recovered in complete enough form to enable metallographic studies to be carried out on them. If hemispherical cavity liners are regarded in the same manner as conical cavity liners with reference to the ratio of mass of the jet to the mass of the liner, and the accompanying relationships between pressure, velocity, and energy, the same theory should apply in both cases.

In the case of cones it appears certain

that the particles that form the jet are ejected by compressional forces. The same probably is equally true of hemispheres. At the time when the detonation wave strikes a hemisphere, the inside layers at the apex are subject to compressional forces. As collapse proceeds, the region of compressional forces moves down the inside of the liner until collapse is complete (Fig 2). If the liner turns inside out the portions of the metal that were subject to compression are in turn subject to tensional forces. It is from the regions of compression that the jet particles must emerge. The region of compression would be composed of a symmetrical section of the hemisphere, beginning as a point and widening into a larger and larger circle as the process of collapse advances. The particles would then be ejected normal to the surface, which would focus them along the axis of the cavity to form the jet.

Apparently the particles thus squeezed out move parallel to the axis of the hemisphere. This is assumed for the following reasons: Cast-iron hemispheres² make holes of relatively small diameters in steel plates, while more ductile metals make funnel-shaped holes with a diameter at the first plate almost equal to the diameter of the hemisphere. This would lead to the belief that with cast-iron hemispheres the process of collapse is interrupted if not terminated by rupture of the liner while collapse is only partially complete. For more ductile metals the process of collapse probably continues down the entire height of the liner, the lower portions of the liner provide a wide jet, which has less penetrating force per unit area and only acts to widen the hole already produced by the portion of the jet emanating from the upper portion of the cavity liner. From the present concepts it appears that jet impact effects for a given explosive vary over a small range for corresponding relatively large changes in the apex angle in cones. Jets from acute-angle cones may penetrate deeper because of the greater length (or the

greater period of duration) of the jet. It is believed, however, that increased penetration is not caused only by increased jet velocity due to a change in the apex angle of the cone but that other factors enter in as well.

EXPLOSIVE FORCE AND STRUCTURE OF METAL IN LINER

A description of the metallographic changes in the microstructure of a cast-iron liner from a 6-in. shaped charge has been given. The time required for the complete deformation of the cone was in the neighborhood of 10 or 15 microseconds, taking the velocity of detonation of 100 pct blasting gelatin as 26,200 ft per sec. This ultra-high-speed deformation involving high pressures applied at velocities that are extremely high in comparison with metal deformation under ordinary conditions had the effect of making the cast iron ductile enough to flow quite readily.

The essential changes that have taken place in the iron of the slug from surface to axis range from a limited amount of deformation at the surface through a phase of more complete deformation, recrystallization of ferrite and agglomeration of graphite to an area of partial spheroidization in the region of the axis of the slug.

Considering the microstructure of the slug in terms of the mechanics of jet formation, there are a number of elements that may be given consideration. The forces acting on the liner during the explosion are represented by vectors of equal magnitude in Fig 3. The only upward force of any magnitude would be one due to the inertia of the slug itself. Hence, the forces involved are mostly compressional forces or those of shear. Microscopically, flow structure varies in character from irregular multidirectional undisturbed patterns to relatively straight lines in regions of shear and greatest flow. Fig 8 represents a region of differential flow; that is, the ferrite and the graphite in the right two thirds of the photograph

have been subject to flow while the pearlite in the upper left seems relatively undisturbed.

In addition, there is an almost complete welding of the grains of the cast iron along the axis of the slug. At the axis, too, the particles of ferrite and the pearlite colonies are very fine, portions of the ferrite being recrystallized. The grain size of ferrite increases toward the outside of the slug and the amount of recrystallization of the ferrite decreases.

Well-developed shear planes are shown in Figs 9 and 11, the upper section in each case showing greater relative motion toward the axis of the slug. This is clearly indicated by the drag on the lower block of metal at the lower left side. The process of collapse apparently involved the movement of rigid colonies of pearlite in a "viscous medium" of ferrite and graphite until portions of this flowing heterogeneous mass reached the vicinity of the axis, where it was probably pulverized or partially spheroidized to form a Munroe jet. The fine-grained iron in Figs 12 and 13 undoubtedly represents the approximate type of material that goes to form a jet. This would be composed, then, of a very high-velocity spray of fine graphite and fine particles of ferrite and pearlite.

SUMMARY AND CONCLUSIONS

1. A theory based upon the microstructure of a collapsed cast-iron cone is offered to explain some of the physical laws involved in jet formation.
2. A study of the microstructure of a collapsed cavity liner shows that cast iron is ductile under conditions of temperature and pressure involved and indicates that jets from cast-iron liners are composed of a fine spray of graphite, partially spheroidized pearlite and ferrite.
3. Collapse of cast-iron conical liners appears to involve processes of compression, shear, and extrusion of particles from the inside of the liner.
4. Jet formation from cones also involves

flow of metal subject to intense pressures and temperatures that are below the melting point of the metal. The metal appears to obey the laws of hydraulic flow.

ACKNOWLEDGMENT

The section on the metallographic survey of the cast-iron slug was written by W. H. Bruckner.

REFERENCES

1. R. S. Lewis and G. B. Clark: Application of Shaped Charges to Mining Operations: Tests on Steel and Rock. *Bull. Univ. of Utah* (July 1946) 37.
2. G. B. Clark: Studies of the Design of Shaped Explosive Charges and Their Effect in Breaking Concrete Blocks. *Mining Tech., AIME* (May 1947—TP 2157).
3. J. B. Hutt: The Shaped Charge—for Cheaper Mine Blasting. *Eng. and Min. Jnl.* (May 1946) 147, 58-63.

DISCUSSION

(S. Epstein and R. D. Chapman presiding)

F. W. SCHONFELD*—I should like to ask the authors if they have any data on a change in chemical analysis of these slugs, since under the intense pressures developed the equation of state may be considerably altered so that the equilibria are completely changed. The method of the authors would seem to be a very interesting tool for developing a knowledge of these relationships.

W. H. BRUCKNER (authors' reply)—Do I understand that you wish me to discuss the question of a change in chemistry?

F. W. SCHONFELD—Yes.

W. H. BRUCKNER—Due to the oxidation?

F. W. SCHONFELD—Yes, for example, a change in carbon content.

W. H. BRUCKNER—As far as we know the slug remains a solid except for some material at the end and interior of the slug where the jet is produced. The explosion of the charge and the formation of the jet are reported to take place within $\frac{1}{10}$ of a microsec. There are oxidizing gases in contact with the exterior of

the slug during this short time which could be responsible for loss of carbon from the surface region of the slug. However the surface of the slug appears to have the same carbon content as the interior thus indicating a negligible loss, if any, due to oxidation. No chemical analysis was made for carbon or other elements in the recovered slug.

E. E. THUM*—I hesitate to make any comment on this because ballistics is something about which I know nothing. The bazooka, however, is an extraordinarily fascinating thing. I know that anyone who ever saw it punch a smooth hole in hardened armor plate could not believe his eyes. Had he not known anything about the "Munroe Effect" he would have gone away thoroughly mystified as to what was going on.

The micrographs exhibited in this paper apparently suggest some instantaneous metallurgy. With due humility, I suggest that this slug under study might within a few thousandths of a second in which it was forming—have passed through a powdery condition and that the slug itself represents a reconsolidation of the fragments.

From the explanation of the jet already given here, I take it that very small particles of metal are blown away from the interior lining of the cone and go out as incandescent solids as a part of the jet. Is it not possible that some portion of this material striking against other particles would reconsolidate and form a sizable portion of this final solid slug? Under this supposition it is not too hard to explain some of the elongated particles observed. The flow of cast iron or any other material, under such conditions of temperature and pressure, is wholly to be anticipated.

A very interesting thing is the apparent change in carbon content from the original structure of the cone to that possessed by the slug. It ought to be very easy to analyze by microchemistry or other means small regions of this slug and actually find out the actual carbon content.

If fragments of cast iron act as indicated above there should be a considerable amount of carbon oxidized almost instantaneously. Carbon diffusion and reaction are very rapid in hot

* University of California, Los Alamos, New Mexico.

* Editor, *Metal Progress*.

steel. Metallurgists generally forget that fact, particularly when we specify that a steel should be heat treated one hour for every inch of cross-section.

W. H. BRUCKNER—We wish to thank Mr. Thum for his interesting discussion. Professor Clark was fortunate in his choice of cast iron for the cone of the shaped charge which became the recovered slug, because with cast iron a metallographic study of plastic flow became possible. In the bazooka slug the structure is mainly ferrite and flow structures are not as easily identified as with the cast iron.

S. EPSTEIN—I think a wrong impression has been given here that cast iron is always brittle. The fact is that if the gray cast iron is heated to hot rolling temperatures it can be rolled. It is possible to hot roll a sheet, for example, out of gray cast iron at a rolling temperature of about 1800°F.

Professor Clark remarked that he found nothing in the metallurgical literature describing the flow of cast iron. True, cast iron is brittle and will not flow at room temperature, but when heated to a red heat it will flow as is evident from the fact that it can be forged and rolled.

W. H. BRUCKNER—There is in the literature a report on the rolling of white, cast iron. Mr. D. P. Forbes in an article entitled "New Cast Irons Heat Treated, Rolled" published in *Metal Progress*, 33, Feb. 1938 p. 137-142, described his successful efforts to hot roll the cast iron. In the liner of the shaped charge the high rate of deformation produced enough heat to cause the solid material to flow easily and form the slug which was recovered. The temperature gradient established in the slug probably ranged from the high temperature of the liquid forming the jet to the lowest temperature on the exterior surface. In the absence of actual temperature measurements it was assumed that wherever ferrite was recrystallized the temperature must have been 1300°F or less and where the pearlite was recrystallized the temperature must have gone above 1300°F.

F. W. SCHONFELD—Now that brings us back to the original point. You say we can, because of the relationships of the microconstituents, eliminate temperature as an unknown factor.

The point I originally tried to make was that under such terrific pressures we do not know what microconstituents or phases would be present, and that therefore attempts to utilize the well-known and ordinary microstructural arrangements may be quite misleading. It is conceivable that another crystal phase of iron might exist under terrific pressure, as in the well known case of ice.

A change in chemistry will, of course, result in a change of microstructure, but extremely large pressure changes might also be responsible for certain differences.

In addition, I do not believe that one should assume that the temperature must have been less than 1800°F because the ferrite has not uncrystallized. Of course pressure shifts the ferrite-austenite transformation temperature downward, but it is likewise true that A_c points are shifted upward by rapid heating. It is also true that ferrite can recrystallize as ferrite at considerably lower temperatures, but perhaps the pressure-temperature cycle is so brief in this case that recrystallization does not occur.

W. H. BRUCKNER—We agree with the last speaker and will say that in the absence of actual measurements of temperature, pressure and rate of deformation the temperatures stated in the paper are an erroneous assumption based on conventional metallurgy in which pressure is considered invariant at 760 mm. At high pressures such as are encountered in firing the shaped charge the known phase relationship of the equilibrium diagram in conventional metallurgy may be changed considerably. It is also possible that a high temperature existing for a short period will give a metallographic product which has the same characteristics as the product resulting from a longer duration at a lower temperature. The last speaker has emphasized the fact that the metallurgy of the shaped charge slug is not the conventional equilibrium metallurgy and we appreciate his comments as an indication of the complexity of the problem of determining the desired values of temperature, pressure and speed of deformation.

G. B. CLARK and W. H. BRUCKNER (authors' closure)—The authors are pleased to have had the evident interest of the various discussers in the problems presented in the paper. Our

knowledge of nonequilibrium, dynamic metallurgy at high pressures and temperatures is limited in scope. When this unknown field is further complicated by plastic action at extremely rapid flow rates the problem becomes one in which conjecture must lead the way to

carefully prepared procedures in which the constants of the reactions involved may be determined. The work is now in this stage with the possibility of the determination of energy, pressure and temperatures resulting from the studies.

Note on the Distribution of Sulphur between Molten Iron and Slag*

BY TERKEL ROSENQVIST†

Few subjects in iron metallurgy and steelmaking have caused so much discussion and have resulted in so many divergent and partly contradictory statements as the theory of the distribution of sulphur between molten iron and slag. An interesting survey of the different points of view is given by Grant and Chipman.¹

Grant and Chipman themselves conclude in their paper that, at least in the open hearth and electric steel furnaces, the governing reaction is a simple distribution like:



They conclude that no significant reaction takes place according to the more classical scheme:



This is the reaction which is regarded by most investigators as the primary sulphur reaction in the blast furnaces, where it is accompanied by the reaction with carbon:



The writer suggests an alternative to the reactions mentioned above.

It is the opinion of the writer that the *a priori* assumption of defined molecular compounds being present in molten steel as well as in molten slag, has retarded rather than promoted a solution of the sulphur problem.

As for the constituents of molten steel, it is taking too much for granted to mention the presence of FeS and MnS. If this infers that the melt contains diatomic molecules, the statement must be made that at least such molecules do not exist in the solid state at room temperature. Solid FeS crystallizes in the nickel-arsenide structure, and MnS (high temperature form) in the sodium-chloride structure. In these structures the sulphur is surrounded by six metal neighbors, and no molecular groups can be isolated. When sulphur is dissolved in molten steel, it is expected to maintain the same coordination number as in the solid state.

We know that sulphur in steel has a certain chemical potential and a chemical activity which can be expressed by the reaction:



where the activity A_s is proportional to the ratio $\frac{P_{\text{H}_2\text{S}}}{P_{\text{H}_2}}$. We know also that this activity is influenced by the presence of other constituents. For instance, there is reason to assume that carbon and silicon increase the sulphur activity and manganese decreases it. However, the exact relationship here is scarcely known, and further investigations are needed.

Concerning the molten slags, if anything should be assumed *a priori* it would be that they are composed of ionic rather than molecular parts. There are indications of this in that solid silicates form ionic structures, and molten slags show high electric conductivity and can be electrolyzed.²

It has been claimed by Taylor and Chipman³ that their activity investigations

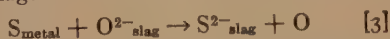
* Issued as Technical Note No. 7, METALS TECHNOLOGY, October 1948. Manuscript received at the office of the Institute August 13, 1948.

† Instructor, Institute for the Study of Metals, University of Chicago.

¹ References are at the end of the note.

in the system $\text{SiO}_2\text{-CaO-FeO}$ give no indication of any ionic nature of the slag, because the activities, when based on an ionic dissociation, do not follow Raoult's law for perfect mixtures. Unfortunately this is not to be expected. Because of interionic reactions and polarization of the different ions, the deviations from perfect mixture must of necessity be large.

On the basis of an ionic theory for molten slags, Lux⁴ and, recently, Flood and Förland⁵ have suggested the oxygen ion O^{2-} as the carrier of the basicity of the slag, and the oxygen ion activity $a_{\text{O}^{2-}}$ or its negative logarithm $p\text{O}$ as an opposite equivalent to $p\text{H}$ in aqueous solution. As it is generally accepted that, high basicity and reducing conditions promote desulphurization, the writer suggests the following formula for sulphur distribution between molten metal and slag:



This is the same equation presented by the writer in another connection.⁶ The equilibrium constant will be:

$$\frac{a_{\text{S}} \cdot a_{\text{O}^{2-}}}{a_{\text{S}^{2-}} \cdot a_{\text{O}}} = K$$

where a_{O} is proportional to $\sqrt{P_{\text{O}_2}}$ in the system. This equilibrium constant is universal, and is based only on the difference in electron affinity of sulphur and oxygen. Eq 3 indicates that good desulphurization is promoted by high oxygen-ion-activity, that is, high basicity, as well as low oxygen pressure—that is, reducing conditions.

In steel slags, where the FeO concentration is high, this will mean a high oxygen

pressure which opposes desulphurization. This effect, however, is partly canceled by the fact that FeO gives off oxygen ions and contributes to the basicity of the slag; and partly by the polarizing action the Fe^{2+} ion is assumed to have on the sulphur ion—an effect which will decrease the activity of the sulphur ion. This can explain why Grant and Chipman find the net effect of FeO small in steel slag.

Most other constituents in the slag and in the iron bath will have similar complex effects. This may be the explanation of the wide difference in the experimental results obtained by various investigators. In most experimental work it has not been possible to study the influence of a single factor alone, as a change in this usually influences one or more of the other factors.

In order to judge if the mechanism which is suggested in Eq 3 is correct, it is necessary to carry out experiments where two of the four activities given in the equation are kept absolutely constant. The writer hopes that, at an early date, he will be able to present the results of work which he is carrying out along this line.

REFERENCES

1. N. J. Grant and J. Chipman: *TP 1988 Metals Tech.* (April 1946); *Trans. AIME* (1946) **167**, 134.
2. A. E. Martin and G. Derge: *Trans. AIME* (1943) **154**, 104.
3. C. R. Taylor and J. Chipman: *Trans. AIME* (1943) **154**, 228.
4. H. Lux: *Ztsch. f. Elektrochemie* (1939) **4**, 303.
5. H. Flood and T. Förland: *Acta Chemica Scandinavica* (1947) **1**, 592.
6. T. Rosenqvist: *Tidskr. f. Kemi, Bergv. och Metallurgi* (1947) **7**, 120.

Institute of Metals Division, Volume 175

Transactions AIME, 1948'

TECHNICAL PAPERS AND DISCUSSIONS

Institute of Metals Division Lecture

Grains, Phases, and Interfaces: An Interpretation of Microstructure. By CYRIL STANLEY SMITH. (*Metals Tech.*, June 1948, TP 2387)

Copper and Copper Alloys

Structure after Working

Preferred Orientation in Drawn and Annealed 70-30 Alpha Brass Tubes. By W. R. HIBBARD, JR. (*Metals Tech.*, Sept. 1947, TP 2245) With discussion

Some Observations of Lineage in Copper Crystals. By W. R. HIBBARD, JR. (*Metals Tech.*, Sept. 1947, TP 2244) With discussion

Deformation Lines in Cold-rolled Copper and Its Binary Alpha Solid Solution Alloys with Aluminum, Nickel and Zinc. By W. R. HIBBARD, JR., R. W. FENN, JR., HAROLD MARGOLIN and H. P. MOORE. (*Metals Tech.*, Feb. 1948, TP 2336) With discussion

Unpredicted Cross-slip in Single Crystals of Alpha Brass. By ROBERT MADDIN, C. H. MATHEWSON and W. R. HIBBARD, JR. (*Metals Tech.*, Feb. 1948, TP 2331) With discussion

The Nature of Strain Markings in Alpha Brass. By J. E. BURKE and C. S. BARRETT. (*Metals Tech.*, Feb. 1948, TP 2327) With discussion

Wire Textures of Copper and Its Binary Alpha Solid Solution Alloys with Aluminum, Nickel and Zinc. By W. R. HIBBARD, JR., and MING-KAO YEN. (*Metals Tech.*, Feb. 1948, TP 2334) With discussion

The Effect of Mechanical Deformation on Grain Growth in Alpha Brass. By J. E. BURKE and Y. G. SHIAU. (*Metals Tech.*, Sept. 1947, TP 2265) With discussion

Kinetics

Grain Growth in 70-30 Brass. By PAUL A. BECK, JOHN TOWERS, JR., and W. D. MANLY. (*Metals Tech.*, Feb. 1948, TP 2326) With discussion

Activity Coefficients in Alpha-brass from Statistical Thermodynamics. By LESTER GUTTMAN. (*Metals Tech.*, Feb. 1948, TP 2330) With discussion

Diffusion, Mobility and Their Interrelation through Free Energy in Binary Metallic Systems. By L. S. DARKEN. (*Metals Tech.*, Jan. 1948, TP 2311) With discussion

Absolute Reaction Rate Theory for Diffusion in Metals. By J. C. FISHER, J. H. HOLLOMON and DAVID TURNBULL. (*Metals Tech.*, Feb. 1948, TP 2344) With discussion

Mechanism of Precipitation in Alloys of Beryllium in Copper. By A. G. GUY, C. S. BARRETT and R. F. MEHL. (*Metals Tech.*, Feb. 1948, TP 2341) With discussion

The Isothermal Transformation of a Eutectoid Aluminum Bronze. By DAVID J. MACK. (*Metals Tech.*, Sept. 1947, TP 2242) With discussion

Constitution and Properties

- The Copper-rich Corner of the Copper-aluminum-silicon Diagram. By F. H. WILSON. (*Metals Tech.*, Feb. 1948, TP 2329) With discussion
- The Constitution and Properties of Copper-rich Copper-chromium and Copper-nickel-chromium Alloys. By WALTER R. HIBBARD, JR., F. D. ROSI, H. T. CLARK, JR., and R. I. O'HERRON. (*Metals Tech.*, Feb. 1948, TP 2317) With supplement and discussion
- The Comparative Properties of Several Types of Commercial Coppers, as Cold Worked and as Recrystallized. By L. R. JACKSON, A. M. HALL and A. D. SCHWOPE. (*Metals Tech.*, Sept. 1947, TP 2274)
- Flow, Fracture and Ductility of Metals. By D. J. McADAM, JR., G. W. GEIL and FRANCES JANE CROMWELL. (*Metals Tech.*, Jan. 1948, TP 2296) With discussion
- Development of Residual Stresses in Strip Rolling. By R. McC. BAKER, R. E. RICKSECKER and W. M. BALDWIN, JR. (*Metals Tech.*, April 1948, TP 2333)

Aluminum and Aluminum Alloys

- Anomalies in the Appearance of Glide Ellipses. By ROBERT MADDIN. (*Metals Tech.*, Feb. 1948, TP 2332) With discussion
- Equilibrium Relations in Aluminum-sodium Alloys of High Purity. By W. L. FINK, L. A. WILLEY and H. C. STUMPF. (*Metals Tech.*, Feb. 1948, TP 2339)
- Grain Growth in High-purity Aluminum and in Aluminum-magnesium Alloy. By P. A. BECK, J. C. KREMER, L. J. DEMER and M. L. HOLZWORTH. (*Metals Tech.*, Sept. 1947, TP 2280) With discussion
- The Use of the Jominy Test in Studying Commercial Age-hardening Aluminum Alloys. By B. M. LORING, W. H. BAER and G. M. CARLTON. (*Metals Tech.*, Feb. 1948, TP 2337) With discussion
- Quenching of 75S Aluminum Alloy. By W. L. FINK and L. A. WILLEY. (*Metals Tech.*, Aug. 1947, TP 2225) With discussion
- The Effect of Tensile and Compressive Stresses on the Corrosion of an Aluminum Alloy. By W. D. ROBERTSON. (*Metals Tech.*, Sept. 1947, TP 2281). With discussion
- Effect of Various Stress Histories on the Flow and Fracture Characteristics of the Aluminum Alloy 24ST. By J. J. LYNCH, E. J. RIPLING and G. SACHS. (*Metals Tech.*, Jan. 1948, TP 2307) With discussion
- Low Cycle Fatigue of the Aluminum Alloy 24ST in Direct Stress. By S. I. LIU, J. J. LYNCH, E. J. RIPLING and G. SACHS. (*Metals Tech.*, Feb. 1948, TP 2338) With discussion
- Purification of Aluminum and Its Alloys. By YVES DARDEL. (*Metals Tech.*, Sept. 1947, TP 2247) With discussion

Magnesium and Magnesium Alloys

- Factors Involved in Heat-treating a Magnesium Alloy. By A. E. FLANIGAN, I. I. CORNET, R. HULTGREN, J. T. LAPSLEY and J. E. DORN. (*Metals Tech.*, Sept. 1947, TP 2282). With discussion
- X Ray Studies of Twinning and Untwinning in Magnesium Alloys. By J. B. HESS and R. L. DIETRICH. (*Metals Tech.*, Feb. 1948, TP 2328) With discussion
- Solubility of Iron in Liquid Magnesium. By D. W. MITCHELL. (*Metals Tech.*, Jan. 1948, TP 2309)
- Low Temperature Transformation in Lithium and Lithium-magnesium Alloys. By C. S. BARRETT and O. R. TRAUTZ. (*Metals Tech.*, April 1948, TP 2346) With discussion

Tungsten, Molybdenum and Chromium

- An Electrolytic Method for Pointing Tungsten Wires. By W. G. PFANN. (*Metals Tech.*, June 1947, TP 2210) With discussion
- Thin Oxide Films on Tungsten. By E. A. GULBRANSEN and W. S. WYSONG. (*Metals Tech.*, Sept. 1947, TP 2224) With discussion
- Thin Oxide Films on Molybdenum. By E. A. GULBRANSEN and W. S. WYSONG. (*Metals Tech.*, Sept. 1947, TP 2226) With discussion
- Plating Molybdenum, Tungsten and Chromium by Thermal Decomposition of Their Carbonyls. By J. J. LANDER and L. H. GERMER. (*Metals Tech.*, Sept. 1947, TP 2259) With discussion
- Plating Chromium by Thermal Decomposition of Chromium Hexacarbonyl. By B. B. OWEN and R. T. WEBBER. (*Metals Tech.*, Jan. 1948, TP 2306) With discussion
- Hydrogen Content of Electrolytic Chromium and Its Removal. By E. V. POTTER and H. C. LÜKENS. (*Metals Tech.*, Jan. 1948, TP 2312)
- Passivity in Chromium-iron Alloys; Adsorbed Iron Films on Chromium. By H. H. UHLIG. (*Metals Tech.*, Sept. 1947, TP 2243). With discussion

Miscellaneous Metals and Alloys

- The Transformation of Cobalt. By A. R. TROIANO and J. L. TOKICH. (*Metals Tech.*, April 1948, TP 2348) With discussion
- Thermal Expansion Properties of Iron-cobalt Alloys. By M. E. FINE and W. C. ELLIS. (*Metals Tech.*, Feb. 1948, TP 2320) With discussion
- The Thermoelectric Properties and Electrical Conductivity of Bismuth-selenium Alloys. By B. D. CULLITY. (*Metals Tech.*, Jan. 1948, TP 2313) With discussion
- A New Graphite Resistor Vacuum Furnace and Its Application in Melting Zirconium. By W. J. KROLL, C. T. ANDERSON and H. L. GILBERT. (*Metals Tech.*, Jan. 1948, TP 2310) With discussion
- Transient Nucleation. By DAVID TURNBULL. (*Metals Tech.*, June 1948, TP 2365)

Powder Metallurgy

- Tantalum Powder by Magnesium Reduction. By J. PRIETO ISAZA, A. J. SHALER and J. WULFF. (*Metals Tech.*, Sept. 1947, TP 2277) With discussion
- Nickel-steels by Powder Metallurgy. By LAURENCE DELISLE and WALTER V. KNOPP. (*Metals Tech.*, Feb. 1948, TP 2340) With discussion
- Evaluation of the Molding, Coining and Sintering Properties of Iron Powder. By JEROME F. KUZMICK. (*Metals Tech.*, Jan. 1948, TP 2308) With discussion
- Magnetic Properties of Iron-powder Compacts. By ROBERT STEINITZ. (*Metals Tech.*, Feb. 1948, TP 2335) With discussion
- The Powder Metallurgy of Porous Metals and Alloys Having a Controlled Porosity. By POL DUWEZ and H. E. MARTENS. (*Metals Tech.*, April 1948, TP 2343) With discussion
- Sintering in the Presence of a Liquid Phase. By F. V. LENEL. (*Metals Tech.*, June 1948, TP 2415) With discussion
- (Powder Metallurgy Seminar) (*Metals Tech.*, Aug. 1948)

TECHNICAL NOTES

- Measurement of Interfacial Tensions. By J. C. FISHER. (*Metals Tech.*, June 1948, TN 1)
- Quick Method for Detecting Preferred Orientation. By P. A. BECK. (*Metals Tech.*, June 1948, TN 2)

Production of Ferrite Single Crystals. By F. G. STONE. (*Metals Tech.*, June 1948, TN 3)

The Effect of Grain Size on the Martensite Transformations. By W. J. BARNETT and A. R. TROIANO (*Metals Tech.*, Aug. 1948, TN 4)

Nucleation of Phase Transformations. By J. C. FISHER, J. H. HOLLOMON, and D. TURNBULL. (*Metals Tech.*, Aug. 1948, TN 5)

An Observation on Diffusion during Homogenization of a Single Crystal of Alpha Brass. By ROBERT MADDIN. (*Metals Tech.*, Sept. 1948, TN 6)

Contents of Vol. 176, Iron and Steel Division, 1948

Index

INDEX

(NOTE: In this index the names of authors of papers and discussions and of men referred to are printed in SMALL CAPITALS, and the titles of papers in *italics*.)

A

- Aging: cast steel: measurements of effect of variations in time and temperature and dependence of aging on thickness of section, 303
- ALEXANDER, B. H.: *Discussion on Anisothermal Formation of Bainite and Proeutectoid Constituents*, 377
- Anelastic effects: in alpha iron, 448
 - measurement: experimental methods, 450
- ASCIK, A. L.: *Discussion on Hydrogen and Nitrogen Contents of Steel during Commercial Melting*, 279
- Austempering. *See* Steel
- Austenite. *See* Steel
- AUSTIN, J. B.: *Discussion on Apparatus for the Hot-extraction Analysis for Hydrogen in Steel*, 258
- AVERBACH, B. L. and COHEN, M.: *X Ray Determination of Retained Austenite by Integrated Intensities*, 401; discussion, 414
- AVERY, H. S.: *Discussion on Wear Tests on Grinding Balls*, 521

B

- Bainite. *See* Steel
- BEVER, M. B.: *Discussion on Hydrogen and Nitrogen Contents of Steel during Commercial Melting*, 278
- Blast-furnace process: desulphurization: probable chemistry, 330
 - distribution of sulphur between molten iron and slag, 540
 - slag-metal interface: sulphur transfer: kinetics, 309
 - sulphur from coke, 343
 - sulphur in iron: interdependence of variables, 330
- Blasting: shaped charges: metal cavity liners: behavior, 527
 - Munroe effect, 527
- BRACE, P. H.: *Discussion on Apparatus for the Hot-extraction Analysis for Hydrogen in Steel*, 259
- BROWER, T. E. and LARSEN, B. M.: *Role of Thermochemical Factors in Basic Open Hearth Production Rate*, 92
 - Some Correlations between Variables Affecting Sulphur in Blast Furnace Iron*, 330
- BROWN, W. F. JR., SACHS, G. and EBERT, L. J.: *Notch-tensile Characteristics of a Partially Austempered, Low Alloy Steel*, 424

- BRUCKNER, W. H. and CLARK, G. B.: *Behavior of Metal Cavity Liners in Shaped Explosive Charges*, 527; discussion, 538

C

- Caspersson ladle: use in casting steel with protection of nitrogen gas, 189
- Cast steel: aging: measurements of effect of variations in time and temperature and dependence of aging on thickness of section, 305
 - ductility: abnormal loss, 283
 - effect of hydrogen, 283
 - temporary loss, 283
- Cavity liners for shaped explosive charges: collapse of conical liners, 527
 - collapse of hemispherical liners: jet formation, 527
 - jet formation: theory, 536
 - metallographic changes in cast iron, 527
- CHANG, LO-CHING and GOLDMAN, K. M.: *Kinetics of the Transfer of Sulphur Across a Slag-metal Interface*, 309; discussion, 327
- CHIPMAN, JOHN: *Discussions: on Direct Oxidation in the Basic Open Hearth Furnace*, 68, 72
 - on Kinetics of the Transfer of Sulphur Across a Slag-metal Interface*, 329
- CLARK, G. B. and BRUCKNER, W. H.: *Behavior of Metal Cavity Liners in Shaped Explosive Charges*, 527; discussion, 538
- COHEN, M.: *Discussion on An Evaluation of Quenching Oils by Means of the End Quench Test*, 422
- COHEN, M. and AVERBACH, B. L.: *X Ray Determination of Retained Austenite by Integrated Intensities*, 401; discussion, 414
- COHEN, MORRIS and HOWARD, R. T., JR.: *Austenite Transformation above and within the Martensite Range*, 384; discussion, 397
- Coke oven: sulphur: tracer study, 343
- Cracking: gun steel: coarse, 482
 - heat checking, 482, 486
 - post-fusion, 483

D

- DARKEN, L. S.: *Discussion on Sampling and Analysis of Steel for Hydrogen*, 246
- DE LONGE, K. A.: *Discussion on Wear Tests on Grinding Balls*, 523
- DERGE, G., PEIFER, W. and RICHARDS, J. H.: *Sampling and Analysis of Steel for Hydrogen*, 219; discussion, 246

DOANE, D. V.: *Discussion on An Evaluation of Quenching Oils by Means of the End Quench Test*, 422

E

EATON, S. E., HYDE, R. W. and OLD, B. S.: *Tracer Study of Sulphur in the Coke Oven*, 343

EBERT, L. J., SACHS, G. and BROWN, W. F. JR.: *Notch-tensile Characteristics of a Partially Austempered, Low Alloy Steel*, 424

ELLIOTT, V. E. and MEYETTE, C. L.: *Method for Determining the Origin of Surface Defects in Rolled Steel Products*, 201; *discussion*, 216

EPSTEIN, S.: *Discussions: on Austenite Transformation above and within the Martensite Range*, 398

on Behavior of Metal Cavity Liners in Shaped Explosive Charges, 539

Explosives. *See* Blasting

F

FEIGENBAUM, S.: *Discussion on Direct Oxidation in the Basic Open Hearth Furnace*, 77

FEILD, A. L.: *Discussion on Direct Oxidation in the Basic Open Hearth Furnace*, 72

FELLOWS, J. A.: *Discussion on X Ray Determination of Retained Austenite by Integrated Intensities*, 414

FLICK, N. C.: *Discussion on Method for Determining the Origin of Surface Defects*, 216

FLYNN, R. A.: *Discussion on Direct Oxidation in the Basic Open Hearth Furnace*, 69

Fracture stress: low-carbon steel: influence of strain aging, 436
meaning of term, 436

G

GAINES, J. W.: *Discussions: on Direct Oxidation in the Basic Open Hearth Furnace*, 73
on Kinetics of the Transfer of Sulphur Across a Slag-metal Interface, 328

GEIL, G. W., McADAM, D. J. JR., WOODARD, D. H. and JENKINS, W. D.: *Influence of Strain Aging on the Fracture Stress of Low-carbon Steel*, 436; *discussion*, 447

GEISLER, A. H.: *Discussion on X Ray Determination of Retained Austenite by Integrated Intensities*, 415

GOLDMAN, K. M. and CHANG, LO-CHING: *Kinetics of the Transfer of Sulphur Across a Slag-metal Interface*, 300; *discussion*, 327

GRANGE, R. A.: *Discussions: on Anisothermal Formation of Bainite and Proeutectoid Constituents*, 376
on Austenite Transformation above and within the Martensite Range, 397

Grinding balls: wear: development of suitable test, 490
effect of abrasive, 516, 520
effect of composition, 498, 520
effect of diameter and weight, 495
mechanism, 497

Grinding balls: wear: rate, 494
short time tests, 490, 518

Gun steel: eroded: heat checking, 482
surface cracking: coarse, 482

heat checking, 482, 486

mechanism of erosion, 487

post-fusion, 483

relation to grain boundaries, 484

testing resistance, 477, 489

testing for resistance to surface cracking, 477, 489

GURRY, R. W.: *Discussion on Apparatus for the Hot-extraction Analysis for Hydrogen in Steel*, 258

H

Hardenability of steel: definition in terms of austenite decomposition, 363

HAWORTH, R. D. JR.: *Discussion on Wear Tests on Grinding Balls*, 520

HESS, W. F.: *Discussion on Anisothermal Formation of Bainite and Proeutectoid Constituents*, 377

HOWARD, R. T. JR. and COHEN, MORRIS: *Austenite Transformation above and within the Martensite Range*, 384; *discussion*, 397

Howe Memorial Lecture: Temperatures in the Open-hearth Furnace, 15

HOYT, S. L.: *Discussion on Structure, Segregation and Solidification of Semikilled Steel Ingots*, 165

HUGHES, EDWARD B. and NORRIS, FRANK G.: *Direct Oxidation in the Basic Open Hearth Process*, 52; *discussion*, 68

HULTGRÉN, AXEL: *Origin of Silicate Inclusions in Basic Electric-arc-furnace Steel of Higher Carbon Contents*, 173

HYDE, R. W., EATON, S. E. and OLD, B. S.: *Tracer Study of Sulphur in the Coke Oven*, 343

Hydrogen in steel: analysis: effect of size and shape of solid sample, 243

gas extracted at high temperature, 248

storage tubes for hydrogen, 240

during commercial melting: quantitative experimental investigation, 260

effect on ductility of cast steel, 283

extraction at low temperatures, 246

hot extraction for analysis: apparatus, Battelle Memorial Institute, 248

rail steel: methods of sampling and analysis, 219

review of literature, 262, 285

vacuum-fusion analysis: rail steel, 219

I

Inclusions: basic electric high-carbon steel: effect of restricting pouring stream for small ingots, 175

research at Söderfors works, Sweden, 173
tapping and pouring tests on large scale, 177

silicate: basic electric high-carbon steel: research at Söderfors works, Sweden, 173

tapping and pouring tests on large scale, 177

effect of restricting pouring stream for small ingots, 175

- INGERSON, EARL: *Testing Gun Steel and Other Alloys and Metals for Resistance to Surface Cracking*, 477; discussion, 489
- Iron: alpha: anelastic effects: interrelation, 449
relaxations, 451
- Puron: anelastic effects, 451
composition, 451
- Iron and steel: grinding balls: wear test: short time, 490, 518
melting: slag-metal interface: sulphur transfer: kinetics, 309
- J
- JAFFE, L. D.: *Anisothermal Formation of Bainite and Proeutectoid Constituents in Steels*, 363; discussion, 376
Discussions: on Anelastic Properties of Iron, 474
on Austenite Transformation above and within the Martensite Range, 398
- JENKINS, W. D., McADAM, D. J. JR., GEIL, G. W. and JENKINS, W. D.: *Influence of Strain Aging on the Fracture Stress of Low-carbon Steel*, 436; discussion, 447
- Jernkontoret: research on origin of silicate inclusions in basic electric steel of higher carbon contents, 173
- JOHNSON, H. W.: *Discussion on Direct Oxidation in the Basic Open Hearth Furnace*, 68
- JOSEPH, T. L.: *Discussion on Kinetics of the Transfer of Sulphur Across a Slag-metal Interface*, 328
- K
- KE, T'ING-SUI: *Anelastic Properties of Iron*, 448; discussion, 474
- Kinetics of transfer of sulphur across a slag-metal interface, 309
- KING, P. P.: *Discussion on Apparatus for the Hot-extraction Analysis for Hydrogen in Steel*, 257, 258
- KNOWLTON, H. B.: *Discussion on An Evaluation of Quenching Oils by Means of the End Quench Test*, 422
- KOH, P. K.: *Discussion on Austenite Transformation above and within the Martensite Range*, 398
- KOMARNITSKY, R. S.: *Discussion on An Evaluation of Quenching Oils by Means of the End Quench Test*, 422
- KULP, R. K.: *Discussion on Structure, Segregation and Solidification of Semikilled Steel Ingots*, 164
- L
- LARSEN, B. M.: *Discussion on Direct Oxidation in the Basic Open Hearth Furnace*, 68
- LARSEN, B. M. and BROWER, T. E.: *Role of Thermochemical Factors in Basic Open Hearth Production Rate*, 92
Some Correlations between Variables Affecting Sulphur in Blast Furnace Iron, 330
- LEBEDEFF, Y. E.: *Discussion on Kinetics of the Transfer of Sulphur Across a Slag-metal Interface*, 327, 329
- LEWIS, J. C.: *Discussion on Apparatus for the Hot-extraction Analysis for Hydrogen in Steel*, 257
- LOEB, C. M. JR. and NORMAN, T. E.: *Wear Tests on Grinding Balls*, 490; discussion, 520
- LORIA, E. A.: *Discussions: on Anisothermal Formation of Bainite and Proeutectoid Constituents*, 377
on Method for Determining the Origin of Surface Defects, 217
on Testing Gun Steel and Other Alloys and Metals, 489
- LOW, J. R. JR.: *Discussion on Influence of Strain Aging on the Fracture Stress of Low-carbon Steel*, 447
- M
- MARSH, J. S.: *Operation of Oxygen-enriched Open-hearth Furnaces*, 78; discussion, 89
Discussion on Structure, Segregation and Solidification of Semikilled Steel Ingots, 164
- MARSHALL, S.: *Discussion on Direct Oxidation in the Basic Open Hearth Furnace*, 73
- Martensite. See Steel
- McADAM, D. J. JR., GEIL, G. W., WOODARD, D. H. and JENKINS, W. D.: *Influence of Strain Aging on the Fracture Stress of Low-carbon Steel*, 436; discussion, 447
- McQUAID, H. W.: *Discussion on Structure, Segregation and Solidification of Semikilled Steel Ingots*, 165
- MEYETTE, C. L. and ELLIOTT, V. E.: *Method for Determining the Origin of Surface Defects in Rolled Steel Products*, 201; discussion, 216
- MOORE, G. A.: *Discussion on Sampling and Analysis of Steel for Hydrogen*, 246
- MOORE, G. A. and SIMS, C. E.: *Apparatus for the Hot-extraction Analysis for Hydrogen in Steel*, 248; discussion, 257
- MOORE, G. A., SIMS, C. E. and WILLIAMS, D. W.: *A Quantitative Experimental Investigation of the Hydrogen and Nitrogen Contents of Steel during Commercial Melting*, 260; discussion, 278
Effect of Hydrogen on the Ductility of Cast Steels, 283
- Munroe effect: shaped charges of explosives, 527
- N
- NELSON, LEON: *Discussion on Structure, Segregation and Solidification of Semikilled Steel Ingots*, 163
- Nitrogen: in steel: during commercial melting: quantitative experimental investigation, 260
protection of steel in casting to prevent oxidation, 189
- NORMAN, T. E. and LOEB, C. M. JR.: *Wear Tests on Grinding Balls*, 490; discussion, 520
- NORRIS, F. G.: *Discussions: on Method for Determining the Origin of Surface Defects*, 216
on Operation of Oxygen-enriched Open-hearth Furnaces, 91
- NORRIS, FRANK G. and HUGHES, EDWARD B.: *Direct Oxidation in the Basic Open Hearth Process*, 52; discussion, 68

O

- Oberhoffer's reagent: use in determining surface defects in rolled steel products, 217, 218
- OLD, B. S., EATON, S. E. and HYDE, R. W., *Tracer Study of Sulphur in the Coke Oven*, 343
- Open-hearth furnaces (*see also* Open-hearth Process):
 basic: liquid fuel: mode of operation, 16
 walls: operating conditions, 41
 heat transfer: methods, 78
 radiation, 79
 oxygen-enriched: effect on scrap and hot-metal ratio, 90
 operation: experimental heats, 78
 refractories: effect of oxygen in operation, 87
 temperatures: flame: increasing, 79
 high: significance, 78
- Open-hearth process (*see also* Open-hearth Furnaces):
 basic: direct oxidation: carbon elimination: control, 56
 carbon elimination: determining rate, 54, 69, 77
 carbon elimination: theory, 60, 72
 definition, 52
 efficiency, 58, 67, 70
 objectives, 53
 pipe life, 71
 practice, 53
 relation to ladle skull, 66
 heat-balance calculations, 93
 heat requirement from charge to melt, net, 106
 mode of operation of furnace, 16
 oxidation: air vs ore: relative amounts, 98
 oxygen blowing: effect on net heat requirement, 101
 production rate: controlling or increasing, 105
 effect of limestone charged, 102
 light vs heavy scrap, 99
 relation to ore in charge and carbon at melt, 100
 role of thermochemical factors, 92
 temperature measurement: air and furnace gases, 47
 Pencoyd Works, 22
 practical plant methods: bath-equalization, 25
 blowing-tube pyrometer, 27
 checking systems, 32
 closed-tube radiation, 26
 rod-boil, 25
 slag bubble, 25
 slag surface, 25
 test-spoon, 24
 purpose, 16, 37
 hydrogen elimination, 272, 273
 temperature measurement: methods: "look," "approach," "touch," 16

P

- PATTERSON, C. T.: *Discussion on Austenite Transformation above and within the Martensite Range*, 398

- PEIFER, W., DERGE, G. and RICHARDS, J. H.: *Sampling and Analysis of Steel for Hydrogen*, 219; *discussion*, 246
- PHILBROOK, W. O.: *Discussion on Structure, Segregation and Solidification of Semikilled Steel Ingots*, 163
- Plastic deformation: influence on fracture stress of low-carbon steel, 436
- Puron (alpha iron): composition, 451
- Pyrometry: in the open-hearth process, 15
 industrial: purposes, 16, 37
 methods in metallurgy: bibliography, 50

Q

- Quenching oils: evaluation by means of end quench test, 416
- QUENEAU, B. R.: *Discussions: on Structure, Segregation and Solidification of Semikilled Steel Ingots*, 169
on X Ray Determination of Retained Austenite by Integrated Intensities, 414

R

- Radioactive pyrite: preparation for tracer study of sulphur in coke oven, 346
- RAUDEBAUGH, R. J.: *Discussion on Direct Oxidation in the Basic Open Hearth Furnace*, 76
- REAGAN, W. J.: *Discussion on Direct Oxidation in the Basic Open Hearth Furnace*, 72
- Refractories: open-hearth furnaces: effect of oxygen in operation, 87
- RICHARDS, J. H., DERGE, G. and PEIFER, W.: *Sampling and Analysis of Steel for Hydrogen*, 219; *discussion*, 246
- Rolled steel: burning: definition of term, 216
 surface defects: burnt: definition of term, 216
 determination with Oberhoffer's reagent, 217, 218
 mechanical type, 201
 method for determining origin by degree of oxide diffusion, 201
 steel type, 201
- ROSENBLATT, D. N.: *Discussion on Austenite Transformation above and within the Martensite Range*, 398
- ROSENQVIST, TERKEL: *Note on the Distribution of Sulphur between Molten Iron and Slag*, 541
- ROWLAND, E. S.: *Discussion on X Ray Determination of Retained Austenite by Integrated Intensities*, 415

S

- SACHS, G., EBERT, L. J. and BROWN, W. F. JR.: *Notch-tensile Characteristics of a Partially Austempered, Low Alloy Steel*, 424
- SANDOZ, G. and SIEBERT, C. A.: *An Evaluation of Quenching Oils by Means of the End Quench Test*, 416; *discussion*, 421
- SCHONFELD, F. W.: *Discussion on Behavior of Metal Cavity Liners in Shaped Explosive Charges*, 538, 539

- SIEBERT, C. A. and SANDOZ, G.: *An Evaluation of Quenching Oils by Means of the End Quench Test*, 416; discussion, 421
- SIMS, C. E.: *Discussions: on Direct Oxidation in the Basic Open Hearth Furnace*, 69
on Kinetics of the Transfer of Sulphur across a Slag-metal Interface, 328
on Method for Determining the Origin of Surface Defects, 216
on Operation of Oxygen-enriched Open-hearth Furnaces, 89, 91
on Structure, Segregation and Solidification of Semikilled Steel Ingots, 164
- SIMS, C. E. and MOORE, G. A.: *Apparatus for the Hot-extraction Analysis for Hydrogen in Steel*, 248; discussion, 257
- SIMS, C. E., MOORE, G. A. and WILLIAMS, D. W.: *Effect of Hydrogen on the Ductility of Cast Steels*, 283
A Quantitative Experimental Investigation of the Hydrogen and Nitrogen Contents of Steel during Commercial Melting, 260; discussion, 278
- Slag-metal interface: kinetics of sulphur transfer, 309
- SLOTTMAN, G. V.: *Discussion on Direct Oxidation in the Basic Open Hearth Furnace*, 72
- SNOEK, J. L.: *Discussion on Anelastic Properties of Iron*, 475
- Söderfors steel works. *See* Inclusions
- SOLER, GILBERT: *Discussion on Structure, Segregation and Solidification of Semikilled Steel Ingots*, 164
- SOSMAN, ROBERT B.: *Temperatures in the Open-hearth Furnace*, 15
- Steel (*see also* Iron and Steel):
 anisothermal formation of bainite and pro-eutectoid constituents: applications, 374, 377
 study, 363
 austenite: anisothermal decomposition: bainite formation, 363, 378
 incubation, nature, 377
 study, 363
 isothermal transformation: bainite formation, 390
 retained in hardened steels, 401
 transformation above and within martensite range: study of TTT curves, 384
 TTT curves, 384
 bainite: anisothermal formation, 363
 burning: definition, 216
 cast. *See* Cast Steel
 casting: nitrogen protection to prevent oxidation, Caspersson ladle, 189
 chromium (SAE 5140): partially austempered and subsequently quenched: notch properties, 424
 notch properties: austempering at 860° and 950°F, 434
 comparison with those of tempered martensites, 432
 relation to hardness, 428
 practical significance of investigation, 434
 gun. *See* Gun Steel
 hardenability: definition in terms of austenite decomposition, 363
- Steel: hardened: austenite: effects, 401
 quantity retained, 401
 X ray determination: based on integrated intensities, 401
 based on integrated intensities: vs lineal analysis, 409
 methods, 401
 high-carbon: inclusions. *See* Inclusions
 hydrogen. *See* Hydrogen in Steel
 low-carbon: fracture stress: influence of strain aging, 436
 martensites: tempered: notch properties, 432
 quenching: evaluating quenchants, 416, 421
 quenching in liquid: three stages of cooling, 416
 quenching in oil: cooling power of oils, 423
 end quench test for evaluation of oil used, 416
 rolled. *See* Rolled Steel
 sampling and analysis for hydrogen, 219
 semikilled: definition, 108
 deoxidation: effect of deoxidizer, 166
 practice, 127
 ingots. *See* Steel Ingots
 liquid: oxygen content, 125
 types: capped, 108, 111, 164
 intermediate, 108, 117
 no mold deoxidation, 108, 122
 tapping: Perrin effect: test heat, 193
- Steel ingots: semikilled: hydrogen content: effect on structure, 169
 segregation characteristics, 130
 solidification characteristics: central part, 159
 structure: capped type, 112
 hydrogen effect, 169
 intermediate type, 117
 no mold deoxidation, 122
 structure, segregation and solidification: review of literature, 109
 study of experimental ingots, 108
- Steelmaking: basic: sulphur flowsheet, 343
 sulphur in bath: distribution between molten iron and slag, 540
- Strain aging: influence on fracture stress of low-carbon steel, 436
- Sulphur: flow in basic steel process, 343
 in blast-furnace iron: variables affecting: correlations, 330
 transfer across slag-metal interface: kinetics, 309
- Swedish Ironmasters' Association. *See* Jernkontoret

T

- TAYLOR, C. R.: *Discussions: on Direct Oxidation in the Basic Open Hearth Furnace*, 68
on Kinetics of the Transfer of Sulphur Across a Slag-metal Interface, 327
on Operation of Oxygen-enriched Open-hearth Furnaces, 89, 91
- TENENBAUM, M.: *Structure, Segregation and Solidification of Semikilled Steel Ingots*, 108; discussion, 163
Discussions: on Direct Oxidation in the Basic Open Hearth Furnace, 68, 71, 72
on Operation of Oxygen-enriched Open-hearth Furnaces, 89

- THOMPSON, J. G.: *Discussion on Sampling and Analysis of Steel for Hydrogen*, 247
- THUM, E. E.: *Discussion on Behavior of Metal Cavity Liners in Shaped Explosive Charges*, 538
- TINER, N.: *Discussion on Method for Determining the Origin of Surface Defects*, 216

W

- WAGSTAFF, J. B.: *Discussions: on Direct Oxidation in the Basic Open Hearth Furnace*, 72
on Operation of Oxygen-enriched Open-hearth Furnaces, 90
- WALKER, H. L.: *Discussion on An Evaluation of Quenching Oils by Means of the End Quench Test*, 421, 422
- Washburn core, 253, 254
- WASHBURN, T. S.: *Discussions: on Direct Oxidation in the Basic Open Hearth Furnace*, 68, 70
on Operation of Oxygen-enriched Open-hearth Furnaces, 90
- WILLIAMS, D. W., SIMS, C. E. and MOORE, G. A.: *Effect of Hydrogen on the Ductility of Cast Steels*, 283

- WILLIAMS, D. W., SIMS, C. E. and MOORE, G. A.: *Quantitative Experimental Investigation of the Hydrogen and Nitrogen Contents of Steel during Commercial Melting*, 260; *discussion*, 278
- WOODARD, D. H., McADAM, D. J. JR., GEIL, G. W. and JENKINS, W. D.: *Influence of Strain Aging on the Fracture Stress of Low-carbon Steel*, 436; *discussion*, 447

X

- X ray determination of retained austenite in hardened steels: method based on integrated intensities, 401

Y

- YAROTSKY, M. F.: *Discussion on Structure, Segregation and Solidification of Semikilled Steel Ingots*, 165

Z

- ZMESKAL, O.: *Discussion on X Ray Determination of Retained Austenite by Integrated Intensities*, 414



3 8198 309 333 464
THE UNIVERSITY OF ILLINOIS AT CHICAGO

**THIS BOOK IS FOR USE
ONLY IN THE LIBRARY
IT DOES NOT CIRCULATE**

